frontiers | Research Topics

Interpretation and implications of variability in ecological systems

Edited by
Robert Klinger, Clare Aslan and
Karen Thorne

Published in
Frontiers in Ecology and Evolution

ISSN 1664-8714
ISBN 978-2-8325-5173-8
DOI 10.3389/978-2-8325-5173-8

About Frontiers

Frontiers is more than just an open access publisher of scholarly articles: it is a pioneering approach to the world of academia, radically improving the way scholarly research is managed. The grand vision of Frontiers is a world where all people have an equal opportunity to seek, share and generate knowledge. Frontiers provides immediate and permanent online open access to all its publications, but this alone is not enough to realize our grand goals.

Frontiers journal series

The Frontiers journal series is a multi-tier and interdisciplinary set of open-access, online journals, promising a paradigm shift from the current review, selection and dissemination processes in academic publishing. All Frontiers journals are driven by researchers for researchers; therefore, they constitute a service to the scholarly community. At the same time, the *Frontiers journal series* operates on a revolutionary invention, the tiered publishing system, initially addressing specific communities of scholars, and gradually climbing up to broader public understanding, thus serving the interests of the lay society, too.

Dedication to quality

Each Frontiers article is a landmark of the highest quality, thanks to genuinely collaborative interactions between authors and review editors, who include some of the world's best academicians. Research must be certified by peers before entering a stream of knowledge that may eventually reach the public - and shape society; therefore, Frontiers only applies the most rigorous and unbiased reviews. Frontiers revolutionizes research publishing by freely delivering the most outstanding research, evaluated with no bias from both the academic and social point of view. By applying the most advanced information technologies, Frontiers is catapulting scholarly publishing into a new generation.

What are Frontiers Research Topics?

Frontiers Research Topics are very popular trademarks of the *Frontiers journals series*: they are collections of at least ten articles, all centered on a particular subject. With their unique mix of varied contributions from Original Research to Review Articles, Frontiers Research Topics unify the most influential researchers, the latest key findings and historical advances in a hot research area.

Find out more on how to host your own Frontiers Research Topic or contribute to one as an author by contacting the Frontiers editorial office: frontiersin.org/about/contact

Interpretation and implications of variability in ecological systems

Topic editors
Robert Klinger — Belize Foundation For Research & Environmental Education, Belize
Clare Aslan — Northern Arizona University, United States
Karen Thorne — Western Ecological Research Center, United States Geological Survey (USGS), United States

Citation
Klinger, R., Aslan, C., Thorne, K., eds. (2024). *Interpretation and implications of variability in ecological systems*. Lausanne: Frontiers Media SA.
doi: 10.3389/978-2-8325-5173-8

Table of contents

Frontiers in Ecology and Evolution

TYPE Original Research
PUBLISHED 23 December 2022
DOI 10.3389/fevo.2022.1053548

OPEN ACCESS

EDITED BY
Luís Borda-de-Água,
Centro de Investigacao em Biodiversidade e Recursos Geneticos (CIBIO-InBIO),
Portugal

REVIEWED BY
Anvar Sanaei,
Leipzig University,
Germany
Yolanda F. Wiersma,
Memorial University of Newfoundland,
Canada

*CORRESPONDENCE
Clare E. Aslan
✉ clare.aslan@nau.edu

SPECIALTY SECTION
This article was submitted to Biogeography and Macroecology, a section of the journal Frontiers in Ecology and Evolution

RECEIVED 25 September 2022
ACCEPTED 02 December 2022
PUBLISHED 23 December 2022

CITATION
Aslan CE, Zachmann L, Epanchin-Niell RS, Brunson MW, Veloz S and Sikes BA (2022) Soil characteristics and bare ground cover differ among jurisdictions and disturbance histories in Western US protected area-centered ecosystems.
Front. Ecol. Evol. 10:1053548.
doi: 10.3389/fevo.2022.1053548

Soil characteristics and bare ground cover differ among jurisdictions and disturbance histories in Western US protected area-centered ecosystems

Clare E. Aslan[1,2]*, Luke Zachmann[2], Rebecca S. Epanchin-Niell[3], Mark W. Brunson[4], Samuel Veloz[5] and Benjamin A. Sikes[6]

[1]Center for Adaptable Western Landscapes, Northern Arizona University, Flagstaff, AZ, United States, [2]Conservation Science Partners, Truckee, CA, United States, [3]College of Agriculture and Natural Resources, University of Maryland, College Park, MD, United States, [4]Environment and Society Department, Utah State University, Logan, UT, United States, [5]Point Blue Conservation Science, Petaluma, CA, United States, [6]Department of Ecology and Evolutionary Biology and Kansas Biological Survey, University of Kansas, Lawrence, KS, United States

Introduction: Ecological conditions at a given site are driven by factors including resource availability, habitat connectivity, and disturbance history. Land managers can influence disturbance history at a site by harvesting resources, creating transportation pathways, introducing new species, and altering the frequency and severity of events such as fires and floods. As a result, locations with different land management histories have also likely experienced different disturbance trajectories that, over time, are likely to result in different ecological characteristics.

Methods: To understand how the presence of different management histories may shape ecological conditions across large landscapes, we examined plant and soil characteristics at matched sampling points across jurisdictional boundaries within four Protected Area-Centered Ecosystems (PACEs) in the western US. We employed Bayesian modeling to explore 1) the extent to which specific ecological variables are linked to disturbance and jurisdiction both among and within individual PACEs, and 2) whether disturbance evidence differs among jurisdictions within each PACE.

Results: Across all jurisdictions we found that disturbances were associated with ecologically meaningful shifts in percent cover of bare ground, forbs, grass, shrubs, and trees, as well as in tree species richness, soil stability, and total carbon. However, the magnitude of shifts varied by PACE. Within PACEs, there were also meaningful associations between some ecological variables and jurisdiction type; the most consistent of these were in soil stability and soil carbon:nitrogen ratios. Disturbance evidence within each PACE was relatively similar across jurisdictions, with strong differences detected between contrast jurisdictions only for the Lassen Volcanic National Park PACE (LAVO).

Discussion: These findings suggest an interaction between management history and geography, such that ecotones appear to manifest at jurisdictional boundaries within some, but not all, contexts of disturbance and location. Additionally, we detected numerous differences between PACEs in the size of disturbance effects on ecological variables, suggesting that while the interplay between disturbance and management explored here appears influential, there remains a large amount of unexplained variance in these landscapes. As continued global change elevates the importance of large landscape habitat connectivity, unaligned management activities among neighboring jurisdictions are likely to influence existing ecological conditions and connectivity, conservation planning, and desired outcomes.

KEYWORDS

anthropogenic disturbance, coupled natural-human systems, cross-boundary management, ecological variability, fire, forest management, grazing, groundcover

1. Introduction

The ecosystem at any given location is driven in part by history of disturbance and stress (e.g., Pierce et al., 2007; Miller et al., 2011). Events and processes that add, reduce, or rearrange resources are key influences on the diversity and function of species assemblages (Powell et al., 2011; Trivellone et al., 2017; Zhang et al., 2019). Human activity shapes these patterns, even in large undeveloped landscapes. Human management type and activity at a given site can affect resources through harvest, restoration, biological invasion, and other processes (Lampert et al., 2014; Goldmann et al., 2015; Innes et al., 2019). Management also affects the types, intensity, and frequency of disturbance, such as through fire suppression, damming and diversion of water, or grazing (Führer, 2000; Alkemade et al., 2013; Schmutz and Moog, 2018). As a result, sites with similar environmental conditions but different management histories may exhibit different biodiversity, function, and adaptive capacity (Bengtsson et al., 2000; Fischer et al., 2006; Levin et al., 2006; Floren et al., 2014; Nicotra et al., 2015; Teague and Barnes, 2017; Huang et al., 2020). Understanding how management may drive such differences among sites is particularly important in light of global change, the emergence of novel ecosystems, and an increasing need for planners and managers to tailor solutions to changing conditions across landscapes (Hobbs et al., 2006).

If management processes shape ecological patterns, over time ecological similarities between jurisdictions may be predicted by similarities in management history (Aslan et al., 2021a). Conversely, initially intact ecosystems that are subjected to unique management histories across jurisdictional boundaries may, over time, diverge to be ecologically distinct even with similar climate, geology, and geography. A primary mechanism driving these management-driven shifts is likely consistent differences between jurisdictions in anthropogenic disturbance. Sites that have been managed primarily for resource extraction such as logging and mining, for example, will exhibit high occurrence of surface disturbance, resource transportation roads, younger forests on average, and possibly active restoration following extraction (DeLong et al., 2004; Zollner et al., 2005; Andrés and Mateos, 2006; Hartmann et al., 2012; Huang et al., 2015; Nelson et al., 2019). Sites managed for recreation, by contrast, may exhibit disturbances clustered in accessible areas such as campgrounds or attractions, passenger car roads and trails, and active restoration such as revegetation projects (Brown et al., 2008; Marzano and Dandy, 2012; Monz et al., 2013; Gutzwiller et al., 2017). Residential sites, including rangelands or forests with subsistence farms, ranches, or private inholdings, may exhibit disturbances that are clustered around built structures, with surrounding undeveloped areas containing trails and further disturbance through off-road vehicle use, harvesting of non-timber forest products, or firewood collection (Maestas et al., 2001; Havlick, 2002; Hansen et al., 2005; Ponstingel, 2020; Gonçalves et al., 2021). Adjacent sites managed for different goals likely provide a key indicator of the potential for management-driven ecological divergence.

Conservation relies on understanding how differing management on the two sides of a boundary may create discontinuities between protected and adjacent areas. These effects may differ across scales. Conservation planning often relies on large, connected landscapes protected from development. In North America, examples include Paseo Pantera: the Path of the Panther (for jaguar movement between Mexico and the United States) and the Yellowstone to Yukon initiative (protecting large mammal migration between Canada and the United States) (Rabinowitz, 2014; Chester, 2015). Smaller, more numerous efforts seek to preserve local habitat connectivity across multi-jurisdictional landscapes through coordinated restorations, watershed, or fire management (e.g., Schultz et al., 2012; Koontz and Newig, 2014; Schultz and Moseley, 2019). Connected landscapes, in turn, allow for dispersal of individuals, gene flow, seasonal migration, recolonization of sites following disturbance, and distributional shifts of populations as a result of climate change (Rudnick et al., 2012; Baguette et al., 2013). However, large landscapes that are divided into multiple distinct management units—as a result of historical events and decisions, distribution of economically-valuable resources, funding allocations, grandfathered practices, and other drivers—are subject to an assortment of internal decisions that result in a patchwork of management practices (Huggard, 2004; Andrew et al., 2012; Aslan et al., 2021a). The result is a management mosaic (*sensu* Epanchin-Niell et al., 2010) that can manifest as an ecological mosaic.

In undeveloped landscapes, management mosaics likely maintain some commonalities that span jurisdictions—for example, broad vegetation type responds to elevation, latitude, and topography and is unlikely to shift across boundaries in response to management except where disturbance has removed all vegetation such as at a mine or quarry. By contrast, changes in plant composition and vegetation pattern and disturbance evidence may respond at smaller spatial and temporal scales to varying management activities, tracking the management mosaic. This mix of factors and scales likely generates an ecological continuum between adjacent management units (Duinker et al., 2010; Andrew et al., 2012; Wiersma et al., 2015). Within that continuum, our aim was to understand how ecological conditions vary as a function of the jurisdictional mosaic within landscape-scale ecosystems.

We placed our study in the landscapes containing four large national parks in the western US: Sequoia-Kings Canyon National Park (SEKI), Lassen Volcanic National Park (LAVO), Grand Canyon National Park and protected areas encompassed in the same ecosystem along the Colorado River (CORI), and Rocky Mountain National Park (ROMO). We selected these case study ecosystems to inform our ongoing conversations with land managers in each park regarding the influences of cross-boundary management challenges. We used field-based data collection to measure ecological characteristics and disturbance evidence across jurisdictional boundaries and employed a Bayesian framework to analyze and understand the resulting patterns, in order to determine whether jurisdiction is predictive of certain ecological characteristics within these large landscapes. We hypothesized that variation in disturbance management is a likely mechanism driving such relationships, so we also analyzed first the relationship between disturbance and ecological variables, then the relationship between disturbance and jurisdiction, and finally the relationship between jurisdiction and measured ecological variables. We piloted the methods used here in the CORI landscape (Aslan et al., 2021b) and in this study refined analyses and extended them across all four landscapes to enable comparison among different geographies. Our findings thus enable us to discuss possible social-ecological influences on ecological conditions within and among landscapes.

With this study, we aimed to examine differences in ecological variables at a point in time that are reflective of mechanisms that span temporal and spatial scales. Knowing that the vegetation and soils at a sampling location are reflective of broad biogeographical influences, geology, historical events, and days to decades to centuries of species interactions and biological processes, we aimed to investigate whether differences in management can manifest in a consistent way detectable in spite of such broad natural variability.

2. Materials and methods

2.1. Study areas

We collected ecological data across jurisdictional boundaries within four focal Protected Area-Centered Ecosystems (PACEs), which served as case study systems for this work. All four PACEs are located in the western US. ROMO occupies a section of the eastern slope and high elevations of the Rocky Mountains in Colorado, spanning vegetation types including oak grasslands, coniferous forests, and tundra. CORI occurs in northern Arizona, southern Utah, and southeastern Nevada and includes sagebrush desert, oak and pinyon-juniper woodlands, and coniferous forests. SEKI occupies a stretch of ridgeline and both western and eastern slopes of the Sierra Nevada in south-central California, ranging from mesic oak grasslands to tundra to high desert. LAVO occurs in temperate coniferous forest in northern California.

2.2. Framework and hypothesis development

Our field sampling protocols and analyses were guided by an *a priori* set of hypotheses linking ecological variables to disturbance and disturbance to jurisdiction (Table 1; Figure 1). At our field sites, we examined the frequency of evidence of disturbance in the form of fire, forest management, grazing, and general human presence. We predicted that vegetation structure would respond to these disturbances. Specifically, we hypothesized that disturbances would be associated with diminished tree cover, and, due to increased light penetration, would be associated with increasing cover of bare ground, grasses, forbs, and, over time, shrubs (Goosem, 2007; Shatford et al., 2007; Schwilk et al., 2009; Stephens et al., 2012; Crotteau et al., 2013; Miller et al., 2014). We also hypothesized that disturbances would reduce soil stability and alter soil chemistry (Kutiel and Shaviv, 1989; Manley et al., 1995; Neff et al., 2005; James et al., 2021). Our detailed hypotheses are presented in Table 1.

We hypothesized that disturbances would vary in frequency and severity across different jurisdictional types (National Park Service-NPS, US Forest Service-USFS-Wilderness and Nonwilderness, and Bureau of Land Management-BLM) in our case study landscapes. Wilderness areas in the US are managed to be "untrammeled," with as little human disturbance as possible (Parsons and Landres, 1996; Zellmer, 2014); as a result, general forest management activities are rare, as are prescribed burns, although natural wildfires may be particularly frequent and extensive. With their dual missions of conservation and recreation, national parks may employ burns and forest management to restore biodiversity or reduce fire hazard, but also aim to support natural processes and patterns, likely resulting in an intermediate level of fire and forest management in such units. National forests are managed to produce the nation's timber crop and thus most likely to use intensive management techniques. Grazing occurs in all sites if

TABLE 1 Conceptual framework and predicted ecological differences among jurisdictions.

Disturbance Type	Response variables affected	Rationale	Citations
Fire	Tree percent cover; shrub percent cover; bare ground percent cover; adult tree density; sapling density; soil carbon; soil phosphorus; soil stability; tree richness	Fire of high enough intensity decreases percent cover of woody plants, particularly trees, initially. Bare ground cover can increase and trees decrease with fire. In the longer term, fire often facilitates shrub and sapling regeneration, resulting in increased densities of those woody plants following fire. Fire can release both carbon and phosphorus from plants into the soil. By removing dominant trees and initiating successional processes, fire can increase tree diversity.	Kutiel and Shaviv (1989), Shatford et al. (2007), Verma and Jayakumar (2012), Crotteau et al. (2013), Miller et al. (2014), Pellegrini et al. (2018)
Forest management	Tree percent cover; grass percent cover; forb percent cover; bare ground percent cover; adult tree density; sapling density; soil carbon; soil stability; adult tree dbh	Forest management consists of chainsaw work and tree/log removal. This reduces cover of trees and allows light penetration, increasing grass and forb and bare ground percent cover. Thinning efforts reduce density of both adult trees and saplings but often leave the largest trees in place, increasing overall average tree size. Soil carbon is released by tree removal and management activities, and soil stability can be reduced by management activities.	Schwilk et al. (2009), Stephens et al. (2012), James et al. (2021)
Human activity	Tree percent cover; grass percent cover; forb percent cover; bare ground percent cover; adult tree density; sapling density; soil carbon; soil stability	Human activity includes forest management work as well as trails and roads. These activities reduce cover of trees and allows light penetration, increasing grass and forb and bare ground percent cover. Such activities also facilitate invasion of non-native grasses and forbs. Soil carbon is released by tree removal and vegetation disturbance, and soil stability can be reduced by vegetation disturbance.	DiTomaso (2000), Pocock and Lawrence (2005), Goosem (2007), Schwilk et al. (2009), Stephens et al., 2012, James et al. (2021)
Grazing	Tree percent cover; shrub percent cover; grass percent cover; forb percent cover; bare ground percent cover; adult tree density; soil carbon; soil stability; C:N ratios	Tree cover and density are diminished where grazing occurs. Grasses and forbs may be facilitated by grazing, although overgrazing can lead to increased shrub cover and increased bare ground cover. Grazing can increase carbon: nitrogen ratios and soil carbon and decrease soil stability.	Manley et al. (1995), Teague et al. (2004), Neff et al. (2005), Best and Arcese (2009), Augustine et al. (2012), D'Odorico et al. (2012), Taboada et al., 2015, Souther et al. (2019), Zheng et al. (2020)

We hypothesized that ecological factors would vary over multijurisdictional landscapes due to systematic differences in frequency and severity of disturbances including fire, grazing management, forest management, and human activity.

grandfathered into NPS or USFS Wilderness (Pinto, 2014; Squillace, 2014), but is excluded from such units if not practiced prior to their protection. Grazing is a primary land use in BLM and USFS Nonwilderness areas. General human presence is likely to be particularly high in those areas as well, since they are considered multiuse (Havlick, 2002; Koontz and Bodine, 2008; Monz et al., 2013; Theobald, 2013; Payne, 2016). In our analytical methods, described below, we examined the strength of relationships between disturbance variables and ecological responses and identified instances in which ecological responses and disturbance evidence contrasted between jurisdictional units within the focal landscapes.

2.3. Field data collection

In 2017, 2018, and 2019 data were collected from public lands under different jurisdictions in all four PACEs. Data were collected from randomly selected sites near jurisdictional boundaries and, at each site, from clustered points such that two points lay on each side of the boundary and points formed a square with sides of 200 m (Supplementary Figure S1). Distance between points was selected to minimize natural differences in elevation and general vegetation type between the points within each square, in order to hold constant sources of natural variation as much as possible. At each point, researchers established two 50 m-long, 6 m-wide belt transects directed away from the jurisdictional boundary and angled 45 and 135 degrees from the boundary line (Supplementary Figure S1). Disturbance was recorded as present/absent within 1-m intervals along each belt transect. Groundcover was recorded by line-point intercept at 0.5-m intervals along the midline of the two transects. Abundance, size, and species richness of adult and sapling trees were recorded within a 100m^2 quadrat established between 20 m and 30 m along each transect and centered on the transect's 25 m mark. Soil stability was assessed at 5-m intervals along each of the transects, using a field soil slake test kit (Herrick et al., 2001). Soil cores to 20 cm depth

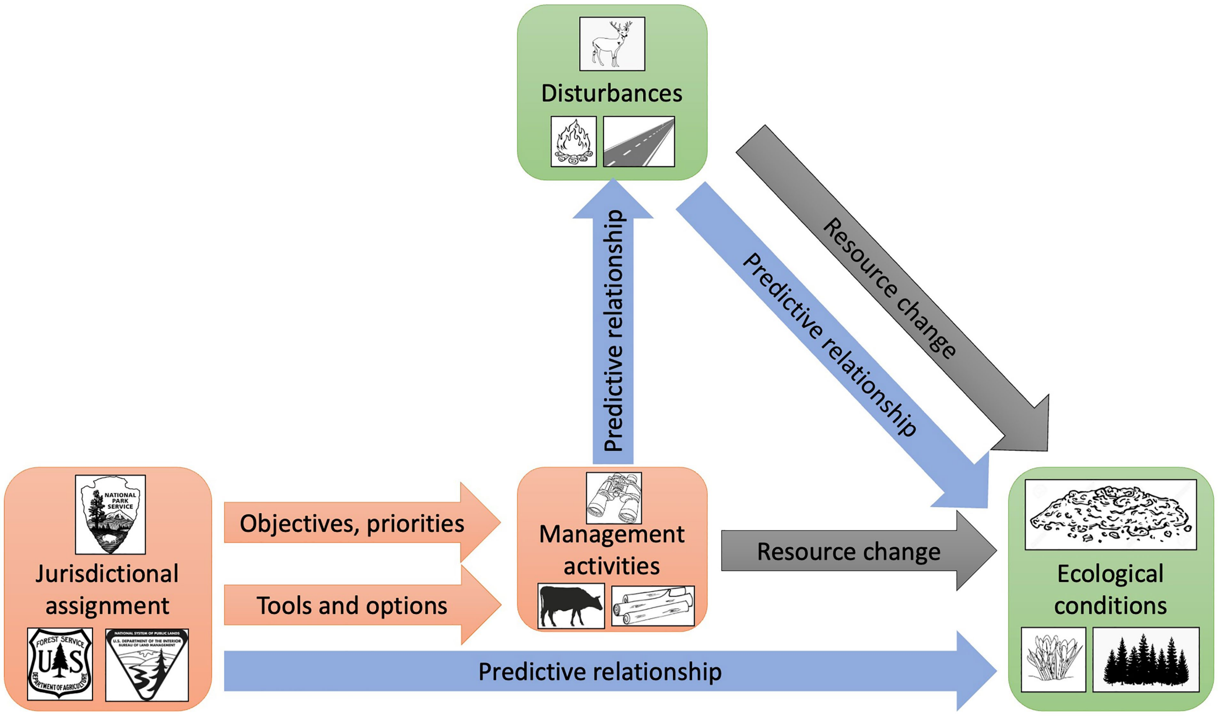

FIGURE 1
Experimental design and analytical flow. Green boxes=measured empirically during this study. Orange boxes and arrows=inferred from established policy and documents; drivers of hypotheses. Gray arrows=hypothesized mechanisms for relationships. Blue arrows=analyzed relationships.

were collected from three locations per transect and homogenized to allow later lab-based chemical and physical analysis (after Aslan et al., 2021b).

We aimed to sample 15 sites (90 points) from each of the following contrasts within each PACE: NPS/USFS Wilderness; NPS/USFS Nonwilderness; NPS/BLM; USFS Wilderness/USFS Nonwilderness; USFS Nonwilderness/BLM; and USFS Wilderness/BLM. In practice, not all contrasts occur within all PACEs, and due to access issues, we were not able to reach the full 15 sites for each contrast. Nevertheless, all management types and at least four contrasts were sampled in each PACE and our final set of sampled sites included 28 (112 points; 224 transects) in ROMO (4 contrasts), 50 (200 points; 400 transects) in LAVO (5 contrasts), 51 (204 points; 416 transects) in SEKI (4 contrasts), and 64 (256 points; 512 transects) in CORI (6 contrasts) (Figure 2).

2.4. Overall modeling and data analysis

To examine the relationships between disturbance and ecological variables (Table 1), disturbance and jurisdiction, and jurisdiction and ecological variables, we modeled data from sites within each PACE using a general, hierarchical formulation for the posterior and joint distribution of unobserved quantities:

$$\mu_{ij} = g\left(\alpha_j + x'_{ij}\beta + w'_{ij}\gamma\right) \tag{1}$$

$$\begin{aligned}&\left[\alpha,\, \beta,\, \gamma,\, \sigma^2,\, \mu_\propto,\, \sigma^2_\propto,\, y_j\right] \\ &\propto \prod_{i=1}^{n_j}\prod_{j=1}^{J}\left[y_{ij} \mid h\left(\mu_{ij}, \sigma^2_j\right)\right]\left[\alpha \mid, \mu_\alpha \mid, \sigma^2_\alpha\right] \\ &\times[\beta][\gamma]\left[\sigma^2\right][\mu_\alpha]\left[\sigma^2_\alpha\right]\end{aligned} \tag{2}$$

Bracket notation (Gelfand and Smith, 1990), $[a \mid b,c]$, reads the probability of a conditional on b and c and implies that any distribution appropriate for the support of the random variable y_{ij} could be used (Supplementary Table S1). Generality in notation is achieved using the moment matching function $h()$ that returns the parameters of a distribution given its first and second central moments (Hobbs and Hooten, 2015). The subscript $i = 1, 2, n_j$ indexes observations within site j; $j = 1, 2, J$ indexes sites within the PACE. The observations come from either of two transects at each of two points in each jurisdiction at a site (Supplementary Figure S1).

Observations were modeled with site-level intercept and, usually, site-specific variance terms. Intercepts for each site, α_j,

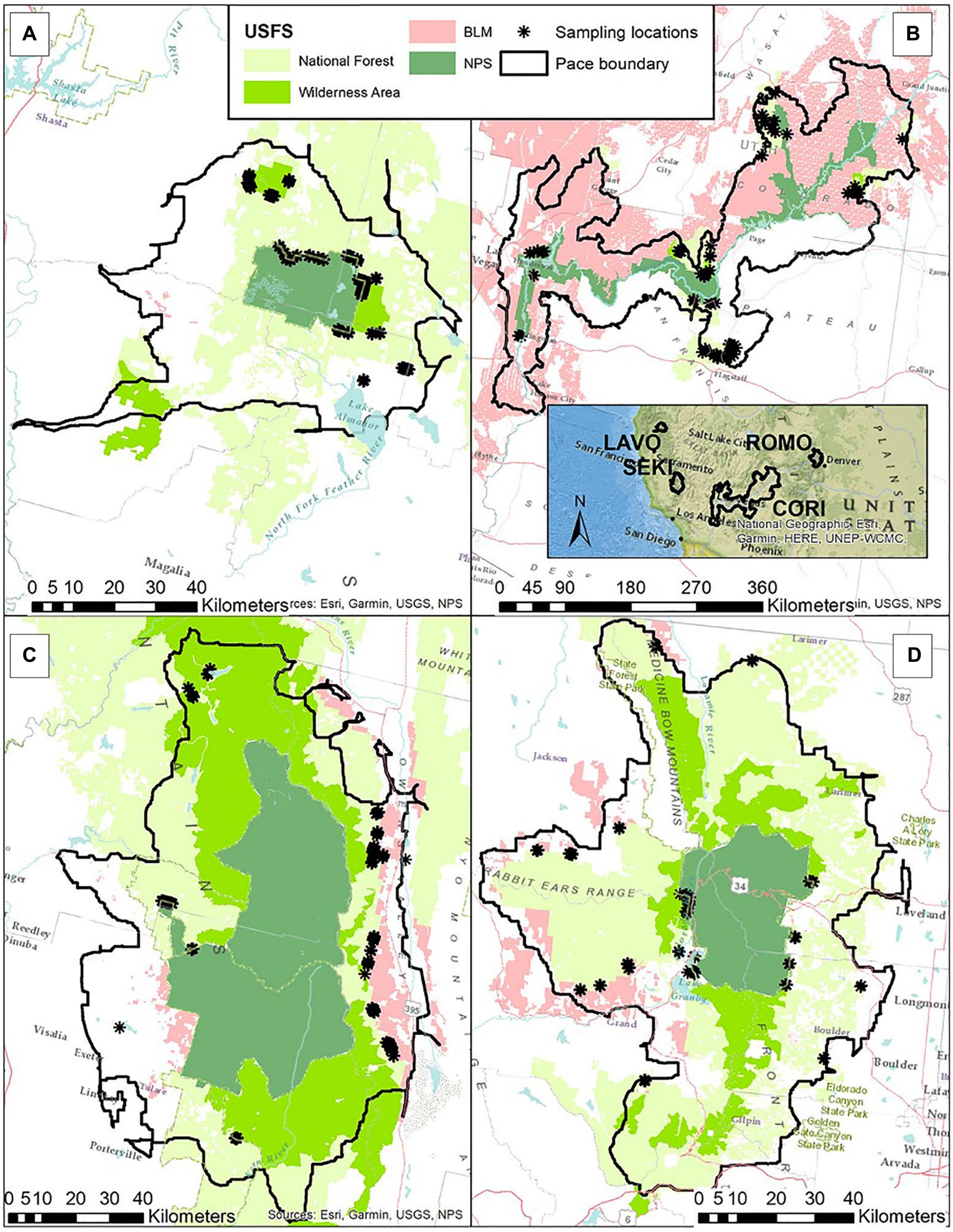

FIGURE 2
Map showing the four protected area centered ecosystems (PACEs) where we collected field samples; **(A)** Lassen LAVO, **(B)** Grand Canyon CORI, **(C)** Sequoia Kings Canyon SEKI, and **(D)** Rocky Mountain ROMO. Colors in the map indicate the different jurisdictions we examined; United States Fish and Wildlife Service (USFWS) wilderness and non-wilderness areas, Bureau of Land Management (BLM) and National Park Service (NPS). The solid black line indicates the boundary of each PACE.

were modeled as a random variable arising from a normal distribution with mean μ_α and variance $\sigma^2_\alpha : \alpha_j \sim \mathrm{N}(\mu_\alpha, \sigma^2_\alpha)$. Site-level variances, σ^2_j, were modeled as a random variable arising from a gamma distribution with parameters matched to moments μ_{σ^2} and $\varsigma^2_{\alpha^2}$: $\sigma^2_j \sim \mathrm{gamma}(\mu^2_{\alpha^2} / \varsigma^2_{\alpha^2}, \mu_{\sigma^2} / \varsigma^2_{\alpha^2})$. We also considered models with.

a simple fixed error term, σ^2, for observations. $\boldsymbol{\beta}$ are jurisdictional effects, and $\boldsymbol{\gamma}$ are other disturbance effects in a generalized linear model (linear, exponential, or logit^{-1}) appropriate for the data, notated by the link function $g()$ (Supplementary Table S1).

The model described above assumes that jurisdictional effects are fixed at the scale of the PACE. Although simple and sensible, such a model does not allow for the possibility that jurisdictional effects are random, and may co-vary with other terms (the intercept, for instance). For example, the influence of jurisdiction in a model of bare ground cover may depend on the proportion of bare ground cover at a site, with more barren sites exhibiting different jurisdictional effects than highly vegetated sites. Thus, we also considered models in which jurisdictional effects were treated as random using random slope terms, $\boldsymbol{\beta}_j$. In this case, α_j and $\boldsymbol{\beta}_j$ are distributed multivariate normal. Their covariance was modeled using the scaled inverse-Wishart distribution with degree of freedom parameter set to $L+1$ to induce a uniform prior distribution on parameter correlations (Gelman and Hill, 2006). L is the dimension of the covariance matrix.

The covariate vector $\boldsymbol{x}_{ij}$ encodes the jurisdiction within which each sample falls. Specifically, jurisdiction was "effect coded." Effect coding uses ones, zeros, and minus ones to convey group membership (BLM, NPS, USFS non-wilderness, or USFS wilderness). With $k=1, 2, K$ groups there are $K-1$ effect-coded variables. The K^{th} effect variable is not needed because the other $K-1$ variables contain all of the information needed to determine the group into which an observation falls. With effect coding, the intercept, α_j, is equal to the overall mean at site j. It is the grand mean of all observations at site j holding all other covariates (disturbance variables, $\mathbf{w}_{ij}$) at their means. The coefficients, $\boldsymbol{\beta}$, are equal to the difference between the mean of the jurisdiction and the overall mean at the site (α_j). The coefficient for the K^{th} variable can be computed as a derived quantity using - $\sum_{k=1}^{K-1}\beta$.

The covariates, $\mathbf{w}_{ij}$, were chosen to explain spatial variation in the response as a result of disturbance factors, including fire, human disturbance, forest management, and grazing. Disturbance factors varied by transect and were defined as the number of point intercepts at which a given disturbance sign was detected. Such sign included indicators of fire (ash, charring, etc.), human disturbance (trail, chainsaw, trash, etc.), forest management (chainsaw, other cutting, etc.), and grazing (cattle prints, scat, etc.; included only for models of CORI and ROMO). Additional covariates in $\mathbf{w}_{ij}$ were derived using remotely sensed or gridded data products, including elevation, and typically varied by point within site according to the spatial resolution of the product from which it was came.

The models of disturbances are meant to reveal whether the frequency/intensity of disturbances is more pronounced on specific jurisdictions. Because disturbance factors are the focus here (appearing on the lefthand side of the model equation) we simplified the model in Eq. 1 by removing $\mathbf{w}'_{ij}\boldsymbol{\gamma}$ and removed all references to $\boldsymbol{\gamma}$ in the expression for the posterior and joint distribution (Eq. 2).

Priors on all parameters were specified to be vague. Priors on model coefficients were normal centered on zero. Variance of these priors was set to assure that dispersion of the prior was much larger than the dispersion of the marginal posterior of the coefficients, except in the case of inverse logit models, where the variance was set to assure a flat distribution of the prediction of proportions (Hobbs and Hooten, 2015). Priors on variances were broad uniform or gamma distributions. Analysis of sensitivity to priors revealed no meaningful effects of priors on marginal posterior distributions of model parameters.

2.5. Model checking and selection

We selected only models that converged using statistics of Brooks and Gelman (1988) and used posterior predictive checks to remove models that were not capable of generating the observed data (Hobbs and Hooten, 2015). We used the minimum posterior predictive loss approach (Gelfand and Ghosh, 1998) to select among the remaining candidate models for each response variable in each PACE.

2.6. Inference

We used the posterior distribution of the coefficients in each model to test our hypotheses about jurisdictional effects and the influence of disturbance factors on each of our ecological variables. Effects were considered positive if estimates of the posterior distributions of their corresponding coefficients had probability density > 0.75 to the right of zero and negative if their coefficients had probability density > 0.75 left of zero.

Contrasts between jurisdictions were computed in the following way. First, at each Markov chain Monte Carlo (MCMC) iteration, m, we make a draw for the intercept term for hypothetical, out-of-sample site $\tilde{j}$ from the underlying distribution of intercepts–e.g., $\alpha_{\tilde{j}}^{m} \sim$ normal (μ_α, σ_α^2). In the model invoking random point jurisdiction effects, draws for the intercept and jurisdiction effects were made concurrently using the multivariate normal. In this case, the intercept and jurisdictional effects will co-vary according to the covariance matrix, Σ. Next, we computed the expected value of the response, $\hat{y}_{\tilde{j}}^{m}$, for each jurisdiction, holding elevation and all disturbance variables at their respective means. Contrasts are formed by computing the difference, $z_{\tilde{j}}^{m}$, in the means between two jurisdictions at each MCMC iteration. For instance, $z_{\tilde{j},BLM-NPS}^{m} = \hat{y}_{\tilde{j},BLM}^{m} - \hat{y}_{\tilde{j},NPS}^{m}$. We summarize the differences between jurisdictions using all M samples in the converged output of the MCMC algorithm. We implemented the algorithm in JAGS (Plummer, 2003), using the R programming language (R Core Team, 2017) to fit all models.

3. Results

Our analysis examined, first, whether field-collected evidence of focal disturbance types was associated with measured ecological groundcover, tree, and soil characteristics across all PACEs; second, whether disturbance evidence varied by jurisdiction and where; and third, whether ecological variables varied by jurisdiction and where. In combination, these outputs allowed us to evaluate the contexts in which jurisdiction was predictive of ecological condition across our focal landscapes, and whether these patterns were consistent with our hypotheses surrounding disturbance variability by management type. We considered relationships to have ecological meaning if a disturbance or jurisdiction type was associated with at least a 75% probability of a shift in an ecological or disturbance variable, and if the magnitude of that shift was at least 10% of the range of that variable, excluding the most extreme observations (Table 2; Supplementary Figures S2, S3).

3.1. Relationships between focal disturbance types and ecological variables

Consistent with our hypotheses (Table 1), we found that each focal disturbance type was related to shifts in groundcover type, soil stability, and soil carbon. However, the magnitude of these relationships varied strongly by PACE. Fire evidence was related to increases in bare ground cover in ROMO, LAVO, and SEKI and a decrease in bare ground in CORI; decreases in soil stability in ROMO and LAVO; increased forb cover in SEKI; and increased shrub cover, decreased tree cover, and decreased tree species richness in ROMO (Table 2). Evidence of forest management (e.g., chainsaw scars) was related to decreased bare ground cover in ROMO and SEKI; increased soil stability in ROMO, SEKI, and CORI; decreased grass cover in ROMO; and decreased shrub cover in SEKI (Table 2). Grazing was associated with both increased bare ground cover and forb cover in ROMO and CORI (Table 2). Finally, evidence of human activity in general (e.g., roads, trails, and disturbance from active forest management) was associated with increased cover of bare ground in CORI, ROMO, and LAVO; decreased soil stability in ROMO and LAVO; increased grass cover in SEKI and LAVO; decreased shrub cover in ROMO; and soil carbon in SEKI (Table 2).

3.2. Relationships between focal disturbance type and jurisdiction

Our analysis detected differences in the occurrence of disturbance evidence between jurisdictional contrasts only for forest management overall and only in LAVO (Table 3).

3.3. Relationships between jurisdiction and ecological variables

We compared pairs of adjacent jurisdictions within each PACE for meaningful differences in ecological variables. Two ecological variables, soil stability and soil carbon: nitrogen ratios, differed between jurisdictions in multiple contrast pairs. Soil stability differed between USFS Wilderness and USFS Nonwilderness in LAVO and SEKI, between NPS and USFS Wilderness in ROMO, and between NPS and USFS Nonwilderness in ROMO and LAVO (Table 4). Carbon: nitrogen ratios differed between BLM and USFS Nonwilderness in LAVO and between NPS and both USFS Nonwilderness and USFS Wilderness in LAVO.

4. Discussion

This study detected two scales of ecological patterns (plant community structure and soil properties) that were predicted by the evidence of disturbances and by the site's jurisdiction. Disturbance was linked to a site's ecological variables, including groundcover type, soil stability, and soil carbon, although these relationships differed among systems. Jurisdictional relationships with soil stability were clear, with additional but less consistent relationships emerging between jurisdiction and soil carbon: nitrogen ratios, bare ground cover, and tree diameter at breast height. Two take-home messages emerge from our findings: first, relationships between ecological variables and disturbance and between ecological variables and jurisdiction varied by PACE. This finding suggests that context is important, with ecotones manifesting at jurisdictional boundaries in certain environmental settings but not in others. Secondly, soil properties showed the strongest and most consistent patterns, both to jurisdiction type and disturbance. Interestingly, then, the signals of jurisdictional boundaries on ecological properties across large landscapes were strongest at the finest spatial scale examined.

Although all disturbance types were linked to ecological responses, no such link was consistent across all the examined PACEs. The greatest number of meaningful shifts in ecological variables associated with disturbance occurred in ROMO, where effects were detected in cover of bare ground, grass, shrubs, and trees, as well as in soil stability. Spanning the continental divide with a national park established in 1915, the ROMO PACE includes wide variation in temperature and precipitation as well as wide variation in human population density, land use, and recreation impacts (Maestas et al., 2001; Kumar et al., 2009; Hansen et al., 2011). From historic cattle ranches to amenity migrants, a blend of human occupants can be found across the Rocky Mountain region (Riebsame et al., 1996; Gosnell and Travis, 2005; Hansen et al., 2014). Furthermore, with a large metropolitan area nearby and steady growth in visitation (national park records report 4 million visitors per year since 2015), it may be that the ecosystems of the ROMO PACE are particularly subject to a relatively constant diversity of anthropogenic disturbances. On the other end of the spectrum, few links between disturbance and ecological responses were observed in the CORI PACE. Although the park itself (established in 1919) receives the highest visitation of those we examined (the National Park Service reported 6.4 million visitors in 2018), visitation is concentrated into a small area and CORI PACE as a whole has low human population density. The large majority of the landscape has been subject to a century and a half of intensive grazing. Fires and forest management are mainly restricted to the forested portions of the PACE, with current forest

TABLE 2 Hypothesized relationships between disturbance types and ecological measures.

Disturbance	Ecological variable	Hypothesis	CORI	ROMO	LAVO	SEKI
Fire	Bare ground cover	(+)	(−) 11.4	(+) 13.1	(+) 12.2	(+) 10.3
Forest management	Bare ground cover	(+)	(−) 9.5	(−) 10.3	(−) 7.6	(−) 20.6
Grazing	Bare ground cover	(+)	(+) 18.7	(+) 19.0		
Human activity	Bare ground cover	(+)	(+) 53.7	(+) 64.7	(+) 44.8	() 9.1
Fire	Carbon-to-nitrogen ratio	(+)	() NA	() 7.6	(−) 21.2	() NA
Forest management	Carbon-to-nitrogen ratio	(+)	(+) NA	(+) 5.5	(+) 7.1	(+) NA
Grazing	Carbon-to-nitrogen ratio	(+)	(−) NA	(+) 10.3		
Human activity	Carbon-to-nitrogen ratio	(+)	(−) NA	(+) 8.1	() 4.8	() NA
Fire	Soil stability	(−)	() 2.9	(−) 27.3	(−) 16.4	() 0.2
Forest management	Soil stability	(−)	(+) 14.7	(+) 21.6	(+) 4.2	(+) 19.3
Grazing	Soil stability	(−)	(−) 4.5	() 2.3		
Human activity	Soil stability	(−)	() 1.0	(−) 26.3	(−) 19.1	() 2.4
Fire	Diameter at breast height	(+)		() NA	(+) NA	(+) NA
Forest management	Diameter at breast height	(+)		(−) NA	(−) NA	(+) NA
Grazing	Diameter at breast height	(−)		(−) NA		
Human activity	Diameter at breast height	(+)		(+) NA	() NA	(−) NA
Fire	Forb cover	(+)	(+) 1.0	(−) 9.0	(+) 3.9	(+) 33.5
Forest management	Forb cover	(+)	(+) 0.9	() 2.9	(−) 1.0	(−) 9.5
Grazing	Forb cover	(−)	() 0.3	(+) 12.7		
Human activity	Forb cover	(−)	(+) 1.4	(+) 8.5	(+) 5.7	() 6.7
Fire	Grass cover	(+)	(+) 8.2	(+) 38.4	(+) 3.1	(+) 5.9
Forest management	Grass cover	(+)	(−) 5.7	(−) 11.9	(−) 1.0	(−) 7.9
Grazing	Grass cover	(+)	(−) 2.4	() 3.5		
Human activity	Grass cover	(+)	(−) 5.3	() 3.4	(+) 12.0	(+) 41.3
Fire	Number of saplings	(+)	(+) NA	() NA		(−) NA
Forest management	Number of saplings	(−)	() NA	(−) NA		(+) NA
Grazing	Number of saplings	(−)	(+) NA	(−) NA		
Human activity	Number of saplings	(−)	(+) NA	(+) NA		(+) NA
Fire	Phosphorus PPM	(+)	(+) NA	(+) NA		(+) NA
Forest management	Phosphorus PPM	()	(+) NA	(−) NA		(−) NA
Grazing	Phosphorus PPM	()	(−) NA	(+) NA		
Human activity	Phosphorus PPM	()	(−) NA	() NA		() NA
Fire	Shrub cover	(+)	(−) 3.0	(+) 19.3	(+) 7.8	() 2.6
Forest management	Shrub cover	(−)	(−) 3.8	() 3.5	(−) 6.6	(−) 40.1
Grazing	Shrub cover	(−)	(+) 5.2	() 1.4		
Human activity	Shrub cover	(+)	(−) 9.7	(−) 16.2	() 4.1	() 5.3
Fire	Total carbon	(+)	(−) 2.2	(+) NA	(−) 7.8	() 1.3
Forest management	Total carbon	(+)	(+) 8.4	(+) NA	(+) 2.8	(+) 5.5
Grazing	Total carbon	(+)	(−) 7.8	(+) NA		
Human activity	Total carbon	(+)	(−) 4.2	() NA	(−) 2.9	(−) 18.8
Fire	Tree cover	(−)	(−) 1.5	(−) 10.3	() 2.0	
Forest management	Tree cover	(−)	(+) 2.1	(+) 8.1	(+) 2.8	

(Continued)

TABLE 2 (Continued)

Disturbance	Ecological variable	Hypothesis	CORI	ROMO	LAVO	SEKI
Grazing	Tree cover	(−)	(−) 3.3	() 6.4		
Human activity	Tree cover	(−)	(−) 2.2	() 1.0	() 1.6	
Fire	Tree species richness	(+)	(+) 2.5	(−) 12.6	(−) NA	
Forest management	Tree species richness	(+)	(+) 4.3	() 0.2	(+) NA	
Grazing	Tree species richness	(−)	() 1.9	(−) 3.5		
Human activity	Tree species richness	(+)	(−) 8.8	(−) 2.7	() NA	

Directionality is indicated parenthetically. A test of each hypothesis is obtained by evaluating the density of the posterior distribution of each coefficient left or right of zero. Negative (−) or positive (+) effects have at least 75% density on either side of zero. Less influential effects are left blank (). An indication of the magnitude of each effect is given next to the sign of each coefficient. This effect size measure is calculated by evaluating the influence of a given covariate (l) on the mean of the response, $\hat{y}$, over its observed range from $\min(w_l)$ to $\max(w_l)$. Because the size of a given effect depends on the native range of the data, we use $\left|\hat{y}^{\max(w_i)} - \hat{y}^{\min(w_i)}\right| \Big/ \left(q(y,0.975) - q(y,0.025)\right) \times 100$, where the denominator represents the range of the data, excluding the most extreme observations.

TABLE 3 Contrast results for forest management.

PACE	Contrast	median(z)	P(z<0)	P(z>0)	$\frac{\lvert\text{median}(z)\rvert}{q(y,0.975)-q(y,0.025)} \times 100$
LAVO	BLM–USFSNONWILDERNESS	−0.031	0.81	0.19	6.3
LAVO	NPS–USFSNONWILDERNESS	0.073	0.01	0.99	14.5
LAVO	NPS–USFSWILDERNESS	0.055	0.07	0.93	11.1
SEKI	NPS–USFSNONWILDERNESS	0	0.17	0.83	0.1
SEKI	USFSNONWILDERNESS–USFSWILDERNESS	0	0.19	0.81	0

We present the median of the expected difference, z, in forest management between each jurisdiction shown. We also present the probability that z is left or right of zero. A value of zero corresponds to no difference. Only contrasts with probability density > 0.75 to either side of zero are included. The final column provides an indication of the magnitude of the difference on the scale of the data. $q(y,p)$ returns the quantile of y at probability p. Thus, the denominator in the expression in the final column corresponds to the range of the data, omitting the most extreme values. For example, a value of 5 would correspond to a median difference between two jurisdictions that is 5% of the range of forest management observations in the corresponding PACE. These results are based on coefficients presented in Supplementary Figure S2.

management trying to mimic the historic fire regime (Holcomb et al., 2011). As a whole, the PACE is arid within only a few high moisture pockets (on the Kaibab Plateau). Aridity as a common environmental stress may play a homogenizing role in the ecology of all jurisdictions across the PACE. That is, the small number of ecological responses to disturbance and jurisdictions likely reflects a consistent effect of low water availability. Fire and grazing have been a consistent part of the landscape so long and may have interacted with water stress to apply strong selective pressures on vegetation communities, such that grazing-intolerant and fire-intolerant species are no longer common in any jurisdiction on the landscape (Moore et al., 1999; Simpson, 2020). A lack of jurisdictional responses may be consistent in areas where disturbance adaptation is consistent across habitat types, including grasslands and savannas (Bowman et al., 2009).

Pre-existing ecological differences among jurisdictions are an important confounding variable that may obscure the relationships we aimed to examine here. The historical assignment of management units to specific jurisdictions was driven by their characteristics—for example, BLM lands are generally rangelands with high forage incidence, and forested landscapes are generally managed by the USFS. Differences in grass or tree cover, therefore, may have driven the assignment of jurisdiction, rather than the other way around. This study, however, was designed with the expectation that both are true—that regions with certain characteristics are indeed more likely to be assigned to certain jurisdictions, but also that the management differences can reinforce divergence of neighboring parcels, such that ecotones may also be products of management itself. Jurisdictional boundaries, drawn on a map at coarse scale, are unlikely to precisely track natural ecotones such as shifts from forests to woodlands to grasslands. By sampling very close to boundaries, at sites matched by elevation and vegetation type, we aimed to keep sources of natural variation as constant as possible in order to discern any divergence emerging at fine scale and directly at the boundary, and thus possibly as a result of management, if it occurs. Our findings that some ecological characteristics do vary in some cases by jurisdiction, but also by PACE, suggest an interplay between the social construct of jurisdictions, the response time of individual ecological characteristics, and the biophysical and geographical characteristics across and between landscapes.

Importantly, we observed relationships between disturbances and ecological variables at the level of full PACEs, as well as between jurisdictions and ecological variables. Our methods only detected disturbances recent enough to leave

TABLE 4 Contrast results for soil stability and carbon-to-nitrogen ratio.

Ecological variable	PACE	Contrast	Median (z)	$P(z<0)$	$P(z>0)$	$\frac{\lvert \text{median}(z) \rvert}{q(y,0.975)-q(y,0.025)}\times 100$
Soil stability						
	CORI	BLM–USFSWILDERNESS	−0.432	0.9	0.1	8.6
	CORI	NPS–USFSWILDERNESS	−0.317	0.81	0.19	6.3
	CORI	USFSNONWILDERNESS–USFSWILDERNESS	−0.373	0.9	0.1	7.5
	ROMO	NPS–USFSNONWILDERNESS	1.219	0.04	0.96	24.4
	ROMO	NPS–USFSWILDERNESS	0.745	0.19	0.81	14.9
	LAVO	NPS–USFSNONWILDERNESS	0.499	0.07	0.93	10
	LAVO	USFSNONWILDERNESS–USFSWILDERNESS	−0.631	0.96	0.04	12.6
	SEKI	BLM–USFSNONWILDERNESS	−0.213	0.83	0.17	4.3
	SEKI	BLM–USFSWILDERNESS	0.322	0.07	0.93	6.4
	SEKI	NPS–USFSNONWILDERNESS	0.379	0.11	0.89	7.6
	SEKI	USFSNONWILDERNESS–USFSWILDERNESS	0.536	0.01	0.99	10.7
Carbon-to-nitrogen ratio						
	CORI	BLM–NPS	1.12	0.13	0.87	2.6
	CORI	BLM–USFSNONWILDERNESS	−0.817	0.82	0.18	1.9
	CORI	BLM–USFSWILDERNESS	−2.325	0.98	0.02	5.4
	CORI	NPS–USFSNONWILDERNESS	−1.928	0.99	0.01	4.5
	CORI	NPS–USFSWILDERNESS	−3.424	1	0	7.9
	CORI	USFSNONWILDERNESS–USFSWILDERNESS	−1.511	0.95	0.04	3.5
	ROMO	BLM–USFSNONWILDERNESS	1.749	0.08	0.92	4.4
	LAVO	BLM–USFSNONWILDERNESS	−2.514	0.99	0.01	11.9
	LAVO	NPS–USFSNONWILDERNESS	−1.598	0.99	0.01	7.5
	LAVO	NPS–USFSWILDERNESS	−2.233	1	0	10.5

We present the median of the expected difference, z, in soil stability or carbon-to-nitrogen ratio between each jurisdiction shown. We also present the probability that z is left or right of zero. A value of zero corresponds to no difference. Only contrasts with probability density > 0.75 to either side of zero are included. The final column provides an indication of the magnitude of the difference on the scale of the data. $q(y,p)$ returns the quantile of y at probability p. Thus, the denominator in the expression in the final column corresponds to the range of the data, omitting the most extreme values. For example, a value of 5 would correspond to a median difference between two jurisdictions that is 5% of the range of soil stability or carbon-to-nitrogen observations in the corresponding PACE. These results are based on coefficients presented in Supplementary Figures S3, S4.

visible traces on the landscape – i.e., charred or downed wood, chainsaw cuts, cattle scat and prints, trails and campsites, etc. High incidences of a disturbance may indicate recent disturbance, but a lack of visible disturbance may indicate either no disturbance or a past disturbance that is simply no longer visible. Future research in which investigations such as these are performed in collaboration with environmental historians might enable longer-term or historical drivers of current conditions to be elucidated, perhaps deepening our understanding of ecological heterogeneity across management mosaics. Furthermore, because we were interested in the degree to which administrative boundaries manifested as ecological boundaries, our empirical data collection took place within 100 m of each jurisdictional boundary. Some disturbance types likely track boundaries closely; for example, livestock grazing in a fenced unit is likely to exert maximum impact immediately along and up to the fenceline and to be absent across the boundary. However, some disturbances (e.g., recreation or fire) and management activities (e.g., fuels or invasives management) may be more spatially diffuse and may become more visible at greater distances from those boundaries. Most of the administrative boundaries we observed in our sampling areas are unmarked or are designated only with rare signage or bits of unmaintained fencing, suggesting that management activities and disturbance effects may not respond to sharp barriers but may instead dissipate more diffusely as they near or cross a boundary. Thus, the temporal persistence and spatial heterogeneity of management effects and disturbance evidence vary in ways that may additionally impede detection of the relationships we examined.

Soil properties, and soil stability particularly, showed the most consistent and well-supported relationships to disturbance or jurisdiction. Soil properties can vary over short distances, due to a combination of parent material, vegetation type, and disturbance (Manley et al., 1995; Lamarche et al., 2004; Neff et al., 2005; Hartmann et al., 2012; Verma and Jayakumar, 2012; Pellegrini et al., 2018). As such, soil properties represent ecological variables at the smallest spatial scale we examined for this study. Soil changes, particularly those in response to disturbances, may be relatively long-lived (Neff et al., 2005; Hartmann et al., 2012; Kuske et al., 2012; Pellegrini et al., 2018), such that their "recovery" may well outlast visible evidence of disturbance. Combined, these facets may make soils the most durable ecological indicators of disturbance and jurisdictional differences. Given their foundational role in ecosystems, divergence in soil properties may have indirect effects that affect the resilience of other components over longer time scales. Different soil properties, however, varied in their responsiveness to the factors investigated here. Despite well-known effects of fire, grazing, and forestry on soil chemistry (Kutiel and Shaviv, 1989; Manley et al., 1995; Neff et al., 2005; Verma and Jayakumar, 2012; Pellegrini et al., 2018), total soil C and N were not related to evidence of these disturbances in our PACEs. In contrast, soil stability was linked to both fire and forest management evidence, and often coincided with changes in ground cover. Soil stability is directly reduced by disturbances that remove plant cover (Belnap, 1995; Duchicela et al., 2012; Chandler et al., 2019) so these patterns are almost certainly mechanistically linked and soil stability changes may continue even after vegetation recovers (Duchicela et al., 2012; Pohl et al., 2012). The broader jurisdictional differences in both soil chemistry and stability may reflect either (1) the gap between visible disturbance sign and past management impacts, (2) soil differences that contributed to different land uses and jurisdictional designations, or (3) a combination of both. Ultimately, though, jurisdictional differences in soil stability and soil fertility (C: N ratio) may impact erosion, hydrology, and vegetation representing both livestock forage and fuels for fire. Better understanding these jurisdictional differences in soils can help with conservation planning and predicting ecosystem resilience.

Large landscape conservation is an ongoing challenge in light of global change drivers, which impact large areas and drive rapid shifts in species composition and distribution, biological invasions, and large-scale disturbances such as megafires and floods (Rudnick et al., 2012; Baldwin et al., 2018). However, such landscapes inevitably encompass multiple jurisdictions, requiring planning and predictions that incorporate cross-boundary effects and multijurisdictional decision-making (Locke, 2011; Bixler et al., 2016; Imperial et al., 2016; Scarlett and McKinney, 2016). Understanding how differing management approaches may lead to ecological differences and thus ecotones, and the scale and context of these effects, will be critical for identifying areas of collaboration and prioritization for cross-boundary decision-making. Our work suggests that anthropogenic disturbances are structuring forces across landscapes, but that their legacies may present in unexpected ways and unequally in different regions. As managers and policymakers aim to support resilient landscapes, it will be important to incorporate history, social landscapes, and the interplay of ecological stress and disturbance into truly interdisciplinary planning, going forward.

Data availability statement

The raw data supporting the conclusions of this article will be made available by the authors, without undue reservation.

Author contributions

CA, RE-N, MB, SV, and BS designed the study and received the funding. LZ analyzed the data. CA led the manuscript writing. CA, LZ, RE-N, MB, SV, and BS contributed to manuscript revisions. All authors contributed to the article and approved the submitted version.

Funding

Funding for this work was provided by National Science Foundation Award #1617309.

Acknowledgments

We thank the National Park Service, US Forest Service, and Bureau of Land Management personnel who provided permits, guidance, and feedback in each of the sampled protected area-centered ecosystems. We are deeply grateful for the hard work of our tireless field crewmembers, including: M. Sample, B. Tiffany, S. Sterner, M. Sotelo, G. Conley, M. Barasha, M. Andrews, J. Collier, M. Bannard, R. Lee, S. Lehman, B. Oxford, and W. Topete.

Conflict of interest

The authors declare that the research was conducted in the absence of any commercial or financial relationships that could be construed as a potential conflict of interest.

Publisher's note

Supplementary material

The Supplementary material for this article can be found online at: https://www.frontiersin.org/articles/10.3389/fevo.2022.1053548/full#supplementary-material

References

Alkemade, R., Reid, R. S., van Den Berg, M., De Leeuw, J., and Jeuken, M. (2013). Assessing the impacts of livestock production on biodiversity in rangeland ecosystems. *Proc. Natl. Acad. Sci. U. S. A.* 110, 20900–20905. doi: 10.1073/pnas.1011013108

Andrés, P., and Mateos, E. (2006). Soil mesofaunal responses to post-mining restoration treatments. *Appl. Soil Ecol.* 33, 67–78. doi: 10.1016/j.apsoil.2005.08.007

Andrew, M. E., Wulder, M. A., and Coops, N. C. (2012). Identification of de facto protected areas in boreal Canada. *Biol. Conserv.* 146, 97–107. doi: 10.1016/j.biocon.2011.11.029

Aslan, C. E., Brunson, M. W., Sikes, B. A., Epanchin-Niell, R. S., Veloz, S., Theobald, D. M., et al. (2021a). Coupled ecological and management connectivity across administrative boundaries in undeveloped landscapes. *Ecosphere* 12:e03329. doi: 10.1002/ecs2.3329

Aslan, C. E., Zachmann, L., McClure, M., Sikes, B. A., Veloz, S., Brunson, M. W., et al. (2021b). Quantifying ecological variation across jurisdictional boundaries in a management mosaic landscape. *Landsc. Ecol.* 36, 1215–1233. doi: 10.1007/s10980-021-01198-7

Augustine, D. J., Booth, D. T., Cox, S. E., and Derner, J. D. (2012). Grazing intensity and spatial heterogeneity in bare soil in a grazing-resistant grassland. *Rangel. Ecol. Manag.* 65, 39–46. doi: 10.2111/REM-D-11-00005.1

Baguette, M., Blanchet, S., Legrand, D., Stevens, V. M., and Turlure, C. (2013). Individual dispersal, landscape connectivity and ecological networks. *Biol. Rev.* 88, 310–326. doi: 10.1111/brv.12000

Baldwin, R. F., Trombulak, S. C., Leonard, P. B., Noss, R. F., Hilty, J. A., Possingham, H. P., et al. (2018). The future of landscape conservation. *Bio Sci.* 68, 60–63. doi: 10.1093/biosci/bix142

Belnap, J. (1995). Surface disturbances: their role in accelerating desertification. *Environ. Monit. Assess.* 37, 39–57. doi: 10.1007/BF00546879

Bengtsson, J., Nilsson, S. G., Franc, A., and Menozzi, P. (2000). Biodiversity, disturbances, ecosystem function and management of European forests. *For. Ecol. Manag.* 132, 39–50. doi: 10.1016/S0378-1127(00)00378-9

Best, R. J., and Arcese, P. (2009). Exotic herbivores directly facilitate the exotic grasses they graze: mechanisms for an unexpected positive feedback between invaders. *Oecologia* 159, 139–150. doi: 10.1007/s00442-008-1172-1

Bixler, R. P., Johnson, S., Emerson, K., Nabatchi, T., Reuling, M., Curtin, C., et al. (2016). Networks and landscapes: a framework for setting goals and evaluating performance at the large landscape scale. *Front. Ecol. Environ.* 14, 145–153. doi: 10.1002/fee.1250

Bowman, D. M. J. S., Balch, J. K., Artaxo, P., Bond, W. J., Carlson, J. M., Cochrane, M. A., et al. (2009). Fire in the earth system. *Science.* 324, 481–484. doi: 10.1126/science.1163886

Brooks, S. P., and Gelman, A. (1988). Alternative methods for monitoring convergence of iterative simulations. *J. Comput. Graph. Stat.* 7, 434–455.

Brown, R. N. K., Rosenberger, R. S., Kline, J. D., Hall, T. E., and Needham, M. D. (2008). Visitor preferences for managing wilderness recreation after wildfire. *J. For.* 106, 9–16. doi: 10.1093/jof/106.1.9

Chandler, D. G., Day, N., Madsen, M. D., and Belnap, J. (2019). Amendments fail to hasten biocrust recovery or soil stability at a disturbed dryland sandy site. *Restor. Ecol.* 27, 289–297. doi: 10.1111/rec.12870

Chester, C. C. (2015). Yellowstone to Yukon: Transborder conservation across a vast international landscape. *Environ. Sci. Pol.* 49, 75–84. doi: 10.1016/j.envsci.2014.08.009

Crotteau, J. S., Morgan Varner, J., and Ritchie, M. W. (2013). Post-fire regeneration across a fire severity gradient in the southern cascades. *For. Ecol. Manag.* 287, 103–112. doi: 10.1016/j.foreco.2012.09.022

D'Odorico, P., Okin, G. S., and Bestelmeyer, B. T. (2012). A synthetic review of feedbacks and drivers of shrub encroachment in arid grasslands. *Ecohydrology* 5, 520–530. doi: 10.1002/eco.259

DeLong, S. C., Fall, S. A., and Sutherland, G. D. (2004). Estimating the impacts of harvest distribution on road-building and snag abundance. *Can. J. For. Res.* 34, 323–331. doi: 10.1139/x03-184

DiTomaso, J. M. (2000). Invasive weeds in rangelands: species, impacts, and management. *Weed Sci.* 48, 255–265. doi: 10.1614/0043-1745(2000)048[0255,IWIRSI]2.0.CO;2

Duchicela, J., Vogelsang, K. M., Schultz, P. A., Kaonongbua, W., Middleton, E. L., and Bever, J. D. (2012). Non-native plants and soil microbes: potential contributors to the consistent reduction in soil aggregate stability caused by the disturbance of north American grasslands. *New Phytol.* 196, 212–222. doi: 10.1111/j.1469-8137.2012.04233.x

Duinker, P. N., Wiersma, Y., Haider, W., Hvenegaard, G. T., and Schmiegelow, F. K. (2010). Protected areas and sustainable forest management: what are we talking about? *For. Chron.* 86, 173–177. doi: 10.5558/tfc86173-2

Epanchin-Niell, R. S., Hufford, M. B., Aslan, C. E., Sexton, J. P., Port, J. D., and Waring, T. M. (2010). Controlling invasive species in complex social landscapes. *Front. Ecol. Environ.* 8, 210–216. doi: 10.1890/090029

Fischer, J., Lindenmayer, D. B., and Manning, A. D. (2006). Biodiversity, ecosystem function, and resilience: ten guiding principles for commodity production landscapes. *Front. Ecol. Environ.* 4, 80–86. doi: 10.1890/1540-9295(2006)004[0080:BEFART]2.0.CO;2

Floren, A., Müller, T., Dittrich, M., Weiss, M., and Linsenmair, K. E. (2014). The influence of tree species, stratum and forest management on beetle assemblages responding to deadwood enrichment. *For. Ecol. Manag.* 323, 57–64. doi: 10.1016/j.foreco.2014.03.028

Führer, E. (2000). Forest functions, ecosystem stability and management. *For. Ecol. Manag.* 132, 29–38. doi: 10.1016/S0378-1127(00)00377-7

Gelfand, A. E., and Ghosh, S. K. (1998). Model choice: a minimum posterior predictive loss approach. *Biometrika* 85, 1–11.

Gelfand, A. E., and Smith, A. F. M. (1990). Sampling-based approaches to calculating marginal densities. *J. Amer. Stat. Assoc.* 85, 398–409.

Gelman, A., and Hill, J. (2006). *Data Analysis Using Regression and Multilevel/Hierarchical Models*. Cambridge, MA, USA: Cambridge University Press.

Goldmann, K., Schöning, I., Buscot, F., and Wubet, T. (2015). Forest management type influences diversity and community composition of soil fungi across temperate Forest ecosystems. *Front. Microbiol.* 6:1300. doi: 10.3389/fmicb.2015.01300

Gonçalves, P. H. S., De Medeiros, P. M., and Albuquerque, U. P. (2021). Effects of domestic wood collection on tree community structure in a human-dominated seasonally dry tropical forest. *J. Arid Environ.* 193:104554. doi: 10.1016/j.jaridenv.2021.104554

Goosem, M. (2007). Fragmentation impacts caused by roads through rainforests. *Curr. Sci.* 93, 1587–1595.

Gosnell, H., and Travis, W. R. (2005). Ranchland ownership dynamics in the Rocky Mountain west. *Rangel. Ecol. Manag.* 58, 191–198. doi: 10.2111/1551-5028(2005)58<191:RODITR>2.0.CO;2

Gutzwiller, K. J., D'Antonio, A. L., and Monz, C. A. (2017). Wildland recreation disturbance: broad-scale spatial analysis and management. *Front. Ecol. Environ.* 15, 517–524. doi: 10.1002/fee.1631

Hansen, A. J., Davis, C. R., Piekielek, N., Gross, J., Theobald, D. M., Goetz, S., et al. (2011). Delineating the ecosystems containing protected areas for monitoring and management. *Bioscience* 61, 363–373. doi: 10.1525/bio.2011.61.5.5

Hansen, A. J., Knight, R. L., Marzluff, J. M., Powell, S., Brown, K., Gude, P. H., et al. (2005). Effects of exurban development on biodiversity: patterns, mechanisms, and research needs. *Ecol. Appl.* 15, 1893–1905. doi: 10.1890/05-5221

Hansen, A. J., Piekielek, N., Davis, C., Haas, J., Theobald, D. M., Gross, J. E., et al. (2014). Exposure of U.S. National Parks to land use and climate change 1900–2100. *Ecol. Appl.* 24, 484–502. doi: 10.1890/13-0905.1

Hartmann, M., Howes, C. G., VanInsberghe, D., Yu, H., Bachar, D., Christen, R., et al. (2012). Significant and persistent impact of timber harvesting on soil microbial communities in Northern coniferous forests. *ISME J.* 6, 2199–2218. doi: 10.1038/ismej.2012.84

Havlick, D. (2002). *No Place Distant: Roads and Motorized Recreation on America's Public Lands*. Chicago: Island Press.

Herrick, J., Whitford, W., Soyza, A., Van Zee, J., Havstad, K., Seybold, C., et al. (2001). Field soil aggregate stability kit for soil quality and rangeland health evaluations. *Catena* 44, 27–35. doi: 10.1016/S0341-8162(00)00173-9

Hobbs, R. J., Arico, S., Aronson, J., Baron, J. S., Bridgewater, P., Cramer, V. A., et al. (2006). Novel ecosystems: theoretical and management aspects of the new ecological world order. *Glob. Ecol. Biogeogr.* 15, 1–7. doi: 10.1111/j.1466-822X.2006.00212.x

Hobbs, N. T., and Hooten, M. B. (2015). *Bayesian Models: A Statistical Primer for Ecologists*. Princeton, NJ, USA: Princeton University Press.

Holcomb, C. M., Sisk, T. D., Dickson, B. D., Sesnie, S. E., and Aumack, E. N. (2011). *Administrative Boundaries and Ecological Divergence: The Divided History and Coordinated Future of Land Management on the Kaibab plateau, Arizona, USA*. Arizona, USA: University of Arizona press.

Huang, L., Jin, C., Zhen, M., Zhou, L., Qian, S., Jim, C. Y., et al. (2020). Biogeographic and anthropogenic factors shaping the distribution and species assemblage of heritage trees in China. *Urban For. Urban Green.* 50:126652. doi: 10.1016/j.ufug.2020.126652

Huang, Y., Tian, F., Wang, Y., Wang, M., and Hu, Z. (2015). Effect of coal mining on vegetation disturbance and associated carbon loss. *Environ. Earth Sci.* 73, 2329–2342. doi: 10.1007/s12665-014-3584-z

Huggard, D. (2004). Establishing representative ecosystems within a managed landscape: an approach to assessment of non-harvestable areas. Report to the sustainable Forest management network, knowledge exchange and technology extension program.

Imperial, M. T., Ospina, S., Johnston, E., O'Leary, R., Thomsen, J., Williams, P., et al. (2016). Understanding leadership in a world of shared problems: advancing network governance in large landscape conservation. *Front. Ecol. Environ.* 14, 126–134. doi: 10.1002/fee.1248

Innes, J., Fitzgerald, N., Binny, R., Byrom, A., Pech, R., Watts, C., et al. (2019). New Zealand ecosanctuaries: types, attributes and outcomes. *J. R. Soc. N. Z.* 49, 370–393. doi: 10.1080/03036758.2019.1620297

James, J., Page-Dumroese, D., Busse, M., Palik, B., Zhang, J., Eaton, B., et al. (2021). Effects of forest harvesting and biomass removal on soil carbon and nitrogen: two complementary meta-analyses. *For. Ecol. Manag.* 485:118935. doi: 10.1016/j.foreco.2021.118935

Koontz, T. M., and Bodine, J. (2008). Implementing ecosystem Management in Public Agencies: lessons from the U.S. Bureau of Land Management and the Forest Service. *Conserv. Biol.* 22, 60–69. doi: 10.1111/j.1523-1739.2007.00860.x

Koontz, T. M., and Newig, J. (2014). From planning to implementation: top-down and bottom-up approaches for collaborative watershed management. *Policy Stud. J.* 42, 416–442. doi: 10.1111/psj.12067

Kumar, S., Simonson, S. E., and Stohlgren, T. J. (2009). Effects of spatial heterogeneity on butterfly species richness in Rocky Mountain National Park, CO USA. *Biodivers. Conserv.* 18, 739–763. doi: 10.1007/s10531-008-9536-8

Kuske, C. R., Yeager, C. M., Johnson, S., Ticknor, L. O., and Belnap, J. (2012). Response and resilience of soil biocrust bacterial communities to chronic physical disturbance in arid shrublands. *ISME J.* 6, 886–897. doi: 10.1038/ismej.2011.153

Kutiel, P., and Shaviv, A. (1989). Effect of simulated forest fire on the availability of N and P in mediterranean soils. *Plant Soil* 120, 57–63. doi: 10.1007/BF02370290

Lamarche, J., Bradley, R. L., Paré, D., Légaré, S., and Bergeron, Y. (2004). Soil parent material may control forest floor properties more than stand type or stand age in mixedwood boreal forests. *Écoscience* 11, 228–237. doi: 10.1080/11956860.2004.11682828

Lampert, A., Hastings, A., Grosholz, E. D., Jardine, S. L., and Sanchirico, J. N. (2014). Optimal approaches for balancing invasive species eradication and endangered species management. *Science* 344, 1028–1031. doi: 10.1126/science.1250763

Levin, P. S., Holmes, E. E., Piner, K. R., and Harvey, C. J. (2006). Shifts in a Pacific Ocean fish assemblage: the potential influence of exploitation. *Conserv. Biol.* 20, 1181–1190. doi: 10.1111/j.1523-1739.2006.00400.x

Locke, H. (2011). Transboundary cooperation to achieve wilderness protection and large landscape conservation. *Park. Sci.* 28, 24–28.

Maestas, J. D., Knight, R. L., and Gilgert, W. C. (2001). Biodiversity and land-use change in the American Mountain west. *Geogr. Rev.* 91, 509–524. doi: 10.1111/j.1931-0846.2001.tb00238.x

Manley, J. T., Schuman, G. E., Reeder, J. D., and Hart, R. H. (1995). Rangeland soil carbon and nitrogen responses to grazing. *J. Soil Water Conserv.* 50, 294–298.

Marzano, M., and Dandy, N. (2012). Recreationist behaviour in forests and the disturbance of wildlife. *Biodivers. Conserv.* 21, 2967–2986. doi: 10.1007/s10531-012-0350-y

Miller, R. F., Ratchford, J., Roundy, B. A., Tausch, R. J., Hulet, A., and Chambers, J. (2014). Response of conifer-encroached Shrublands in the Great Basin to prescribed fire and mechanical treatments. *Rangel. Ecol. Manag.* 67, 468–481. doi: 10.2111/REM-D-13-00003.1

Miller, A. D., Roxburgh, S. H., and Shea, K. (2011). How frequency and intensity shape diversity–disturbance relationships. *Proc. Natl. Acad. Sci.* 108, 5643–5648. doi: 10.1073/pnas.1018594108

Monz, C. A., Pickering, C. M., and Hadwen, W. L. (2013). Recent advances in recreation ecology and the implications of different relationships between recreation use and ecological impacts. *Front. Ecol. Environ.* 11, 441–446. doi: 10.1890/120358

Moore, M. M., Covington, W. W., and Fulé, P. Z. (1999). Reference conditions and ecological restoration: a southwestern ponderosa pine perspective. *Ecol. Appl.* 9, 1266–1277. doi: 10.1890/1051-0761(1999)009[1266:RCAERA]2.0.CO;2

Neff, J. C., Reynolds, R. L., Belnap, J., and Lamothe, P. (2005). Multi-decadal impacts of grazing on soil physical and biogeochemical properties in Southeast Utah. *Ecol. Appl.* 15, 87–95. doi: 10.1890/04-0268

Nelson, D. L., Kellner, K. F., and Swihart, R. K. (2019). Rodent population density and survival respond to disturbance induced by timber harvest. *J. Mammal.* 100, 1253–1262. doi: 10.1093/jmammal/gyz094

Nicotra, A. B., Beever, E. A., Robertson, A. L., Hofmann, G. E., and O'Leary, J. (2015). Assessing the components of adaptive capacity to improve conservation and management efforts under global change. *Conserv. Biol.* 29, 1268–1278. doi: 10.1111/cobi.12522

Parsons, D. J., and Landres, P. B. (1996). "Restoring natural fire to wilderness: how are we doing?" in *Fire in Ecosystem Management: Shifting the Paradigm from Suppression to Prescription*. eds. L. P. Theresa and A. B. Leonard (Lawrence, Kansas, USA: Allen Press), 366–373.

Payne, W. A. (2016). Tragedy of the commons revisited grazing, land degradation and desertification on multi-use. *Public Lands of Nevada.* 沙漠研究 26, 121–128. doi: 10.14976/jals.26.3_121

Pellegrini, A. F. A., Ahlström, A., Hobbie, S. E., Reich, P. B., Nieradzik, L. P., Staver, A. C., et al. (2018). Fire frequency drives decadal changes in soil carbon and nitrogen and ecosystem productivity. *Nature* 553, 194–198. doi: 10.1038/nature24668

Pierce, S., Luzzaro, A., Caccianiga, M., Ceriani, R. M., and Cerabolini, B. (2007). Disturbance is the principal α-scale filter determining niche differentiation, coexistence and biodiversity in an alpine community. *J. Ecol.* 95, 698–706. doi: 10.1111/j.1365-2745.2007.01242.x

Pinto, R. L. (2014). Cattle grazing in the national parks: historical development and history of management in three Southern Arizona parks. Available at: https://search.proquest.com/docview/1556771557/abstract/ABC83D75101B4C48PQ/1 (Accessed March 24, 2020).

Plummer, M. (2003). JAGS: a program for analysis of Bayesian graphical models using Gibbs sampling. *Work. Pap.* 8, 1–10.

Pocock, Z., and Lawrence, R. E. (2005). "How far into a forest does the effect of a road extend? Defining road edge effect in eucalypt forests of South-Eastern Australia." in *Proceedings of the 2005 International Conference on Ecology and Transportation* (North Carolina State University, Raleigh, North Carolina, USA: Center for Transportation and the Environment), 397–405.

Pohl, M., Graf, F., Buttler, A., and Rixen, C. (2012). The relationship between plant species richness and soil aggregate stability can depend on disturbance. *Plant Soil* 355, 87–102. doi: 10.1007/s11104-011-1083-5

Ponstingel, D. (2020). The impact of exurban development on forested areas in Kurgan City, Russia. *Land Use Policy* 94:104485. doi: 10.1016/j.landusepol.2020.104485

Powell, S., Costa, A. N., Lopes, C. T., and Vasconcelos, H. L. (2011). Canopy connectivity and the availability of diverse nesting resources affect species coexistence in arboreal ants. *J. Anim. Ecol.* 80, 352–360. doi: 10.1111/j.1365-2656.2010.01779.x

R Core Team (2017). *R: A Language and Environment for Statistical Computing.* Vienna, Austria: R Foundation for Statistical Computing.

Rabinowitz, A. (2014). "The underground railway of the jaguar," in *An Indomitable Beast*. ed. A. Rabinowitz (Berlin: Springer), 133–149.

Riebsame, W. E., Gosnell, H., and Theobald, D. M. (1996). Land use and landscape change in the Colorado Mountains I: theory, scale, and pattern. *Mt. Res. Dev.* 16, 395–405. doi: 10.2307/3673989

Rudnick, D., Ryan, S., Beier, P., Cushman, S., Dieffenbach, F., Epps, C. W., et al. (2012). The role of landscape connectivity in planning and implementing conservation and restoration priorities. Issues in ecology. undefined. Available at: https://www.semanticscholar.org/paper/The-Role-of-Landscape-Connectivity-in-Planning-and-Rudnick-Ryan/e0ea58e8cbc592d5e0c9c704334b9f2334483355 (Accessed August 9, 2021).

Scarlett, L., and McKinney, M. (2016). Connecting people and places: the emerging role of network governance in large landscape conservation. *Front. Ecol. Environ.* 14, 116–125. doi: 10.1002/fee.1247

Schmutz, S., and Moog, O. (2018). "Dams: ecological impacts and management," in *Riverine Ecosystem Management*. eds. S. Shmutz and J. Sendzimir (Cham: Springer), 111–127.

Schultz, C. A., Jedd, T., and Beam, R. D. (2012). The collaborative Forest landscape restoration program: a history and overview of the first projects. *J. For.* 110, 381–391. doi: 10.5849/jof.11-082

Schultz, C. A., and Moseley, C. (2019). Collaborations and capacities to transform fire management. *Science* 366, 38–40. doi: 10.1126/science.aay3727

Schwilk, D. W., Keeley, J. E., Knapp, E. E., McIver, J., Bailey, J. D., Fettig, C. J., et al. (2009). The national fire and fire surrogate study: effects of fuel reduction methods on forest vegetation structure and fuels. *Ecol. Appl.* 19, 285–304. doi: 10.1890/07-1747.1

Shatford, J. P. A., Hibbs, D. E., and Puettmann, K. J. (2007). Conifer regeneration after Forest fire in the Klamath-Siskiyous: how much, how soon? *J. For.* 105, 139–146. doi: 10.1093/jof/105.3.139

Simpson, A. C. (2020). Evidence for state change in an arid grassland-steppe: limited recovery of vegetation after intermediate to long-term cattle exclusion in the southwestern U.S. Available at: https://www.proquest.com/docview/2415358997/abstract/5ED27A5099DF4FB1PQ/1 (Accessed February 2, 2022).

Souther, S., Loeser, M., Crews, T. E., and Sisk, T. (2019). Complex response of vegetation to grazing suggests need for coordinated, landscape-level approaches to grazing management. *Glob. Ecol. Conserv.* 20:e00770. doi: 10.1016/j.gecco.2019.e00770

Squillace, M. (2014). Grazing in wilderness areas. *Environ. Law* 44, 415–445.

Stephens, S. L., McIver, J. D., Boerner, R. E. J., Fettig, C. J., Fontaine, J. B., Hartsough, B. R., et al. (2012). The effects of Forest fuel-reduction treatments in the United States. *Bioscience* 62, 549–560. doi: 10.1525/bio.2012.62.6.6

Taboada, M. A., Rubio, G., and Chaneton, E. J. (2015). "Grazing impacts on soil physical, chemical, and ecological properties in forage production systems," in *Soil Management: Building a Stable Base for Agriculture* (New York, John Wiley & Sons, Ltd), 301–320.

Teague, R., and Barnes, M. (2017). Grazing management that regenerates ecosystem function and grazingland livelihoods. *Afr. J. Range Forage Sci.* 34, 77–86. doi: 10.2989/10220119.2017.1334706

Teague, W. R., Dowhower, S. L., and Waggoner, J. A. (2004). Drought and grazing patch dynamics under different grazing management. *J. Arid Environ.* 58, 97–117. doi: 10.1016/S0140-1963(03)00122-8

Theobald, D. M. (2013). A general model to quantify ecological integrity for landscape assessments and US application. *Landsc. Ecol.* 28, 1859–1874. doi: 10.1007/s10980-013-9941-6

Trivellone, V., Bougeard, S., Giavi, S., Krebs, P., Balseiro, D., Dray, S., et al. (2017). Factors shaping community assemblages and species co-occurrence of different trophic levels. *Ecol. Evol.* 7, 4745–4754. doi: 10.1002/ece3.3061

Verma, S., and Jayakumar, S. (2012). Impact of forest fire on physical, chemical and biological properties of soil: a review. *Proc. Int. Acad. Ecol. Environ. Sci.* 2:168.

Wiersma, Y. F., Duinker, P. N., Haider, W., Hvenegaard, G. T., and Schmiegelow, F. K. A. (2015). Introduction: relationships between protected areas and sustainable Forest management: where are we heading? *Conserv. Soc.* 13, 1–12. doi: 10.4103/0972-4923.161206

Zellmer, S. (2014). Wilderness imperatives and untrammeled nature. College of Law Faculty Publications. Available at: https://digitalcommons.unl.edu/lawfacpub/193 (Accessed December 11, 2022).

Zhang, C., Settele, J., Sun, W., Wiemers, M., Zhang, Y., and Schweiger, O. (2019). Resource availability drives trait composition of butterfly assemblages. *Oecologia* 190, 913–926. doi: 10.1007/s00442-019-04454-5

Zheng, Y., Zhou, G., Zhuang, Q., and Shimizu, H. (2020). Long-term elimination of grazing reverses the effects of shrub encroachment on soil and vegetation on the Ordos plateau. *J. Geophys. Res. Biogeosciences* 125:e2019JG005439. doi: 10.1029/2019JG005439

Zollner, P. A., Gustafson, E. J., He, H. S., Radeloff, V. C., and Mladenoff, D. J. (2005). Modeling the influence of dynamic zoning of Forest harvesting on ecological succession in a northern hardwoods landscape. *Environ. Manag.* 35, 410–425. doi: 10.1007/s00267-003-0217-9

frontiers | Frontiers in Ecology and Evolution

TYPE Original Research
PUBLISHED 07 February 2023
DOI 10.3389/fevo.2022.1040114

Sierra Nevada amphibians demonstrate stable occupancy despite precipitation volatility in the early 21st Century

Brian J. Halstead[1]*, Patrick M. Kleeman[2], Jonathan P. Rose[3] and Gary M. Fellers[2]†

[1]U.S. Geological Survey, Western Ecological Research Center, Dixon Field Station, Dixon, CA, United States, [2]U.S. Geological Survey, Western Ecological Research Center, Point Reyes Field Station, Point Reyes Station, CA, United States, [3]U.S. Geological Survey, Western Ecological Research Center, Santa Cruz Field Station, Santa Cruz, CA, United States

OPEN ACCESS

EDITED BY
Clare Aslan,
Northern Arizona University,
United States

REVIEWED BY
Diogo Alagador,
University of Évora,
Portugal
Erin Muths,
United States Department of the Interior,
United States

*CORRESPONDENCE
Brian J. Halstead
✉ bhalstead@usgs.gov

†Deceased

SPECIALTY SECTION
This article was submitted to
Biogeography and Macroecology,
a section of the journal
Frontiers in Ecology and Evolution

RECEIVED 08 September 2022
ACCEPTED 12 December 2022
PUBLISHED 07 February 2023

CITATION
Halstead BJ, Kleeman PM, Rose JP and Fellers GM (2023) Sierra Nevada amphibians demonstrate stable occupancy despite precipitation volatility in the early 21st Century.
Front. Ecol. Evol. 10:1040114.
doi: 10.3389/fevo.2022.1040114

Climate can have a strong influence on species distributions, and amphibians with different life histories might be affected by annual variability in precipitation in different ways. The Sierra Nevada of California, United States, experienced some of the driest and wettest years on record in the early 21st Century, with variability in annual precipitation predicted to increase with climate change. We examined the relationship between adult occupancy dynamics of three high elevation anurans and site and annual variation in measures of winter severity, summer wetness, and cumulative drought. We further evaluated how these weather conditions affected the probability that each species would reproduce, conditional on their occurrence at a site. We found that although different aspects of weather affected the occupancy dynamics of each species differently, adult occupancy probabilities were generally stable throughout our 15-year study period. The probability of reproduction, although slightly more variable than adult occupancy, was similarly stable throughout the study. Although occurrence of the three species was resilient to recent extremes in precipitation, more detailed demographic study would inform the extent to which amphibian populations will remain resilient to increasing severity, duration, and frequency of drought and flood cycles.

KEYWORDS

anuran, climate change, drought, multi-state occupancy model, occurrence, reproduction, Yosemite National Park

1. Introduction

Climate is one of the most important drivers of species distributions. The influence of climate can take many forms, ranging from obvious effects like climatic extremes that exceed the physiological tolerances of species (Evans et al., 2015) to subtle influences of climate on interspecific interactions (Dallalio et al., 2017). The current velocity of anthropogenic climate change, however, likely exceeds the pace at which species can adapt to new or more variable climates (Menéndez et al., 2006; Merkle et al., 2022). One aspect of global anthropogenic change that can be particularly important in limiting species distributions is climate variability.

Climate change is expected to influence the climate in different ways in different places. In California, United States, one of the major anticipated effects of climate change is to increase annual variability in precipitation, despite small changes to mean annual precipitation (Swain et al., 2018). Already in the early 21st Century, the Sierra Nevada has experienced some of the wettest and driest years on record, and the southwestern United States is currently in the midst of a multi-year "megadrought" (Williams et al., 2022). The predicted increase in the frequency and severity of droughts and floods (Huang and Swain, 2022) will likely have a large influence on many taxa, especially aquatic organisms or those that require surface waters for reproduction, like amphibians.

The anuran (frogs and toads) fauna of the high elevations of the Sierra Nevada, California, United States, is dominated by three species that differ substantially in life history strategies. The Sierra Nevada yellow-legged frog (*Rana sierrae*) historically inhabited naturally fishless, high elevation, permanent waterbodies. Long-lived adults of the species are semiaquatic, and larvae usually overwinter two or more times before undergoing metamorphosis (Fellers et al., 2013). Population declines following the historical introduction of trout (Knapp and Matthews, 2000; Knapp, 2005) and later lethal chytridiomycosis caused by the fungal pathogen *Batrachochytrium dendrobatidis* (*Bd*) caused extensive population declines and extirpations of the species (Briggs et al., 2005; Vredenburg et al., 2010), precipitating the listing of the frogs as endangered under the U.S. Endangered Species Act (ESA; U.S. Fish and Wildlife Service, 2014).

Population declines, potentially caused by chytridiomycosis (Lindauer and Voyles, 2019), also led to the listing of Yosemite toads (*Anaxyrus canorus*) as threatened under the ESA (U.S. Fish and Wildlife Service, 2014). Like Sierra Nevada yellow-legged frogs, Yosemite toads have a long-lived adult stage, but Yosemite toad adults are predominantly terrestrial (Morton and Pereyra, 2010; Liang, 2013). Adults breed at snowmelt in the shallow margins of wetlands, usually in meadows, and eggs and larvae develop quickly and metamorphose into juvenile toads in a few months (Mullaly, 1953; Kagarise Sherman and Morton, 1993). The reliance on shallow wetlands likely increases the chances of annual reproductive failure in this species (Kagarise Sherman and Morton, 1993; Sadinski et al., 2020). This toad, however, is less sensitive to introduced fish than Sierra Nevada yellow-legged frogs because Yosemite toad larvae are unpalatable to trout, the dominant introduced fish in the Sierra Nevada (Grasso et al., 2010).

In contrast to Sierra Nevada yellow-legged frogs and Yosemite toads, sierran treefrogs (*Pseudacris sierra*) are widespread in California and have a shorter adult lifespan (Ethier et al., 2021). Sierran treefrogs breed in a diversity of wetlands and, like Yosemite toads, typically undergo metamorphosis in a single season (Ethier et al., 2021). Like Sierra Nevada yellow-legged frogs, however, sierran treefrogs are palatable to fish (Grasso et al., 2010) and their occurrence is negatively related to the presence of fish (Matthews et al., 2001; Knapp, 2005).

These three anurans have different life history strategies, but all are adapted to the strongly seasonal environments of high elevations in the Sierra Nevada, and all are dependent on aquatic breeding sites. We sought to examine how recent extremes in annual precipitation affected adult occupancy dynamics and probability of reproduction of these anurans. Specifically, we estimated the influence of three climatic variables related to different aspects of water availability: winter severity (Snow Water Equivalent [SWE] in April), drought (minimum Palmer Drought Severity Index [PDSI] in September), and active season water balance (3-month Standardized Precipitation and Evapotranspiration Index [SPEI] in September) on probabilities of colonization, extirpation, and reproduction of each species. We relate our results to the life history strategy of each species and discuss how life history variation affects susceptibility and resilience to weather variability.

2. Materials and methods

2.1. Study area

We studied amphibian occupancy dynamics in Yosemite National Park (hereafter, Yosemite), California, from 2007 to 2021 (Figure 1). Yosemite is located in the central Sierra Nevada at elevations ranging from 648 to 3,997 m and is drained by two major rivers: the Merced River in the southern portion of the park and the Tuolumne River in the northern portion of the park. At high elevations, dominant trees are lodgepole pine (*Pinus contorta*), red fir (*Abies magnifica*), and white fir (*Abies concolor*). Lower elevations include additional *Pinus* spp., and meadows and riparian areas contain willows (*Salix jepsoni*), corn lily (*Veratrum californicum*), small camas (*Camassia quamash*), broad-leaf lupine (*Lupinus latifolius*), sedges (Cyperaceae), and grasses (Poaceae). Most precipitation at higher elevations falls as snow in the winter and early spring.

We divided Yosemite into 220 watershed units, each with 10–25 potential breeding sites, and randomly selected six watersheds from the Merced River basin and eight watersheds from the Tuolumne River basin (Figure 1; Fellers et al., 2015). The boundaries between our watershed units usually followed natural features and drainages, but they did not strictly conform to Hydrologic Unit Code (HUC) units mapped in the U.S. Geological Survey Watershed Boundary Dataset because of the great variation in the number of sites among mapped HUCs.

2.2. Field methods

We surveyed all potential breeding sites in each selected watershed unit using independent double observer Visual

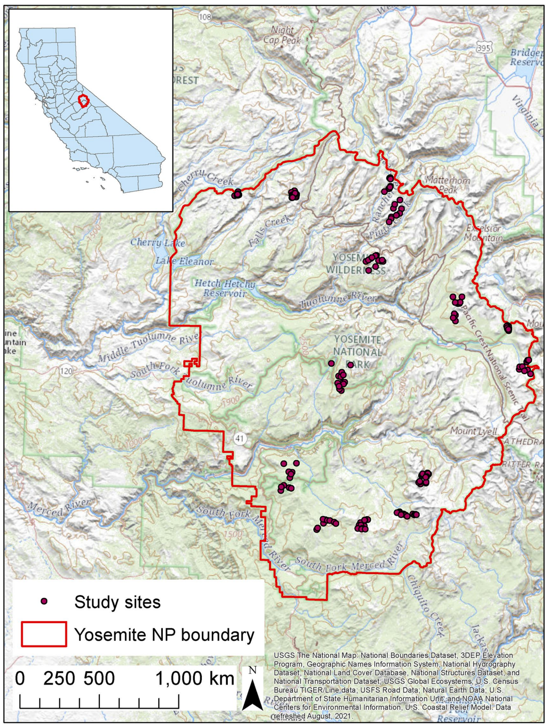

USGS The National Map: National Boundaries Dataset, 3DEP Elevation Program, Geographic Names Information System, National Hydrography Dataset, National Land Cover Database, National Structures Dataset, and National Transportation Dataset; USGS Global Ecosystems; U.S. Census Bureau TIGER/Line data; USFS Road Data; Natural Earth Data; U.S. Department of State Humanitarian Information Unit; and NOAA National Centers for Environmental Information, U.S. Coastal Relief Model. Data refreshed August, 2021

FIGURE 1
Locations of sites surveyed for amphibians in Yosemite National Park, California, United States, 2007–2021. All potential breeding sites in each of 14 watershed units were surveyed.

Encounter Surveys (VES; Crump and Scott, 1994; Fellers et al., 2015). Each site was independently surveyed by two biologists with surveys timed to start 15–60 min apart to help ensure independence between biologists while allowing time for disturbed amphibians to resume normal activity and be available for detection. To conduct surveys, each biologist walked slowly around the perimeter of ponds, lakes, and streams, or through meadows, while searching for eggs, larvae, subadults, and adults of each amphibian species. Biologists used a dip net to flush hiding amphibians and to capture larvae for positive identification when necessary. Each biologist maintained an independent count of the number of each life stage for each species at each site. In addition to counts of each life stage of each species, we recorded biologist identity, air and water temperature, maximum water depth, and site dimensions (length and width). The datasets generated for this study can be found on ScienceBase (Kleeman et al., 2022; doi: 10.5066/P9X6SKT8).

2.3. Analytical methods

We used multi-state dynamic occupancy models (Duarte et al., 2020; Rose et al., 2022) to estimate amphibian occurrence and breeding dynamics in Yosemite. These models allow for transitions between different occurrence states (i.e., unoccupied, occupied by adults only, and occupied by adults and pre-metamorphic life stages [eggs or larvae]) while accounting for imperfect state observations. Our model included three possible occurrence states for sites: (1) unoccupied by amphibians; (2) occupied by juvenile or adult amphibians only; and (3) occupied by adults and pre-metamorphic life stages indicative of breeding (whether or not adults were observed; i.e., breeding was conditional on adult occurrence). Our observation states matched the occurrence states, but our model allowed mis-classification without false positive detections. Specifically, we assumed that amphibians of any life stage could be missed during surveys. In other words, a site with only adults present (state 2) could be correctly classified with adults observed or misclassified as no amphibians observed, and a site with pre-metamorphic life stages (state 3) could be correctly classified with eggs or larvae observed or misclassified with only adults observed or with no amphibians observed.

In addition to these site-specific states, we also included additional hierarchical structure into the model to account for our clustering of sites within watershed units. We did this in two different ways, depending on the species. For widespread sierran treefrogs, which were observed in all sampled watersheds each year, we allowed mean probability of occurrence, extirpation probability, and colonization probability to vary among watersheds as a logit-normal random intercept for watershed. For Sierra Nevada yellow-legged frogs and Yosemite toads, which did not occur in all watersheds during all years, we added an additional level to the model to allow for occurrence dynamics at the watershed scale, and conditioned site occupancy on occurrence within the watershed using a multi-scale occupancy model. The multi-scale multi-state dynamic occupancy model was parameterized in terms of an initial occupancy state, extirpation probabilities, and colonization probabilities as follows.

For watershed-scale occupancy dynamics, we modeled the initial occurrence state in watershed i as

$$\Psi \sim beta\left(\alpha = 1, \beta = 1\right),$$

$$z_{i,1} \sim Bernoulli\left(\Psi\right),$$

where ψ is the watershed-scale probability of occurrence and $z_{i,1}$ is an indicator variable for presence (1) or absence (0) of the species in watershed i at the beginning of the study. For watershed-scale occupancy in subsequent years, we modeled occupancy dynamics as

$$\gamma_{WS} \sim beta\left(1,1\right),$$

$$\phi \sim beta(1,1)$$

$$\mu_{z_{i,t}} = z_{i,t-1} \times \phi + (1 - z_{i,t-1}) \times \gamma_{WS},$$

$$z_{i,t} \sim Bernoulli(\mu_{z_{i,t}}),$$

where γ_{WS} is the probability an unoccupied watershed is colonized by the species, ϕ is the probability an occupied watershed remains occupied, $\mu_{z\_i,t}$ is the probability watershed i is occupied in year t, given its occurrence status in year t – 1, and $z_{i,t}$ is an indicator for presence (1) or absence (0) of the species in watershed i in year t. We then modeled the initial occurrence state at site j, conditional on occurrence in the watershed in which site j was found, as

$$initial\_state_{1,j} = (1 - \theta_j) \times z_{i,1} + (1 - z_{i,1}),$$

$$initial\_state_{2,j} = \theta_j \times (1 - r_{j,1}) \times z_{i,1},$$

$$initial\_state_{3,j} = \theta_j \times r_{j,1} \times z_{i,1},$$

$$occ\_mtx_{j,1} \sim categorical\left(initial\_state_{[1:3],j}\right),$$

where *initial_state* defines a vector of multinomial probabilities for each site j, with states defined as 1 = unoccupied, 2 = occupied by adults only, and 3 = occupied by adults and pre-metamorphic life stages (i.e., used for breeding); θ is the probability the site is occupied by adult amphibians; $z_{i,1}$ is the indicator variable for whether the watershed in which the site is found is occupied by the species; $r_{j,1}$ is the conditional (on adult occurrence) probability that breeding occurred at the site in the initial year of the study; $occ\_mtx_{j,1}$ is a matrix of the true occupancy state of each site j in year 1; and *categorical* represents a categorical distribution. θ and r were further modeled as logit-linear functions of covariates using binomial regression (Table 1). Variables included in the model were based on knowledge of the ecology of the species and prior research (Knapp, 2005; Fellers et al., 2015; Halstead et al., 2021). Occurrence dynamics at the site scale were then modeled, conditional on watershed occurrence as for initial occupancy, with the transition matrix

$$\begin{array}{ccccc}
 & & & \textbf{State at } t & \\
 & & \textbf{Unoccupied} & \textbf{Adults only} & \textbf{Used for reproduction} \\
 & \textbf{Unoccupied} & (1-\gamma_{j,t-1}) \times z_{i,t} + (1-z_{i,t}) & \varepsilon_{j,t-1} \times z_{i,t} + (1-z_{i,t}) & \varepsilon_{j,t-1} \times z_{i,t} + (1-z_{i,t}) \\
\textbf{State at } t+1 & \textbf{Adults only} & \gamma_{j,t-1} \times (1-r_{j,t}) \times z_{i,t} & (1-\varepsilon_{j,t-1}) \times (1-r_{j,t}) \times z_{i,t} & (1-\varepsilon_{j,t-1}) \times (1-r_{j,t}) \times z_{i,t} \\
 & \textbf{Used for reproduction} & \gamma_{j,t-1} \times r_{j,t} \times z_{i,t} & (1-\varepsilon_{j,t-1}) \times r_{j,t} \times z_{i,t} & (1-\varepsilon_{j,t-1}) \times r_{j,t} \times z_{i,t}
\end{array},$$

$$occ\_mtx_{j,t} \sim categorical\left(trans\_mtx_{j,t-1,occ\_mtx_{j,t-1},[1:3]}\right),$$

where γ is the probability unoccupied site j is colonized by adults in year t; ε is the probability adults are extirpated from occupied site j in year t; r is the probability reproduction occurs at site j (conditional on adult occurrence at site j in year t); $z_{i,t}$ are indicator variables that do not allow sites in watersheds unoccupied in year t to be colonized that year and force occupied sites to become extirpated if the watershed in which they occur is not occupied the following year; and $occ\_mtx_{j,t}$ is a matrix of the true occupancy state of each site j in year t. The transition matrix for sierran treefrogs, for which we did not use a multi-scale model but instead allowed mean probability of occurrence at sites to vary across watersheds, was identical except that all $z_{i,t}$ were fixed at 1. All probabilities (γ, ε, and r) were further modeled as logit-linear functions of covariates using binomial regression, with variables included in the model tailored to the ecology of each species (Table 1).

Conditional on the occurrence state of the site, the observation matrix was defined as

$$\begin{array}{ccccc}
 & & & \textbf{Observed state} & \\
 & & \textbf{\textit{None}} & \textbf{\textit{Adults}} & \textbf{\textit{Larvae or eggs}} \\
 & \textbf{\textit{Unoccupied}} & 1 & 0 & 0 \\
\textbf{True state} & \textbf{\textit{Adults only}} & 1 - p_{Aj,t,k} & p_{Aj,t,k} & 0 \\
 & \textbf{\textit{Used for reproduction}} & (1 - p_{Aj,t,k})(1 - p_{Lj,t,k}) & p_{Aj,t,k}(1 - p_{Lj,t,k}) & p_{Lj,t,k}
\end{array},$$

$$obs\_array_{j,t,k} \sim categorical\left(p_{j,t,k,occ\_mtx_{j,t},[1:3]}\right),$$

where p is the probability of detecting each life stage, adult (A) or pre-metamorphic (L), at site j in year t and survey k and $obs\_array_{j,t,k}$ is the observed state at site j in year t and survey k. Note that we assumed that no false positives occurred: adults could not be detected if they were not present, nor could pre-metamorphic

TABLE 1 Processes affected by and summaries of predictor variables included in the multi-scale multi-state models of amphibian occurrence and reproduction.

Variable	Processes (species) affected	Scale	Mean	SD	Range
Snow-water equivalent in April (kg/m^2)	Probabilities of reproduction (PSSI and ANCA) and colonization (all)	Site × year	295	233	0–1,718
3-month standardized precipitation and evapotranspiration index in September	Probability of colonization (all)	Site × year	−0.85	1.27	−3.09 to 1.57
Minimum Palmer drought severity index in September	Probabilities of reproduction (RASI) and extirpation (all)	Site × year	−1.28	1.94	−4.21 to 4.81
Elevation (m)	Initial site occurrence (all)	Site	2,776	272	2,100–3,336
Area (m^2)	Initial site occurrence (all); probabilities of colonization and extirpation (all); probability of detection (PSSI)	Site	15,400	35,000	0–230,000
Fish (binary)	Initial site occurrence (PSSI and RASI); probabilities of reproduction, colonization, and extirpation (PSSI and RASI)	Site	0.09	0.29	0–1
Permanence (binary)	Initial site occurrence (all); probabilities of reproduction, colonization, and extirpation (all)	Site	0.70	0.46	0–1
Days since snowmelt	probability of detection (PSSI)	Site × year	65	25	0–132
Air temperature (°C)	probability of detection (all except RASI larvae)	Site × year × survey	17.5	3.8	1.0–35.0

PSSI = sierran treefrog (*Pseudacris sierra*); ANCA = Yosemite toad (*Anaxyrus canorus*); RASI = Sierra Nevada yellow-legged frog (*Rana sierrae*).

life stages be detected if breeding did not occur at the site. We allowed p to vary with site, year, and survey-specific variables based on prior research for each species (Fellers et al., 2015) using binomial regression with a logit link function (Table 1).

We selected variables to influence each parameter based on prior research in Yosemite (Table 1; Knapp, 2005; Fellers et al., 2015; Halstead et al., 2021) plus the three variables related to water availability above. In addition to variables recorded in the field, we used U.S. Geological Survey topographic maps to assign wetland hydroperiods, and we determined presence of fish based on gill net surveys (Fellers et al., 2015; Knapp et al., 2020). Date of snowmelt (earliest date at which all snow has melted) was estimated using a snow sensor at Gin Flat (2,070 m elevation near the western boundary of Yosemite between the Merced and Tuolumne rivers), and the number of days since snowmelt used as a potential variable affecting amphibian detection (Fellers et al., 2015). We used snow-water equivalent (SWE) in April, the month at which SWE typically reaches its maximum, from Daymet as a measure of the severity of the preceding winter and the amount of water available in snowpack (Thornton et al., 2020). To assess short-term effects of precipitation and evapotranspiration on occupancy dynamics and reproduction, we used the 3-month standardized precipitation and evapotranspiration index (SPEI03; Vose et al., 2014) in September, which integrated precipitation and evapotranspiration during the driest part of the year (June–August), when amphibians in this system are most active. We used the minimum Palmer Drought Severity Index (PDSI) in September to account for cumulative water deficits integrated across years as measured at the driest time of year (Vose et al., 2014). Each of these water availability variables was extracted for each site and year of the study.

We analyzed the model for each species using the package "NIMBLE" (de Valpine et al., 2022) in R 4.1.3 (R Core Team, 2022). Priors for each parameter in the model were selected to be uninformative but weakly regularizing: $beta(\alpha = 1, \beta = 1)$ for all probabilities, $exponential(\lambda = 1)$ for all standard deviations, and $Gaussian(mean = 0, SD = 1)$ for all logit-linear coefficients. We ran each model on 5 chains of 100,000 iterations each after a burn-in phase of 10,000 iterations and thinned each chain by a factor of 5, basing inference on 100,000 samples from the posterior distribution. The minimum effective sample size (the estimated number of statistically independent samples from the Markov chain Monte Carlo output after accounting for serial autocorrelation) across all parameters and species was 639 (Tables 2–4). We assessed convergence with the $\hat{R}$ statistic (Gelman and Rubin, 1992) and examination of history plots. All plots appeared stationary and well-mixed, and the maximum $\hat{R}$ across all monitored parameters was 1.02. Model code to reproduce analyses is available on GitLab (Halstead et al., 2022; doi: 10.5066/P9VR4SH3). Unless otherwise indicated, we summarize posterior distributions as median (95% equal-tailed interval).

3. Results

Across 6,169 surveys of 174 sites in 14 watersheds and 15 years, we detected sierran treefrog adults 290 times and evidence of reproduction (eggs or larvae) 2,546 times. For Sierra Nevada yellow-legged frogs, we detected adults 637 times and evidence of reproduction 715 times. We had the fewest detections

TABLE 2 Posterior summaries and Markov chain Monte Carlo (MCMC) diagnostics of parameters for the multi-state dynamic occupancy model for sierran treefrogs (*Pseudacris sierra*) in Yosemite National Park, California, United States, 2007–2021.

Model component	Parameter	Mean	SD	Median	95% CRI	P(dir)	BF dir.	Rhat	n.eff
Initial site occupancy	$\mu_{\theta\_perm\_fishless}$	0.93	0.06	0.94	0.76 to >0.99			1.00	11,649
	$\mu_{\theta\_perm\_fish}$	0.30	0.20	0.27	0.04–0.76			1.00	11,417
	μ_{θ_seas}	0.77	0.15	0.79	0.4–0.97			1.00	8,517
	$\beta_{0\_perm\_fishless}$	2.94	1.12	2.81	1.14–5.54			1.00	9,784
	$\beta_{0\_perm\_fish}$	−1.03	1.12	−1.02	−3.27 to 1.14			1.00	11,108
	β_{0_seas}	1.41	1.01	1.35	−0.39 to 3.55			1.00	8,120
	β_{elev}	−0.66	0.66	−0.62	−2.06 to 0.55	0.85	5.6	1.00	12,657
	$\beta_{elev\wedge 2}$	0.24	0.60	0.20	−0.8 to 1.53	0.64	1.8	1.00	8,640
	β_{area}	0.64	0.60	0.62	−0.49 to 1.88	0.86	6.2	1.00	7,626
	σ_{θ_WS}	1.37	0.80	1.29	0.12–3.19			1.00	2,962
Reproduction	$\mu_{r\_perm\_fishless}$	0.94	0.06	0.96	0.78–0.99			1.01	639
	$\mu_{r\_perm\_fish}$	0.77	0.16	0.81	0.36–0.97			1.01	943
	μ_{r_seas}	0.92	0.08	0.94	0.68–0.99			1.01	647
	$\iota_{0\_perm\_fishless}$	3.25	0.99	3.27	1.28–5.17			1.01	726
	$\iota_{0\_perm\_fish}$	1.46	1.02	1.48	−0.57 to 3.44			1.01	950
	ι_{0_seas}	2.81	1.03	2.82	0.77–4.83			1.01	767
	$\iota_{SWE\_\times\_perm\_fishless}$	0.28	0.44	0.26	−0.52 to 1.19	0.73	2.7	1.00	8,739
	$\iota_{SWE\_\times\_perm\_fish}$	0.14	0.61	0.12	−0.99 to 1.4	0.58	1.4	1.00	12,769
	$\iota_{SWE\_\times\_seas}$	0.29	0.50	0.28	−0.65 to 1.31	0.72	2.6	1.00	8,218
	σ_{r_WS}	3.64	1.28	3.41	1.83–6.77			1.00	2,095
	σ_{r_year}	1.79	0.54	1.71	1–3.07			1.00	7,641
Colonization	$\mu_{\gamma\_perm\_fishless}$	0.65	0.12	0.66	0.41–0.88			1.00	5,593
	$\mu_{\gamma\_perm\_fish}$	0.27	0.17	0.24	0.05–0.69			1.01	2,580
	μ_{γ_seas}	0.53	0.15	0.53	0.23–0.81			1.01	4,406
	$\zeta_{0\_perm\_fishless}$	0.69	0.59	0.66	−0.37 to 1.96			1.00	5,123
	$\zeta_{0\_perm\_fish}$	−1.15	0.98	−1.16	−3.02 to 0.81			1.01	2,390
	ζ_{0_seas}	0.12	0.67	0.13	−1.22 to 1.45			1.01	4,431
	ζ_{SWE}	−0.12	0.36	−0.11	−0.87 to 0.56	0.63	1.7	1.00	6,973
	ζ_{SPEI03}	0.37	0.31	0.36	−0.22 to 1.03	0.90	8.7	1.00	11,472
	ζ_{area}	0.10	0.46	0.10	−0.8 to 1.02	0.59	1.4	1.00	1,866
	σ_{γ_WS}	1.29	0.60	1.24	0.15–2.65			1.02	2,336
	σ_{γ_year}	0.58	0.43	0.49	0.04–1.66			1.00	1,664
Extirpation	$\mu_{\varepsilon\_perm\_fishless}$	0.06	0.02	0.05	0.02–0.11			1.01	3,573
	$\mu_{\varepsilon\_perm\_fish}$	0.08	0.07	0.06	0.01–0.26			1.00	7,069
	μ_{ε_seas}	0.07	0.03	0.06	0.03–0.14			1.00	4,142
	$\nu_{0\_perm\_fishless}$	−2.88	0.41	−2.88	−3.69 to −2.06			1.00	3,850
	$\nu_{0\_perm\_fish}$	−2.80	1.06	−2.70	−5.21 to −1.05			1.00	5,288
	ν_{0_seas}	−2.70	0.46	−2.70	−3.62 to −1.8			1.00	4,277
	$\nu_{PDSI\_\times\_perm\_fishless}$	−0.49	0.34	−0.47	−1.22 to 0.12	0.94	14.8	1.00	12,004
	$\nu_{PDSI\_\times\_perm\_fish}$	−0.53	0.81	−0.51	−2.19 to 0.98	0.73	2.8	1.00	23,707
	$\nu_{PDSI\_\times\_seas}$	0.15	0.35	0.17	−0.6 to 0.79	0.68	2.1	1.00	12,323

(Continued)

TABLE 2 (Continued)

Model component	Parameter	Mean	SD	Median	95% CRI	P(dir)	BF dir.	Rhat	n.eff
	ν_{area}	−0.71	0.22	−0.70	−1.14 to −0.29	1.00	2856.1	1.00	8,864
	σ_{ε_WS}	0.82	0.28	0.77	0.4–1.48			1.00	10,424
	$\sigma_{\varepsilon\_year}$	0.92	0.30	0.87	0.47–1.63			1.00	10,812
Detection	μ_{p_adults}	0.36	0.07	0.36	0.23–0.5			1.00	2,303
	ξ_{0_adults}	−0.59	0.30	−0.60	−1.19 to 0			1.00	2,254
	ξ_{adults_dssm}	−0.61	0.13	−0.61	−0.86 to −0.36	>0.99	∞	1.00	9,021
	ξ_{adults_temp}	0.15	0.09	0.15	−0.03 to 0.32	0.95	17.4	1.00	52,220
	ξ_{adults_area}	0.68	0.29	0.68	0.11–1.24	0.99	110.6	1.00	2,442
	μ_{p_larvae}	0.78	0.05	0.78	0.66–0.86			1.00	1,966
	ξ_{0_larvae}	1.26	0.30	1.26	0.68–1.85			1.00	1,947
	ξ_{larvae_dssm}	0.40	0.13	0.40	0.14–0.66	1.00	1161.8	1.00	8,150
	ξ_{larvae_temp}	0.19	0.06	0.19	0.06–0.31	1.00	616.3	1.00	41,530
	ξ_{larvae_area}	0.15	0.27	0.15	−0.38 to 0.66	0.71	2.4	1.00	2,216
	σ_{p_site}	2.90	0.23	2.89	2.48–3.38			1.00	12,810
	σ_{p_year}	0.42	0.12	0.40	0.22–0.7			1.00	16,211
	$\sigma_{p\_observer}$	0.39	0.13	0.38	0.19–0.69			1.00	9,938

SD = standard deviation; 95% CRI = 95% equal-tailed interval; P(dir) = proportion of posterior probability distribution with the same sign as the median (model coefficients only); BF dir. = posterior odds of a directional effect based on prior expectation of 0.5 (model coefficients only); Rhat = Gelman-Rubin convergence diagnostic; n.eff = effective sample size (the estimated number of statistically independent samples from the Markov chain Monte Carlo output after accounting for serial autocorrelation).

of Yosemite toads, with adults detected 274 times and evidence of reproduction 622 times.

The three climatic variables related to water availability that we evaluated varied substantially over the study period, but exhibited different patterns (Figure 2; Table 1). Across sites, annual April SWE averaged 295 kg/m^2 (SD = 197; range = 29–695), reaching its maximum value in 2010 and its minimum value in 2013 (Figure 2; Table 1). Annual September minimum PDSI averaged −1.28 (SD = 1.86; range = −3.44 to 3.57) reaching maximum and minimum values in 2011 and 2008, respectively (Figure 2; Table 1). Annual SPEI03 in September averaged −0.85 (SD = 1.22, range = −2.90 to 1.05), with maximum and minimum values observed in 2017 and 2008, respectively (Figure 2; Table 1).

Sierran treefrogs occurred in all watersheds in all years, but Sierra Nevada yellow-legged frogs and Yosemite toads occurred in only a subset of watersheds. In 2007, probability of occurrence of Sierra Nevada yellow-legged frogs in watersheds was median 0.70 (95% equal-tailed interval = 0.45–0.88). Colonization probability was low (0.02 [<0.01–0.07]) and watershed persistence probability was high (0.97 [0.93–0.99]); nonetheless, the probability of occurrence for Sierra Nevada yellow-legged frogs at the watershed scale decreased from 2007 to 2021 (Figure 3). Initial probability of occurrence for Yosemite toads (0.52 [0.26–0.78]) was lower than for Sierra Nevada yellow-legged frogs, but both colonization and watershed persistence probabilities were estimated to be higher (0.07 [0.01–0.18] and 0.99 [0.96–>0.99], respectively), resulting in an increase in the probability of occurrence of Yosemite toads at the watershed scale from 2007 to 2021 (Figure 3).

Species varied in their probability of occurrence in 2007 and in their responses to elevation and area. The initial probability of occurrence of sierran treefrogs was generally much higher than for the other species (Tables 2–4; Figure 4). The initial probability of occurrence for both sierran treefrogs and Sierra Nevada yellow-legged frogs was highest in permanent fishless waterbodies, lower in seasonal wetlands, and lowest in permanent waterbodies with fish (Tables 2, 3; Figure 4). In contrast, the initial probability of occurrence for Yosemite toads was higher in seasonal wetlands than permanent waterbodies (Table 4; Figure 4). In sierran treefrogs, initial probability of occurrence was generally higher at lower elevations (Table 2; Figure 4). Relative to elevation, initial probability of occurrence for Sierra Nevada yellow-legged frogs peaked near 2,700 m elevation, whereas initial probability of occurrence for Yosemite toads was highest at the lowest and highest elevations sampled (Tables 3, 4; Figure 4). For all species and breeding site types, larger sites were more likely to be occupied initially than smaller sites (Tables 2–4; Figure 4).

The probability of colonization varied across species, and was lowest for sierran treefrogs and Sierra Nevada yellow-legged frogs in permanent waterbodies with fish (Tables 2–4; Figure 5). Probability of colonization for all species was positively related to 3-month SPEI in September (Tables 2–4; Figure 5). April snow-water equivalent had a negative effect on colonization probability for Sierra Nevada yellow-legged frogs (Table 3; Figure 5), but a positive effect on colonization probability for Yosemite toads

TABLE 3 Posterior summaries and Markov chain Monte Carlo (MCMC) diagnostics of parameters for the multi-state dynamic occupancy model for Sierra Nevada yellow-legged frogs (*Rana sierrae*) in Yosemite National Park, California, United States, 2007–2021.

Model component	Parameter	Mean	SD	Median	95% CRI	P(dir)	BF dir.	Rhat	n.eff
Watershed occupancy	ψ	0.69	0.11	0.70	0.45–0.88			1.00	100,000
	γ_{WS}	0.02	0.02	0.01	<0.01–0.07			1.00	34,072
	ϕ_{WS}	0.97	0.02	0.97	0.93–0.99			1.00	15,673
Initial site occupancy	$\mu_{\theta\_perm\_fishless}$	0.67	0.08	0.67	0.51–0.8			1.00	33,091
	$\mu_{\theta\_perm\_fish}$	0.19	0.12	0.16	0.03–0.48			1.00	54,000
	μ_{θ_seas}	0.46	0.13	0.45	0.21–0.72			1.00	47,200
	$\beta_{0\_perm\_fishless}$	0.71	0.35	0.70	0.04–1.41			1.00	32,947
	$\beta_{0\_perm\_fish}$	−1.69	0.88	−1.65	−3.51 to −0.06			1.00	56,689
	β_{0_seas}	−0.19	0.58	−0.18	−1.35 to 0.93			1.00	47,269
	β_{elev}	−0.41	0.23	−0.40	−0.88 to 0.04	0.96	25.8	1.00	55,128
	$\beta_{elev^\wedge 2}$	−0.52	0.19	−0.52	−0.92 to −0.15	1.00	383.6	1.00	29,062
	β_{area}	1.02	0.30	1.01	0.45–1.64	1.00	11110.1	1.00	41,556
Reproduction	$\mu_{r\_perm\_fishless}$	0.57	0.03	0.57	0.51–0.62			1.00	26,598
	$\mu_{r\_perm\_fish}$	0.09	0.05	0.08	0.02–0.22			1.00	60,187
	μ_{r_seas}	0.13	0.03	0.13	0.08–0.2			1.00	50,646
	$\iota_{0\_perm\_fishless}$	0.26	0.11	0.26	0.04–0.49			1.00	26,542
	$\iota_{0\_perm\_fish}$	−2.47	0.70	−2.42	−3.99 to −1.26			1.00	63,237
	ι_{0_seas}	−1.90	0.26	−1.89	−2.43 to −1.41			1.00	50,653
	$\iota_{PDSI\_\times\_perm\_fishless}$	0.27	0.11	0.27	0.07–0.49	1.00	259.4	1.00	34,959
	$\iota_{PDSI\_\times\_perm\_fish}$	−0.37	0.64	−0.33	−1.71 to 0.78	0.71	2.4	1.00	74,172
	$\iota_{PDSI\_\times\_seas}$	0.17	0.26	0.17	−0.37 to 0.67	0.74	2.8	1.00	64,680
	σ_{r_year}	0.22	0.14	0.21	0.02–0.54			1.01	2,750
Colonization	$\mu_{\gamma\_perm\_fishless}$	0.09	0.02	0.09	0.05–0.14			1.00	11,441
	$\mu_{\gamma\_perm\_fish}$	0.02	0.02	0.01	0–0.06			1.00	29,034
	μ_{γ_seas}	0.08	0.03	0.08	0.04–0.15			1.00	12,746
	$\zeta_{0\_perm\_fishless}$	−2.30	0.27	−2.30	−2.87 to −1.79			1.00	12,646
	$\zeta_{0\_perm\_fish}$	−4.66	1.31	−4.46	−7.78 to −2.68			1.00	39,648
	ζ_{0_seas}	−2.45	0.37	−2.45	−3.2 to −1.74			1.00	14,075
	ζ_{SWE}	−0.47	0.26	−0.44	−1.06 to −0.05	0.99	82.9	1.00	5,693
	ζ_{SPEI03}	0.37	0.23	0.36	−0.05 to 0.86	0.96	24.1	1.00	15,597
	ζ_{area}	−0.47	0.20	−0.47	−0.88 to −0.08	0.99	109.0	1.00	20,016
	σ_{γ_year}	0.52	0.36	0.46	0.03–1.38			1.00	2,197
Extirpation	$\mu_{\varepsilon\_perm\_fishless}$	0.08	0.02	0.08	0.05–0.12			1.00	15,102
	$\mu_{\varepsilon\_perm\_fish}$	0.08	0.08	0.06	0–0.31			1.00	34,165
	μ_{ε_seas}	0.13	0.04	0.13	0.06–0.23			1.00	18,717
	$\nu_{0\_perm\_fishless}$	−2.45	0.25	−2.45	−2.96 to −1.96			1.00	16,197
	$\nu_{0\_perm\_fish}$	−2.97	1.39	−2.77	−6.26 to −0.81			1.00	37,501
	ν_{0_seas}	−1.94	0.39	−1.92	−2.75 to −1.21			1.00	18,621
	$\nu_{PDSI\_\times\_perm\_fishless}$	−0.41	0.27	−0.39	−1 to 0.07	0.95	18.5	1.00	27,578
	$\nu_{PDSI\_\times\_perm\_fish}$	−0.13	0.76	−0.10	−1.71 to 1.28	0.55	1.2	1.00	79,877
	$\nu_{PDSI\_\times\_seas}$	−0.43	0.48	−0.38	−1.49 to 0.41	0.81	4.3	1.00	22,452

(Continued)

TABLE 3 (Continued)

Model component	Parameter	Mean	SD	Median	95% CRI	P(dir)	BF dir.	Rhat	n.eff
	ν_{area}	−0.54	0.17	−0.54	−0.87 to −0.21	1.00	1723.1	1.00	31,275
	$\sigma_{\varepsilon\_year}$	0.41	0.29	0.35	0.03–1.12			1.00	2,705
Detection	μ_{p_adults}	0.58	0.03	0.58	0.52–0.64			1.00	12,514
	ξ_{0_adults}	0.32	0.13	0.32	0.07–0.57			1.00	12,514
	ξ_{adults_temp}	0.21	0.07	0.21	0.07–0.35	1.00	688.7	1.00	51,918
	μ_{p_larvae}	0.80	0.02	0.81	0.75–0.85			1.00	18,062
	ξ_{0_larvae}	1.42	0.15	1.42	1.12–1.72			1.00	18,232
	σ_{p_year}	0.18	0.13	0.16	0.01–0.47			1.02	1,805
	$\sigma_{p\_observer}$	0.23	0.11	0.22	0.04–0.48			1.01	3,733

SD = standard deviation; 95% CRI = 95% equal-tailed interval; P(dir) = proportion of posterior probability distribution with the same sign as the mean (model coefficients only); BF dir. = posterior odds of a directional effect based on prior expectation of 0.5 (model coefficients only); Rhat = Gelman-Rubin statistic; n.eff = effective sample size (the estimated number of statistically independent samples from the Markov chain Monte Carlo output after accounting for serial autocorrelation).

(Table 4; Figure 5). Colonization probabilities were higher in waterbodies without fish than waterbodies with fish, regardless of seasonality, for sierran treefrogs and Sierra Nevada yellow-legged frogs (Tables 2, 3; Figure 5). In addition to weather variables, site colonization probability for Sierra Nevada yellow-legged frogs was negatively related to site area (Table 3).

Extirpation probabilities of all species were affected by minimum September PDSI, but the direction of effects and their magnitude varied across species and breeding site types (Tables 2–4; Figure 6). Extirpation probability for Sierra Nevada yellow-legged frogs was negatively related to minimum September PDSI (i.e., a lower extirpation probability when conditions were wetter in September) in all breeding site types, but evidence for an effect of PDSI on permanent sites with fish was weaker than for other breeding site types (Table 3; Figure 6). Minimum September PDSI had a negative effect on extirpation of Yosemite toads in seasonal wetlands, but a positive effect in permanent waterbodies (Table 4; Figure 6). Evidence of an effect of PDSI on the probability of extirpation for sierran treefrogs was substantial only for permanent fishless breeding sites, for which it had a negative effect (Table 2; Figure 6). Site area was negatively related to extirpation probability for all three species (Tables 2–4).

Although weather affected the probability of reproduction for Sierra Nevada yellow-legged frogs and Yosemite toads, evidence for an effect of weather variables on sierran treefrogs was weak (Tables 2–4; Figure 7). Probability of reproduction for Sierra Nevada yellow-legged frogs was positively related to minimum September PDSI in occupied permanent fishless waterbodies, but evidence for an effect of weather on reproduction in other breeding site types was weak (Table 3; Figure 7). Probability of reproduction for Yosemite toads was negatively related to April SWE regardless of whether wetlands were permanent or seasonal, but the effect was stronger in permanent waterbodies (Table 4; Figure 7). Probability of reproduction for sierran treefrogs was highest in permanent fishless waterbodies and lowest in permanent waterbodies with fish (Table 2; Figure 7). The effects of weather, breeding site type, and random annual variation resulted in differing patterns of annual probabilities of reproduction at occupied sites across species (Figure 8).

Annual probability of site occurrence for adults of all species was relatively stable, but varied by breeding site type (Figure 9). For Sierra Nevada yellow-legged frogs and sierran treefrogs, probability of occurrence was consistently higher in permanent fishless and seasonal wetlands than in permanent waterbodies with fish (Figure 9). Adult Yosemite toads had moderately higher probability of occurrence in seasonal than permanent sites (Figure 9). Site occupancy growth rates were generally near 1 and turnover rates were generally low except for Yosemite toads between 2007 and 2008 and sierran treefrogs in permanent fishless sites in the same interval (Figure 9), when both species colonized a number of previously unoccupied sites.

On average, detection probabilities for larvae were higher than detection probabilities for adults for all species (Tables 2–4; Figure 10). For all species, air temperature had a positive effect on detection probability for all life stages (Tables 2–4; Figure 10). In addition to air temperature, sierran treefrogs were more likely to be detected at larger occupied sites (Table 2; Figure 10). Days since snowmelt had opposite effects on adults and larvae of sierran treefrogs; adults had higher detection probability sooner after snowmelt, whereas larvae had higher detection probability longer after snowmelt (Table 2; Figure 10). For sierran treefrogs, detection probabilities varied substantially among sites (Table 2).

4. Discussion

Despite substantial variation in climatic conditions related to water availability, occurrence of adult amphibians in Yosemite was stable. Although climatic variables affected transitions between adult occupancy states, these responses were not so strong as to

TABLE 4 **Posterior summaries and Markov chain Monte Carlo (MCMC) diagnostics of parameters for the multi-state dynamic occupancy model for Yosemite toads (*Anaxyrus canorus*) in Yosemite National Park, California, United States, 2007–2021.**

Model component	Parameter	Mean	SD	Median	95% CRI	P(dir)	BF dir.	Rhat	n.eff
Watershed occupancy	ψ	0.52	0.13	0.52	0.26–0.78			1.00	51,345
	γ_{WS}	0.08	0.04	0.07	0.01–0.18			1.00	24,261
	ϕ_{WS}	0.99	0.01	0.99	0.96–1			1.00	19,190
Initial site occupancy	μ_{θ_seas}	0.23	0.11	0.21	0.07–0.5			1.00	22,612
	μ_{θ_perm}	0.09	0.05	0.08	0.02–0.23			1.00	15,607
	β_{0_seas}	−1.32	0.66	−1.33	−2.6 to −0.01			1.00	22,340
	β_{0_perm}	−2.47	0.66	−2.46	−3.82 to −1.22			1.00	15,649
	β_{elev}	0.28	0.34	0.28	−0.37 to 0.96	0.80	4.1	1.00	51,180
	$\beta_{elev^\wedge 2}$	1.38	0.41	1.35	0.65–2.26	1.00	9089.9	1.00	16,030
	β_{area}	0.30	0.40	0.30	−0.47 to 1.11	0.78	3.5	1.00	39,262
Reproduction	μ_{r_seas}	0.47	0.06	0.47	0.35–0.59			1.00	11,909
	μ_{r_perm}	0.51	0.06	0.51	0.4–0.62			1.00	10,329
	ι_{0_seas}	−0.13	0.25	−0.13	−0.61 to 0.37			1.00	11,822
	ι_{0_perm}	0.03	0.23	0.03	−0.42 to 0.48			1.00	10,266
	$\iota_{SWE\_\times\_seas}$	−0.16	0.22	−0.15	−0.59 to 0.26	0.77	3.3	1.00	19,122
	$\iota_{SWE\_\times\_perm}$	−0.35	0.16	−0.34	−0.67 to −0.04	0.99	86.5	1.00	18,736
	σ_{r_year}	0.72	0.21	0.70	0.39–1.21			1.00	17,016
Colonization	μ_{γ}	0.04	0.02	0.04	0.02–0.08			1.00	6,201
	ζ_0	−3.23	0.43	−3.20	−4.15 to −2.46			1.00	5,572
	ζ_{SWE}	0.78	0.27	0.78	0.25–1.33	1.00	504.1	1.00	13,707
	ζ_{SPEI03}	0.88	0.36	0.86	0.21–1.64	0.99	184.2	1.00	9,109
	ζ_{area}	0.03	0.16	0.03	−0.29 to 0.35	0.58	1.4	1.00	30,328
	σ_{γ_year}	1.08	0.42	1.02	0.45–2.09			1.00	8,511
Extirpation	μ_{ε_seas}	0.06	0.02	0.06	0.02–0.12			1.00	15,857
	μ_{ε_perm}	0.16	0.04	0.15	0.08–0.25			1.00	15,815
	ν_{0_seas}	−2.80	0.42	−2.78	−3.68 to −2.04			1.00	14,257
	ν_{0_perm}	−1.72	0.34	−1.70	−2.44 to −1.09			1.00	14,429
	$\nu_{PDSI\_\times\_seas}$	−0.59	0.47	−0.56	−1.57 to 0.25	0.91	9.6	1.00	23,386
	$\nu_{PDSI\_\times\_perm}$	0.45	0.25	0.46	−0.05 to 0.93	0.96	25.6	1.00	19,112
	ν_{area}	−0.98	0.26	−0.97	−1.51 to −0.5	1.00	∞	1.00	15,108
	$\sigma_{\varepsilon\_year}$	0.49	0.35	0.43	0.03–1.32			1.01	2,449
Detection	μ_{p_adults}	0.39	0.05	0.39	0.3–0.49			1.00	9,139
	ξ_{0_adults}	−0.44	0.21	−0.44	−0.84 to −0.02			1.00	9,143
	ξ_{adults_temp}	0.16	0.11	0.16	−0.05 to 0.38	0.93	13.5	1.00	57,122
	μ_{p_larvae}	0.87	0.03	0.87	0.81–0.92			1.00	11,369
	ξ_{0_larvae}	1.91	0.23	1.91	1.46–2.39			1.00	11,044
	ξ_{larvae_temp}	0.14	0.13	0.14	−0.13 to 0.4	0.85	5.8	1.00	61,398
	σ_{p_year}	0.51	0.17	0.49	0.22–0.9			1.00	12,158
	$\sigma_{p\_observer}$	0.30	0.18	0.28	0.02–0.71			1.01	2,247

SD = standard deviation; 95% CRI = 95% equal-tailed interval; P(dir) = proportion of posterior probability distribution with the same sign as the mean (model coefficients only); BF dir. = posterior odds of a directional effect based on prior expectation of 0.5 (model coefficients only); Rhat = Gelman-Rubin statistic; n.eff = effective sample size (the estimated number of statistically independent samples from the Markov chain Monte Carlo output after accounting for serial autocorrelation).

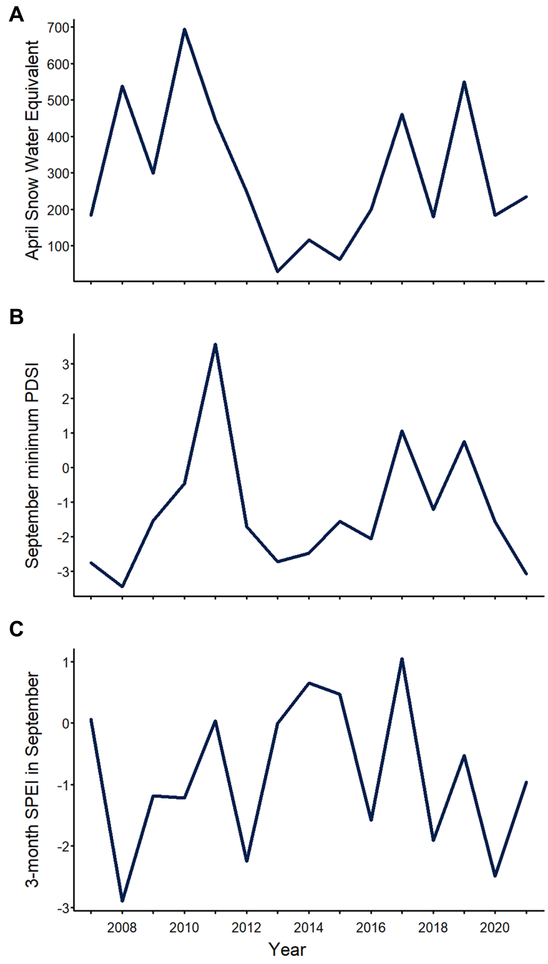

FIGURE 2
Mean annual **(A)** April snow water equivalent, **(B)** September minimum Palmer Drought Severity Index (PDSI; lower values=drier conditions), and **(C)** 3-month Standardized Precipitation Evapotranspiration Index (SPEI) in September in Yosemite National Park, California, United States, 2007–2021, averaged across surveyed sites.

result in large changes to the proportion of sites occupied in most years. Indeed, after the first 2 years of study, adult occupancy growth rates of all species were near 1.0. Thus, similar to native amphibians in the San Francisco Bay Area of California, United States (Moss et al., 2021), the occurrence of all three anurans was resilient to extremes in winter severity, summer precipitation, and drought over the last 15 years. Individual species, however, often responded differently to weather variables, and in some cases the response varied within species across wetland types.

Although the extirpation probability of all species was affected by the minimum PDSI in September, the response was quite variable across species and wetland types. For example, little evidence existed for an effect of PDSI on sierran treefrog extirpation for seasonal wetlands and permanent waterbodies containing fish, but moderately strong support existed for a negative effect of PDSI on extirpation in permanent waterbodies without fish (i.e., wetter site × year combinations were less likely to be extirpated). A similar pattern was observed for Sierra Nevada yellow-legged frogs: some support existed for a negative effect of PDSI on extirpation in seasonal wetlands, but support for a negative effect of PDSI on extirpation in permanent fishless wetlands was stronger. For both Sierra Nevada yellow-legged frogs and sierran treefrogs, lower probability of occurrence in waterbodies containing fish (Knapp and Matthews, 2000; Matthews et al., 2001; Knapp, 2005) likely superseded any effects of weather on extirpation of these species in these waterbodies. Thus, site characteristics, including co-occurring species, can influence the extent to which climate affects occupancy dynamics (Moss et al., 2021).

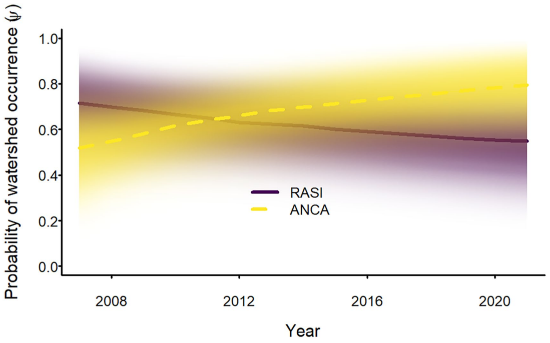

FIGURE 3
Annual probability of occurrence of adult Sierra Nevada yellow-legged frogs (*Rana sierrae*; RASI) and Yosemite toads (*Anaxyrus canorus*; ANCA) at the watershed scale in Yosemite National Park, California, United States, 2007–2021. Bold lines indicate posterior modes and the intensity of shading represents the posterior probability density.

Yosemite toads, which were not affected by fish in our models (Knapp, 2005; Grasso et al., 2010; Fellers et al., 2015), exhibited even more context-dependence in the influence of weather on extirpation probabilities. Some support existed for a negative effect of PDSI on extirpation in seasonal sites for Yosemite toads, whereas support was strong for a positive effect of PDSI on Yosemite toad extirpation in permanent sites. The finding that wetter conditions were related to extirpation of Yosemite toads in permanent sites was unexpected. Related to our findings, in high elevation populations of the related boreal toad (*Anaxyrus boreas boreas*) larval survival was lower in permanent sites than in ephemeral sites (Crockett et al., 2020). We suspect, however, that the terrestrial adults of Yosemite toads might be more strongly tied to permanent waterbodies in dry years, but disperse to more favored meadow habitats in wet years (Berlow et al., 2013; Liang, 2013; Sadinski et al., 2020). Our models cannot distinguish whether extirpation is a result of mortality or emigration, and it is likely that in the case of Yosemite toad extirpation at permanent sites, migration might be the dominant process (Morton and Pereyra, 2010; Liang, 2013).

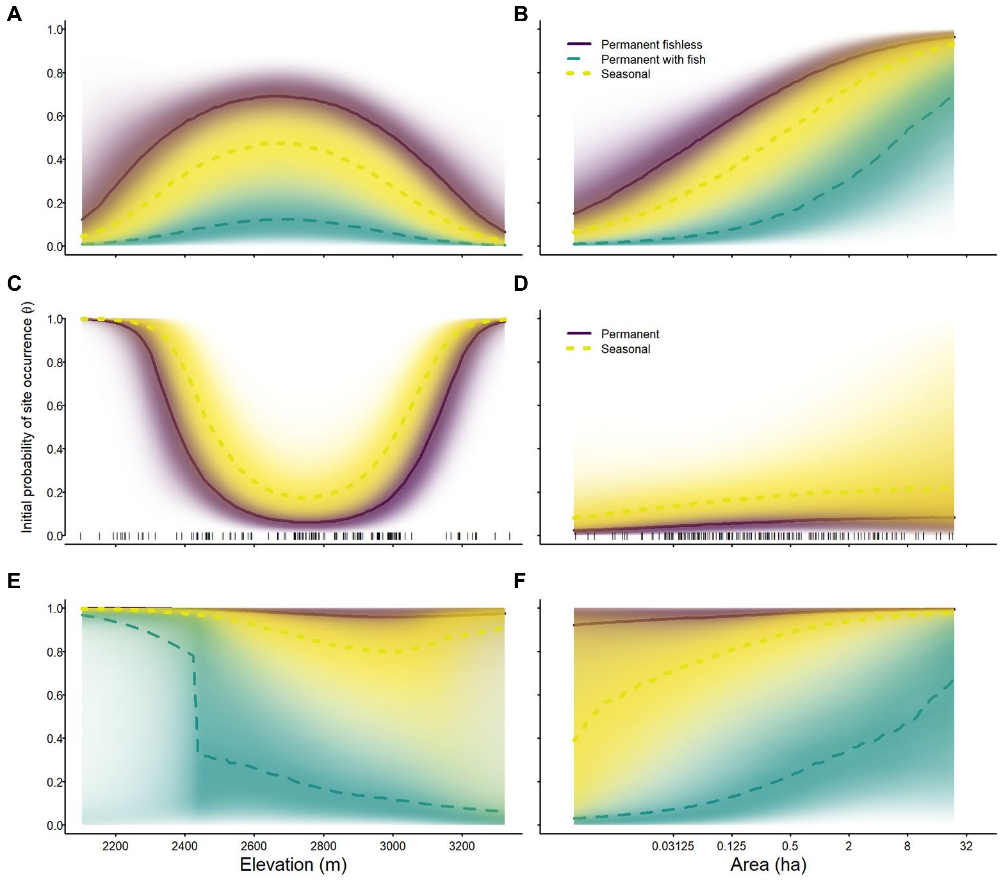

FIGURE 4
Initial probability of occurrence of Sierra Nevada yellow-legged frogs [*Rana sierrae*; **(A,B)**], Yosemite toads [*Anaxyrus canorus*; **(C,D)**], and sierran treefrogs [*Pseudacris sierra*; **(E,F)**] in relation to elevation **(A,C,E)**, site area [**(B,D,F)**; plotted on a log scale], and site type (indigo shading and solid line=permanent [and fishless for panels **(A–D)**]; aqua shading and dashed line=permanent with fish; gold shading and dotted line=seasonal) in Yosemite National Park, California, United States, 2007. Lines represent posterior modes and shading intensity represents the posterior probability distribution.

The colonization of unoccupied sites by all three species was positively related to SPEI03 in September. SPEI03 in September was chosen as a measure of active season (June–August) climatic wetness, and the positive relationship between colonization of unoccupied sites and wetness is likely because wetter conditions facilitate terrestrial activity of amphibians (Bartelt et al., 2004; Schmetterling and Young, 2008). For more aquatic species in particular, a wetter summer environment might allow them to disperse farther from wetlands and facilitate colonization of unoccupied sites, provided the active season is long enough for dispersal to occur.

Winter severity, in contrast to summer wetness, had contrasting effects on colonization probabilities of Sierra Nevada yellow-legged frogs and Yosemite toads. Yosemite toads were more likely to colonize unoccupied sites following more severe winters. Winter severity generally has two major effects on amphibians in the following active season. In high elevation systems snowpack dominates moisture availability, and soil moisture is generally high following severe winters (Bales et al., 2006). Higher soil moisture likely facilitates dispersal of terrestrial amphibians because they can more easily find moist refugia to maintain water balance as they move across the landscape (Baldwin et al., 2006). This is likely the dominant process increasing Yosemite toad colonization probability following severe winters. The other major effect of severe winters is to shorten the subsequent active season because snowmelt occurs later in the year (Bales et al., 2006). In the case of Sierra Nevada yellow-legged frogs, which had decreased colonization probabilities following severe winters, the short duration of the active season might have limited time for colonization of unoccupied sites. This might be especially true if colonization events are dominated by recently metamorphosed subadults, which would disperse through the landscape after undergoing metamorphosis in mid- to late summer. Colonization is not only affected by dispersal, however, but also by successful establishment at unoccupied sites.

In addition to weather, fish had a negative influence on colonization probabilities for Sierra Nevada yellow-legged frogs and sierran treefrogs. The negative effects of introduced fish on

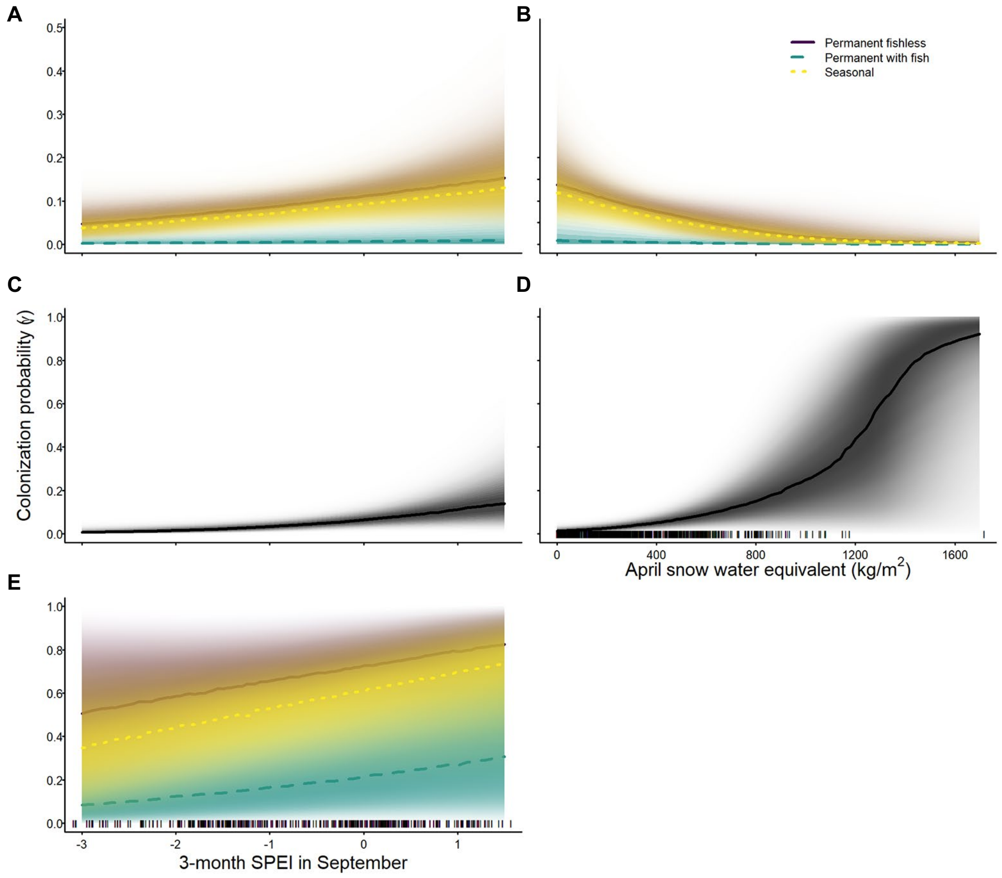

FIGURE 5
Probability of colonization for Sierra Nevada yellow-legged frogs [*Rana sierrae*; **(A,B)**], Yosemite toads [*Anaxyrus canorus*; **(C,D)**], and sierran treefrogs [*Pseudacris sierra*; **(E)**] in relation to 3-month Standardized Precipitation and Evapotranspiration Index (SPEI) in September **(A,C,E)**, April snow water equivalent **(B,D)**, and site type (indigo shading and solid line=permanent without fish; aqua shading and dashed line=permanent with fish; gold shading and dotted line=seasonal; black solid lines and shading=no distinction among site types) in Yosemite National Park, California, United States, 2007–2021. Lines represent posterior modes and shading intensity represents the posterior probability distribution.

amphibian populations are well-known, and introduced trout are negatively related to the occurrence of Sierra Nevada and mountain yellow-legged frogs (*Rana muscosa*) and sierran treefrogs in the high elevations of the Sierra Nevada (Knapp and Matthews, 2000; Matthews et al., 2001; Knapp, 2005; Fellers et al., 2015). Sierra Nevada and mountain yellow-legged frog populations can rapidly increase in abundance following the removal of non-native fish (Knapp et al., 2007); our study provides additional evidence that introduced fishes inhibit colonization of sites by native amphibians, which further fragments the landscape and impairs the function of healthy amphibian metapopulations (Knapp et al., 2003).

Weather not only affected occupancy dynamics of adult anurans, it also affected the probability that both Sierra Nevada yellow-legged frogs and Yosemite toads would breed. Although support for an effect of April SWE on the probability Yosemite toads would breed was only weakly supported for seasonal wetlands, evidence for a negative effect of winter severity on the probability Yosemite toads would reproduce in permanent wetlands was strong. Yosemite toads typically breed at snowmelt in the shallow margins of wetlands, often in meadows (Liang et al., 2017; Sadinski et al., 2020). In more severe winters, when snowmelt occurs later, conditions might be less favorable for Yosemite toads to reproduce. The stronger relationship between probability of reproduction and winter severity in permanent sites might be caused by reduced snowpack limiting opportunities for Yosemite toads to breed in more favored meadow sites (Liang et al., 2017; Sadinski et al., 2020). For Sierra Nevada yellow-legged frogs, overwhelming support for a positive effect of wetness on the probability of larval occurrence existed for permanent fishless waterbodies, but little support existed for the effects of weather on the probability of larval occurrence in seasonal wetlands or those with fish, likely because these wetland types are unsuitable for Sierra Nevada yellow-legged frog reproduction (Knapp and Matthews, 2000; Knapp, 2005; Fellers et al., 2013). Thus, like extirpation, the influence of weather variables might be context-specific and secondary to the effects of habitat conditions and biotic relationships.

As expected, fish had a negative effect on the probability of larval occurrence for both Sierra Nevada yellow-legged frogs and

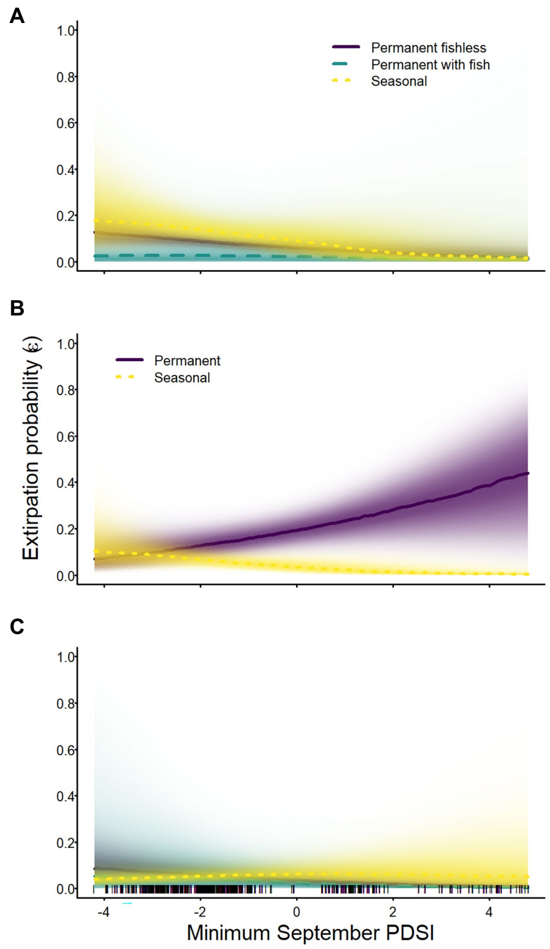

FIGURE 6
Probability of extirpation for Sierra Nevada yellow-legged frogs [*Rana sierrae*; **(A)**], Yosemite toads [*Anaxyrus canorus*; **(B)**], and sierran treefrogs [*Pseudacris sierra*; **(C)**] in relation to the minimum Palmer Drought Severity Index (PDSI) in September and site type (indigo shading and solid line=permanent [and fishless for panels **(A,C)**]; aqua shading and dashed line=permanent with fish; gold shading and dotted line=seasonal) in Yosemite National Park, California, United States, 2007–2021. Lines represent posterior modes and shading intensity represents the posterior probability distribution.

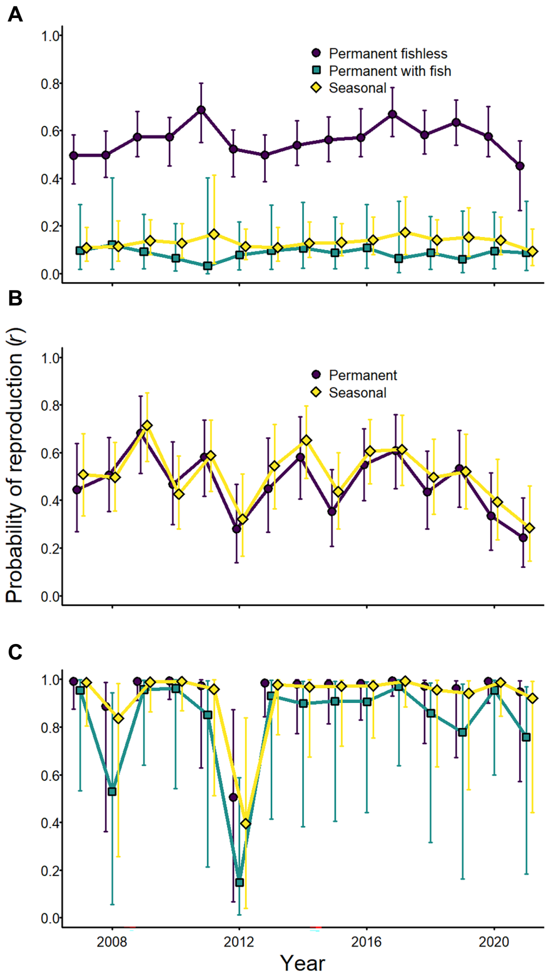

FIGURE 8
Annual probabilities of reproduction (conditional on adult occurrence) for Sierra Nevada yellow-legged frogs [*Rana sierrae*; **(A)**], Yosemite toads [*Anaxyrus canorus*; **(B)**], and sierran treefrogs [*Pseudacris sierra*; **(C)**] by site type (indigo circles and line=permanent [and fishless for panels **(A,C)**]; aqua squares and line=permanent with fish; gold diamonds and line=seasonal) based on modeled relationships with climate variables and random annual variation in Yosemite National Park, California, United States, 2007–2021. Points represent posterior medians; error bars represent 95% equal-tailed intervals.

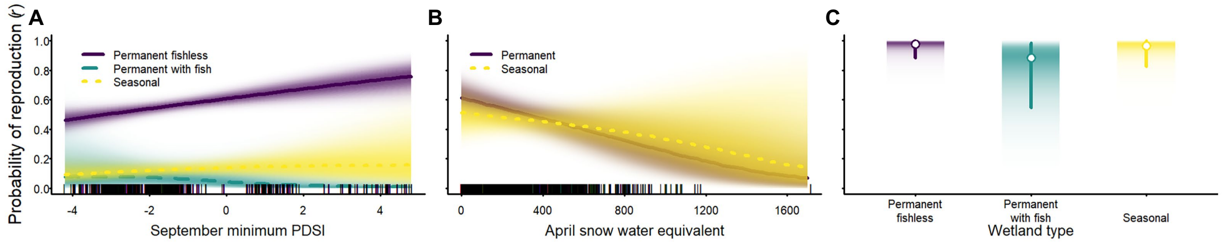

FIGURE 7
Probability of reproduction for Sierra Nevada yellow-legged frogs [*Rana sierrae*; **(A)**], Yosemite toads [*Anaxyrus canorus*; **(B)**], and sierran treefrogs [*Pseudacris sierra*; **(C)**] in relation to the minimum Palmer Drought Severity Index (PDSI) in September **(A)**, April snow water equivalent [SWE; **(B)**], and site type (indigo shading and solid line=permanent [and fishless for panels **(A,C)**]; aqua shading and dashed line=permanent with fish; gold shading and dotted line=seasonal) in Yosemite National Park, California, United States, 2007–2021. Lines represent posterior modes and shading intensity represents the posterior probability distribution. In **(C)**, white circles represent posterior modes, vertical lines represent 95% highest posterior density intervals, and the intensity of shading represents posterior probability densities.

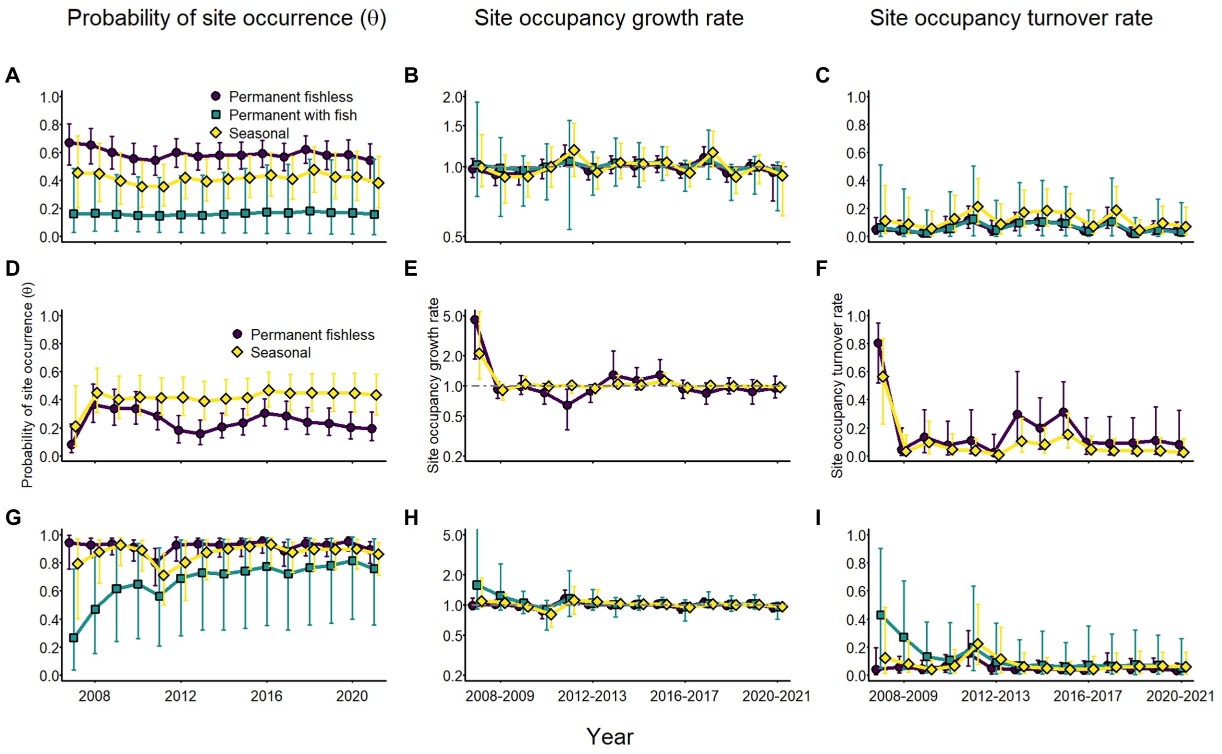

FIGURE 9
Annual estimates of site occupancy probability **(A,D,G)**, site occupancy growth rate **(B,E,H)**, and site occupancy turnover rate **(C,F,I)** for Sierra Nevada yellow-legged frogs [*Rana sierrae*; **(A–C)**], Yosemite toads [*Anaxyrus canorus*; **(D–F)**], and sierran treefrogs [*Pseudacris sierra*; **(G–I)**] by site type (indigo circles and line=permanent [and fishless for panels **(A–C)** and **(G–I)**]; aqua squares and line=permanent with fish; gold diamonds and line=seasonal) based on modeled relationships with climate variables and random annual variation in colonization and extirpation probabilities in Yosemite National Park, California, United States, 2007–2021. Points represent posterior medians; error bars represent 95% equal-tailed intervals. The gray horizontal dot-dash line at 1.0 in panels **(B,E,H)** indicates stable occupancy.

sierran treefrogs (Knapp and Matthews, 2000; Matthews et al., 2001; Knapp, 2005). The negative effect of fish on reproduction was especially strong for Sierra Nevada yellow-legged frogs, which were 15 (5–71) times more likely to reproduce in permanent waterbodies without fish than those with fish. The negative effect of fish on these frogs is therefore evident for multiple processes and life stages, including the initial occupancy and colonization of adult life stages and the probability that adults will reproduce at the few sites where they co-occur with fish.

Annual probability of reproduction was more variable than adult occupancy, especially for Yosemite toads. Nonetheless, the probability of reproduction remained relatively stable when compared to the high variability in weather variables affecting Yosemite toad and Sierra Nevada yellow-legged frog reproduction. For Sierra Nevada yellow-legged frogs, annual probability of reproduction in permanent waterbodies without fish was remarkably stable. Two main mechanisms likely lead to this stability. First, the alpine lakes in which Sierra Nevada yellow-legged frogs typically breed are permanent and contain water in all years. Second, because Sierra Nevada yellow-legged frog tadpoles overwinter (Fellers et al., 2013), more than one cohort is typically available to be observed. As long as sites maintain water, therefore, observation of pre-metamorphic life stages integrates conditions for up to 3 years. Annual reproduction of Yosemite toads, on the other hand, was more variable. This annual variability was likely caused by the greater response of seasonal wetlands than permanent waterbodies to climatic variation (Moss et al., 2021). In particular, April SWE was highly variable among years and affected the probability of Yosemite toad reproduction in both permanent and seasonal sites. Additional variation might be caused by female toads skipping breeding in some years (Morton and Pereyra, 2010), as occurs with high elevation populations of the related boreal toad (Muths et al., 2010). Sierran treefrogs reproduced with high probability in all site types, regardless of weather conditions. The apparent exception in 2012 was likely caused by aberrant timing of surveys (i.e., after eggs had hatched and before tadpoles had matured enough to be easily sampled in a dip net). Although our model structure accounted for annual variation in larval detection probabilities, the nearly universally high detection probability of sierran treefrog tadpoles resulted in what we suspect is an artificially low probability of reproduction (and high probability of detection) when the timing of surveys relative to tadpole development was mismatched.

Initial occurrence probabilities largely agreed with past research on these species. For example, a positive relationship between site area and occupancy is generally expected across

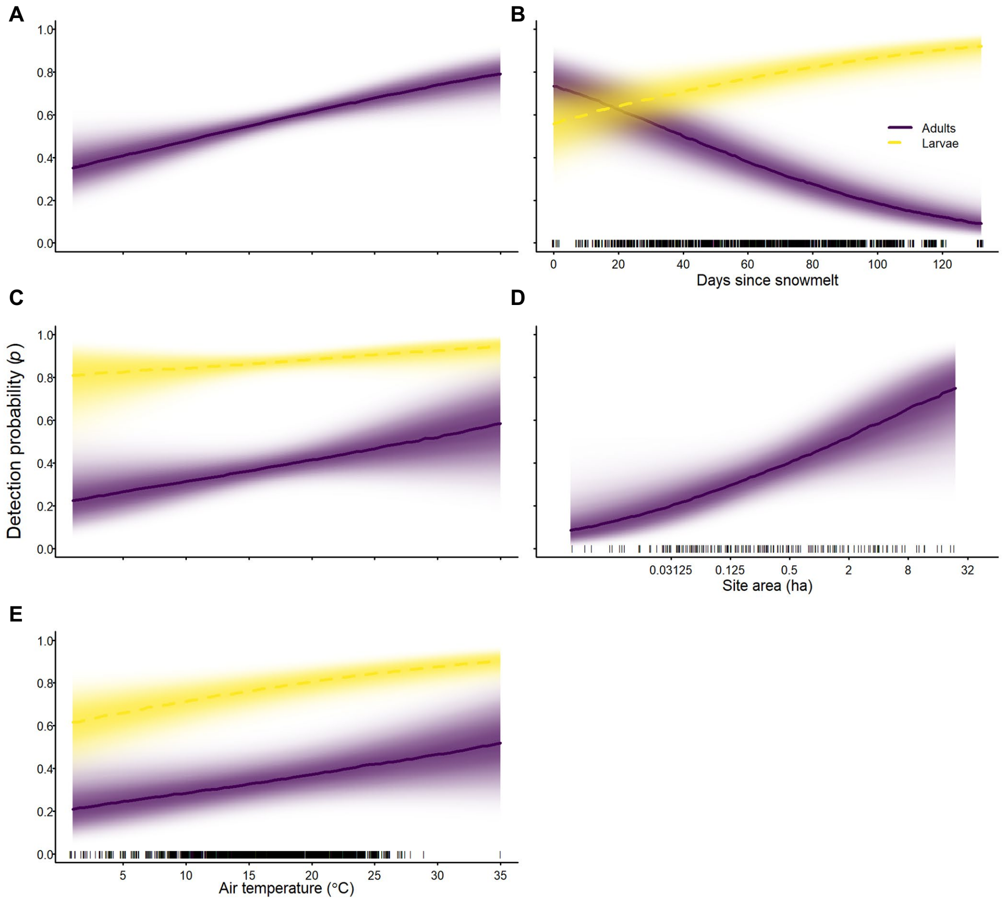

FIGURE 10
Probability of detection of Sierra Nevada yellow-legged frogs [*Rana sierrae*; **(A)**], Yosemite toads [*Anaxyrus canorus*; **(C)**], and sierran treefrogs [*Pseudacris sierra*; **(B,D,E)**] in relation to air temperature **(A,C,E)**, days since snowmelt **(B)**, site area **(D)**, and life stage [adults (indigo solid lines and shading), larvae (gold dashed lines and shading)] in Yosemite National Park, California, United States, 2007–2021. Lines represent posterior modes; intensity of shading represents the posterior probability density.

taxa (Gleason, 1922; Storch et al., 2005). A negative relationship between the occurrence of introduced fish and many anurans also is well-documented (Knapp and Matthews, 2000; Matthews et al., 2001; Knapp, 2005; Fellers et al., 2015). We did not evaluate the influence of introduced fish on Yosemite toads because past research does not suggest that toads are affected negatively by fish, and laboratory trials suggest that Yosemite toad larvae are unpalatable to trout, the dominant introduced fish in the Sierra Nevada (Knapp, 2005; Grasso et al., 2010; Fellers et al., 2015). The peak in initial occurrence for Sierra Nevada yellow-legged frogs near 2,700 m elevation and the corresponding trough for Yosemite toads at the same elevation might be an artifact of the composition of sites in our selected watersheds. A relatively high proportion of sites at the lowest and highest elevation watersheds we sampled were meadows, whereas lakes, ponds, and streams dominated mid-elevation sites. Therefore, the relationship between elevation and initial probability of occurrence for these species might be indicative of this artifact rather than representing larger patterns throughout the ranges of these species (Knapp, 2005).

Occurrence is a blunt instrument for evaluating effects of any variable on the status or trends of populations. Demographic changes leading to changes in abundance might be masked by using occupancy as the response variable of interest, and populations often decline substantially in abundance before becoming extirpated. Another limitation of our study was that we visited each site once when we expected that larval anurans would be present. Therefore, our measure of reproduction at each site did not indicate whether larvae successfully underwent metamorphosis and recruited into the subadult population. Additional follow-up visits to evaluate successful recruitment following reproduction would have limited the number of sites visited each year. Our measures of adult occupancy and probability of reproduction are nonetheless valuable for the long time series and large spatial extent.

Although our study found that amphibian occurrence and reproduction were robust to recent variability in water availability, as the climate becomes more variable in the Sierra Nevada (Swain et al., 2018), the life history strategies that amphibians have evolved over millennia might be inadequate to ensure the persistence of these species. For example, the reliance of Sierra Nevada yellow-legged frogs on permanent fishless waterbodies places them at risk of extirpation if sites shift from permanent lakes and streams to semi-permanent or seasonal wetlands. For a species that has already been extirpated from many historical sites, further extirpations could be costly. Limiting other stressors, such as removing invasive fish from permanent lakes and streams, would help to increase colonization probabilities and maintain the connectivity necessary for functioning Sierra Nevada yellow-legged frog metapopulations and foster resilience to climate change (Knapp et al., 2003, 2007). Yosemite toads are likely susceptible to further increases in the variability of precipitation in the Sierra Nevada as well. Although these toads are adapted to periodic, perhaps even frequent, recruitment failure (Morton and Pereyra, 2010; Liang et al., 2017; Sadinski et al., 2020), it is unclear whether the longevity of adult toads will enable persistence of the toads through megadroughts or severe winters associated with megafloods (Ault et al., 2016; Huang and Swain, 2022). A better understanding of the demography of Yosemite toads, especially the relationship between weather variables and adult survival and recruitment, would be necessary to evaluate the probability of this species persisting in a changing climate.

The occurrence of anurans in Yosemite has so far been resilient to recent extreme climatic events. Despite the influences of weather on adult occupancy dynamics and probability of reproduction, the occurrence of anurans in Yosemite has remained stable over the past 15 years. As the climate continues to change, changes to the hydrology of breeding sites and ecological communities might result in changes to the distribution and occurrence of anurans in the Sierra Nevada. Our study provides insight into the mechanisms exacerbating extirpations and facilitating colonization and reproduction of native anurans in the Sierra Nevada to inform conservation and management of these species.

Data availability statement

Data presented in the study are deposited in ScienceBase and are accessible at https://doi.org/10.5066/P9X6SKT8 (Kleeman et al., 2022). Code used to analyze the data are deposited on GitLab and is accessible at https://doi.org/10.5066/P9VR4SH3 (Halstead et al., 2022).

Ethics statement

The animal study was reviewed and approved by USGS Western Ecological Research Center Animal Care and Use Committee (protocol WERC-2014-01).

Author contributions

BH: conceptualization, methodology, formal analysis, investigation, writing–original draft, writing–review and editing, visualization, and supervision. PK: conceptualization, methodology, data curation, writing–review and editing, and supervision. JR: conceptualization, writing–review and editing, and visualization. GF: conceptualization, methodology, investigation, supervision, and project administration. All authors contributed to the article and approved the submitted version.

Funding

This project was funded by the U.S. Geological Survey (USGS) Ecosystems Mission Area through the USGS Amphibian Research and Monitoring Initiative (ARMI).

Acknowledgments

We thank the numerous technicians that contributed to this project, including Isaac Chellman, Kathryn Cooney, Jennifer Dhundale, David Dimitrie, Sara Dykman, Devon Edmonds, Emmy Johnson, Jane Lester, Patrick Lien, Mike McDonald, Britt Ousterhout, Anjana Parandhaman, John Romansic, Kelsey Ruehling, Heyo Tjarks, Andy Valencia, Liz Williams, and JP Zegarra. Surveys were conducted under U.S. Fish and Wildlife Service Permit TE-844852 and Yosemite National Park annual permits for Study ID 00544, and followed IACUC protocol WERC-2014-01. This work is publication 859 of the USGS ARMI. Any use of trade, product, or firm names is for descriptive purposes only and does not imply endorsement by the U.S. Government.

Conflict of interest

The authors declare that the research was conducted in the absence of any commercial or financial relationships that could be construed as a potential conflict of interest.

Publisher's note

References

Ault, T. R., Mankin, J. S., Cook, B. I., and Smerdon, J. E. (2016). Relative impacts of mitigation, temperature, and precipitation on 21st-century megadrought risk in the American southwest. *Sci. Adv.* 2:e1600873. doi: 10.1126/sciadv.1600873

Baldwin, R. F., Calhoun, A. J. K., and Demaynadier, P. G. (2006). Conservation planning for amphibian species with complex habitat requirements: a case study using movements and habitat selection of the wood frog Rana sylvatica. *J. Herpetol.* 40, 442–453. doi: 10.1670/0022-1511(2006)40[442:CPFASW]2.0.CO;2

Bales, R. C., Molotch, N. P., Painter, T. H., Dettinger, M. D., Rice, R., and Dozier, J. (2006). Mountain hydrology of the western United States. *Water Resour. Res.* 42, 1–13. doi: 10.1029/2005WR004387

Bartelt, P. E., Peterson, C. R., and Klaver, R. W. (2004). Sexual differences in the post-breeding movements and habitats selected by Western toads (Bufo boreas) in southeastern Idaho. *Herpetologica* 60, 455–467. doi: 10.1655/01-50

Berlow, E. L., Knapp, R. A., Ostoja, S. M., Williams, R. J., McKenny, H., Matchett, J. R., et al. (2013). A network extension of species occupancy models in a patchy environment applied to the Yosemite toad (*Anaxyrus canorus*). *PLoS One* 8:e72200. doi: 10.1371/journal.pone.0072200

Briggs, C. J., Vredenburg, V. T., Knapp, R. A., and Rachowicz, L. J. (2005). Investigating the population-level effects of chytridiomycosis: an emerging infectuous disease of amphibians. *Ecology* 86, 3149–3159. doi: 10.1890/04-1428

Crockett, J. G., Bailey, L. L., and Muths, E. (2020). Highly variable rates of survival to metamorphosis in wild boreal toads (*Anaxyrus boreas boreas*). *Popul. Ecol.* 62, 258–268. doi: 10.1002/1438-390X.12044

Crump, M. L., and Scott, N. J. J. (1994). "Visual encounter surveys" in *Measuring and Monitoring Biological Diversity: Standard Methods for Amphibians*. eds. W. R. Heyer, M. A. Donnelly, R. W. McDiarmid, L.-A. C. Hayek and M. S. Foster (Washington and London: Smithsonian Institution Press), 84–92.

Dallalio, E. A., Brand, A. B., and Grant, E. H. C. (2017). Climate-mediated competition in a high-elevation salamander community. *J. Herpetol.* 51, 190–196. doi: 10.1670/15-157

de Valpine, P., Paciorek, C., Turek, D., Michaud, N., Anderson-Bergman, C., Obermeyer, F., et al. (2022). NIMBLE: MCMC, Particle Filtering, and Programmable Hierarchical Modeling. *R package version 0.12.2*. Available at: https://cran.r-project-org/package=nimble doi: 10.5281/zenodo.1211190

Duarte, A., Peterson, J. T., Pearl, C. A., Rowe, J. C., McCreary, B., Galvan, S. K., et al. (2020). Estimation of metademographic rates and landscape connectivity for a conservation-reliant anuran. *Landsc. Ecol.* 35, 1459–1479. doi: 10.1007/s10980-020-01030-8

Ethier, J. P., Fayard, A., Soroye, P., Choi, D., Mazerolle, M. J., and Trudeau, V. L. (2021). Life history traits and reproductive ecology of north American chorus frogs of the genus *Pseudacris* (Hylidae). *Front. Zool.* 18:40. doi: 10.1186/s12983-021-00425-w

Evans, T. G., Diamond, S. E., and Kelly, M. W. (2015). Mechanistic species distribution modelling as a link between physiology and conservation. *Conserv. Physiol.* 3, 1–16. doi: 10.1093/conphys/cov056

Fellers, G. M., Kleeman, P. M., and Miller, D. A. W. (2015). Wetland occupancy of pond-breeding amphibians in Yosemite National Park, USA. *J. North Am. Herpetol.* 2015, 22–33. doi: 10.17161/jnah.vi1.11903

Fellers, G. M., Kleeman, P. M., Miller, D. A. W., Halstead, B. J., and Link, W. A. (2013). Population size, survival, growth, and movements of *Rana sierrae*. *Herpetologica* 69, 147–162. doi: 10.1655/herpetologica-d-12-00045

Gelman, A., and Rubin, D. B. (1992). Inference from iterative simulation using multiple sequences. *Stat. Sci.* 7, 457–472. doi: 10.1214/ss/1177011136

Gleason, H. A. (1922). On the relation between species and area. *Ecology* 3, 158–162. doi: 10.2307/1929150

Grasso, R. L., Coleman, R. M., and Davidson, C. (2010). Palatability and antipredator response of Yosemite toads (*Anaxyrus canorus*) to nonnative brook trout (*Salvelinus fontinalis*) in the Sierra Nevada Mountains of California. *Copeia* 2010, 457–462. doi: 10.1643/ch-09-033

Halstead, B. J., Kleeman, P. M., Rose, J. P., and Fellers, G. M. (2022). "Code to Analyze Multi-State, Multi-Scale Dynamic Occupancy Models for Amphibians in Yosemite National Park," in *U.S. Geological Survey Code Release*. doi: 10.5066/P9VR4SH3

Halstead, B. J., Rose, J. P., and Kleeman, P. M. (2021). Time-to-detection occupancy methods: performance and utility for improving efficiency of surveys. *Ecol. Appl.* 31:e02267. doi: 10.1002/eap.2267

Huang, X., and Swain, D. L. (2022). Climate change is increasing the risk of a California megaflood. *Sci. Adv.* 8:eabq0995. doi: 10.1126/sciadv.abq0995

Kagarise Sherman, C., and Morton, M. L. (1993). Population declines of Yosemite toads in the eastern Sierra Nevada of California. *J. Herpetol.* 27, 186–198. doi: 10.2307/1564935

Kleeman, P. M., Halstead, B. J., Rose, J. P., and Fellers, G. M. (2022). "Multi-state occurrence data and predictors for amphibians in Yosemite National Park, 2007–2021," in *U.S. Geological Survey Data Release*. doi: 10.5066/P9X6SKT8

Knapp, R. A. (2005). Effects of nonnative fish and habitat characteristics on lentic herpetofauna in Yosemite National Park, USA. *Biol. Conserv.* 121, 265–279. doi: 10.1016/j.biocon.2004.05.003

Knapp, R. A., Boiano, D. M., and Vredenburg, V. T. (2007). Removal of nonnative fish results in population expansion of a declining amphibian (mountain yellow-legged frog, *Rana muscosa*). *Biol. Conserv.* 135, 11–20. doi: 10.1016/j.biocon.2006.09.013

Knapp, R. A., and Matthews, K. R. (2000). Non-native fish introductions and the decline of the mountain yellow-legged frog from within protected areas. *Conserv. Biol.* 14, 428–438. doi: 10.1046/j.1523-1739.2000.99099.x

Knapp, R. A., Matthews, K. R., Preisler, H. K., and Jellison, R. (2003). Developing probabilistic models to predict amphibian site occupancy in a patchy landscape. *Ecol. Appl.* 13, 1069–1082. doi: 10.1890/1051-0761(2003)13[1069,DPMTPA]2.0.CO;2

Knapp, R. A., Pavelka, C., Hegeman, E. E., and Smith, T. C. (2020). The Sierra Lakes inventory project: non-native fish and community composition of lakes and ponds in the Sierra Nevada, California version 2. *Environ. Data Initiative*. doi: 10.6073/pasta/d835832d7fd00d9e4466e44eea87fab3

Liang, C. T. (2013). Movements and habitat use of Yosemite toads (*Anaxyrus* (formerly *Bufo*) *canorus*) in the sierra National Forest, California. *J. Herpetol.* 47, 555–564. doi: 10.1670/12-054

Liang, C. T., Grasso, R. L., Nelson-Paul, J. J., Vincent, K. E., and Lind, A. J. (2017). Fine-scale habitat characteristics related to occupancy of the Yosemite toad, *Anaxyrus canorus*. *Copeia* 105, 120–127. doi: 10.1643/ch-15-290

Lindauer, A. L., and Voyles, J. (2019). Out of the frying pan, into the fire? Yosemite toad (*Anaxyrus canorus*) susceptibility to *Batrachochytrium dendobatidis* after development under drying conditions. *Herpetol. Conserv. Biol.* 14, 185–198.

Matthews, K. R., Pope, K. L., Preisler, H. K., and Knapp, R. A. (2001). Effects of nonnative trout on Pacific treefrogs (*Hyla regilla*) in the Sierra Nevada. *Copeia* 2001, 1130–1137. doi: 10.1643/0045-8511(2001)001[1130:eontop]2.0.co;2

Menéndez, R., Megías, A. G., Hill, J. K., Braschler, B., Willis, S. G., Collingham, Y., et al. (2006). Species richness changes lag behind climate change. *Proc. R. Soc. B Biol. Sci.* 273, 1465–1470. doi: 10.1098/rspb.2006.3484

Merkle, J. A., Abrahms, B., Armstrong, J. B., Sawyer, H., Costa, D. P., and Chalfoun, A. D. (2022). Site fidelity as a maladaptive behavior in the Anthropocene. *Front. Ecol. Environ.* 20, 187–194. doi: 10.1002/fee.2456

Morton, M. L., and Pereyra, M. E. (2010). Habitat use by Yosemite toads: life history traits and implications for conservation. *Herpetol. Conserv. Biol.* 5, 388–394.

Moss, W. E., McDevitt-Galles, T., Muths, E., Bobzien, S., Purificato, J., and Johnson, P. T. J. (2021). Resilience of native amphibian communities following catastrophic drought: evidence from a decade of regional-scale monitoring. *Biol. Conserv.* 263:109352. doi: 10.1016/j.biocon.2021.109352

Mullaly, D. P. (1953). Observations on the ecology of the toad *Bufo canorus*. *Copeia* 1953, 182–183. doi: 10.2307/1439932

Muths, E., Scherer, R. D., and Lambert, B. A. (2010). Unbiased survival estimates and evidence for skipped breeding opportunities in females. *Methods Ecol. Evol.* 1, 123–130. doi: 10.1111/j.2041-210x.2010.00019.x

R Core Team (2022). *R: A Language and Environment for Statistical Computing*. Vienna, Austria: R Foundation for Statistical Computing.

Rose, J. P., Kleeman, P. M., and Halstead, B. J. (2022). Hot, wet and rare: modelling the occupancy dynamics of the narrowly distributed Dixie Valley toad. *Wildl. Res.* (in press). doi: 10.1071/WR22029

Sadinski, W., Gallant, A. L., and Cleaver, J. E. (2020). Climate's cascading effects on disease, predation, and hatching success in *Anaxyrus canorus*, the threatened Yosemite toad. *Glob. Ecol. Conserv.* 23:e01173. doi: 10.1016/j.gecco.2020.e01173

Schmetterling, D. A., and Young, M. K. (2008). Summer movements of boreal toads (*Bufo boreas boreas*) in two western Montana basins. *J. Herpetol.* 42, 111–123. doi: 10.1670/07-125r1.1

Storch, D., Evans, K. L., and Gaston, K. J. (2005). The species-area-energy relationship. *Ecol. Lett.* 8, 487–492. doi: 10.1111/j.1461-0248.2005.00740.x

Swain, D. L., Langenbrunner, B., Neelin, J. D., and Hall, A. (2018). Increasing precipitation volatility in twenty-first-century California. *Nat. Clim. Chang.* 8, 427–433. doi: 10.1038/s41558-018-0140-y

Thornton, M. M., Shrestha, R., Wei, Y., Thornton, P. E., Kao, S., and Wilson, B. E. (2020). *Daymet: Monthly Climate Summaries on a 1-km Grid for North America, Version 4*. ORNL DAAC, Oak Ridge, TN. (Accessed August 16, 2022).

U.S. Fish and Wildlife Service (2014). Endangered and threatened wildlife and plants; endangered species status for Sierra Nevada yellow-legged frog and northern distinct population segment of the mountain yellow-legged frog, and threatened species status for Yosemite toad. *Fed. Regist.* 79, 24256–24310.

Vose, R. S., Applequist, S., Squires, M., Durre, I., Menne, M. J., Williams, C. N. Jr., et al. (2014). Improved historical temperature and precipitation time series for U.S. climate divisions. *J. Appl. Meteorol. Climatol.* 53, 1232–1251. doi: 10.1175/JAMC-D-13-0248.1

Vredenburg, V. T., Knapp, R. A., Tunstall, T. S., and Briggs, C. J. (2010). Dynamics of an emerging disease drive large-scale amphibian population extinctions. *Proc. Natl. Acad. Sci. U. S. A.* 107, 9689–9694. doi: 10.1073/pnas.0914111107

Williams, A. P., Cook, B. I., and Smerdon, J. E. (2022). Rapid intensification of the emerging southwestern north American megadrought in 2020–2021. *Nat. Clim. Chang.* 12, 232–234. doi: 10.1038/s41558-022-01290-z

frontiers | Frontiers in Ecology and Evolution

TYPE Original Research
PUBLISHED 18 May 2023
DOI 10.3389/fevo.2023.1157700

OPEN ACCESS

EDITED BY
Clare Aslan,
Northern Arizona University, United States

REVIEWED BY
Craig Stephen,
University of Saskatchewan, Canada
Erik Petersson,
Swedish University of Agricultural Sciences,
Sweden

*CORRESPONDENCE
Lizabeth Bowen
✉ lbowen@ucdavis.edu;
✉ lbowen@usgs.gov

RECEIVED 02 February 2023
ACCEPTED 20 April 2023
PUBLISHED 18 May 2023

CITATION
Bowen L, Yee J, Bodkin J, Waters S, Murray M, Coletti H, Ballachey B, Monson D and Miles AK (2023) Gene expression and wildlife health: varied interpretations based on perspective.
Front. Ecol. Evol. 11:1157700.
doi: 10.3389/fevo.2023.1157700

Gene expression and wildlife health: varied interpretations based on perspective

Lizabeth Bowen[1]*, Julie Yee[1], James Bodkin[2], Shannon Waters[1], Michael Murray[3], Heather Coletti[4], Brenda Ballachey[2], Daniel Monson[2] and A. Keith Miles[1]

[1]U.S. Geological Survey, Western Ecological Research Center, Davis, CA, United States, [2]U.S. Geological Survey, Alaska Science Center, Anchorage, AK, United States, [3]Monterey Bay Aquarium, Monterey, CA, United States, [4]National Park Service, Anchorage, AK, United States

We evaluated wildlife population health from the perspective of statistical means vs. variances. We outlined the choices necessary to provide the framework for our study. These consisted of spatial and temporal boundaries (e.g., choice of sentinel species, populations, time frame), measurement techniques (molecular to population level), and appropriate statistical analyses. We chose to assess the health of 19 sea otter populations, located in the north Pacific from the Aleutian Islands, AK, to Santa Barbara, CA, and varying in population growth rates and length of occupancy. Our focal metric was gene expression (i.e., mRNA transcripts) data that we had previously generated across sea otter populations as a measure of population health. We used statistical methods with different approaches (i.e., means vs. variances) and examined the subsequent interpretive outcomes and how these influence our assessment of "health." Interpretations based on analyses using variances versus means overlapped to some degree. In general, sea otter populations with low variation in gene expression were limited by food resources and at or near carrying capacity. In populations where the variation in gene expression was moderate or high, four out of five populations were increasing in abundance, or had been recently increasing. Where we had additional information on sources of stressors at the level of the population, we were able to draw inferences from those stressors to specific gene expression results. For example, gene expression patterns of sea otters from Western Prince William Sound were consistent with long term exposure to petroleum hydrocarbons, whereas in Kachemak Bay, patterns were consistent with exposure to algal toxins. Ultimately, determination of population or ecosystem health will be most informative when multiple metrics are examined across disciplines in the context of specific scenarios and goals.

KEYWORDS

gene expression, sea otter, variability, wildlife health, stressor

1. Introduction

Marine habitats worldwide are facing unprecedented challenges due to expanded industrial development and associated contaminants (Álvarez-Muñoz et al., 2016), resource extraction (Pauly et al., 1998; Herbert-Read et al., 2022), and climate change (IPCC, 2022), all of which have the potential to substantially degrade and alter biological resources in coastal ecosystems. Additional consequences of climate change include modifications of hydrological processes that can transport pathogens, pollutants, nutrients, and sediments across watersheds that ultimately deposit into estuarine and nearshore marine environments with potentially adverse biological effects. While our understanding of physical processes resulting from climate change, such as sea level rise and ocean acidification, is advancing due to accumulating data and refined models, the implications for biological systems are only beginning to be explored. In recent decades, much effort has been expended on monitoring the health and productivity of nearshore ecosystems, with focused studies targeting species of economic, social, and ecologic importance (Harley et al., 2006; Halpern et al., 2015; Bowen et al., 2020a). As such, there is increased understanding of the interdependence of health across wildlife, ecosystems, and humans.

A definition of health specific to wildlife and ecosystems is provided by Hanisch et al. (2012): "Wildlife health is a multidisciplinary concept and is concerned with multiple stressors that affect wildlife. Wildlife health can be applied to individuals, populations, and ecosystems, but its most important defining characteristics are whether a population can respond appropriately to stresses and sustain itself." As such, the term "health" may be used to indicate resilience that reflects the capacity of a population or ecosystem to cope with and respond to natural and anthropogenic challenges. This definition of health includes and embraces the dynamic nature of wildlife populations and allows for assessment of change within the boundaries of resilience and outside those boundaries in the realm of catastrophic failure.

How does wildlife population health translate into ecosystem health? Ecosystems are certainly affected if physiological or ecological functions of a significant number of individuals, or species, are altered (Khalid et al., 2021). According to Rapport (2007), the focus of ecosystem health practice is twofold: (1) to "diagnose," through indicators, situations in which ecosystem function (and structure) have become compromised, owing to anthropogenic stress or other causes; and (2) to devise diagnostic protocols to assess the causes of dysfunction and propose interventions that may restore ecosystem health. Improved knowledge of the health status of a population or ecosystem considered vulnerable or at-risk provides valuable information for wildlife management, conservation assessments, and decision making (Blanchong et al., 2016; Campbell et al., 2018; DeCandia et al., 2018).

The concept of sentinel species used as proxies for the measurement of ecosystem health has widely been accepted (Fossi and Panti, 2017), with different sentinels perhaps providing distinct measurements and interpretations of ecosystem health. Using "keystone species," i.e., those that have a disproportionate effect on the organization and function of ecosystems (Paine, 1966; Power et al., 1996), as sentinels provides another approach to translating individual or population health to ecosystem health. A well-known example of a keystone species is the sea otter (*Enhydra lutris*), which was extirpated across most of its range in the north Pacific due to intensive hunting. Following protection, sea otters rebounded in many areas, allowing for studies comparing nearshore communities in coastal ecosystems in the presence and absence of sea otters. A common finding was that in the presence of sea otters, the relative abundance of kelp increased, and herbivorous sea urchins, on which the otters preyed, declined (Kenyon, 1969; Estes and Palmisano, 1974; Estes and Duggins, 1995). Worldwide, kelp forest communities support higher biodiversity and biomass than urchin barrens and are indicative of a healthy coastal ecosystem (Mann, 1973; Harold and Reed, 1985).

Wildlife health currently may be measured using a variety of tools, from the cellular and molecular to the population levels. Traditional evaluation of the health status of wildlife generally has been based on a combination of population history (e.g., trends in abundance, movement, diet, reproductive and survival rates), physical examinations of individuals, and clinical pathology data. Many studies focusing on sensitive populations are disease-centric; however, infectious diseases occur in all ecosystems, both healthy and unhealthy, and play an important role in structuring biological communities (Tracy et al., 2019). Although the exact cause(s) of species declines frequently is unknown, declines are often associated with multiple and potentially synergistic environmental stressors (Tinker et al., 2021; Tyack et al., 2022).

Health assessments of individuals and populations at the molecular level are rapidly increasing (Snape et al., 2004; Trego et al., 2019). Gene-based health diagnostics provide an opportunity for an alternate, whole-system or holistic assessment of health not only in individuals or populations but potentially in ecosystems (Bowen et al., 2012). Gene expression is physiologically driven by intrinsic and extrinsic stimuli including toxins, pathogens, contaminants, trauma, or nutrition. As key indicators of pathophysiologic status, the earliest observable signs of health impairment are altered levels of gene transcripts, evident prior to clinical manifestation (McLoughlin et al., 2006), thus providing an early warning of potentially compromised health of individuals, populations, and ecosystems (Bowen et al., 2020b). Broad-scale identification of gene expression patterns can provide mechanistic understanding as a proxy for health (Pedersen and Babayan, 2011; Portnoy et al., 2020) that can then be extrapolated to populations. Identifying causal links between exposure to stressors and gene transcript patterns, and then from individual responses to change in population abundance, provides a link between perturbation at the individual level to shifts in structure at the population level and possibly function at the ecosystem level.

We now have a working definition of health (Hanisch et al. 2012), a technique for measurement of health at the individual and population levels, and a conceptual link for extension of the concept of health to the ecosystem level. Essentially, we have the picture but not the perspective. The perspective can dramatically influence our interpretation, and consequently, the management decisions and actions that may be recommended. When we are assigning a level of health to a population or an ecosystem, we must ask the question - in relation to what? Often in ecology, comparisons are made to a standard or baseline from which a relative identifier can be assigned (e.g., this population is unhealthy relative to our baseline population). Especially in wildlife biology and ecology, absence of reliable baseline data presents a challenge when trying to quantify health, and changes in health, in an era of rapid global change (Tracy et al., 2019). Additionally, acceptance of presumed baseline conditions can be problematic, given that nearly all systems are non-stationary and baselines can be variable or shift over time (Klein and Thurstan, 2016). Other aspects of perspective that could be considered are: temporal (do we have a time series of data on a single population or ecosystem in the absence of a known baseline?); spatial (what are the levels of separation or interactions between the populations we are comparing?) and inclusivity (can we identify all factors that define separate populations, and can we sample those in ways to justify inferences?).

As we are discussing stressors and organisms' transcriptional responses to these stressors, we must also consider how the response that we are using for our determination of health may vary over time. For example, when exposed to a stressor, an animal may have a non-linear transcriptional response (Androulakis et al., 2007; Jo et al., 2021), and therefore, we need to understand at which point in the curve have we sampled, as it may greatly influence our interpretation. Finally, is the response "healthy" in that it allows continued normal existence, or does it indicate a shift from equilibrium that may be deleterious for the population?

1.1. Objectives

This represents a case study on populations of sea otters throughout their range. We have utilized gene expression as a tool to enhance our understanding of how environmental conditions and stressors may be linked to the health of sea otters in studies on populations ranging from Southern California to the Aleutian Islands in Alaska (Table 1; Miles et al., 2012; Bowen et al., 2015, 2016; Tinker et al., 2021). Notable stressors suggested by our findings include nutritional stress at Adak and Western Prince William Sound (2010–2012), hydrocarbons in Western Prince William Sound (2006–2008), hydrocarbons or dioxin-like substances in Kodiak, wildfire contaminants in Big Sur, and algal toxins in Kachemak Bay (Bowen et al., 2015, 2016, 2022). In this study, our objective was to compare the interpretive outcomes of statistical approaches (i.e., means vs. variances) to analyze gene expression data previously generated across sea otter populations that vary in several metrics such as population abundance and energy intake rates. These data (19 populations) have not been previously analyzed together.

2. Materials and methods

2.1. Study area

The 19 sea otter populations we have chosen to include in this study are located from near Santa Barbara, California, north to Prince William Sound (WPWS), Alaska and west to Adak, Alaska (ADAK) (Figure 1; Table 1). Our "reference" (REF) group of sea otters were under permanent human care and were sampled from aquaria within the United States and Canada (Bowen et al., 2012). Each reference sea otter was classified as "clinically normal" by associated veterinarians. Although stress is inherent in life under permanent human care for wildlife species, environmental stressors are thought to be minimized in an aquarium setting. Additionally, gene expression levels in reference sea otters were not statistically different from gene expression levels in free-ranging sea otters inhabiting an area with minimal environmental stressors (Alaska Peninsula) (Bowen et al., 2016). In CA, the current range of the sea otter extends from near Los Angeles in the south to near San Francisco in the north, areas of relatively high human impacts. However, the range includes some coastline along the Big Sur coast, in Central CA, where human densities are low, and the watersheds are protected to some extent by governmental resource agencies. The sea otter populations occurring in Washington state (WASH1 & 2), British Columbia (CLAY, NUCH), and Southeast Alaska (ELFI, WHAL) resulted from reintroductions in the 1960's and 1970's to restore the species (Jameson et al., 1982). Sea otters in south-central and south-west Alaska (WPWS1 & 2, KBAY, KATM, KOD, APEN, ADAK) are the descendants of remnant populations that survived near those locations. Human densities along the north Pacific coastline generally decline from south to north, and given the areas in which our study animals were sampled, we expect that human degradation of watersheds likely diminish along this gradient. Within each distinct sea otter population, the full range of nearshore habitats are occupied, including sandy shorelines, protected soft sediment bays and estuaries, and exposed rocky shorelines.

Sea otters were captured using Wilson traps (Wendell et al., 1996) or tangle nets and brought immediately to a shipboard or shore station for processing. All sea otters were anesthetized with fentanyl citrate and midazolam hydrochloride (Monson et al., 2001; Murray, 2015) prior to processing. Nearly all the animals (exception AK Pen) were captured with the Wilson trap that targeted resting groups of animals without knowledge of age or sex. At the Alaska Peninsula site, sea otters were captured using tangle nets that targeted active animals, also without regard to age or sex. Because the true age and sex composition could not be determined for each population, we were unable to evaluate the composition of the sampled population relative to the entire population. However, as the capture methods were not known to be biased toward age or sex, we concluded that the captured individuals were representative of the population being sampled.

2.2. Blood collection and RNA extraction

A 2.5 ml sample from each sea otter was drawn directly into a PAXgene blood RNA collection tube (PreAnalytiX, Zurich, Switzerland) from either the jugular or popliteal veins and then frozen at −80°C until extraction of RNA (Bowen et al., 2012). The RNA from blood in PAXgene tubes was isolated according to manufacturer's standard protocols, which included an on-column DNase treatment to remove contaminating gDNA (silica-based microspin technology), and the extracted RNA stored at −80°C until analysis. We measured the concentration and clarity on a Qubit 3.0 Fluorometer using the RNA, DNA and RNA IQ Assay Kits (Life Technologies, Carlsbad, CA, USA).

2.3. cDNA synthesis

A standard cDNA synthesis was performed on 2 ug of RNA template from each animal. Reaction conditions included 4 units reverse transcriptase (Omniscript®, Qiagen, Valencia, CA), 1 μM random hexamers, 0.5 mM each dNTP, and 10 units RNase inhibitor, in RT buffer (Qiagen, Valencia, CA). Reactions were incubated for 60 min at 37°C, followed by an enzyme inactivation step of 5 min at 93°C, and then stored at −20°C until further analysis.

2.4. Real-time PCR

The 13 genes chosen for the expression profile analysis represent multiple physiological systems that play roles in immuno-modulation, inflammation, cell protection, tumor suppression, cellular stress-response, xenobiotic metabolizing enzymes and antioxidant enzymes

TABLE 1 Population locations, number of samples, sex, age class, and sampling year.

						Sex		Age class				
	Location code	Location	Region	Ocean current	N	M	F	Pup	Juvenile	Adult	Aged adult	Year(s) sampled
1	WPWS1	Western Prince William Sound1	Gulf of AK	Alaska Coastal Current	80	20	60	3	13	49	15	2006–8
2	WPWS2	Western Prince William Sound2	Gulf of AK	Alaska Coastal Current	88	19	69	9	6	53	20	2008–10
3	KBAY	Kachemak Bay	Gulf of AK	Alaska Coastal Current	20	0	20	0	0	10	10	2019
4	KATM	Katmai	Aleutian/AK Peninsula	Alaska Coastal Current	30	12	18	2	4	24	0	2009
5	KOD	Kodiak	Gulf of AK	Alaska Coastal Current	25	9	16	0	2	23	0	2005
6	APEN	Alaska Peninsula	Aleutian/AK Peninsula	Alaska Coastal Current	27	14	13	0	8	19	0	2009
7	ELFI	Elfin Cove	SE Alaska	Alaska Coastal Current	30	6	24	3	3	21	3	2011
8	WHAL	Whale Bay	SE Alaska	Alaska Coastal Current	29	6	23	1	1	22	5	2011
9	ADAK	Adak Island/ Clam Lagoon	Aleutian/AK Peninsula	Alaska Coastal Current	24	12	12	0	17	4	3	2012
10	NUCH	Nuchatlitz	BC/WA	Bifurcation	29	12	17	0	1	21	7	2010
11	CLAY	Clayoquot Sound	BC/WA	Bifurcation	25	9	16	0	4	18	3	2010–11
12	WASH1	Washington1	BC/WA	Bifurcation	16	10	6	0	0	11	5	2011
13	WASH2	Washington2	BC/WA	Bifurcation	14	1	13	0	0	12	2	2011
14	ES	Elkhorn Slough	CA	California Current	23	8	15	2	2	19	0	2013
15	MONT	Monterey	CA	California Current	27	6	21	0	2	17	8	2009/10/13
16	BIGS	Big Sur	CA	California Current	50	13	37	0	5	34	11	2008–10
17	DC	Diablo Canyon	CA	California Current	55	10	45	0	10	42	3	2012
18	SB	Santa Barbara	CA	California Current	41	21	20	2	3	36	0	2012/13
19	REF	Reference	Under Permanent Human Care	Under Permanent Human Care	17	7	10	0	3	6	8	2008–10

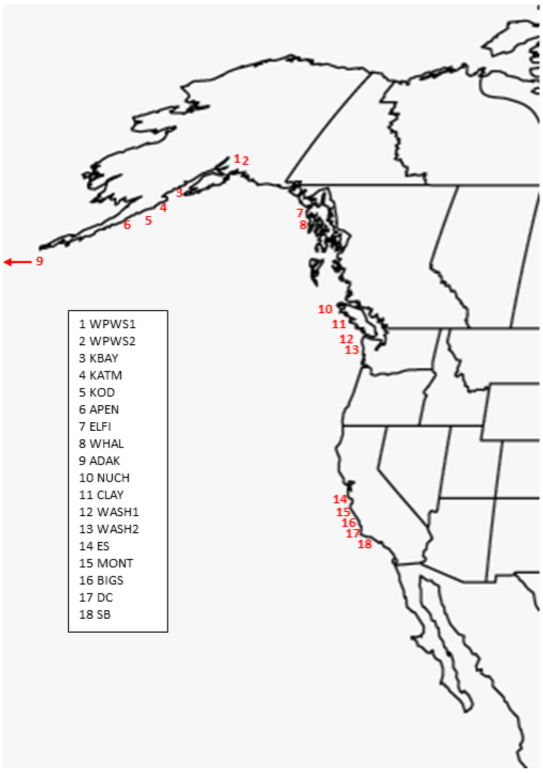

FIGURE 1
Population locations of sea otters included in the analysis. Locations numbered from North to South (Table 1). Captive otters (*N*=17) not shown (see Bowen et al., 2012 for details).

(Table 2). These genes can be modified by biological, physical, or anthropogenic impacts and consequently can provide information on the general type of stressors present in a given environment.

Real-time PCR systems for the individual, sea otter-specific reference or housekeeping gene (S9) and genes of interest were run in separate wells (see Supplementary Table S1 for primer sequences). Briefly, 1 μL of cDNA was added to a mix containing 12.5 μL of Quanti-Tect SYBR Green Master Mix [5 mM Mg2+] (Qiagen, Valencia, CA), 0.5 μL each of forward and reverse sequence specific primers, and 10.0 μL of RNase-free water; total reaction mixture was 25 μL. The reaction mixture cDNA samples for each gene of interest and the S9 gene were loaded into 96 well plates in duplicate and sealed with optical sealing tape (Applied Biosystems, Foster City, CA). Reaction mixtures containing water, but no cDNA, were used as negative controls; thus approximately 3–4 individual sea otter samples were run per plate.

Amplifications were conducted on a Step-One Plus Real-time Thermal Cycler (Applied Biosystems, Foster City, CA). Reaction conditions were as follows: 50°C for 2 min, 95°C for 15 min, 40 cycles of 94°C for 30 s, 60°C for 30 s, 72°C for 31 s, and an extended elongation phase at 72°C for 10 min. Reaction specificity was monitored by melting curve analysis using a final data acquisition phase of 60 cycles of 65°C for 30 s and verified by direct sequencing of randomly selected amplicons. Cycle threshold crossing values (C_T) for each of the genes of interest were normalized to the S9 housekeeping gene.

2.5. Statistical analysis

We used statistical methods with different approaches to examine the interpretive outcomes of different statistical perspectives and how these influence our assessment of "health." Traditionally, gene expression data are presented as C_T (Threshold crossing) values. According to the ΔC_T method (Livak and Schmittgen, 2001), we normalized values (internal reference gene C_T subtracted from the gene of interest C_T). Often, $\Delta\Delta C_T$ (Livak and Schmittgen, 2001) is used; in that case the normalized value of the target gene is compared with the C_T of a calibrator sample (reference population). In some instances, $\Delta\Delta C_T$ values are then transformed. Real-time PCR data are represented as normalized C_T values; the lower the C_T, the higher the quantity of transcripts. We used generalized linear multivariate models (GLMV) to visually describe gene transcript profiles by location (Figure 2) [Note: KOD was included in the GLMV analysis but not in further analyses, because at the time of sampling and analysis for KOD, three genes were yet to be included in the expression panel (CCR3, HTT5, CaM)].We then evaluated the association between gene transcription levels and location with redundancy analysis (RDA) (Figure 3; Legendre and Legendre, 2012). Redundancy analysis allows the analysis of multiple response variables (in this case the 13 genes in our transcript panel) by combining multiple regression and principal components analysis (PCA). Two types of ordination scores are derived in an RDA (Legendre and Legendre, 2012): (1) those quantifying relationships between response and predictor variables (linear combinations of predictor variables, i.e., the multiple regression component); and (2) those that quantify the associations between response variables and sampling units (weighted sampling unit scores, i.e., the PCA component). Our sampling units comprised 625 sea otters separated into 18 groups based on location (Table 1). We evaluated significance of the overall ordination with Monte Carlo tests (*N* = 999; Legendre and Legendre, 2012). We conditioned the Monte Carlo simulations on location, which we specified as a random effect in the RDA.

Subsequent to RDA, and in order to illustrate within population differences, we used gene profiling based on per gene and per otter response correlation for the Kachemak Bay (KBAY) otters, using normalized qPCR data obtained from each individual otter, which were subjected to hierarchical clustering using Genesis software (Genesis, Graz, Switzerland). Average dot product metric, with complete linkage clustering, was used to generate a heatmap profile of gene expression (Figure 4; Connon et al., 2012).

We used a generalized linear latent variable analysis (GLLVA), a key approach for modeling multivariate abundance data, to identify associations between population/location and transcript level (Figure 5; Skrondal and Rabe-Hesketh, 2004). The generalized linear latent variable model (GLLVM) extends the basic generalized linear model to multivariate data using a factor analytic approach, incorporating a small number of latent variables (interpreted as ordination axes) for each site accompanied by factor loadings to model correlations between responses (Niku et al., 2019).

We evaluated homogeneity of the variance–covariance matrices among the groups with a distance-based test (beta dispersion test; Anderson et al., 2006; Figure 6).

All analyses (except the heatmap analysis, Genesis, Graz, Switzerland, Figure 4) were conducted in Program R (R Development

TABLE 2 Thirteen genes selected for sea otter-specific qPCR analytical panel and their functions.

Gene	Gene function
HDC	The HDCMB21P gene codes for a translationally controlled tumor protein (TCTP) implicated in cell growth, cell cycle progression, malignant transformation, tumor progression, and in the protection of cells against various stress conditions and apoptosis (Bommer and Thiele, 2004; Tuynder et al., 2004; Ma et al., 2010). Up-regulation of HDC is indicative of the development or existence of cancer. Environmental triggers may be responsible for population-based, up-regulation of HDC. HDC transcription is known to increase with exposure to carcinogenic compounds such as polycyclic aromatic hydrocarbons (Bowen et al., 2007; Raisuddin et al., 2007; Zheng et al., 2008).
COX2	Cyclooxygenase-2 catalyzes the production of prostaglandins that are responsible for promoting inflammation (Goldsby et al., 2003). Cox2 is responsible for the conversion of arachidonic acid to prostaglandin H2, a lipoprotein critical to the promotion of inflammation (Harris et al., 2002). Up-regulation of Cox2 is indicative of cellular or tissue damage and an associated inflammatory response.
CYT	The complement cytolysis inhibitor protects against cell death (Jenne and Tschopp, 1989). The upregulation of CYT is indicative of cell or tissue death. It is now believed that domoic acid-induced altered Ca2+ homeostasis is key in excitotoxic apoptosis, which is consistent with our finding of significantly higher levels of CYT in KBay otters (Portnoy et al., 2020); increased levels of CYT have also been associated with cardiomyopathy (Oksjoki et al., 2007; Ehrlenbach et al., 2013).
AHR	The arylhydrocarbon receptor responds to classes of environmental toxicants including polycyclic aromatic hydrocarbons, polyhalogenated hydrocarbons, dibenzofurans, and dioxin (Oesch-Bartlomowicz and Oesch, 2005). Depending upon the ligand, AHR signaling can modulate T-regulatory (TREG) (immune-suppressive) or T-helper type 17 (TH17) (pro-inflammatory) immunologic activity (Quintana et al., 2008; Veldhoen et al., 2008. Wang et al., 2009) were the first to identify substantial activation of AHR by domoic acid exposure in fish, a transcriptional response of phase I XME through ligand-activated AHR and ARNT to domoic acid exposure. AHR binds to toxins, initiating a detoxification cascade and an altered immune response. Activation of the AHR pathway also contributes to cardiac malformation (Incardona, 2017).
THRb	The thyroid hormone receptor beta can be used as a mechanistically based means of characterizing the thyroid-toxic potential of complex contaminant mixtures (Tabuchi et al., 2006). Thus, increases in THR transcription may indicate exposure to organic compounds including PCBs and associated potential health effects such as developmental abnormalities and neurotoxicity (Tabuchi et al., 2006). Hormone-activated transcription factors bind DNA in the absence of hormone, usually leading to transcriptional repression (Tsai and O'Malley, 1994).
HSP 70	The heat shock protein 70 is produced in response to thermal or other stress (Iwama et al., 1999; Tsan and Gao, 2004). In addition to being expressed in response to a wide array of stressors (including hyperthermia, oxygen radicals, heavy metals, and ethanol) heat shock proteins act as molecular chaperones (De Maio, 1999). For example, heat shock proteins aid the transport of the AHR/toxin complex in the initiation of detoxification (Tanabe et al., 1994).
IL-18	Interleukin-18 is a pro-inflammatory cytokine (Goldsby et al., 2003). Plays an important role in inflammation and host defense against microbes (Krumm et al., 2008).
IL-10	Interleukin-10 is an anti-inflammatory cytokine (Goldsby et al., 2003). Levels of IL-10 have been correlated with relative health of free-ranging harbor porpoises, e.g., increased amounts of IL-10 correlated with chronic disease whereas the cytokine was relatively reduced in apparently fit animals experiencing acute disease (Beineke et al., 2007). Association of IL-10 transcription with chronic disease has also been documented in humans (Rigopoulou et al., 2005).
DRB	A component of the major histocompatibility complex, the DRB class II gene, is responsible for the binding and presentation of processed antigen to T_H lymphocytes, thereby facilitating the initiation of an immune response (Goldsby et al., 2003; Bowen et al., 2006). Up-regulation of MHC genes has been positively correlated with parasite load (Wegner et al., 2006), whereas down-regulation of MHC has been associated with contaminant exposure (Dong et al., 1997).
Mx1	The Mx1 gene responds to viral infection (Tumpey et al., 2007). Vertebrates have an early strong innate immune response against viral infection, characterized by the induction and secretion of cytokines that mediate an antiviral state, leading to the up-regulation of the MX-1 gene (Kibenge et al., 2005).
CCR3	The chemokine receptor 3 binds at least seven different chemokines and is expressed on eosinophils, mast cells (MC), and a subset of Th cells (Th2) that generate cytokines implicated in mucosal immune responses (Gurish et al., 2002; Kringel et al., 2006). Up-regulation of CCR3 occurs in the presence of parasites (Gurish et al., 2002; Kringel et al., 2006).
5HTT	The serotonin transport gene codes for an integral membrane protein that transports the neurotransmitter serotonin from the synaptic spaces into presynaptic neurons. This transport of serotonin by the SERT protein terminates the action of serotonin and recycles it in a sodium-dependent manner (Jennings et al., 2006; Squire et al., 2008). Algal toxins have been associated with increased expression of HTT5 (Pazos et al., 2017); at the cellular level, domoic acid is an excitatory amino acid analog of glutamate, a major excitatory neurotransmitter in the brain known to activate glutamate receptors (Pulido, 2008). Exposure to hydrocarbons has also been linked with altered levels of neurotransmitters (Gesto et al., 2006; Sriram et al., 2022).
CaM	Calmodulin (CaM) is a small acidic Ca2+−binding protein, with a structure and function that is highly conserved in all eukaryotes. CaM activates various Ca2+−dependent enzyme reactions, thereby modulating a wide range of cellular events, including metabolism control, muscle contraction, exocytosis of hormones and neurotransmitters, and cell division and differentiation (Chen et al., 2012). CaM has also been reported to be a pivotal calcium metabolism regulator in shell formation (Li et al., 2004). Algal toxicity is associated with increased intracellular Ca2+ (Choi, 1992; Choi, 1994; Berman et al., 2002; Shalbuyeva et al., 2006; Plested and Mayer, 2007; Pulido, 2008). This intracellular excess is toxic to the cells and triggers the activation of several detrimental cascading effects (Portnoy et al., 2020).

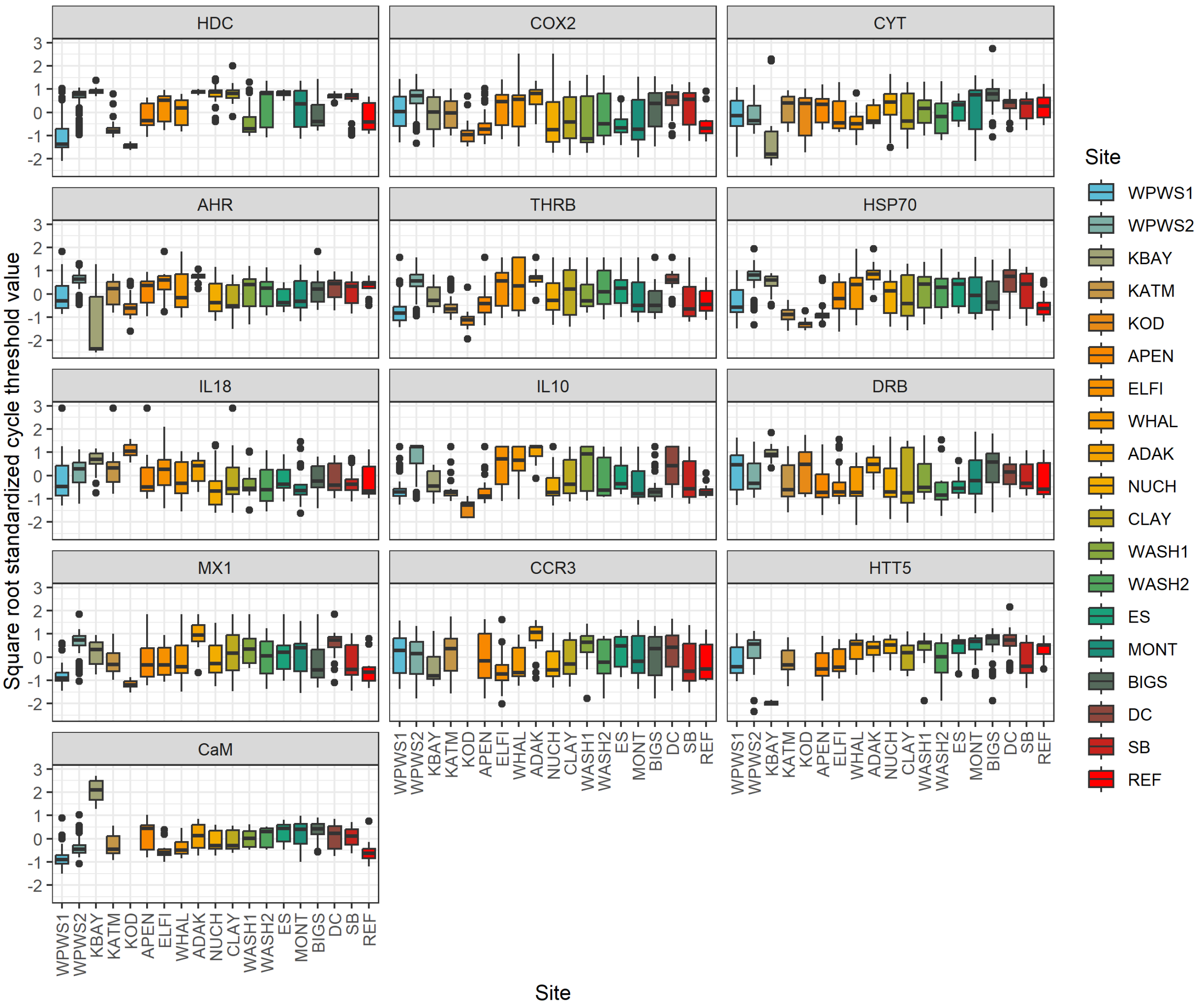

FIGURE 2
Generalized linear multivariate models (GLMV) were used to visually describe gene transcript profiles by location. Distribution of mean cycle threshold (C_T) values and confidence intervals across genes targeted by the panel of 13 primer pairs for 19 populations. Note: KOD is missing data for CCR3, HTT5, and CaM. Real-time PCR data are represented as normalized values (NVs); the lower the NV, the higher the quantity of transcripts. All values were pre-standardized to mean 0 and sd 1 in order to visualize inter-site variation on common scale. Data was then transformed based on the square root standardized C_T values (Negative values are transformed by taking the sqrt of the absolute value and reattaching the negative sign). This transformation reduces the kurtosis (heavy tails) above and below the 0 and enables outliers to be included in the graph without flattening the variation patterns in the midsection of the graph. Sites have one of 3 general patterns: (1) otters distributed widely above and below average gene expression (boxes that encompass 0), (2) otters generally expressing more than average (boxes below 0), and (3) otters that are generally under-expressing (boxes above 0).

Core Team, 2012). We used the vegan package for the RDA and beta dispersion test.

3. Results

Using a generalized linear multivariate model (GLMV) to visually describe gene transcript profiles by gene and population (Table 3), Figure 2 illustrates the distribution of mean cycle threshold (C_T) values and confidence intervals across genes targeted by the panel of 13 primer pairs for 19 populations. Although most population responses were overlapping to some degree, clear differences exist among responses for genes and populations (Figure 2; Table 3). The most striking differences occurred for (1) HDC, for which Western Prince William Sound 1 (WPWS1) had significantly higher expression than WPWS2 and any of the other populations, (2) CYT, for which Big Sur (BIGS) had significantly lower expression than any of the other populations, and CaM which had lower levels of expression in KBAY than in any other population.

The RDA of the occurrence of 13 genes in 18 populations of sea otters captured between 2006 and 2019 is depicted in Figures 3A,B. The variation in Figure 3A is dominated by the differences between KBAY and other locations. The same analysis was repeated (Figure 3B) with KBAY omitted, showing WPWS1 as the most transcriptionally divergent population. In the RDA, location explained 32% of the total variation in transcription levels; 87% of this can be explained by the first three axes (accumulated constrained eigenvalues); 68% of the variation is under the influence of variables that were not included in the model or measured. Hierarchical cluster analysis and subsequent heat map generation were conducted using individual sea otter

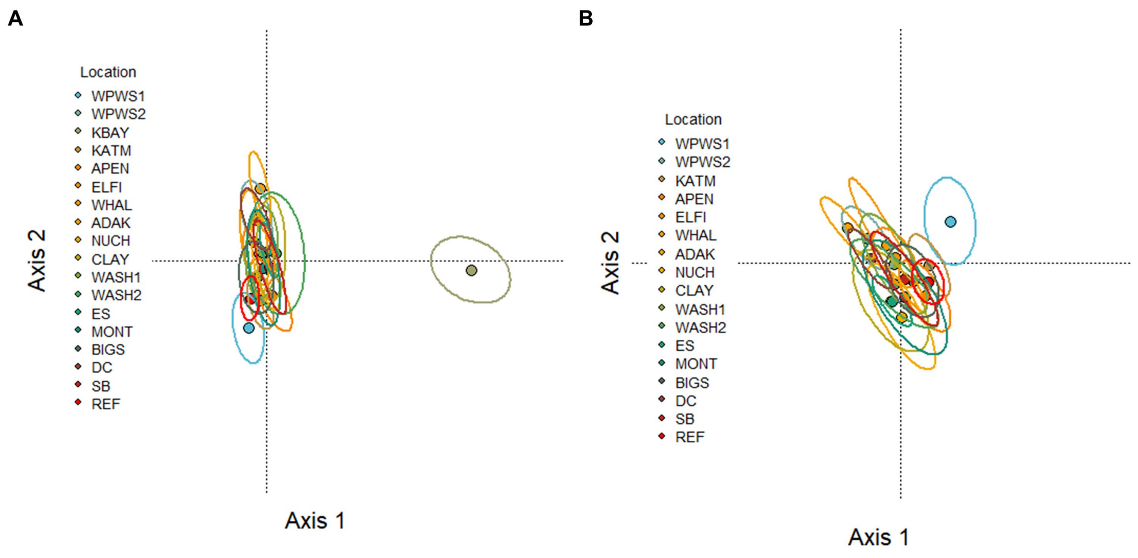

FIGURE 3
(A,B) RDA Redundancy analysis of the occurrence of 13 genes in 18 populations of sea otters (small circles) captured between 2006 and 2019. Large circles indicate population centroids. KOD sites omitted due to lack of CCR3, HTT5, and CaM (KOD samples were analyzed prior to development of CCR3, HTT5, and CaM assays). **(A)** The differences between KBAY and other sites are dominating the variation in this figure, making it difficult to pick out the differences among the other locations. **(B)** The same analysis is repeated with KBAY omitted. Figures with individual otters plotted are shown in Supplementary Figure 1.

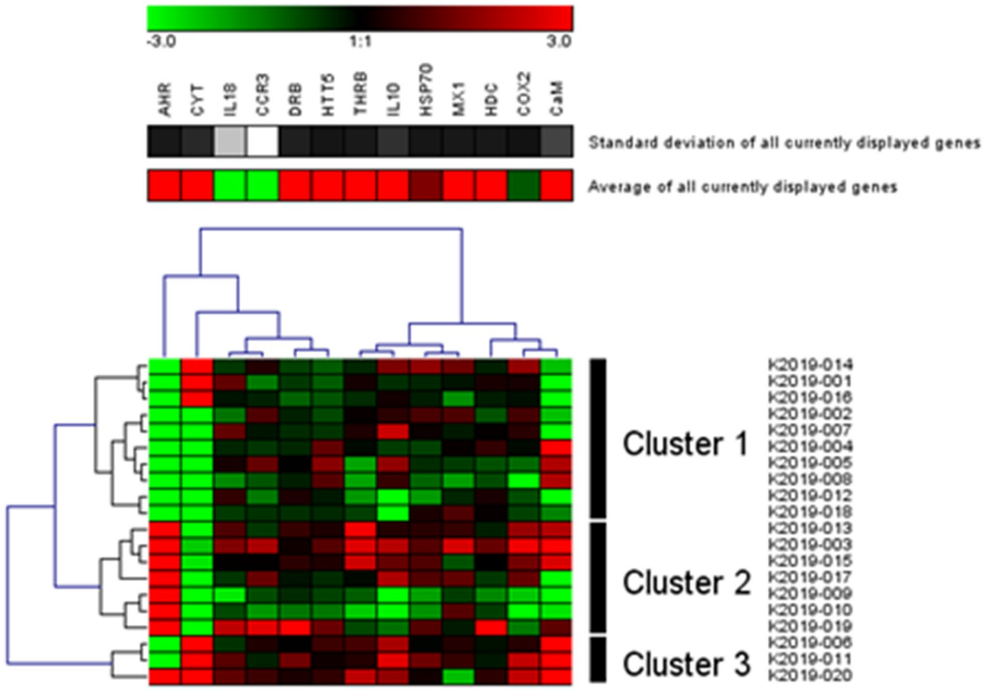

FIGURE 4
Gene profiling: Transcription matrix of 13 target genes in sea otters captured in 2019 in Kachemak Bay, AK (Hierarchical clustering with complete linkage disequilibrium; Genesis, Graz, Switzerland). Green indicates higher relative transcription levels and red indicates lower relative transcription levels.

transcription data (Figure 4). Heat map analysis was successful in demonstrating structuring of the KBAY population based on transcriptional differences. Cluster 1 was defined predominately by relatively high levels of AHR and CYT expression as well as by elevated CaM in 7 out of 10 otters. Cluster 2 was defined by relatively lower levels of AHR expression, high CYT expression and mixed CaM. Cluster 3 was identified by mixed AHR and relatively low CYT and CaM expression.

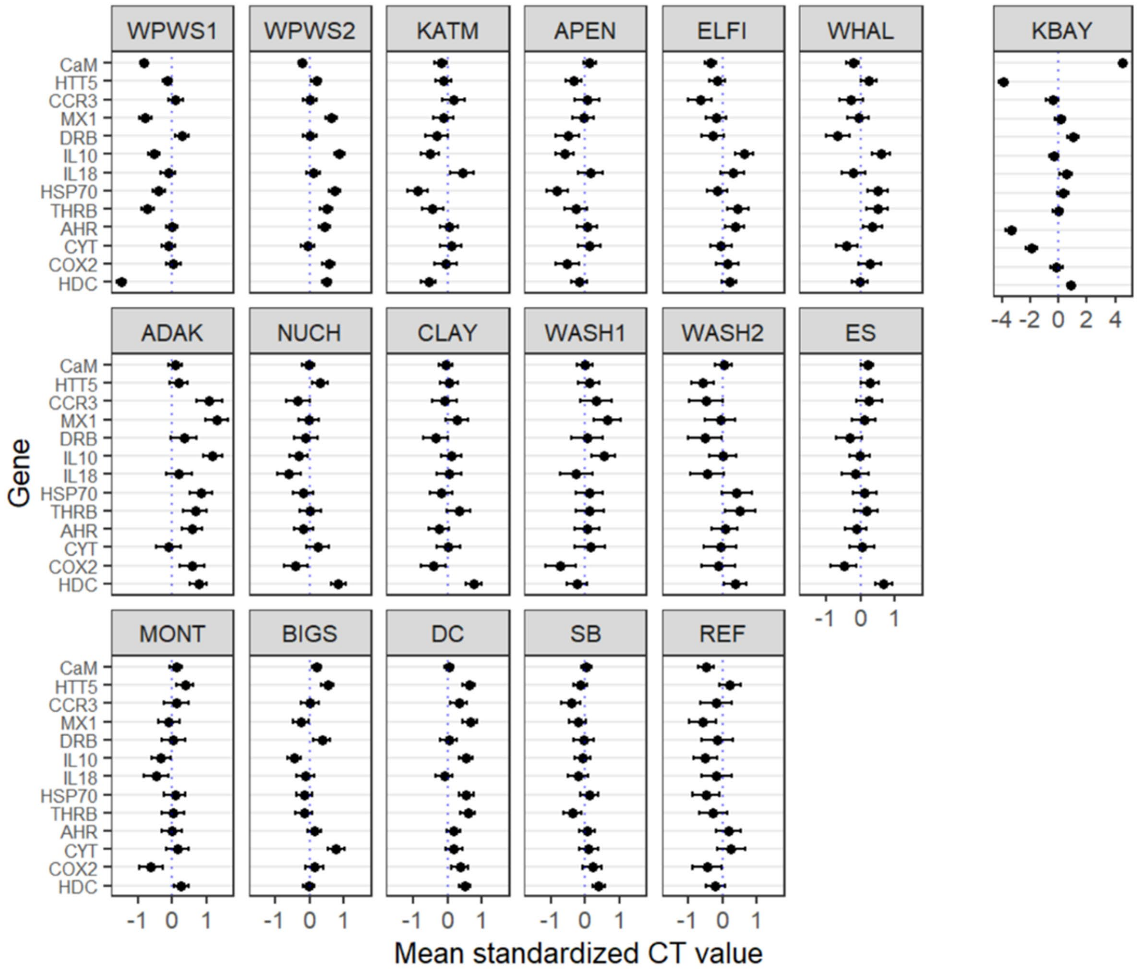

FIGURE 5
Generalized linear latent variable analysis (GLLVA). Plots of the point estimates (ticks) for coefficients of the genes and their 95% confidence intervals (lines) for the GLLVM. X axes represent transcription level estimates (deviations from the mean) after accounting for within and across population deviations. The vertical 0 reference line the mean transcription level across all populations. Y axes represent genes of interest. Many of the 95% confidence intervals do not include zero, indicating that many of the genes exhibit evidence of a strong association between population/location and transcript level. The KBAY population is plotted separately on the right on a different scale due to wider variations compared to the other populations.

The GLLVA identified many 95% confidence intervals that do not include zero, indicating that many of the genes exhibit evidence of a strong association between population/location and transcript level (Figure 5). The GLLVA identifies strong associations between population and transcript levels for at least one gene in each population: WPWS1 (7), WPWS2 (7), KATM (4), APEN (4), ELFI (4), WHAL (4), KATM (6), ADAK (8), NUCH (2), CLAY (1), WASH1 (3), WASH2 (1), ES (2), MONT (1), BIGS (4), DC (7), SB (3), and REF (3).

We evaluated homogeneity of the variance–covariance matrices among the groups with a distance-based test (beta dispersion test; Figure 6; Table 4; Anderson et al., 2006). For each wild population, abundance was estimated more than once (often annually) prior to sampling, allowing the classification of each population as either stable, declining, or increasing. Populations were assigned the status of "core" or "periphery" (Table 4); core indicates "long established" (10–20 years minimum), while periphery indicates relatively newly established (<10 years). Population groups are sorted from North to South (latitudes) geographically. The null hypothesis, no differences among populations, was rejected with distance to centroid beta dispersion $p < 0.001$.

4. Discussion

This study reveals some of the challenges and possible uses of gene expression data for describing wildlife health and brings into question choices of study design, methods of statistical analysis, and interpretation. For example, using distribution of mean cycle threshold (C_T) values and confidence intervals for individual genes of interest to describe population differences leads to complicated conclusions about population health and resilience (Figures 2, 5). Before we can interpret this data, we should determine whether it is "good" or "bad" for a gene to be up- or down-regulated. If a gene has relatively high(er) levels of expression, is that necessarily a negative indication? Higher levels of expression indicate a response to something, perhaps a stressor, but if it's an appropriate response resulting in mitigation of a stressor, that should have a positive outcome for the individual or population. For example, in Figure 5, there are four predominant patterns: (1) populations distributed above and below average gene expression (boxes that encompass 0), (2) populations generally expressing more than average (boxes below 0),

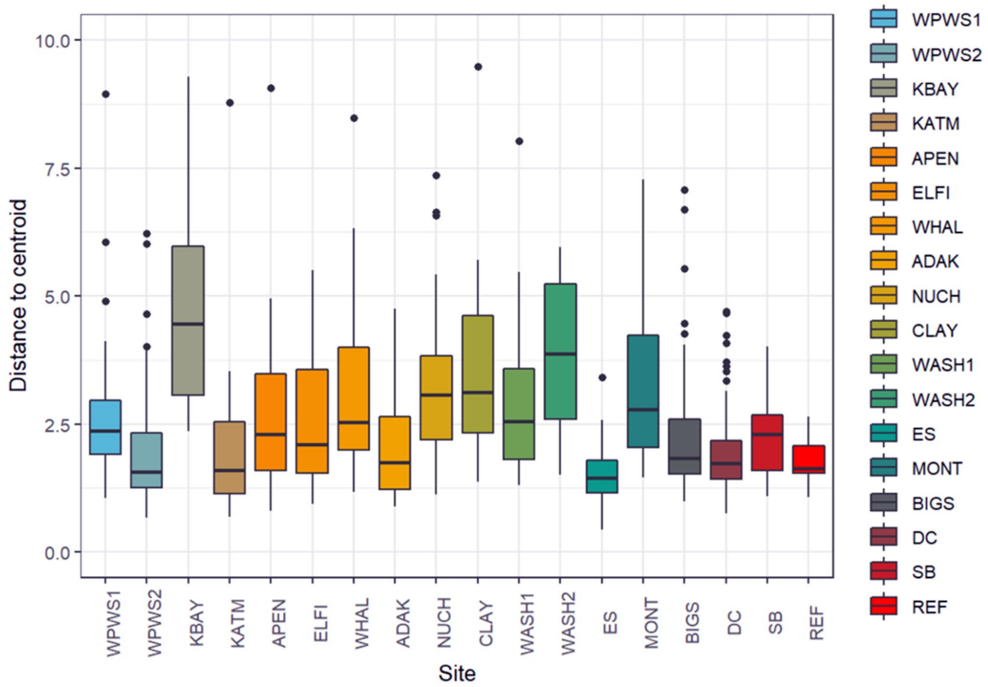

FIGURE 6
We evaluated homogeneity of the variance–covariance matrices among the groups with a distance-based test (beta dispersion test; Anderson et al., 2006). Population groups are sorted from North to South geographically. The null hypothesis was rejected with distance to centroid beta dispersion $p<1.106e^{-12}$.

(3) populations that are generally under-expressing (boxes above 0), and (4) populations whose values are generally very close to the mean, with little variation across the 13 genes. Moderate (i.e., close to the average) levels of gene expression may be indicative of ecosystem or population equilibrium; while very low levels of gene expression could indicate either a lack of stressors, or potentially an inability to mount a molecular response, perhaps due to a lack of biological resources. Additional data on individuals or the population would be needed to clarify and support interpretation of the gene expression results (Vera-Massieu et al., 2015; Weiße et al., 2015; Strandin et al., 2018).

Although similar in output, GLMV (Figure 2) and GLLVA (Figure 5) use slightly different approaches to identify gene contributions to the separation of populations in statistical space. In fact, GLMV depicts raw data and is thus purely descriptive, identifying general patterns. Conversely, GLLVA is model based and identifies statistical significance, allowing for interpretations and conclusions. However, the outcome of the two analyses lead to similar interpretations. For example, we can say with certainty that WPWS1 has by far the highest level of HDC expression of the groups in our study. The HDC gene codes for a translationally controlled tumor protein (TCTP) implicated in cell growth, cell cycle progression, malignant transformation, tumor progression, and in the protection of cells against various stress conditions and apoptosis (Bommer and Thiele, 2004; Tuynder et al., 2004; Ma et al., 2010; Table 1). HDC transcription is known to increase with exposure to carcinogenic compounds such as polycyclic aromatic hydrocarbons (PAH; Bowen et al., 2007; Raisuddin et al., 2007; Zheng et al., 2008). We can hypothesize that HDC might be responding to lingering oil from the *Exxon Valdez* oil spill (EVOS) in 1989 (Bodkin et al., 2012), which is consistent with WPWS sea otters having continued EVOS-related survival effects lasting until ~2010 (Monson et al., 2001; Ballachey et al., 2014). Again, although an appropriate response can be interpreted as a "good" thing, there are associated costs. Molecular activity is physiologically costly (Vera-Massieu et al., 2015; Weiße et al., 2015; Strandin et al., 2018). Perhaps the largest cost is the reallocation of nutrients and energy from one portion of an individual's resource budget to other metabolic functions. Mitigation of stressors imposes demands on animals above those normally required to sustain life and may result in reduction of fitness evidenced by decreased reproductive capability, increased susceptibility to disease, or disadvantageous behavioral changes (Martin et al., 2010; Graham et al., 2011).

Other differences in distribution of mean cycle threshold (C_T) values and confidence intervals of note include relatively low levels of CYT in the BIGS population and the relatively low levels of eight of the 13 genes in the WPWS2 population. CYT, the complement cytolysis inhibitor, protects against or inhibits cell death (Jenne and Tschopp, 1989). Relatively low levels of CYT expression might be indicative of an inability to or lack of a need to kill pathogens. Again, population level context would help with interpretation. The low expression levels seen in WPWS2 sea otters could be consistent with an inability to mount effective responses to pathogens, contaminants, injury, or other stressors when compared to other groups. In fact, disease and mortality do not necessarily indicate a disease-induced population decline, because the elevated frequency of disease is a common manifestation of resource limitation in many wildlife species, which in turn is influenced by prey availability and environmental conditions (Post et al., 2013; Wobeser, 2013). For example, WPWS2 may no longer have mortality level stressors related to

TABLE 3 Means and variances for all populations.

	WPWS1		WPWS2		KBAY		KATM		KOD		APEN	
	Mean	Variance	Mean	Variance	Mean	Variance	Mean	Variance	Mean	Variance	Mean	Variance
AHR	10.38	5.71	12.15	1.93	−3.31	160.17	10.62	2.16	7.51	13.19	10.64	3.56
HDC	0.83	21.34	9.20	3.39	10.68	1.47	4.78	2.64	−1.84	1.40	6.39	2.99
COX2	8.17	3.09	9.43	2.37	7.73	4.02	7.95	2.10	5.67	2.61	6.77	3.16
CYT	1.62	5.44	1.75	1.02	−3.71	93.06	2.25	1.63	0.69	12.80	2.29	1.63
THRB	11.70	9.38	16.32	8.53	14.25	2.44	12.80	2.29	8.94	11.20	13.40	10.21
HSP70	10.09	5.40	13.84	6.66	12.42	1.14	8.51	3.21	5.70	2.52	8.65	2.47
IL18	1.91	9.35	2.44	1.05	3.55	1.48	3.32	16.30	5.40	2.43	2.65	19.58
IL10	13.60	7.58	20.66	14.45	14.74	5.72	13.81	6.63	6.60	19.42	13.32	8.76
DRB	0.38	2.19	−0.07	0.67	1.48	1.20	−0.57	2.29	0.42	2.69	−0.87	2.37
MX1	10.53	2.41	15.11	5.75	13.47	1.39	12.73	2.41	8.39	2.25	12.90	13.07
CCR3	5.18	2.00	5.04	1.59	4.31	1.38	5.30	2.95	N/A	N/A	5.11	5.40
HTT5	9.99	1.62	10.92	6.12	−1.03	0.84	10.01	1.93	N/A	N/A	9.39	5.65
CaM	−1.76	0.85	−0.68	0.19	7.48	11.15	−0.65	0.30	N/A	N/A	−0.09	0.47

	ELFI		WHAL		ADAK		NUCH		CLAY		WASH1	
	Mean	Variance	Mean	Variance	Mean	Variance	Mean	Variance	Mean	Variance	Mean	Variance
AHR	11.82	7.57	11.81	16.24	12.81	0.89	9.67	9.65	9.39	6.69	10.66	10.27
HDC	7.91	3.04	7.02	2.81	10.31	0.33	10.56	7.21	10.34	10.86	6.11	10.47
COX2	8.38	3.35	8.76	12.54	9.54	1.76	7.06	21.77	7.06	9.59	6.28	14.34
CYT	1.80	2.88	0.76	3.48	1.66	0.38	2.62	11.67	2.00	6.89	2.36	4.59
THRB	16.15	18.04	16.36	25.03	17.04	8.05	14.52	16.31	15.71	27.22	14.98	8.57
HSP70	10.88	5.72	13.08	31.42	14.24	6.49	10.74	7.62	10.78	14.98	11.81	11.01
IL18	2.96	12.31	1.68	3.35	2.72	1.19	0.63	8.66	2.35	25.91	1.55	3.69
IL10	19.41	21.67	19.40	19.40	22.28	7.92	14.62	14.71	16.91	20.31	19.01	29.27
DRB	−0.53	1.72	−1.11	3.60	0.46	0.63	−0.26	6.35	−0.61	6.97	0.04	3.11
MX1	12.41	2.69	12.86	10.55	17.32	17.15	13.00	6.88	13.96	11.85	15.19	14.62
CCR3	3.96	3.07	4.60	0.98	6.71	1.84	4.48	0.94	4.89	1.50	5.50	3.06
HTT5	9.92	1.11	11.11	1.24	10.96	0.95	11.25	1.25	10.52	1.61	10.71	8.99
CaM	−0.94	0.18	−0.71	0.19	−0.17	0.34	−0.40	0.14	−0.41	0.10	−0.31	0.08

(Continued)

TABLE 3 (Continued)

	WASH2		ES		MONT		BIGS		DC		SB	
	Mean	Variance	Mean	Variance	Mean	Variance	Mean	Variance	Mean	Variance	Mean	Variance
AHR	10.61	5.00	9.88	1.04	10.37	6.29	10.94	5.43	11.10	1.46	10.60	2.44
HDC	8.61	13.76	9.94	0.65	8.22	13.43	6.91	4.00	9.24	0.39	8.75	3.48
COX2	7.76	11.39	6.86	1.86	6.51	14.27	8.41	3.74	8.98	2.00	8.61	3.63
CYT	1.72	9.28	2.10	0.58	2.40	14.08	4.20	11.08	2.51	0.60	2.25	0.70
THRB	16.37	21.76	15.11	6.24	14.58	17.50	13.79	9.34	16.73	7.54	13.05	8.78
HSP70	12.80	17.72	11.83	2.48	11.71	10.99	10.92	5.29	13.29	9.22	11.82	6.21
IL18	1.06	7.62	1.85	1.30	1.00	6.47	1.89	1.72	1.98	1.42	1.70	1.00
IL10	16.34	22.55	16.23	5.66	14.70	19.38	14.02	7.90	18.96	16.27	15.91	25.14
DRB	−0.88	6.63	−0.58	0.29	−0.01	6.19	0.47	1.99	−0.03	0.29	−0.14	0.50
MX1	12.81	9.19	13.39	7.72	12.77	11.40	12.26	10.04	15.19	7.75	12.35	5.84
CCR3	4.24	5.76	5.42	0.84	5.20	2.52	5.01	2.63	5.55	2.37	4.37	2.78
HTT5	8.65	23.47	11.20	1.28	11.47	1.35	11.90	4.81	12.21	4.33	9.95	4.34
CaM	−0.26	0.10	0.02	0.15	−0.11	0.66	0.04	0.23	−0.22	0.32	−0.26	0.14

	REF	
	Mean	Variance
AHR	11.04	0.81
HDC	6.17	3.32
COX2	6.95	2.38
CYT	2.67	1.87
THRB	13.39	2.51
HSP70	9.78	2.95
IL18	1.74	2.73
IL10	13.77	1.99
DRB	−0.33	1.09
MX1	11.18	4.31
CCR3	4.71	1.22
HTT5	11.00	0.68
CaM	−1.17	0.77

TABLE 4 Beta diversity by population.

	Core/ Perip	Population growth	Average distance to median	Diversity category
WPWS1	Core	Increasing	7.912	Moderate
WPWS2	Core	Stable	6.592	Low
KBAY	Core	Stable/Increasing	15.457	High
KATM	Periphery	Increasing	5.546	Low
APEN	Core	Stable	7.519	Moderate
ELFI	Core	Stable	8.288	Moderate
WHAL	Periphery	Increasing	10.312	High
ADAK	Core	Stable	6.079	Low
NUCH	Core	Stable	9.615	Moderate
CLAY	Periphery	Increasing	10.83	High
WASH1	Periphery	Increasing	9.963	Moderate
WASH2	Core	Stable	11.459	High
ES	Core	Increasing	4.802	Low
MONT	Core	Stable	10.077	High
BIGS	Core	Stable	7.020	Moderate
DC	Core	Stable	6.647	Low
SB	Periphery	Increasing	7.532	Moderate
REF	N/A	N/A	4.951	Low

Average distance to median identified for each population. Diversity category (Low, Moderate, High) assigned by arbitrarily designated groups (Low = 4–6; Moderate = 7–9; High = 10+). Populations are identified as core or periphery and population growth is categorized as stable, increasing, or decreasing. The reference otters are not categorized in terms of population metrics as they are not free-ranging and are permanently under human care.

PAHs but may continue to have non-lethal, yet disadvantageous, levels of stressors still related to oil spill effects. Infectious diseases occur in all ecosystems, both healthy and unhealthy, and play an important role in structuring biological communities (Tracy et al., 2019). A determination of WPWS2 at or exceeding carrying capacity and thus likely nutrient limited would help support the theory of resource limitation. Energy intake rates have been shown to be a useful indicator of resource availability in sea otters (Dean et al., 2002; Coletti et al., 2016). Estimated energy intake rates for sea otters living in WPWS averaged ~6.5 kcal/min between 2010 and 2012 (Coletti and Wilson, 2015), which is consistent with a population near carrying capacity and supports the theory of resource limitation.

Previous work by Bowen et al. (2022), identified abnormally high levels of AHR and CYT as well as low levels of CaM in KBAY otters; these differences are also identified in our current analyses. Brief interpretation indicates possible exposure to an algal toxin; the KBay sea otters had transcript profiles very different from those of otters with suspected oil exposure (WPWS1), and in fact, oil exposure is not suspected to be a factor influencing transcript profiles in KBay (Bowen et al., 2022). At the time of sampling in 2019, the KBAY population was stable or increasing (Table 1). Intuitively, this may conflict with the extremely divergent gene expression patterns identified in KBAY otters. We can surmise that the KBAY otters were responding to a stressor, and, at least in the short-term, providing some level of mitigation of that stressor. However, we do not know the longer-term consequences of this exposure. Even without near-term morbidity or mortality, will exposure to this particular stressor affect population health in the long-term?

KBAY was also remarkable from the analysis of population centroids in the RDA (Figure 3), in which it was separated from all other groups along axis 1. As stated above, we identified a very high level of CYT, AHR, and HTT5, and low level of CaM expression in KBAY in relation to the other groups. Little discernable separation occurred along axis 2 in the RDA and population centroids were obscured. In general, there are still unmeasured factors influencing the gene expression levels, however, the environmental variables have a very strong influence. What about within population variation? For example, the gene expression KBAY profile appears to split into two groups. Although we found no statistical link among age, sex, or capture location, and gene expression profile within this population, further examination revealed stark differences in gene expression levels within the KBAY otter population (Figure 4). The KBAY population may have been exposed to one or more harmful algal toxins (Bowen et al., 2022). Harmful algal blooms may not be uniformly distributed, and prey items may concentrate or bioaccumulate toxins differently. As well, dietary specialization is a well-known attribute of the sea otter; the diet of sea otters in KBAY is diverse, including clams and mussels that may sequester biotoxins and crustaceans that may not (Tinker et al., 2008). Therefore, we could predict that this within-population split has to do with foraging location or prey preferences.

Due to the degree KBAY drove placement of the other otter populations in RDA space, we repeated the analysis without KBAY otters (Figure 3B). When KBAY is removed, the remaining otter populations spread out somewhat in RDA space, The most notable separation in this case is WPWS1, which separated from all other groups along axis 1 and 2 (Figure 3B). We identified very high levels of HDC expression in WPWS1 in relation to the other groups (Figure 2). As described in Miles et al. (2012), expression profiles of WPWS1 otters in comparison with clinically normal reference otters indicated exposure to lingering oil.

Historically, the term beta diversity has been used in an ecological context to represent the difference in species composition between local and regional assemblages (de Juan et al., 2013). Thus, diversity has been suggested as a measure of ecosystem resilience (de Juan et al., 2013); greater variation in beta diversity could be an early warning sign of declining host health (Fackelmann and Sommer, 2019). However, considering the current and rapidly increasing nearshore marine ecosystem degradation due to cumulative stressors associated largely with climate change, there is an urgent need to identify variables that might indicate changes in ecosystem state (de Juan et al., 2013). Although beta diversity is a promising measure of ecosystem resilience in the context of species richness, can we apply this to levels of gene expression? Our beta dispersion test identified significantly different levels of variation in quantities of gene expression across populations (Figure 6). Additionally, the captive population had the smallest amount of diversity in terms of gene expression, which might indicate more stable environments with fewer stressors.

Research in unicellular organisms has linked noise (heterogeneity/variation) in gene expression to population growth rate (Keren et al., 2015). We have not found studies that used levels of beta dispersion in gene expression as a measure of population or ecosystem health or resilience. However, extrapolation from the unicellular model to the population level may be possible. For example, variability in expression in unicellular organisms is anti-correlated to population average gene expression, which in turn is tightly coupled to growth rate (Tyson et al., 1979; Ingraham et al., 1983; Bar-Even et al., 2006; Newman et al., 2006; Brauer et al., 2008; Klumpp et al., 2009; Taniguchi et al., 2010; Keren et al., 2013, 2015). This brings us to two distinct approaches of quantifying variation in gene expression, intrinsic vs. extrinsic variability. Intrinsic variability describes the variation at the level of a single gene due to the stochastic nature of the transcriptional process, while extrinsic variability relates to the variability across different genes as a result of population dynamics and environment (Keren et al.'s, 2015). As far as we know these concepts have not yet been applied to gene expression studies in wildlife; accurate interpretation will require further exploration.

In terms of growth, work to date has focused on growth of a cell, not a population. However, the concept therein may be applied (with modifications) to wildlife populations. For example, in Keren et al. (2015) study of gene expression in yeast, harsher environmental conditions were found to reduce growth rates. At least conceptually, this also applies to wildlife populations; greater environmental pressures require greater levels of mitigation, evidenced by greater levels of variation in gene expression. Gene expression mitigation uses resources normally reserved for maintenance of growth and reproduction. An ensuing resource allocation imbalance occurs, ultimately resulting in slower growth rates, either at the cellular or population level (Martin et al., 2010; Graham et al., 2011). However, this may not be immediately evident. For example, otters in the KBAY population demonstrate the highest amount of variation in our study, and yet as of 2019 the KBAY population was stable (Esslinger et al., 2021); what we do not know are the long-term effects of the particular stressor and the resulting molecular mitigation strategies. How do we interpret the relatively little variation demonstrated by several populations (see Figure 6)? From what we know, we can speculate that the low variation in the WPWS2 and ADAK populations is because those populations are nutritionally limited, making increased expression difficult if not impossible. Just recently, the KATM population was determined to be food-limited but is an area with little or no known remarkable environmental stressors (Coletti et al., 2016; Tinker et al., 2021). The ES population may exhibit low variability because of its small size and homogenous landscape. The REF population includes only animals under permanent human care. As such, their environment is tightly regulated with little variation in extrinsic stimuli, which can result in limited variability. Moderate variability (WPWS1, APEN, ELFI, NUCH, WASH1, BIGS, SB) includes populations clearly responding to stressors as well as populations thought to be at equilibrium. Aside from KBAY, populations categorized as having highly variable gene expression (KBAY, WHAL, CLAY, WASH2, MONT) showed significant differences in gene expression from other populations. Note that three or four of these five populations may be periphery populations, which may account for the high variation. However, in this exercise, we examined variability across a gene panel. For a more complete picture and more refined interpretation as it relates to individual and population health, we should consider variation on a per gene basis. We should also consider formally collecting (if needed) and incorporating (when available) other measurements at both the ecosystem level and individual level that may aid in interpretation (such as prey availability and body condition). Level of variation might also reflect where the population is heading, rather than where it has been. It is important to recognize that our determination of population status based on length of occupation and surveys of abundance are by design, hindcasting, in terms of what the population has been doing, not where the next data point might lie on that trend.

In our study, interpretations based on variances and means overlapped to some degree. For example, those populations in the low diversity category all had suppressed or low levels of gene expression, representing limited nutritional resources or limited extrinsic stressors, respectively. These two states are quite different, and interpretation of results requires additional knowledge of the system as a whole. In contrast, populations in the moderate and high diversity categories (with the exception of KBAY) did not align with analyses focused on mean expression levels. Clearly there are interpretations and inferences we are not yet making based on these findings.

5. Implications

Determination of population "health" will require several choices and definitions (including of health itself): perspective (including choice of sentinel species, population inclusions, time frame, etc.), measurement techniques (molecular to population level), and statistical analysis choices (focus on population means or population variation). Ultimately, determination of population or ecosystem health will require information from many disciplines, contextualized to specific scenarios and goals. Inclusion of fine scale, mechanistic tools such as gene expression are necessary to begin to understand why populations are healthy or not, and to formulate strategies for recovery. Without these, we are left with only a simple and partial answer regarding population status. At some point, which we have not quite reached on a global scale, gene expression may be linked to wildlife population status as measure of health. A conceptualized example of the relationship between variation in gene expression and population status is provided in Table 5.

This brings us back to one of our original questions: is divergent gene expression good or bad? Similarly, is divergent variation in gene expression good or bad? Both appear to be context dependent, and neither can be answered without first defining the optimum or healthy system. Long-term monitoring programs could be leveraged to

TABLE 5 Using gene expression to conceptualize wildlife population status as a measure of health.

Population Status	Gene expression		
	Elevated	Suppressed	Baseline
Increasing	Appropriate response to stressor (McLoughlin et al., 2006; Trego et al., 2019)	Unbalanced resource allocation (Bowen et al., 2016)	At physiological equilibrium (Bowen et al., 2012, 2016)
Decreasing	Immunopathology (Thacker et al., 2007; Channappanavar and Perlman, 2017) Unbalanced resource allocation (Martin et al., 2010; Graham et al., 2011)	Nutritionally limited (Spitz et al., 2015; Weiße et al., 2015; Strandin et al., 2018) Increased susceptibility (Pedersen and Babayan, 2011; Bowen et al., 2016)	Top-down pressure (e.g., predation) (Coletti et al., 2021)
At equilibrium	Appropriate response to stressor (McLoughlin et al., 2006)	Unbalanced resource allocation (Bowen et al., 2016)	At physiological equilibrium (Bowen et al., 2012, 2016)

address data gaps and provide consistent ecosystem level-inputs of a variety of metrics, which would allow for interpretation of these results more fully.

Data availability statement

The raw data supporting the conclusions of this article will be made available by the authors, without undue reservation.

Ethics statement

Field activities were conducted under the Marine Mammal Protection Act USFWS permit (MA041309). No animals were used in the current study. Animal care and permit information can be found in the cited literature.

Author contributions

LB, JY, AM, and JB contributed to conception and design of the study. SW organized the database. JY and LB performed the statistical analyses. LB wrote the first draft of the manuscript. DM, BB, HC, JY, MM, and JB wrote sections of the manuscript. All authors contributed to the article and approved the submitted version.

Funding

USGS Ecosystems Mission Area provided funding for original field study, data analyses, interpretation, and writing.

Acknowledgments

The authors would like to thank Rob Klinger for his invaluable assistance as a statistical sounding board. They greatly appreciate the hard work of all who participated in gathering samples and data for this project; you are far too many to list here, but this research would not have been possible without you. Any use of trade, firm, or product names is for descriptive purposes only and does not imply endorsement by the U.S. Government.

Conflict of interest

The authors declare that the research was conducted in the absence of any commercial or financial relationships that could be construed as a potential conflict of interest.

Publisher's note

Supplementary material

The Supplementary material for this article can be found online at: https://www.frontiersin.org/articles/10.3389/fevo.2023.1157700/full#supplementary-material

References

Álvarez-Muñoz, D., Llorca, M., Blasco, J., and Barceló, D. (2016). "Chapter 1–Contaminants in the marine environment" in *Marine ecotoxicology*. eds. J. Blasco, P. M. Chapman, O. Campana and M. Hampel (Cambridge, MA: Academic Press), 1–34.

Anderson, M. J., Ellingsen, K. E., and McArdle, B. H. (2006). Multivariate dispersion as a measure of beta diversity. *Ecol. Lett.* 9, 683–693. doi: 10.1111/j.1461-0248.2006.00926.x

Androulakis, I. P., Yang, E., and Almon, R. R. (2007). Analysis of time-series gene expression data: methods, challenges, and opportunities. *Annu. Rev. Biomed. Eng.* 9, 205–228. doi: 10.1146/annurev.bioeng.9.060906.151904

Ballachey, B. E., Bodkin, J. L., Esler, D., and Rice, S. D. (2014). "Lessons from the 1989 Exxon Valdez oil spill: a biological perspective" in *Impacts of oil spill disasters on marine habitats and fisheries in North America* (Milton Park: Taylor & Francis), 181.

Bar-Even, A., Paulsson, J., Maheshri, N., Carmi, M., O'Shea, E., Pilpel, Y., et al. (2006). Noise in protein expression scales with natural protein abundance. *Nat. Genet.* 38, 636–643. doi: 10.1038/ng1807

Beineke, A., Siebert, U., Muller, G., and Baumgartner, W. (2007). Increased blood interleukin-10 mRNA levels in diseased free-ranging harbor porpoises (*Phocoena phocoena*). *Vet. Immunol. Immunopathol.* 115, 100–106. doi: 10.1016/j.vetimm.2006.09.006

Berman, F. W., LePage, K. T., and Murray, T. F. (2002). Domoic acid neurotoxicity in cultured cerebellar granule neurons is controlled preferentially by the NMDA receptor Ca2+ influx pathway. *Brain Res.* 924, 20–29. doi: 10.1016/s0006-8993(01)03221-8

Blanchong, J. A., Robinson, S. J., Samuel, M. D., and Foster, J. T. (2016). Application of genetics and genomics to wildlife epidemiology. *J. Wildl. Manag.* 80, 593–608. doi: 10.1002/jwmg.1064

Bodkin, J. L., Ballachey, B. E., Coletti, H. A., Esslinger, G. G., Kloecker, K. A., Rice, S. D., et al. (2012). Long-term effects of the 'Exxon Valdez'oil spill: sea otter foraging in the intertidal as a pathway of exposure to lingering oil. *Marine Ecol. Prog. Ser.* 447, 273–287. doi: 10.1073/pnas.120163397

Bommer, U. A., and Thiele, B. J. (2004). The translationally controlled tumour protein (TCTP). *Int. J. Biochem. Cell Biol.* 36, 379–385. doi: 10.1007/978-3-319-67591-6_4

Bowen, L., Aldridge, B. M., Miles, A. K., and Stott, J. L. (2006). Expressed MHC class II genes in sea otters (*Enhydra lutris*) from geographically disparate populations. *Tissue Antigens* 67, 402–408. doi: 10.1111/j.1399-0039.2006.00559.x

Bowen, L., Counihan, K. L., Ballachey, B., Coletti, H., Hollmen, T., Pister, B., et al. (2020a). Monitoring nearshore ecosystem health using Pacific razor clams (*Siliqua patula*) as an indicator species. *PeerJ* 8:e8761. doi: 10.7717/peerj.8761

Bowen, L., Longshore, K., Wolff, P., Klinger, R., Cox, M., Bullock, S., et al. (2020b). Gene transcript profiling in desert bighorn sheep. *Wildl. Soc. Bull.* 44, 323–332. doi: 10.1002/wsb.1078

Bowen, L., Miles, A. K., Ballachey, B., Waters, S., and Bodkin, J. (2016). Gene transcript profiling in sea otters post-Exxon Valdez oil spill: a tool for marine ecosystem health assessment. *J. Mar. Sci. Eng.* 4:39. doi: 10.3390/jmse4020039

Bowen, L., Miles, A. K., Kolden, C. A., Saarinen, J. A., Bodkin, J. L., Murray, M. J., et al. (2015). Effects of wildfire on sea otter (*Enhydra lutris*) gene transcript profiles. *Mar. Mamm. Sci.* 31, 191–210. doi: 10.1111/mms.12151

Bowen, L., Miles, A. K., Murray, M., Haulena, M., Tuttle, J., Van Bonn, W., et al. (2012). Gene transcription in sea otters (*Enhydra lutris*); development of a diagnostic tool for sea otter and ecosystem health. *Mol. Ecol. Resour.* 12, 67–74. doi: 10.1111/j.1755-0998.2011.03060.x

Bowen, L., Riva, F., Mohr, C., Aldridge, B., Schwartz, J., Miles, A. K., et al. (2007). Differential gene expression induced by exposure of captive mink to fuel oil: a model for the sea otter. *EcoHealth* 4, 298–309. doi: 10.1007/s10393-007-0113-5

Bowen, L., Waters, S., Stott, J. L., Duncan, A., Meyerson, R., and Woodhouse, S. (2022). Baseline gene expression levels in Falkland-Malvinas Island penguins: towards a new monitoring paradigm. *Life* 12:258. doi: 10.3390/life12020258

Brauer, M. J., Huttenhower, C., Airoldi, E. M., Rosenstein, R., Matese, J. C., Gresham, D., et al. (2008). Coordination of growth rate, cell cycle, stress response, and metabolic activity in yeast. *Mol. Biol. Cell* 19, 352–367. doi: 10.1091/mbc.e07-08-0779

Campbell, L. J., Hammond, S. A., Price, S. J., Sharma, M. D., Garner, T. W. J., Birol, I., et al. (2018). A novel approach to wildlife transcriptomics provides evidence of disease-mediated differential expression and changes to the microbiome of amphibian populations. *Mol. Ecol.* 27, 1413–1427. doi: 10.1111/mec.14528

Channappanavar, R., and Perlman, S. (2017). Pathogenic human coronavirus infections: causes and consequences of cytokine storm and immunopathology. *Semin. Immunopathol.* 39, 529–539. doi: 10.1007/s00281-017-0629-x

Chen, Z., Wang, H., Matsumura, K., and Qian, P. (2012). Expression of calmodulin and myosin light chain kinase during larval settlement of the barnacle *Balanus Amphitrite*. *PLoS One* 7:e31337. doi: 10.1371/journal.pone.0031337

Choi, D. W. (1992). Excitotoxic cell death. *J. Neurobiol.* 23, 1261–1276. doi: 10.1002/neu.480230915

Choi, D. W. (1994). Calcium and excitotoxic neuronal injury. *Ann. N. Y. Acad. Sci.* 747, 162–171. doi: 10.1111/j.1749-6632.1994.tb44407.x

Coletti, H. A., Bodkin, J. L., Monson, D. H., Ballachey, B. E., and Dean, T. A. (2016). Detecting and inferring cause of change in an Alaska nearshore marine ecosystem. *Ecosphere* 7:e01489. doi: 10.1002/ecs2.1489

Coletti, H. A., Bowen, L., Ballachey, B. E., Wilson, T. L., Waters, S., Booz, M., et al. (2021). Gene expression profiles in two razor clam populations: discerning drivers of population status. *Life* 11:1288. doi: 10.3390/life11121288

Coletti, H. A., and Wilson, T. L.. (2015). *Nearshore marine bird surveys: Data synthesis, analysis and recommendations for sampling frequency and intensity to detect population trends. Exxon Valdez oil spill restoration project final report (restoration project 12120114-F)*, National Park Service, Anchorage, Alaska.

Connon, R. E., D'Abronzo, L. S., Hostetter, N. J., Javidmehr, A., Roby, D. D., Evans, A. F., et al. (2012). Transcription profiling in environmental diagnostics: health assessments in Columbia River basin steelhead (*Oncorhynchus mykiss*). *Environ. Sci. Technol.* 46, 6081–6087. doi: 10.1021/es3005128

de Juan, S., Thrush, S. F., and Hewitt, J. E. (2013). Counting on β-diversity to safeguard the resilience of estuaries. *PLoS One* 8:e65575. doi: 10.1371/journal.pone.0065575

De Maio, A. (1999). Heat shock proteins: facts, thoughts, and dreams. *Shock* 11, 1–12. doi: 10.1097/00024382-199901000-00001

Dean, T. A., Bodkin, J. L., Fukuyama, A. K., Jewett, S. C., Monson, D. H., and O'Clair, C. E. (2002). Food limitation and the recovery of sea otters following the 'Exxon Valdez' oil spill. *Mar. Ecol. Prog. Ser.* 241, 255–270. doi: 10.3354/meps241255

DeCandia, A. L., Dobson, A. P., and vonHoldt, B. M. (2018). Toward an integrative molecular approach to wildlife disease. *Conserv. Biol.* 32, 798–807. doi: 10.1111/cobi.13083

Dong, L., Ma, Q., and Whitlock, J. P. Jr. (1997). Down-regulation of major histocompatibility complex Q1b gene expression by 2,3,7,8-tetrachlorodibenzo-p-dioxin. *J. Biol. Chem.* 272, 29614–29619. doi: 10.1074/jbc.272.47.29614

Ehrlenbach, S., Rosales, A., Posch, W., Wilflingseder, D., Hermann, M., Brockmeyer, J., et al. (2013). Shiga toxin 2 reduces complement inhibitor CD59 expression on human renal tubular epithelial and glomerular endothelial cells. *Infect. Immun.* 81, 2678–2685. doi: 10.1128/IAI.01079-12

Esslinger, G. G., Robinson, B. H., Monson, D. H., Taylor, R. L., Esler, D., Weitzman, B. P., et al. (2021). Abundance and distribution of sea otters (Enhydra lutris) in the southcentral Alaska stock, 2014, 2017 and 2019. U.S. Geological Survey Open-File Report 2021–1122, 19.

Estes, J. A., and Duggins, D. O. (1995). Sea otters and kelp forests in Alaska: generality and variation in a community ecological paradigm. *Ecol. Monogr.* 65, 75–100. doi: 10.2307/2937159

Estes, J. A., and Palmisano, J. F. (1974). Sea otters: their role in structuring nearshore communities. *Science* 185, 1058–1060. doi: 10.1126/science.185.4156.1058

Fackelmann, G., and Sommer, S. (2019). Microplastics and the gut microbiome: how chronically exposed species may suffer from gut dysbiosis. *Mar. Pollut. Bull.* 143, 193–203. doi: 10.1016/j.marpolbul.2019.04.030

Fossi, M. C., and Panti, C. (2017). "Sentinel species of marine ecosystems" in *Oxford research encyclopedia of environmental science* (Oxford: Oxford University Press), 27.

Gesto, M., Tintos, A., Soengas, J. L., and Miguez, J. M. (2006). Effects of acute and prolonged naphthalene exposure on brain monoaminergic neurotransmitters in rainbow trout (*Oncorhynchus mykiss*). *Comp. Biochem. Physiol. C* 144, 173–183. doi: 10.1016/j.cbpc.2006.08.002

Goldsby, R. A., Kindt, T. J., Osborne, B. A., and Kuby, J. (2003). *Immunology*, *5th Edn*. New York: WH Freeman and Company.

Graham, A. L., Shuker, D. M., Pollitt, L. C., Auld, S. K. J. R., Wilson, A. J., and Little, T. J. (2011). Fitness consequences of immune responses: strengthening the empirical framework for ecoimmunology. *Funct. Ecol.* 25, 5–17. doi: 10.1111/j.1365-2435.2010.01777.x

Gurish, M. F., Humbles, A., Tao, H., Finkelstein, S., Boyce, J. A., Gerard, C., et al. (2002). CCR3 is required for tissue eosinophilia and larval cytotoxicity after infection with Trichinella spiralis. *J. Immunol.* 168, 5730–5736. doi: 10.4049/jimmunol.168.11.5730

Halpern, B. S., Longo, C., Lowndes, J. S. S., Best, B. D., Frazier, M., Katona, S. K., et al. (2015). Patterns and emerging trends in global ocean health. *PLoS One* 10:e0117863. doi: 10.1371/journal.pone.0117863

Hanisch, S. L., Riley, S. J., and Nelson, M. P. (2012). Promoting wildlife health or fighting wildlife disease: insights from history, philosophy, and science. *Wildl. Soc. Bull.* 36, 477–482. doi: 10.1002/wsb.163

Harley, C. D., Randall Hughes, A., Hultgren, K. M., Miner, B. G., Sorte, C. J., Thornber, C. S., et al. (2006). The impacts of climate change in coastal marine systems. *Ecol. Lett.* 9, 228–241. doi: 10.1111/j.1461-0248.2005.00871.x

Harold, C., and Reed, D. C. (1985). Food availability, sea urchin grazing, and kelp forest community structure. *Ecology* 66, 1160–1169. doi: 10.2307/1939168

Harris, S. G., Padilla, J., Koumas, L., Ray, D., and Phipps, R. P. (2002). Prostaglandins as modulators of immunity. *Trends Immunol.* 23, 144–150. doi: 10.1016/S1471-4906(01)02154-8

Herbert-Read, J. E., Thornton, A., Amon, D. J., Birchenough, S. N., Côté, I. M., Dias, M. P., et al. (2022). A global horizon scan of issues impacting marine and coastal biodiversity conservation. *Nat. Ecol. Evol.* 6, 1262–1270. doi: 10.1038/s41559-022-01812-0

Incardona, J. P. (2017). Molecular mechanisms of crude oil developmental toxicity in fish. *Arch. Environ. Contam. Toxicol.* 73, 19–32. doi: 10.1007/s00244-017-0381-1

Ingraham, J. L., Maaløe, O., and Neidhardt, F. C. (1983). *Growth of the bacterial cell*. Massachusetts: Sinauer Associates.

IPCC (2022). "Climate change 2022: impacts, adaptation, and vulnerability" in *Contribution of working group II to the sixth assessment report of the intergovernmental panel on climate change*. eds. H. O. Pörtner, D. C. Roberts, M. Tignor, E. S. Poloczanska, K. Mintenbeck and A. Alegríaet al. (New York: Cambridge University Press), 3056.

Iwama, G. K., Mathilakath, M. V., Forsyth, R. B., and Ackerman, P. A. (1999). Heat shock proteins and physiological stress in fish. *Am. Zool.* 39, 901–909. doi: 10.1093/icb/39.6.901

Jameson, R. J., Kenyon, K. W., Johnson, A. M., and Wight, H. M. (1982). History and status of translocated sea otter populations in North America. *Wildlife Society Bulletin*, 100–107.

Jenne, D. E., and Tschopp, J. (1989). Molecular structure and functional characterization of a human complement cytolysis inhibitor found in blood and seminal plasma: identity to sulfated glycoprotein 2, a constituent of rat testis fluid. *Proc. Natl. Acad. Sci.* 86, 7123–7127. doi: 10.1073/pnas.86.18.7123

Jennings, K. A., Loder, M. K., and Sheward, W. J. (2006). Increased expression of the 5-HT transporter confers a low-anxiety phenotype linked to decreased 5-HT transmission. *J. Neurosci.* 26, 8955–8964. doi: 10.1523/JNEUROSCI.5356-05.2006

Jo, K., Sung, I., Lee, D., Jang, H., and Kim, S. (2021). Inferring transcriptomic cell states and transitions only from time series transcriptome data. *Sci. Rep.* 11:12566. doi: 10.1038/s41598-021-91752-9

Kenyon, K. W. (1969). The sea otter in the eastern Pacific Ocean. *North American Fauna* 68, 1–352. doi: 10.3996/nafa.68.0001

Keren, L., van Dijk, D., Weingarten-Gabbay, S., Dan Davidi, D., Jona, G., Weinberger, A., et al. (2015). Noise in gene expression is coupled to growth rate. *Genome Res.* 25, 1893–1902. doi: 10.1101/gr.191635.115

Keren, L., Zackay, O., Lotan-Pompan, M., Barenholz, U., Dekel, E., Sasson, V., et al. (2013). Promoters maintain their relative activity levels under different growth conditions. *Mol. Syst. Biol.* 9:701. doi: 10.1038/msb.2013.59

Khalid, N., Aqeel, M., Noman, A., Hashem, M., Mostafa, Y. S., Alhaithloul, H. A., et al. (2021). Linking effects of microplastics to ecological impacts in marine environments. *Chemosphere* 264:128541. doi: 10.1016/j.chemosphere.2020.128541

Kibenge, M. J. T., Munir, K., and Kibenge, F. S. B. (2005). Constitutive expression of Atlantic salmon Mx1 protein in CHSE-214 cells confers resistance to infectious *Salmon Anaemia* virus. *Virol. J.* 2:75. doi: 10.1186/1743-422X-2-75

Klein, E. S., and Thurstan, R. H. (2016). "Acknowledging long-term ecological change: the problem of shifting baselines" in *Perspectives on oceans past*. eds. K. S. Máñez and B. Poulsen (Dordrecht: Springer), 11–29.

Klumpp, S., Zhang, Z., and Hwa, T. (2009). Growth rate-dependent global effects on gene expression in bacteria. *Cells* 139, 1366–1375. doi: 10.1016/j.cell.2009.12.001

Kringel, H., Iburg, T., Dawson, H., Aasted, B., and Roepstorff, A. (2006). A time course study of immunological responses in Trichuris suis infected pigs demonstrates induction of a local type 2 response associated with worm burden. *Int. J. Parasitol.* 36, 915–924. doi: 10.1016/j.ijpara.2006.04.008

Krumm, B., Mengb, X., Lia, Y., Xiangb, Y., and Denga, J. (2008). Structural basis for antagonism of human interleukin 18 by poxvirus interleukin 18-binding protein. *Proc. Natl. Acad. Sci. U. S. A.* 105, 20711–20715. doi: 10.1073/pnas.0809086106

Legendre, P., and Legendre, L. (2012). "Chapter 11: canonical analysis" in *Developments in environmental modelling*. eds. P. Legendre and L. Legendre (Amsterdam: Elsevier), 625–710.

Li, S., Xie, L., Zhang, C., Zhang, Y., and Gu, M. (2004). Cloning and expression of a pivotal calcium metabolism regulator: calmodulin involved in shell formation from pearl oyster (*Pinctada fucata*). *Comp. Biochem. Physiol. B* 138, 235–243. doi: 10.1016/j.cbpc.2004.03.012

Livak, K. J., and Schmittgen, T. D. (2001). Analysis of relative gene expression data using real-time quantitative PCR and the 2(-Delta Delta C(T)) method. *Methods* 25, 402–408. doi: 10.1006/meth.2001.1262

Ma, Q., Geng, Y., Xu, W., Wu, Y., He, F., Shu, W., et al. (2010). The role of translationally controlled tumor protein in tumor growth and metastasis of colon adenocarcinoma cells. *J. Proteome Res.* 9, 40–49. doi: 10.1021/pr9001367

Mann, K. H. (1973). Seaweeds: their productivity and strategy for growth. *Science* 182, 975–981. doi: 10.1126/science.182.4116.975

Martin, L. B., Hopkins, W. A., Mydlarz, L. D., and Rohr, J. R. (2010). The effects of anthropogenic global changes on immune functions and disease resistance. *Trans. NY Acad. Sci.* 1195, 129–148. doi: 10.1111/j.1749-6632.2010.05454.x

McLoughlin, K., Turteltaub, K., Bankaitis-Davis, D., Gerren, R., Siconolfi, L., Storm, K., et al. (2006). Limited dynamic range of immune response gene expression observed in healthy blood donors using RT-PCR. *Mol. Med.* 12, 185–195. doi: 10.2119/2006-00018.McLoughlin

Miles, A. K., Bowen, L., Ballachey, B., Bodkin, J. L., Murray, M., Estes, J. L., et al. (2012). Variations of transcript profiles between sea otters *Enhydra lutris* from Prince William sound, Alaska, and clinically normal reference otters. *Mar. Ecol. Prog. Ser.* 451, 201–212. doi: 10.3354/meps09572

Monson, D. H., McCormick, C., and Ballachey, B. E. (2001). Chemical anesthesia of northern sea otters (*Enhydra lutris*): results of past field studies. *J. Zoo Wildl. Med.* 32, 181–189. doi: 10.1638/1042-7260(2001)032[0181:CAONSO]2.0.CO;2

Murray, M. J. (2015). "Chapter 7 - veterinary medicine and sea otter conservation" in *Sea otter conservation*. eds. S. E. Larson, J. L. Bodkin and G. R. VanBlaricom (Cambridge, MA: Academic Press), 159–195.

Newman, J. R., Ghaemmaghami, S., Ihmels, J., Breslow, D. K., Noble, M., DeRisi, J. L., et al. (2006). Single-cell proteomic analysis of *S. cerevisiae* reveals architecture of biological noise. *Nature* 441, 840–846. doi: 10.1038/nature04785

Niku, J., Brooks, W., Herliansyah, R., Hui, F. K., Taskinen, S., and Warton, D. I. (2019). Efficient estimation of generalized linear latent variable models. *PLoS One* 14:e0216129. doi: 10.1371/journal.pone.0216129

Oesch-Bartlomowicz, B., and Oesch, F. (2005). Phosphorylation of cytochromes P450: first discovery of a posttranslational modification of a drug-metabolizing enzyme. *Biochem. Biophys. Res. Commun.* 338, 446–449. doi: 10.1016/j.bbrc.2005.08.092

Oksjoki, R., Kovanen, P. T., Meri, S., and Pentikainen, M. O. (2007). Function and regulation of the complement system in cardiovascular diseases. *Front. Biosci.* 12, 4696–4708. doi: 10.2741/2419

Paine, R. T. (1966). Food web complexity and species diversity. *Am. Nat.* 100, 65–75. doi: 10.1086/282400

Pauly, D., Christensen, V., Dalsgaard, J., Froese, R., and Torres, F. Jr. (1998). Fishing down marine food webs. *Science* 279, 860–863. doi: 10.1126/science.279.5352.860

Pazos, A. J., Ventoso, P., Martínez-Escauriaza, R., Pérez-Parallé, M. L., Blanco, J., Triviño, J. C., et al. (2017). Transcriptional response after exposure to domoic acid-producing pseudo-nitzschia in the digestive gland of the mussel *Mytilus galloprovincialis*. *Toxicon* 140, 60–71. doi: 10.1016/j.toxicon.2017.10.002

Pedersen, A. B., and Babayan, S. A. (2011). Wild immunology. *Mol. Ecol.* 20, 872–880. doi: 10.1111/j.1365-294X.2010.04938.x

Plested, A. J., and Mayer, M. L. (2007). Structure and mechanism of kainate receptor modulation by anions. *Neuron* 53, 829–841. doi: 10.1016/j.neuron.2007.02.025

Portnoy, D. S., Fields, A. T., Greer, J. B., and Schlenk, D. (2020). "Genetics and oil: transcriptomics, epigenetics, and population genomics as tools to understand animal responses to exposure across different time scales" in *Deep oil spills-facts, fate, and effects*. eds. A. Murawski, C. H. Ainsworth, S. Gilbert, S. D. J. Hollander, C. B. Paris and M. Schlüteret al. (Switzerland: Springer Nature), 515–532.

Post, E., Bhatt, U. S., Bitz, C. M., Brodie, J. F., Fulton, T. L., Hebblewhite, M., et al. (2013). Ecological consequences of sea-ice decline. *Science* 341, 519–524. doi: 10.1126/science.1235225

Power, M. E., Tilman, D., Estes, J. A., Menge, B. A., Bond, W. J., Mills, L. S., et al. (1996). Challenges in the quest for keystones: identifying keystone species is difficult-but essential to understanding how loss of species will affect ecosystems. *Bioscience* 46, 609–620. doi: 10.2307/1312990

Pulido, O. M. (2008). Domoic acid toxicologic pathology: a review. *Mar. Drugs* 6, 180–219. doi: 10.3390/md20080010

Quintana, F. J., Basso, A. S., Iglesias, A. H., Korn, T., Farez, M. F., Bettelli, E., et al. (2008). Control of T(reg) and T(H)17 cell differentiation by the aryl hydrocarbon receptor. *Nature* 453, 65–71. doi: 10.1038/nature06880

R Development Core Team (2012). R: A language and environment for statistical computing. Vienna, Austria, R Foundation for Statistical Computing. Available at: http://www.R-project.org/ (Accessed October 12, 2022)

Raisuddin, S., Kwok, K. W. H., Leung, K. M. Y., Schlenk, D., and Lee, J. (2007). The copepod Tigriopus-a promising marine model organism for ecotoxicology and environmental genomics. *Aquat. Toxicol.* 83, 161–173. doi: 10.1016/j.aquatox.2007.04.005

Rapport, D. J. (2007). Sustainability science: an ecohealth perspective. *Sustain. Sci.* 2, 77–84. doi: 10.1007/s11625-006-0016-3

Rigopoulou, E. I., Abbott, W. G., Haigh, P., and Naoumov, N. V. (2005). Blocking of interleukin-10 receptor—a novel approach to stimulate T-helper cell type 1 responses to hepatitis C virus. *Clin. Immunol.* 117, 57–64. doi: 10.1016/j.clim.2005.06.003

Shalbuyeva, N., Brustovetsky, T., Bolshakov, A., and Brustovetsky, N. (2006). Calcium-dependent spontaneously reversible remodeling of brain mitochondria. *J. Biol. Chem.* 281, 37547–37558. doi: 10.1074/jbc.M607263200

Skrondal, A., and Rabe-Hesketh, S. (2004). *Generalized latent variable modeling: Multilevel, longitudinal, and structural equation models*. New York: Chapman and Hall/CRC.

Snape, J. R., Maund, S. J., Pickford, D. B., and Hutchinson, T. H. (2004). Ecotoxicogenomics: the challenge of integrating genomics into aquatic and terrestrial ecotoxicology. *Aquat. Toxicol.* 67, 143–154. doi: 10.1016/j.aquatox.2003.11.011

Spitz, J., Becquet, V., Rosen, D. A. S., and Trites, A. W. (2015). A nutrigenomic approach to detect nutritional stress from gene expression in blood samples drawn from Steller Sea lions. *Comp. Biochem. Phys. A* 187, 214–223. doi: 10.1016/j.cbpa.2015.02.006

Squire, L., Berg, D., Bloom, F. E., du Lac, S., Ghosh, A., and Spitzer, N. C.. (2008). *Fundamental neuroscience*. Amsterdam: Elsevier Academic Press.

Sriram, K., Lin, G. X., Jefferson, A. M., McKinney, W., Jackson, M. C., Cumpston, J. L., et al. (2022). Biological effects of inhaled crude oil vapor V. altered biogenic amine neurotransmitters and neural protein expression. *Toxicol. Appl. Pharmacol.* 449:116137. doi: 10.1016/j.taap.2022.116137

Strandin, T., Babayan, S. A., and Forbes, K. M. (2018). Reviewing the effects of food provisioning on wildlife immunity. *Philos. Trans. R. Soc. B: Biol. Sci.* 373:20170088. doi: 10.1098/rstb.2017.0088

Tabuchi, M., Veldhoen, N., Dangerfield, N., Jeffries, S., Helbing, C. C., and Ros, P. S. (2006). PCB-related alteration of thyroid hormones and thyroid hormone receptor gene expression in free-ranging harbor seals (*Phoca vitulina*). *Environ. Health Perspect.* 114, 1024–1031. doi: 10.1289/ehp.8661

Tanabe, S., Iwat, H., and Tatsukawa, R. (1994). Global contamination by persistent organochlorines and their ecotoxicological impact on marine mammals. *Sci. Total Environ.* 154, 163–177. doi: 10.1016/0048-9697(94)90086-8

Taniguchi, Y., Choi, P. J., Li, G. W., Chen, H., Babu, M., Hearn, J., et al. (2010). Quantifying *E. coli* proteome and transcriptome with single-molecule sensitivity in single cells. *Science* 329, 533–538. doi: 10.1126/science.1188308

Thacker, T. C., Palmer, M. V., and Waters, W. R. (2007). Associations between cytokine gene expression and pathology in *Mycobacterium bovis* infected cattle. *Vet. Immunol. Immunop.* 119, 204–213. doi: 10.1016/j.vetimm.2007.05.009

Tinker, M. T., Bentall, G., and Estes, J. A. (2008). Food limitation leads to behavioral diversification and dietary specialization in sea otters. *P. Natl. A. Sci.-Biol.* 105, 560–565. doi: 10.1073/pnas.0709263105

Tinker, M. T., Bodkin, J. L., Bowen, L., Ballachey, B., Bentall, G., Burdin, A., et al. (2021). Sea otter population collapse in Southwest Alaska: assessing ecological covariates, consequences, and causal factors. *Ecol. Monogr.* 91:e01472. doi: 10.1002/ecm.1472

Tracy, A. M., Pielmeier, M. L., Yoshioka, R. M., Heron, S. F., and Harvell, C. D. (2019). Increases and decreases in marine disease reports in an era of global change. *Proc. R. Soc. B* 286:20191718. doi: 10.1098/rspb.2019.1718

Trego, M. L., Whitehead, A., Kellar, N. M., Lauf, M., and Lewison, R. L. (2019). Tracking transcriptomic responses to endogenous and exogenous variation in cetaceans in the Southern California bight. *Conserv. Physiol.* 7:coz018. doi: 10.1093/conphys/coz018

Tsai, M. J., and O'Malley, B. W. (1994). Molecular mechanisms of action of steroid/thyroid receptor superfamily members. *Annu. Rev. Biochem.* 63, 451–486. doi: 10.1146/annurev.bi.63.070194.002315

Tsan, M., and Gao, B. (2004). Cytokine function of heat shock proteins. *Am. J. Physiol Cell. Physiol.* 286, C739–C744. doi: 10.1152/ajpcell.00364.2003

Tumpey, T. M., Szretter, K. J., Van Hoeven, N., Katz, J. M., Kochs, G., Haller, O., et al. (2007). The Mx1 gene protects mice against the pandemic 1918 and highly lethal human H5N1 influenza viruses. *J. Virol.* 81, 10818–10821. doi: 10.1128/JVI.01116-07

Tuynder, M., Fiucci, G., Prieur, S., Lespagnol, A., Géant, A., Beaucour, S., et al. (2004). Translationally controlled tumor protein is a target of tumor reversion. *Proc. Natl. Acad. Sci.* 101, 15364–15369. doi: 10.1073/pnas.0406776101

Tyack, P. L., Thomas, L., Costa, D. P., Hall, A. J., Harris, C. M., Harwood, J., et al. (2022). Managing the effects of multiple stressors on wildlife populations in their ecosystems: developing a cumulative risk approach. *Proc. R. Soc. B* 289:20222058. doi: 10.1098/rspb.2022.2058

Tyson, C. B., Lord, P. G., and Wheals, A. E. (1979). Dependency of size of *Saccharomyces cerevisiae* cells on growth rate. *J. Bacteriol.* 138, 92–98. doi: 10.1128/jb.138.1.92-98.1979

Veldhoen, M., Hirota, K., Westendorf, A. M., Buer, J., Dumoutier, L., Renauld, J. C., et al. (2008). The aryl hydrocarbon receptor links TH17-cell-mediated autoimmunity to environmental toxins. *Nature* 453, 106–109. doi: 10.1038/nature06881

Vera-Massieu, C., Brock, P. M., Godínez-Reyes, C., and Acevedo-Whitehouse, K. (2015). Activation of an inflammatory response is context-dependent during early development of the California Sea lion. *R. Soc. Open Sci.* 2:150108. doi: 10.1098/rsos.150108

Wang, L., Liang, X. F., Zhang, W. B., Mai, K. S., Huang, Y., and Shen, D. (2009). Amnesic shellfish poisoning toxin stimulates the transcription of CYP1A possibly through AHR and ARNT in the liver of red sea bream *Pagrus major*. *Mar. Pollut. Bull.* 58, 1643–1648. doi: 10.1016/j.marpolbul.2009.07.004

Wegner, K. M., Kalbe, M., Rauch, G., Kurtz, J., Schaschl, H., and Reusch, T. B. H. (2006). Genetic variation in MHC class II expression and interactions with MHC sequence polymorphism in three-spined sticklebacks. *Mol. Ecol.* 15, 1153–1164. doi: 10.1111/j.1365-294X.2006.02855.x

Weiße, A. Y., Oyarzún, D. A., Danos, V., and Swain, P. S. (2015). Mechanistic links between cellular trade-offs, gene expression, and growth. *Proc. Natl. Acad. Sci.* 112, E1038–E1047. doi: 10.1073/pnas.1416533112

Wendell, F. E., Pattison, C. A., and Harris, M. D. (1996). Sea otter, Enhydra lutris, containment management: Field studies and feasibility assessment. California Department of Fish and Game Marine Resources Division. Available at: http://hdl.handle.net/1834/18339 (Accessed November 3, 2022)

Wobeser, G. A. (2013). *Essentials of disease in wild animals*. New York: John Wiley & Sons.

Zheng, S., Song, Y., Qiu, X., Sun, T., Ackland, M. L., and Zhang, W. (2008). Annetocin and TCTP expressions in the earthworm *Eisenia fetida* exposed to PAHs in artificial soil. *Ecotoxicol. Environ. Saf.* 71, 566–573. doi: 10.1016/j.ecoenv.2007.10.025

frontiers | Frontiers in Ecology and Evolution

TYPE Original Research
PUBLISHED 24 July 2023
DOI 10.3389/fevo.2023.1158265

EDITED BY
Karen Thorne,
United States Geological Survey (USGS),
United States

REVIEWED BY
Carl R. Gosper,
Conservation and Attractions
(DBCA), Australia
Rachel Mitchell,
University of Arizona, United States

*CORRESPONDENCE
Emma C. Underwood
eunderwoodrussell@ucdavis.edu

RECEIVED 03 February 2023
ACCEPTED 01 June 2023
PUBLISHED 24 July 2023

CITATION
Underwood EC, Sorenson QM, Schrader-Patton CC, Molinari NA and Safford HD (2023) Assessing spatial and temporal variation in obligate resprouting, obligate seeding, and facultative seeding shrub species in California's Mediterranean-type climate region. *Front. Ecol. Evol.* 11:1158265. doi: 10.3389/fevo.2023.1158265

Assessing spatial and temporal variation in obligate resprouting, obligate seeding, and facultative seeding shrub species in California's Mediterranean-type climate region

Emma C. Underwood[1]*, Quinn M. Sorenson[1], Charlie C. Schrader-Patton[2], Nicole A. Molinari[3] and Hugh D. Safford[1,4]

[1]Department of Environmental Science and Policy, University of California, Davis, Davis, CA, United States, [2]RedCastle Resources, Inc., Contractor to: US Department of Agriculture Forest Service Western Wildlands Environmental Threat Assessment Center (WWETAC), Bend, OR, United States, [3]US Department of Agriculture Forest Service, Los Padres National Forest, Solvang, CA, United States, [4]Vibrant Planet, Incline Village, NV, United States

Mediterranean-climate region (MCR) shrublands have evolved a set of regeneration strategies in response to periodic, high intensity wildfires: obligate seeding (OS), obligate resprouting (OR), and facultative seeding (FS) species. In the North American MCR, data on their spatial and temporal variability is currently lacking, which is a significant information gap for resource managers. We developed a multinomial model using dynamic and static variables to predict the distribution of the three shrub post-fire regeneration strategies, plus trees and herbs, in southern California. Cross-validation showed 50% of the predicted values for each of the five plant groups were within 8–24 percent of the actual value. We assessed variation in shrub regeneration strategies in three ways. First, we found the three major shrub community types (mixed chaparral, chamise-redshank chaparral, and coastal sage scrub) had proportionally greater biomass of FS (37–43% of total biomass) than OR or OS. Second, we assessed the spatial variability using (a) moisture availability (climatic water deficit and solar radiation) and found FS accounted for an increasingly greater proportion of total aboveground live biomass as water became limited, while OR biomass decreased; and (b) ecosystem productivity (NDVI) which showed the proportion of OS, OR, and tree biomass increased with productivity (with a corresponding dramatic decrease in herb biomass). We also assessed temporal variability using time since fire and found OS represented an initially small proportion of total biomass immediately post-fire (8–10%) which increased with time since fire (13–17%). Third, spatial outputs from the multinomial model indicated FS dominated pixels were most widely distributed across the study area (~3.4 million ha, 71%), compared to OR and OS covering 5% each. FS also occurred more frequently on warmer, south facing slopes and summits whereas OR preferred cooler, north facing slopes and valleys ($p < 0.0001$). Better understanding the distribution of OS, OR, and FS shrubs is important for resource management, including quantifying shrubland carbon storage and identifying areas for post-fire restoration, as described in a case study of the Bobcat Fire on the Angeles National Forest.

KEYWORDS

biomass, climatic water deficit, national forests, NDVI, resource management, solar radiation, time since last fire, wildfire

Introduction

All of the world's Mediterranean-climate regions (MCRs) are characterized by expansive evergreen, sclerophyllous shrublands known by a variety of regional names including fynbos in South Africa, kwongan in western Australia, and case chaparral in the North American MCR. These shrubland ecosystems are highly species diverse (Cowling et al., 1996; Rundel, 2018) and – except in Chile, where fire was largely absent before European settlement – they are also characterized by a set of shared regeneration strategies driven by adaptation to intense wildfire (Bond and Midgley, 2001; Bond and Midgley, 2003; Keeley et al., 2011; Clarke et al., 2015; Keeley and Safford, 2016). These regeneration strategies include fire-stimulated germination of soil-stored seeds, serotiny, and resprouts from apical, basal, epicormic, or underground structures (Clarke et al., 2013; Lawes et al., 2022).

In the ecological literature, shrub species exhibiting different combinations of these syndromes are typically placed in three groups (Keeley, 1991). "Obligate seeders" (OS) are shrub taxa that have lost the ability to resprout – which is a trait of most woody angiosperm taxa – but whose seed germination is stimulated by fire (this group technically includes serotinous taxa, which are not found in shrubs in the North American MCR but rather in some associated conifer tree taxa). "Obligate resprouters" (OR) are taxa that lack fire-stimulated seed germination and rely entirely on resprouting to regenerate after fire; the OR group includes taxa with and without specialized underground storage structures. A third group, "facultative seeders" (FS), is composed of taxa whose post-fire regeneration occurs *via* resprouting as well as *via* fire-stimulated seedling recruitment. The evolutionary relationships between these groups are incompletely understood. Resprouting post-fire is thought to be an ancestral trait across woody plants, with facultative seeding derived from resprouting species (Bond and Midgley, 2003; Pausas and Keeley, 2014). Non-resprouting obligate seeders are hypothesized to be subsequently derived from facultative seeders within lineages of resprouters experiencing reliably intense, but relatively infrequent, fires (Pausas and Keeley, 2014).

Spatial variation of different regeneration strategies is seen at multiple spatial scales. At a global scale, resprouting has a strong relationship with productivity (Pausas and Bradstock, 2007; Clarke et al., 2015). For example, in a study in Australia, Lawes et al. (2022) recorded an increase in resprouting ability with higher productivity (rainfall, primary productivity), albeit mediated by fire regimes. More productive environments provided ample resources for the provision and protection of resprouting organs and/or provide a selective force through relatively frequent disturbance by fires (Gosper et al., 2019). Alternatively, obligate seeding is strongly associated with aridity and vegetation prone to infrequent but intense crown fires – such as heath in Australia (Bellingham and Sparrow, 2000; Bond and Midgley, 2001; Bond and Midgley, 2003; Pausas and Keeley, 2014; Lawes et al., 2022). At a finer spatial resolution, within shrubland ecosystems in California, Meentemeyer et al. (2001) found shrub abundance at the landscape scale most strongly associated with annual soil moisture and solar radiation. OR species were found to have a higher abundance in mesic environments: their non-refractory seeds generally germinate during longer fire-free intervals on sheltered, north facing slopes with moist, cool, shaded soil conditions with ample litter (Gordon and White, 1994; Meentemeyer et al., 2001). In addition, OR seeds are short-lived, do not accumulate in the seedbank, and are sensitive to higher temperatures (Keeley, 1991). OR species develop deep, extensive root systems to avoid drought stress (Poole and Miller, 1975). In contrast, OS species have a higher abundance in xeric environments, with shallow roots which must survive summer water stress in the first year of growth. In southern Australia, for example, Clarke et al. (2015) found proportionally more obligate seeders in drier Mediterranean to semi-arid climates. The ability for OS to survive dry periods has been attributed to highly sclerophyllous leaves, cryptic stomata, and the resistance of stem xylem to water stress-induced embolism (Davis et al., 1999; Meentemeyer and Moody, 2002; Jacobson et al., 2007).

In turn, different regeneration strategies, and their relative proportions, confer different levels of shrub environmental fitness, influencing the resilience of ecosystems to disturbance from fire (Bellingham and Sparrow, 2000; Bond and Midgley, 2003). In post-fire environments with suitable moisture conditions, OR shrubs can respond with vigorous and aggressive resprouting from surviving biomass (often belowground). For example, in the California MCR, OR quickly refill the space previously occupied by the mature plant and can reach reproductive maturity sooner than OS and even FS species (which do not resprout as vigorously as OR under good site conditions), demonstrating little demographic change post-fire (Keeley, 1986). This post-fire advantage has been attributed to deep roots, high root-to-shoot ratios, and high nutrient stores in the root and root crown (Desouza et al., 1986), which allows for rapid recovery and resprouting of OR post-fire. Recovery of FS and OS from seed is typically delayed until the rainy season when germination is triggered. OS recruitment is largely restricted to the first-year post-fire which produces an even-aged cohort that suffers extreme mortality after fire (Keeley, 1986). Seedlings of OS establish more successfully post-fire than seedlings of FS as OS have greater tolerance to water stress (Keeley and Zedler, 1978; Jacobson et al., 2007) and because FS species also resprout, making them more successful post-fire regenerators under most conditions. Note that for OS species, the longer time to maturity and slow accumulation of seed in the seed bank presents an immaturity risk in instances of short fire intervals (Zedler, 1995; Enright et al., 1998).

Consequently, excessive short interval, frequent fire in California has a major influence on shrubland dynamics and on the distribution of regeneration strategies (Syphard et al., 2018; Safford et al., 2022). Southern California experiences very high ignition densities associated with expanding human development and increasing cover of highly flammable invasive grasses. Short interval fires (specifically time since last fire) can have major impacts on the reproductive ability and regeneration potential of shrubs. For example, most post-fire obligate seeding *Ceanothus* species are negatively impacted by time since last fire of <10 years, while obligate seeding *Arctostaphylos* species require much longer fire return intervals (Keeley and Davis, 2007). These negative impacts of short interval, high frequency fire on OS species are multiplied as subsequent fires occur, and the seed pool is progressively reduced, with consequences for population growth and genetic variability of OS (Zedler et al., 1983; Clarke et al., 2015). Very high fire frequencies can lead to local extirpation of OS species, resulting in the increased dominance of (often non-native) grasses and forbs, which then feeds back into even more frequent fire (Franklin, 2002; Syphard et al., 2018).

Understanding spatial and temporal variation in the distribution of OR, OS, and FS species will allow resource managers to better predict vegetation response and prioritize management activities that aid the recovery from ecosystem disturbances and stressors, such as short interval fire and drought. This is especially valuable in southern California, where shrublands account for more than half of the vegetation of four federally-managed National Forests and where resource managers are actively engaged in managing wildfires, addressing non-native annual species, planning for a warmer and drier climate, and attempting to maximize and balance a variety of ecosystem services (Safford et al., 2018; USFS, 2022). In addition, an improved understanding of the spatial variation in shrub regeneration strategies can support the quantification of belowground, standing dead, and litter carbon pools in shrublands whose carbon storage and sequestration capacities have traditionally been ignored or undervalued (Langley et al., 2002; Jenerette et al., 2018; Underwood et al., 2018).

In this study, we describe the development of a multinomial model to predict the relative biomass proportions of five plant groups – three shrub regeneration types (OR, OS, and FS), and herb and tree life forms – across the southern California ecoregion. Previous attempts to determine the distribution of species with different regeneration strategies have relied on temperature, annual precipitation, solar radiation, slope, topographic moisture index and soil type (Syphard and Franklin, 2010), or soil moisture and substrate rockiness (Meentemeyer et al., 2001). Here, we build on previous efforts by increasing the number of environmental variables to consider both static and dynamic predictors, using field plots with high spatial accuracy to train our model, and generating data over a larger spatial area.

Using the results from our model, in this contribution we: (a) describe variation in the proportions of OS, FS, OR, herb and tree by three shrub community types (mixed chaparral, chamise redshank chaparral and coastal sage scrub); (b) assess the influence of two moisture – related variables (climatic water deficit and solar radiation), productivity (NDVI) and temporal variation in time since last fire; (c) quantify spatial variation in regeneration strategies at the landscape scale; and finally (d) to highlight the implications of our results for resource managers, we provide a case study of the Bobcat Fire on the Angeles National Forest describing the use of OS data to support decision making.

Materials and methods

Study area

Our study area consists of shrublands within a 31,069 km^2 (7,677,317 acres) footprint that encompasses all Level 4 USGS ecoregions (Omernik and Griffith, 2014) that overlap with the Angeles, Cleveland, Los Padres, and San Bernardino National Forests in southern California, USA, ranging from sea level to 3,506 m. National forest lands account for over 50% of the study area (15,920 km^2 or 3,933,992 ac). The region is characterized by a Mediterranean-type climate with a warm to hot dry season and a cool wet season of three to five months. Vegetation physiognomic types in the study region are dominated by shrubland [62% (determined using FVEG; FRAP, 2015)], grassland (16%), broadleaf woodland (8%), and conifer and mixed conifer-broadleaf forests (8%). We base our vegetation type delineations on the California Wildlife Habitat Relations classification (Barbour et al., 2007; https://wildlife.ca.gov/Data/CWHR/Wildlife-Habitats), which is widely used in California. In shrublands the major communities are mixed chaparral (29%; dominated by scrub oak [*Quercus berberidifolia*], various species of *Ceanothus* and manzanita [*Arctostaphylos*], and other mostly resprouting shrub species); sage scrub (12%; dominated by California sagebrush [*Artemisia californica*], purple sage [*Salvia leucophylla*], black sage [*Salvia mellifera*], and California buckwheat [*Eriogonum fasiculatum*]); and chamise/redshank chaparral (6%; dominated by chamise [*Adenostoma fasciculatum*] and/or redshank [*Adenostoma sparsifolium*]). The chaparral-dominated communities (evergreen, sclerophyllous shrubs), are found at higher elevations while coastal sage scrub (drought-deciduous, soft-leaved shrubs) are found at lower elevations and inland desert margins with lower precipitation and shorter growing seasons (Gray, 1982).

Plot data

To estimate the proportion of biomass for shrubs with different regeneration strategies we used plot data from the USDA Forest Service Forest Inventory and Analysis (FIA) program (Burkman, 2005). We analyzed 222 of the 434 total FIA plots available omitting 212 owing to incomplete data, occurrence within uncommon vegetation types (defined as <1% of the study area, FRAP, 2015), or insufficient sample size (i.e., where there were <10 plots in a vegetation type). Many of these less common vegetation types were dominated by trees with limited shrub abundance, e.g., CWHR types blue-oak foothill pine, Eastside pine, Ponderosa Pine, valley foothill riparian, redwood, sierra mixed conifer, and coastal oak woodland. We also removed any plot that had more than 90% of total biomass comprised of trees to avoid the possibility of including plots that were misclassified as shrublands. One note, is the FIA program is designed to measure forest conditions across the US and therefore does not typically include non-forest plots, but the National Forests in southern California extended the FIA sampling to include shrubland plots. Since coastal and desert scrub communities are not well represented on Forest Service lands in southern California, OS present in these communities may be underrepresented in the plots.

FIA plots are comprised of four, 14.64-m diameter circular subplots arranged triangularly with one subplot at plot center and 3 subplots positioned 36.6 m from plot center at angles of 0°, 120° and 240° (Burkman, 2005). FIA permanent plots are remeasured periodically with the goal of a complete remeasurement of all plots every ten years (https://frap.fire.ca.gov/research-monitoring/forest-inventory-and-analysis/), thus 10% of the plots are visited each year. The plots used in this study were visited in 2001, 2002, 2004, 2008, 2010 or 2012. Plot measurements included species, crown diameter, and height of all individual shrubs in each subplot. To estimate shrub aboveground biomass, we applied species-specific allometric equations to shrub species where possible (Wakimoto, 1978; McGinnis et al., 2010), otherwise, we used a generalized shrub-herb biomass equation (Lutes et al., 2006, see Schrader-Patton and Underwood, 2021 for details).

We assigned each species in the FIA plot to one of three lifeform categories: shrub, tree or herb (forbs and grasses). Shrub species (the focus of this current study) were further categorized into one of three post-fire regeneration strategies: obligate seeder (OS), facultative seeder (FS), or obligate resprouter (OR) using descriptions of regeneration strategy and life history reported in primary literature and public databases (Gordon and White, 1994; Borchert et al., 2004; CNPS, 2021; FEIS, 2021). For each plot, we calculated the proportion of aboveground live biomass for each of these five plant groups: OS, FS, OR, tree, and herb, by dividing the estimated biomass of each by the summed total biomass across all groups.

Predicting the distribution and variation of shrub regeneration strategies

To predict the distribution of the three shrub regeneration strategies (OS, FS, OR), along with trees and herbs, we modeled changes in the proportion of biomass within each regeneration strategy using a multinomial regression model in the statistical software R (R Core Team, 2016) with the package 'nnet' (Ripley and Venables, 2021).

We analyzed the following variables using the function *multinom* to predict the distribution of the five plant groups: average annual solar radiation, actual evapotranspiration (AET), climate water deficit (CWD), average annual precipitation, the normalized difference vegetation index (NDVI, using the maximum composite value from July to August each year), modeled aboveground biomass (a proxy for productivity), eastness (a measure of continentality and dryness), slope, flow accumulation, soil bulk density, soil clay content, and soil percent carbon (see Table S1). Finally, we included vegetation type from the CWHR classification system from the FVEG vegetation data (FRAP, 2015) and time since last fire from the Fire Return Interval Departure geodatabase (Safford and Van de Water, 2014; USDA, 2015). We selected time since last fire rather than, for example, average fire return interval, as we wanted to account for the transition from early seral fire-following species to the dominance of other regeneration strategies over time. The time since last fire temporal variable was calculated for each plot by first intersecting the plot with the fire perimeter data obtained (https://frap.fire.ca.gov/frap-projects/fire-perimeters/). Next, we subtracted the year of the most recent fire from the year the FIA plot was visited.

To avoid variance inflation, we did not include variables that were strongly correlated ($r > 0.55$). We considered the predictor variables northness and elevation but excluded them because they were closely correlated ($r > 0.57$) with other variables (solar radiation, AET, and CWD). We retained solar radiation, AET, and CWD because they are more mechanistically linked to water stress and productivity (Stephenson, 1998). Total aboveground biomass, flow accumulation, time since fire were natural-log transformed to improve model fit. To reduce the number of parameters included, we only tested interactions that were biologically meaningful, such as an interaction between CWD and solar radiation.

To select the best model, we started with a full model and removed predictors sequentially using Akaike Information Criteria (AIC) to evaluate model fit. Predictor variables remained in the final model if they improved model fit by a minimum ΔAIC of -2 (Anderson and Burnham, 2004). For the final model, p-values were generated with a Wald-z test. Obligate seeder shrubs were selected as the baseline variable for the multinomial model against which the other four plant groups are calculated (therefore OS are not displayed in Results). We chose OS as a baseline because our focus was on determining differences among different shrub regeneration strategies and we expected OS to differ most from FS and OR. The p-values reported (Table 1) for FS, OR, tree and herb indicate how likely the estimate is different from 0, i.e., relative to OS. To evaluate the performance of the final model, we performed leave-k-out cross validation with $k = 8$ (Hastie et al., 2009, see code in Supplementary Material). To do this, we randomly withheld eight observations from the dataset, refit the model, and evaluated the difference between predicted and observed values of

TABLE 1 Model estimates (log-odds) from the final multinomial model and standard error.

	Facultative Seeder			Obligate Resprouter			Tree			Herb		
	Est.	Std. Error	P	Est.	Std. Error	p	Est.	Std. Error	p	Est.	Std. Error	P
Intercept	0.816	0.063	<0.0E+13	0.069	0.074	3.54E-01	−1.745	0.130	<0.0E+13	0.030	0.074	6.90E-01
CWHR-Coastal Scrub	0.758	0.136	2.47E-08	1.167	0.154	3.40E-14	1.517	0.202	6.62E-14	0.409	0.147	5.41E-03
CWHR-Mixed Chaparral	0.190	0.069	5.86E-03	0.515	0.080	1.31E-10	1.422	0.134	<0.0E+13	0.011	0.081	8.97E-01
CWHR-Chamise Redshank Chaparral	0.541	0.188	4.02E-03	−0.439	0.218	4.44E-02	−0.466	0.252	6.46E-02	0.288	0.220	1.89E-01
Time Since Fire (ln+1)	−0.477	0.033	<0.0E+13	−0.572	0.035	<0.0E+13	−0.496	0.039	<0.0E+13	−0.622	0.036	<0.0E+13
Total Aboveground Biomass (ln)	0.128	0.035	2.48E-04	0.105	0.038	6.36E-03	1.810	0.054	<0.0E+13	0.312	0.043	2.48E-13
Average Annual Solar Radiation	0.236	0.028	<0.0E+13	−0.221	0.029	5.91E-14	0.167	0.035	1.39E-06	0.019	0.034	5.71E-01
Average Annual Precipitation	−0.303	0.039	4.44E-15	−0.194	0.041	2.09E-06	−0.366	0.050	2.91E-13	−0.147	0.045	1.12E-03
Actual Evapotranspiration (AET)	−0.044	0.034	2.01E-01	−0.350	0.037	<0.0E+13	−0.439	0.042	<0.0E+13	0.332	0.042	3.55E-15
Climate Water Deficit (CWD)	−0.037	0.041	3.57E-01	−0.372	0.044	<0.0E+13	−0.421	0.051	2.22E-16	−0.323	0.049	3.21E-11
Normalized Difference Vegetation Index (NDVI)	−0.158	0.036	1.35E-05	0.009	0.039	8.29E-01	0.018	0.045	6.94E-01	−0.777	0.044	<0.0E+13
Aspect-Eastness	0.173	0.024	1.03E-12	0.095	0.027	4.43E-04	0.274	0.032	<0.0E+13	0.175	0.029	1.39E-09
Slope	0.036	0.028	2.03E-01	−0.058	0.031	6.13E-02	0.221	0.037	1.76E-09	0.051	0.034	1.34E-01
Soil Bulk Density	0.062	0.040	1.21E-01	−0.319	0.044	4.81E-13	0.267	0.052	2.45E-07	0.335	0.048	2.22E-12
% Clay	−0.250	0.028	<0.0E+13	−0.201	0.031	1.22E-10	0.518	0.040	<0.0E+13	−0.074	0.033	2.42E-02
‰ Carbon	0.083	0.045	6.50E-02	−0.318	0.050	2.53E-10	−0.539	0.055	<0.0E+13	0.034	0.053	5.29E-01
Flow accumulation (ln)	0.082	0.030	5.64E-03	0.093	0.032	4.02E-03	0.241	0.035	3.77E-12	0.133	0.034	9.39E-05
Solar Radiation: Precipitation	−0.050	0.029	8.30E-02	−0.085	0.028	2.74E-03	−0.412	0.032	<0.0E+13	−0.085	0.033	1.06E-02

Obligate seeder (OS) shrubs were selected as the baseline variable for the multinomial model against which the other four classes are calculated against, therefore OS are not displayed. P-values were generated by Wald-z tests.

the excluded observations. This procedure was iterated 3,000 times to generate a distribution of model accuracy. To fully evaluate the predictive accuracy and fit of the model, we examined the distribution of cross-validation errors: mean, standard deviation, kurtosis, skew, and interquartile range.

We then used the raster surfaces corresponding to each predictor (Table S1) as model inputs into the 'predict' function in R software (R Core Team, 2016). We created a raster spatial layer (30 m resolution) with the proportion of biomass for each of the five plant groups. This process essentially applies the model predictions of the proportion of each plant group to each pixel in our study area. Finally, to investigate distribution patterns of the three types of shrub regeneration strategies across southern California, we created three raster outputs based on a query of: shrub proportion in a pixel is >33% and where OS or FS or OR is >33%, to identify pixels dominated by shrubs with different regeneration strategies.

Using these data, we report on variation in shrub regeneration strategies by the following three areas: first, we assessed variation in the five groups across the three major CWHR shrub communities in southern California: mixed chaparral, chamise redshank chaparral, and coastal sage scrub (https://wildlife.ca.gov/Data/CWHR/Wildlife-Habitats), by estimating the proportion of OR, OS, FS, trees, and herbs as predicted from the model while holding all other variables at their median value. Second, to examine influence of water availability and time in explaining the variation of shrub regeneration types across the landscape, we calculated the proportion of biomass in the five groups in response to two moisture-related variables (climatic water deficit and solar radiation) and productivity (NDVI), and time since last fire. Third, we summarized the distribution of shrub regeneration types at the landscape scale. We tested for differences in the mean proportion of shrub reproductive strategy using a linear regression (using *lm* function in the 'stats' package in R, R Core Team, 2016) to assess differences in the dominance of OR and OS between warmer, south facing slopes, summits and ridges, and cooler, north facing slopes, valleys and depressions by calculating the mean average value of OS, FS, and OR by topographic facet (vegetation x aspect x topographic units; Hollander and Underwood, 2021). Model performance assumptions were checked for residual normality and homoscedasticity, and P-values were corrected using the Tukey method.

Results

The final selected model for determining the biomass of the five plant groups included vegetation type, time since fire), estimated aboveground live biomass, NDVI, slope, eastness, AET, CWD, flow accumulation, soil bulk density, percent clay, carbon (grams per kg of fine earth soil), and the interaction between mean annual solar radiation and mean annual precipitation (Figure S1; Tables 1, 2). Cross validation indicated that the model can predict the relative proportion of biomass represented by each of the five plant groups (OS, FS, OR, tree and herb) with 50% of predictions falling within 5 to 24 percent of the actual value depending on the type of regeneration strategy, as shown by the interquartile ranges (Table 3). Of the shrub regeneration strategies, OS are best predicted, with the narrowest interquartile range of −4.98–11.42%, while FS and OR showed a broader range of prediction with interquartile ranges of −19.7–23.3%, and −14.8–16.5% respectively. Trees and herbs had more narrow ranges of predictability with interquartile ranges of 0.50–4.83% and −4.11–10.1%, respectively (Table 3; Figure 1). All five plant groups had a high level of accuracy, with the error distribution closely centered around 0 (−0.57 to 1.24, Table 3).

Variation of the five plant groups within three shrub communities

We found FS biomass dominated in the three shrub communities – mixed chaparral, chamise redshank chaparral, and coastal sage scrub – accounting for 37%, 41% and 43% respectively of the total biomass (Figure 2). There was slightly more OS than OR biomass (20% versus 16%) in chamise redshank chaparral, and slightly more OR than OS biomass (20% versus 15%) in mixed chaparral. However, OR biomass was proportionally greater (25%) than OS (10%) in coastal sage scrub. Among vegetation types, model outputs indicated tree biomass is greatest in mixed chaparral (13%) and herb biomass greatest in chamise redshank chaparral (18%, Figure 2) compared to the other two shrub communities.

Influence of time since fire, water availability, and productivity on the proportion of each shrub regeneration strategy

The influence of time since fire across all shrub communities was most notable for OS species. OS represent a small fraction of biomass immediately after fire, but this increased steeply (from an average of 5% to an average of 18%) in the first 25 years post-fire, and then more gradually as time since fire increased (Figure 3A). A closer examination of the first 25 years post-fire shows the relative proportions of OS, FS and OR is similar in the first two decades post-fire [with the exception of OS biomass in chamise redshank chaparral, which increased more rapidly than OS in mixed chaparral or coastal sage scrub (Figure S2)]. All other groups decreased slightly to account for the increase in OS biomass, and OR and herb decreased most sharply during the first decade post-fire. The proportion of FS biomass on the landscape dominated all time points following fire compared to the other plant groups and stayed relatively constant over time, accounting for 35%–38% of the total biomass.

We found a similar response of shrub regeneration strategies to two indicators of water availability, CWD and solar radiation. As CWD increased (less available water), FS and OS accounted for an increasingly greater proportion of the total biomass (Figure 3B), with the inverse pattern in OR. Similarly, across the gradient of solar radiation values, FS increased from around 25% to 40% as

TABLE 2 Change in Akaike Information Criteria for each parameter when each was removed from the biomass model.

Var	dAIC
Total Aboveground Biomass (ln)	−1817.07
WHR	−710.74
% Clay	−576.46
Normalized Difference Vegetation Index (NDVI)	−526.31
Actual Evapotranspiration (AET)	−479.61
Average Annual Solar Radiation	−396.04
Time Since Fire (ln+1)	−365.09
Soil Bulk Density	−279.45
Average Annual Solar Radiation:Average Annual Precipitation	−255.01
‰ Carbon	−243.29
Climate Water Deficit (CWD)	−169.75
Aspect-Eastness	−84.38
Average Annual Precipitation	−75.58
Slope	−63.17
Flow accumulation (ln)	−48.15

TABLE 3 Summary of cross validation distributions: mean, standard deviation, 25th percentile, 75th percentile.

	Mean	Standard deviation	Skewness	Kurtosis	25th percentile	75th percentile
Obligate Seeder	1.24	17.8	−1.37	5.28	−4.98	11.42
Facultative Seeder	−0.10	29.0	−0.51	2.4	−19.7	23.3
Obligate Resprouter	−0.08	23.7	−0.99	3.66	−14.8	16.5
Tree	−0.57	30.32	−0.73	4.14	0.50	4.83.
Herb	−.46	21.7	−1.54	6.07	−4.11	10.1

solar radiation increased while OR decreased at a similar rate (Figure 3C). However, unlike with increasing CWD, an increase in solar radiation does not impact the proportion of OS biomass, which remained relatively constant at 15–18% of the total biomass. Results showed tree biomass decreased with increasing CWD as conditions became drier, but increased at higher levels of solar radiation. Herb biomass decreased slightly as both CWD and solar radiation increased.

There was a notable interaction between solar radiation and average annual precipitation, most influentially for tree biomass. At higher precipitation, the proportion of tree biomass did not differ with solar radiation. In contrast, at lower precipitation, the proportion of tree biomass strongly increased with solar radiation (Figure S1). For this reason, we focused on the effect of solar radiation in general at a median value of precipitation (Figure 3C). Across all levels of precipitation, as solar radiation increased, the proportion of OR biomass strongly declined, while the proportion of FS biomass strongly increased. Trees increased slightly with higher solar radiation, but the proportions of OS and herbs were unaffected.

The proportion of biomass contributed by OS and OR shrub species increased with productivity, as captured by NDVI, while FS biomass increased and then plateaued at higher NDVI. Herb biomass declined dramatically with increasing NDVI, from 38% to 2% (likely owing to the closing shrub canopy, Figure 3D), while trees remained relatively stable across NDVI values.

Variation in shrub regeneration strategies at the landscape scale

Analyzing the spatial rasters depicting OS-, OR- or FS-dominated pixels, we found dramatically different spatial patterns between the three shrub regeneration strategies. FS species covered the greatest spatial distribution, accounting for 3,372,125 ha (71%) of shrub dominated pixels in the study area (Figure 4): the FS group covered a range of productivity gradients and vegetation types (reflecting findings in Figure 3D), although it was notably absent from high elevation areas. In contrast, OS-dominated pixels covered the smallest spatial area (21,899 ha, 5% of shrub dominated pixels) occurring throughout the study area from coastal Big Sur and the Santa Ynez Mountains on the Los Padres National Forest to interior locations including the eastern fringes of the San Jacinto mountains (desert shrub vegetation) in the south (Figure 4, see case study in Supplementary Materials). Finally, pixels dominated by OR species covered 25,075 ha (5% of shrub dominated pixels in the study area), showing aggregations in the San Bernardino and San Gorgonio Mountains on the San Bernardino National Forest; San Gabriel Mountains on the Angeles National Forest, and throughout higher elevations on the Los Padres National Forest. OR-dominated pixels were notably absent in lower elevation areas with low water availability, as indicated in the relationship with CWD and solar radiation (Figures 3B, C).

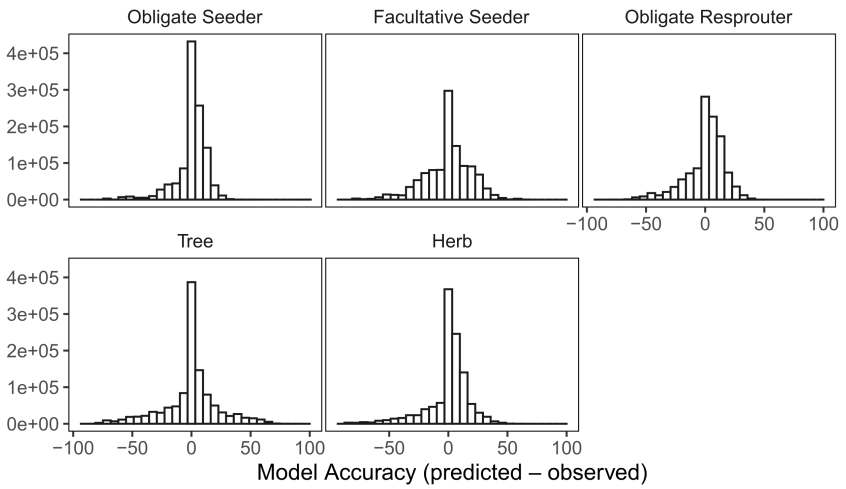

FIGURE 1
Cross validation distribution of model accuracy. Each histogram represents the observed minus the predicted value for eight randomly selected plots iterated 3,000 times.

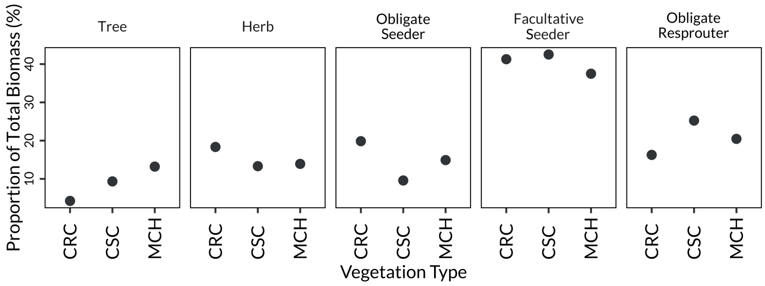

FIGURE 2
Estimated proportion of biomass by different life history types as predicted from the model of life history types within the three major shrubland vegetation types: MCH = mixed chaparral, CRC = chamise redshank chaparral; and CSC = coastal sage scrub. Note, all other variables in model are held at their median value.

More specifically, using the mean proportion of each of the shrub groups on each of 12 topographic facets (Hollander and Underwood, 2021), we found FS showed statistically significant higher mean biomass proportions on south facing slopes, summits, and ridges and lower biomass proportions on north facing slopes, valleys and depressions across all three shrub community types ($p < 0.0001$, Figure 5; Tables S2, S3). In contrast, OR had a higher mean value in cooler topographic facets (i.e., north facing slopes, valleys and depressions) versus warmer facets Figure 5; Tables S2, S3).

Discussion

Using FIA plots and a variety of static and dynamic environmental variables, we modeled the distribution of five plant groups – three shrub regeneration strategies: obligate seeders (OS), facultative seeders (FS), obligate resprouters (OR); and trees and herbs – by estimating the proportion of biomass within each of the five groups. Overall, model cross-validation showed the accuracy achieved 50% of predicted value within 8 to 24 percent of the actual value, with prediction accuracy highest for herb biomass and lowest for OR. Of the three shrub regeneration strategies, OS biomass was predicted with the highest accuracy and narrowest environmental range (Table 3; Figure 1). Our results reinforced findings from Syphard and Franklin (2010) who studied a subset of our southern California ecoregion: species distribution models showed obligate seeding species were mapped with highest accuracy, potentially due to their limited seed dispersal. In contrast, both Syphard and Franklin (2010) and this study mapped OR with less accuracy (incidentally, OR have a variety of seed dispersal mechanisms including long-distance dispersal by birds [Bullock, 1978; Syphard and Franklin, 2010]). One caveat to these findings is the bias of FIA plots to sample upland interior, moister sites which contain trees, thereby possibly underrepresenting OS species in coastal and desert scrub communities. In addition, research has shown some shrub species, such as *Ceanothus leucodermis*, vary temporarily and spatially in their post-fire regeneration strategy, changing from OR to OS with longer fire-fire intervals (Keeley, 2023).

The results reported relating to temporal variation and time since fire on shrub regeneration strategies reflect our understanding of chaparral communities and successional pathways. Relative to OS, species with resprouting ability (FS and OR) are able to rapidly dominate post-fire sites (Figure S2). OS represented a small proportion of the initial post-fire biomass (5–7% depending on the shrub community type), however OS increased to 17–21% a century following fire (available fire history data date back 100 years). Studies indicate OS regeneration in California shrublands is largely resilient after fire when the time since last fire is long enough to support mature shrub growth and several years of seed set (Keeley, 1986). For example, in mixed chaparral communities, which have a higher proportion of OS than chamise redshank chaparral, stands >30 years old had twice the amount of live OS biomass (Bohlman et al., 2018). In comparison, the proportion of FS biomass increases immediately post-fire, reflecting the resprouting ability of this type, but then decreases slightly over time as OS species grow and become established. This pattern reflects other studies which suggest seedlings of OS are more successful post-fire than seedlings of FS (Keeley and Zedler, 1978). The proportion of herb biomass decreases dramatically in the first two decades as the shrub canopy closes.

Our findings highlight notable variation among the five plant groups with respect to their responses to water availability, as indicated in our analyses of CWD and solar radiation effects. As CWD increased, we found a trade-off in the relationship between OS, FS and OR, such that OR decreased dramatically with increasing CWD, while FS and OS increased (Figure 3B). These findings reflect the general understanding in the literature that OS have undergone greater selection for physiological and morphological tolerances to drought (and higher insolation) due to the higher frequency of sexual reproduction when compared to species with the capacity to resprout (Keeley, 1998; Meentemeyer et al., 2001). Furthermore, seedlings of OS are more tolerant of water stress and tissue dehydration, and more efficient at conducting water (Pratt et al., 2010; Vilagrosa et al., 2013). Consequently, OS (and presumably FS which harbor similar regeneration traits) can do better in xeric sites with more stressful drought conditions, while OR predominate in sites with more reliable moisture (thus lower CWD) (Meentemeyer and Moody, 2002). OR are less physiologically and morphologically able to tolerate water stress: their leaves are less sclerophyllous and they have a lower resistance to water stress-induced cavitation of their stems (Meentemeyer and Moody, 2002). We also found an increase in CWD resulted in a decrease in the proportions of herbs and trees.

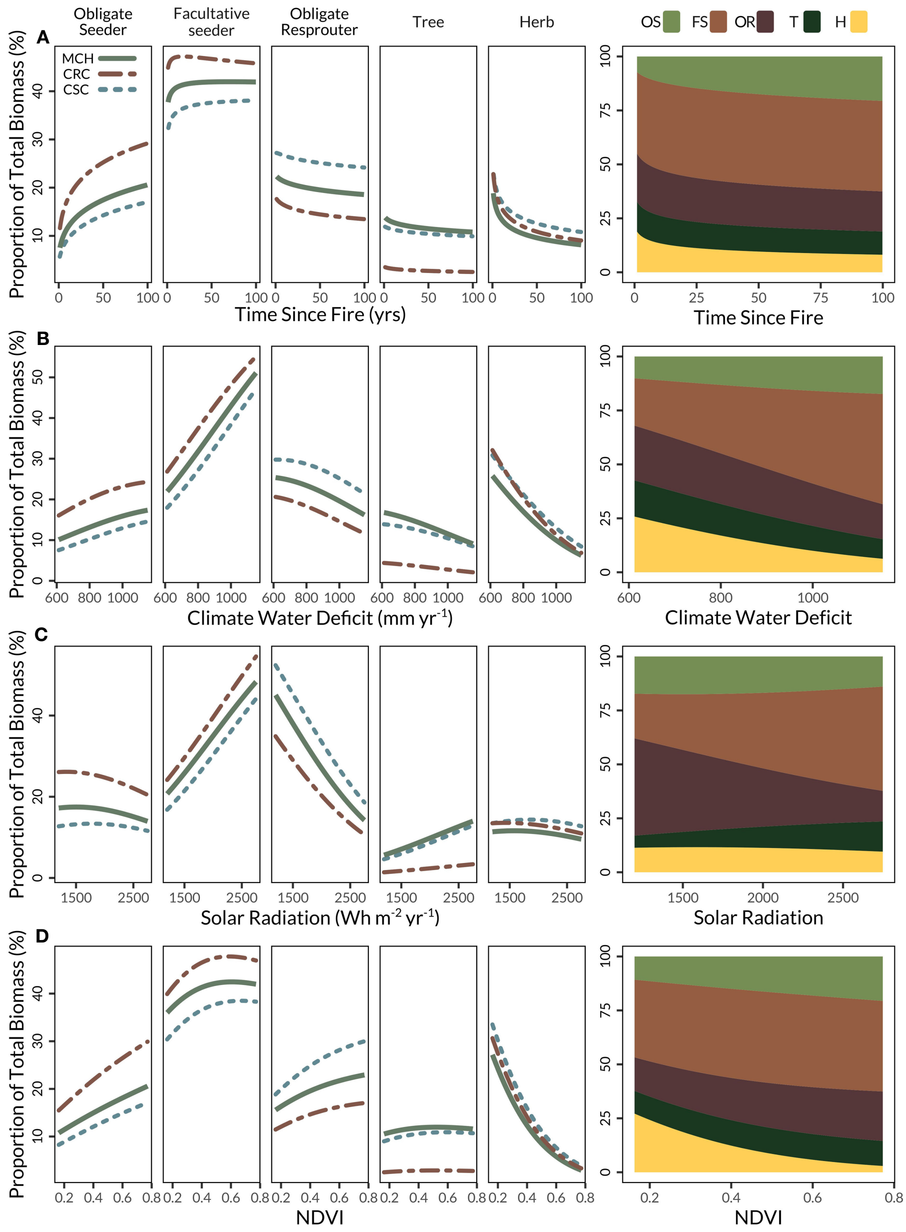

FIGURE 3
Proportion of biomass by life history type in response to differences in **(A)** time since fire, **(B)** climatic water deficit, **(C)** solar radiation, **(D)** normalized difference vegetation index (NDVI). Proportions are generated from marginal effects for each variable with all other variables in the model held at median values. Right panel displays the proportions of life history types from the most common vegetation type represented in FIA plots: mixed chaparral.

As solar radiation increased, we found the same tradeoff in OR and FS as with CWD, with decreased OR biomass. The lower abundance of OR on hotter slopes and ridges with high solar exposure may be reflecting the sensitivity of OR seed viability to drought and high soil temperatures, as has been suggested in other studies in California (e.g., Meentemeyer et al., 2001). In contrast to CWD, increasing solar radiation drove a slight decrease in OS (Figure 3C), which is counter to the increase with higher insolation suggested by Keeley (1998). Also, somewhat counterintuitive, is the increase in the proportion of tree biomass at higher levels of solar radiation.

The variation found in the proportion of biomass in the five plant groups and productivity (NDVI) was intuitive. Herb biomass was influenced most strongly and drastically declined (38% to 2%) as productivity increased, while OR, OS, and tree biomass increased with productivity. The pattern for OR reflects findings in the literature: resprouting is optimal in moist and fertile environments (Pausas and Keeley, 2014). Of note is the response of FS, whose biomass is relatively stable across the range of NDVI values (Figure 3D). One reason is that FS shrubs are benefitting from both seeding traits (better able to cope in water stressed environments) and resprouting traits (e.g., deep roots and higher

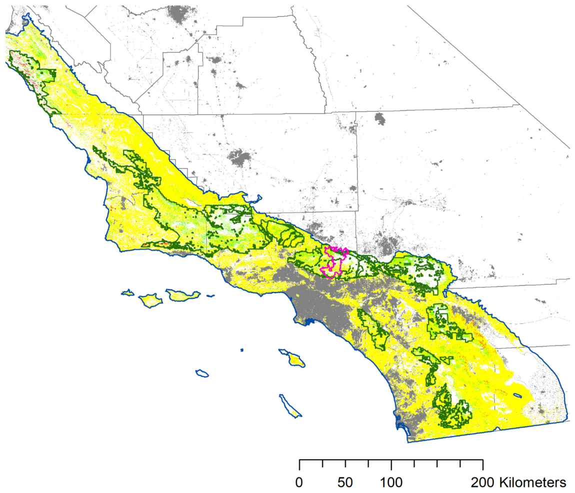

FIGURE 4
Maps depicting the proportion of shrub regeneration strategies: obligate seeders (OS), facultative seeders (FS), and obligate resprouters (OR). ANF = Angeles National Forest, CNF = Cleveland National Forest, LPNF = Los Padres National Forest, SBNF = San Bernardino National Forest. Inset map shows study area in the grey.

root to shoot ratios). Levin (1990) suggested that seeding traits make a species better suited to changing environments as seed banks are a source of genetic variation, which might explain the widespread distribution of OS over a range of productivity values.

The three shrub regeneration strategies showed notable spatial variation at the landscape scale. FS species accounted for over a third of the biomass in all three shrub communities and FS dominated pixels were much more broadly distributed than OR or OS, reflecting findings relating to the influence of productivity (NDVI) on the proportion of FS biomass (Figure 3D). OR dominated pixels occurred in loose aggregations including in higher elevation areas of the San Bernardino and Angeles National Forests. OS dominated pixels occupied the smallest spatial area and occurred in scattered pixels throughout the ecoregion. Our findings reflect suggestions that in many Mediterranean-type climate regions, there is some spatial segregation between OS and OR, where OS occupy parts of the landscape where water is more susceptible to strong oscillations, and OR occupy areas where water is more reliable (Pausas and Keeley, 2014). The analysis using topographic facets supports our understanding from the literature (e.g., Gordon and White, 1994): the mean proportion of FS and OS in mixed chaparral and chamise redshank chaparral was higher in warmer, south facing slopes, summits and ridge facets (except for OS in coastal sage scrub), while the mean proportion of OR was higher in cooler, north facing slopes, valleys and depression facets (Figure 5; Tables S2, S3).

Implications of study

Modeling the distribution of shrub regeneration strategies can support resource management in a number of ways. First, spatial data outputs lay the foundation for improved estimates of carbon storage across multiple shrub biomass pools. Existing regional data on aboveground live biomass (Schrader-Patton and Underwood, 2021) can be used in conjunction with the proportion of OS, FS, and OR to estimate belowground biomass using root to shoot ratios, standing dead biomass, and litter, which differ by species with different post-fire regeneration strategies (e.g., Green, 1970; Kummerow et al., 1977; Miller and Ng, 1977; Riggan et al., 1988; Schrader-Patton et al., 2023). In turn, for resource managers this provides a powerful dataset for carbon accounting and monitoring.

Second, information on the proportion of OS versus resprouting species can help identify areas at risk of conversion to non-native grasslands owing to high frequency fire (Syphard et al., 2013; Syphard et al., 2018), and contribute to prioritization of areas for post-fire restoration (see case study on Bobcat Fire in Supplementary Materials). Although resprouting shrubs can also decline when experiencing (very) short fire return intervals, they are much more resilient than the OS group (Zedler et al., 1983; Pausas et al., 2016).

The results we report used field data and static and dynamic variables to assess spatial and temporal variation in shrub post-fire regeneration strategies at the ecoregional scale in California. This study provides a contribution from the North American

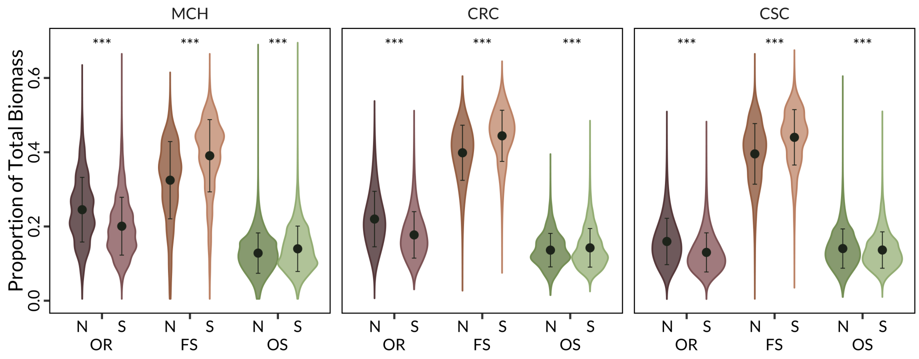

FIGURE 5
Mean proportion of shrub regeneration strategy in the three main shrub vegetation types: MCH = mixed chaparral; CRC= chamise redshank chaparral; CSC = coastal sage scrub, by topographic facets. N = north facing slopes, valleys and depressions and S = south facing slopes, summits and ridges. OR = Obligate Resprouters, FS = Facultative Seeders, and OS = Obligate Seeders. Error bars are +/− SD. *** Indicates statistically significant (P<0.0001).

Mediterranean-Climate Region which joins studies of spatial variation in post-fire regeneration types from other MCRs including Australia (Clarke et al., 2015; Lawes et al., 2022), South Africa (Bond and Midgley, 2003; Cowling et al., 2018), and the Mediterranean Basin (Parra and Moreno, 2018).

Data availability statement

The data presented in this study are available on request from the corresponding author.

Author contributions

Project idea was conceived of by EU, HS and NM. Data processing and analyses were undertaken by QS, CS-P and EU. EU led the writing of the manuscript with contributions from QS, and all authors reviewed and edited the manuscript. All authors contributed to the article and approved the submitted version.

Funding

The work contributing to this study was funded by the California Department of Forestry and Fire Protection (CalFire), the USDA Forest Service Western Wildlands Environmental Threat Assessment Centre, and the USDA Forest Service Pacific Southwest Region.

Acknowledgments

We are grateful to Alex Syphard and Jon Keeley for valuable discussions and Kama Kennedy (USDA Forest Service Remote Sensing Lab) for contributions in applying allometric equations to the FIA plot data.

Conflict of interest

The authors declare that the research was conducted in the absence of any commercial or financial relationships that could be construed as a potential conflict of interest.

Publisher's note

Supplementary material

The Supplementary Material for this article can be found online at: https://www.frontiersin.org/articles/10.3389/fevo.2023.1158265/full#supplementary-material

References

Anderson, D., and Burnham, K. (2004). *Model selection and multi-model inference (2nd edition)* (New York: NY: Springer-Verlag).

Barbour, M. G., Keeler-Wolf, T., and Schoenherr, A. A. (2007). *Terrestrial vegetation of California* (Berkeley, CA: University of California Press).

Bellingham, P. J., and Sparrow, A. D. (2000). Resprouting as a life history strategy in woody plant communities. *Oikos* 89, 409–416. doi: 10.1034/j.16000706.2000.890224.x

Bohlman, G. N., Underwood, E. C., and Safford, H. D. (2018). Estimating biomass in California's chaparral and coastal sage scrub shrublands. *Madroño* 65, 28–46. doi: 10.3120/0024-9637-65.1.28

Bond, W. J., and Midgley, J. J. (2001). Ecology of sprouting in woody plants: the persistence niche. *Trends Ecol. Evol.* 16, 45–51. doi: 10.1016/S0169-5347(00)02033-4

Bond, W. J., and Midgley, J. J. (2003). The evolutionary ecology of sprouting in woody plants. *Int. J. Plant Sci.* 164, S103–S114. doi: 10.1086/374191

Borchert, M., Lopez, A., Bauer, C., and Knowd, T. (2004). *Field guide to coastal sage scrub and chaparral alliances of Los Padres National Forest, USDA Forest Service Region 5, Ecological Field Guide.*

Bullock, S. H. (1978). Plant abundance and distribution in relation to types of seed dispersal in chaparral. *Madroño* 25, 104–105.

Burkman, B. (2005). "Forest inventory and analysis sampling and plot design; FIA fact sheet series," in *USDA Forest Service forest inventory and analysis national program* (Washington DC, USA: USDA Forest Service). Available at: https://www.fia.fs.usda.gov/library/fact-sheets/data-collections/Sampling%20and%20Plot%20Design.pdf.

Clarke, P. J., Lawes, M. J., Midgley, J. J., Lamont, B. B., Ojeda, F., Burrows, G. E., et al. (2013). Resprouting as a key functional trait: how buds, protection and resources drive persistence after fire. *New Phytol.* 197, 19–35. doi: 10.1111/nph.12001

Clarke, P. J., Lawes, M. J., Murphy, B. P., Russell-Smith, J., Nano, C. E. M., Bradstock, R., et al. (2015). A synthesis of postfire recovery traits of woody plants in Australian ecosystems. *Sci. Total Environ.* 534, 31–42. doi: 10.1016/j.scitotenv.2015.04.002

CNPS (California Native Plant Society). (2021). *A manual of California vegetation, online edition* (Sacramento, CA: California Native Plant Society). Available at: http://www.cnps.org/cnps/vegetation/.

Cowling, R. M., Gallien, L., Richardson, D. M., and Ojeda, F. (2018). What predicts the richness of seeder and resprouter species in fire-prone cape fynbos: rainfall reliability or vegetation density? *Austral. Ecol.* 43, 614–622. doi: 10.1111/aec.12606

Cowling, R. M., Rundel, P. W., Lamont, B. B., Arroyo, M. K., and Arianoutsou, M. (1996). Plant diversity in Mediterranean-climate regions. *Trends Ecol. Evol.* 11, 362–366. doi: 10.1016/0169-5347(96)10044-6

Davis, S. D., Ewers, F. W., Wood, J., Reeves, J. J., and Kolb, K. J. (1999). Differential susceptibility to xylem cavitation among three pairs of *Ceanothus* species in the transverse mountain ranges of southern California. *Ecoscience* 6, 180–186. doi: 10.1080/11956860.1999.11682519

Desouza, J., Silka, P. A., and Davis, S. D. (1986). Comparative physiology of burned and unburned *Rhus laurina* after chaparral wildfire. *Oecologia* 71, 63–68. doi: 10.1007/BF00377322

Enright, N. J., Marsula, R., Lamont, B. B., and Wissel, C. (1998). The ecological significance of canopy seed storage in fireprone environments: a model for nonsprouting shrubs. *J. Ecol.* 86, 946–959. doi: 10.1046/j.1365-2745.1998.00312.x

FEIS. (2021). *(Fire effects information system).* Available at: https://www.feis-crs.org/feis/.

Franklin, J. (2002). Enhancing a regional vegetation map with predictive models of dominant plant species in chaparral. *Appl. Veg Sci.* 5, 135–146. doi: 10.1111/j.1654-109X.2002.tb00543.x

FRAP (Fire and Resource Assessment Program). (2015). *Data from: Fveg15_1 vegetation data. California department of forestry and fire protection's CALFIRE fire and resource assessment program (FRAP).* Available at: http://frap.fire.ca.gov/data/frapgisdata-sw-fveg_download.

Gordon, H., and White, T. C. (1994). *Ecological guide to southern California chaparral plant series. transverse and peninsular ranges: Angeles, Cleveland, and San*

Bernardino national forests. report R5-ECOL-TF-005 (Albany WA: USDA Forest Service Pacific Southwest Region).

Gosper, C. R., Hopley, T., Byren, M., Hopper, S. D., Prober, S. M., and Yates, C. J. (2019). Phylogenomics shows lignotuber state is taxonomically informative in closely related eucalypts. *Mol. Phylogenet Evol.* 135, 236–248. doi: 10.1016/j.ympev.2019.03.016

Gray, J. T. (1982). Community structure and productivity in *Ceanothus* chaparral and coastal sage scrub of southern California. *Ecol. Monogr.* 52 (4), 415–435. doi: 10.2307/2937353

Green, L. R. (1970). *An experimental prescribed burn to reduce fuel hazard in chaparral. research note PSWRN-216* (Berkeley, CA: USDA Pacific Southwest Forest and Range Experimental Forest).

Hastie, T., Tibshirani, R., and Friedman, J. (2009). *The elements of statistical learning: data mining, inference, and prediction. 2nd ed* (New York: Springer).

Hollander, A. D., and Underwood, E. C. (2021). Data from: shrubland vegetation topographic facets of southern California. *Dryad Digital Repository*. doi: 10.25338/B8JW59

Jacobson, A. L., Pratt, B. R., Ewers, F. W., and Davis, S. D. (2007). Cavitation resistance among 26 chaparral species of southern California. *Ecol. Monogr.* 77 (1), 99–115. doi: 10.1890/05-1879

Jenerette, G. D., Park, I. W., Andrews, H. M., and Eberwein, J. R. (2018). "Biogeochemical cycling of carbon and nitrogen in chaparral dominated ecosystems," in *Valuing chaparral*. Eds. E. C. Underwood, H. D. Safford, N. A. Molinari and J. E. Keeley (Cham, Switzerland: Springer International Publishing), 141–179.

Keeley, J. E. (1986). "Resilience of Mediterranean shrub communities to fires," in *Resilience in Mediterranean-type ecosystems: tasks for vegetation science*. Eds. B. Dell, A. J. M. Hopkins and B. B. Lamont (Dordrecht, Germany: Springer). doi: 10.1007/978-94-009-4822-8_7

Keeley, J. E. (1991). Seed germination and life history syndromes in the California chaparral. *Bot. Rev.* 57, 81–116. doi: 10.1007/BF02858766

Keeley, J. E. (1998). "Coupling demography, physiology and evolution in chaparral shrubs," in *Landscape degradation and biodiversity in Mediterranean-type ecosystems*. Eds. P. W. Rundel G. Montenegro and F. M. Jaksic (Berlin, Germany: Springer-Verlag), 237–264.

Keeley, J. E. (2023). Spatial and temporal strategies of resprouting and seeding in a chaparral shrub species. *Ecology* 104 (4), e3984. doi: 10.1002/ecy.39844of4KEELEY

Keeley, J. E., and Davis, F. W. (2007). "Chaparral," in *Terrestrial vegetation of California*, *3rd Edition*. Eds. M. G. Barbour, T. Keeler-Wolf and A. A. Schoenherr (Berkeley, CA: University of California Press).

Keeley, J. E., Pausas, J. G., Rundel, P. W., Bond, W. J., and Bradstock, R. A. (2011). Fire as an evolutionary pressure shaping plant traits. *Trends Plant Sci.* 16, 406–411. doi: 10.1016/j.tplants.2011.04.002

Keeley, J. E., and Safford, H. D. (2016). "Fire as an ecosystem process," in *Ecosystems of California*. Eds. H. A. Mooney and E. Zavaleta (Berkeley, CA: University of California Press).

Keeley, J. E., and Zedler, P. H. (1978). Reproduction of chaparral shrubs after fire: a comparison of sprouting and seedling strategies. *Am. Midl. Nat.* 99, 142–161. doi: 10.2307/2424939

Kummerow, J., Krause, D., and Jow, W. (1977). Root systems of chaparral shrubs. *Oecologia* 29, 163–177. doi: 10.1007/BF00345795

Langley, J. A., Drake, B. G., and Hungate, B. A. (2002). Extensive belowground carbon storage supports roots and mycorrhizae in regenerating scrub oaks. *Oecologia* 131, 542–548. doi: 10.1007/s00442-002-0932-6

Lawes, M. J., Crisp, M. D., Clarke, P. J., Murphy, B. P., Midgley, J. J., Russell-Smith, J., et al. (2022). Appraising widespread resprouting but variable levels of postfire seeding in Australian ecosystems: the effect of phylogeny, fire regime and productivity. *Aus. J. Bot.* 70 (2), 114–130. doi: 10.1071/BT21110

Levin, D. A. (1990). The seed bank as a source of genetic novelty in plants. *Amer. Nat.* 135, 563–572. doi: 10.1086/285062

Lutes, D., Keane, R., Caratti, J., Key, C., Benson, N., Sutherland, S., et al. (2006). *FIREMON: fire effects monitoring and inventory system* (Fort Collins, CO: Rocky Mountain Research Station).

McGinnis, T. W., Shook, C. D., and Keeley, J. E. (2010). Estimating aboveground biomass for broadleaf woody plants and young conifers in Sierra Nevada, California, forests. *West J. App. For.* 25, 203–209. doi: 10.1093/wjaf/25.4.203

Meentemeyer, R., and Moody, A. (2002). Distribution of plant life history types in California chaparral: the role of topographically-determined drought severity. *J. Veg. Sci.* 13, 67–78. doi: 10.1111/j.1654-1103.2002.tb02024.x

Meentemeyer, R. K., Moody, A., and Franklin, J. (2001). Landscape-scale patterns of shrub-species abundance in California chaparral. *Plant Ecol.* 156, 19–41. doi: 10.1023/A:1011944805738

Miller, P. C., and Ng, R. (1977). Root:shoot biomass ratios in shrubs in southern California and central Chile. *Madroño* 24, 215–223.

Omernik, J. M., and Griffith, G. E. (2014). Ecoregions of the conterminous united states: evolution of a hierarchical spatial framework. *Environ. Manag.* 54, 1249–1266. doi: 10.1007/s00267-014-0364-1

Parra, A., and Moreno, J. M. (2018). Drought differentially affects the post-fire dynamics of seeders and resprouters in a Mediterranean shrubland. *Sci. Total Environ.* 626, 1219–1229. doi: 10.1016/j.scitotenv.2018.01.174

Pausas, J. G., and Bradstock, R. A. (2007). Fire persistence traits of plants along a productivity and disturbance gradient in mediterranean shrublands of south-east Australia. *Glob Ecol. Biogeogr.* 16, 330–340. doi: 10.1111/j.1466-8238.2006.00283.x

Pausas, J. G., and Keeley, J. E. (2014). Evolutionary ecology of resprouting and seeding in fireprone ecosystems. *New Phytol.* 204, 55–65. doi: 10.1111/nph.12921

Pausas, J. G., Pratt, R. B., Keeley, J. E., Jacobsen, A. L., Ramirez, A. R., Vilagrosa, A., et al. (2016). Towards understanding resprouting at the global scale. *New Phytol.* 209, 945–954. doi: 10.1111/nph.13644

Poole, D. K., and Miller, P. C. (1975). Water relations of selected species of chaparral and coastal sage communities. *Ecology* 56, 1118–1128. doi: 10.2307/1936151

Pratt, R. B., North, G. B., Jacobsen, A. L., Ewers, F. W., and Davis, S. D. (2010). Xylem root and shoot hydraulics is linked to life history type in chaparral seedlings. *Funct. Ecol.* 24, 70–81. doi: 10.1111/j.1365-2435.2009.01613.x

R Core Team (2016). *R: a language and environment for statistical computing* (Vienna, Austria: R Foundation for Statistical Computing).

Riggan, P. J., Goode, S., Jacks, P. M., and Lockwood, R. N. (1988). Interaction of fire and community development in chaparral of southern California. *Ecol. Monogr.* 58, 155–176. doi: 10.2307/2937023

Ripley, B., and Venables, W. (2021). *Nnet: feed-forward neural networks and multinomial log-linear models* (R Package).

Rundel, P. (2018). "California Chaparral and its global significance," in *Valuing chaparral*. Eds. E. C. Underwood, H. D. Safford, N. A. Molinari and J. E. Keeley (Cham, Switzerland: Springer International Publishing), 1–27.

Safford, H. D., Paulson, A. K., Steel, Z. L., Young, D. J. N., and Wayman, R. B. (2022). The 2020 California fire season: a year like no other, a return to the past, or a harbinger of the future? *Glob Ecol. Biogeogr.* 00, 1–21. doi: 10.1111/geb.13498

Safford, H. D., Underwood, E. C., and Molinari, N. A. (2018). "Managing chaparral resources on public lands," in *Valuing chaparral*. Eds. E. C. Underwood, H. D. Safford, N. A. Molinari and J. E. Keeley (Cham, Switzerland: Springer International Publishing), 411–448.

Safford, H. D., and Van de Water, K. M. (2014). *Using fire return interval departure (FRID) analysis to map spatial and temporal changes in fire frequency on national forest lands in california. research paper PSW-RP-266* (Albany, CA: USDA Forest Service, Pacific Southwest Research Station).

Schrader-Patton, C. C., and Underwood, E. C. (2021). New biomass estimates for chaparral-dominated southern California landscapes. *Remote Sens.* 13 (8), 1581. doi: 10.3390/rs13081581

Schrader-Patton, C. C., Underwood, E. C., and Sorenson, Q. M. (2023). Annual biomass spatial data for southern California, (2001–2021): above- and belowground, standing dead, and litter. *Ecology*, e4031. doi: 10.1002/ecy.4031

Stephenson, N. L. (1998). Actual evapotranspiration and deficit: biologically meaningful correlates of vegetation distribution across spatial scales. *J. Biogeog.* 25, 855–870. doi: 10.1046/j.1365-2699.1998.00233.x

Syphard, A. D., Bar Massada, A., Butsic, V., and Keeley, J. E. (2013). Land use planning and wildfire: development policies influence future probability of housing loss. *PloS One* 8 (8), e71708. doi: 10.1371/journal.pone.0071708

Syphard, A. D., Brennan, T. J., and Keeley, J. E. (2018). "Chaparral landscape conversion in southern California," in *Valuing chaparral*. Eds. E. C. Underwood, H. D. Safford, N. A. Molinari and J. E. Keeley (Cham, Switzerland: Springer International Publishing), 323–336.

Syphard, A., and Franklin, J. (2010). Species traits affect the performance of species distribution models for plants in southern California. *J. Veg. Sci.* 21, 177–189. doi: 10.1111/j.1654-1103.2009.01133.x

Underwood, E. C., Safford, H. D., Molinari, N. A., and Keeley, J. E. (2018). *Valuing chaparral: ecological, socio-economic, and management perspectives* (Cham, Switzerland: Springer International Publishing).

USDA [US Department of Agriculture]. (2015). *Data from: fire-return interval departure (FRID) geodatabase*. Available at: http://www.fs.usda.gov/detail/r5/landmanagement/gis/?cid=STELPRDB5327836.

USFS (USDA Forest Service). (2022). *Confronting the wildfire crisis: a strategy for protecting communities and improving resilience in america's forests. report: FS-1187a*. Available at: https://www.fs.usda.gov/sites/default/files/Confronting-Wildfire-Crisis.pdf.

Vilagrosa, A., Hernandez, E., Luis, V. C., Cochard, H., and Pausas, J. G. (2013). Physiological differences explain the co-existence of different regeneration strategies in Mediterranean ecosystems. *New Phytol.* 201, 1277–1288. doi: 10.1111/nph.12584

Wakimoto, R. H. (1978). *Responses of southern California brushland vegetation to fuel manipulation [dissertation]* (Berkeley (CA: University of California).

Zedler, P. H. (1995). "Fire frequency in southern California shrublands: biological effects and management options," in *Brushfires in California wildlands: ecology and resource management*. Eds. J. E. Keeley and T. Scott (Fairfield, Washington DC: International Association of Wildland Fire), 101–112.

Zedler, P. H., Gautier, C. R., and McMaster, G. S. (1983). Vegetation change in response to extreme events – the effect of a short interval between fires in California chaparral and coastal scrub. *Ecology* 64 (4), 809–818. doi: 10.2307/1937204

Frontiers in Ecology and Evolution

TYPE Original Research
PUBLISHED 25 July 2023
DOI 10.3389/fevo.2023.1202610

OPEN ACCESS

EDITED BY
Robert Klinger,
United States Department of the Interior,
United States

REVIEWED BY
Charles Krebs,
University of British Columbia, Canada
Daniel Scherrer,
Swiss Federal Institute for Forest, Snow and Landscape Research (WSL), Switzerland

*CORRESPONDENCE
Peter D. Billman
peter.billman@uconn.edu

RECEIVED 08 April 2023
ACCEPTED 14 June 2023
PUBLISHED 25 July 2023

CITATION
Billman PD, Beever EA, Westover ML and Ryals DK (2023) Spatio-temporal variability in the strength, directionality, and relative importance of climate on occupancy and population densities in a philopatric mammal, the American pika (*Ochotona princeps*). *Front. Ecol. Evol.* 11:1202610. doi: 10.3389/fevo.2023.1202610

Spatio-temporal variability in the strength, directionality, and relative importance of climate on occupancy and population densities in a philopatric mammal, the American pika (*Ochotona princeps*)

Peter D. Billman[1]*, Erik A. Beever[2,3], Marie L. Westover[4] and Dylan K. Ryals[2,5]

[1]Department of Ecology and Evolutionary Biology, University of Connecticut, Storrs, CT, United States, [2]U.S. Geological Survey Northern Rocky Mountain Science Center, Bozeman, MT, United States, [3]Department of Ecology, Montana State University, Bozeman, MT, United States, [4]Department of Biological Sciences, Los Rios Community College District, Sacramento, CA, United States, [5]Department of Entomology, Purdue University, West Lafayette, IN, United States

Species distribution models (SDMs) have been widely employed to evaluate species–environment relationships. However, when extrapolated over broad spatial scales or through time, these models decline in their predictive ability due to variation in how species respond to their environment. Many models assume species–environment relationships remain constant over space and time, hindering their ability to accurately forecast distributions. Therefore, there is growing recognition that models could be improved by accounting for spatio-temporal nonstationarity – a phenomenon wherein the factors governing ecological processes change over space or time. Here, we investigated nonstationarity in American pika (*Ochotona princeps*) relationships with climatic variables in the Rocky Mountains (USA). We first compared broad-scale differences in pika–climate patterns for occupancy and population density across the Southern, Central, and Northern Rockies. Next, we investigated within-ecoregion variation across four mountain ranges nested within the Northern Rockies. Lastly, we tested whether species–climate relationships changed over time within the Central Rockies ecoregion. Across all analyses, we found varying levels of nonstationarity among the climate metrics for both occupancy and density. Although we found general congruence in temperature metrics, which consistently had negative coefficients, and moisture metrics (e.g., relative humidity), which had positive coefficients, nonstationarity was greatest for summer and winter precipitation over both space and time. These results suggest that interpretations from one ecoregion should not be applied to other regions universally – especially when using precipitation metrics. The within-ecoregion analysis found much greater variation in the strength-of-relationship coefficients among the four mountain ranges, relative to the inter-regional analysis, possibly attributable to smaller sample sizes per mountain range. Lastly, the importance of several variables shifted through time from significant to insignificant in the temporal analysis. Our results collectively reveal the overall complexity underlying species–environment relationships. With rapidly shifting conditions globally, this work adds to the growing body of literature highlighting how issues of spatio-temporal nonstationarity can limit the accuracy, transferability, and reliability of models and that interpretations will likely be most robust at local to regional scales. Diagnosing, describing, and incorporating nonstationarity of species–climate relationships into models over space and time could serve as a pivotal step in creating more informative models.

KEYWORDS

nonstationarity, spatio-temporal analysis, Rocky Mountains, species–climate relationships, distribution models, density, American pikas

1 Introduction

Contemporary climate change continues to shape species' distributions and biological communities globally. Observational and experimental studies have now documented responses spanning shifts in distributions, abundance, body size, phenology, behavior, and biotic interactions, among many others (Eastman et al., 2012; Thurman and Garcia, 2019; Goodman et al., 2022; Calabrese and Pfennig, 2023; Kerner et al., 2023). Shifts in distributions and declines in abundance have caused particular concern, given that both indicate species may not be evolving rapidly enough to cope with the impacts of recent climate change, thereby increasing risks of extirpation and extinction (Radchuk et al., 2019). Accordingly, understanding the underlying biological processes (i.e., mechanisms) that influence species responses remains a priority for management decision-making and species-distribution modeling efforts (Urban et al., 2016).

Pinpointing the factors that limit distributions, and how these factors vary in importance over space and time, has long been of interest in ecology (Darwin, 1859). To understand and model multidimensional niche spaces, species-specific life histories should be well understood; simultaneously, investigators should also consider how factors constraining populations might vary across temporal and spatial scales. For example, Brown (1984), emphasized that the abiotic factors constraining distributions differ between cool- and warm-edge range limits. Although rising temperatures may cause declines in occupancy at warm limits, they may concurrently allow greater survival and expansion beyond current cold-edge range limits (e.g., Sultaire et al., 2022). Given the recent motivation to identify evolutionary "winners" and "losers" under climate change based on biological traits, a binary classification of species' vulnerability would be an oversimplification, considering that species often simultaneously benefit and suffer from climate shifts, depending on populations' range position and numerous other factors (Somero, 2010). This, along with spatial variability in local adaptation, microrefugia, disturbances, and biotic interactions, may partially explain why species–climate relationships tend to be markedly heterogeneous over space and, thus, difficult to predict.

Given the large variability in the relative importance of environmental constraints across species ranges, species distribution models (SDMs) have recently sought to account for some of this heterogeneity (Peterson et al., 2011; Guisan et al., 2017; Martínez-Minaya et al., 2018). Broadly, correlative SDMs aim to statistically and spatially model distributions using known or suspected relationships between organisms and environmental conditions. One recent meta-analysis concluded that SDMs generally perform best when predicting species occurrences, but sequentially decline in predictive ability for population abundance, fitness, and genetic diversity (Lee-Yaw et al., 2022). Although SDMs have had increasing success (i.e., predictive accuracy) in recent years, one major limitation is they generally cannot be applied elsewhere in a species' range other than where the training data originated (Charney et al., 2021; Rousseau and Betts, 2022). Mechanistic modeling offers an alternative to correlative approaches by modeling distributions based on individual-level, physiological processes that are hypothesized to constrain species (Riddell et al., 2017; Briscoe et al., 2022), such as water requirements necessary to dissipate heat (Riddell et al., 2019). Nonetheless, mechanistic models require high-quality biological data that explain how species experience their environment and are therefore limited by our understanding of how environmental factors actually constrain species (Kearney et al., 2010; Urban et al., 2016).

Both correlative and mechanistic modeling approaches currently struggle with accommodating nonstationarity, a phenomenon wherein ecological processes and relationships vary in strength, direction, and relative importance over space and time (Rollinson et al., 2021). Nonstationarity can arise from shifts in species' relationships with environmental variables both spatially and temporally, as well as from shifts in environmental conditions. For example, one recent study found that snowshoe hares (*Lepus americanus*) are primarily constrained in their distribution by snow-cover duration, but the degree of the snow's importance interacts strongly with maximum temperature across the species' range (Sultaire et al., 2022). Mounting evidence suggests that due to widespread nonstationarity in ecological relationships, inferences from one time period and region should not be used to infer or predict range dynamics elsewhere or in other time periods (Pardi et al., 2020); accordingly, heavy reliance on range-wide distribution models could create the possibility of overgeneralizations and inaccurate models for more-localized climate-adaptation management and decision-making. Collectively, these observations raise the following questions: 1) What are the most appropriate scales to investigate to best understand species–environment relationships (e.g., Guisan et al., 2007), especially to be most useful for resource managers (Carroll et al., 2022)?; 2) Should future monitoring efforts ideally focus on local, regional, or continental scales?, and, accordingly, 3) Where should model training and validation data be acquired from (e.g., Scherrer et al., 2021)?; 4) When are SDMs transferable over time in a reliable manner (e.g., Smith et al., 2013)?; and 5) What range of environmental conditions are necessary to survey to ensure models are robust (e.g., Thuiller et al., 2004)? Ecological forecasts remain limited today by our overall nascent understanding of varying degrees of nonstationarity across both space and time, and climate is only one niche component that makes SDM transferability difficult (e.g., these models often ignore biotic interactions and habitat fragmentation and loss, Díaz et al., 2019).

Further complicating advances in forecasting climate-driven responses, rates of warming are remarkably heterogeneous over earth, with high-elevation and high-latitude regions generally experiencing much faster rates than elsewhere (Wang Q et al., 2016). For example, warming across four of earth's largest mountain chains (the Alps, Andes, Himalayas, and Rockies) has been notably faster than surrounding lowlands, whereas differences in precipitation have been less consistent (Pepin et al., 2022). The variable rates of warming may therefore leave mountain-dwelling populations at greater risk relative to their low-elevation counterparts under shifting conditions. Complex topography in mountains provides a high diversity of local climates for species to exploit, highlighting how mountain systems may now act as exceptional testing grounds for questions related to ecological nonstationarity in species responses to climate over local and regional scales, as well as through time.

Here, we evaluate species–climate relationships using occupancy and population density data to evaluate the degree of spatiotemporal nonstationarity in a small mammal. To do so, we tested relationships at several scales including within ecoregions, across ecoregions, and over time, using the American pika (*Ochotona princeps*, Richardson, 1828) as our focal species. American pikas ("pikas," hereafter) are small, climate-sensitive lagomorphs that occupy patchily distributed, broken-rock (e.g., talus) habitats in western North America, predominantly in mountainous areas (Hafner and Sullivan, 1995). We used a newly integrated dataset of occupied and historically occupied patches that were surveyed between 2011 and 2021. These data cover three expansive ecoregions, and all field surveys used identical sampling protocols. Because shifts in climate often cause contrasting demographic responses across seasons (e.g., Cordes et al., 2020), we examined both summer and winter metrics that we hypothesized act as proxies of specific, mechanism-based pathways that shape population dynamics (SI, Table 1). Accordingly, we incorporated seasonal metrics for temperature, precipitation, and moisture. In this study, we specifically predicted the following:

1. Across ecoregions, the strength and direction of climate relationships of both response metrics (occupancy and density) will exhibit high spatial nonstationarity, with coefficients displaying large variability within each climate metric.
2. Within an ecoregion, species–climate relationships will show higher congruence in strength and directionality among mountain ranges that are in close geographic proximity, compared to those further away.
3. Between two closely spaced time periods, the strength and direction of species–climate relationships will not change within each climate metric. In other words, such relationships will exhibit relative temporal stationarity.

2 Methods

2.1 Model organism

We focus on American pikas here given their often-high detectability ($p > 0.90$, Beever et al., 2010; Ray et al., 2016) as well as our ability to quantify population density from patch-level surveys using visual and auditory detections. Due to their limited physiological thermoregulation, pikas occupy broken-rock features, like talus fields and lavascapes, that buffer against fluctuating ambient temperatures (Benedict et al., 2020). This habitat is also readily delineated using satellite imagery prior to field surveys and persists over centuries to millennia with little structural change. Studies that have incorporated mechanistically-informed variables suggest that heat and cold stress are often the best predictors of pika distribution and density across various ecoregions (e.g., Beever et al., 2003; Wilkening et al., 2011; Johnston et al., 2019; Billman et al., 2021), and abundance has often been linked strongly to precipitation and water-balance (Beever et al., 2013; Johnston et al., 2019), highlighting the species' overall responsiveness to the direct effects of weather and climate. In addition to direct exposure, the indirect effects of climate have also been found to shape occupancy and/or population density, such as precipitation's role on the quality, diversity, and availability of forage (e.g., Erb et al., 2014; Ray et al., 2016; Varner et al., 2023). Although temperate mountain regions exhibit high seasonality throughout the year, pikas do not hibernate, which can leave them vulnerable to both winter conditions, such as low snowpack, and summer conditions. Due to numerous life-history characteristics, pikas appear to have a comparatively lower adaptative capacity in the face of climate change than many other montane mammals in western North America, making them an ideal model organism for testing climate-responsiveness theory and questions (Beever et al., 2023).

2.2 Field surveys: occupancy and population density

We surveyed for evidence of current or historical pika occupancy in talus patches across the Rocky Mountains (USA) between 2011 and 2021. Patches – each defined as a contiguous area of broken-rock habitat separated from all other such areas by >25 m – were identified using satellite imagery on the online mapping platform CalTopo.com prior to fieldwork. Field surveys occurred from June to September and were restricted to crepuscular hours, to achieve the highest detectability (few surveys between 12:00 and 16:00; these occurred only when conditions were cooler, with fully overcast skies). To survey, we walked 50-m transects across each talus patch, spaced 15 m apart elevationally, to obtain estimates of population density while avoiding double-counting individuals (# of pikas/50 m, *sensu* Beever et al., 2011). We considered a patch occupied if we unequivocally detected pikas visually, aurally, or if we found fresh haypiles with at least 10 fresh sprigs (green with chlorophyll) of herbaceous vegetation in them. A patch was considered historically occupied or extirpated if we only found old evidence such as old fecal pellets or degrading haypiles with no fresh vegetation present. Patches that appeared unoccupied were sampled with additional time and effort to be confident in their unoccupied classification. Additional information regarding field-survey protocol can be found in Beever et al. (2011; 2013) and Billman et al. (2021).

Our surveys spanned three scales to assess variability in species-climate relationships: inter-regional (among ecoregions), intra-regional (i.e., among mountain ranges within a single ecoregion), and between two sampling periods. The inter-regional comparison included data from the Southern Rockies (New Mexico), Central Rockies (Wyoming and Montana), and the Northern Rockies (Montana and Idaho) which represent three of six recognized lineages of *O. princeps* (Schmidt et al., in prep, Galbreath et al., 2010). Site-selection protocol differed slightly among ecoregions (e.g., elevational-transect design in Northern Rockies vs a near-census in Southern Rockies), so we provide an in-depth description of each region's site-selection protocol in the Supplemental Information. The intra-regional dataset covers the Beaverhead Mountains, Italian Peaks, Lemhi Range, and the Tobacco Root Mountains nested within the Northern Rockies, which were surveyed in 2018–19. The temporal-analysis data were collected in the Central Rockies, with the "historical sampling period" spanning 2011–2016 and a "recent sampling period" from 2019–2021. These sites were all located within the Greater Yellowstone Ecosystem, including Yellowstone and Grand Teton National Park. All sites included in the temporal analysis were surveyed in both periods. However, several fewer sites were occupied in the latter period and excluded from the density analysis but retained (marked as unoccupied) in the occupancy analysis. Although these time periods seem relatively short when examining changes in occupancy, interannual patch turnover has been documented to be high for pikas in response to weather variability (e.g., Rodhouse et al., 2018). We excluded all talus patches without evidence of current or past pika occupancy, as these sites may not always have been structurally or otherwise suitable (following Billman et al., 2021). However, this may create minor differences between our study and others that have retained such no-evidence sites.

2.3 Climate data

Seasonal climate data were extracted from the standalone program, ClimateNA (Wang T et al., 2016). These data are locally downscaled from PRISM climate rasters using bilinear interpolation and account for site-specific elevation, latitude, and longitude. Summer (JJA) and winter conditions (DJF) are hypothesized to be the most stressful to pikas, so we extracted Summer: minimum, mean, and maximum temperature (respectively, T_{min}, T_{mean}, T_{max}), precipitation, relative humidity (RH), and climate moisture index (CMI), and Winter: T_{mean} and precipitation. We hypothesized each of these variables represents a mechanistic pathway of climatic influence on pikas. For example, winter precipitation (i.e., snowfall) has been shown to have a positive effect on site occupancy as higher snowpacks buffer pikas from sub-zero temperatures that occur above the snow (Beever et al., 2010; Johnston et al., 2019). Similarly, snowfall may be associated with higher population densities as heavy snowpacks provide a water source for high-quality forage in spring and summer in montane systems (Yandow et al., 2015). Full descriptions of the hypothesized mechanisms tied to each climate stressor can be found in Table 1 of the SI appendix.

For occupancy, we calculated the average climate conditions over the four years' seasons prior to surveying. Winter metrics included the winter immediately preceding surveys and the previous three winters, whereas summer metrics comprised the previous four summers. The 4-year window minimized overlap in the temporal dataset in the Central Rockies (i.e., ~95% resurveys were 4+ years after initial surveys, mean = 5.2 years). We excluded current summer conditions for occupancy because a large proportion of surveys occurred in June, so current-season metrics would therefore represent future conditions (after surveys occurred) in many instances. For density predictors, we included only the winter conditions immediately preceding surveys, as well the previous year's summer conditions (to avoid using data from after the date when a survey occurred in early summer).

2.4 Data analysis

For each region separately, climate metrics were scaled and centered using Z-scores to evaluate the relative importance of metrics that often differed by one to several orders of magnitude. Numerous studies have already sought to identify the top models and predictors of pika occupancy and density using multivariate modeling and AIC (e.g., Beever et al., 2011; Johnston et al., 2019; Billman et al., 2021), so we explicitly did not include that objective in this study. Rather, we examined the univariate effects of each climate variable on both responses. We used simple linear regression modeling for population density and logistic regression modeling for occupancy. As expected, density estimates showed a strong positive skew, so estimates were log-transformed to better meet the assumptions of parametric testing. We excluded unoccupied patches in the density analyses to differentiate the possible divergent drivers of occupancy and density. Given the species' consistently high detectability ($p \geq 0.90$, Beever et al., 2013; Ray et al., 2016), we used naive logistic regression models for occupancy, which assume perfect detectability ($p = 1$); naive models for this species have already been shown to be robust against parameter estimate bias in previous investigations (e.g., Rodhouse et al., 2010). We used the *lm()* function in base R for density analyses, and the *glm()* function in the *lme4* package (Bates et al., 2015). All plots were created using *ggplot2* (Wickham, 2011). Effect sizes and 95% confidence intervals were extracted from all model summaries. Coefficients for the logistic regression models are on the log-odds scale. Principal component analysis (PCA) plots were created using the *ggfortify* package (Tang et al., 2016), more specifically the *prcomp()* and *autoplot()* functions which scaled the eight climate variables prior to plotting (Figure 1). All analyses were conducted in R Statistical Software (v.4.2.2; R Core Team, 2021). Overall, we evaluated effect size strength (i.e., magnitude), directionality (+/−/non-significant if 95% CI included zero), and relative importance compared to other variables.

3 Results

There was marked heterogeneity in species–climate relationships across space and time. We surveyed and included a total of 1,867 talus patches for the inter-ecoregional dataset, 734 patches for the intra-regional dataset in the Northern Rockies, and 264 patches for the temporal dataset in the Central Rockies. Inter-regionally, approximately 30% of sites ($N = 565$) were historically occupied (i.e., possibly extirpated). Patches were distributed between 1,381 and 3,884 m above sea level, and breakdowns of patch occupancy by region and mountain range can be found in Table 2 of the SI Appendix. Patch sizes ranged from 1 pika home range (~315 m^2, ~20-m-diameter circle) to patches in Grand Teton NP that spanned >1 km^2. Lastly, patch-level population densities ranged from 0.23 to 4.0 pikas/50 m surveyed.

3.1 Inter-regional analysis

Across the three ecoregions, occupancy and density were all significantly negatively associated with the four temperatures metrics (mean β coefficient ± 1 SD; occupancy: −0.90 ± 0.21, density: −0.23 ± 0.08) and positively associated with the two moisture metrics (RH and CMI, mean β coefficient ± SD; occupancy: 0.62 ± 0.25; density: 0.25 ± 0.11). However, there was more nonstationarity in precipitation metrics across space than other metrics (Figure 2). Winter precipitation (i.e., snowfall) was positively associated with both responses in the Northern and Central Rockies, but unexpectedly not in the Southern Rockies. On the other hand, summer precipitation was only positively associated with both response metrics in the Northern Rockies, as well as occupancy in the Southern Rockies, but there were no relationships between summer precipitation and density in the Southern Rockies and both responses in the Central Rockies. The overall strength of species–climate relationships was stronger in the Northern and Central Rockies relative to the Southern Rockies. Notably, the precision of coefficient estimates did not consistently increase with greater sample sizes across regions.

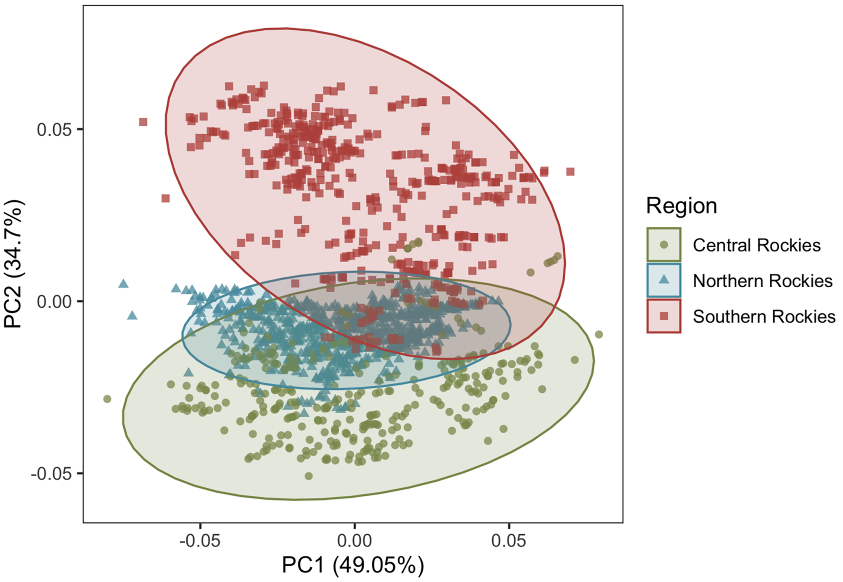

FIGURE 1
PCA plot illustrating the climate space of all sites across the three ecoregions. This PCA included all eight climate variables and explains 83.75% of the variance on the first two axes. For the Central Rockies cluster, we excluded the historical survey period to be more consistent with the timing of the surveying in the other two periods (~2016–2021).

3.2 Intra-regional analysis

All relationships coefficients were significant and consistent in directionality (within variables) across mountain ranges, with the exception of all Italian Peaks density variables, and T_{mean} in winter and relative humidity in summer for occupancy (Figure 2). Temperature was, again, consistently negative for both response metrics (when excluding the Italian Peaks, for density). Moisture and precipitation metrics were all positively associated with occupancy and density, as hypothesized (when excluding the Italian Peaks). For occupancy, the Beaverhead Mountains overwhelmingly displayed stronger species–climate relationships (i.e., larger coefficients) than did the other three mountain ranges, with only a few exceptions (Figure 2). Overall, coefficients showed a greater range across the various climate metrics in the intra-regional analysis relative to the inter-regional analysis (*occupancy*: inter-regional range = −1.18 to 1.47, intra-regional range = −1.76 to 3.30; *density*: inter-regional range = −0.39 to 0.36, intra-regional range = −0.41 to 0.64).

3.3 Temporal analysis

Similar to the inter- and intra-regional analyses, temperature consistently had a negative effect on both occupancy and density over time, with the exception of T_{max} in summer for density (Figure 3). Variability in the strength of relationships to temperature was notably greater for density than for occupancy. Relative humidity was significant only in the historical sampling period for both response metrics. Climate moisture index was positively associated with occupancy in both periods and density in the historical period, but negatively associated with density in the current period. Winter precipitation (i.e., snowfall) consistently had a positive effect on both responses in both periods, whereas summer precipitation had no effect on occupancy in either period, and was only significant for density in the current period. However, this summer-precipitation effect on density was surprisingly negative ($\beta = -0.38$, 95% CI: −0.52 to −0.23). Overall, there was lower congruency in the strength and directionality than expected between the two time periods that were only several years apart (e.g., only ~69% of cases showed consistent directionality).

4 Discussion

Here, we examined how species–climate relationships vary across spatial and temporal scales using a readily detectable small mammal whose range spans approximately one-third of North America. Overarchingly, we found higher temperatures consistently had a negative effect on both pika occupancy and densities, while moisture metrics mostly had positive effects on both responses. However, the importance of precipitation in summer and winter showed the highest nonstationarity across space, with winter snowpack having no effect on either response in the Southern Rockies, and summer precipitation having no effect on either response in the Central Rockies. Moreover, the precision of effect sizes was generally the lowest for precipitation metrics, both at inter- and intra-regional scales. Our findings illustrate the existence of some nonstationarity of biotic responses to certain climate factors, cautioning extrapolation beyond single regions or time periods.

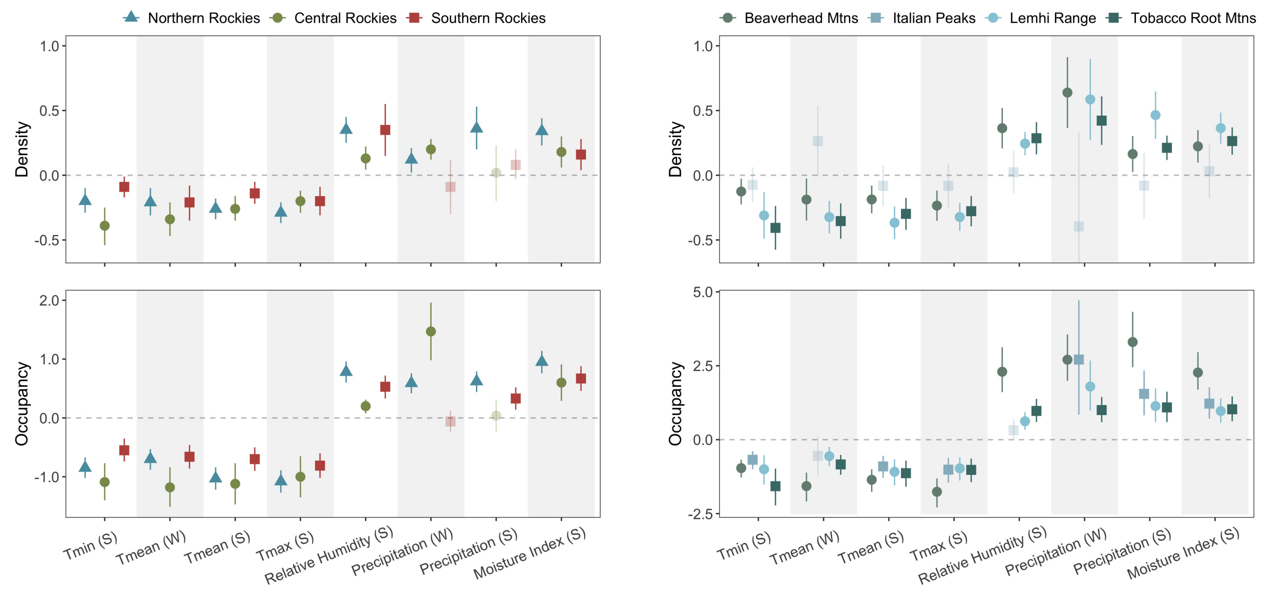

FIGURE 2
Coefficient estimates from univariate parameter estimates by climate metric and season in parentheses (S = summer, W = winter) for inter- and intra-regional analyses. Significant relationships between each response and climate variable (CIs do not overlap 0) are colored and opaque, whereas insignificant relationships (CIs overlap 0) are partially transparent. Coefficient estimates above the horizontal zero line suggest that variable has a positive effect on occupancy and density, and vice versa for estimates below the line. The cropped lower CI limit for the Italian Peaks' winter precipitation for density extends down to −1.12.

4.1 Among-ecoregion variability

At the inter-regional scale, which spans over twelve degrees of latitude and nearly ten degrees of longitude, there was general congruence in approximate coefficient size and directionality of temperature metrics for both responses. Overwhelmingly, warmer temperatures had a negative effect on both pika occupancy and density across the three vast ecoregions. In winter, warmer temperatures are typically correlated with lower snowpack, followed by lower snow retention into summer, which may explain why warmer winters have a negative effect. These results corroborate numerous other studies that highlight the sensitivity of pikas to warmer temperatures across seasons (Beever et al., 2003; Wilkening et al., 2011; Stewart et al., 2015). In contrast, several other investigations have found the effect of temperature on pikas to vary across study areas (Jeffress et al., 2013; Rodhouse et al., 2018). Nevertheless, high summertime temperatures have also been implicated in constraining dispersal abilities and corridors used by pikas (Henry et al., 2012; Castillo et al., 2014), suggesting that the previously occupied sites in hotter areas may be less likely to be recolonized. Given that all three ecoregions have warmed in recent decades, our results indicate that further temperature-related patch-level extirpations seem likely for the species, unless increases in precipitation possibly ameliorate thermal stress.

In addition to temperature, we found full congruence in the directionality of the two moisture metrics across ecoregions, suggesting that water balance constitutes a predictable selective pressure on pikas. However, the two seasonal-precipitation metrics were less consistently significant, showing several insignificant relationships depending on the ecoregion and response metric. Such differences appear to align with the amount of snowfall received and its duration, across our study regions. Downscaled data from ClimateNA are tightly correlated with weather-station measurements for temperature metrics ($R^2 \geq 0.99$) but not as much with precipitation metrics ($R^2 \geq 0.64$), leading to substantially lower predictive power for precipitation metrics (Wang T et al., 2016). Therefore, we cannot rule out possible climate-downscaling discrepancies as a contributor to insignificant relationships with precipitation. Still, we suspect the lack of consistent relationships with precipitation may be due to unaccounted-for interactions with temperature that may be biologically relevant. For example, another study found that high temperatures were indeed more influential on pika occupancy in drier national parks (Jeffress et al., 2013). Whereas Erb et al. (2011) found that annual precipitation best predicted pika occupancy across 69 sites in the Southern Rockies, we found that only precipitation in summer had a small positive effect on occupancy, whereas winter precipitation surprisingly had no effect in the Southern Rockies. West of the Rocky Mountains, in

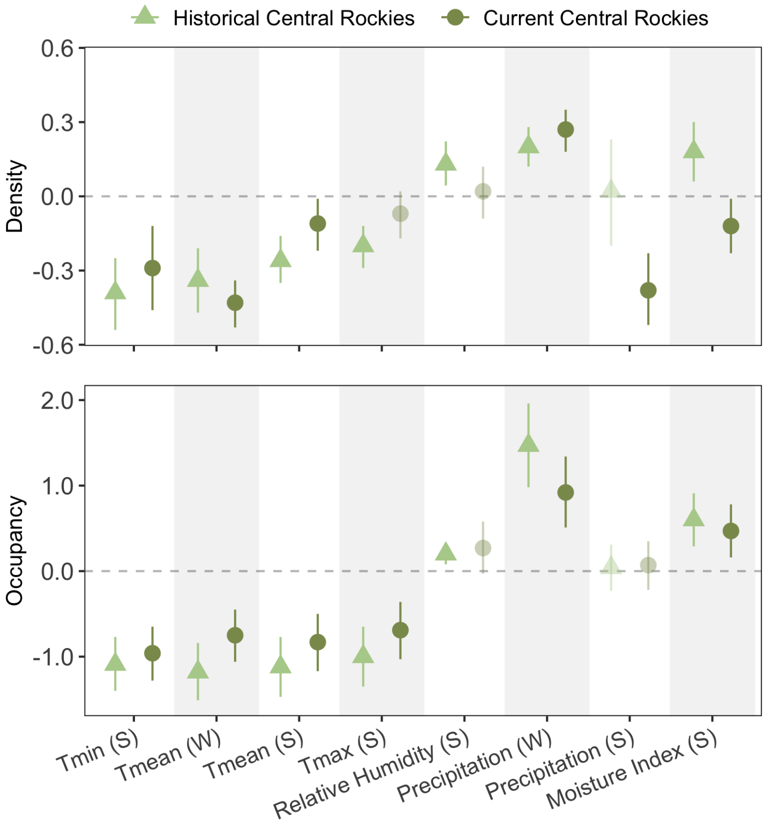

FIGURE 3
Coefficient estimates for univariate parameter estimates by climate metric and season for the Central Rockies temporal analysis. The light green triangle points represent the historical-period sampling (2011–2016), whereas the dark green circle points represent the recent-period sampling (2019–2021).

the Great Basin ecoregion, Millar et al. (2018) described the climate envelope of pika-extant sites as ranging from 7–83 mm for summer precipitation, whereas our pika-occupied sites had consistently more summer precipitation (Southern Rockies: 137–392 mm, Central: 68–247 mm, and Northern: 82–203 mm). Millar et al. (2018) suggested that Great Basin pikas can accommodate substantially more-arid summer conditions than what we have found in the Rocky Mountains, indicating that thresholds of pika sensitivity may vary across ecoregions. For example, 99.4% of our historically occupied (possibly extirpated) sites in the Rockies were still wetter in term of summer precipitation (Southern Rockies: 135–387 mm, Central: 57–239 mm, and Northern: 75–208 mm) than pika-occupied sites in the Great Basin (Millar et al., 2018). For summer T_{max}, Millar et al. (2018) reported their pika-extant sites ranged from 11.4 to 29.9°C; our extant sites fell entirely within their ranges (14.4–26.8°C). However, our warmest (T_{max}) historically occupied sites across our three regions only reached 27.4–29.1°C, suggesting a possible lower threshold for summer heat tolerance in the Rocky Mountains relative to the Great Basin.

Across temperature and precipitation metrics, our results continue to illustrate how climate-envelope thresholds may differ substantially across species' ranges. Such differences may also, in part, reflect genetic, behavioral, habitat (e.g., microrefugia, forage quality), or other differences among populations that remain difficult to model. Our findings reiterate other studies' calls for consideration of the context-dependencies of scale prior to formulating range-wide generalities (Schwalm et al., 2016). Nonstationarity in precipitation metrics especially warrants caution of their inclusion in broad-scale modeling, whereas temperature and moisture metrics appeared to play a more predictable role in shaping occupancy and population densities, herein. For precipitation metrics, the use of spatially varying coefficients (SVCs) in distribution modeling may be one effective solution to account for this large spatial variation in the relative and absolute importance of these metrics.

Investigations into spatial nonstationarity in species-environment relationships have been growing in recent years, with studies often documenting the greatest spatial nonstationarity in climate metrics specifically (Pease et al., 2022b). Identifying the key drivers of variability in these relationships is especially important for management decision-making and policy. Given that management actions are generally implemented at local- to regional-scales, results from one region applied elsewhere should be evaluated with particular care since species–climate relationships vary across spatial and temporal extents, over which environmental stressors can differ (Pease et al., 2022a). Yet, species-specific data limitations may constrain robust modeling efforts at local scales when resources and data are limited. This may be especially pronounced in rural areas, where species occurrence records are less common than near urban settings (Bowler et al., 2022). One solution to fill spatial gaps at local scales may involve heavier reliance on citizen-science data for additional occurrence and density records in some instances, but experts may still need to determine true absences for presence-absence models. In addition, there are widespread biases in occurrence records across species due to various reasons (e.g., body size, rarity, and group size, Callaghan et al., 2021), but intraspecific species–environment relationships often do not correlate to patterns with heterospecifics in the same community or in closely related species (e.g., Rossi et al., 2023). Accordingly, considerations may be necessary at the species level. Our results show that the level of species-specific nonstationarity depends on which climate metrics are evaluated in modeling (i.e., some metrics, like temperature, exhibited surprising levels of stationarity over large spatial domains), a pattern that is likely prevalent across taxa. We therefore caution that community-scale modeling that does not account for species-specific relationships with climate may be ineffective for predicting the future distributions of species, especially when extrapolating into novel conditions and the distant future.

4.2 Within-ecoregion variability

Relative to the inter-regional comparison, intra-regional coefficients were more variable, showing a larger range of strengths (*occupancy*: within-region: −1.76 to 3.30, among-regions: −1.18 to 1.47; *density*: within-region: −0.41 to 0.64, among-regions: −0.39 to 0.36). However, this may partially be due to smaller sample sizes within mountain ranges relative to across mountain ranges (Table 2, SI Appendix). Excluding the Italian Peaks, responses in the other three mountain ranges showed consistent directionality of each response to climate, with both summer and winter precipitation and moisture-related metrics having reliably positive effects. For these four variables, coefficients still varied widely in most cases (e.g., relative humidity for occupancy, coefficient range: 0.32–2.3 on the log-odds scale). Temperature had consistently negative effects on both occupancy and abundance, in alignment with the inter-regional analyses. The general consistency of response directionality among the three mountain ranges provides some promise that within ecoregions, results from one mountain range may be relevant (to some extent) to other nearby mountain ranges for both occupancy and density in a given time period.

Results from the Italian Peaks diverged from the other three ranges, whereby all climate relationships were insignificant for density, and winter T_{mean} and summer relative humidity were insignificant for occupancy. To note, the Italians Peaks were the only mountain range where pika population densities decreased slightly with elevation (see Figure S2 in Billman et al., 2021). The underlying geology of the Italian Peaks is predominantly limestone. Unlike the larger metamorphic and igneous talus found throughout the other mountain ranges, limestone talus in this mountain range was typically smaller in size (10- to 50-cm-diameter rocks, on average) and, consequently, shallower than larger-clast talus slopes. Although numerous studies have promoted optimism for the microclimate buffering capacity of talus as a long-term refugia for pikas (e.g., Millar et al., 2013), one recent study found that deep, subsurface temperatures in talus in Colorado (USA) had still warmed substantially between 1963–64 and 2009–21 (Monk and

Ray, 2022). Accordingly, we suspect that the lack of pika–climate relationships for density in the Italian Peaks may largely be due to poor thermal buffering of the small, limestone talus; smaller rock diameters and shallower talus depth likely translate to warmer interstitial temperatures at low elevations and colder temperatures at high elevations. Thermally stressful conditions at the lowest and highest elevations in this mountain range would suggest a linear relationship for density would have no detectable effect; instead, the relationships may be quadratic, with the most favorable conditions for population densities at the mid elevations. On the contrary, the Beaverhead Mountains generally showed the strongest effect sizes, particularly for occupancy (Figure 2), which may have been due to topographic similarity of sampled watersheds in this mountain range. This range is especially linear and all watersheds on the west have comparable elevational spans of habitat and minimum elevations of occupancy, whereas the east-side watersheds retracted very little and also have comparable minimum elevations of current occupancy to one another (Billman et al., 2021). These elevational patterns of occupancy (vs extirpation) likely explain why the pika-climate relationships there were often the strongest compared to the other ranges. Lastly, the Beaverhead sites exhibited the broadest climate space in a PCA that included all eight climate variables (Figure S1). Overall, these context-dependencies highlight necessary caution when applying interpretations among mountain ranges with differing topography and geology, for example.

Although some empirical studies found that species–climate relationships become more stationary, and predictable, at broader scales (e.g., Miller and Hanham, 2011), others have found stationarity decreases at larger scales, such as when study regions are spaced far apart (e.g., McAlpine et al., 2008). Discrepancies here likely arise because far-apart study domains may or may not be similar in terms of climate, vegetation, and species composition, among other factors. Because the four mountain ranges in our Northern Rockies intra-regional analysis had similar climatic conditions and other similarities, like vegetation, we predicted that stationarity would be higher in terms of coefficient directionality and magnitude relative to the inter-regional analysis. However, we surprisingly found less congruence in effect-size magnitude and more consistency in climate-relationship directionality (when excluding the Italian Peaks). Interestingly, pika–climate relationships for precipitation and moisture metrics were consistently stronger (i.e., larger magnitudes) at local scales relative to the inter-regional analysis, suggesting that variability in range-wide modeling datasets may dampen the overall strength of species–climate relationships at local scales, which are more relevant to managers.

On the contrary, we found comparable coefficients for temperature metrics between intra- and inter-regional analyses for density (mean temperature β coefficient: −0.22 vs. −0.23, respectively), and occupancy (−1.06 vs. −0.90, respectively). Because eco-evolutionary processes are hierarchically structured in nature, patterns found at local scales often do not align with those at much broader scales (Osborne et al., 2007), making these findings particularly surprising. For species with large distributions that span immense climate gradients, species–climate relationships should generally be examined at the ecoregional scale when possible due to comparable topography, geology, vegetation, and climatic conditions (Smith et al., 2019). Within said ecoregions, we advise sampling efforts span the largest gradient of environmental conditions possible to evaluate variability in relationships over space. Given what we found intra-regionally, anomalous conditions in select mountain ranges (within an ecoregion) may warrant their exclusion from regional models, but they should also receive additional sampling efforts in the future would be beneficial to better understand and predict species–climate relationships therewithin.

In this case, pika–climate relationships for temperature metrics may be more practical than precipitation and moisture metrics for extrapolating to new regions or at different scales if necessary, but further exploration seem warranted. Our findings overall have important implications for species distribution modeling in the face of climate change, given that temperatures are rising across most of the planet, but changes in precipitation vary considerably and are less predictable (IPCC, 2022). Yet, precipitation and moisture are predicted to grow increasingly important for terrestrial species moving forward to maintain body cooling requirements with rising temperatures (Riddell et al., 2019). Provided that extirpations often occur at the hottest and driest sites within a species range, understanding spatial nonstationarity in precipitation and moisture metrics are critical for informing and modeling extinction risks.

4.3 Temporal variability

In general, we found high agreement of directionality within climate metrics over time, but less so for climate-density relationships than for climate-occupancy. For both responses, we identified only one case where the directionality of an effect changed sign through time; density was positively influenced by climate moisture index in the historical period, but CMI had a negative effect in the more-recent survey period. In contrast, the results from the occupancy analysis suggested moisture had a consistently positive effect in both periods, highlighting how the drivers of occupancy and density may not always align, a result documented in other studies as well (e.g., Dibner et al., 2017). Climate-density relationships are often less predictable than occupancy, since shorter-term processes generally drive population densities whereas changes in occupancy occur over longer periods and are often influenced by larger-scale processes like macroclimate (Beever et al., 2013; Schulz et al., 2019).

There were several cases where species–climate relationships were significant in one period but not the other in our analysis. This temporal nonstationarity appeared unpredictable and was found in temperature, moisture, and precipitation metrics (*density*: T_{max}, relative humidity, and summer precipitation; *occupancy*: relative humidity). One possible explanation for temporal divergence is that correlations among climate metrics are often nonstationary themselves over time, whereby changes in temperature do not always correlate with changes in precipitation, for example (e.g., Bueno de Mesquita et al., 2021). In our case, summer relative humidity had a positive effect on occupancy in the historical period but not the more-recent period, whereas all other relationships with occupancy and climate were significant (except summer precipitation in both periods). This may indicate that temperature, winter precipitation, and CMI were more limiting in the more-recent survey period than relative humidity. Similarly, the relative importance of climate variables may have changed over time (Marcinkowski et al., 2015). Our mixed results regarding temporal nonstationarity somewhat stand in contrast to another pika study that found relatively high temporal transferability of SDMs in California (Stewart et al., 2015). Although the ecological explanations discussed above may indeed account for this change in variable importance over time, the range of climate values could differ between periods, where conditions may never have reached some stress threshold in the more-recent period. However, this possibility is unlikely in the case of relative humidity, given that the historical-period range was 44.5–70.5% and the recent-period range was 44.5–71.6% – nearly identical. In fact, the overall climate space of surveyed sites between periods had remarkable overlap when using a PCA that included all eight climate metrics (Figure S2). Overall, these patterns caution interpretations of results from single-time period surveys, including those in the two spatial analyses above. While biological interpretations of nonstationarity in species–climate relationships remain important, mathematical evaluation of whether the range of predictor values (prior to scaling and centering) might vary substantially over time over time would provide a valuable complement; this, in turn, could strongly alter the magnitude and directionality of predictors on the response across time periods.

A majority of studies on temporal stationarity in ecology thus far have focused on tree rings. These studies have frequently found that correlations between ring growth and climate fluctuate between significant and non-significant; such fluctuations have been attributed to changes in weather patterns through time. For example, one study found that the effect of winter precipitation on ring growth has decreased over time and become insignificant, whereas the effects of spring temperature and prior-year summer temperatures have become significant recently (Marcinkowski et al., 2015). This often unpredictable de-coupling of species–climate relationships on interannual and interdecadal timescales has wide-ranging implications for SDMs, which typically assume temporal stationarity (i.e., mean and variance change do not over time). However, assuming stationarity is unlikely to capture the complexity of underlying ecological processes and how variable they can be through time. Similar to previous tree-ring studies, our temporal-scale results highlight how assuming stationarity, even over a short time span, could also be misleading and generate incorrect interpretations of animal–climate relationships as well (Bueno de Mesquita et al., 2021). Accordingly, recent studies have recommended that temporal nonstationarity (rather than stationarity) should be the baseline assumption when modeling species–climate relationships through time (Tumajer et al., 2023).

Responses to weather and climate conditions are also highly variable across species (Rossi et al., 2023). Therefore, the degree of nonstationarity can be expected to differ markedly among species within the same community and site (Hereş et al., 2022). This adds an additional layer of complexity when modeling but must be considered prior to applying interpretations from one species to another. Collectively, a stronger emphasis should be placed on understanding temporal nonstationarity in animals to more effectively inform future SDMs, as well as management strategies that rely on timely, near-term forecasts. More broadly, in the face of deterministic climate change, directional selection across species may be an important evolutionary process for many populations over time (decades to centuries); however, increased frequency of extreme events may instead lead to destabilizing selection as well.

4.4 Important considerations and caveats

The primary goal of this study was not to identify top models for predicting occupancy and density, but rather to evaluate variability in species–climate relationships over space and time using univariate climatic factors. Accordingly, there are key interactions among climate factors that likely also explain important mechanisms of stress in this species. We only modeled linear relationships for density, which may or may not be the most descriptive model structure. We acknowledge these simple models constitute a great over-simplification of the full dynamics governing species occupancy and abundance. However, given 1) particular questions that we and our management partners sought to address in the various regions, and 2) our primary objective in this study to assess nonstationarity in species–climate relationships across space and time, we believe our current approach most directly addresses this objective. In addition, our study did not model relationships with non-climatic factors that are also important for occupancy and density, such as habitat suitability and connectivity, forage quality and abundance, interspecific interactions, microclimate temperatures, among others. As described elsewhere, metapopulation dynamics, Allee effects, human disturbances, and other transient processes also cloud the relationship between species and their environment (Holt, 2020). We acknowledge that, particularly relevant for our analyses of density, error and uncertainties are not propagated in other ways through our analysis; Bayesian approaches may better account for this noisiness, explicitly.

Given that American pikas have been considered a sentinel species for understanding metapopulation dynamics and the impact of climate change on alpine species, our findings of consistently strong species–climate relationships for most variables and scales are particularly exciting and highlight how strongly macro-climate appears to influence this species along with micro-climate conditions. Although our sampling design differed slightly among the Southern, Central, and Northern Rockies, we found many consistent relationships among regions (i.e., stationarity, see T_{max} in summer) which suggests that methodological differences in study design may not always lead to divergent results and interpretations. Nevertheless, we do not encourage applying different survey designs over space when it's possible to avoid. The presence of local adaptation across regions and the two pika lineage here was also beyond the scope of this study but may well be an important factor in species–climate relationships when comparing multiple ecoregions that have long had vastly different climatic conditions. These considerations are important when evaluating the applicability of SDMs for any given species, or otherwise projecting results from one study region or timescale to another. However, further studies examining species' relationships with univariate climate factors would be beneficial to improving our understanding of species' ecology, physiology, and conservation.

Nonstationarity, if unaccounted for, decreases model performance and reliability, but so does climate novelty when models aim to predict species' responses beyond the range of the calibration data. Nonstationarity can reflect true biological or mechanistic changes in species–environment relationships over space or time; in contrast, model error can emerge simply due to inappropriate extrapolation into novel conditions. Whereas the focus of our investigation was to examine issues related to nonstationarity, ignoring climate novelty during SDM creation and application will also provide biologically unrealistic inferences and deteriorate model predictability. In addition, novel conditions and nonstationarity may act synergistically in influencing model performance and thus, overall utility. The development of increasingly flexible model structures should seek to account for both ecological nonstationarity and novel conditions when possible, as both are predicted to increase under continuing contemporary climate change (Radeloff et al., 2015).

5 Implications

The impending loss of global biodiversity underscores the need to evaluate species' vulnerabilities to further shifts in climate, overexploitation, invasive species, and land-use patterns (Díaz et al., 2019). Species' exposure and adaptive capacities are now recognized to vary widely across spatial scales (Beever et al., 2023) but given that ecological relationships are notoriously variable over multiple spatial and temporal dimensions, understanding patterns in new places, time periods, and under no-analog conditions can be difficult. However, there are growing opportunities to now capitalize on "big-data" systems that span many disciplines to better evaluate the importance of scale. Growing recognition of nonstationarity in ecological processes has highlighted remaining questions related to the appropriate scales for investigations, the limits of extrapolation, and the overall usefulness of spatially explicit models. Although our results were mostly comparable across three of the four ranges within the single ecoregion, range-wide modeling using climate envelopes from one region and time period would provide inaccurate and unrealistic results in most cases – particularly for precipitation, according to our results. Holistically, our results stress how a better understanding of the appropriate spatial and temporal scales of species–climate responses could create more effective, tailored climate-adaptation strategies under shifting conditions.

Analyses in recent years have begun exploring new mathematical methods in their models, like spatially varying coefficients (SVCs), to account for nonstationarity in species–climate relationships over space and time (e.g., Humphreys et al., 2022; Sultaire et al., 2022), justification for which is further supported by our analyses. Similarly, geographically and temporally weighted regression and machine learning in ecology should be considered in more instances, given their often-superior performance relative to other methods in forecasting processes in cases where nonstationarity is high (Feng et al., 2021). Nevertheless, model structure choice should ultimately be motivated by the study question at hand (Segurado et al., 2006). While we encourage additional investigations into nonstationarity in species–climate relationships across spatial domains, we anticipate future investigations into how these relationships change through time will yield the greatest insights in a rapidly changing world. Although the full complexity of ecological networks can never be fully modeled, we hope the results here provide further motivation to continue discussions surrounding the relationships of patterns and scale in order to improve biodiversity management and forecasts moving forward.

Data availability statement

The original contributions presented in the study are publicly available. This data can be found here: USGS Science Data Catalog (SDC), https://doi.org/10.5066/P9WB1EWC.

Ethics statement

Ethical review and approval was not required for the animal study because this study only included observational data.

Author contributions

PB, conceptualization, methodology, data collection and curation, formal analysis, investigation, writing–original draft, writing–review and editing, visualization, and supervision. EB, conceptualization, methodology, data collection and curation, investigation, writing–original draft, writing–review, and editing. MW and DR, data collection and curation, writing–original draft, and writing–review and editing. All authors contributed to the article and approved the submitted version.

Funding

This work was funded by numerous organizations and grants, including the American Society of Mammalogists GIAR (PB, MW), Northwest Scientific Association (PB), Sigma Xi (PB), American Alpine Club (PB), Western National Parks Association (EB), U.S. Geological Survey (EB), University of New Mexico Joseph Gaudin Scholarship (MW), and the New Mexico Research Grant (MW). Any use of trade, firm, or product names is for descriptive purposes only and does not imply endorsement by the U.S. Government.

Conflict of interest

The authors declare that the research was conducted in the absence of any commercial or financial relationships that could be construed as a potential conflict of interest.

Publisher's note

Supplementary material

The Supplementary Material for this article can be found online at: https://www.frontiersin.org/articles/10.3389/fevo.2023.1202610/full#supplementary-material

References

Bates, D., Maechler, M., Bolker, B., and Walker, S. (2015). Fitting linear mixed-effects model using lme4. *J. Stat. Softw.* 67 (1), 1–48. doi: 10.18637/jss.v067.i01

Beever, E., Brussard, P. E., and Berger, J. (2003). Patterns of apparent extirpation among isolated populations of pikas (*Ochotona princeps*) in the great basin. *J. Mammal.* 84 (1), 37–54. doi: 10.1644/1545-1542(2003)084<0037:POAEAI>2.0.CO;2

Beever, E. A., Dobrowski, S. Z., Long, J., Mynsberge, A. R., and Piekielek, N. B. (2013). Understanding relationships among abundance, extirpation, and climate at ecoregional scales. *Ecology* 94 (7), 1563–1571. doi: 10.1890/12-2174.1

Beever, E. A., Ray, C., Mote, P. W., and Wilkening, J. L. (2010). Testing alternative models of climate-mediated extirpations. *Ecol. Appl.* 20 (1), 164–178. doi: 10.1890/08-1011.1

Beever, E. A., Ray, C., Wilkening, J. L., Brussard, P. F., and Mote, P. W. (2011). Contemporary climate change alters the pace and drivers of extinction. *Global Change Biol.* 17 (6), 2054–2070. doi: 10.1111/j.1365-2486.2010.02389.x

Beever, E. A., Wilkening, J. L., Billman, P. D., Thurman, L. L., Ernest, K. A., Wright, D. H., et al. (2023). Geographic and taxonomic variation in adaptive capacity among mountain-dwelling small mammals: implications for conservation status and actions. *Biol. Conserv.* 282, 109942. doi: 10.1016/j.biocon.2023.109942

Benedict, L. M., Wiebe, M., Plichta, M., Batts, H., Johnson, J., Monk, E., et al. (2020). Microclimate and summer surface activity in the American pika (Ochotona princeps). *Western North Am. Nat.* 80 (3), 316–329. doi: 10.3398/064.080.0303

Billman, P. D., Beever, E. A., McWethy, D. B., Thurman, L. L., and Wilson, K. C. (2021). Factors influencing distributional shifts and abundance at the range core of a climate-sensitive mammal. *Glob. Chang. Biol.* 27 (19), 4498–4515. doi: 10.1111/gcb.15793

Bowler, D. E., Callaghan, C. T., Bhandari, N., Henle, K., Benjamin Barth, M., Koppitz, C., et al. (2022). Temporal trends in the spatial bias of species occurrence records. *Ecography* 2022 (8), e06219. doi: 10.1111/ecog.06219

Briscoe, N. J., Morris, S. D., Mathewson, P. D., Buckley, L. B., Jusup, M., Levy, O., et al. (2022). Mechanistic forecasts of species responses to climate change: the promise of biophysical ecology. *Global Change Biol.* 1451-1470. doi: 10.1111/gcb.16557

Brown, J. H. (1984). On the relationship between abundance and distribution of species. *Am. Nat.* 124 (2), 255–279. doi: 10.1086/284267

Bueno de Mesquita, C. P., White, C. T., Farrer, E. C., Hallett, L. M., and Suding, K. N. (2021). Taking climate change into account: non-stationarity in climate drivers of ecological response. *J. Ecol.* 109 (3), 1491–1500. doi: 10.1111/1365-2745.13572

Calabrese, G. M., and Pfennig, K. S. (2023). Climate change alters sexual signaling in a desert-adapted frog. *Am. Nat.* 201 (1), 91–105. doi: 10.1086/722174

Callaghan, C. T., Poore, A. G., Hofmann, M., Roberts, C. J., and Pereira, H. M. (2021). Large-Bodied birds are over-represented in unstructured citizen science data. *Sci. Rep.* 11 (1), 19073. doi: 10.1038/s41598-021-98584-7

Carroll, K. A., Farwell, L. S., Pidgeon, A. M., Razenkova, E., Gudex-Cross, D., Helmers, D. P., et al. (2022). Mapping breeding bird species richness at management-relevant resolutions across the united states. *Ecol. Appl.* 32 (6), e2624. doi: 10.1002/eap.2624

Castillo, J. A., Epps, C. W., Davis, A. R., and Cushman, S. A. (2014). Landscape effects on gene flow for a climate-sensitive montane species, the American pika. *Mol. Ecol.* 23 (4), 843–856. doi: 10.1111/mec.12650

Charney, N. D., Record, S., Gerstner, B. E., Merow, C., Zarnetske, P. L., and Enquist, B. J. (2021). A test of species distribution model transferability across environmental and geographic space for 108 western north American tree species. *Front. Ecol. Evol.* 9, 689295. doi: 10.3389/fevo.2021.689295

Cordes, L. S., Blumstein, D. T., Armitage, K. B., CaraDonna, P. J., Childs, D. Z., Gerber, B. D., et al. (2020). Contrasting effects of climate change on seasonal survival of a hibernating mammal. *Proc. Natl. Acad. Sci. U. S. A.* 18119-18126. doi: 10.1073/pnas.1918584117

Darwin, C. (1859). *On the origin of species* (London, UK: Routledge).

Díaz, S. M., Settele, J., Brondízio, E., Ngo, H., Guèze, M., Agard, J., et al. (2019). *The global assessment report on biodiversity and ecosystem services: summary for policy makers.*

Dibner, R. R., Doak, D. F., and Murphy, M. (2017). Discrepancies in occupancy and abundance approaches to identifying and protecting habitat for an at-risk species. *Ecol. Evol.* 7 (15), 5692–5702. doi: 10.1002/ece3.3131

Eastman, L. M., Morelli, T. L., Rowe, K. C., Conroy, C. J., and Moritz, C. (2012). Size increase in high elevation ground squirrels over the last century. *Global Change Biol.* 18 (5), 1499–1508. doi: 10.1111/j.1365-2486.2012.02644.x

Erb, L. P., Ray, C., and Guralnick, R. (2011). On the generality of a climate-mediated shift in the distribution of the American pika (*Ochotona princeps*). *Ecology* 92 (9), 1730–1735. doi: 10.1890/11-0175.1

Erb, L. P., Ray, C., and Guralnick, R. (2014). Determinants of pika population density vs. occupancy in the southern rocky mountains. *Ecol. Appl.* 24 (3), 429–435. doi: 10.1890/13-1072.1

Feng, L., Wang, Y., Zhang, Z., and Du, Q. (2021). Geographically and temporally weighted neural network for winter wheat yield prediction. *Remote Sens. Environ.* 262, 112514. doi: 10.1016/j.rse.2021.112514

Galbreath, K. E., Hafner, D. J., Zamudio, K. R., and Agnew, K. (2010). Isolation and introgression in the intermountain West: contrasting gene genealogies reveal the complex biogeographic history of the American pika (*Ochotona princeps*). *J. Biogeogr.* 37 (2), 344–362. doi: 10.1111/j.1365-2699.2009.02201.x

Goodman, M. C., Carroll, G., Brodie, S., Grüss, A., Thorson, J. T., Kotwicki, S., et al. (2022). Shifting fish distributions impact predation intensity in a sub-Arctic ecosystem. *Ecography* 2022 (9), e06084. doi: 10.1111/ecog.06084

Guisan, A., Graham, C. H., Elith, J., Huettmann, F., and Group, N. S. D. M. (2007). Sensitivity of predictive species distribution models to change in grain size. *Diversity Distrib.* 13 (3), 332–340. doi: 10.1111/j.1472-4642.2007.00342.x

Guisan, A., Thuiller, W., and Zimmermann, N. E. (2017). *Habitat suitability and distribution models: with applications in r* (Cambridge, UK: Cambridge University Press).

Hafner, D. J., and Sullivan, R. M. (1995). Historical and ecological biogeography of nearctic pikas (Lagomorpha, ochotonidae). *J. Mammal.* 76 (2), 302–321. doi: 10.2307/1382343

Henry, P., Sim, Z. J., and Russello, M. A. (2012). Genetic evidence for restricted dispersal along continuous altitudinal gradients in a climate change-sensitive mammal: the American pika. *PloS One* 7 (6), 10. doi: 10.1371/journal.pone.0039077

Hereş, A.-M., Polanco-Martínez, J. M., Petritan, I. C., Petritan, A. M., and Yuste, J. C. (2022). The stationary and non-stationary character of the silver fir, black pine and scots pine tree-growth-climate relationships. *Agric. For. Meteorol.* 325, 109146. doi: 10.1016/j.agrformet.2022.109146

Holt, R. D. (2020). Reflections on niches and numbers. *Ecography* 43 (3), 387–390. doi: 10.1111/ecog.04828

Humphreys, J. M., Srygley, R. B., Lawton, D., Hudson, A. R., and Branson, D. H. (2022). Grasshoppers exhibit asynchrony and spatial non-stationarity in response to the El Niño/Southern and pacific decadal oscillations. *Ecol. Model.* 471, 110043. doi: 10.1016/j.ecolmodel.2022.110043

IPCC. (2022). *Climate Change 2022: Impacts, Adaptation, and Vulnerability. Contribution of Working Group II to the Sixth Assessment Report of the Intergovernmental Panel on Climate Change.* [Pörtner, H.-O., Roberts, D. C., Tignor, M., Poloczanska, E. S., Mintenbeck, K., Alegría, A., Craig, M., Langsdorf, S., Löschke, S., Möller, A. , Okem, A. , and Rama, B. (Eds.)] (Cambridge University Press. Cambridge

University Press, Cambridge, UK and New York, NY, USA) 3056 pp. doi: 10.1017/9781009325844

Jeffress, M. R., Rodhouse, T. J., Ray, C., Wolff, S., and Epps, C. (2013). The idiosyncrasies of place: geographic variation in the climate-distribution relationships of the American pika. *Ecol. Appl.* 23 (4), 864–878. doi: 10.1890/12-0979.1

Johnston, A. N., Bruggerman, J., Beers, A. T., Beever, E. A., Christopherson, R. G., and Ransom, J. I. (2019). Ecological consequences of anomalies in atmospheric moisture and snowpack. *Ecology* 100 (4), e02638. doi: 10.1002/ecy.2638

Kearney, M. R., Wintle, B. A., and Porter, W. P. (2010). Correlative and mechanistic models of species distribution provide congruent forecasts under climate change. *Conserv. Lett.* 3 (3), 203–213. doi: 10.1111/j.1755-263X.2010.00097.x

Kerner, J. M., Krauss, J., Maihoff, F., Bofinger, L., and Classen, A. (2023). Alpine butterflies want to fly high: species and communities shift upwards faster than their host plants. *Ecology* 104 (1), e3848. doi: 10.1002/ecy.3848

Lee-Yaw, J. A., McCune, L., Pironon, S., and Sheth, S. N. (2022). Species distribution models rarely predict the biology of real populations. *Ecography* 2022 (6), e05877. doi: 10.1111/ecog.05877

Marcinkowski, K., Peterson, D. L., and Ettl, G. J. (2015). Nonstationary temporal response of mountain hemlock growth to climatic variability in the north cascade range, Washington, USA. *Can. J. For. Res.* 45 (6), 676–688. doi: 10.1139/cjfr-2014-0231

Martínez-Minaya, J., Cameletti, M., Conesa, D., and Pennino, M. G. (2018). Species distribution modeling: a statistical review with focus in spatio-temporal issues. *Stoch. Environ. Res. Risk Assess.* 32, 3227–3244. doi: 10.1007/s00477-018-1548-7

McAlpine, C., Rhodes, J., Bowen, M., Lunney, D., Callaghan, J., Mitchell, D., et al. (2008). Can multiscale models of species' distribution be generalized from region to region? a case study of the koala. *J. Appl. Ecol.* 45 (2), 558–567. doi: 10.1111/j.1365-2664.2007.01431.x

Millar, C. I., Delany, D. L., Hersey, K. A., Jeffress, M. R., Smith, A. T., Van Gunst, K. J., et al. (2018). Distribution, climatic relationships, and status of American pikas (Ochotona princeps) in the great basin, USA. *Arctic Antarctic Alpine Res.* 50 (1). doi: 10.1080/15230430.2018.1436296

Millar, C. I., Westfall, R. D., and Delany, D. L. (2013). Thermal and hydrologic attributes of rock glaciers and periglacial talus landforms: Sierra Nevada, California, USA. *Quat. Int.* 310, 169–180. doi: 10.1016/j.quaint.2012.07.019

Miller, J. A., and Hanham, R. Q. (2011). Spatial nonstationarity and the scale of species–environment relationships in the Mojave desert, California, USA. *Int. J. Geographical Inf. Sci.* 25 (3), 423–438. doi: 10.1080/13658816.2010.518147

Monk, E. M., and Ray, C. (2022). Revisiting talus and free-air temperatures after 50 years of change at an American pika (Ochotona princeps) study site in the southern Rockies. *PloS Climate* 1 (7), e0000049. doi: 10.1371/journal.pclm.0000049

Osborne, P. E., Foody, G. M., and Suárez-Seoane, S. (2007). Non-stationarity and local approaches to modelling the distributions of wildlife. *Diversity Distrib.* 13 (3), 313–323. doi: 10.1111/j.1472-4642.2007.00344.x

Pardi, M. I., Terry, R. C., Rickart, E. A., and Rowe, R. J. (2020). Testing climate tracking of montane rodent distributions over the past century within the great basin ecoregion. *Global Ecol. Conserv.* 24, e01238. doi: 10.1016/j.gecco.2020.e01238

Pease, B. S., Pacifici, K., and Kays, R. (2022a). Exploring spatial nonstationarity for four mammal species reveals regional variation in environmental relationships. *Ecosphere* 13 (8), e4166. doi: 10.1002/ecs2.4166

Pease, B. S., Pacifici, K., Kays, R., and Reich, B. (2022b). What drives spatially varying ecological relationships in a wide-ranging species? *Diversity Distrib.* 28 (9), 1752–1768. doi: 10.1111/ddi.13594

Pepin, N. C., Arnone, E., Gobiet, A., Haslinger, K., Kotlarski, S., Notarnicola, C., et al. (2022). Climate changes and their elevational patterns in the mountains of the world. *Rev. Geophys.* 60 (1), 1-40. doi: 10.1029/2020rg000730

Peterson, A. T., Soberon, J., Pearson, R. G., Anderson, R. P., Martinez-Meyer, E., Nakamura, M., et al. (2011). *Ecological niches and geographic distributions* Vol. Vol. 49) (Princeton, NJ: Princeton University Press).

Radchuk, V., Reed, T., Teplitsky, C., van de Pol, M., Charmantier, A., Hassall, C., et al. (2019). Adaptive responses of animals to climate change are most likely insufficient. *Nat. Commun.* 10 (1), 3109. doi: 10.1038/s41467-019-10924-4

Radeloff, V. C., Williams, J. W., Bateman, B. L., Burke, K. D., Carter, S. K., Childress, E. S., et al. (2015). The rise of novelty in ecosystems. *Ecol. Appl.* 25 (8), 2051–2068. doi: 10.1890/14-1781.1

Ray, C., Beever, E. A., and Rodhouse, T. J. (2016). Distribution of a climate-sensitive species at an interior range margin. *Ecosphere* 7 (6), e01379. doi: 10.1002/ecs2.1379

R Core Team (2021). R: A Language and Environment for Statistical Computing. R Foundation for Statistical Computing. Vienna, Austria. Available at: https://www.R-project.org.

Riddell, E. A., Apanovitch, E. K., Odom, J. P., and Sears, M. W. (2017). Physical calculations of resistance to water loss improve predictions of species range models. *Ecol. Monogr.* 87 (1), 21–33. doi: 10.1002/ecm.1240

Riddell, E. A., Iknayan, K. J., Wolf, B. O., Sinervo, B., and Beissinger, S. R. (2019). Cooling requirements fueled the collapse of a desert bird community from climate change. *Proc. Natl. Acad. Sci. U. S. A.* 116 (43), 21609–21615. doi: 10.1073/pnas.1908791116

Rodhouse, T. J., Beever, E. A., Garrett, L. K., Irvine, K. M., Jeffress, M. R., Munts, M., et al. (2010). Distribution of American pikas in a low-elevation lava landscape: conservation implications from the range periphery. *J. Mammal.* 91 (5), 1287–1299. doi: 10.1644/09-mamm-a-334.1

Rodhouse, T. J., Jeffress, M. R., Sherrill, K. R., Mohren, S. R., Nordensten, N. J., Magnuson, M. L., et al. (2018). Geographical variation in the influence of habitat and climate on site occupancy turnover in American pika (Ochotona princeps). *Diversity Distrib.* 24 (11), 1506–1520. doi: 10.1111/ddi.12791

Rollinson, C. R., Finley, A. O., Alexander, M. R., Banerjee, S., Dixon Hamil, K.-A., Koenig, L. E., et al. (2021). Working across space and time: nonstationarity in ecological research and application. *Front. Ecol. Environ.* 19 (1), 66–72. doi: 10.1002/fee.2298

Rossi, A. J., Klinger, R. C., Hellwig, E. C., and Van Vuren, D. H. (2023). Niches of three sympatric montane ground-dwelling squirrels: relative importance of climate, topography, and landcover. *Ecol. Evol.* 13 (4), e9949. doi: 10.1002/ece3.9949

Rousseau, J. S., and Betts, M. G. (2022). Factors influencing transferability in species distribution models. *Ecography* 2022 (7), e06060. doi: 10.1111/ecog.06060

Scherrer, D., Esperon-Rodriguez, M., Beaumont, L. J., Barradas, V. L., and Guisan, A. (2021). National assessments of species vulnerability to climate change strongly depend on selected data sources. *Diversity Distrib.* 27 (8), 1367–1382. doi: 10.1111/ddi.13275

Schulz, T., Vanhatalo, J., and Saastamoinen, M. (2019). Long-term demographic surveys reveal a consistent relationship between average occupancy and abundance within local populations of a butterfly metapopulation. *Ecography* 43 (2), 306–317. doi: 10.1111/ecog.04799

Schwalm, D., Epps, C. W., Rodhouse, T. J., Monahan, W. B., Castillo, J. A., Ray, C., et al. (2016). Habitat availability and gene flow influence diverging local population trajectories under scenarios of climate change: a place-based approach. *Global Change Biol.* 22 (4), 1572–1584. doi: 10.1111/gcb.13189

Segurado, P., Araujo, M. B., and Kunin, W. (2006). Consequences of spatial autocorrelation for niche-based models. *J. Appl. Ecol.* 43 (3), 433–444. doi: 10.1111/j.1365-2664.2006.01162.x

Smith, A., Beever, E. A., Kessler, A. E., Johnston, A. N., Ray, C., Epps, C. W., et al. (2019). Alternatives to genetic affinity as a context for within-species response to climate. *Nat. Climate Change* 9 (10), 787–794. doi: 10.1038/s41558-019-0584-8

Smith, A. B., Santos, M. J., Koo, M. S., Rowe, K. M., Rowe, K. C., Patton, J. L., et al. (2013). Evaluation of species distribution models by resampling of sites surveyed a century ago by Joseph grinnell. *Ecography* 36 (9), 1017–1031. doi: 10.1111/j.1600-0587.2013.00107.x

Somero, G. (2010). The physiology of climate change: how potentials for acclimatization and genetic adaptation will determine 'winners' and 'losers'. *J. Exp. Biol.* 213 (6), 912–920. doi: 10.1242/jeb.037473

Stewart, J. A. E., Perrine, J. D., Nichols, L. B., Thorne, J. H., Millar, C. I., Goehring, K. E., et al. (2015). Revisiting the past to foretell the future: summer temperature and habitat area predict pika extirpations in California. *J. Biogeogr.* 42 (5), 880–890. doi: 10.1111/jbi.12466

Sultaire, S. M., Humphreys, J. M., Zuckerberg, B., Pauli, J. N., and Roloff, G. J. (2022). Spatial variation in bioclimatic relationships for a snow-adapted species along a discontinuous southern range boundary. *J. Biogeogr.* 49 (1), 66–78. doi: 10.1111/jbi.14279

Tang, Y., Horikoshi, M., and Li, W. (2016). ggfortify: unified interface to visualize statistical result of popular r packages. *R J.* 8 (2), 474–485. doi: 10.32614/RJ-2016-060

Thuiller, W., Brotons, L., Araújo, M. B., and Lavorel, S. (2004). Effects of restricting environmental range of data to project current and future species distributions. *Ecography* 27 (2), 165–172. doi: 10.1111/j.0906-7590.2004.03673.x

Thurman, L. L., and Garcia, T. S. (2019). Asymmetric competition shapes amphibian response to rapid environmental change. *Ecosphere* 10 (12), e02950. doi: 10.1002/ecs2.2950

Tumajer, J., Begović, K., Čada, V., Jenicek, M., Lange, J., Mašek, J., et al. (2023). Ecological and methodological drivers of non-stationarity in tree growth response to climate. *Global Change Biol.* 29 (2), 462–476. doi: 10.1111/gcb.16470

Urban, M. C., Bocedi, G., Hendry, A. P., Mihoub, J.-B., Pe'er, G., Singer, A., et al. (2016). Improving the forecast for biodiversity under climate change. *Science* 353 (6304). doi: 10.1126/science.aad8466

Varner, J., Carnes-Douglas, Z. J., Monk, E., Benedict, L. M., Whipple, A., Dearing, M. D., et al. (2023). Sampling a pika's pantry: temporal shifts in nutritional quality and winter preservation of American pika food caches. *Ecosphere* 14 (5), e4494. doi: 10.1002/ecs2.4494

Wang, Q., Fan, X., and Wang, M. (2016). Evidence of high-elevation amplification versus Arctic amplification. *Sci. Rep.* 6 (1), 19219.

Wang, T., Hamann, A., Spittlehouse, D., and Carroll, C. (2016). Locally downscaled and spatially customizable climate data for historical and future periods for north America. *PloS One* 11 (6), e0156720. doi: 10.1371/journal.pone.0156720

Wickham, H. (2011). *"ggplot2." Wiley interdisciplinary reviews: computational statistics 3.2.* 180-185.

Wilkening, J. L., Ray, C., Beever, E. A., and Brussard, P. F. (2011). Modeling contemporary range retraction in great basin pikas (*Ochotona princeps*) using data on microclimate and microhabitat. *Quat. Int.* 235, 77–88. doi: 10.1016/j.quaint.2010.05.004

Yandow, L. H., Chalfoun, A. D., and Doak, D. F. (2015). Climate tolerances and habitat requirements jointly shape the elevational distribution of the American pika (*Ochotona princeps*), with implications for climate change effects. *PloS One* 10 (8). doi: 10.1371/journal.pone.0131082

Frontiers in Ecology and Evolution

TYPE Original Research
PUBLISHED 28 July 2023
DOI 10.3389/fevo.2023.1164050

Variations in climate drive behavior and survival of small desert tortoises

Kristin H. Berry[1]*, Jeremy S. Mack[1]† and Kemp M. Anderson[2]

[1]U.S. Geological Survey, Western Ecological Research Center, Reno, NV, United States, [2]Center for Innovation in Teaching and Learning, Bajada Ecology LLC, Seal Beach, CA, United States

OPEN ACCESS

EDITED BY
Clare Aslan,
Northern Arizona University, United States

REVIEWED BY
Amanda Goldberg,
Virginia Tech, United States
Cameron Barrows,
University of California, Riverside,
United States

*CORRESPONDENCE
Kristin H. Berry
✉ kristin_berry@usgs.gov

†PRESENT ADDRESS
Jeremy S. Mack,
Lehigh University, Bethlehem,
PA, United States

RECEIVED 11 February 2023
ACCEPTED 04 July 2023
PUBLISHED 28 July 2023

CITATION
Berry KH, Mack JS and Anderson KM (2023) Variations in climate drive behavior and survival of small desert tortoises. *Front. Ecol. Evol.* 11:1164050.
doi: 10.3389/fevo.2023.1164050

In the Mojave Desert, timing and amounts of precipitation profoundly affect the availability of water and annual plant foods necessary for the threatened Agassiz's desert tortoise (*Gopherus agassizii*) to survive, especially during prolonged droughts. As part of recovery actions to increase declining populations, we translocated 83 juvenile and young desert tortoises raised in head-start pens for 4–10 years to a new location 15 km away during the fall of 2013 and 2014. We tracked them for 9 years during a megadrought, during multiple years of low rainfall, and a few years when precipitation neared or exceeded long-term norms. We evaluated behaviors and how precipitation and forage availability affected survival. At the end of the study, 21.6% of tortoises were alive, and six had grown to adulthood. Annual models of survival indicated that tortoise size was the driving variable in most years, followed by the number of repeatedly used burrows during periods of temperature extremes. Other variables affecting survival in ≥1 year were vegetation, movements during the first 2 years post-translocation, and condition index, a measure of health. Tortoises moved more, expanded home ranges, and grew rapidly in years when winter rainfall approached or exceeded long-term norms and annual plants were available to eat. During dry years, movements and growth were limited. Exceptions to this pattern occurred in the last year of study, a dry year: tortoises grew and moved more, and home ranges increased. The increase in size and approaching adulthood may have stimulated greater traveling. Some left the study area, indicating a need for large release areas. We may have aided survival by offering water twice yearly when handling because some tortoises drank and increased in mass up to 40%. Prolonged droughts and hotter temperatures can limit the recovery of populations, reduce the survival of young tortoises, and increase the time to maturity.

KEYWORDS

***Gopherus agassizii*, growth, behavior, juvenile, Mojave Desert, precipitation**

1 Introduction

Throughout the globe, many species of tortoises and turtles are endangered or threatened with extinction (Rhodin et al., 2018). Agassiz's desert tortoise (*Gopherus agassizii*), an iconic desert species in the American Southwest, is a federally listed, threatened species (U.S. Fish and Wildlife Service [USFWS] 1990). Numerous human activities contributed to the listing, e.g., collecting, vandalism, deaths on roads, diseases, and hyper-predation by expanding predator populations. Habitat was degraded, fragmented, or lost from livestock grazing; mining; development for agriculture, urbanization, road networks, solar energy, and utilities; military uses; invasive species and fires; and uncontrolled recreational vehicle use. Despite recovery efforts, the species continued to decline rapidly, and Allison and McLuckie (2018) reported that the desert tortoise was on the path to extinction under current conditions. In 2021, the International Union for Conservation of Nature placed *G. agassizii* on the Red List as critically endangered (Berry et al., 2021). Numerous anthropogenic activities and diseases resulted in continued population and habitat losses and habitat degradation (USFWS 2011, Berry and Murphy, 2019).

The latest test for survival is climate warming. According to Williams et al. (2020); Stahle (2020), and Cook et al. (2021), the worst megadrought occurred in the 16th century and the second worst from 1999 to 2020 in southwestern North America. Anthropogenic influences added to the severity. Without the anthropogenic influence, Stahle (2020:1,584) wrote: "…the 2000–2018 interval would have been just another episode of reduced precipitation, low soil moisture, and poor tree growth…" The warming temperatures drove greater aridity, including drier soil conditions, more severe droughts, and the die-off of trees (Overpeck and Udall, 2020). As climate warming continues, the American Southwest is expected to become more arid with "…widespread, prolonged, and severe dry spells and drought almost a sure bet" (Overpeck and Udall, 2020:11,857; Cook et al., 2021). More extreme heat waves and dust storms are part of the pattern.

Life in the Mojave, western Sonoran, and southern edge of the Great Basin deserts is harsh: rainfall is low and unpredictable, summer air temperatures exceed 46°C, and freezing days range from 2 to ~120 per year, depending on region (Rowlands et al., 1982; Rowlands, 1995). Desert tortoises have adaptations to survive but are vulnerable in part because of their k-selected life history traits: a long period of 17 to 20 years or more to reach sexual maturity, low fecundity, and an estimated longevity of >60 years (Woodbury and Hardy, 1948; Hardy, 1976; Turner et al., 1987; Medica et al., 2012; Berry and Murphy, 2019). Survival is low in the early years, increasing as tortoises grow from hatching to adulthood (Turner et al., 1987; Berry et al., 2020). Tortoises seek refuge in burrows, caves, and dens to avoid temperature extremes, lack of forage and moisture, and probably predators; they spend >95% of their lives underground (Woodbury and Hardy, 1948; Nagy and Medica, 1986; Henen et al., 1998).

The herbivorous tortoise depends on winter and summer rains for water for drinking and producing native annual forbs and herbaceous perennial plants for forage. Tortoises are highly selective in choosing species of plants to eat (Oftedal, 2002; Oftedal et al., 2002; Jennings and Berry, 2015). Growth occurs after emergence from brumation in late winter, if food is available, and ceases by late summer or fall (Nagy and Medica, 1986; Medica et al., 2012). Tortoises will emerge to drink with rain and when fresh forage is available (Medica et al., 1980; Henen et al., 1998).

Periods of drought and precipitation have profound effects on the physiology, health, and above-ground activities of adult desert tortoises (Henen et al., 1998; Christopher et al., 1999; Duda et al., 1999; Jennings and Berry, 2015). Drought can lead to dehydration and starvation and may have more severe effects on small, young tortoises because soft shells with developing bone and scute are vulnerable to desiccation and overheating (e.g., Berry et al., 2002; Longshore et al., 2003; Nagy et al., 2015a).

The augmentation of declining populations through head-starting and translocation was part of the revised recovery plan for the tortoise (U.S. Fish and Wildlife Service [USFWS], 2011). The International Union for Conservation of Nature (IUCN, International Union for the Conservation of Nature, Species Survival Commission, 2013) published guidelines on head-starting, translocation of animals, and conservation techniques used for endangered species. For desert tortoises, head-starting involves rearing juveniles in predator-proof pens experimentally either to learn more about early life stages or to grow them to predator-resistant sizes to augment depleted populations. Previous research indicated that survival and growth were negatively affected when rainfall was low (Berry et al., 2002; Medica et al., 2012). Existing knowledge of small tortoises involved studies of wild tortoise behaviors, use of burrows, and temperatures when active (Berry and Turner, 1984; 1986). Studies of tortoises kept in large, open pens provided data on growth, activities, survival (Nagy and Medica, 1986; Medica et al., 2012), and other traits. Research on head-started and translocated small tortoises has provided several advances in identifying important variables associated with survival (e.g., Nagy et al., 2015a; Nagy et al., 2015b; Nafus et al., 2016; Germano et al., 2017; Nagy et al., 2020). Most publications on the translocation of head-started tortoises were limited to 1–3 years.

Our overarching objective was to translocate tortoises from predator-proof head-start pens to an appropriate site, monitor behavioral responses to the megadrought for several years, and identify factors affecting survival. The tortoises were in pens from 2003 to 2014, where most experienced poor husbandry (Mack et al., 2018). Thus, the translocation began under conditions lacking the desirable protocols later published by the IUCN, International Union for the Conservation of Nature, Species Survival Commission (2013) and Swaisgood and Ruiz-Miranda (2019). We translocated tortoises in 2013 and 2014 and monitored them for 9 years. We asked four questions:

(1) Did timing and amounts of precipitation and forage availability using the normalized difference vegetation index (NDVI) affect tortoise behaviors, e.g., settling, movements and dispersal, and home ranges?

(2) Were growth and size affected by precipitation and forage availability?

(3) Was health a factor in survival?

(4) What variables affected survivorship annually and at the end of 9 years?

We addressed the questions by 1) evaluating amounts and timing of precipitation and NDVI during the study, 2) comparing behaviors with timing and amounts of rainfall and NDVI, 3) tracking size and growth during the life of each tortoise and evaluating relationships to precipitation and NDVI, and 4) modeling survival annually using multiple variables to identify important variables.

2 Study area

The study area was at Edwards Air Force Base (EAFB) in the western Mojave Desert, Kern County, California, USA. Because the tortoises were pen-raised on EAFB, a release there was a requirement. To maximize survival to adulthood, we used four criteria for site selection: an area formerly supporting a population of desert tortoises but severely reduced to one to two adults (Allison and McLuckie, 2018; Berry et al., 2020), ease of access (limited restrictions on use and surface disturbance), soils suitable for juveniles to dig burrows, and a vegetation association comparable to the head-start pens—a diverse creosote bush community with *Larrea tridentata* and western Joshua trees, *Yucca brevifolia* (Mack et al., 2018; https://www.wildlife.ca.gov/Data/VegCAMP/Natural-Communities, accessed 1 Oct 2022). We sought a site with large (2 m) creosote bushes and clones with well-developed coppice mounds where old and recently dug burrows by rodents and other animals were evident because wild juvenile tortoises select large shrubs, such as creosote bushes, for constructing burrows (Berry and Turner, 1984; 1986). We selected a 15-km^2 site on the north-facing slope and alluvial fan of Leuhman Ridge at elevations of 750 to 850 m (Figure 1). Typical of the region, the site was fragmented by linear disturbances: 13.74 km of dirt roads (density of 0.91 km/km^2 and in use), a fence forming the southern boundary at the base of Leuhman Ridge, a paved road on the west, and railroad tracks forming the eastern boundary. The site was within 2 km of a landfill, settlements, and military facilities. Historically, sheep grazed the area.

Predators likely to kill juvenile tortoises included gopher snakes (*Pituophis melanoleucus*), Mohave rattlesnakes (*Crotalus scutulatus*), antelope ground squirrels (*Ammospermophilus leucurus*), Mohave ground squirrels (*Xerospermophilus mohavensis*), loggerhead shrikes (*Lanius ludovicianus*), common ravens (*Corvus corax*), kit fox (*Vulpes macrotis*), and coyotes (*Canis latrans*). Ravens and the canids were common to abundant, supported by nearby anthropogenic sources of water, food, perches, and nest sites.

3 Materials and methods

3.1 Precipitation

In this region of the Mojave Desert, most precipitation falls between 1 Oct and 31 Mar, the fall and winter seasons, seasons with approximately 80 freezing days (Rowlands, 1995). We accessed total monthly precipitation data from the PRISM Climate Group in a 4-km grid cell raster dataset. We extracted data from the grid cell centered at latitude 34.9565, longitude −117.7047, and elevation 760

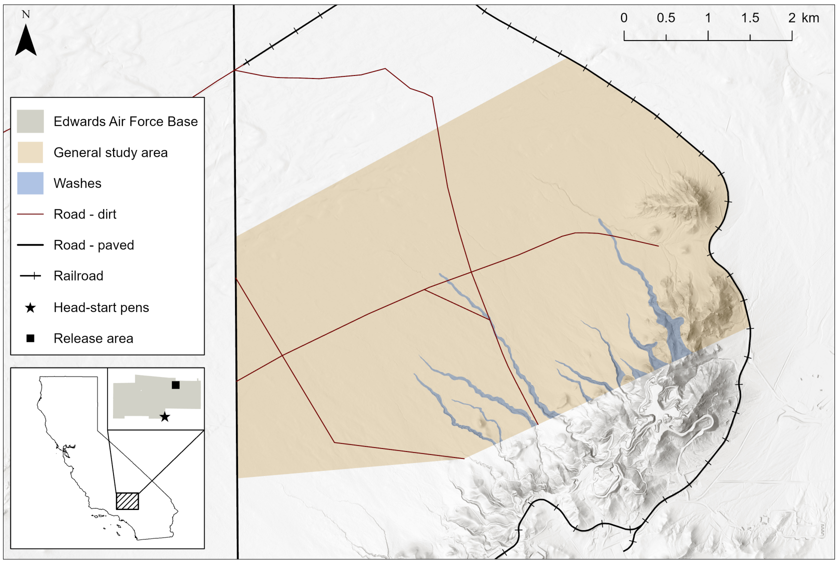

FIGURE 1
Locations of the head-start pens and study area where 83 small Agassiz's desert tortoises (*Gopherus agassizii*) were translocated in 2013–2014 on Edwards Air Force Base in the western Mojave Desert, California, USA.

(prism_archive_ls function in package prism; Edmund et al., 2020). We calculated water year from 1 Oct to 30 Sep, and winter totals from 1 Oct to 31 Mar (Manning, 1992; Hereford et al., 2006). Our monthly series began Oct 1969 and ended Sep 2022 to allow the calculation of two long-term averages: 30 years prior to the study (1982–2012) and 30 years prior to the megadrought (1969–1999).

3.2 Vegetation

We obtained data on the NDVI through the U.S. Geological Survey's (USGS's) Earth Resources Observation and Science Center Science Processing Architecture On Demand Interface (U.S. Geological Survey [USGS], 2022). We used NDVI as a measure of food availability, given its strong correlation with the production of vegetation and productivity in a broad range of systems (Petorelli, 2013). We compiled Landsat NDVI and cloud cover (%) data (30-m spatial resolution, 16-day temporal resolution) from 2013 through 2022. All images were corrected following standard methods including radiometrically calibrated, orthorectified, and corrected for top of atmospheric reflectance. We extracted mean monthly NDVI values within each tortoise home range annually and derived a time series of two indices of vegetation production: mean growing season (MGS) NDVI and peak growing season (PGS) NDVI. We collected data at randomly selected sites on the composition and cover of perennial vegetation using 50 line intercepts (50 m each) during Apr 2017, a non-drought year. Also in April, the biomass of annual plants was collected from 20 randomly selected quadrats, 20 × 50 cm each from beneath shrub canopies and in intershrub spaces.

3.3 Desert tortoises

3.3.1 Histories and selection of tortoises

The tortoises were from the head-start program and pens and from cohorts hatched in summer or early fall annually between 2003 and 2010 (Mack et al., 2018; Figure 1). They were in three life stages or size classes (carapace length at the midline, MCL in mm): juvenile 1, <60; juvenile 2, 60–99; and immature 1, 100–139 (Berry and Christopher, 2001). In the fall of 2013, a few days prior to release, we removed 35 tortoises from the pens to prepare them for release. We collected metrics (mm, g) from each tortoise: MCL, carapace width at the fifth or sixth marginal scute, maximum height, and mass. The metrics were used to assess growth and calculate a body condition index developed by Nagy et al. (2002). The prime condition index was 0.64 g/cm^3 (0.6–0.7 g/cm^3). We also evaluated clinical signs of health and disease using a form modified by Berry and Christopher (2001). These tortoises were from cohorts hatched in 2003–2007, were 6–10 years old, and averaged (± SE) 85.2 ± 2.6 mm MCL (range, 69.0–132.0 mm). We repeated this process in the fall of 2014 and removed the 48 remaining tortoises from cohorts 2005, 2007–2010, and aged 4–9 years; they averaged 64.2 ± 1.5 mm MCL (range, 50.6–112.2 mm).

Prior to release, we attached radio transmitters of increasing size and lifespan as the tortoises grew larger, starting with the smaller sizes (BD-2, 2.4 g; PD-2, 3.6 g; and later, R1–2B, 10 g; Holohil Systems Ltd., Carp, Ontario, Canada). Transmitter weights were <10% of the body weights of the tortoises. Before release, tortoises were placed in individual containers in ~1.5 cm of water to drink for 15–20 min.

3.3.2 Site visits and tracking status of tortoises

Throughout the study, unless described elsewhere, we tracked and searched for live, missing, and dead tortoises monthly using two types of receivers (R2000, Advanced Telemetry Systems Inc., Isanti, MN, USA; R-1000, Communications Specialists, Inc., Orange, CA, USA), and recorded locations with Global Positioning Systems (GPS, Garmin GPS Map 62s, Garmin Ltd., Olanthe, KS, USA). Locations were accurate within the error range of the GPS (~3 m). After translocating the 2013 tortoises, we tracked them daily for 7 days, then on alternate days for 2 weeks, and then twice monthly through February. After that, the tortoises were tracked monthly. The 2014 tortoises were checked 24 h after initial release and then monitored monthly.

During each monthly visit, we recorded data on date, time (PST), weather conditions, location (Universal Transverse Mercator [UTM] system, NAD 83), details of location (whether the tortoise was above or below ground), description of the burrow (if at a burrow), and activities. If a tortoise was missing and pulses were not heard in the vicinity of known locations or from a high point in the study area, we searched previously used activity areas, nearby coyote or kit fox dens, and raven perches. If the tortoise was dead, we recorded the location (UTMs), condition of remains, and evidence for the cause of death; photographed the site and remains; and collected the remains for further analysis. We determined probable causes of death, drawing on previously described observations for clinical signs of poor health, forensic evidence of lesions from trauma (Berry and Christopher, 2001; Berry et al., 2002; Mack et al., 2018), and evidence of predation by ground squirrels and other rodents, ants, common ravens, kit foxes, and coyotes and other species (Boarman, 1993; Boarman and Berry, 1995; Berry et al., 2006; Mack et al., 2018). We used tracks, scats, the size of tooth marks, and the condition of the shell to determine the probable predator.

In spring and fall, we changed transmitters, collected data on metrics and health, took digital images (carapace, plastron, limbs, head, and posterior shell), and evaluated health and lesions from trauma or other sources. If a tortoise was deep in a burrow when the transmitter was to be changed, we tapped it to encourage emergence (Medica et al., 1980), sprayed water at the entrance to simulate rain, or returned later to determine accessibility. After handling, we offered the tortoises water to drink. From 2018 to the end of the study, we conducted more comprehensive health assessments (Berry and Christopher, 2001, updated). If the tortoise was injured, additional notes and photographs were taken. From the fall of 2019 through 2022 (end of the project), we measured the mass of tortoises before and after they were offered water to drink. When tortoises grew to >165 mm MCL, they were fitted with transmitters lasting approximately a year. Handling only occurred when ambient temperatures were ≤35°C and generally for <30 min.

3.4 Data analysis

3.4.1 Precipitation and vegetation

We compared precipitation totals for water year and winter for the study years (2013–2022) with long-term averages: 30-year norms for the 30 years prior to the study and the 30 years prior to the beginning of the megadrought in 1999 (Cook et al., 2021). We explored the linear relationship between precipitation totals (winter and water year) and measures of NDVI (MGS and PGS) using general linear models. We conducted all calculations and statistical analyses in R (version 4.1.0; R Core Team, 2021).

3.4.2 Desert tortoises

3.4.2.1 Settling behavior

We described initial settling behaviors for tortoises released in 2013, estimating the time to establish a first burrow (tortoise covered and stayed overnight), noting how many were self-dug or developed by expanding mammal or reptile burrows, dates of entering and staying in a burrow for brumation, and straight-line distances traveled from the release site to 1) first burrow and 2) burrow occupied for brumation. We calculated two measures of dispersal: 1) dispersal after 24 h and 2) dispersal after 1 year. For dispersal after 24 h, we calculated the straight-line distance from the release point to where a tortoise was located at the 24-h post-release check. For dispersal after 1 year, we calculated the straight-line distance from the release point to the center of the home range (see below) developed during the first year (Oct-to-Oct). For both releases, we compared dispersal distances using an unpaired two-sample *t*-test. For these analyses, we included tortoises that were alive at the end of both time intervals.

3.4.2.2 Movements and home range

We calculated the distance that a tortoise moved between observations (hereafter movements) as a straight-line distance (i.e., the minimum distance moved). We then calculated the total distance traveled as the sum of tortoise movements and average movement as the total movements divided by the number of observations.

Home ranges were estimated by fitting a minimum convex polygon (MCP) to monthly locations (mcp function in package adehabitatHR; Calenge, 2006). To calculate an area from the MCP, we removed tortoises with <3 unique locations. Traditional methods like MCP were recommended for studies of herpetofauna, even though these methods may include areas of unusable habitat or underestimate areas of habitat use (Row and Blouin-Demers, 2006; Fleming et al., 2015; Averill-Murray et al., 2020).

We compared differences in movements, home ranges, and growth between years by fitting a linear mixed-effects (LME) model that controlled for random variation between tortoises. Differences between years were explored with Tukey's *post-hoc* multiple comparisons. LME models were fitted with the lme4 package (Bates et al., 2023).

3.4.2.3 Repeat burrows

We used periods of temperature extremes (i.e., fall–winter and summer) to quantify the number of repeatedly used burrows (hereafter repeat burrows) because locations recorded during these periods were likely to be below ground. To compensate for errors in GPS accuracy, we treated burrows within a 3-m radius as a single location (spDists function in package sp; Pebesma et al., 2021). We further defined a repeat burrow as one used among seasons with temperature extremes but not used during a single season within a single year.

3.4.2.4 Growth

We used carapace measurements recorded during transmitter changes to calculate growth rates. Because growth is dependent on food supply and foraging in spring, we focused on fall-to-fall measurements (i.e., water year cycle) and calculated annual growth rates for each tortoise after release until death or the end of the study. We compared growth between years with an LME model that controlled for variation between tortoises and explored differences with Tukey's *post-hoc* multiple comparisons. For tortoises with a known status (i.e., live or dead) at the end of the study, we calculated an overall growth rate by fitting a linear model of size by time since release and compared overall growth rates between status with an unpaired two-sample *t*-test. For each tortoise smaller than the minimum adult size at the end of the study, we estimated years to reach adult size based on cohort year, years prior to release, and an average of post-release annual growth.

3.4.2.5 Status (live, dead, or missing) of tortoises and survivorship

We summarized the status and metrics for live, dead, and missing tortoises annually. We calculated death rates for single years as D/n, where D is the number of dead tortoises and n is the number of known dead and live tortoises. For annualized death rates for >1 year, we used the equation

$$(1 - [1 - D/n]^{1/t}) \times 100\%$$

where D is the number of dead tortoises with transmitters in a given period, n is the number of known live and dead tortoises with transmitters in a specific year, and t is the number of years. Annual or annualized survival was the reciprocal of the annual or annualized mortality rate. We summarized probable causes of death for dead tortoises. We summarized data on the status of tortoises annually.

3.4.2.6 Annual models of survival for tortoises

We identified important predictor variables of survival using generalized linear models (GLMs) with a logit link for binary outcomes. Models were run each year with cumulative data collected through December. We started modeling efforts in 2014 with 15 months of data collected for the tortoises released in October 2013. Tortoises were either removed from modeling efforts because they were missing, with unknown status, or missing a value for a variable included in the model. Only live and dead tortoises were included in each annual model.

Nine potential variables were considered for the survival models: age, size (MCL), condition index, total distance traveled, distance traveled per observation, size of home range, the total number of unique locations, number of repeat burrows, and average MGS NDVI within a tortoise home range. Before including all proposed variables, we conducted a Pearson's correlation analysis to identify variables correlated with one another. We removed highly correlated variables to reduce redundant information and simplify the model structure without reducing the quality of prediction (Dormann et al., 2013). We removed the total distance traveled and size of the home range because of the correlation with distance traveled per observation, total number of unique locations because of the correlation with the number of repeat burrows, and age because of the correlation with size. Therefore, the final set of models considered five variables: size (MCL), mean MGS NDVI, condition index, distance traveled per observation, and number of repeat burrows. These variables created 32 main effects models with all possible variable combinations for each year.

Model fit was based on second-order Akaike's information criterion (AIC_c; corrected for sample size). We identified the best-fit annual model as the model with the lowest AIC_c, then compared each model to the best-fit model, and ranked the models based on the difference between AIC_c values (ΔAIC_c). In addition to the best-fit model, we reported models with ΔAIC_c values <2 units, highlighting the most parsimonious model, or one with the simplest structure (i.e., fewest parameters) and a similar model fit (Burnham and Anderson, 2002). We also calculated additional metrics of model fit including Akaike weights and evidence ratios.

For each of the five explanatory variables, we estimated relative variable importance and model-averaged coefficients annually. Relative importance was calculated by taking the sum of the Akaike weights for all models in which a specific variable occurred. Similarly, model-averaged coefficients were calculated by averaging coefficient estimates for each variable over the models in which they occurred. We constructed the model set and ran the GLMs with the package ModelInference (version 1.70, https://www.usgs.gov/staff-profiles/mark-herzog, accessed Jul 2021). Additionally, we described two relationships with survival based on the size and number of repeat burrows by fitting separate logistic regression models. Based on model fits, we highlighted the size of tortoises and the number of repeat burrows that corresponded to a 50% level of survival.

4 Results

4.1 Precipitation and vegetation

During the study, rainfall exceeded the 30-year normal for the water year in 2 of 9 years (2018–2019 and 2019–2020) and for winter in 3 of 9 years (2016–2017, 2018–2019, and 2019–2020; Figure 2). However, amounts of precipitation reflected the megadrought. Average precipitation was 69.8% of normal for the water year ($\bar{x}$ = 103.2 mm; range, 45.8–204.0 mm) and winter rain was 68.0% of normal ($\bar{x}$ = 85.4; range, 38.5–163.6) when compared to the norms for the previous 30 years (water year, 147.8 mm; winter, 125.6 mm). Differences in precipitation (65.2, 65.1%) were more pronounced when totals were compared with norms from 30 years prior to the beginning of the megadrought (1999): water year and winter averages were 158.4 and 131.2 mm, respectively. Although totals of precipitation varied from the norms, timing remained consistent. Winter precipitation accounted for 82.7% of total precipitation during the study, which was comparable to 30 years prior to the study (85.0%) and prior to 1999 (82.8%).

Both vegetation indices (MGS and PGS NDVI) closely tracked precipitation (Figure 2). Overall, a linear relationship existed between precipitation and the average NDVI value within tortoise home ranges, which was significant for MGS (water year and winter: t = 2.5, df = 8, $p \leq 0.05$). The average MGS value increased by 0.25 and 0.21 with a 1-mm increase in precipitation for winter and water year precipitation, respectively, and accounted for the same amount of variability (adjusted partial $R^2 = 0.360$).

The composition of shrubs and trees was dominated by creosote bushes (76.2%) and white bur-sage (18.5%, *Ambrosia dumosa*). The western Joshua tree made up 2.3%, Cooper's thornbush (*Lycium cooperi*) 1.2%, and cheesebush (*Ambrosia salsola*), California joint fir (*Ephedra californica*), and giant Eriastrum (*Eriastrum densifolium* ssp. *elongatum*) 0.6% each. Biomass of annual forbs and grasses averaged 107 g/m^2 beneath shrub canopies and 18.1 g/m^2 in the intershrub spaces. Non-native forbs (*Brassica tournefortii* and *Erodium cicutarium*) and grasses (*Bromus* spp., *Schismus* spp.) composed 23.4% of the biomass beneath canopies and 47.8% of the biomass in the intershrub spaces. During the study, African mustard (*B. tournefortii*) arrived along the paved road and rapidly spread into the study area.

4.2 Settling and dispersal

Between 2 Oct and 6 Dec 2013, each tortoise was observed an average (± SE) of 18.6 ± 0.4 times (range, 17.0–26.0) unless an unusual circumstance dictated otherwise. Most (58.8%, 20/34) tortoises established first burrows within ~24 h and an additional 38.2% (13/34) within 48 h. One exploring tortoise excavated its first burrow after 6 days. The average distance between the release and construction of the first burrow was 64.5 ± 19.0 m (range, 0–642.7 m). Tortoises began settling into burrows for brumation starting the day of release and continued through 17 Oct, although most settled after 6 days (58.8%, 20/34). We considered settling for brumation when the tortoise remained in a single burrow for the remainder of the fall and early winter unless rainfall caused a burrow to collapse or a tortoise emerged to drink. The average distance between release sites and burrows used for brumation was 75.8 ± 18.3 m (range, 0–603 m). Rain may have disturbed five settled tortoises in November, and they re-settled to additional burrows. Most burrows used by tortoises were modified rodent burrows, although some occupied larger mammal and reptile burrows. No rodent burrows were of sufficient size to support the three larger tortoises; overall ≥9 tortoises dug ≥1 of their own burrows. We observed one to six excavated or modified burrows for each tortoise; most were in coppice mounds under creosote bushes and camouflaged by overhanging live and dead branches and dried plants. Dispersal distances within 24 h were larger ($p < 0.005$) for tortoises released in 2013 (46.6 ± 7.2 m; range, 0.0–166.1 m) compared to tortoises released in 2014 (23.6 ± 3.0 m; range, 0.0–117.2). One year after release, dispersal distances were no longer different ($p = 0.865$)

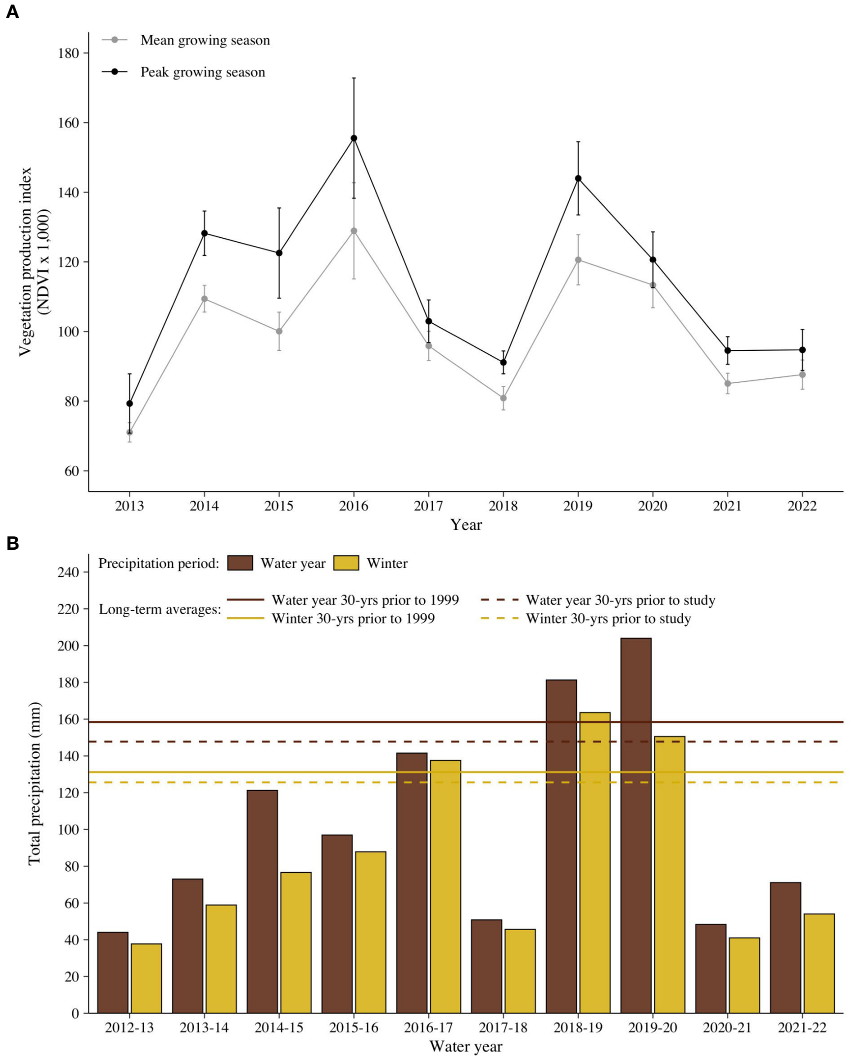

FIGURE 2
(A) Mean growing season and peak growing season of vegetation, part of the normalized difference vegetation index (NDVI), and **(B)** yearly precipitation for water year and winter precipitation for the 2013–2022 study of translocated small Agassiz's desert tortoise (*Gopherus agassizii*) from head-start pens to a site on Edwards Air Force Base in the western Mojave Desert, California, USA. Norms for 30 years pre-megadrought (1999) and the 30 years prior to the study are shown.

between tortoises released in 2013 (49.4 ± 6.7 m; range, 4.8–149.6) and those released in 2014 (47.5 ± 8.2 m; range, 5.5–204.6).

4.3 Movements, home ranges, and growth

Movements varied between years. Tortoises moved larger distances per observation in 2020 and 2022 compared to all other years ($p < 0.05$; Figure 3A). The first year of significantly larger movements (2020) followed two above-average years of precipitation and vegetation growth. Conversely, the second year (2022) followed two below-average years of precipitation (Table 1). Comparable to movements, home range size varied between years. Following the large movements in 2020 and 2022, the home range size significantly increased to its largest size in 2022 ($p < 0.05$; Figure 3B). Home ranges also grew consistently in size over time, even when movements were low, suggesting tortoises were exploring new areas. At the end of the study, tortoise size had a linear relationship with movement and home range, where both increased by 0.25 m and 0.001 km^2, respectively, with an increase in 1-mm MCL (Figure 4; adjusted partial R^2 movement = 0.454 and home range = 0.323). A marked increase in movements and home range size appeared to occur at approximately 145–150 mm MCL. Two tortoises missing at the end of the study undertook long trips and left the study area; one was last seen on a paved road >3 km to the south after moving little and having a small home range for 8 years.

4.4 Growth

Growth varied between years and mostly tracked precipitation and vegetation patterns, except for 2022 (Table 1; Figure 3C).

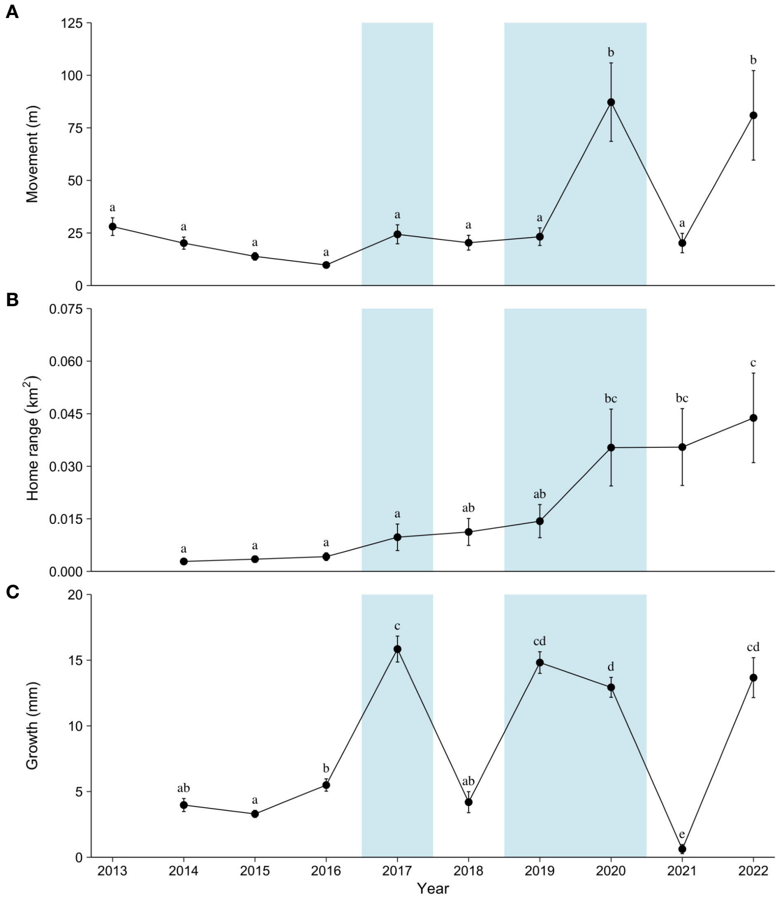

FIGURE 3
Annual averages of movements between observations **(A)**, total home range **(B)**, and growth **(C)** for small Agassiz's desert tortoises (*Gopherus agassizii*) translocated to a study area at Edwards Air Force Base in the western Mojave Desert, California, USA. Blue boxes indicate years with precipitation above the long-term norms. Different small letters indicate significant differences in years within each figure ($p < 0.05$).

TABLE 1 Comparisons of yearly averages of precipitation data with growth, average movement, and home ranges of Agassiz's desert tortoises (*Gopherus agassizii*) after translocation in 2013 and 2014 to a site on Edwards Air Force Base in the western Mojave Desert, California, USA.

	Precipitation		NDVI		Tortoise variables		
Year	Water year (mm)	Winter (mm)	Peak	Mean	Growth (mm)	Movement (m)	Home range (km^2)
2014	73.03	58.92	128.23	109.41	3.98	20.17	0.003
2015	121.27	76.64	122.55	100.07	3.30	13.85	0.006
2016	96.96	87.86	155.55	128.94	5.50	9.78	0.008
2017	141.55	137.60	102.96	95.87	15.84	29.00	0.012
2018	50.80	45.67	91.12	80.86	4.19	20.37	0.015
2019	181.32	163.55	144.00	120.60	14.82	23.23	0.022
2020	204.00	150.56	120.60	113.34	12.93	87.23	0.071
2021	48.30	41.01	94.54	85.08	0.62	20.20	0.071
2022	71.07	54.01	94.73	87.62	13.7	80.97	0.090

The blue-shaded rows are years when water year or winter precipitation totals were greater than 30-year long-term averages prior to the study. Movement = annual averages of movements between observations.

NDVI, normalized difference vegetation index.

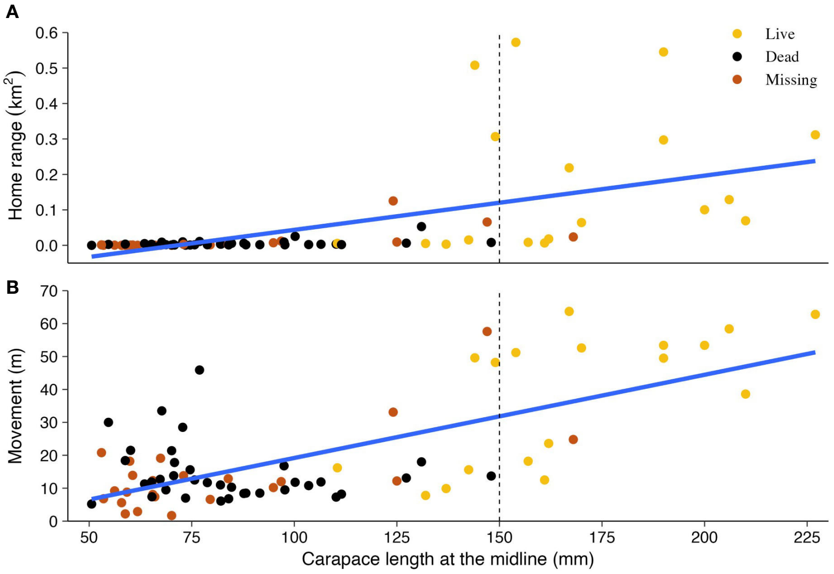

FIGURE 4
Annual averages of total home range **(A)** and movements between observations **(B)** by size (MCL in mm, carapace at the midline) of small Agassiz's desert tortoises (*Gopherus agassizii*) translocated from head-start pens to a study area on Edwards Air Force Base in the western Mojave Desert, California, USA.

Growth was higher in years of above-average precipitation (2017, 2019, 2020, and 2022) compared to all other years ($p < 0.05$). The large growth in 2022 again suggested that tortoises had reached a critical size permitting increases in behavioral (movement) and physiological (growth) patterns. The fastest-growing tortoise, 80 mm MCL at release, grew 12.4 mm/year on average, whereas the slowest-growing tortoise (and still alive) was 92.3 mm MCL when released and averaged 6.1 mm/year. Growth rates calculated from linear model fits also showed that tortoises grew at different overall rates (Figure 5). On average, tortoises alive at the end of the study grew 9.42 mm/year (range, 5.16–12.4 mm/year), which was higher ($p < 0.005$) compared to those that died, which grew 4.26 mm/year (range, 0–11.6 mm/year). Differences in hatching year (cohort year) and individual growth rates resulted in differences in years to reach a minimum size at sexual maturity, 180 mm MCL. At the end of the study, six female tortoises (77.5 to 126 mm MCL at release) reached and surpassed 180 mm MCL at 14–17 years of age. The remaining live tortoises probably will require up to 25 years post-hatching to achieve minimum adult size.

4.5 Hydration

Each tortoise was offered opportunities to drink after handling and responded in a variety of ways from not drinking to drinking copiously. For tortoises that drank, gains in body mass ranged from 0.97% to 39.7% and varied by year (Table 2). Tortoises drank and gained mass during years when precipitation was above the norm and during droughts. The proportions of non-drinking tortoises were similar in drought and wet years.

4.6 Status of tortoises

By the end of the study, 18 tortoises were alive, 41 were dead, and 24 were missing with unknown status (Figure 6). Fifteen of 18 tortoises surviving to the end of the study were <100 mm MCL when released, averaging 81.3 mm MCL (range, 61.6–99.0 mm). Annualized survivorship for all the tortoises for 2013–2022 was 92.97%; concomitantly, mortality rates were 7.03% (Table 3). When evaluated by year or groups of years, mortality rates ranged from 4.51 to 18.60%. Mortality in the 1.25 years between Oct 2014 and Dec 2015 was high (15.91%) following the translocation of the 48 remaining tortoises from the head-start pens; an additional 14 tortoises were lost during this time. Other years with high mortality rates were 2017 and 2021.

Tortoises found dead were <100 mm MCL when released, and most (36/41) were ≤100 mm MCL at death. Most missing tortoises also were <100 mm MCL when released (22/24) and when lost (Table 4). Most small missing tortoises were probably prey, carried off the study area, although some tortoises may have left the plot. Most surviving tortoises (15/18) were older when released, from 7 to 10 years old; only three were 4 to 6 years old.

Probable causes of death included predation by avian and mammalian predators; a combination of starvation, dehydration, and exposure; and unknown (Table 5). For all dead tortoises, more died from predators than other causes: common ravens, 31.7% (13/41); and mesocarnivores [kit fox, coyote, and generic canid (kit fox or coyote)], 48.78% (20/41). Sizes of tortoises differed depending on the cause of death. Tortoises dying of a combination of dehydration, starvation, and exposure were the smallest and averaged 58.1 mm MCL (n = 6; range, 50.6–65.2), whereas for kills by common ravens, the mean was 74.4 mm MCL (n = 13; range, 54.7–106.5). Kills by mesocarnivores (kit fox, coyote, and canids) were larger, averaging

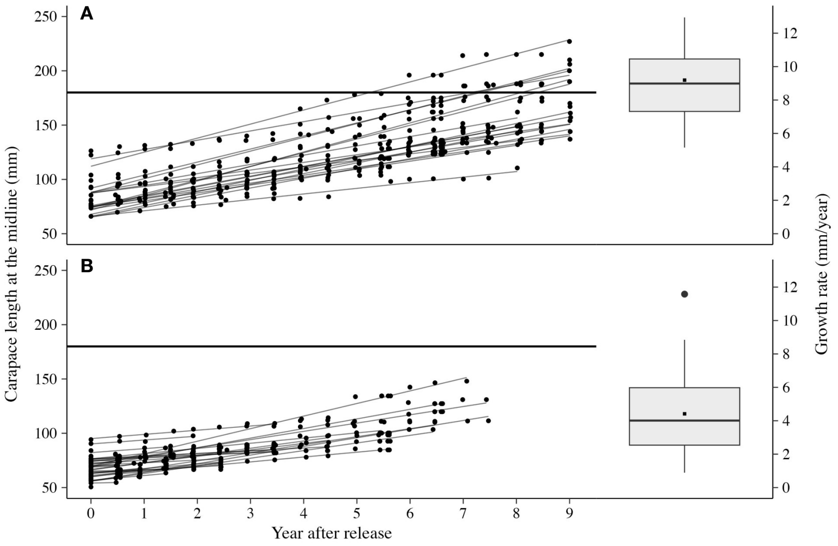

FIGURE 5
Growth rates and linear model fits of live **(A)** and dead **(B)** small Agassiz's desert tortoises (*Gopherus agassizii*) translocated from head-start pens to a study area on Edwards Air Force Base in the western Mojave Desert, California, USA.

90.3 mm MCL (n = 21; range, 63–148). The distances that dead tortoises were found from the last known locations when alive depended on the cause of death and predator. Tortoises dying of starvation, dehydration, or exposure were at or close to the last known location when alive, $\bar{x}$ = 0.8 m (n = 6; range, 0–5.8 m), whereas predators appeared to transport their prey at greater distances. On average, tortoises killed by mammals were 113.4 m (range, 3.2–1,109.2 m) distant from the last known locality, whereas those killed by common ravens were an average of 450.6 m (8.9–2,405 m) distant. More tortoises died in spring (19/41), the season when most likely to be above ground, than in summer (10/41), fall (9/41), or winter (3/41).

4.7 Annual models of survival for tortoises

The sample sizes of tortoises in the annual models of survival ranged from 31 in 2014, which included only the first release of tortoises, to 65 in 2015, after the second release of tortoises. By the end of the study, the final model included 57 tortoises (18 alive and 39 dead; Table 6). In terms of variable importance, tortoise size (MCL) ranked highest in 8 of 9 years with positive model coefficients, indicating that larger tortoises were more likely to survive (Table 7). The logistic regression model indicated that tortoises that reached a size (MCL) of 125 mm had a 50% chance of survival (Figure 7A). The importance value of repeat burrows was greater than 0.5 in 6 years of the study (2014–2017, 2019, and 2021); tortoises with more repeat burrows were more likely to survive; however, this pattern was not consistent across years, with a negative model coefficient in 2014 (Table 6). Model coefficients in this first year, however, had very high standard errors, which were likely caused by low sample sizes between live and dead tortoises (28 live and three dead) and should be interpreted with caution. The logistic regression model indicated that tortoises with approximately four repeat burrows had a 50% chance of survival, and chances of survival increased with increasing numbers of repeat burrows (Figure 7B). Additional variables with importance values ≥0.50 in one or more years were distance traveled per observation in the first 2 years, MGS NDVI in 2 years of low rainfall, and condition index in 2015, the year after 48 tortoises were released in 2014 and

TABLE 2 Annual gains in mass following handling and hydration for juvenile, immature, and young adult Agassiz's desert tortoises (*Gopherus agassizii*) in fall for 4 years (2019–2022) at the study site on Edwards Air Force Base in the western Mojave Desert of California, USA.

Sample year, fall	N	No. tortoises that did not drink	Increased mass (%) after drinking	
				Range
2019	27	6	24.7	11.9–32.7
2020	24	7	20.9	6.01–29.9
2021	21	6	15.64	3.2–37.9
2022	18	4	13.24	0.97–39.72

Years 2019 and 2020 were years of above-average rainfall, whereas years 2021 and 2022 were drought years. Nevertheless, tortoises drank in both wet and dry years. The blue-shaded rows are years when water year or winter precipitation totals were greater than 30-year long-term averages prior to the study.

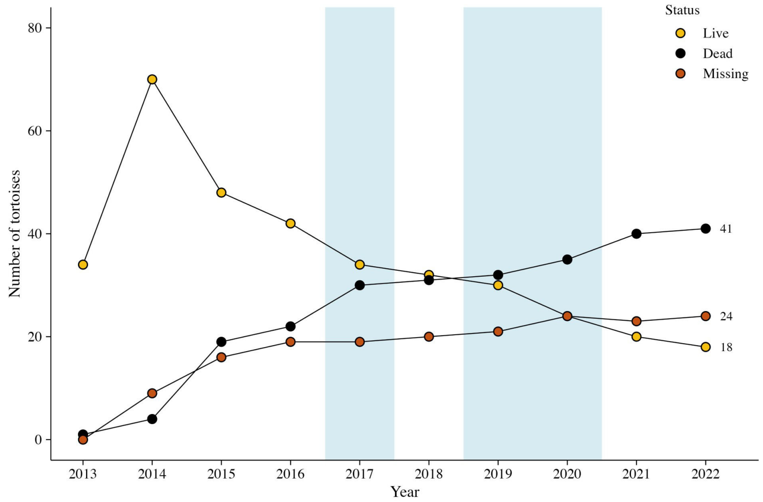

FIGURE 6
Status (live, dead, and missing) of small Agassiz's desert tortoises (*Gopherus agassizii*) translocated from head-start pens to a study area on Edwards Air Force Base in 2013–2014 in the western Mojave Desert, California, USA. The shaded blue boxes indicate years with precipitation above the long-term norms.

deaths were high (Table 7). Model fit and the number of models that performed similarly to the best-fit model (i.e., $\Delta AIC_c < 2$) varied by year (Table 6). Starting in 2018, a model with size as the sole variable became the most parsimonious model.

5 Discussion

5.1 Translocation during the megadrought and a warming climate

The megadrought resulted in prolonged years of drought with precipitation 65% to 70% below pre-megadrought and pre-study norms. The megadrought resulted in hotter air temperatures, hot droughts, evaporative losses of soil moisture, and stressed plants, presenting a bleak outlook for tortoises (Dannenberg et al., 2022). According to Cook et al. (2021), an estimated 50% chance exists for another similar drought before the end of the century. Low levels of precipitation and hotter temperatures affect almost every aspect of life for all sizes of tortoises, from the reduced cover of shrubs used for protection (Hereford et al., 2006) to health and physiology (Henen et al., 1998; Christopher et al., 1999). With this study and previous publications on adults, above-ground activities, such as movements and home range size, are limited (Duda et al., 1999), more years may be required to achieve reproductive maturity (Medica et al., 2012), and egg production is more limited (Turner et al., 1986; Turner et al., 1987; Henen, 1997; Henen, 2002a; Henen,

TABLE 3 Death rates, annualized mortality rates, and survivorship of translocated small Agassiz's desert tortoises between 1 October 2013 and 31 December 2022 at Edwards Air Force Base in the western Mojave Desert, California, USA.

Time period	D	N	Years	Mortality rate	Survivorship
Oct 2013–Dec 2022	41	83	9.25	7.03	92.97
Oct 2013–Dec 2015	19	83	2.25	10.91	89.09
Oct 2013–Sep 2014	4	35	1	11.43	88.57
Oct 2014–Dec 2015	15	77	1.25	15.91	84.09
Jan–Dec 2016	3	48	1	6.25	93.75
Jan–Dec 2017	8	43	1	18.60	81.40
Jan–Dec 2018–2019	3	34	2	4.51	95.49
Jan–Dec 2019–2020	5	33	2	7.89	92.11
Jan–Dec 2020	3	30	1	10.00	90.00
Jan–Dec 2021	4	25	1	16.00	84.00
Jan–Dec 2021–2022	5	25	2	10.56	89.44

Mortality was calculated using simple death rates for 1 year and annualized mortality rates for multiple years. Years with N ≤ 25 are not shown.

TABLE 4 Size classes and sizes (mm carapace lengths at the mid-line, MCL) of Agassiz's desert tortoises (*Gopherus agassizii*) at release and fates of live, dead, and missing at the end of the project at Edwards Air Force Base in the western Mojave Desert, California, USA.

	Sample size and range of sizes in carapace length, mm MCL; total sample includes sample size, mean, and range in carapace lengths			
Size class	Alive at start	Alive at end	Dead	Missing
Juv1	18 (50.6–58.8)	0	6 (50.6–58.8)	7 (53–59)
Juv2	60 (74.2 (60–99)	0	27 (60.1–97.7)	13(60.6–94.9)
Imm1	5 (104–132)	3 (110.5–137)	7 (100.2–131)	2 (124.1, 125)
Imm2		9 (144–170)	1 (146.5)	2 (147, 168)
Adult		6 (189–227)		
Total sample	83	18	41	24
Mean, range	73.1 (50.6–132)	110.5–227	81.8, 50.6–146.5	53–168

Size classes (mm, MCL): Juvenile 1 (Juv1), 45–59; Juvenile 2 (Juv2), 60–99; Immature 1 (Imm1), 100–139; Immature 2 (Imm2), 140–179; and Adult (≥180). Average not shown for totals unless sample size ≥25.

2002b). Higher death rates are likely for all sizes of tortoises, and juveniles in head-start pens may be especially vulnerable (Berry et al., 2002: Mack et al., 2018). More females than males may be produced, as suggested by Nagy et al. (2016), and this has been observed in other species of turtles (Roberts et al., 2023).

5.2 Survival and contributing factors

Survival of juvenile tortoises to adult sizes is essential to achieve viable populations (Congdon et al., 1993, Turner et al., 1987; Berry et al., 2020). Despite challenging circumstances for the small tortoises coupled with the megadrought, 21.7% survived. Most survivors were <100 mm MCL when released, and six reached an adult size at 14–17 years old, slightly younger than reported in a long-term study of penned tortoises in Nevada (Medica et al., 2012) but within the ages suggested for a population in the eastern Mojave Desert (Turner et al., 1987). Low rainfall and persistent drought did not appear to slow growth overall or increase the time to maturity for some survivors. The larger tortoises followed a pattern of tortoises in Nevada pens: little or no growth during drought and rapid growth when winter rains produced annual plant foods (Medica et al., 2012). Nevertheless, this pattern changed at EAFB in 2021 and 2022, both dry years: home ranges increased, and in 2022, movements, home range, and growth were comparable to those during wet years. The cause may be size-related, genetics, or physiology, with tortoises in the large immature class (140–179 mm MCL) approaching or becoming adults. Larger tortoises have more mass and nutritional resources and can travel more to obtain food. Forbs were uncommon and widely spaced in those dry years, and tortoises sought them out and ate them.

The availability of drinking water twice per year during handling may have partially offset the effects of drought. During the last 2 years of study, available drinking water possibly contributed to increased growth and movements. The added water had an important physiological function, potentially allowing tortoises to dump concentrated wastes from the bladder, refilling it with diluted urine, rehydrating, and ridding them of concentrations of waste in the blood. Consumption of dried plants could follow, thereby improving nutritional status (Peterson, 1996; Oftedal, 2002).

Models of survival indicated that size (MCL) ranked the highest among the variables, and larger tortoises were more likely to survive. Some tortoises <100 mm MCL at release survived to large immature and adult sizes, suggesting that release may be

TABLE 5 Probable causes of death for 41 small, head-started Agassiz's desert tortoises (*Gopherus agassizii*) translocated in 2013 and 2014 to the study site at Edwards Air Force Base in the western Mojave Desert, California, USA.

Probable cause of death	Tortoises released in 2013	Tortoises released in 2014
Common raven	5	8
Kit fox	1	4
Generic canid (kit fox and coyote)	6	6
Coyote	2	2
Starvation, dehydration, and exposure		6
Unknown	1	
Total	15	26

Deaths occurred between 2013 and 2022.

TABLE 6 Models for evaluating variables associated with survival of translocated juvenile and young desert tortoises raised in head-start pens at Edwards Air Force Base, California, USA.

Year	Model	AIC_c	ΔAIC_c	Akaike weight	Cumulative weight	Evidence ratio
2014	Movement, MCL, Burrows	9.5	0.000	0.52	0.52	1.00
2015	Movement, Burrows	61.6	0.000	0.15	0.15	1.00
	Movement, CI, Burrows	62.0	0.411	0.12	0.27	1.23
	CI, Burrows	62.3	0.627	0.11	0.38	1.37
	CI, MGS, Burrows	62.8	1.166	0.08	0.46	1.79
	Movement, MGS, Burrows	62.9	1.222	0.08	0.54	1.84
	Movement, CI, MGS, Burrows	63.0	1.345	0.08	0.62	1.96
	Movement, MCL, Burrows	63.2	1.598	0.07	0.69	2.22
2016	Movement, MCL, MGS	39.1	0.000	0.20	0.20	1.00
	MCL, MGS, Burrows	39.3	0.107	0.19	0.40	1.06
	Movement, MCL, MGS, Burrows	39.9	0.753	0.14	0.54	1.46
	MCL, MGS	40.4	1.210	0.11	0.65	1.83
	MCL, CI, MGS, Burrows	40.6	1.442	0.10	0.75	2.06
2017	MCL, Burrows	56.7	0.000	0.25	0.25	1.00
	MCL, MGS, Burrows	57.6	0.904	0.16	0.41	1.57
	Movement, MCL, Burrows	58.7	1.958	0.09	0.50	2.66
2018	MCL, MGS, Burrows	40.0	0.000	0.18	0.18	1.00
	MCL, MGS	40.2	0.204	0.16	0.34	1.11
	MCL	40.4	0.483	0.14	0.48	1.27
	MCL, Burrows	41.9	1.892	0.07	0.55	2.58
2019	MCL, Burrows	37.8	0.000	0.24	0.24	1.00
	MCL, CI, Burrows	38.9	1.135	0.14	0.37	1.76
	MCL	39.6	1.764	0.10	0.47	2.42
	MCL, MGS, Burrows	39.6	1.833	0.10	0.57	2.50
2020	MCL	27.2	0.000	0.15	0.15	1.00
	MCL, CI, Burrows	27.6	0.327	0.12	0.27	1.18
	MCL, Burrows	27.9	0.625	0.11	0.37	1.37
	MCL, MGS	28.0	0.766	0.10	0.47	1.47
	MCL, CI	28.4	1.159	0.08	0.55	1.79
	MCL, CI, MGS	28.6	1.406	0.07	0.63	2.02
	MCL, CI, MGS, Burrows	28.7	1.493	0.07	0.69	2.11
2021	MCL, Burrows	27.5	0.000	0.22	0.22	1.00
	MCL	27.7	0.152	0.20	0.42	1.08
2022	MCL	25.2	0.000	0.24	0.24	1.00
	Movement, MCL	26.4	1.180	0.13	0.37	1.80
	MCL, CI	26.6	1.376	0.12	0.48	1.99
	MCL, Burrows	27.1	1.881	0.09	0.58	2.56

We measured the performance of generalized linear models ranked according to corrected Akaike's Information Criterion (AICc), the difference in AICc relative to the best model (ΔAICc), Akaike weight, cumulative weight, and evidence ratios. MCL = size based on carapace length at the midline of tortoises; CI = condition index; Movement = average distance that a tortoise traveled per observation; Burrows = number of repeatedly used burrows during times of extreme temperatures (late fall, winter, and summer); MGS = average mean value of growing season NDVI within a home range calculated using minimum convex polygons.

NDVI, normalized difference vegetation index.

TABLE 7 Importance values of predictor variables used to explain the survival of small Agassiz's desert tortoises (*Gopherus agassizii*) released in 2013 and 2014 at a study area on Edwards Air Force Base, in the western Mojave Desert, California, USA.

	Variable likelihood by year								
	2014	2015	2016	2017	2018	2019	2020	2021	2022
Size of tortoise	0.978		0.949	0.746	0.996	0.974	0.997	1.0	0.995
Movements	0.964	0.633							
Repeat burrows	0.819	0.953	0.554	0.984		0.732		0.502	
Condition index		0.540							
MGS NDVI			0.968		0.611				

The total model set (main effects only) included 32 models for each year of study. For each year, variables included the size of the tortoise (carapace length at the midline, mm); movements = average distance (m) traveled per observation; repeat burrows = number of repeatedly used burrows during periods of temperature extremes (fall–winter and summer); condition index = a measure of health; and MGS NDVI = value of mean growing season. Only those variables with a likelihood of >0.500 are shown.
NDVI, normalized difference vegetation index.

possible at smaller sizes, i.e., 75–80 mm MCL. Nagy et al, 2011; Nagy et al, 2015a; Nagy et al, 2015b) considered size and shell hardness to be vital components of decisions on timing for releases of small, head-started tortoises and suggested sizes >100 mm MCL. For 50% survival based on size, our findings suggest 125 mm MCL.

The number of repeatedly used burrows during periods of temperature extremes ranked second in model importance for survival, not surprisingly, considering the importance of burrows in the lives of adults and the fidelity that adults show to these retreats (Woodbury and Hardy, 1948; Burge, 1978; Freilich et al., 2000; Drake et al., 2015). Juvenile and immature tortoises rapidly prepared burrows during settling and showed behaviors comparable to those of adults, constructing and using burrows during temperature extremes. Burrow use also figured prominently in short-term experimental studies of translocated juvenile and immature tortoises; burrow abundance (Nafus et al., 2016) and use (Germano et al., 2017) were powerful predictors of survival. Burrows will have an important role in buffering against the increasingly hot and dry conditions forecast for the entire range of the tortoise, especially if long and deep burrows allow a reduction in metabolic rates (Nagy et al., 1997). Repeatedly used burrows were also an important component of survival for translocated adults in the central Mojave Desert in a long-term study (Mack and Berry, 2023).

Other variables with high importance values contributed to post-release survival in ≥1 year: distance traveled per observation (high in the first 2 years post translocation) and mean growing season ranked high in 2 dry years. Condition index held a high value in 2015 only, the year following the release of small tortoises in 2014 and when mortality rates were high and many tortoises disappeared.

5.3 Reducing dispersal in the future

Finding methods to anchor animals to the release site can be important for positive outcomes for translocation because excessive dispersal is associated with higher mortality rates (e.g., Field et al., 2003; Nussear et al., 2012; Swaisgood and Ruiz-Miranda, 2019). In our study, the timing of the release in early October was likely a factor in reducing dispersal distances, homing, and rejection of the release site in the short-term (Stamps and Swaisgood, 2007; Berger-Tal et al., 2020). The fall release coincided with the time that tortoises enter brumation (Woodbury and Hardy, 1948; Rautenstrauch et al., 2002; Mack et al., 2015). Comparable to the pattern for wild adults, the small tortoises settled into burrows within several days of release in October and remained until late winter, unless precipitation stimulated brief emergence (Medica et al., 1980; Henen et al., 1998).

The choice of a release site can provide an anchor for settling, particularly if the habitat is comparable to the home site. In a long-distance translocation study, Nussear et al. (2012) observed less dispersal and more rapid settling when tortoises were translocated to typical habitats. We selected a site like the head-start pens and where large creosote bushes had live and dead overhanging branches and soils contained numerous rodent burrows, evidence of easy digging. Wild tortoises of all sizes selected canopies of large shrubs to place burrows throughout much of the geographic range (Burge, 1978; Berry and Turner, 1984; 1986). Nafus et al. (2016) reported that the abundance of small mammal burrows was the most powerful predictor of survival among translocated juvenile desert tortoises in a Nevada study. However, if tortoises 70–100 mm MCL are released, some are likely to require larger rodent burrows than used by heteromyid rodents, i.e., burrows used by ground squirrels, because many rodent burrows are too small for larger juvenile and immature tortoises. The presence of rodent burrows beneath shrubs signals easy digging.

5.4 Selecting translocation sites

Locating places to translocate tortoises for recovery purposes presents major challenges because habitats are degraded and fragmented due to historic, recent, and current anthropogenic disturbances typical throughout the geographic range and generally in the West (U.S. Fish and Wildlife Service [USFWS], 1994; Leu et al., 2008; U.S. Fish and Wildlife Service [USFWS], 2011; Berry and Murphy, 2019). Importantly, substantial blocks of land, whether managed by agencies within the Departments of Defense or the Interior, have histories of uses and current commitments often limiting compatibility for recovery (e.g., U.S. Bureau of Land Management, 2019).

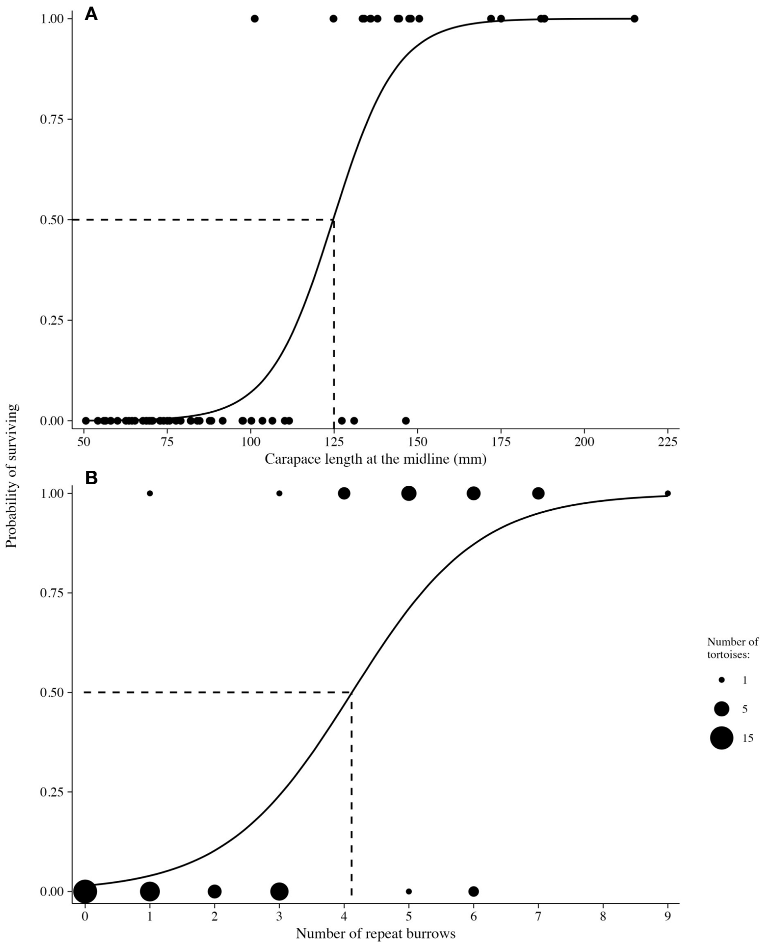

FIGURE 7
Probability of survival for 83 small Agassiz's desert tortoises (*Gopherus agassizii*) based on **(A)** size (carapace length at the midline, MCL, mm) and **(B)** number of repeat burrows (repeatedly used burrows during periods of temperature extremes) after translocation to a site on Edwards Air Force Base in the western Mojave Desert, California, USA. Size of the tortoise was the principal driver of survival in annual models of survival, followed by repeatedly used burrows.

The USFWS (2011) has a goal of restoring tortoise populations to viability, and head-starting is one method of augmenting diminished populations. Translocated tortoises need space. Based on our study, the 15-km^2 site was too small because some tortoises dispersed after reaching 145–150 mm MCL (or smaller). Depending on location, the translocation site may need fencing to reduce unauthorized uses (e.g., Berry et al., 2014a; Berry et al., 2020) or protect the tortoises from vehicle kills on paved and well-used dirt roads (von Seckendorff Hoff and Marlow 2002; Nafus et al., 2013).

Tortoise habitats will gain from the reduction of non-native grasses and harmful non-native forbs (e.g., African mustard). Grasses, whether native or non-native, are poor forage and harmful for juveniles and all sizes of tortoises if forbs are not consumed as part of the diet (Hazard et al., 2009; 2010; Drake et al., 2016). Much of the geographic range, including the study area on EAFB, has invasive, non-native annual grasses, and African mustard has rapidly invaded parts of the Mojave Desert (Brooks and Berry, 2006; Minnich and Sanders, 2000). Non-native, annual grasses are flammable and have contributed to severe damage from fires to critical habitat units for the tortoise, particularly in the central, eastern, and northeastern Mojave Desert regions (Brooks and Matchett, 2006; Klinger et al., 2021). Non-native grasses and forbs effectively compete with the native forbs preferred by tortoises (Brooks, 2000; Brooks, 2003; Berry et al., 2014b; Jennings and Berry, 2015). The situation is acute during drought years because non-native species (e.g., *Schismus* spp., *Bromus* spp.) composed 91% of the biomass in dry years in the western Mojave (Brooks and Berry, 2006). Production of annual forbs following winter rains is essential for the growth of small tortoises: forbs provide energy, nutrients, and minerals (Nagy and Medica, 1986; Hazard et al., 2009; Hazard et al., 2010). The altered food supply, when coupled with prolonged years of drought, reduces the capacity of juveniles to grow and increases the time to reach sexual maturity. Habitat restoration is likely essential to the recovery of tortoise populations (Abella et al., 2023).

5.5 Hyper-predation by ravens and coyotes

Reductions in predators that kill tortoises would benefit the survival of small, translocated tortoises. Populations of ravens and coyotes have grown in the Mojave Desert because of subsidies from anthropogenic sources of food and water and, for ravens, the addition of nest and perch sites (Kristan and Boarman., 2003; Esque et al., 2010; Cypher et al., 2018). At EAFB, the two species of predators benefitted locally from animal kills on nearby roads and highways, trash, and other food and water sources available from nearby settlements and on-base housing, military offices and facilities, and perches in Joshua trees and cultivated trees. These predators were the sources of most deaths of tortoises in our study and other projects (e.g., Nagy et al., 2015b). Recent efforts to reduce the population growth of ravens throughout the Mojave Desert in California have focused on lethal measures and oiling of eggs (e.g., U.S. Fish and Wildlife Service [USFWS] 2008; Shields et al., 2019), but neither measure occurred on EAFB during the time frame of the study (W.E. King, 412 CEG/CEVA, EAFB, personal communication, 2 Feb 2023).

6 Implications

The translocation of head-started tortoises began under difficult circumstances because of several factors, including the condition of tortoises to be translocated (Mack et al., 2018). In the future, head-starting projects would benefit from guidelines in IUCN, International Union for the Conservation of Nature, Species Survival Commission (2013) and Swaisgood and Ruiz-Miranda (2019). These publications provide roadmaps to successful projects, especially when a team of knowledgeable and committed parties and multiple government agencies can be assembled in advance of project initiation and meet frequently as conditions warrant.

Climate change, with increasing temperatures, megadroughts, and more hot and dry years forecasted, poses new challenges to survival for tortoises, especially when existing and projected climate variations are coupled with long-term habitat degradation. Although tortoises have physiological and behavioral adaptations for living in deserts, these adaptations may be insufficient during prolonged droughts. For small tortoises, deeper burrows with more soil cover and longer tunnels may allow greater protection from increasing temperatures and declining soil moisture but may be beyond the capacity of small tortoises to dig. Experimental testing of pre-dug, deep burrows, and drinking water is another option, especially when associated with telemetered individuals.

Protection and restoration of habitats and controlling subsidized predators are potential routes forward. Improvements in head-start methods (e.g., Nagy et al., 2020) with translocations delayed until juveniles are ≥70–100 mm MCL are likely to aid in higher survival. Fall translocations to appropriate sites can allow for rapid construction of burrows, settling, and brumation. Fall releases result in tortoises moving underground, whereas spring releases contribute to above-ground activity and likely predation. Release sites of high quality (large, protected from ongoing and future surface disturbances) could enhance survival. Future options include the exploration of sites beyond the current distributional limits in the northern Mojave at higher elevations. Desirable sites likely to benefit the tortoise would be free of historic and recent livestock grazing, feral burros, horses, mining, and other developments, especially if those areas support food plants preferred by the tortoises.

Data availability statement

The senior author will need to obtain permission from the U.S. Air Force base at Edwards, California, before sharing the data. Research is continuing on the remaining live study animals by Dr. Ron Swaisgood's team at the San Diego Zoo Wildlife Alliance, California and he should also be contacted, at least to approve sharing. Requests to access the datasets should be directed to kristin_berry@usgs.gov.

Ethics statement

The animal study was reviewed and approved by U.S. Fish and Wildlife Service Endangered Species Permits. We worked under USFWS Permits for Endangered Species and the study plan received multiple reviews. All permit numbers are listed in the paper.

Author contributions

The authors are listed in order of the level of contributions. KB is first, JM is second, and KA is third. All authors contributed to the article and approved the submitted version.

Funding

Edwards Air Force Base provided funds to the U.S. Geological Survey for the project.

Acknowledgments

We thank D. Essary, R. Newman, T. Shields, A. Spenceley, and M. Tuma for assistance in the field; M. Tuma for assistance with two reports; R. Klinger for assistance with NDVI; R. Swaisgood for sharing plant data; and R. Swaisgood, D. Elam, and three reviewers for constructive reviews. We appreciated the support of T. Mull early in the project and W. King, who managed long-term monitoring; both were employees of EAFB. Handling during translocation and subsequent monitoring were under permits from the U.S. Fish and Wildlife Service: TE-32004C-0-2, TE-87850B-0, TE-45827D-0, and TE-46010D-0. Any use of trade firm or product names is for descriptive purposes only and does not imply endorsement by the U.S. government.

Conflict of interest

Author KA was employed by the company Bajada Ecology LLC.

The remaining authors declare that the research was conducted in the absence of any commercial or financial relationships that could be construed as a potential conflict of interest.

Publisher's note

References

Abella, S. R., Berry, K. H., and Ferrazzano, S. (2023). Techniques for restoring damaged Mojave and western Sonoran habitats, including those for threatened desert tortoises and Joshua trees. *Desert Plants* 38, 4–52.

Allison, L. J., and McLuckie, A. M. (2018). Population trends in Mojave desert tortoises (*Gopherus agassizii*). *Herpetol. Conserv. Biol.* 13, 433–452.

Averill-Murray, R. C., Fleming, C. H., and Riedle, J. D. (2020). Reptile home ranges revisited: a case study of space use of Sonoran desert tortoises (*Gopherus morafkai*). *Herpetol. Conserv. Biol.* 15, 253–271.

Bates, D., Maechler, M., Bolker, B., Walker, S., Christensen, R. H. B., Singmann, H., et al. (2023) *lme4: linear mixed-effects models using "Eigen" and S4*. Available at: https://cran.r-project.org/package=lme4 (Accessed Jun 2023).

Berger-Tal, O., Blumstein, D. T., and Swaisgood, R. R. (2020). Conservation translocations: a review of common difficulties and promising directions. *Anim. Conserv.* 23, 121–131. doi: 10.1111/acv.12534

Berry, K. H., Allison, L. J., McLuckie, A. M., Vaughn, M., and Murphy, R. W. (2021). *Gopherus agassizii, Mojave Desert tortoise. The International Union for Conservation of Nature Red List of Threatened Species*™ (IUCN 2021). Available at: https://www.iucnredlist.org/species/97246272/3150871 (Accessed July 14, 2023).

Berry, K. H., Bailey, T. Y., and Anderson, K. M. (2006). Attributes of desert tortoise populations at the National Training Center, central Mojave Desert, California, USA. *J. Arid Environ.* 67 (Supplement), 165–191. doi: 10.1016/j.jaridenv.2006.09.026

Berry, K. H., and Christopher, M. M. (2001). Guidelines for the field evaluation of desert tortoise health and disease. *J. Wildl. Dis.* 37, 427–450. doi: 10.7589/0090-3558-37.3.427

Berry, K. H., Gowan, T. A., Miller, D. M., and Brooks, M. L. (2014b). Models of invasion and establishment for African mustard (*Brassica tournefortii*). *Invasive Plant Sci. Manage.* 7, 599–616. doi: 10.1614/IPSM-D-14-00023.1

Berry, K. H., Lyren, L. M., Yee, J. L., and Bailey, T. Y. (2014a). Protection benefits desert tortoise (*Gopherus agassizii*) abundance: the influence of three management strategies on a threatened species. *Herpetological Mongr.* 28, 66–92. doi: 10.1655/HERPMONOGRAPHS-D-14-00002

Berry, K. H., and Murphy, R. W. (2019). *Gopherus agassizii* (Cooper 1861) – Mojave Desert Tortoise, Agassiz's Desert Tortoise. *Chelonian Res. Monogr.* 5, 1–45. doi: 10.3854/crm.5.109.agassizii.v1.2019

Berry, K. H., Spangenberg, E. K., Homer, B. L., and Jacobson, E. R. (2002). Deaths of desert tortoises following periods of drought and research manipulation. *Chelonian Conserv. Biol.* 4, 436–448.

Berry, K. H., and Turner, F. B. (1984). "Notes on the behavior and habitat preferences of juvenile desert tortoises (*Gopherus agassizii*) in California," in *Proc. Ninth Ann. Desert Tortoise Council Symp* (Lake Havasu City, AZ, USA: The Desert Tortoise Council), 111–130. Available at: https://deserttortoise.org (Accessed January 2, 2023).

Berry, K. H., and Turner, F. B. (1986). Spring activities and habits of juvenile desert tortoises, *Gopherus agassizii*, in California. *Copeia* 4), 1010–1012. doi: 10.2307/1445302

Berry, K. H., Yee, J. L., Shields, T. A., and Stockton, L. (2020). The catastrophic decline of tortoises at a fenced Natural Area. *Wildl. Monogr.* 205, 1–53. doi: 10.1002/wmon.1052

Boarman, W. I. (1993). "When a native predator becomes a pest: A case study," in *Conservation and Resource Management*. Eds. S. K. Majumdar, E. W. Miller, D. E. Baker, E. K. Brown, J. R. Pratt and R. F. Schmalz (Easton, PA: The Pennsylvania Academy of Science), 191–206.

Boarman, W. I., and Berry, K. H. (1995). "Common ravens in the southwestern United States 1968–92," in *Our Living Resources. A Report to the Nation on the Abundance, and Health of U.S. Plants, Animals, and Ecosystems*. Eds. E. T. LaRoe, G. S. Farris, C. E. Puckett, P. D. Doran and M. J. Mac (Washington, DC: U.S. Department of the Interior, National Biological Service), 73–75.

Brooks, M. L. (2000). Competition between alien annual grasses and native annual plants in the Mojave Desert. *Am. Midl. Nat.* 144, 92–108. doi: 10.1674/0003-0031(2000)144[0092:CBAAGA]2.0.CO;2

Brooks, M. L. (2003). Effects of increased soil nitrogen on the dominance of alien annual plants in the Mojave Desert. *J. Appl. Ecol.* 40, 344–353. doi: 10.1046/j.1365-2664.2003.00789.x

Brooks, M. L., and Berry, K. H. (2006). Dominance and environmental correlates of alien annual plants in the Mojave Desert, USA. *J. Arid Environ.* 67 (Supplement), 100–124. doi: 10.1016/j.jaridenv.2006.09.021

Brooks, M. L., and Matchett, J. R. (2006). Spatial and temporal patterns of wildfires in the Mojave Deser–2004. *J. Arid Environ.* 67 (Supplement), 148–164. doi: 10.1016/j.jaridenv.2006.09.027

Burge, B. L. (1978). "Physical characteristics and patterns of utilization of cover sites used by *Gopherus agassizi* in southern Nevada," in *Proc. 3rd Ann. Desert Tortoise Council Symp* (Las Vegas, Nevada, USA: The Desert Tortoise Council), 80–111. Available at: https://desertortoise.org (Accessed January 2, 2023).

Burnham, K. P., and Anderson, D. R. (2002). *Model Selection and Multimodel Inference: a Practical Information-theoretic Approach. 2nd ed.* (New York: Spring Science Business Media).

Calenge, C. (2006). The package adehabitat for the R software: tool for the analysis of space and habitat use by animals. *Ecol. Modell.* 197, 1035. doi: 10.1016/j.ecolmodel.2006.03.017

Christopher, M. M., Berry, K. H., Wallis, I. R., Nagy, K. A., Henen, B. T., and Peterson, C. C. (1999). Reference intervals and physiologic alternations in hematologic and biochemical values of free-ranging desert tortoises in the Mojave Desert. *J. Wildl. Dis.* 35, 212–238. doi: 10.7589/0090-3558-35.2.212

Congdon, J. D., Dunham, A. E., and Van Loben Sels, R. C. (1993). Delayed sexual maturity and demographics of Blanding's turtles (*Emydoidea blandingii*): implications for conservation and management of long-lived organisms. *Conserv. Biol.* 7, 826–833. doi: 10.1046/j.1523-1739.1993.740826.x

Cook, B. I., Mankin, J. S., Williams, A. P., Marvel, K. D., Smerdon, J. E., and Liu, H. (2021). Uncertainties, limits, and benefits of climate change mitigation for soil moisture drought in southwestern North America. *Earth's Future* 9, e2021ER002013. doi: 10.1029/2021EF002014

Cypher, B. L., Kelly, E. C., Westall, T. L., and Van Horn Job, C. L. (2018). Coyote diet patterns in the Mojave Desert: implications for threatened desert tortoises. *Pac. Conserv. Biol.* 24, 44–54. doi: 10.1071/PC17039

Dannenberg, M. P., Yan, D., Barnes, M. L., Smith, W. K., Johnston, M. R., Scott, R. L., et al. (2022). Exceptional heat and atmospheric dryness amplified losses of primary production during the 2020 U.S. Southwest hot drought. *Global Change Biol.* 22, 4794–4806. doi: 10.111/gcb.16214

Dormann, C. F., Elith, J., Bacher, S., Buchmann, C., Carl, G., Carré, G., et al. (2013). Collinearity: a review of methods to deal with it and a simulation study evaluating their performance. *Ecography* 5, 027–046. doi: 10.1111/j.1600-0587.2012.07348.x

Drake, K. K., Bowen, L., Nussear, K. E., Esque, T. C., Berger, A. J., Custer, N. A., et al. (2016). Negative impacts of invasive plants on conservation of sensitive desert wildlife. *Ecosphere* 7, e01531. doi: 10.1002/ecs2.1531

Drake, K. K., Esque, T. C., Nussear, K. E., DeFalco, L. A., Scoles-Sciulla, S. J., Modlin, A. T., et al. (2015). Desert tortoise use of burned habitat in the eastern Mojave Desert. *J. Wildl. Manage.* 79, 618–629. doi: 10.1002/jwmg.874

Duda, J. J., Krzysik, A. J., and Freilich, J. E. (1999). Effects of drought on desert tortoise movement and activity. *J. Wildl. Manage.* 63, 1181–1192. doi: 10.2307/3802836

Edmund, H., Bell, K., and Butler, A. (2020) *Prism: access data from the Oregon State Prism Climate Project*. Available at: https://github.com/ropensci/prism.

Esque, T. C., Nussear, K. E., Drake, K. K., Walde, A. D., Berry, K. H., Averill-Murray, R. C., et al. (2010). Effects of subsidized predators, resource variability, and human population density on desert tortoise populations in the Mojave Desert, USA. *Endangered Species Res.* 12, 167–177. doi: 10.3354/esr00298

Field, K. J., Tracy, C. R., Medica, P. A., Marlow, R. W., and Corn, P. S. (2003). "Spring, fall, or winter? Success of desert tortoise translocation as affected by season of release," in *Proc. 27th Ann. Desert Tortoise Council Symp* (Las Vegas, Nevada, USA: The Desert Tortoise Council), 107–109. Available at: https://deserttortoise.org (Accessed October 10, 2021).

Fleming, C. H., Fagan, W. F., Mueller, T., Olson, K. A., Leimgruber, P., and Calabrese, J. M. (2015). Rigorous home range estimation with movement data: a new autocorrelated kernel density estimator. *Ecology* 96, 1182–1188. doi: 10.1890/14-2010.1

Freilich, J. E., Burnham, K. P., Collins, C. M., and Garry, C. A. (2000). Factors affecting population assessments of desert tortoises. *Conserv. Bio.* 14, 1479–1489. doi: 10.1046/j.1523-1739.2000.98360.x

Germano, J. M., Nafus, M. G., Perry, J. A., Hall, D. B., and Swaisgood, R. R. (2017). Predicting translocation outcomes with personality for desert tortoises. *Behav. Ecol.* 28, 1075–1084. doi: 10.1093/beheco/arx064

Hardy, R. (1976). "The Utah population—a look in the 1970's," in *Proc. First Ann. Desert Tortoise Council Symp., 23–24 March 1976* (Las Vegas, Nevada, USA: The Desert Tortoise Council), 84–88. Available at: https://deserttortoise.org (Accessed August 15, 2022).

Hazard, L. C., Shemanski, D. R., and Nagy, K. A. (2009). Nutritional quality of natural foods of juvenile desert tortoises (*Gopherus agassizii*): energy, nitrogen, and fiber digestibility. *J. Herpetol.* 43, 38–48. doi: 10.1670/07-160R1.1

Hazard, L. C., Shemanski, D. R., and Nagy, K. A. (2010). Nutritional quality of natural foods of juvenile and adult desert tortoises (*Gopherus agassizii*): calcium, phosphorus, and magnesium digestibility. *J. Herpetol.* 44, 135–147. doi: 10.1670/08-134.1

Henen, B. T. (1997). Seasonal and annual energy budgets of female desert tortoises (*Gopherus agassizii*). *Ecology* 78, 283–296. doi: 10.1890/0012-9658(1997)078[0283:SAAEBO]2.0.CO;2

Henen, B. T. (2002a). Energy and water balance, diet, and reproduction of female desert tortoises (*Gopherus agassizii*). *Chelonian Conserv. Biol.* 4, 319–329.

Henen, B. T. (2002b). Reproductive effort and reproductive nutrition of female desert tortoises: essential field methods. *Integr. Comp. Biol.* 42, 43–50. doi: 10.1093/icb/42.1.43

Henen, B. T., Peterson, C. C., Wallis, I. R., Berry, K. H., and Nagy, K. A. (1998). Effects of climatic variation on field metabolism and water relations of desert tortoises. *Oecologia* 117, 365–373. doi: 10.1007/s004420050669

Hereford, R., Webb, R. H., and Longpré, C. I. (2006). Precipitation history and ecosystem response to multidecadal precipitation variability in the Mojave Desert regio–2001. *J. Arid Environ.* 67 (Supplement), 13–34. doi: 10.1016/j.jaridenv.2006.09.019

IUCN, International Union for the Conservation of Nature, Species Survival Commission. (2013). *Guidelines for reintroductions and other conservation translocations. The Reintroduction and Invasive Species Specialist Groups' Task Force on Moving Plants and Animals for Conservation Purposes. Version 1.0* (Gland, Switzerland: IUCN Species Survival Commission). Available at: https://www.iucn.org/content/guidelines-reintroductions-and-other-conservation-translocations (Accessed 11 Jun 2021).

Jennings, W. B., and Berry, K. H. (2015). Desert tortoises (*Gopherus agassizii*) are selective herbivores that track the flowering phenology of their preferred food plants. *PloS One* 10, e0116716. doi: 10.1371/journal.pone.0116716

Klinger, R., Underwood, E. C., McKinley, R., and Brooks, M. L. (2021). Contrasting geographic patterns of ignition probability and burn severity in the Mojave Desert. *Front. Ecol. Evol.* 9, 593167. doi: 10.3389/fevo.2021.593167

Kristan, W. B.III, and Boarman., W. I. (2003). Spatial pattern of risk of common raven predation on desert tortoises. *Ecology* 84, 2432–2443. doi: 10.1890/02-0448

Leu, M., Hanser, S. E., and Knick, S. T. (2008). The human footprint in the West: A large-scale analysis of anthropogenic impacts. *Ecol. Appl.* 18, 1119–1139. doi: 10.1890/07-0480.1

Longshore, K. M., Jaeger, J. R., and Sappington, J. M. (2003). Desert tortoise (*Gopherus agassizii*) survival at two eastern Mojave Desert sites: death by short-term drought? *J. Herpetol.* 37, 169–172. doi: 10.1670/0022-1511(2003)037[0169:DTGASA]2.0.CO;2

Mack, J. S., and Berry, K. H. (2023). Drivers of survival of translocated tortoises. *J. Wildl. Manage.* 87, e22352. doi: 10.1002/jwmg.22352

Mack, J. S., Berry, K. H., Miller, D. M., and Carlson, A. S. (2015). Factors affecting the thermal environment of Agassiz's desert tortoise (*Gopherus agassizii*) cover sites in the Central Mojave Desert during periods of temperature extremes. *J. Herpetol.* 49, 405–414. doi: 10.1670/13-080

Mack, J. S., Schneider, H. E., and Berry, K. H. (2018). Crowding affects health, growth, and behavior in headstart pens for Agassiz's desert tortoise. *Chelonian Conserv. Biol.* 17, 14–26. doi: 10.2744/CCB-1248.1

Manning, J. C. (1992). *Applied principles of hydrology. 2nd edition* (New York: Macmillan).

Medica, P. A., Bury, R. B., and Luckenbach, R. A. (1980). Drinking and construction of water catchments by the desert tortoise, *Gopherus agassizii*, in the Mojave Desert. *Herpetologica* 36, 301–304.

Medica, P. A., Nussear, K. E., Esque, T. C., and Saethre, M. B. (2012). Long-term growth of desert tortoises (*Gopherus agassizii*) in a southern Nevada population. *J. Herpetol.* 46, 213–220. doi: 10.1670/11-327

Minnich, R. A., and Saunders, A. C. (2000). "*Brassica tournefortii* Gouan," in *Invasive Plants of California's Wildlands*. Eds. C. C. Bossard, J. M. Randall and M. C. Hoshovsky (Berkeley, CA: University of California Press), 68–72.

Nafus, M. G., Esque, T. C., Averill-Murray, R. C., Nussear, K. E., and Swaisgood, R. R. (2016). Habitat drives dispersal and survival of translocated juvenile desert tortoises. *J. Appl. Ecol.* doi: 10.1111/1365–2664.12774

Nafus, M. F., Tuberville, T. D., Buhlmann, K. A., and Todd, B. D. (2013). Relative abundance and demographic structure of Agassiz's desert tortoise (*Gopherus agassizii*) along roads of varying size and traffic. *Biol. Conserv.* 162, 100–106. doi: 10.1016/j.biocon.2013.04.009

Nagy, K. A., Henen, B. T., and Hillard, L. S. (2020). Head-started Agassiz's desert tortoise *Gopherus agassizii* achieved high survival, growth, and body condition in natural field enclosures. *Endangered Species Res.* 43, 305–321. doi: 10.3354/esr01067

Nagy, K. A., Henen, B. T., Vyas, D. B., and Wallis, I. R. (2002). A condition index for the desert tortoise (*Gopherus agassizii*). *Chelonian Conserv. Biol.* 4, 425–429.

Nagy, K. A., Hillard, S., Dickson, S., and Morafka, D. J. (2015a). Effects of artificial rain on survivorship, body condition, and growth of head-started desert tortoises (*Gopherus agassizii*) released to the open desert. *Herpetological Conserv. Biol.* 10, 535–549.

Nagy, K., Hillard, L. S., Tuma, M. W., and Morafka, D. J. (2015b). Head-started desert tortoises (*Gopherus agassizii*): Movements, survivorship and mortality causes following their release. *Herpetological Conserv. Biol.* 10, 203–215.

Nagy, K. A., Kuchling, G., Hillard, L. S., and Henen, B. T. (2016). Weather and sex ratios of head-started Agassiz's desert tortoise *Gopherus agassizii* juveniles hatched in natural habitat enclosures. *Endangered Species Res.* 30, 145–155. doi: 10.3354/esr00737

Nagy, K. A., and Medica, P. A. (1986). Physiological ecology of desert tortoises in southern Nevada. *Herpetologica* 42, 73–92.

Nagy, K. A., Morafka, D. J., and Yates, R. A. (1997). Young desert tortoise survival—energy, water, and food requirements in the field. *Chelonian Conserv. Biol.* 2, 396–404.

Nagy, K. A., Tuma, M. W., and Hillard, L. S. (2011). Shell hardness measurement in juvenile desert tortoises, *Gopherus agassizii*. *Herpetological Rev.* 42, 191–195.

Nussear, K. E., Tracy, C. R., Medica, P. A., Wilson, D. S., Marlow, R. W., and Corn, P. S. (2012). Translocation as a conservation tool for Agassiz's desert tortoises: survivorship, reproduction, and movements. *J. Wildl. Manage.* 76, 1341–1353. doi: 10.1002/jwmg.390

Oftedal, O. T. (2002). "Nutritional ecology of the desert tortoise in the Mohave and Sonoran deserts," in *The Sonoran Desert Tortoise: Natural History, Biology, and Conservation*. Ed. T. R. Van Devender (Tucson, AZ: University of Arizona Press and the Arizona-Sonora Desert Museum), 194–241.

Oftedal, O. T., Hillard, S., and Morafka, D. J. (2002). Selective spring foraging by juvenile desert tortoises (*Gopherus agassizii*) in the Mojave Desert: evidence of an adaptive nutritional strategy. *Chelonian Conserv. Biol.* 4, 341–352.

Overpeck, J. T., and Udall, B. (2020). Climate change and the aridification of North America. *Proc. Natl. Acad. Sci. U.S.A.* 117, 11856–11858. doi: 10.1073/pnas.2006323117

Pebesma, E., Bivand, R., Rowlingson, B., Gomez-Rubio, V., Hijmans, R., Sumner, M., et al. (2021). Sp: classes and methods for spatial data. R package version 1.4.5. Available at: https://github.com/edzer/sp/ (Accessed September 2022).

Peterson, C. C. (1996). Anhomeostasis: seasonal water and solute relations in two populations of the desert tortoise (*Gopherus agassizii*) during chronic drought. *Physiol. Zool.* 69, 1324–1358. doi: 10.1086/physzool.69.6.30164263

Petorelli, N. (2013). *The normalized difference vegetation index* (Oxford, UK: Oxford University Press).

Rautenstrauch, K. R., Rakestraw, D. L., Brown, G. A., Boone, J. L., and Lederle, P. E. (2002). Patterns of burrow use by desert tortoises (*Gopherus agassizii*) in southcentral Nevada. *Chelonian Conserv. Biol.* 4, 398–405.

R Core Team. (2021). *R: a language and environment for statistical computing* (Vienna, Austria: R Foundation for Statistical Computing).

Rhodin, A. G. J., Stanford, C. B., van Dijk, P. P., Eisemberg, C., Goode, E. V., Luiselli, L., et al. (2018). Global conservation status of turtles and tortoises (Order Testudines). *Chelonian Conserv. Biol.* 17, 135–161. doi: 10.2744/ccb-1348.1

Roberts, H. P., Willey, L. L., Jones, M. T., Akre, T. S. B., King, D. I., Kleopfer, J., et al. (2023). Is the future female for turtles? Climate change and wetland configuration predict sex ratios of a freshwater species. *Global Change Biol.* 29, 2643–2654. doi: 10.1111/gcb.16625

Row, J. R., and Blouin-Demers, G. (2006). Kernels are not accurate estimators of home-range size for herpetofauna. *Copeia* 2006 (4), 797–802. doi: 10.1643/0045-8511(2006)6[797:KANAEO]2.0.CO;2

Rowlands, P. G. (1995). "Regional bioclimatology of the California Desert," in *The California Desert: An Introduction to Natural Resources and Man's Impact*. Eds. J. Latting and P. G. Rowlands (Riverside, CA: June Latting Books), 95–134.

Rowlands, P., Johnson, H., Ritter, E., and Endo, A. (1982). "The Mojave Desert," in *Reference Handbook on the Deserts of North America*. Ed. G. Bender (Westport, CT: Greenwood Press), 103–162.

Shields, T., Currylow, A., Hanley, B., Boland, S., Boarman, B., and Vaughn, M. (2019). Novel management tools for subsidized avian predators and a case study in the conservation of a threatened species. *Ecosphere* 10 (10), e02895. doi: 10.1002/ecs2.2895

Stahle, D. W. (2020). Anthropogenic megadrought. *Science* 368 (6488), 238–239. doi: 10.1126/science.abb6902

Stamps, J. A., and Swaisgood, R. R. (2007). Someplace like home: experience, habitat selection and conservation biology. *Appl. Anim. Behav. Sci.* 102, 392–409. doi: 10.1016/j.applanim.2006.05.038

Swaisgood, R. R., and Ruiz-Miranda, C. (2019). “Moving animals in the right direction: making conservation translocation an effective tool,” in *International Wildlife Management: Conservation Challenges in a Changing World*. Eds. J. L. Koprowski and P. R. Krausman (Baltimore, MD: Johns Hopkins Univ Press), 141–156.

Turner, F. B., Berry, K. H., Randall, D. C., and White, G. C. (1987). *Population ecology of the desert tortoise at Goffs, Californ–1986* (Rosemead, California, USA: Southern California Edison).

Turner, F. B., Hayden, P., Burge, B. L., and Roberson, J. B. (1986). Egg production by the Desert Tortoise (*Gopherus agassizii*) in California. *Herpetologica* 42, 93–104.

U.S. Bureau of Land Management. (2019). *West Mojave route network project. Final supplemental environmental impact statement for the California Desert District* (California, USA: USBLM, Moreno Valley).

U.S. Fish and Wildlife Service [USFWS]. (1990). Endangered and threatened wildlife and plants; determination of threatened status for the Mojave population of the desert tortoise. *Fed. Regist.* 55, 12178–12191.

U.S. Fish and Wildlife Service [USFWS]. (1994). *esert tortoise (Mojave population) recovery plan* (Portland, Oregon. USA: USFWS).

U.S. Fish and Wildlife Service [USFWS]. (2008). *Environmental assessment to implement a desert tortoise recovery plan task; reduce common raven predation on the desert tortoise* (Ventura, California, USA: U.S. Department of the Interior, Fish and Wildlife Service).

U.S. Fish and Wildlife Service [USFWS]. (2011). *Revised Recovery Plan for the Mojave Population of the desert tortoise (Gopherus agassizii)* (Reno, Nevada, USA: USFWS).

U.S. Geological Survey [USGS]. (2022). *User guide. Earth Resources Observation and Science (EROS) Center Science Processing Architecture (ESPA) On Demand Interface, version 13.0. Department of the Interior, U.S. Geological Survey*. Available at: https://www.usgs.gov/media/files/eros-science=processing-architecture-demand-interface-user-guide.

von Seckendorff Hoff, K., and Marlow, R. W. (2002). Impacts of vehicle road traffic on Desert Tortoise populations with consideration of conservation of tortoise habitat in southern Nevada. *Chelonian Conserv. Biol.* 4, 449–456.

Williams, A. P., Cook, E. R., Smerdon, J. E., Cook, B. I., Abatzoglou, J. T., Bolles, K., et al. (2020). Large contribution from anthropogenic warming to an emerging North American megadrought. *Science* 368, 314–318. doi: 10.1126/science.aaz9600

Woodbury, A. M., and Hardy, R. (1948). Studies of the desert tortoise, *Gopherus agassizii*. *Ecol. Monogr.* 18, 145–200. doi: 10.2307/1948638

frontiers | Frontiers in Ecology and Evolution

TYPE Original Research
PUBLISHED 09 October 2023
DOI 10.3389/fevo.2023.1229123

OPEN ACCESS

EDITED BY
Matteo Marcantonio,
Université catholique de Louvain, Belgium

REVIEWED BY
Kristen Shive,
University of California, Berkeley,
United States
Andreas P. Wion,
Colorado State University, United States

*CORRESPONDENCE
Micah Wright
✉ mcwright@usgs.gov

RECEIVED 25 May 2023
ACCEPTED 18 September 2023
PUBLISHED 09 October 2023

CITATION
Wright M, van Mantgem P, Buffington K, Thorne K, Engber E and Smith S (2023) Spatially explicit models of seed availability improve predictions of conifer regeneration following the 2018 Carr Fire in northern California.
Front. Ecol. Evol. 11:1229123.
doi: 10.3389/fevo.2023.1229123

Spatially explicit models of seed availability improve predictions of conifer regeneration following the 2018 Carr Fire in northern California

Micah Wright[1]*, Phillip van Mantgem[1], Kevin Buffington[2], Karen Thorne[2], Eamon Engber[3] and Sean Smith[4]

[1]U.S. Geological Survey, Western Ecological Research Center, Arcata, CA, United States, [2]U.S. Geological Survey, Western Ecological Research Center, Davis, CA, United States, [3]National Park Service, Klamath Network Fire Ecology Program, Orick, CA, United States, [4]National Park Service, Klamath Inventory and Monitoring Network, Ashland, OR, United States

For many conifer species in dry conifer forests of North America, seeds must be present for postfire regeneration to occur, suggesting that seed dispersal from surviving trees plays a critical role in postfire forest recovery. However, the application of tree fecundity and spatial arrangement to postfire conifer recovery predictions have only recently become more common, and is often included at relatively coarse scales (i.e., 30 meters). In this study, we mapped surviving trees using lidar and created a spatially explicit estimate of seed density (seed shadows) with 10 m, 50 m, and 100 m median dispersal distances. We estimated the number of seeds produced by each tree using allometric relationships between tree size and fecundity. Along with the seed shadows, we used a suite of topographic variables as inputs to negative binomial hurdle models to predict conifer seedling abundance in 131 plots following the 2018 Carr Fire in northern California, USA. We compared models using each of the seed shadows to each other as well as to a model using the distance to the nearest surviving tree, which served as a baseline. All model formulations indicated that estimated seed availability was positively associated with conifer regeneration. Despite the importance of seed availability plays in regeneration and the substantial differences in seed availability represented by the different seed shadows in our analysis, we found surprisingly little difference in model performance regardless of which seed shadow was used. However, the models employing seed shadows outperformed the models with distance to the nearest live tree. Although we have demonstrated a modest improvement in predicting postfire conifer regeneration, the uncertainty in our results highlights the importance of tree detection and classification in future studies of this kind. Future studies may find it useful to consider other factors such as predation, site suitability, and seed mortality as potential drivers of discrepancies between total and realized dispersal kernels.

KEYWORDS

wildland fire, conifer regeneration, dispersal kernel, Bayesian modeling, lidar

1 Introduction

In recent years, wildfires in the western region of the U.S. have become more frequent, larger, and more severe (Stevens et al., 2017; Williams et al., 2019; Goss et al., 2020), and long-term warming and prolonged droughts due to climate change are projected to increase wildfire severity and length of season over the coming decades (Wehner et al., 2017). As fire size and severity has increased, so has the scale of tree mortality, with large, high severity patches becoming increasingly common (Collins et al., 2017; Williams et al., 2023). Therefore, there is an urgent need to understand the mechanisms of forest regeneration. Nearly all conifers in the western U.S. are obligate seeders, implying that natural reforestation following fire requires a locally available seed source, either from surviving trees or via adaptations such as serotinous cones or soil seed banks (Turner et al., 1998; Stevens-Rumann and Morgan, 2019). Many of the dominant species in the mixed conifer forests of northern California are wind dispersed and lack either serotinous cones or soil seed banks (Burns and Honkala, 1990), though serotinous knobcone pine *Pinus attenuata* (Lemmon) is found in the region (Reilly et al., 2019). In species lacking these adaptations, the probability of postfire seedling establishment for non-serotinous species typically declines with increasing distance from the nearest surviving tree because wind dispersed seeds are less likely to fall further from the source (Chambers et al., 2016; Coop et al., 2019). Most conifer seed dispersal occurs over relatively short distances, with most wind dispersed seeds falling within 100 m of the parent tree, though distances may vary by tree height (Greene and Johnson, 1989; Katul et al., 2005; Bullock et al., 2017). If seeds rarely travel more than 100m, this suggests that the time required for forests to naturally regenerate in the interior of large patches of high tree mortality may be substantially more than areas closer to the patch edge, as seed dispersal into areas further from the edge relies on infrequent long-distance dispersal or the maturation and subsequent reproduction from initial colonizers (Turner et al., 1998). This timeline may be extended further by competition from shrubs and hardwoods, which can more rapidly recolonize severely burned areas via resprouting or persistent soil seed banks (Knapp et al., 2012; Welch et al., 2016) and may compete with regenerating conifers (Collins and Roller, 2013; Crotteau et al., 2013; Tepley et al., 2017).

Seed availability is a critical component of the postfire recovery process (Gill et al., 2022). One common approach is to approximate seed availability with simple metrics such as distance to the nearest surviving tree or unburned forest edge, which are easy to measure and have a proven utility in predicting conifer regeneration (Chambers et al., 2016; Korb et al., 2019). However, these methods do not capture fine scale variation in seed availability, which may be especially important in areas that experienced high tree mortality but where there are multiple locations with surviving trees within the range of most seed dispersal. For example, the center of a circular patch of high tree mortality may receive substantially more seed than would be suggested by simply determining the nearest surviving tree, since the area would be receiving seed from all trees within dispersal range (Peeler and Smithwick, 2020). Simple distance models may also be less optimal when seed production capability varies across the landscape due to variations in tree size, density, or both. While recent efforts have been made to incorporate the fecundity and spatial arrangement of trees into predictions of postfire regeneration (Tepley et al., 2017; Shive et al., 2018; Downing et al., 2019; Peeler and Smithwick, 2020; Stewart et al., 2021), few studies have attempted to do so at the scale of individual trees (but see Landesmann and Morales, 2018).

Seed availability can be modeled using estimates for fecundity and dispersal. Dispersal functions (kernels) use the distance from the parent tree to create a spatially uniform (i.e., isotropic) distribution describing the probability a seed will fall to the ground a given distance from the source (Greene et al., 2004; Nathan et al., 2008; Bullock et al., 2017). When combined with allometrically derived estimates of annual seed production (fecundity) (Greene and Johnson, 1994), these distributions can be used to estimate seed availability at a given distance from a surviving tree or group of trees for a given time after a fire event. The combination of dispersal probability and fecundity is known as a seed shadow (Clark et al., 1999a). Seed shadows have been used to approximate seed availability across geographic space when modeling the probability of postfire conifer regeneration (Shive et al., 2018; Stewart et al., 2021). However, these recent modeling efforts have relied on moderate resolution data such as 30 m burn severity maps from Monitoring Trends in Burn Severity (MTBS, https://www.mtbs.gov/), which may obscure fine-scale variation in seed availability. Fine scale maps of surviving trees, such as those created using fine scale imagery or lidar data, may more accurately reflect the variation in seed source availability on the landscape, and thus more closely represent true seed availability (Barber et al., 2022).

In this study, we used data from one to three years after a severe wildlife event (the 2018 Carr Fire) at Whiskeytown National Recreation Area (WHIS) to assess the ability of seed shadows derived from high-resolution maps of individual trees to predict short-term postfire conifer regeneration. We also tested whether the models using seed shadows outperformed models using distance to the nearest live tree, assuming that the high performance and simplicity of the distance models makes them an appropriate baseline. In addition to estimates of seed availability, our models also included variables for topography and shrub cover to assess the influence of site characteristics on postfire conifer regeneration.

2 Materials and methods

2.1 Study area

Whiskeytown National Recreation Area is located at the southeastern edge of the Klamath bioregion (Skinner et al., 2006) in Shasta and Trinity Counties, just west of the city of Redding in northern California. WHIS is over 17,000 hectares in size, and is characterized by steep topography and high biodiversity, with a wide variety of forest types including oak woodlands, knobcone pine woodlands, mixed conifer and yellow pine forests, with true fir (red and white) at high elevations (Fry and Stephens, 2006). Elevation in WHIS ranges from 250 to 1,890 meters above sea level. The park also includes large areas of shrubland and sparsely-treed woodlands, especially on the south-facing slopes north of Whiskeytown Lake.

Common conifer species include ponderosa pine (*Pinus ponderosa*), Jeffrey pine (*Pinus jeffreyi*), incense cedar (*Calocedrus decurrens* (Torr.) Floren.), Douglas fir, sugar pine (*Pinus lambertiana* Dougl.), and white fir (*Abies concolor* (Gord. & Glend.) Lindl.). Knobcone and gray pine (*Pinus sabiniana*) are common at low elevations, and some red fir (*Abies magnifica* var. *shastensis*) is found in the high elevations of the park. A variety of hardwood species are also found throughout the park, including California black oak (*Quercus kelloggii* Newb.), canyon live oak (*Quercus chrysolepis* Liebm.), tanoak (*Notholithocarpus densiflorus*), golden chinquapin (*Chrysolepis chrysophylla*), and dogwood (*Cornus nuttallii* Audubon). See Smith et al. (2021) for a detailed description of vegetation found in the park.

Fires were historically common in the area but decreased in frequency after 1850, with an almost complete absence of fire in the latter half of the 20th century following the widespread adoption of fire suppression (Fry and Stephens, 2006). However, fire has not been completely absent in the last few decades. Starting in the mid-1990s, the National Park Service introduced fuels reduction and other restoration projects, often involving the use of prescribed fire. In addition to these treatments, wildfire has also occurred within the park boundary. Most notably, the Shasta-Trinity Unit Lightning Complex Fire burned through the park in 2008, which burned 4% of the park area at high severity (MTBS, 2018).

The Carr Fire started on July 23rd, 2018, and actively burned for 38 days before containment on August 30th the same year (https://www.fire.ca.gov/incidents/2018/7/23/carr-fire). The fire burned nearly 93,000 hectares, including nearly the entire area of WHIS, destroyed over 1,000 homes in nearby communities, resulted in 8 human deaths, and had an estimated damage cost of >$1.6 billion (USD). The fire occurred under abnormally hot, dry, and windy conditions, and made significant runs when terrain and wind aligned, burning a large portion of WHIS in a single 24-hour period.

Our study focused on the yellow pine and mixed conifer forests of WHIS, which covered over 5,200 ha within the park prior to the Carr Fire (Figure 1). According to data produced by MTBS, over 65% of the conifer forests (3,450 ha) burned at high severity (Figure 1, MTBS, 2020). High severity patches were extensive, especially on the steep slopes of the Brandy, Boulder, and Mill Creek drainages.

2.2 Field data

We leveraged field data from two separate sources for this analysis. We used data from a preexisting network of 0.1 ha fire monitoring (FMH) plots in WHIS, which are designed to monitor changes in fuels and forest structure at random locations following fire (USDI National Park Service, 2003). We selected all plots where seedling density and overstory trees (>15 cm diameter at breast height or 1.37 m, hereafter DBH) were sampled after the Carr Fire, for a total of 23 plots. The FMH plot data captured species, DBH, and status for all overstory trees in the plot based on a 15 cm DBH threshold. The same information was collected for pole size trees (stems ≤ 15 cm DBH) in 0.025 ha subplots. The FMH plots also captured seedling tallies (stems ≤ 2.5 cm DBH) by size class, species, and status in a 50 m^2 subplot (0.005 ha). The FMH plots also captured vegetation cover using two 50 m point intercept transects, where species and height of vegetation was recorded at 30 cm intervals for a total of 166 points per transect. We averaged the shrub cover estimates from both transects to get a plot level estimate of shrub cover.

In addition to the FMH plots, we established a total of 108 0.1 ha plots in the summers of 2020 and 2021 (Figure 1). We sampled plots over most of the elevation range of the park, with plot elevations ranging from 330 to 1,870 m. For most of these plots (n = 76) we used GIS to randomly select sampling locations within conifer forests according to the following criteria: no slopes > 50%, > 50 m and < 500 m from a road, 100 m from non-vegetated areas

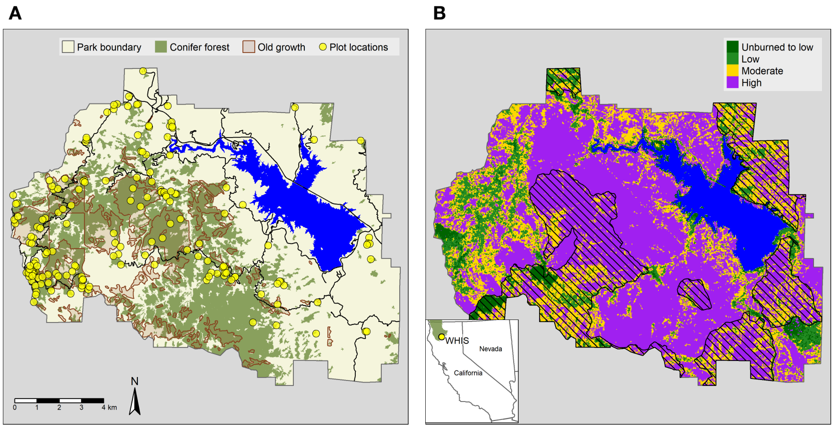

FIGURE 1
(A) Location of forest plots, old growth, and conifer forests at Whiskeytown National Recreation Area. Forest types and old growth polygons were derived from park data products circa 2006. **(B)** Monitoring Trends in Burn Severity (MTBS) burn severity map with previous fire perimeters (pattern fill) overlayed. The inset shows the location of WHIS and the Klamath bioregion (in green). Klamath bioregion data downloaded from https://databasin.org/datasets/4996c7e61a0e48f2bef646903f51b82b.

(e.g., Whiskeytown Lake), and at least 50 m from one another. The sampling locations were stratified across burn severity and predicted regeneration. Regeneration was predicted using the models developed in (Stewart et al., 2021) using the poscrptR R package (Wright et al., 2020). We used vegetation alliance polygons created for the National Park Service (Fox et al., 2006) to identify conifer forests by selecting polygons with Douglas fir, mixed conifer, ponderosa pine, or red fir forest alliance types. We established 12 of the plots specifically in random locations within unoccupied aerial survey (UAS) sampling areas to assist with future vegetation mapping projects using the same criteria described above, with the exception that plot locations were stratified by burn severity and whether the forest alliance was conifer (described above) or oak, including black oak, blue oak, canyon live oak, interior live oak, Oregon white oak, and tanoak forest and woodland alliances. We established an additional 20 plots to match earlier randomly sampled plot surveys of old-growth conifer forests (Leonzo and Keyes, 2010). Three of the original plots from Leonzo and Keyes (2010) could not be reached due to unsafe conditions, so we sampled three replacement plots using the same random sampling criteria outlined in Leonzo and Keyes (2010).

At each plot, we recorded DBH, species identity, and live and dead status for all standing trees > 15 cm DBH over a 0.1 ha circular plot. We measured sapling (stems 0.1 to 15.0 cm DBH) stem diameter, species location and status in a 0.011 ha subplot at the plot center. We also collected tallies of live seedlings (stems < 1.37 m in height) in the subplot, recording species and height class (0.1–5, 5–10, 11–25, 26–50, 51–75, 76–100, and 100–136 cm). On nine occasions the seedling subplot was reduced in size to 0.001 ha or 0.005 ha because the large numbers of seedlings present made larger subplot sizes impractical. We also visually estimated the cover of shrubs, forbs, and grasses within the plot area. Cover estimates were binned into the following classes: 0–1%, 2–5%, 6–25%, 26–50%, 51–75%, 76–95%, and 96–100%.

We normalized the data for each plot type (FMH and 0.1 ha field plots) by putting basal area and seedlings on a common per hectare scale and binning shrub cover into 25% class bins. Seedlings were not always identifiable beyond the genus level, and we could not determine the species of the lidar mapped trees from aerial imagery. Therefore, we report results for our analyses on seedling density for all conifers combined. We initially performed the analysis at the genus level, with broadly similar results. Plot sizes were similar between plot types, so we expected that any difference in seedling detection probability between plot types due to sampled area is likely to be small.

2.3 Seed availability

2.3.1 Individual tree delineation and classification

We mapped surviving tree locations using a combination of lidar and high-resolution imagery. The detection of individual trees from lidar works best on dominant trees whose crowns are clearly visible from above (Maltamo et al., 2004). WHIS is structurally diverse, with a substantial understory component (Leonzo and Keyes, 2010). Therefore, we assumed that trees detected using the lidar data are in reality “tree approximate objects” (North et al., 2017; Jeronimo et al., 2018) and may represent more than one individual tree, though we refer to them as individual trees for simplicity. Given the forest structure at WHIS, we likely underestimated surviving trees and their associated seed production. However, larger trees are of local interest (Leonzo and Keyes, 2010) and generally produce more seed (Greene and Johnson, 1994), so we expect that we have captured the overall spatial trends in tree survival and seed production, even where the absolute values deviate.

We developed a model for mapping individual tree mortality status across the park. We used the lidR R package (Roussel et al., 2020; Roussel and Auty, 2021) to create a 0.5 m resolution canopy height model for the Whiskeytown footprint (grid_canopy and p2r functions) from lidar collected in 2019 (8 points/m^2, U.S. Geological Survey, 2021). We further processed the lidar to find individual tree points (locate_trees and lmf functions, 5 m moving window and 7 m height threshold) and crowns (dalponte2016 function, Dalponte and Coomes, 2016). We derived point cloud-based metrics for each crown following methods outlined in Marrs and Ni-Meister (2019). We resampled high resolution (12 inch) multispectral orthomosaic imagery (collected November 2018 for the National Park Service by Eagle Digital Imaging, Inc.) to 1 m resolution, which we then used to calculate the green normalized difference vegetation index (GNDVI; [NIR-green]/[NIR+green]). GNDVI was less sensitive to shadows than NDVI in our exploration of potential model predictors. We then extracted summary statistics of GNDVI for each crown. We generated points for live (n=609) and dead (n=758) trees from manual interpretation of the color infrared imagery and 2020 NAIP imagery (https://www.usgs.gov/centers/eros/science/usgs-eros-archive-aerial-photography-national-agriculture-imagery-program-naip). We used a parameter selection algorithm model (rf.modelSel from the rfUtilities package, parsimony=0.025, Murphy et al., 2010) to reduce the number of predictor variables for the final random forest model (randomForest R package, Breiman, 2001; Liaw et al., 2002). Seven GNDVI metrics and four lidar metrics were included in the final model (Table 1). We partitioned the data into 80/20% training/testing data sets to assess model performance. We used a random forest model with default parameters to classify trees by their mortality status.

The tree mortality status model performed well, with 93.4% overall accuracy, a Cohens’s Kappa of 0.87, sensitivity of 0.96, and specificity of 0.91. The model correctly identified live trees with an accuracy of 90.3% when we compared it to a separate validation data set of live and dead trees generated using UAS imagery (Thorne et al., 2023). Of the 2.23 million individual trees detected across WHIS, 77.1% were classified as dead. However, we noticed that there were occasional trees incorrectly classified as live within large high severity patches, likely due to the presence of shrubs or herbaceous vegetation within the tree crown footprint. Though these trees were likely to have little to no influence on many of our analyses, they would have a strong influence on calculating metrics such as distance to the nearest surviving tree. Based on this assumption, we used 2020 NAIP aerial imagery to manually

TABLE 1 Final predictor variables and model importance for tree mortality random forest model.

Predictors	Source	Importance
GNDVI Median	Orthoimagery	346.0
GNDVI Mean	Orthoimagery	286.7
GNDVI 90th percentile	Orthoimagery	217.2
GNDVI Sum	Orthoimagery	187.9
GNDVI Min	Orthoimagery	81.7
Lidar Intensity SD	Lidar	65.7
Proportion of 1st returns	Lidar	43.4
GNDVI Max	Orthoimagery	34.8
Proportion of 3rd returns	Lidar	34.7
GNDVI SD	Orthoimagery	16.4
Proportion of 2nd returns	Lidar	15.5

Metrics were extracted from each tree approximate object crown. GNDVI, green normalized difference vegetation index; SD, standard deviation. We sourced the orthoimagery from the National Park Service and the lidar data from the USGS National Map Lidar Explorer.

check the mortality classification on all trees classified as alive that were greater than 70 m from the nearest other surviving tree (n=374); of these, 186 were manually reclassified as dead for further analyses, often because of the presence of resprouting shrubs underneath the dead tree. Of course, manually correcting these trees did not address incorrectly classified dead trees in these areas or any incorrectly classified trees in areas of greater tree density. Regardless, due to the outsize influence an isolated tree can have on the availability of seed, we felt that correcting the misclassified isolated trees was the more conservative approach.

Rather than misclassification, we assumed that the omission of smaller surviving trees would be the most likely error in areas of high tree density and stand complexity because tree detection is more difficult under these conditions (Jeronimo et al., 2018). Omitting small trees likely lead to a subsequent underestimation of available seed in these locations. However, large trees account for the most basal area and produce the most seed (Greene and Johnson, 1994), so we assume that the overall pattern of seed dispersal is maintained.

We estimated diameter for each mapped tree using a height-diameter allometric equation from (Parker and Evans, 2004), which we parameterized using data from the Klamath Inventory and Monitoring Network plots in WHIS (I&M, Odion et al., 2011). Some sampling variability has been observed in the I&M tree height measurements, so we averaged heights and diameters by tree from the 2012 and 2015 sample dates. We fit the models using the brms package (Bürkner, 2017) in R using a gamma likelihood with a log link. It has been shown that including other predictors such as crown diameter improves the predictive accuracy of height-diameter equations (Jucker et al., 2017). However, since we did not have access to field measurements of crown diameter, we elected to use the univariate model. Model predictions are shown in Supplementary Figure 1.

2.3.2 Dispersal kernels

We produced isotropic kernels at 1m resolution for each of the mapped surviving trees (described above) using a lognormal dispersal function (Greene et al., 2004), shown below.

$$f(x) = (\frac{1}{(2\pi)^{1.5}Sx^2})exp(-\frac{ln(x/L)^2}{2S^2})$$

The values from the lognormal dispersal function represent an estimate of the probability of seed dispersal at a given distance (x in the equation above) from the parent tree on a two-dimensional plane. The parameters L and S determine the median dispersal distance and the standard deviation of the log distances, respectively (Greene et al., 2004).

We were unable to estimate the parameters in the kernel functions directly from our field data. Therefore, we calculated seed dispersal probability for three parameterizations for each kernel: short, medium, and long-distance, with the shape parameter held constant at one following recommendations in Greene et al. (2004) and scale parameter (median dispersal distance) at 10, 50, and 100m respectively (Figure 2). During preliminary analysis, we tried several other dispersal functions including the WALD, log-hyperbolic secant, exponential power, and inverse Gaussian, all of which had similar performance to the lognormal function. We selected these functions because they received good support in the literature (Katul et al., 2005; Bullock et al., 2017; but see Cousens et al., 2018).

2.3.3 Fecundity and seed shadows

Larger trees are likely to produce more seeds (Greene and Johnson, 1994; Krannitz and Duralia, 2004), so we calculated the expected annual seed production of each tree using equations from Greene and Johnson (1994). We estimated the individual seed mass using average seeds per kilogram by species from Bonner and Karrfalt (2008), using regionally specific values where possible. Since we did not know the species for the lidar mapped trees, we created a weighted seed weight coefficient for each field plot based on the proportion of each species by basal area in the plot. We then used the median of the plot-level values as the seed coefficient for the fire. The equations in Greene and Johnson (1994) derive leaf mass from basal area, which we estimated from the modeled tree diameters described above. We converted the annual seed estimates for each tree location to a raster surface with 1m resolution and applied the lognormal dispersal function using a moving window function from the terra package in R (Hijmans, 2022) to create the seed shadows for each of the different kernel parameterizations. Finally, we extracted the estimated seed rain for each seedling subplot and converted it to the estimated total expected seed availability at the plot in seedlings per hectare by multiplying the predicted seed rain by the number of seed-producing seasons between when the fire was contained and when the plot was sampled. We assumed that the seed producing season was from September to December.

To visually demonstrate the variation in different kernel parameterizations, we plotted the seed shadows for the area

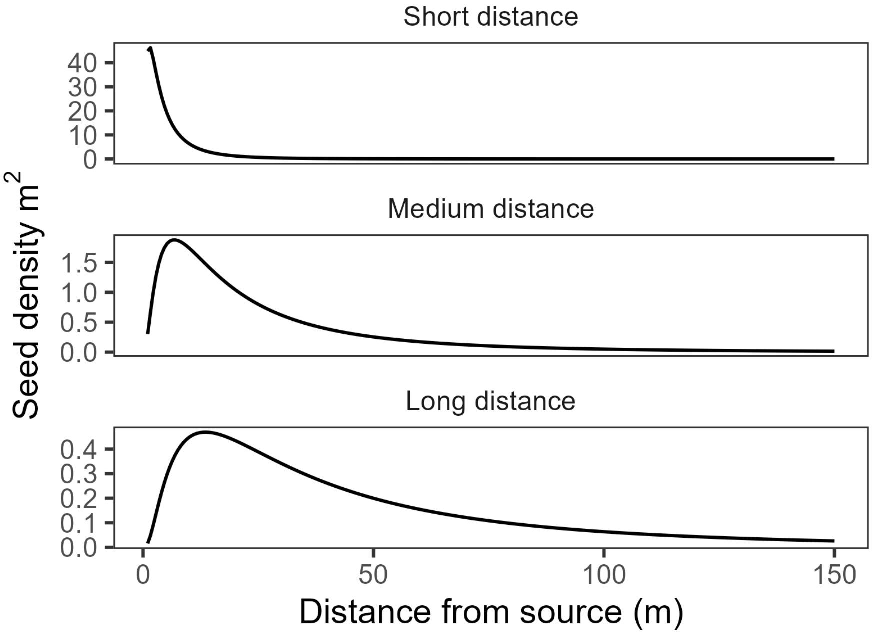

FIGURE 2
Estimated seed density for each of the kernel function parameterizations for a hypothetical tree producing 10,000 seeds.

200 m surrounding a plot that burned at high severity with complete basal area mortality (Figure 3). The plot is >70 m from the nearest surviving tree, but with many surviving trees in the surrounding area, especially to the north and west. We subjectively selected the area surrounding this plot because there were few surviving trees in the area immediately surrounding the plot but many surviving trees nearby. This image shows the potential effect of different kernel parameterizations on estimated seed availability.

2.3.4 Distance to live tree

We calculated the distance to the nearest surviving tree to use as a comparison with expected seed availability at each plot. This estimate is not a seed shadow, though we assumed that it functioned as a proxy for the amount of seed available at the plot location.

2.4 Topography

We used whitebox tools (Wu, 2021) to estimate topographic wetness index from a 1 m-resolution lidar digital elevation model (DEM). First, we breached depressions to remove sinks. We then calculated D-infinity flow direction and flow accumulation for each cell, which we used to calculate topographic wetness index:

$$wetness\ index = Ln(flow\ accumulation/tan(slope)))$$

We calculated heat load index following methods outlined in McCune and Keon (2002) using the spatialEco package (Evans, 2021). We extracted the average heat load index, topographic wetness index, slope, and elevation from the 1 m DEM for the area of each seedling subplot.

2.5 Analysis

We used the brms package (Bürkner, 2017) in R (R Core Team, 2021) to fit Bayesian generalized linear models estimating the influence of estimated seed availability, shrub cover, topographic wetness index, elevation, and heat load index on postfire conifer regeneration. There were several plots without seedlings, so we used negative binomial hurdle models to estimate both the influence of covariates on the probability of encountering no conifer seedlings as well as the effects on conifer seedling abundance, conditional on their being present (Steel et al., 2013). The model takes the following form:

$$P(Y_i = y_i) = \begin{cases} p_i = logit(\beta_0 + \beta_{x_i} x_i) & y_i = 0 \\ (1 - p_i)\frac{NB(\mu,\phi)}{1-NB(\mu,\phi)} & y_i > 0 \end{cases}$$

Where NB is the negative binomial distribution, β_0 is the intercept, and β_{x_i} are the regression coefficients for the *ith* predictor. The count portion of the model is a zero truncated negative binomial with a log link and shape parameter ϕ:

$$NB(\mu = exp(\beta_0 + \beta_{x_i} x_i), \phi)$$

We used the same predictors in the hurdle and count portions of the model.

We fit separate models with different seed availability variables: three models with seed shadows derived using each of the three dispersal function parameterizations, and an additional model that used the distance to the nearest surviving tree. We standardized all continuous predictors by subtracting the mean and dividing by two standard deviations, which puts continuous and binary predictors on a common scale (Gelman, 2008). We used weakly informative

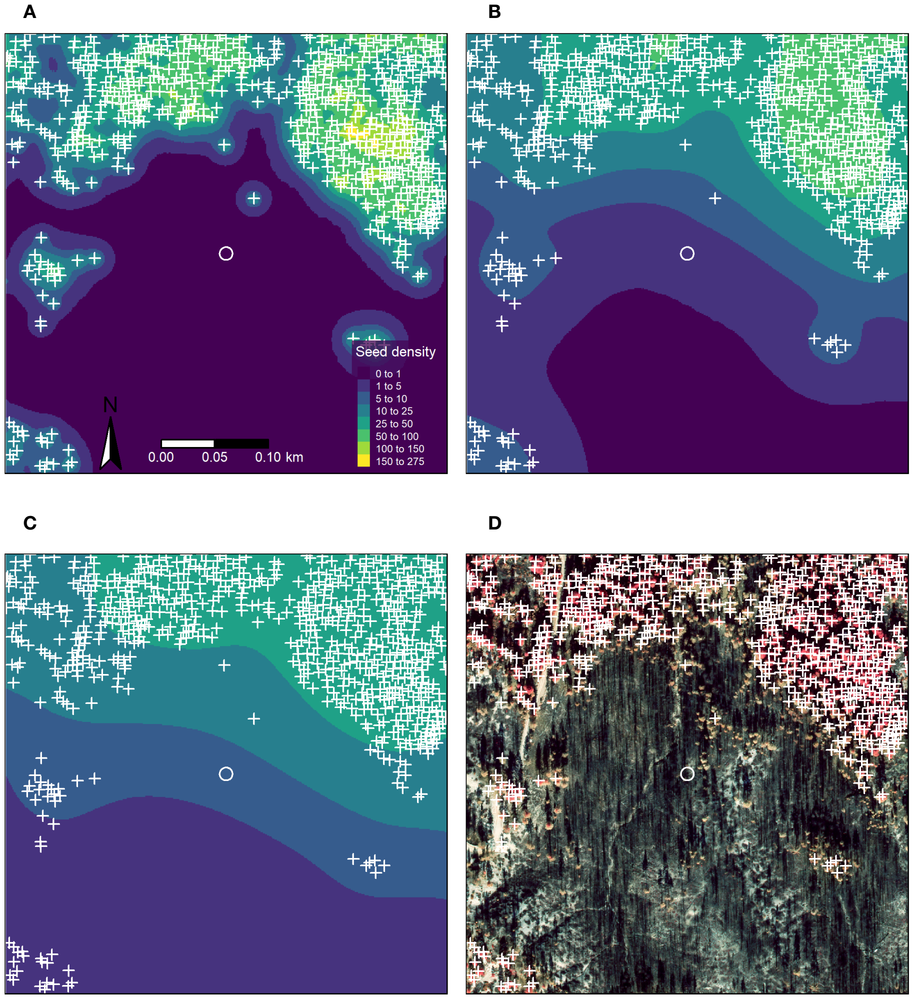

FIGURE 3
Orthophoto and maps of seed shadows for a 200 m area surrounding a plot in a high severity patch with extensive tree mortality. The plot area is shown as a white circle, plot area is to scale. Orthophoto shown in false color infrared. **(A)** 10 m median dispersal distance. **(B)** 50 m median dispersal distance. **(C)** 100 m median dispersal distance. **(D)** False color infrared orthophoto (National Park Service, unpublished data).

priors in all models, where β_0 is the intercept, β_x are the regression coefficients, and ϕ is the shape parameter of the negative binomial distribution:

$$\beta_0 \sim \mathcal{N}(0, 10)$$

$$\beta_x \sim \mathcal{N}(0, 5)$$

$$\phi \sim G(0.2, 0.2)$$

We ran all models for 2,000 iterations and ensured that all $\hat{R}$ values did not exceed 1.01. We checked the model fit using posterior predictive checks and leave-one-out cross-validation (LOO, Vehtari et al., 2017). We compared models using the expected log pointwise predictive density ($\widehat{elpd}$), which estimates the predictive accuracy of the model for each data point held out during LOO (Vehtari et al., 2017). Models can be compared by differencing $\widehat{elpd}$ estimates ($\Delta\widehat{elpd}$), and the standard error of $\Delta\widehat{elpd}$ can characterize the uncertainty in the model comparison. Generally, models with $\Delta\widehat{elpd}$ of less than four have similar predictive performance (Sivula et al., 2020). Here, we report the on the parameters for the model with the highest $\widehat{elpd}$. We calculated mean absolute error (MAE) for each model as an additional measure of model performance. Along with conditional effects for the hurdle and count portions of the model, we report the probability of direction, which describes the probability that the parameter is the same sign as the median of the posterior distribution (Makowski et al., 2019).

Several plots were located in areas that burned multiple times, including 26 in the 2008 Shasta-Trinity Unit Lightning Complex fire. Reburned areas may have lower conifer regeneration than similar areas that have not experienced recent burns if surviving seed trees are killed (Tepley et al., 2017; McCord et al., 2020). We assumed that multiple burns would largely effect any regeneration we observed by removing potential parent trees. We modeled seed availability from the mapped surviving trees, so we elected not to include whether a plot was reburned in any of the models as this was unlikely to add additional information. The data can be found at Wright et al. (2023).

3 Results

Conifer recruitment was found at most plots throughout the park. Out of the 131 plots, 35 (27%) did not have any conifer seedlings. Average seedling density for all conifers combined was 2,265 stems per hectare (Figure 4). *Abies*, *Pinus* and *Calocedrus* had the similar average seedling densities, with 703, 635, and 737 stems per hectare, respectively. *Pseudotsuga* seedlings were rare, found in only 29 plots, with the lowest average seedling density of 189 stems per hectare.

Oak regeneration was also widespread throughout the fire; 101 plots had either *Quercus* or *Notholithocarpus* regenerating in the plot, usually resprouting from topkilled trees.

There were considerable differences in the seed shadows we produced, depending on parameterizations (Figure 3). Unsurprisingly, seed shadows parameterized with short distance kernels (10m median dispersal distance) were much more concentrated around the source trees, with no predicted seed presence in the plot. In contrast, the estimates created with medium and long-distance parameterizations (50 and 100 m median dispersal distance, respectively) showed more widespread seed availability but at relatively low densities, especially for the long-distance parameterization.

All plots were within 321 meters of at least one surviving tree (Figure 5), with a median distance of 21 meters and 119 plots within 100 meters of a surviving tree.

3.1 Model results

LOO suggested that the models using seed availability extracted from seed shadows modestly outperformed the model using simple distance to live trees (Supplementary Table 1, Figure 6), with $\widehat{elpd}$ greater than four at least one standard error from zero. The medium distance model had the highest $\widehat{elpd}$, though there was little evidence for major differences between the models using seed availability extracted from seed shadows with $\widehat{elpd}$ less than four in all cases. The short distance dispersal model had the lowest MAE, but MAE was similar across the seed shadow models. As with LOO, MAE suggested that the distance to live tree model had the worst performance, with Δ MAE of 186 then the next best model. As with LOO, MAE for the models using dispersal kernels were very similar, although the model using the short-distance dispersal had lower MAE than the medium-distance model.

The medium distance model selected by LOO suggested that increased seed availability was associated with increased conifer seedling presence and density (Figures 7, 8), with probability of direction approaching 1 for both the hurdle and count components of the model. The effects of elevation were more uncertain. The best performing model indicated that increasing elevation resulted in fewer seedling observations (probability of direction 0.96), though there was little strength of evidence for a similar effect on seedling abundance (probability of direction 0.58). There was also little evidence for a consistent effect of topographic wetness index on either seedling presence or abundance, with probability of direction 0.78 and 0.56, respectively). There was some evidence that conifer seedlings were less likely to be found in areas with a high heat load index (probability of direction 0.95). The effect of heat load index on seedling density was more uncertain, but also suggested a positive relationship (probability of direction 0.87).

The effects of shrub cover were mixed. The model suggested that conifer seedlings were more likely to be observed (hurdle portion of the model) with shrub cover in the 26–50% range than in 0–25% (probability of direction 0.91), though the model also suggested that seedling abundance (density portion of the model) was lower in the 26–50% shrub cover class than in lower shrub densities (probability of direction 0.94). Evidence was much weaker for effects in the higher shrub cover classes (probability of direction below 85% in all cases), though it should be noted that the highest two shrub cover classes had very few observations (five and six plots, respectively).

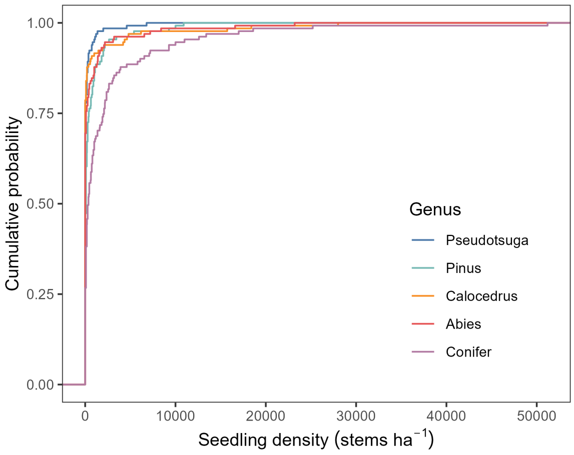

FIGURE 4
Empirical cumulative distribution function of conifer seedling density by genus.

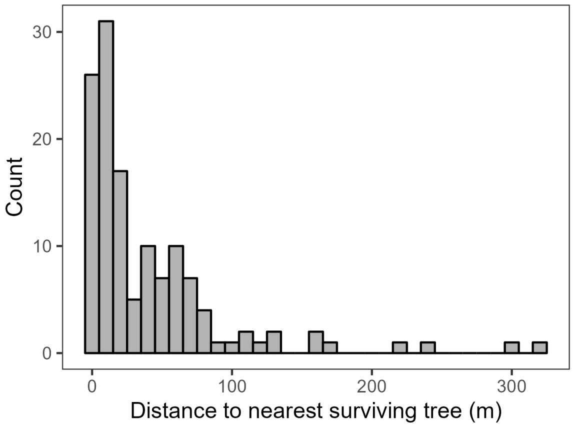

FIGURE 5
Histogram of the distance to the nearest surviving tree to each plot in meters.

4 Discussion

For the bulk of obligate seeding conifers lacking serotinous cones, spatial variability in fire-related tree mortality will determine the availability of seeds and thus the spatial variability in regeneration following the fire event (Gill et al., 2022). There is a vast literature demonstrating this using a variety of methodologies at a variety of scales (Korb et al., 2019; Peeler and Smithwick, 2020; Gill et al., 2022). However, relatively few studies have incorporated variation in the spatial arrangement and fecundity of surviving trees at fine spatial scales. Our results suggest that incorporating fine scale estimates of seed availability can improve estimates of variability in postfire conifer regeneration.

Though the models with seed availability derived from seed shadows generally outperformed the models using the distance to the nearest surviving tree, the performance gain from the simple distance model was less than expected. This may be explained in part by species-specific variation in postfire dispersal capability. For example, the presence of serotinous knobcone pine in 15 of the low-elevation plots might have muted the effects of any dispersal model since the parent tree does not need to survive the fire for seeds to disperse. In addition to species-level differences, we were unable to precisely determine the species of the lidar mapped trees, including whether each mapped tree was indeed a conifer. Though our study was largely performed in conifer dominated areas and all but two plots had conifers present, tree misclassification as either conifer or live almost certainly drove a large part of the uncertainty in our results.

As expected, seed availability was associated with increased seedling presence and density. However, we did not observe the highest seedling densities in the places with the greatest estimated seed availability. Instead, the highest seedling densities were observed in plots with estimates of between 50 and 100 seeds per square meter (Supplementary Figure 2). High seed availability was most often observed in areas with a high density of surviving trees. This may be due to competition and shading from surviving trees, which can inhibit seed germination (Kroiss and HilleRisLambers, 2015). This pattern is also reminiscent of the Janzen-Connel effect (Janzen, 1970; Connell, 1971), which suggests that seeds and seedlings face higher predation levels where they are most

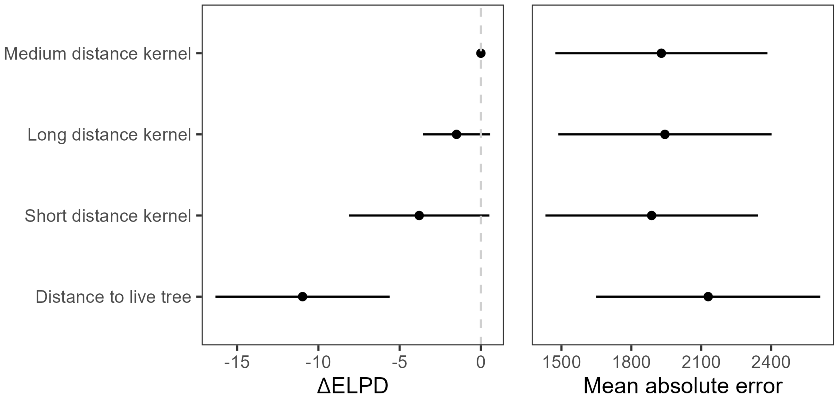

FIGURE 6
$\Delta el\hat{p}d$ and mean absolute error (MAE, ± SE) for all models. $\Delta el\hat{p}d$ is a relative measure against the model with the best $el\hat{p}d$ in the set, so the models with the greatest predictive power have $\Delta el\hat{p}d$ estimates of zero.

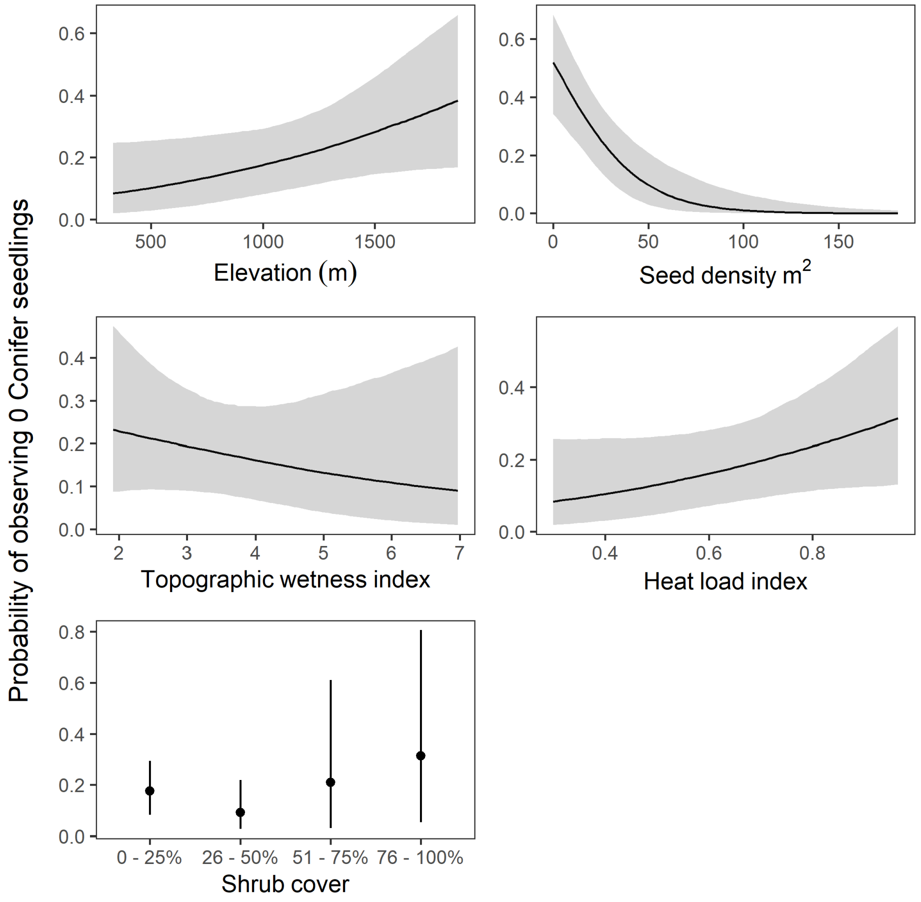

FIGURE 7
Model predictions of probability of observing zero conifer seedlings (± 95% credible intervals) for each predictor in the model with the highest $\widehat{elpd}$. Predictions are made holding all other variables constant. Note the different axes scales.

abundant, that is near the parent tree. These effects have been demonstrated in some forest types (Steinitz et al., 2011; but see Hyatt et al., 2003). While an investigation of the Janzen-Connel effect is beyond the scope of this work, we mention it here as another possible mechanism contributing the uncertainty in our results.

Elevation had the most influence on conifer regeneration of all the topographic variables in the hurdle portions of the model. This is likely due in part to the prefire distribution of conifer trees throughout the park. Conifers are more prevalent with increasing elevation and are typically only dominant above ~1,500 m at WHIS (Smith et al., 2021). The effect of elevation may also be attributed to increased moisture availability and lower temperatures (Dodson and Root, 2013). The lack of a notable effect of elevation on seedling abundance may have been affected by the distribution of species along the elevation gradient, especially due to the presence of serotinous knobcone pine at lower elevations which reproduce in great numbers following fire events (Keeley et al., 1999). However, without reliable species identification for the potential parent trees, we were unable to disentangle the effects of species distribution from other potential mechanisms.

Our model indicated that the probability of seedling establishment was lower in areas with higher heat load index, though the strength of evidence for this effect was relatively low. This is similar to the findings of Boag et al. (2020), who found that greater heat load index resulted in a reduced probability of conifer regeneration, though the strength of the effect varied by species. As with elevation, species distributions may explain some of the uncertainty in our results. There was also little evidence for a consistent effect of topographic wetness index. We expected that conifers would be more likely to regenerate in more mesic areas, so the reason for the uncertainty in our results is unclear. Harvey et al. (2016) did not find a substantial relationship between *Pseudotsuga* regeneration and drought severity, noting that it is relatively drought tolerant. However, the variation in drought tolerant species in our study area suggests that this explanation may be insufficient at WHIS.

We found considerable uncertainty in the relationship between shrub cover and conifer regeneration, though there was some evidence for a facilitative effect for up to 50% shrub cover on seedling establishment but not density. These results are consistent with previous work. Observations from the nearby Sierra Nevada have shown shrub cover to have a complex association with postfire conifer recruitment, with both facilitative and competitive effects (Gray et al., 2005; Collins and Roller, 2013). Within the Klamath bioregion, the prevalence of shade tolerant conifers (Donato et al., 2009) and the facilitative effects of shrubs on local microsite

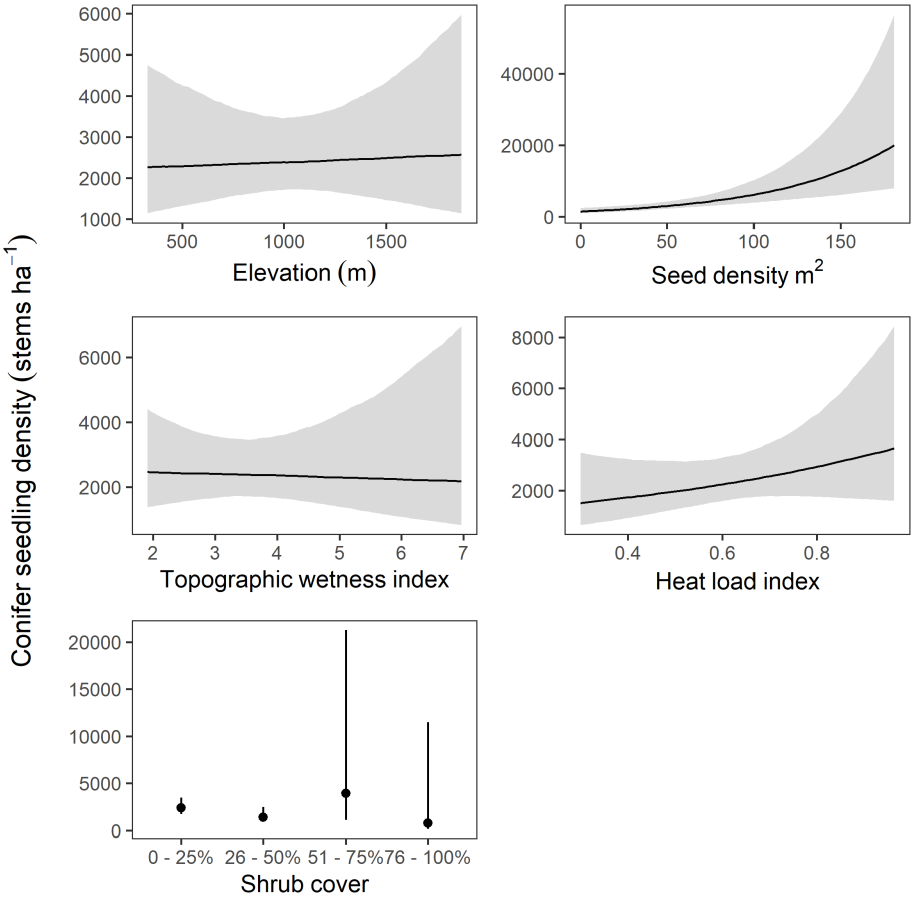

FIGURE 8
Model predictions of conifer seedling density in stems per hectare (± 95% credible intervals) for each predictor in the model with the highest $\widehat{elpd}$. Predictions are made holding all other variables constant. Note the different axes scales.

conditions (Irvine et al., 2009) may enhance postfire recruitment. Shatford et al. (2007) found that while shrubs did seem to influence seedling density, the effect varied by species and competition from shrub cover did not seem to meaningfully affect the presence of conifer regeneration. We suspect the uncertainty in our results was likely influenced at least in part by relatively few observations we had in high (i.e., >50%) shrub cover. Additionally, our study occurred relatively soon after the fire, when the initial pulse of regenerating conifers established at a similar time to the shrubs, giving these conifers a competitive advantage relative to conifers that may establish later (Tepley et al., 2017).

Approaches such as we have presented here can be used to help improve postfire conifer regeneration tools such as poscrptR (Wright et al., 2020), particularly by incorporating fine scale seed dispersal and tree mortality information. Incorporating finer scale (i.e., less than 30 m resolution) mortality and regeneration data into future modeling efforts may be particularly important given the projections of a warmer and dryer climate in dry conifer forest regions, which is linked to more severe and frequent wildfires (Abatzoglou et al., 2017; Williams et al., 2019). Furthering the understanding of fine-scale variation in regeneration potential will help inform management intervention and future modeling efforts.

4.1 Limitations

We were unable to directly parameterize the dispersal kernels we used to create the seed shadows, so we chose to limit our analysis to isotropic kernels, even though anisotropic kernels generally outperform simple isotropic kernels where they have been applied (Savage et al., 2011). Because we selected the parameterizations *a priori*, we were necessarily limited in the possible number of parameterizations that could reasonably be assessed, as well as the number of potential variables that may influence the seed shadows. For example, we elected to ignore the influence of terrain and wind. The effect of wind on seed dispersal is well documented (Greene and Johnson, 1996; Sánchez et al., 2011; van Putten et al., 2012), though the results for the influence of terrain have been more mixed and are likely scale- and species-dependent (Donato et al., 2009; Katul and Poggi, 2012; Peeler and Smithwick, 2020). There is little doubt the rugged, steep terrain in WHIS had some influence on seed dispersal, not the least of which is the effect terrain would have on local wind patterns. We also ignored the effect neighboring trees and other obstacles might have had on seed dispersal, which likely contributed to model error because seeds can disperse further when the parent tree is in or near an open area than when it is surrounded by neighbors (Greene and Johnson, 1996). Our models also attempted to associate established seedlings with seed shadows that were modeled assuming a single dispersal agent (i.e., wind), ignoring any potential additional dispersal agents that may have changed the distribution of seeds, such as the movement of cones or seeds by animals (Rogers et al., 2019).

Additionally, seed availability does not necessarily directly translate to seed establishment and survival. Millerón et al. (2013) found large disparities between seed dispersal kernels and kernels from established saplings, suggesting that dispersal alone is insufficient to capture patterns in recruitment and survival. Although we attempted to include variables that might distinguish between site quality and thus the probability of seedling establishment, we simply could not precisely determine the effects of site quality (i.e., soil moisture or temperature, see Wooten et al., 2022) with our data. For example, the presence of downed logs and shrubs can provide protection and increase soil moisture for regenerating seedlings (Tappeiner and Helms, 1971; Landesmann and Morales, 2018; Marcolin et al., 2019). Furthermore, many conifer seeds are consumed by small mammals and birds before germination (Gashwiler, 1970; Zwolak et al., 2010), which would change the distribution of available seed if the predation pressure was not spatially uniform (Janzen, 1970; Connell, 1971). Beyond predation, the factors influencing seed germination and seedling survival are complex, and include climate, competition, and abiotic factors (Irvine et al., 2009; Tepley et al., 2017; Stewart et al., 2021). We expect that the influence of climatic variables on postfire recruitment will become more apparent in coming years, especially since temperature has been unusually high in the postfire years (data not shown).

We tried to account for variation in fecundity with tree size when calculating estimates of seed availability, and to consider the amount of time available for seeds to disperse by including the number of seasons between the fire and when the plot was sampled. However, there is temporal variation in seed production in most conifer species (Clark et al., 1999b). Masting, the synchronization of periodic seed production between plants (Kelly, 1994), may also have influenced conifer regeneration after the Carr Fire. Masting has been demonstrated in many conifer species, including many of the species included in this study (Wright et al., 2021). Whether or not we sampled following a mast year undoubtedly influenced the total number of seedlings available, and thus the error between real and estimated seed availability. Finally, there was likely substantial model error arising from our inability to identify the species or even survival status of trees using aerial imagery or lidar, which may have obscured the advantages of modeling seed dispersal using individual tree locations.

5 Implications

Understanding the spatial variation in tree survival and seed availability is fundamental to understanding variability in postfire conifer regeneration, and therefore ecosystem recovery. However, simple metrics such as distance to surviving tree may not adequately capture the potential variation in seed dispersal or establishment. Indeed, our analysis demonstrates that models of dispersal at the tree level may also be inadequate to fully describe regeneration if they do not accurately capture variation in fecundity and dispersal (i.e., masting and anisotropy) or in establishment and survival (i.e., variation in microsite and predation). Spatial variation in conifer regeneration will drive forest recovery and structure in the years to come, including determining future fires through their effects on fuel availability (Tepley et al., 2018).

Our analysis suggest that successful postfire conifer regeneration is most likely to occur in areas where seed sources are available within a relatively short distance, at least in the years immediately after fire. These results highlight the importance of isolated surviving trees, which may serve as the only locally available seed source in areas of extensive tree mortality. The spatial arrangement, seed production, and seed dispersal characteristics of these surviving trees control both the rate and the possibility of forest recovery at WHIS. These results also highlight the importance of future disturbances such as drought and wildfire to forest recovery trajectories, since the death of isolated trees and those in small refugia may have an outsize influence on forest structure for years to come.

Data availability statement

The datasets presented in this study can be found on sciencebase, the U.S. Geological Survey data repository. A full citation for the data releases is as follows: Wright, M.C., Smith, S.B., Engber, E., Thorne, K.M., Buffington, K.J., and van Mantgem, P.J., 2023, Data describing site characteristics including conifer regeneration following the 2018 Carr Fire in Whiskeytown National Recreation Area: U.S. Geological Survey data release, https://doi.org/10.5066/P95G11FE.

Author contributions

MW combined the data, performed the Bayesian analysis, and wrote the manuscript. KB performed the tree location and mortality analyses and assisted in the manuscript writing and editing. SS provided the inventory and monitoring data, EE provided the FMH data, and SS, EE, PM, and KT secured the funding for the project, organized the remaining data collection efforts, and assisted in the manuscript writing and editing. All authors contributed to the article and approved the submitted version.

Funding

This work was supported by H.R. 2157 Additional Supplemental Appropriations for Disaster Relief Act 2019 (Public Law 116-20), the National Park Service, and the U.S. Geological Survey Ecosystems Mission Area.

Acknowledgments

We thank the NPS and USGS crews who collected the field data. Thanks to C. Freeman and A. Colley for spatial data and processing, and to Laura Shaskey for logistical support.

Conflict of interest

The authors declare that the research was conducted in the absence of any commercial or financial relationships that could be construed as a potential conflict of interest.

Publisher's note

Author disclaimer

Any use of trade, firm, or product names is for descriptive purposes only and does not imply endorsement by the U.S. Government.

Supplementary material

The Supplementary Material for this article can be found online at: https://www.frontiersin.org/articles/10.3389/fevo.2023.1229123/full#supplementary-material

References

Abatzoglou, J. T., Kolden, C. A., Williams, A. P., Lutz, J. A., and Smith, A. M. (2017). Climatic influences on interannual variability in regional burn severity across western US forests. *Int. J. Wildland Fire* 26, 269–275. doi: 10.1071/WF16165

Barber, C., Graves, S. J., Hall, J. S., Zuidema, P. A., Brandt, J., Bohlman, S. A., et al. (2022). Species-level tree crown maps improve predictions of tree recruit abundance in a tropical landscape. *Ecol. Appl.* 32, e2585. doi: 10.1002/eap.2585

Boag, A. E., Ducey, M. J., Palace, M. W., and Hartter, J. (2020). Topography and fire legacies drive variable post-fire juvenile conifer regeneration in eastern Oregon, USA. *For. Ecol. Manage.* 474, 118312. doi: 10.1016/j.foreco.2020.118312

F. T. Bonner and R. P. Karrfalt (Eds.) (2008). *The woody plant seed manual* (U.S. Department of Agriculture, Forest Service, Washington, DC).

Breiman, L. (2001). Random forests. *Mach. Learn.* 45, 5–32. doi: 10.1023/A:1010933404324

Bullock, J. M., Mallada González, L., Tamme, R., Götzenberger, L., White, S. M., Pärtel, M., et al. (2017). A synthesis of empirical plant dispersal kernels. *J. Ecol.* 105, 6–19. doi: 10.1111/1365-2745.12666

Bürkner, P.-C. (2017). brms: An R package for Bayesian multilevel models using Stan. *J. Stat. Software* 80, 1–28. doi: 10.18637/jss.v080.i01

Burns, R. M., and Honkala, B. H. (1990). *Silvics of North America. Volume 1. Conifers*. United States Department of Agriculture (USDA), Forest Service. Available at: https://www.fs.usda.gov/research/treesearch/1547.

Chambers, M. E., Fornwalt, P. J., Malone, S. L., and Battaglia, M. A. (2016). Patterns of conifer regeneration following high severity wildfire in ponderosa pine–dominated forests of the Colorado Front Range. *For. Ecol. Manage.* 378, 57–67. doi: 10.1016/j.foreco.2016.07.001

Clark, J., Beckage, B., Camill, P., Cleveland, B., HilleRisLambers, J., Lichter, J., et al. (1999b). Interpreting recruitment limitation in forests. *Am. J. Bot.* 86, 1–16. doi: 10.2307/2656950

Clark, J. S., Silman, M., Kern, R., Macklin, E., and HilleRisLambers, J. (1999a). Seed dispersal near and far: Patterns across temperate and tropical forests. *Ecology* 80, 1475–1494. doi: 10.1890/0012-9658(1999)080[1475:SDNAFP]2.0.CO;2

Collins, B. M., and Roller, G. B. (2013). Early forest dynamics in stand-replacing fire patches in the northern Sierra Nevada, California, USA. *Landscape Ecol.* 28, 1801–1813. doi: 10.1007/s10980-013-9923-8

Collins, B. M., Stevens, J. T., Miller, J. D., Stephens, S. L., Brown, P. M., and North, M. P. (2017). Alternative characterization of forest fire regimes: Incorporating spatial patterns. *Landscape Ecol.* 32, 1543–1552. doi: 10.1007/s10980-017-0528-5

Connell, J. H. (1971). On the role of natural enemies in preventing competitive exclusion in some marine animals and in rain forest trees. *Dynamics populations* 298, 298–310.

Coop, J. D., DeLory, T. J., Downing, W. M., Haire, S. L., Krawchuk, M. A., Miller, C., et al. (2019). Contributions of fire refugia to resilient ponderosa pine and dry mixed-conifer forest landscapes. *Ecosphere* 10, 1–24. doi: 10.1002/ecs2.2809

Cousens, R. D., Hughes, B. D., and Mesgaran, M. B. (2018). Why we do not expect dispersal probability density functions based on a single mechanism to fit real seed shadows. *J. Ecol.* 106, 903–906. doi: 10.1111/1365-2745.12891

Crotteau, J. S., Varner, J. M. III, and Ritchie, M. W. (2013). Post-fire regeneration across a fire severity gradient in the southern Cascades. *For. Ecol. Manage.* 287, 103–112. doi: 10.1016/j.foreco.2012.09.022

Dalponte, M., and Coomes, D. A. (2016). Tree-centric mapping of forest carbon density from airborne laser scanning and hyperspectral data. *Methods Ecol. Evol.* 7, 1236–1245. doi: 10.1111/2041-210X.12575

Dodson, E. K., and Root, H. T. (2013). Conifer regeneration following stand-replacing wildfire varies along an elevation gradient in a ponderosa pine forest, Oregon, USA. *For. Ecol. Manage.* 302, 163–170. doi: 10.1016/j.foreco.2013.03.050

Donato, D. C., Fontaine, J. B., Campbell, J. L., Robinson, W. D., Kauffman, J. B., and Law, B. E. (2009). Conifer regeneration in stand-replacement portions of a large mixed-severity wildfire in the Klamath–Siskiyou Mountains. *Can. J. For. Res.* 39, 823–838. doi: 10.1139/X09-016

Downing, W. M., Krawchuk, M. A., Meigs, G. W., Haire, S. L., Coop, J. D., Walker, R. B., et al. (2019). Influence of fire refugia spatial pattern on post-fire forest recovery in Oregon's Blue Mountains. *Landscape Ecol.* 34, 771–792. doi: 10.1007/s10980-019-00802-1

Evans, J. S. (2021) *spatialEco*. Available at: https://github.com/jeffreyevans/spatialEco.

Fox, L. I., Stuart, J. D., and Steinberg, S. J. (2006). *Using high resolution satellite imagery and feature extraction software for vegetation mapping at the Whiskeytown National Recreation Area, Redding, California*.

Fry, D. L., and Stephens, S. L. (2006). Influence of humans and climate on the fire history of a ponderosa pine-mixed conifer forest in the southeastern Klamath Mountains, California. *For. Ecol. Manage.* 223, 428–438. doi: 10.1016/j.foreco.2005.12.021

Gashwiler, J. S. (1970). Further study of conifer seed survival in a western Oregon clearcut. *Ecology* 51, 849–854. doi: 10.2307/1933977

Gelman, A. (2008). Scaling regression inputs by dividing by two standard deviations. *Stat Med.* 27, 2865–2873. doi: 10.1002/sim.3107

Gill, N. S., Turner, M. G., Brown, C. D., Glassman, S. I., Haire, S. L., Hansen, W. D., et al (2022). Limitations to propagule dispersal will constrain postfire recovery of plants and fungi in western coniferous forests. *BioScience.* 7, 347–364 doi: 10.1093/biosci/biab139

Goss, M., Swain, D. L., Abatzoglou, J. T., Sarhadi, A., Kolden, C. A., Williams, A. P., et al. (2020). Climate change is increasing the likelihood of extreme autumn wildfire conditions across California. *Environ. Res. Lett.* 15, 094016. doi: 10.1088/1748-9326/ab83a7

Gray, A. N., Zald, H. S., Kern, R. A., and North, M. (2005). Stand conditions associated with tree regeneration in Sierran mixed-conifer forests. *For. Sci.* 51, 198–210. doi: 10.1093/forestscience/51.3.198

Greene, D. F., Canham, C. D., Coates, K. D., and Lepage, P. T. (2004). An evaluation of alternative dispersal functions for trees. *J. Ecol.* 92, 758–766. doi: 10.1111/j.0022-0477.2004.00921.x

Greene, D., and Johnson, E. (1989). A model of wind dispersal of winged or plumed seeds. *Ecology* 70, 339–347. doi: 10.2307/1937538

Greene, D., and Johnson, E. (1994). Estimating the mean annual seed production of trees. *Ecology* 75, 642–647. doi: 10.2307/1941722

Greene, D., and Johnson, E. (1996). Wind dispersal of seeds from a forest into a clearing. *Ecology* 77, 595–609. doi: 10.2307/2265633

Harvey, B. J., Donato, D. C., and Turner, M. G. (2016). High and dry: Post-fire tree seedling establishment in subalpine forests decreases with post-fire drought and large stand-replacing burn patches. *Global Ecol. Biogeography* 25, 655–669. doi: 10.1111/geb.12443

Hijmans, R. J. (2022) *terra: Spatial Data Analysis*. Available at: https://CRAN.R-project.org/package=terra.

Hyatt, L. A., Rosenberg, M. S., Howard, T. G., Bole, G., Fang, W., Anastasia, J., et al. (2003). The distance dependence prediction of the Janzen-Connell hypothesis: a meta-analysis. *Oikos* 103, 590–602. doi: 10.1034/j.1600-0706.2003.12235.x

Irvine, D. R., Hibbs, D. E., and Shatford, J. P. (2009). The relative importance of biotic and abiotic controls on young conifer growth after fire in the Klamath-Siskiyou region. *Northwest Sci.* 83, 334–347. doi: 10.3955/046.083.0405

Janzen, D. H. (1970). Herbivores and the number of tree species in tropical forests. *Am. Nat.* 104, 501–528. doi: 10.1086/282687

Jeronimo, S. M., Kane, V. R., Churchill, D. J., McGaughey, R. J., and Franklin, J. F. (2018). Applying LiDAR individual tree detection to management of structurally diverse forest landscapes. *J. Forestry* 116, 336–346. doi: 10.1093/jofore/fvy023

Jucker, T., Caspersen, J., Chave, J., Antin, C., Barbier, N., Bongers, F., et al. (2017). Allometric equations for integrating remote sensing imagery into forest monitoring programmes. *Global Change Biol.* 23, 177–190. doi: 10.1111/gcb.13388

Katul, G., and Poggi, D. (2012). The effects of gentle topographic variation on dispersal kernels of inertial particles. *Geophysical Res. Lett.* 39. doi: 10.1029/2011GL050811

Katul, G., Porporato, A., Nathan, R., Siqueira, M., Soons, M., Poggi, D., et al. (2005). Mechanistic analytical models for long-distance seed dispersal by wind. *Am. Nat.* 166, 368–381. doi: 10.1086/432589

Keeley, J. E., Ne'eman, G., and Fotheringham, C. (1999). Immaturity risk in a fire-dependent pine. *J. Mediterr. Ecol.* 1, 41–48.

Kelly, D. (1994). The evolutionary ecology of mast seeding. *Trends Ecol. Evol.* 9, 465–470. doi: 10.1016/0169-5347(94)90310-7

Knapp, E. E., Weatherspoon, C. P., and Skinner, C. N. (2012). Shrub seed banks in mixed conifer forests of northern California and the role of fire in regulating abundance. *Fire Ecol.* 8, 32–48. doi: 10.4996/fireecology.0801032

Korb, J. E., Fornwalt, P. J., and Stevens-Rumann, C. S. (2019). What drives ponderosa pine regeneration following wildfire in the western United States? *For. Ecol. Manage.* 454, 117663. doi: 10.1016/j.foreco.2019.117663

Krannitz, P. G., and Duralia, T. E. (2004). Cone and seed production in *Pinus ponderosa*: a review. *Western North Am. Nat.* 64, 208–218.

Kroiss, S. J., and HilleRisLambers, J. (2015). Recruitment limitation of long-lived conifers: Implications for climate change responses. *Ecology* 96, 1286–1297. doi: 10.1890/14-0595.1

Landesmann, J. B., and Morales, J. M. (2018). The importance of fire refugia in the recolonization of a fire-sensitive conifer in northern Patagonia. *Plant Ecol.* 219, 455–466. doi: 10.1007/s11258-018-0808-4

Leonzo, C. M., and Keyes, C. R. (2010). Fire-excluded relict forests in the southeastern Klamath Mountains, California, USA. *Fire Ecol.* 6, 62–76. doi: 10.4996/fireecology.0603062

Liaw, A., and Wiener, M. (2002). Classification and regression by randomForest. *R News* 2, 18–22.

Makowski, D., Ben-Shachar, M. S., and Lüdecke, D. (2019). bayestestR: Describing effects and their uncertainty, existence and significance within the Bayesian framework. *J. Open Source Software* 4, 1541. doi: 10.21105/joss.01541

Maltamo, M., Eerikäinen, K., Pitkänen, J., Hyyppä, J., and Vehmas, M. (2004). Estimation of timber volume and stem density based on scanning laser altimetry and expected tree size distribution functions. *Remote Sens. Environ.* 90, 319–330. doi: 10.1016/j.rse.2004.01.006

Marcolin, E., Marzano, R., Vitali, A., Garbarino, M. , and Lingua, E. (2019). Post-fire management impact on natural forest regeneration through altered microsite conditions. *Forests* 10 1014. doi: 10.3390/f10111014

Marrs, J., and Ni-Meister, W. (2019). Machine learning techniques for tree species classification using co-registered LiDAR and hyperspectral data. *Remote Sens.* 11, 819. doi: 10.3390/rs11070819

McCord, M., Reilly, M. J., Butz, R. J., and Jules, E. S. (2020). Early seral pathways of vegetation change following repeated short-interval, high-severity wildfire in a low-elevation, mixed conifer–hardwood forest landscape of the Klamath Mountains, California. *Can. J. For. Res.* 50, 13–23. doi: 10.1139/cjfr-2019-0161

McCune, B., and Keon, D. (2002). Equations for potential annual direct incident radiation and heat load. *J. Vegetation Sci.* 13, 603–606. doi: 10.1111/j.1654-1103.2002.tb02087.x

Millerón, M., López de Heredia, U., Lorenzo, Z., Alonso, J., Dounavi, A., Gil, L., et al. (2013). Assessment of spatial discordance of primary and effective seed dispersal of European beech (*Fagus sylvatica L.*) by ecological and genetic methods. *Mol. Ecol.* 22, 1531–1545. doi: 10.1111/mec.12200

MTBS (2018) *MTBS Data Access: Fire Level Geospatial Data. MTBS Project* (USDA Forest Service/U.S. Geological Survey) (Accessed 2022-07-18).

MTBS (2020). *Monitoring trends in burn severity assessment of event ID - ca4069812251020080622* (U.S. Geological Survey and USDA Forest Service). doi: 10.5066/P9IED7RZ

Murphy, M. A., Evans, J. S., and Storfer, A. (2010). Quantifying *Bufo boreas* connectivity in Yellowstone National Park with landscape genetics. *Ecology* 91, 252–261. doi: 10.1890/08-0879.1

Nathan, R., Schurr, F. M., Spiegel, O., Steinitz, O., Trakhtenbrot, A., and Tsoar, A. (2008). Mechanisms of long-distance seed dispersal. *Trends Ecol. Evol.* 23, 638–647. doi: 10.1016/j.tree.2008.08.003

North, M. P., Kane, J. T., Kane, V. R., Asner, G. P., Berigan, W., Churchill, D. J., et al. (2017). Cover of tall trees best predicts California spotted owl habitat. *For. Ecol. Manage.* 405, 166–178. doi: 10.1016/j.foreco.2017.09.019

Odion, D., Sarr, D., Mohren, S., and Smith, S. (2011). *Monitoring vegetation composition, structure and function in the parks of the Klamath Network Parks* (Fort Collins, Colorado: National Park Service).

Parker, R. C., and Evans, D. L. (2004). An application of LiDAR in a double-sample forest inventory. *Western J. Appl. Forestry* 19, 95–101. doi: 10.1093/wjaf/19.2.95

Peeler, J. L., and Smithwick, E. A. (2020). Seed source pattern and terrain have scale-dependent effects on post-fire tree recovery. *Landscape Ecol.* 35, 1945–1959. doi: 10.1007/s10980-020-01071-z

R Core Team (2021). *R: A Language and Environment for Statistical Computing* (Vienna, Austria: R Foundation for Statistical Computing). Available at: https://www.R-project.org/.

Reilly, M. J., Monleon, V. J., Jules, E. S., and Butz, R. J. (2019). Range-wide population structure and dynamics of a serotinous conifer, knobcone pine (*Pinus attenuata L.*), under an anthropogenically-altered disturbance regime. *For. Ecol. Manage.* 441, 182–191. doi: 10.1016/j.foreco.2019.03.017

Rogers, H. S., Beckman, N. G., Hartig, F., Johnson, J. S., Pufal, G., Shea, K., et al. (2019). The total dispersal kernel: A review and future directions. *AoB Plants* 11, plz042. doi: 10.1093/aobpla/plz042

Roussel, J., and Auty, D. (2021) *Airborne LiDAR data manipulation and visualization for forestry applications*. Available at: https://cran.r-project.org/package=lidR.

Roussel, J.-R., Auty, D., Coops, N. C., Tompalski, P., Goodbody, T. R., Meador, A. S., et al. (2020). lidR: An R package for analysis of Airborne Laser Scanning (ALS) data. *Remote Sens. Environ.* 251, 112061. doi: 10.1016/j.rse.2020.112061

Sánchez, J. M. C., Greene, D. F., and Quesada, M. (2011). A field test of inverse modeling of seed dispersal. *Am. J. Bot.* 98, 698–703. doi: 10.3732/ajb.1000152

Savage, D., Barbetti, M. J., MacLeod, W. J., Salam, M. U., and Renton, M. (2011). Can mechanistically parameterised, anisotropic dispersal kernels provide a reliable estimate of wind-assisted dispersal? *Ecol. Model.* 222, 1673–1682. doi: 10.1016/j.ecolmodel.2011.03.003

Shatford, J., Hibbs, D., and Puettmann, K. (2007). Conifer regeneration after forest fire in the Klamath-Siskiyous: how much, how soon? *J. Forestry* 105, 139–146. doi: 10.1093/jof/105.3.139

Shive, K. L., Preisler, H. K., Welch, K. R., Safford, H. D., Butz, R. J., O'Hara, K. L., et al. (2018). From the stand scale to the landscape scale: Predicting the spatial patterns of forest regeneration after disturbance. *Ecol. Appl.* 28, 1626–1639. doi: 10.1002/eap.1756

Sivula, T., Magnusson, M., and Vehtari, A. (2020). Uncertainty in Bayesian leave-one-out cross-validation based model comparison. *arXiv preprint arXiv:2008.10296.* 1–88. doi: 10.48550/arXiv.2008.10296

Skinner, C. N., Taylor, A. H., and Agee, J. K. (2006). "Klamath mountains bioregion," in *Fire in California's ecosystems*. Eds. N. G. Sugihara, J. W. v. Wagtendonk, J. Fites-Kaufmann, K. E. Shaffer and A. E. Thode (Berkeley: University of California Press), 170–194.

Smith, S. B., van Mantgem, P. J., and Odion, D. (2021). *Vegetation community monitoring: Species composition and biophysical gradients in Klamath Network parks* (National Park Service, Fort Collins, Colorado).

Steel, E. A., Kennedy, M. C., Cunningham, P. G., and Stanovick, J. S. (2013). Applied statistics in ecology: Common pitfalls and simple solutions. *Ecosphere* 4, 1–13. doi: 10.1890/ES13-00160.1

Steinitz, O., Troupin, D., Vendramin, G., and Nathan, R. (2011). Genetic evidence for a Janzen–Connell recruitment pattern in reproductive offspring of *Pinus halepensis* trees. *Mol. Ecol.* 20, 4152–4164. doi: 10.1111/j.1365-294X.2011.05203.x

Stevens, J. T., Collins, B. M., Miller, J. D., North, M. P., and Stephens, S. L. (2017). Changing spatial patterns of stand-replacing fire in California conifer forests. *For. Ecol. Manage.* 406, 28–36. doi: 10.1016/j.foreco.2017.08.051

Stevens-Rumann, C. S., and Morgan, P. (2019). Tree regeneration following wildfires in the western US: a review. *Fire Ecol.* 15, 1–17. doi: 10.1186/s42408-019-0032-1

Stewart, J. A., van Mantgem, P. J., Young, D. J., Shive, K. L., Preisler, H. K., Das, A. J., et al. (2021). Effects of postfire climate and seed availability on postfire conifer regeneration. *Ecol. Appl.* 31, e02280. doi: 10.1002/eap.2280

Tappeiner, J. C., and Helms, J. A. (1971). Natural regeneration of Douglas fir and white fir on exposed sites in the Sierra Nevada of California. *Am. Midland Nat.* 86, 358–370. doi: 10.2307/2423629

Tepley, A. J., Thomann, E., Veblen, T. T., Perry, G. L., Holz, A., Paritsis, J., et al. (2018). Influences of fire–vegetation feedbacks and post-fire recovery rates on forest landscape vulnerability to altered fire regimes. *J. Ecol.* 106, 1925–1940. doi: 10.1111/1365-2745.12950

Tepley, A. J., Thompson, J. R., Epstein, H. E., and Anderson-Teixeira, K. J. (2017). Vulnerability to forest loss through altered postfire recovery dynamics in a warming climate in the Klamath Mountains. *Global Change Biol.* 23, 4117–4132. doi: 10.1111/gcb.13704

Thorne, K. M., Freeman, C. M., and Rankin, L. L. (2023). UAS Imagery at whiskeytown national recreation area in 2018 and 2019 following the carr fire. U.S. geological survey data release. *ScienceBase*. https://doi.org/10.5066/P9GS9V1J

Turner, M. G., Baker, W. L., Peterson, C. J., and Peet, R. K. (1998). Factors influencing succession: Lessons from large, infrequent natural disturbances. *Ecosystems* 1, 511–523. doi: 10.1007/s100219900047

USDI National Park Service (2003). *Fire monitoring handbook* (Boise (ID: Fire Management Program Center, National Interagency Fire Center).

U.S. Geological Survey (2021) *Lidar Point Cloud CA_CarrHirzDeltaFires_2019* (Accessed 2022-05-13).

van Putten, B., Visser, M. D., Muller-Landau, H. C., and Jansen, P. A. (2012). Distorted-distance models for directional dispersal: A general framework with application to a wind-dispersed tree. *Methods Ecol. Evol.* 3, 642–652. doi: 10.1111/j.2041-210X.2012.00208.x

Vehtari, A., Gelman, A., and Gabry, J. (2017). Practical Bayesian model evaluation using leave-one-out cross-validation and WAIC. *Stat Computing* 27, 1413–1432. doi: 10.1007/s11222-016-9696-4

Wehner, M. F., Arnold, J. R., Knutson, T., Kunkel, K. E., and LeGrande, A. N. (2017). “Droughts, floods, and wildfires,” In *Climate Science Special Report: Fourth National Climate Assessment, Volume I* [D. J. Wuebbles, D. W. Fahey, K. A. Hibbard, D. J. Dokken, B. C. Stewart and T. K. Maycock (Eds.)]. U.S. Global Change Research Program, Washington, DC, USA, pp. 231–256.doi: 10.7930/J0CJ8BNN

Welch, K. R., Safford, H. D., and Young, T. P. (2016). Predicting conifer establishment post wildfire in mixed conifer forests of the North American Mediterranean-climate zone. *Ecosphere* 7, e01609. doi: 10.1002/ecs2.1609

Williams, A. P., Abatzoglou, J. T., Gershunov, A., Guzman-Morales, J., Bishop, D. A., Balch, J. K., et al. (2019). Observed impacts of anthropogenic climate change on wildfire in California. *Earth’s Future* 7, 892–910. doi: 10.1029/2019EF001210

Williams, J., Safford, H., Enstice, N., Steel, Z., and Paulson, A. (2023). High-severity burned area and proportion exceed historic conditions in Sierra Nevada, California, and adjacent ranges. *Ecosphere* 14, e4397. doi: 10.1002/ecs2.4397

Wooten, J. T., Stevens-Rumann, C. S., Schapira, Z. H., and Rocca, M. E. (2022). Microenvironment characteristics and early regeneration after the 2018 Spring Creek Wildfire and post-fire logging in Colorado, USA. *Fire Ecol.* 18, 10. doi: 10.1186/s42408-022-00133-8

Wright, M. C., Mantgem, P., Stephenson, N. L., Das, A. J., and Keeley, J. E. (2021). Seed production patterns of surviving Sierra Nevada conifers show minimal change following drought. *For. Ecol. Manage.* 480, 118598. doi: 10.1016/j.foreco.2020.118598

Wright, M. C., Stewart, J. A. E., van Mantgem, P. J., Young, D. J. N., Shive, K. L., Preisler, H. K., et al. (2020). *poscrptR. R package and U.S. Geological Survey software release*. U.S. Geological Survey software release, https://code.usgs.gov/

Wright, M. C., Smith, S. B., Engber, E., Thorne, K. M., Buffington, K. J., van Mantgem, P. J., et al (2023) *Data describing site characteristics including conifer regeneration following the 2018 Carr Fire in Whiskeytown National Recreation Area: U.S. Geological Survey data release*. doi: 10.5066/P95G11FE

Wu, Q. (2021) *whitebox: ‘WhiteboxTools’ R Frontend. R package version 2.0.0. https://CRAN.R-project.org/package=whitebox*. doi: 10.5066/P95G11FE.

Zwolak, R., Pearson, D. E., Ortega, Y. K., and Crone, E. E. (2010). Fire and mice: Seed predation moderates fire’s influence on conifer recruitment. *Ecology* 91, 1124–1131. doi: 10.1890/09-0332.1

frontiers | Frontiers in Ecology and Evolution

TYPE Original Research
PUBLISHED 23 October 2023
DOI 10.3389/fevo.2023.1232704

OPEN ACCESS

EDITED BY
Clare Aslan,
Northern Arizona University, United States

REVIEWED BY
Ryan Askren,
University of Arkansas at Monticello,
United States
Dominik Marchowski,
Polish Academy of Sciences, Poland

*CORRESPONDENCE
Cory T. Overton
coverton@usgs.gov

RECEIVED 01 June 2023
ACCEPTED 02 October 2023
PUBLISHED 23 October 2023

CITATION
Overton CT and Casazza ML (2023) Movement behavior, habitat selection, and functional responses to habitat availability among four species of wintering waterfowl in California. *Front. Ecol. Evol.* 11:1232704. doi: 10.3389/fevo.2023.1232704

Movement behavior, habitat selection, and functional responses to habitat availability among four species of wintering waterfowl in California

Cory T. Overton* and Michael L. Casazza

U.S. Geological Survey, Western Ecological Research Center, Dixon Field Station, Dixon, CA, United States

Introduction: Habitat selection analyses provide a window into the perceived value of habitats by animals and how those perceptions compare with other animals, change across time, or change in relation to availability (termed functional responses). Habitat selection analysis and functional responses can be used to develop strategies to avoid habitat limitations, guide habitat management, and set attainable conservation goals. GPS relocations of marked animals are the principal data used in habitat selection analysis. The accuracy and frequency with which tracking devices collect data are increasing and may result in non-stationary point processes that result from latent behaviors previously unidentifiable in sparse data.

Methods: We investigated non-stationary step length distributions and integrated a two-mixture model of animal movement with step selection analysis to identify patterns of activity among four species of co-occurring waterfowl that winter in the Central Valley of California, United States. We evaluated relative strength of selection and compared functional responses across a range of habitat types for two goose and two dabbling duck species.

Results: Goose species (greater white-fronted goose [*Anser albifrons*] and lesser snow goose [*Anser caerulescens caerulescens*]) used habitats similarly and displayed similar functional responses with habitat availability. Northern pintail (*Anas acuta*) displayed functional responses for habitats that provided primary food resources and sanctuary from hunting that were more similar to geese than to mallard (*Anas platyrhynchos*), which expressed a more generalist pattern of habitat selection.

Discussion: Our results define conditions where food resource competition between geese and ducks could operate, which indicate that some species may be more impacted than others. Specifically, early season food limitation may manifest more strongly in snow geese due to longer movements and stronger functional response with rice availability. Late season limitations may manifest in northern pintail, which remain reliant on rice later but may not be reflected in habitat selection patterns due to a consistent functional response with rice availability. We show that multiple movement processes present in high-resolution data can be used to obtain a variety of information about animal behavior and that subsequent step selection analyses may demonstrate unique functional responses relative to alternate habitat selection methods that warrant additional investigation.

KEYWORDS

telemetry, GPS, step selection, *Anas acuta*, *Anas platyrhynchos*, *Anser albifrons*, *Anser caerulescens*

Introduction

Habitat selection analysis is a generic term for many approaches that relate use of a habitat/resource and the availability of that habitat (Neu et al., 1974; Johnson, 1980; Manly et al., 2002; Johnson et al., 2008; Thurfjell et al., 2014). Patterns of selection and avoidance of habitats provide information on individual resource requirements (Osborn et al., 2017) and comparative indicators of habitat value (Avgar et al., 2016), inform population abundance estimates (Boyce et al., 2016), and more broadly reflect levels of fitness across individuals (Northrup et al., 2022). Habitat selection patterns may change due to changes in relative use among multiple habitat types or changes in availability of habitat types. Changes in habitat use may result from internal drivers such as changing life history needs (Groff et al., 2017) or dietary requirements (Mitchell et al., 2020). Changes in habitat availability involves external factors such as resource phenology (Resano-Mayor et al., 2019), environmental disturbance (Brussee et al., 2022), or anthropogenic change (Knopff et al., 2014). Comparisons of resource selection patterns across individuals, species, or regions can identify overlap and potential avenues for competition (Rosenzweig, 1981) and identify density-dependent processes (Morris, 1989). Some methods of quantifying habitat selection allow for the identification of individual patterns of selection (Leclerc et al., 2016; Muff et al., 2020) or inclusion of random effects (Gillies et al., 2006; Duchesne et al., 2010) to quantify individual patterns of selection and assess functional responses of use or selection relative to habitat availability (Mysterud and Ims, 1998; Holbrook et al., 2019).

Used habitat measures that comprise part of habitat selection analyses can be obtained from surveys and occupancy information but is more commonly obtained with repeated observations of the same individual(s) through time and typically using tracking devices (Manly et al., 2002). These tracking devices provide increasingly complete and accurate spatial information about animal locations (Kays et al., 2015). Increasing data frequency and accuracy are also likely to manifest animal movement patterns or activities that were not apparent with coarser data (Nathan et al., 2022). This can allow the identification of multiple behavior states or constituent activities and context-dependent analysis of resource use (Patterson et al., 2009; Bergen et al., 2022; Overton et al., 2022). It is often crucial to identify constituent behaviors within individual tracks since non-stationary processes (a time series that has statistical properties, metrics, or moments [such as mean or variance] that vary in time) resulting in imbalanced movement or habitat selection can bias selection analyses when quantifying use (Osborne et al., 2007) or identifying available habitats (Aarts et al., 2013; Pay et al., 2022). Methods to reduce the impact of non-stationary processes include data thinning (Schabenberger and Gotway, 2005), path segmentation (Patterson et al., 2009; Nathan et al., 2022), and autocorrelation weighting (Alston et al., 2023).

Across the globe, bird species often co-occur and concentrate in regions with favorable seasonal climatic conditions and where food or other resources occur predictably, and their concentrations are high. These locations, such as the Baltic Sea, may attract millions of birds during the winter, often substantial proportions of global or flyway populations, into regions where anthropogenic activities may both positively or negatively affect habitat quality, resource values, and ultimately the carrying capacity of the landscape (Skov et al., 2011; Marchowski and Leitner, 2019). Where bird concentrations are exceptionally high, such as California's Central Valley and Poland's Odra Estuary, understanding space use and resource selection patterns are a principal component of effective land management, setting conservation targets and developing habitat restoration and enhancement activities (Marchowski et al., 2015; Marchowski and Leitner, 2019; CVJV, 2020). Increasingly abundant goose populations (~2 million, Olson, 2022) in the Central Valley that are overpopulation targets, co-occur with 4.76 to 6.27 million dabbling ducks (Fleming et al., 2019) that are largely below conservation targets (CVJV, 2020). In this region, dabbling ducks and geese utilize similar food resources, occupy the region during the same periods, and many times restrict use to limited, often publicly owned, lands where they are not subject to hunting (sanctuary) and can roost during daylight hours without disturbance. Owing to this apparent niche overlap, habitat selection patterns to identify resource use and needs in this region are necessary for public area habitat management plans.

Furthermore, comparison of selection patterns across species is needed to assess the potential for competition between geese and ducks and to parameterize landscape energetics models and estimate carrying capacity (CVJV, 2020, Miller et al., 2014; Williams et al., 2014; Petrie et al., 2016). Understanding functional responses in habitat selection patterns relative to habitat availability can guide conservation objectives and landscape planning in a region where drought is increasingly common (Diffenbaugh et al., 2015) and affects agricultural and water management practices that determine food accessibility and how the landscape provisions resources for wildlife (Petrie et al., 2016; Pathak et al., 2018).

Here, we present analyses of movement activity and resource selection for four waterfowl species that winter in the Central Valley. These include two goose species, the lesser snow goose (LSGO, *Anser caerulescens caerulescens*) and greater white-fronted goose (GWFG, *Anser albifrons*), which was represented by two sympatric subspecies, Pacific greater white-fronted goose (*A. a. frontalis*) and Tule goose (*A. a. elegans*). We also tracked two species of dabbling duck including the migratory northern pintail (NOPI, *Anas acuta*) and mallard (MALL, *Anas platyrhynchos*), which include individuals that both breed locally and migrate. Snow geese are the most abundant goose in the region, and northern pintails are the most abundant duck (Olson, 2022). Agriculture is the principal land use with rice providing a major food resource for waterfowl (Miller et al., 2010; CVJV, 2020). Corn is more limited in availability but present and may be locally abundant. Rainfall is the principal form of precipitation and occurs mostly from November to March. Following winter rains and coincident with increasing temperatures beginning in January, both goose species may switch diet from principally seeds to emerging grass (Ely and Raveling, 2011). Late in winter, ducks will also switch from principally seeds in their diet to also include aquatic invertebrates (Euliss and Harris, 1987; Miller, 1987). Persistent drought has affected the region in recent years and resulted in fallowing of agricultural lands and reduction in potential food supplies. These variable conditions allowed us to quantify resource selection patterns and compare functional responses across a variety of habitat types and among species with different ecological traits.

Materials and methods

Waterfowl were captured and fit with GPS logging transmitters using multiple methods between 2015 and 2022 at locations in California, Oregon, and within the arctic (McDuie et al., 2019; Casazza et al., 2021). Mallards were captured in the fall via rocket nets, box nets, or using dip nets from airboats while night lighting. Mallards were also captured during spring using baited swim-in traps and dip nets while incubating. Most pintails were captured via rocket nets in the fall. Some pintails were captured in the spring using rocket nets or swim-in traps. Greater white-fronted geese and lesser snow geese were captured using rocket nets in the fall. Some lesser snow geese were also caught in arctic molting regions using walk-in corral traps. Snow goose captures in the arctic were associated with breeding colonies on Wrangel Island, Russia; Banks Island, Northwest Territories, Canada; and colonies at both the Colville and Ikpikpuk River deltas on the North Slope of Alaska. Ducks were fit with various transmitter packages ranging from 10 to 25 g and affixed with backpack-style harnesses using Teflon$^{\text{TM}}$ ribbon or nylon-neoprene elastic harness material. Geese were fit with 35- to 42-mm-diameter collar transmitters. Transmitters collected GPS data and metadata on transmitter performance (e.g., battery, charging current, and temperature) and most also collected accelerometry data. Data collection frequency varied from every 15 min to once per day corresponding to battery voltage capacity in order to maximize the duration of tracking. All data were transmitted once or twice per day via the cellular (GSM) network when in cellular range and stored on-board when out of range. Both GPS locations and secondary data such as temperature and accelerometry were used to identify mortality events and suspend active deployment periods. Data used for analysis were limited to the Central Valley Joint Venture planning region in central California and occurred primarily in the Sacramento Valley and Sacramento–San Joaquin Delta. Telemetry data were subset to hourly GPS collection intervals with continual tracking for at least 3 days to remove any bias in selection or movement resulting from intermittent GPS collection when battery levels were low (e.g., hourly data only available during daylight hours). Data periods for analysis extended from October through April.

We conducted a step selection analysis (SSA) following the methods of Fieberg et al. (2021). We used 100 replicate movement steps for each observed movement with a circular uniform turning angle distribution. We evaluated random step length patterns using two commonly used parametric distributions, exponential and gamma, using the “amt” package (Signer et al., 2019). However, we anticipated that hourly movement data of waterfowl across long time frames would reflect a non-stationary movement process with at least two states of activity, inactive and moving. Strictly speaking, the “inactive” movement process includes multiple behaviors such as loafing, swimming, or walking that consistently reflect short and slow activity. Similarly, the “moving” state reflects both rapid and long movements indicative of flight, though also some overlapping behaviors such as directional foraging or gleaning that entail rapid, but ground-based, movements. To account for non-stationarity movement processes, we estimated step lengths using a two-mixture log-normal distribution that provides mean and variance parameters as well as mixing probabilities for two distributions of step lengths and the ability to randomly sample from estimated distributions (package “mixtools”, Benaglia et al., 2009). We estimated one two-mixture distribution using 50,000 randomly selected movements from all four species to identify inactive and moving behaviors and allow comparisons of movement activity among four waterfowl species using the same underlying model of movement. For SSA, we first estimated species-specific two-mixture movement distributions, then subset locations to those identified as moving, and finally produced random steps using the mixture component that represented movement. Inactive step distribution median step length was approximately nominal GPS location error (~20 m) and are largely non-informative for habitat selection (all 100 random steps generally were within the same habitat patch/landcover type as the observed use step). Moving step distribution, on the other hand, reflected both within-patch movements (e.g., while actively foraging) and between-patch movements (e.g., large-scale disturbance and flights from sanctuary to foraging patches).

Inactive steps were used to describe temporal patterns of mobility, the inverse of the probability of inactive movements, both within a single day and across the winter season when birds used the Central Valley (October through April). Mobility was also used to quantify the probability of moving when a location occurred within different landcover types. A linear trend through the season in mobility was calculated using logistic regression that included tests for differences in mobility and trends among species. Circadian (midnight to midnight) patterns in mobility for each species were estimated using a high-order (sixth-order) polynomial linear model to account for complex movement dynamics during crepuscular periods with significance of the trends assessed with *t*-statistics. Difference in patterns among species was tested using an ANOVA. Interpretation of differences was assessed graphically by contrasting trends including confidence bands among species. The log-odds of mobility within different habitats were assessed using an ANOVA separately for each species. Statistical tests were performed using Tableau Desktop software v 2022.4 (©Salesforce, San Francisco, CA).

Habitat types used in analyses were delineated for each agricultural year (May 1 through April) using the National Agricultural Statistics Service Crop Data Layer (CDL; Boryan et al., 2011). Crop and other landcover categories were condensed to six classes. Two represented primary food resources used by both ducks and geese in California ("corn" and "rice"). Two habitat types represented secondary food resources used predominantly by a single taxon in California, namely, agricultural fields and crops, including pasture, alfalfa, and idle cropland (hereafter, "PAI") that produce grass in late winter consumed by geese, and various seasonal, permanent, and semi-permanent "wetlands" with food resources (seeds and invertebrates) consumed by ducks. CDL classification of wetlands is complicated by highly heterogenous vegetation and water extents throughout the year, which results in lower accuracy than other crop types (Lark et al., 2021). Therefore, we supplemented wetland classification using the National Wetlands Inventory (USFWS, 2018) and, within the Sacramento–San Joaquin River Delta, using the California Aquatic Resource Inventory (SFEI, 2022). This combined wetland map was produced by converting CDL raster layers to vector (polygon) representation and isolating the resulting wetland polygons. These polygons were merging to the vector layers provided in the National Wetlands Inventory or California Aquatic Resource Inventory to produce a complete wetland only polygon layer. This combined wetland-only layer was then merged with the original CDL polygons to replace wetlands that were unidentified in the CDL layers. Two non-habitat classes were also included ("urban" and "other" including various landcover and crop types). Lastly, we established a seventh habitat class ("protected" lands) to represent land parcels conferring some measure of habitat protection (GAP Status 1 and 2) using the California Protected Area Database (GreenInfo Network, 2022). Within the region used by waterfowl, this class contained state, federal, and non-governmental ownership that typically provide some measure of spatial refuge from hunting pressure but also consisted of a variety of landcover types. The final map containing seven habitat classes was extracted to points. All geospatial processing was performed in R using packages "sf", "rgee", and "rgdal" (Pebesma, 2018; Aybar, 2022; Bivand et al., 2022).

Step selection functions were developed for individual birds during both day and night and for two winter periods (early season, October to January 15, and late season, January 15 to April). We chose to estimate selection for each individual separately during day and night because it is known that foraging activity and, during hunting season, the need for refuge differ between taxa during both day and night (McNeil et al., 1992; McDuie et al., 2021). We divided the wintering period in half to account for seasonal diet shifts, as temperatures warm, to a greater reliance on newly emerged grasses for geese and to invertebrates for ducks (Euliss and Harris, 1987; Miller, 1987; Ely and Raveling, 2011). Although there are other factors that may influence habitat selection such as weather-induced and anthropogenic flooding, intensity of hunting pressure, or other disturbance factors (Mott, 2022), our ability to capture those impacts as habitat features was limited. Therefore, we rely on data collected across a number of years and under varying environmental conditions to provide a generalizable interpretation of resource selection across habitat types reflecting resources that are already recognized among regional conservation efforts (CVJV, 2020). Since our goal was to evaluate the functional relationships between relative importance of a habitat and the availability of that habitat, we ran step selection models for each combination of individual, photoperiod, and seasonal periods that were developed independently for each habitat type. We only considered one habitat at a time because interpretation of beta estimates for categorical covariates in step selection models is the relative selection of the covariate versus all categories not in the model. Also, including multiple covariates would incorporate habitat dependences that obscure the functional response of habitat selection with habitat availability that we were investigating. Development and interpretation of a full habitat selection model would of course benefit from a more complex model structure with consideration of statistical processes such as multicollinearity, perhaps with assessments of temporal autocorrelation of within individual random variation. Such approaches are worthwhile but appear unable to evaluate functional response for the relative strength of selection (RSS) estimates due to dependence among parameter estimates (Fieberg et al., 2021).

We compiled all RSS estimates produced for each habitat type in a conditional logit model run for each combination of individual, photoperiod, and seasonal period and contrasted the average availability of the habitat with those RSS estimates to investigate functional responses. When either use or availability of a habitat class is very low, sampling may fail to produce adequate samples for those classes resulting in highly variable and potentially biased estimates of selection (Northrup et al., 2022). For this reason, we assessed the RSS estimates, which are provided by the beta parameter estimate in each step selection model (Fieberg et al., 2021) and removed four extreme RSS estimates, each of which had large standard errors and high leverage on mean parameter estimates (Figure 1). Functional relationships between mean RSS and average availability of each habitat were investigated qualitatively using previously identified functional response patterns (Holbrook et al., 2019) but patterns were not formally

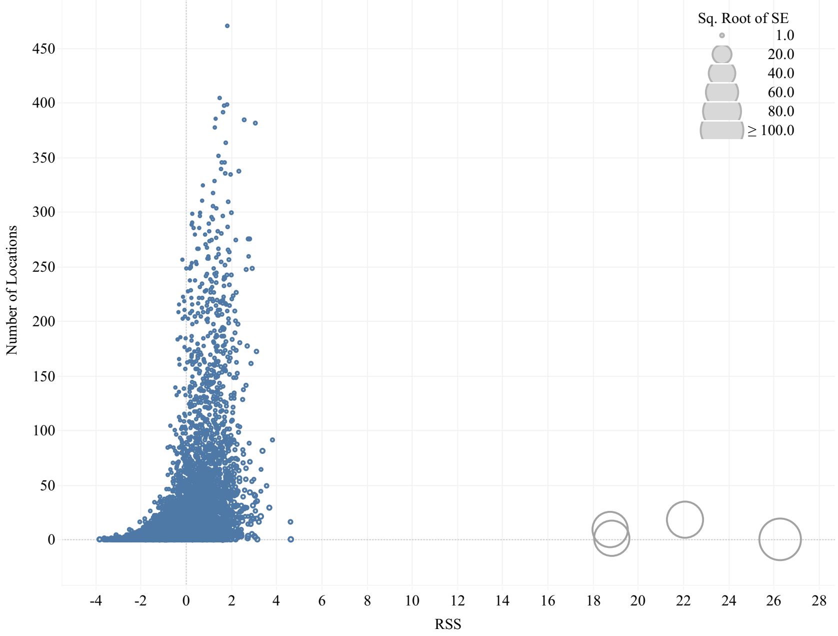

FIGURE 1
Distribution of relative strength of selection (RSS) estimates for seven habitat types by four species of waterfowl during day and night periods in two seasons (early and late winter). Symbol size is scaled to the square root of estimated RSS standard errors. Four RSS estimates with extreme values and high uncertainty were removed from subsequent analyses (gray symbols).

subjected to statistical testing. We interpreted these functional relationship patterns as indications of how habitat value (relative to other habitats) changes as the availability of that habitat changes.

Results

A total of 691 individual waterfowl were tracked within California's Central Valley between April 2015 and January 2023, which provided data across 971 individual bird-years and produced over 3.5 million GPS locations at intervals ranging from once per day to every minute. Our final dataset filtered GPS locations to the wintering period (October through April) and to continuous hourly intervals lasting a minimum of 3 days, resulting in 169,716 locations (Table 1; Overton and Casazza, 2023). Random step lengths estimated using both exponential and gamma distributions failed to capture the clear bi-model pattern in the empirical distribution of waterfowl movements, but the two-mixture model estimated the log-normal movement distribution accurately (Figure 2) and was used in subsequent analyses (Overton and Casazza, 2023). A step length distribution derived equally across all species (Table 2) produced estimates for one component that was approximately equal to the GPS location error among our tags (median = 21.1 m) and 69.1% of all step lengths reflected this "inactive" movement process. The remaining 30.9% of locations reflected "moving" activity with a median movement of 504 m (95% CI: 158–16,026 m). Each species demonstrated different relative proportions of these two movement activities. Each duck species indicated greater proportion of inactive movements (>80%) than geese (<70%), particularly lesser snow geese, among which just over half of movements were inactive (Table 2). Species-specific differences in movement activity were accentuated when step length distributions were calculated independently for each species, which indicated shorter median movements among geese and larger among ducks (Table 2).

Each species started the season with different rates of movement ($F_{6,20726} = 731.35$, $p < 0.0001$) with mallards moving the least

TABLE 1 Data from greater white-fronted geese (GWFG), lesser snow geese (LSGO), mallard (MALL), and northern pintail (NOPI) fit with GPS tracking units and occurring within California between April 2015 through January 2023 including number of marked individuals, number of unique annual periods extending from May through April (bird-years), and total number of locations collected at intervals ranging from once per minute to once per day.

	GWFG	LSGO	MALL	NOPI	Total
Individuals	120	154	211	206	691
Bird-years	173	231	319	248	971
Total locations	1,409,941	1,172,357	583,018	432,468	3,594,784
Analyzed locations	189,332	208,751	59,882	148,151	606,116

Analyzed locations were subset to hourly intervals with sequences occurring for at least 72 h and occurring from October 1 to April 30 of the following calendar year.

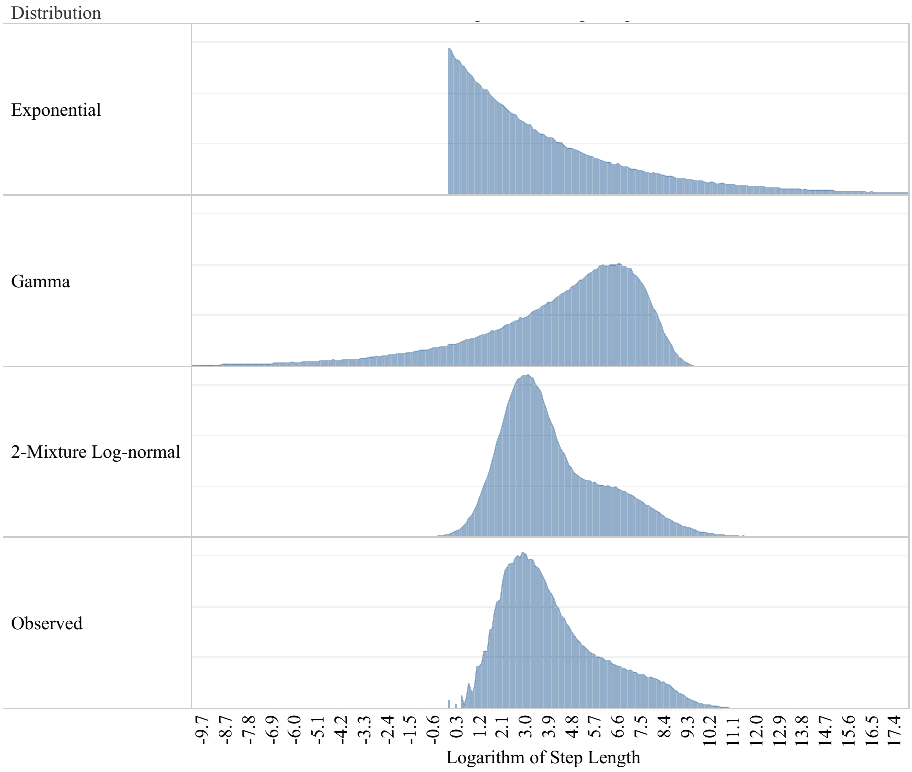

FIGURE 2
Two commonly used step length distributions used to define available habitat in step selection models, exponential and gamma, poorly approximated the empirical distribution of step lengths represented in waterfowl movement data. An alternative step length distribution using a two-mixture log-normal distribution produced a more accurate approximation of the observed data.

TABLE 2 Step length distributions were estimated using a 2-mixture log-normal distribution and a random sample of 50,000 steps across all four species (GWFG = greater white-fronted goose, LSGO = lesser snow goose, MALL = mallard, NOPI = northern pintail) of waterfowl (A) and species-specific step length distributions were also estimated using all available movements for each species (B).

(A)				
		Combined		
Step type		**Inactive**	**Moved**	
Median step length (m)		21.1	504	
95% CI		2.58–172	15.8–16,026	
Proportion		0.691	0.309	
Species	**GWFG**	**LSGO**	**MALL**	**NOPI**
Proportion inactive	0.696	0.505	0.888	0.845
Proportion moving	0.304	0.495	0.112	0.155
(B)				
Species	**GWFG**		**LSGO**	
Step type	**Inactive**	**Moved**	**Inactive**	**Moved**
Median step length (m)	18.8	389	15.19	366
± 2 SD	2.6–137	11–13,762	2.6–90.5	8.7–15,387
Proportion	0.644	0.356	0.456	0.544

(Continued)

TABLE 2 Continued

(B)				
Species	MALL		NOPI	
Step type	Inactive	Moved	Inactive	Moved
Mean log-normal step length	28.14	1,152	24.53	1,339
± 2 SD	2.5–312	63.3–20,964	2.7–221	136–13,152
Proportion	0.826	0.174	0.882	0.118

frequently and snow geese the most. Each species' mobility increased significantly through the season (GWFG: $t_{6037} = 4.39$, $p < 0.0001$; LSGO: $t_{7052} = 5.36$ $p < 0.0001$; MALL: $t_{2470} = 6.075$, $p < 0.0001$) except for Northern Pintail ($t_{5167} = 0.515$, $p = 0.606$), although they still maintained higher movement rates than mallard throughout the season (Figure 3). Circadian patterns also differed significantly between species ($F_{21,8821} = 126.977$, $p < 0.0001$). Nocturnal rates of movement were lower and diurnal rates were higher for all species, and ducks showed a stronger peak of movement activity at dawn and dusk with fewer mid-day movements than geese (Figure 4). Mobility also varied depending on the habitat occupied (Figure 5). Non-habitats (urban and other) generally had the highest rates of movement, and habitats reflecting either higher food value (rice, corn, and wetlands) or sanctuary from disturbance (protected lands) had the lowest rates of movement (Figure 5). Mallards were more inactive across all habitat types except urban, and lesser snow geese were the most mobile among all habitat types.

Each species, except mallards, used rice habitats the most and rice was also the most available habitat type at normal ranges of movement. Protected lands were both the most used and the most available habitat for mallards (Table 3). The second most used habitat for species other than mallard was protected land, while mallards used PAI habitats (i.e., pasture, alfalfa, and idle cropland) the second most frequently (Table 3). All species used urban lands the least, which were not always the least available habitat within

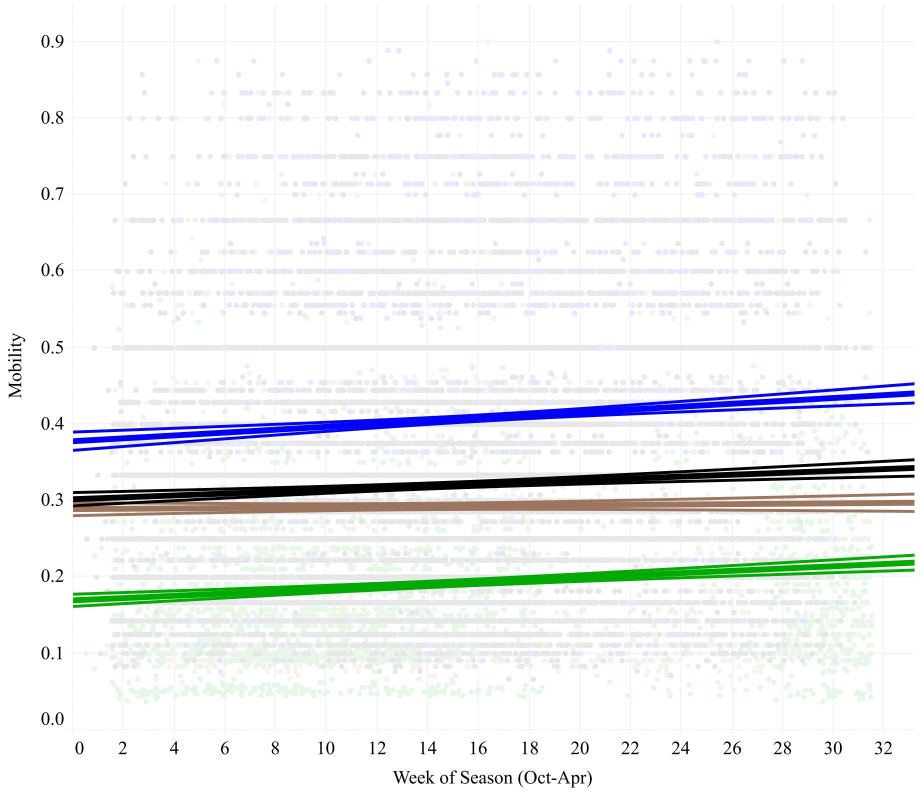

FIGURE 3
Movement activity increased for three of four species of waterfowl [greater white-fronted goose (black), lesser snow goose (blue), and mallard (green)] tracked in the Central Valley of California from October through April. Pintail (brown) began the season with a similar movement rate to greater white-fronted geese, but the increase in movement rate for pintail throughout the season was not significant ($p = 0.42$). Lesser snow geese had the highest movement rates, and mallard the lowest, throughout the season. Daily movement estimates were plotted as background points. Trend lines were plotted with 95% confidence regions.

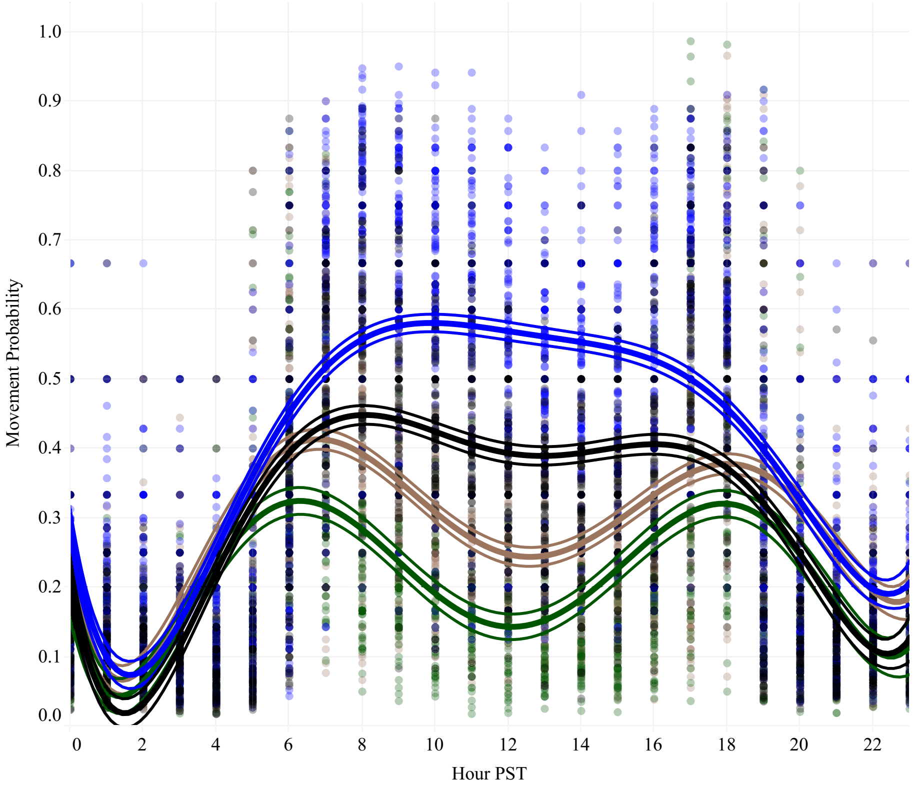

FIGURE 4
Circadian patterns of movement activity showed a similar pattern of reduced movement probability overnight across species. Diurnal movement activity was greater among geese, greater white-fronted goose (black) and lesser snow goose (blue), which produced a strong crepuscular peak in movement activity among ducks, mallard (green), and northern pintail (brown). Hourly estimated movement probability was plotted for each bird-year as background points. Trend lines were plotted with 95% confidence regions.

normal movement ranges (Table 3). Rice, corn, and protected lands had significantly higher selection than alternative habitats based on RSS for most species in the early winter (Figure 6). The RSS for rice declined for all species during the late winter and only pintail retained significant selection for rice after January 15. Greater white-fronted geese did not significantly select sanctuary in the early winter period and mallard did not select sanctuary in the late winter, nor did they select corn in either period (Figure 6). In the early winter, private wetlands were avoided by goose species and selected for only by mallard. In the late winter, private wetlands were significantly selected for only by snow geese (Figure 6). Urban habitats were always avoided by all species, but not significantly by mallards in the late winter. PAI habitats were avoided by all species in the early winter, but less so in the late winter when only lesser snow geese and northern pintail significantly avoided PAI relative to other habitats (Figure 6). Other non-habitat landcovers were avoided by each species in both periods (Figure 6).

Functional relationships describing the relative strength of selection a species had for a habitat compared with the average availability of habitat demonstrated differences in how each species used or avoided the seven habitat types. For each species and habitat, these patterns did not differ between early and late winter periods, so both periods were combined for subsequent interpretations. Differences in functional response were greatest between geese and ducks, and most similar between snow geese and greater white-fronted geese (Figure 7). Rice, which was selected by all species, had increasing RSS with availability among geese and consistent RSS across availability for ducks (Figure 7). Corn was available in limited quantities in most individuals, and though selected for by most species, the RSS did not change across availability for either goose species, nor for mallards, and the RSS for corn declined with increasing availability for pintail (Figure 7). Protected lands were also generally selected for by most individuals, and all species except mallards showed increasing RSS with availability; mallards' RSS was constant across all availabilities of protected lands (Figure 7). Although the wetlands were avoided relative to other habitats for geese, and used equally as other habitats by pintail, a significant increase in the RSS of wetlands existed for all species except for mallard, for which RSS was constant across availability (Figure 7). Each species avoided urban habitats and showed constant RSS among the limited amount of urban land that was available. Although PAI habitats were generally avoided throughout the winter, the RSS increased with availability for each species except mallard, for which it remained constant (Figure 7). Among geese, the estimated increase in RSS for PAI as availability increased suggests that geese will select for PAI habitats when more than 45% of available habitat within their movement range is PAI (Figure 7). Other, mostly non-habitat, landcover classes were also avoided by each species and RSS increased with availability.

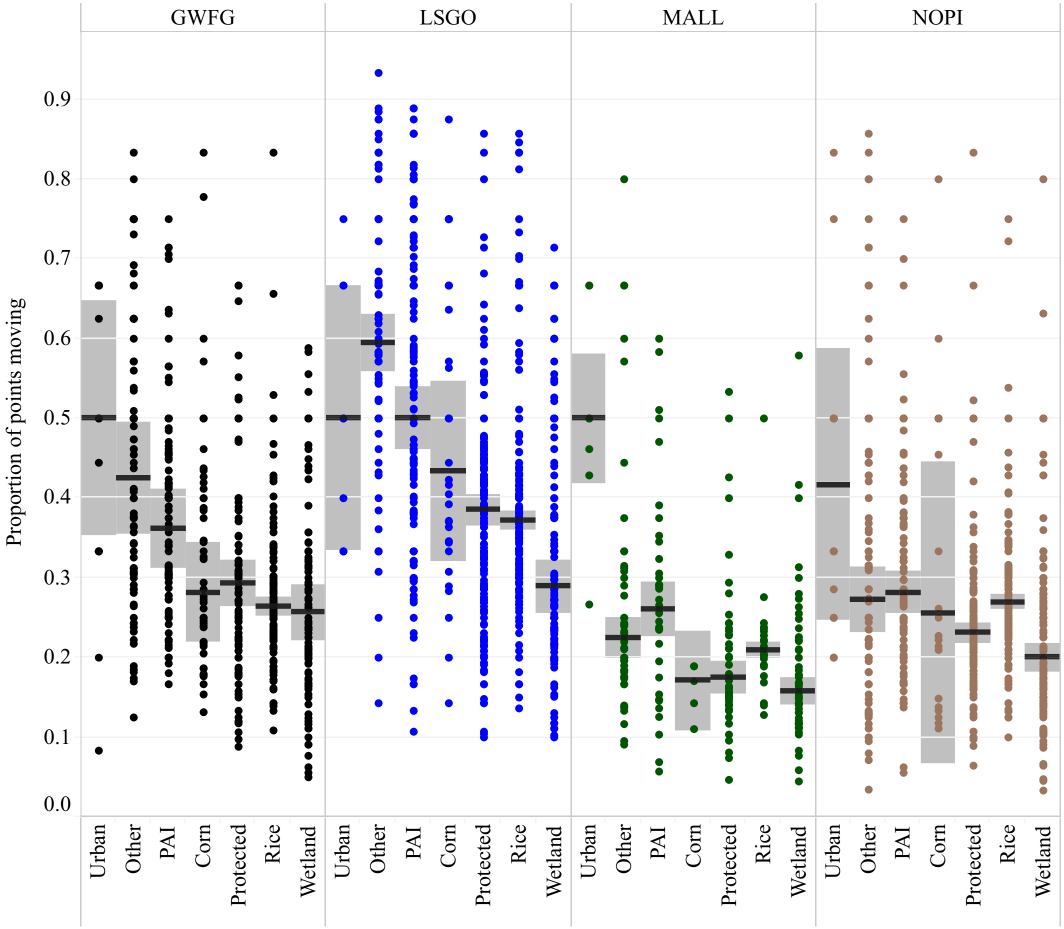

FIGURE 5
Movement activity among four species of waterfowl, greater white-fronted goose (black), lesser snow goose (blue), mallard (green), and northern pintail (brown), and among habitats being occupied. Points represent the proportion of movements in each habitat and by each species that best fit the "moving" component of a two-mixture log-normal step length distribution. Bar represents the median proportion of points identified as moving, and shaded regions indicate 95% confidence regions. PAI indicates pasture, alfalfa, and idle croplands.

TABLE 3 Proportion of telemetry locations occurring within seven habitat types ("Used") by four species (GWFG = greater white-fronted goose, LSGO = lesser snow goose, MALL = mallard, and NOPI = northern pintail) of wintering waterfowl ("Used") in the Central Valley of California, and the average proportion of 100 random movements into each habitat type that originate from each observed location ("Available").

		Corn	PAI	Other	Protected	Rice	Urban	Wetland
GWFG	Used	7.47%	14.94%	6.98%	15.68%	43.80%	0.53%	10.59%
	Available	5.83%	17.67%	13.58%	14.10%	35.98%	2.29%	10.55%
LSGO	Used	2.64%	10.96%	6.25%	23.41%	48.44%	0.40%	7.89%
	Available	2.17%	13.65%	12.78%	20.04%	41.65%	1.89%	7.81%
MALL	Used	0.70%	14.34%	7.27%	40.49%	12.51%	0.45%	24.24%
	Available	0.69%	27.54%	14.29%	28.56%	9.07%	2.36%	17.49%
NOPI	Used	0.91%	9.62%	4.85%	24.67%	45.20%	0.43%	14.33%
	Available	1.12%	22.75%	14.16%	17.16%	29.04%	2.85%	12.93%

PAI indicates pasture, alfalfa, and idle croplands.

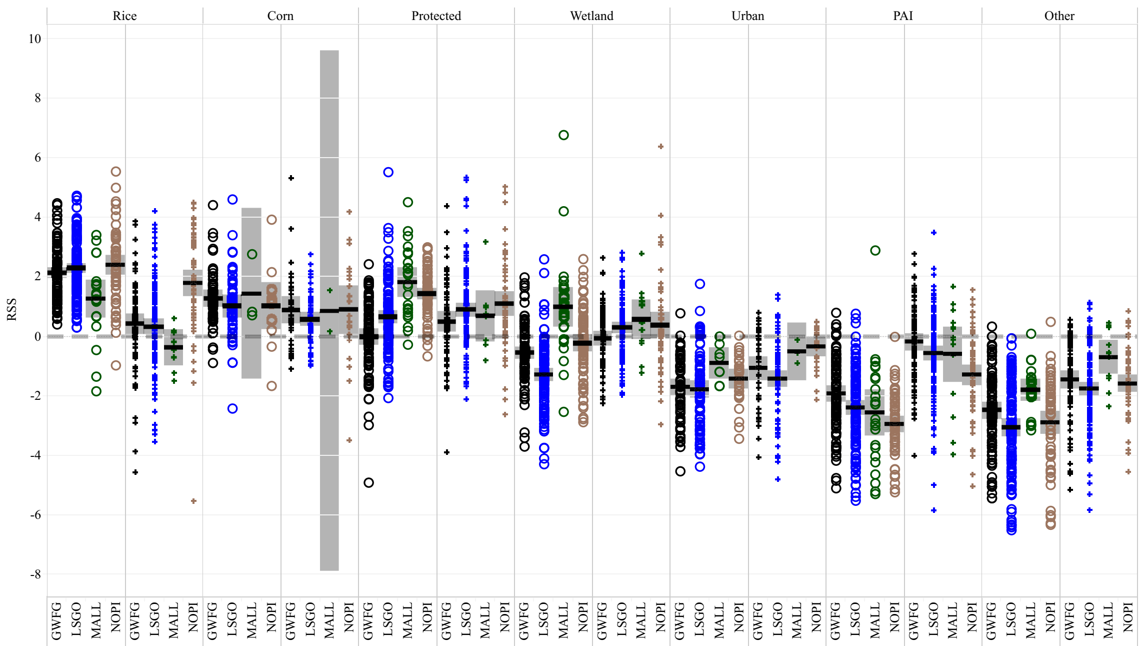

FIGURES 6

Relative strength of selection estimates among seven habitat classes and four species of waterfowl, greater white-fronted goose (black), lesser snow goose (blue), mallard (green), and northern pintail (brown), wintering in the Central Valley of California. Estimates were calculated for individual birds in both diurnal and nocturnal periods and within early (October to January 15; circles) and late (January 16 through April, crosses) periods. Species × habitat combinations marked with asterisks did not show a significant difference in relative use between the indicated habitat and other habitats available with that species' movement range. All other habitats indicated significant selection or avoidance relative to other available habitats. Habitat types ranked by mean RSS across individuals from highest (left) to lowest (right) average RSS. PAI indicates pasture, alfalfa, and idle croplands.

Discussion

Step lengths derived from hourly movements of wintering waterfowl exhibited a high degree of non-stationarity that resulted from multiple types of movement occurring at that temporal scale. Standard, single-component, step length distributions were not able to accurately replicate the empirical pattern of movement, but a mixture model did produce similar step length distributions. The two-mixture log-normal distribution we used should improve calculation of integrated step selection analysis (iSSA; Avgar et al., 2016). Incorporating multimodal parametric movement distributions extends the utility of iSSA to efforts that currently require empirical distributions of observed step lengths (Fortin et al., 2005; Forester et al., 2009), track segmentation (Patterson et al., 2009), or destructive sampling (Schabenberger and Gotway, 2005) to accurately reflect the available landscape.

The ability to distinguish between inactivity and movement in each birds' track also allowed effective comparisons of movement patterns among our wintering waterfowl species. The circadian pattern in waterfowl activity described by waterfowl movements is well documented among individual species (Paulus, 1988) but has yet to be described among multiple co-occurring taxa and provides valuable estimates for agent-based modeling (Miller et al., 2014) and more accurate scenario planning in energetics models (CVJV, 2020). The seasonal increase in movement frequency observed among most waterfowl warrants closer attention. There are a variety of reasons why increased movement may occur later in the winter ranging from increased foraging effort resulting from exploitative competition (Legagneux et al., 2009; Davis and Afton, 2010) to seasonal behavioral and physiological changes related to breeding activity (McKinney, 1965). However, prior work indicates that increased frequency of movement may not correspond to increased movement distance, which was not shown to broadly increase across species or sexes of dabbling duck in the Central Valley (McDuie et al., 2019), and the increased probability of movement we estimated was small (~4% increase in April compared to October for most species, <2% for northern pintail). This suggests that increased movement frequency is not related to lower food supplies and is more likely related to social interactions associated with courtship behavior and the reduction of disturbance following the completion of hunting seasons.

A major concern in the wintering ranges of many animal species is the potential for food resource competition or other limitations (Marchowski et al., 2015; Petrie et al., 2016). Similarities in food resources across taxa, habitat dynamics that increase or decrease food accessibility, overabundant co-occurring species, reliance on variable water supplies during extended droughts, and the dependence on agricultural practices to provide many of the food resources animals depend on the increased potential that, under some conditions, food resource competition could affect the fitness of individuals and prevent achievement of conservation goals (CVJV, 2020, Williams et al., 2014; Petrie et al., 2016). Habitat types we assumed *a priori* to provide the most, or highest-quality, resources (e.g., rice, corn, protected lands, and wetlands, CVJV, 2020, Miller, 1987; Petrie et al., 2016) were the habitats with the lowest rates of mobility, indicating that birds remained localized in

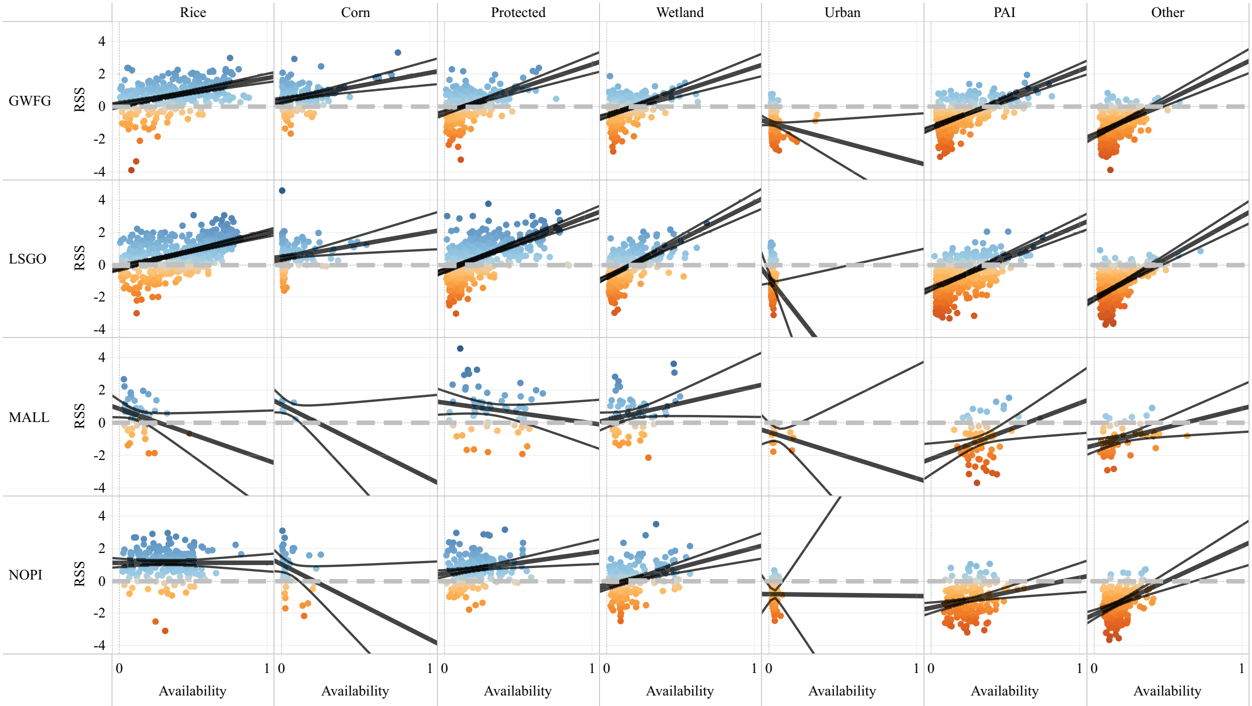

FIGURE 7
Functional response in the relative strength of selection (RSS) for seven habitats among four species of wintering waterfowl (GWFG = greater white-fronted goose, LSGO = lesser snow goose, MALL = mallard, and NOPI = northern pintail) using the Central Valley in California from October through April. Points represent RSS estimates from step selection analyses for each species during both diurnal and nocturnal periods and early (October to January 15) and late (January 16 through April) seasons. Color of points represents the RSS (blue = positive/selection, brown = negative/avoidance). Linear functional response (thick black line) relates RSS with average habitat availability and includes 95% confidence region (thin black lines). Reference line (dashed gray) indicates equal selection ratio between the indicated habitat and other habitats available within the normal movement range of the species. Habitat types ranked by mean RSS across individuals from highest (left) to lowest (right) average RSS. PAI indicates pasture, alfalfa, and idle croplands.

those habitats more than alternatives. Additionally, movements among geese were more common than among ducks, indicating potentially higher energetic demand. Within-taxa differences were also apparent as mallards were only 75% as mobile as northern pintail, and snow geese was nearly 40% more mobile than greater white-fronted geese. These differences can be used to parameterize species-specific demand in landscape energetics models (e.g., CVJV, 2020, Petrie et al, 2016) or agent-based models (Miller et al., 2014; Williams et al., 2014) and for scenario planning and establishing conservation objectives. They may also indicate which species are likely to demonstrate impacts of food limitations first. Based on our assessment, snow geese are likely to demonstrate physiological or behavioral response to food limitation first, if foods are limited prior to diet shifts during the late winter, due to their high movement rate, higher relative use of rice, and stronger functional response with rice availability. Food limitations occurring later in the season are likely to manifest in pintail first since they remain reliant on rice; however, such limitation may not reflect change in resource selection due to the constant functional response with respect to availability for this species.

Relative habitat value as indicated by step selection functions matched our *a priori* expectations; specifically, habitats providing key food resources and habitats providing sanctuary during the hunting season were selected more than the alternative habitats available to individuals. However, habitat use patterns also indicated important differences between taxa. Mallards were the only species that show significantly stronger selection for wetlands than alternate habitats and were also the species with the strongest RSS for protected areas (e.g., National Wildlife Refuges, State Wildlife Areas, and conservation easements), which, in the Central Valley, are often specifically managed to provide seasonal or semi-permanent wetlands (CVJV, 2020). Compared to the other species, mallard appear to benefit particularly from the management of both public and private emergent seasonal wetlands. The consequence is that mallard may be insulated from any future changes in agricultural practices that reduce the value of primary waterfowl food crops such as conversion from rice or reduction in winter flooding due to drought. In addition, mallard may be a better indicator than other species of the benefits of conservation actions such as wetland enhancements or costs of practices that reduce wetland function such as changes in timing or quantity of water delivery.

Variability in functional responses between RSS and habitat availability existed across both habitat classes and between species and illustrated important behavioral and ecological differences between them. Specifically, pintail RSS functional responses were more different from mallards than from geese for four of the seven habitat types. In particular, they were different for three of four habitats with the highest average RSS (rice, protected, and wetland). This indicates that among resources shared by multiple species, such as primary food sources, plasticity in individual's response to availability may limit competition. That is, northern pintail may be more likely to experience competition with greater white-fronted and snow geese because their functional responses were more similar to those two species. Mallards, which showed a more constant functional response with availability of selected habitats (Holbrook et al., 2019), are, by comparison, a habitat generalist. Differences in RSS and in functional relationships between goose species were minor for all habitats and indicated similar patterns of reliance on Central Valley habitats. However, seasonal diet shifts, particularly by geese that transition in the late winter from grains to grazing on emerging grasses in pasture, idle cropland, and other formerly bare ground, may affect the relationship between RSS and habitat availability. Increase in relative use of PAI coincided with decreases in RSS for rice for all species except pintail. This supports the idea that many species transition diet from grains to grasses and/or invertebrates prior to the breeding season (Euliss and Harris, 1987; Miller, 1987; Ely and Raveling, 2011). Only pintail maintain strong selection for rice over other habitats. Because none of the late winter RSS values for non-rice habitats indicate both selection for the habitat and a significant increase from the early winter, northern pintail may be particularly impacted by changes to the timing or patterns of agricultural activities related to rice such as drying fields to prepare them for planting in the spring.

Prior work that has interpretated behavior patterns related to different functional responses have assessed a variety of habitat selection analysis methods (Holbrook et al., 2019). Many behaviors (e.g., proportional use, trade-offs, and avoidance) result in different mathematical relationships between selection metrics (e.g., use, use: availability ratios, and RSF coefficients) and habitat availability (Holbrook et al., 2019). RSS metrics resulting from SSA have not yet been similarly analyzed. SSA and iSSA (Avgar et al., 2016) identify habitat availability based not only on the composition and configuration of the landscape but also on the cognitive/behavioral process that governs movements and navigation (Nathan et al., 2022). Availability, in SSA, is defined at each location by the joint distributions of behaviorally mediated movement processes (step lengths and turning angles) and the configuration and composition of habitats in a spatially explicit landscape. This means functional response can then be estimated within individuals, which allows investigation of individual plasticity in resource selection (Muff et al., 2020; Northrup et al., 2022). However, the functional relationships between RSS metrics and estimates of resource availability derived using SSA likely have different mathematical forms compared to other habitat selection metrics because SSA may describe habitat at different (and multiple) scales and orders of selection (Johnson, 1980; Thurfjell et al., 2014) compared to some alternate habitat selection methods. Our results indicate that among several categorical habitat types, the relationship between the relative strength of selection and habitat availability indicates avoidance at low availability and selection at high availability, which did not match any previously described selection behaviors (Holbrook et al., 2019). This might be expected in a landscape of patchy or clustered resources when availability is determined to be greater near an animal's current location. Spatial and temporal autocorrelation in habitat use and availability are likely to create difficult computational and methodological issues to resolve where it is appropriate to do so (Alston et al., 2023). Our segmentation of the movement process into "inactive" and "moving" modalities was a partial solution to reduce autocorrelation. Newer approaches such as autocorrelation weighting may both increase precision of functional responses and reduce bias in selection functions (Alston et al., 2023).

Our use of path segmentation to develop behavior-specific step selection functions (i.e., by separating inactive movement periods from the step length distribution) may have made resulting functions more accurate and/or improved computational efficiencies and is one of the multiple approaches to separate tracks into specific behavior states (Roever et al., 2014; Mott, 2022; Pay et al., 2022). Without segmenting and removal of the inactive step lengths, 45% to 89% of our sample of available habitat would likely be at functionally the same location as the observed step and require a greater sample of available steps to obtain representation of other habitat types. This would reduce the magnitude of RSS for occupied habitats since, at each location, the used habitat class would be identical to a greater portion of available habitat samples. This may be a particular problem for flighted birds that often have a greater disparity in movement capacity between movement activity modes, which result in bi- or multi-modal distributions of step lengths that are not accurately reflected in single-component distributions.

We developed species-specific step length distributions for our SSA because we anticipated individual species to have different biologically relevant movement processes such as period of feeding (diurnal vs. nocturnal), food acquisition methods (rotational feeding vs. dabbling), and susceptibility to disturbance. Although we used the same temporal scale (hourly) for each species, it is possible that the non-stationary movement patterns may reflect different behaviors for ducks and geese, for example, differences in foraging behavior. Evidence for this lies in that median step length when "moving" was nearly four times further in ducks than geese. Mallard and northern pintail generally feed by dabbling, tipping to reach submerged food, in flooded fields. Geese will feed in flooded fields, but also forage in dry or puddled fields where they both walk and periodically fly to the leading edge of foraging flocks where food resources are gained at the quickest rate (Black et al., 1992). Therefore, the "moving" steps for geese may reflect a greater proportion of intra-patch movements related to foraging while "moving" ducks tend to be moving between habitat patches. Our results are likely robust to this potential disparity in movement activity, because most habitat patches in the Central Valley are either smaller in scale than the median movements of geese (e.g., wetlands) or larger in extent than median movements of ducks (e.g., rice). Thus, both taxa would have been affected in approximately the same manner by the spatial structure of habitats.

Conclusion

Co-occurring species that seasonally concentrate and utilize similar food or other resources may show differences in functional responses between relative strengths of habitat selection and availability of habitats due to niche differentiation or they may show similarities that could indicate interspecific competition.

Wintering waterfowl's movements and selection of habitats in California's Central Valley show differences between taxonomic groups (geese versus ducks), differences within taxonomic groups (mallard versus northern pintail), seasonal patterns, and different functional responses. These complex patterns reflect well understood behavioral differences (patterns of foraging activity), resource needs (preference for sanctuary areas during the hunting season), and species phenology (diet shifts). Functional responses also suggest that for most habitats, the relative importance of the habitat increases with the relative abundance of that habitat within the normal range of a single movement. This likely reflects waterfowl's (and birds in general) tendency for limited movements within patches while foraging and their ability to move long distances between patches quickly. Habitat importance across all habitats for mallards was least affected by availability, suggesting that they are more of a generalist species. Pintails were additively selecting (Holbrook et al., 2019) for their principal food resource, rice, indicating that rice was equally important regardless of availability whereas the importance of rice to geese increased as more rice was available, implying that geese may be focusing their space use at higher scales (second order) where rice is more available to them (Holbrook et al., 2019). Our results identify the habitat selection patterns, species, and habitat types that may be most likely to reflect impacts of competition and food resource limitation. Conservation and scenario planners may use these predictions to develop landscape energy budgets and management responses to environmental limitations such as drought or changing agricultural practices during periods when food resources may become limited.

Data availability statement

The datasets presented in this study can be found in online repositories. The names of the repository/repositories and accession number(s) can be found below: U.S. Geological Survey ScienceBase Digital Repository (https://www.sciencebase.gov/catalog/), https://doi.org/10.5066/P9ELSUHN.

Ethics statement

The animal study was approved by the U.S. Geological Survey Western Ecological Research Center Institutional Animal Use and Care Committee. The study was conducted in accordance with the local legislation and institutional requirements.

Author contributions

MC conceived the original idea and design. CO conducted analyses and authored the manuscript with edits by MC. All authors contributed to the article and approved the submitted version.

Funding

We thank the Arctic Goose Joint Venture, California Department of Water Resources, Ducks Unlimited, and the USGS Ecosystems Mission Area for funding that enabled this work.

Acknowledgments

We wish to thank F. McDuie, E. Matchett, A. Mott, D. Mackell, and many technicians from the U.S. Geological Survey (USGS) Dixon Field Station; V. Patil and staff at the USGS Alaska Science Center; E. Reed and staff at the Environment and Climate Change Canada–Yellowknife; and the California Waterfowl Association for conducting the field work to collect and complete quality control for the data used in this manuscript. We thank personnel at Grizzly Island Wildlife Area, Upper Butte Basin Wildlife Area, Summer Lake Wildlife Area, and the Sacramento National Wildlife Refuge for land access and logistical support.

Conflict of interest

The authors declare that the research was conducted in the absence of any commercial or financial relationships that could be construed as a potential conflict of interest.

Publisher's note

Author disclaimer

Any use of trade, firm, or product names is for descriptive purposes only and does not imply endorsement by the U.S. Government.

References

Aarts, G., Fieberg, J., Brasseur, S., and Matthiopoulos, J. (2013). Quantifying the effect of habitat availability on species distributions. *J. Anim. Ecol.* 82, 1135–1145. doi: 10.1111/1365-2656.12061

Alston, J. M., Fleming, C. H., Kays, R., Streicher, J. P., Downs, C. T., Ramesh, T., et al. (2023). Mitigating pseudoreplication and bias in resource selection functions with autocorrelation-informed weighting. *Methods Ecol. Evol.* 14, 643–654. doi: 10.1111/2041-210X.14025

Avgar, T., Potts, J. R., Lewis, M. A., and Boyce, M. S. (2016). Integrated step selection analysis: bridging the gap between resource selection and animal movement. *Methods Ecol. Evol.* 7, 619–630. doi: 10.1111/2041-210X.12528

Aybar, C. (2022). "Rgee: R bindings for calling the 'Earth Engine' API," in *R package version 1.1.5*. Available at: https://CRAN.R-project.org/package=rgee.

Benaglia, T., Chauveau, D., Hunter, D. R., and Young, D. (2009). mixtools: an *R* package for analyzing finite mixture models. *J. Stat. Soft* 32, 1-29. doi: 10.18637/jss.v032.i06

Bergen, S., Huso, M. M., Duerr, A. E., Braham, M. A., Katzner, T. E., Schmuecker, S., et al. (2022). Classifying behavior from short-interval biologging data: An example with GPS tracking of birds. *Ecol. Evol.* 12, e08395. doi: 10.1002/ece3.8395

Bivand, R., Keitt, T., and Rowlingson, B. (2022). "rgdal: bindings for the 'Geospatial' Data abstraction library," in *R package version 1*. Available at: https://CRAN.R-project.org/package=rgdal.

Black, J. M., Carbone, C., Wells, R. L., and and Owen, M.. (1992). Foraging dynamics in goose flocks: The cost of living on the edge. *Animal Behav.* 44 (1), 41–50.. doi: 10.1016/S0003-3472(05)80752-3

Boryan, C., Yang, Z., Mueller, R., and Craig, M. (2011). Monitoring US agriculture: the US department of agriculture, national agricultural statistics service, cropland data layer program. *Geocarto Int.* 26, 341–358. doi: 10.1080/10106049.2011.562309

Boyce, M. S., Johnson, C. J., Merrill, E. H., Nielsen, S. E., Solberg, E. J., and Van Moorter, B. (2016). REVIEW: Can habitat selection predict abundance? *J. Anim. Ecol.* 85, 11–20. doi: 10.1111/1365-2656.12359

Brussee, B. E., Coates, P. S., O'Neil, S. T., Casazza, M. L., Espinosa, S. P., Boone, J. D., et al. (2022). Invasion of annual grasses following wildfire corresponds to maladaptive habitat selection by a sagebrush ecosystem indicator species. *Global Ecol. Conserv.* 37, e02147. doi: 10.1016/j.gecco.2022.e02147

Casazza, M. L., McDuie, F., Jones, S., Lorenz, A. A., Overton, C. T., Yee, J., et al. (2021). Waterfowl use of wetland habitats informs wetland restoration designs for multi-species benefits. *J. Appl. Ecol.* 58, 1910–1920. doi: 10.1111/1365-2664.13845

CVJV (2020). *Central valley joint venture 2020 implementation plan* (Sacramento, CA: US Fish and Wildlife Service).

Davis, B. E., and Afton, A. D. (2010). Movement distances and habitat switching by female mallards wintering in the lower mississippi alluvial valley. *Waterbirds* 33, 349–356. doi: 10.1675/063.033.0311

Diffenbaugh, N. S., Swain, D. L., and Touma, D. (2015). Anthropogenic warming has increased drought risk in California. *Proc. Natl. Acad. Sci. U.S.A.* 112, 3931–3936. doi: 10.1073/pnas.1422385112

Duchesne, T., Fortin, D., and Courbin, N. (2010). Mixed conditional logistic regression for habitat selection studies. *J. Anim. Ecol.* 79, 548–555. doi: 10.1111/j.1365-2656.2010.01670.x

Ely, C. R., and Raveling, D. G. (2011). Seasonal variation in nutritional characteristics of the diet of greater white-fronted geese: White-Fronted Goose Diet. *J. Wildlife Manage.* 75, 78–91. doi: 10.1002/jwmg.13

Euliss, N. H., and Harris, S. W. (1987). Feeding ecology of northern pintails and green-winged teal wintering in california. *J. Wildlife Manage.* 51, 724. doi: 10.2307/3801733

Fieberg, J., Signer, J., Smith, B., and Avgar, T. (2021). A 'How to' guide for interpreting parameters in habitat-selection analyses. *J. Anim. Ecol.* 90, 1027–1043. doi: 10.1111/1365-2656.13441

Fleming, K. K., Mitchell, M. K., Brasher, M. G., Colluccy, J. M., James, J. D., Petrie, M. J., et al. (2019). "Derivation of regional, non-breeding duck population abundance objectives to inform conservation planning in North America. 2019 revision. North American Waterfowl Management Plan Science Support Team Technical Report 1," in *Central valley joint venture (CVJV), 2020. Central valley joint venture 2020 implementation plan* (Sacramento, CA: US Fish and Wildlife Service).

Forester, J. D., Im, H. K., and Rathouz, P. J. (2009). Accounting for animal movement in estimation of resource selection functions: sampling and data analysis. *Ecology* 90, 3554–3565. doi: 10.1890/08-0874.1

Fortin, D., Beyer, H. L., Boyce, M. S., Smith, D. W., Duchesne, T., and Mao, J. S. (2005). Wolves influence elk movements: Behavior shapes a trophic cascade in Yellowstone National Park. *Ecology* 86, 1320–1330. doi: 10.1890/04-0953

Gillies, C. S., Hebblewhite, M., Nielsen, S. E., Krawchuk, M. A., Aldridge, C. L., Frair, J. L., et al. (2006). Application of random effects to the study of resource selection by animals: Random effects in resource selection. *J. Anim. Ecol.* 75, 887–898. doi: 10.1111/j.1365-2656.2006.01106.x

GreenInfo Network (2022) *California Protected Areas Database 2022b release*. Available at: https://data.cnra.ca.gov/dataset/california-protected-areas-database.

Groff, L. A., Calhoun, A. J. K., and Loftin, C. S. (2017). Amphibian terrestrial habitat selection and movement patterns vary with annual life-history period. *Can. J. Zool.* 95, 433–442. doi: 10.1139/cjz-2016-0148

Holbrook, J. D., Olson, L. E., DeCesare, N. J., Hebblewhite, M., Squires, J. R., and Steenweg, R. (2019). Functional responses in habitat selection: clarifying hypotheses and interpretations. *Ecol. Appl.* 29, e01852. doi: 10.1002/eap.1852

Johnson, D. H. (1980). The comparison of usage and availability measurements for evaluating resource preference. *Ecology* 61, 65–71. doi: 10.2307/1937156

Johnson, D. S., Thomas, D. L., Ver Hoef, J. M., and Christ, A. (2008). A general framework for the analysis of animal resource selection from telemetry data. *Biometrics* 64, 968–976. doi: 10.1111/j.1541-0420.2007.00943.x

Kays, R., Crofoot, M. C., Jetz, W., and Wikelski, M. (2015). Terrestrial animal tracking as an eye on life and planet. *Science* 348, aaa2478. doi: 10.1126/science.aaa2478

Knopff, A. A., Knopff, K. H., Boyce, M. S., and St. Clair, C. C. (2014). Flexible habitat selection by cougars in response to anthropogenic development. *Biol. Conserv.* 178, 136–145. doi: 10.1016/j.biocon.2014.07.017

Lark, T. J., Schelly, I. H., and Gibbs, H. K. (2021). Accuracy, bias, and improvements in mapping crops and cropland across the United States using the USDA cropland data layer. *Remote Sens.* 13, 968. doi: 10.3390/rs13050968

Leclerc, M., Vander Wal, E., Zedrosser, A., Swenson, J. E., Kindberg, J., and Pelletier, F. (2016). Quantifying consistent individual differences in habitat selection. *Oecologia* 180, 697–705. doi: 10.1007/s00442-015-3500-6

Legagneux, P., Blaize, C., Latraube, F., Gautier, J., and Bretagnolle, V. (2009). Variation in home-range size and movements of wintering dabbling ducks. *J. Ornithol* 150, 183–193. doi: 10.1007/s10336-008-0333-7

Manly, B. F. J., McDonald, L. L., Thomas, D. L., McDonald, T., and Erickson, W. P. (2002). *Resource selection by animals: statistical design and analysis for field studies. 2nd ed* (Boston: Kluwer Academic Publishers, Dordrecht).

Marchowski, D., and Leitner, M. (2019). Conservation implications of extraordinary Greater Scaup (Aythya marila) concentrations in the Odra Estuary, Poland. *Condor* 121, duz013. doi: 10.1093/condor/duz013

Marchowski, D., Neubauer, G., Ławicki, Ł., Woźniczka, A., Wysocki, D., Guentzel, S., et al. (2015). The Importance of Non-Native Prey, the Zebra Mussel Dreissena polymorpha, for the Declining Greater Scaup Aythya marila: A Case Study at a Key European Staging and Wintering Site. *PloS One* 10, e0145496. doi: 10.1371/journal.pone.0145496

McDuie, F., Casazza, M. L., Overton, C. T., Herzog, M. P., Hartman, C. A., Peterson, S. H., et al. (2019). GPS tracking data reveals daily spatio-temporal movement patterns of waterfowl. *Mov Ecol.* 7, 6. doi: 10.1186/s40462-019-0146-8

McDuie, F., Lorenz, A. A., Klinger, R. C., Overton, C. T., Feldheim, C. L., Ackerman, J. T., et al. (2021). Informing wetland management with waterfowl movement and sanctuary use responses to human-induced disturbance. *J. Environ. Manage.* 297, 113170. doi: 10.1016/j.jenvman.2021.113170

McKinney, F. (1965). Spacing and chasing in breeding ducks. *Wildfowl* 16, 15.

McNeil, R., Drapeau, P., and Goss-Custard, J. D. (1992). The occurrence and adaptive signficance of nocturnal habits in waterfowl. *Biol. Rev.* 67, 381–419. doi: 10.1111/j.1469-185X.1992.tb01188.x

Miller, M. R. (1987). Fall and winter foods of northern pintails in the sacramento valley, california. *J. Wildlife Manage.* 51, 405. doi: 10.2307/3801027

Miller, M. R., Garr, J. D., and Coates, P. S. (2010). Changes in the status of harvested rice fields in the sacramento valley, california: implications for wintering waterfowl. *Wetlands* 30, 939–947. doi: 10.1007/s13157-010-0090-2

Miller, M. L., Ringelman, K. M., Schank, J. C., and Eadie, J. M. (2014). SWAMP: An agent-based model for wetland and waterfowl conservation management. *SIMULATION* 90, 52–68. doi: 10.1177/0037549713511864

Mitchell, L. J., Kohler, T., White, P. C. L., and Arnold, K. E. (2020). High interindividual variability in habitat selection and functional habitat relationships in European nightjars over a period of habitat change. *Ecol. Evol.* 10, 5932–5945. doi: 10.1002/ece3.6331

Morris, D. W. (1989). Density-dependent habitat selection: Testing the theory with fitness data. *Evol. Ecol.* 3, 80–94. doi: 10.1007/BF02147934

Mott, A. (2022). "*Habitat use and distribution implications of four goose species wintering in California's Sacramento Valley*," (Davis, CA: University of California-Davis).

Muff, S., Signer, J., and Fieberg, J. (2020). Accounting for individual-specific variation in habitat-selection studies: Efficient estimation of mixed-effects models using Bayesian or frequentist computation. *J. Anim. Ecol.* 89, 80–92. doi: 10.1111/1365-2656.13087

Mysterud, A., and Ims, R. A. (1998). Functional responses in habitat use: availability influences relative use in trade-off situations. *Ecol* 79, 1435–1441. doi: 10.1890/0012-9658(1998)079[1435:FRIHUA]2.0.CO;2

Nathan, R., Monk, C. T., Arlinghaus, R., Adam, T., Alós, J., Assaf, M., et al. (2022). Big-data approaches lead to an increased understanding of the ecology of animal movement. *Science* 375, eabg1780. doi: 10.1126/science.abg1780

Neu, C. W., Byers, C. R., and Peek, J. M. (1974). A technique for analysis of utilization-availability data. *J. Wildlife Manage.* 38, 541. doi: 10.2307/3800887

Northrup, J. M., Vander Wal, E., Bonar, M., Fieberg, J., Laforge, M. P., Leclerc, M., et al. (2022). Conceptual and methodological advances in habitat-selection modeling: guidelines for ecology and evolution. *Ecol. Appl.* 32, e02470. doi: 10.1002/eap.2470

Olson, S. M.2022*Pacific Flyway Data Book 2022: Migratory bird abundance, harvest, and hunter activity*. Helena, MT: (US Fish and Wildlife Service, Division of Migratory Bird Management).

Osborn, J. M., Hagy, H. M., Mcclanahan, M. D., Davis, J. B., and Gray, M. J. (2017). Habitat selection and activities of dabbling ducks during non-breeding periods: Dabbling Duck Habitat Selection. *Jour. Wild. Mgmt.* 81, 1482–1493. doi: 10.1002/jwmg.21324

Osborne, P. E., Foody, G. M., and Suárez-Seoane, S. (2007). Non-stationarity and local approaches to modelling the distributions of wildlife. *Diversity Distributions* 13, 313–323. doi: 10.1111/j.1472-4642.2007.00344.x

Overton, C., Casazza, M., Bretz, J., McDuie, F., Matchett, E., Mackell, D., et al. (2022). Machine learned daily life history classification using low frequency tracking data and automated modelling pipelines: application to North American waterfowl. *Mov Ecol.* 10, 23. doi: 10.1186/s40462-022-00324-7

Overton, C., and Casazza, M.. (2023). Movements, used habitats, and available habitats identified using step selection procedures for four species of waterfowl in California's Central Valley, 2015-2022. U.S. Geological Survey Data Release. *Mov Ecol.* doi: 10.5066/P9ELSUHN

Pathak, T., Maskey, M., Dahlberg, J., Kearns, F., Bali, K., and Zaccaria, D. (2018). Climate change trends and impacts on california agriculture: A detailed review. *Agronomy* 8, 25. doi: 10.3390/agronomy8030025

Patterson, T. A., Basson, M., Bravington, M. V., and Gunn, J. S. (2009). Classifying movement behaviour in relation to environmental conditions using hidden Markov models. *J. Anim. Ecol.* 78, 1113–1123. doi: 10.1111/j.1365-2656.2009.01583.x

Paulus, S. L. (1988). Time-activity budgets of nonbreeding Anatidae: a review, In Waterfowl in Winter. Ed. Weller, M. W. (Minneapolis, MN: University of Minnesota Press).

Pay, J. M., Patterson, T. A., Proft, K. M., Cameron, E. Z., Hawkins, C. E., Koch, A. J., et al. (2022). Considering behavioral state when predicting habitat use: Behavior-specific spatial models for the endangered Tasmanian wedge-tailed eagle. *Biol. Conserv.* 274, 109743. doi: 10.1016/j.biocon.2022.109743

Pebesma, E. (2018). Simple features for R: Standardized support for spatial vector data. *R J.* 10, 439–446. doi: 10.32614/RJ-2018-009

Petrie, M. J., Fleskes, J. P., Wolder, M. A., Isola, C. R., Yarris, G. S., and Skalos, D. A. (2016). Potential effects of drought on carrying capacity for wintering waterfowl in the central valley of california. *J. Fish Wildlife Manage.* 7, 408–422. doi: 10.3996/082015-JFWM-082

Resano-Mayor, J., Korner-Nievergelt, F., Vignali, S., Horrenberger, N., Barras, A. G., Braunisch, V., et al. (2019). Snow cover phenology is the main driver of foraging habitat selection for a high-alpine passerine during breeding: implications for species persistence in the face of climate change. *Biodivers Conserv.* 28, 2669–2685. doi: 10.1007/s10531-019-01786-9

Roever, C. L., Beyer, H. L., Chase, M. J., and and Van Aarde, R. J.. (2014). The pitfalls of ignoring behaviour when quantifying habitat selection. *Div. Distrib.* 20 (3), 322–333. doi: 10.1111/ddi.12164

Rosenzweig, M. L. (1981). A theory of habitat selection. *Ecology* 62, 327–335. doi: 10.2307/1936707

SFEI (2022) *California Aquatic Resource Inventory (CARI) version 1.1*. Available at: https://www.sfei.org/data/california-aquatic-resource-inventory-cari-version-11-gis-data.

Schabenberger, O., and Gotway, C. A. (2005). *Statistical methods for spatial data analysis, Texts in statistical science* (Boca Raton: Chapman & Hall/CRC).

Signer, J., Fieberg, J., and Avgar, T. (2019). Animal movement tools (amt): R package for managing tracking data and conducting habitat selection analyses. *Ecol. Evol.* 9, 880–890. doi: 10.1002/ece3.4823

Skov, H., Heinänen, S., Žydelis, R., Bellebaum, J., Bzoma, S., Dagys, M., et al. (2011). *Waterbird populations and pressures in the Baltic Sea* (Copenhagen: Nordic Council of Ministers).

Thurfjell, H., Ciuti, S., and Boyce, M. S. (2014). Applications of step-selection functions in ecology and conservation. *Mov Ecol.* 2, 4. doi: 10.1186/2051-3933-2-4

USFWS (2018) *National wetlands inventory*. Available at: https://data.nal.usda.gov/dataset/national-wetlands-inventory.

Williams, C. K., Dugger, B. D., Brasher, M. G., Coluccy, J. M., Cramer, D. M., Eadie, J. M., et al. (2014). Estimating habitat carrying capacity for migrating and wintering waterfowl: considerations, pitfalls and improvements. *Wildfowl* 4, 407–435.

frontiers | Frontiers in Ecology and Evolution

TYPE Original Research
PUBLISHED 21 November 2023
DOI 10.3389/fevo.2023.1215964

OPEN ACCESS

EDITED BY
Thomas George Bornman,
South African Environmental Observation Network (SAEON), South Africa

REVIEWED BY
Peter M.J. Herman,
Delft University of Technology, Netherlands
David Burdick,
University of New Hampshire, United States

*CORRESPONDENCE
Lyndsay L. Rankin
✉ lrankin@usgs.gov

RECEIVED 02 May 2023
ACCEPTED 20 October 2023
PUBLISHED 21 November 2023

CITATION
Rankin LL, Jones SF, Janousek CN, Buffington KJ, Takekawa JY and Thorne KM (2023) Stress gradients structure spatial variability in coastal tidal marsh plant composition and diversity in a major Pacific coast estuary.
Front. Ecol. Evol. 11:1215964.
doi: 10.3389/fevo.2023.1215964

Stress gradients structure spatial variability in coastal tidal marsh plant composition and diversity in a major Pacific coast estuary

Lyndsay L. Rankin[1*], Scott F. Jones[1,2], Christopher N. Janousek[3], Kevin J. Buffington[1], John Y. Takekawa[4] and Karen M. Thorne[1]

[1]U.S. Geological Survey, Western Ecological Research Center, Davis, CA, United States, [2]Department of Biology, University of North Florida, Jacksonville, FL, United States, [3]Oregon State University, Department of Fisheries, Wildlife and Conservation Sciences, Corvallis, OR, United States, [4]Suisun Resource Conservation District, Suisun City, CA, United States

Understanding the drivers of variability in plant diversity from local to landscape spatial scales is a challenge in ecological systems. Environmental gradients exist at several spatial scales and can be nested hierarchically, influencing patterns of plant diversity in complex ways. As plant community dynamics influence ecosystem function, understanding the drivers of plant community variability across space is paramount for predicting potential shifts in ecosystem function from global change. Determining the scales at which stress gradients influence vegetation composition is crucial to inform management and restoration of tidal marshes for specific functions. Here, we analyzed vegetation community composition in 51 tidal marshes from the San Francisco Bay Estuary, California, USA. We used model-based compositional analysis and rank abundance curves to quantify environmental (elevation/tidal frame position, distance to channel, and channel salinity) and species trait (species form, wetland indicator status, and native status) influences on plant community variability at the marsh site and estuary scales. While environmental impacts on plant diversity varied by species and their relationships to each other, overall impacts increased in strength from marsh to estuary scales. Relative species abundance was important in structuring these tidal marsh communities even with the limited species pools dominated by a few species. Rank abundance curves revealed different community structures by region with higher species evenness at plots higher in the tidal frame and adjacent to freshwater channels. By identifying interactions (species–species, species–environment, and environment–trait) at multiple scales (local, landscape), we begin to understand how variability measurements could be interpreted for conservation and land management decisions.

KEYWORDS

plant diversity, tidal marsh, environmental gradient, GLLVM, environment–trait association, abundance modeling, rank abundance curve

1 Introduction

Natural and physical processes determine plant community organization along environmental gradients; yet, understanding these relationships is challenging given that numerous processes occur across multiple spatial scales. Vegetation communities are often influenced by biotic and abiotic factors (and their interactions) such as weather (temperature and precipitation); substrate (e.g., moisture, nutrients, microbes); topography; competition and facilitation; and disturbances such as drought, fire, and herbivory (Bridge and Johnson, 2000; Van der Heijden et al., 2008, Brooker et al., 2008; Clarke et al., 2010; Mokany et al., 2022; Xi et al., 2022). Climate-driven vegetation changes are well documented globally over the Holocene (e.g., Neumann et al., 2010; Marquer et al., 2017) and in multiple ecosystems from alpine and tundra to temperate forests (Michelsen et al., 2011; Oakes et al., 2014; Maliniemi et al., 2018; Song et al., 2018). Impacts from disturbances and changes in diversity drivers have also been shown to be scale dependent (Graham et al., 1990; Chaneton and Facelli, 1991; Bernhardt-Römermann et al., 2015). In managed tidal wetlands, plant diversity at local versus landscape scales was dependent on variables such as salinity gradients and water management (Jones et al., 2021). Differences in species rank and relative abundance across temporal and spatial scales can result from changes in community diversity and response to the environment (Jones et al., 2017; Avolio et al., 2019).

Tidal marshes are highly productive, dynamic ecosystems that help support estuarine biodiversity, confer flood protection, and have aesthetic and recreational value (Barbier et al., 2011). Marsh environmental gradients are guided by elevation and tidal range (Rogers and Woodroffe, 2015) as well as past hydrological manipulations (Oosterlee et al., 2018). Tidal marshes are dominated by halophytic plants adapted to natural flooding regimes (Adam, 1993), with flooding controlling local site geomorphology, nutrient availability, soil and water salinity, and soil redox. These flooding regimes influence the zonation and productivity of marsh halophytic plant species (Engels et al., 2011; Janousek et al., 2016). Species zonation is also impacted by species-level interactions (Bertness, 1991; Crain et al., 2004). Human activities and disturbances have had profound influences in tidal marshes, altering environmental conditions such as flooding patterns, sediment availability, nutrient levels, contaminants, water quality, and the introduction of invasive species (Takekawa et al., 2006; Gilby et al., 2021) and affecting species distributions (Gedan et al., 2009).

Vegetation patterns are important indicators of ecosystem transformations from anthropogenic stressors such as land-use change (Tasser and Tappeiner 2002), non-native species invasion (Sundaram and Hiremath, 2012), and water diversion (Elmore et al., 2003). For example, land area may change when freshwater diversion or reconnections occurs (White et al., 2023) and plant communities may change with diking of low tidal lands (Mora and Burdick, 2013) or seasonal impoundment of tidal marshes (Jones et al., 2021). Large scale ecosystem transformations have been documented over the last century primarily due to human disturbance, including modification to hydrologic conditions (Busch et al., 1998). In the Everglades of southeast Florida, USA, the marsh vegetation communities have changed over the last 80 years due to road and levee building and sea-level rise (SLR) (Ross et al., 2000). A similar type of comparison study documented a stable vegetation community in Greenland over 40 years, possibly due to the small magnitude of temperature change (Daniëls et al., 2011).

The *stress gradient hypothesis* is one framework for understanding plant community organization (Bertness and Callaway, 1994; Maestre et al., 2005; Lortie and Callaway, 2006; Maestre et al., 2009). The hypothesis states that biotic interactions are driven by facilitation (positive interactions) under conditions of high abiotic stresses (e.g., temperature, salinity, inundation) and competition under more benign conditions (Maestre et al., 2006). Considering that tidal marshes are naturally a stressful environment it can be difficult to determine if plant community organization is driven by facilitation or competition as outlined by the stress gradient hypothesis. A conceptual model for tidal marshes states that plant community composition is driven primarily by the abiotic factors of the system (Kirwan and Guntenspergen, 2015). In a mesocosm experiment, Schile et al. (2017) demonstrated that facilitation did not occur between two marsh sedges when increased flooding was simulated. In a field and greenhouse experiment, Morzaria-Luna and Zedler (2014) found that the type of stress gradient, salt marsh species, and experiment duration determined the role of competition and facilitation. The spatial scale of a study could also feasibly impact how environmental gradients shape species interactions and diversity.

Understanding the influence of stress gradients on plant communities is also important in preparing for future climate impacts (Bertness and Ewanchuk, 2002). Climate change and SLR will cause a substantial shift in several fundamental abiotic characteristics of estuaries (Parker and Boyer, 2019) but impacts to vegetation communities may be less clear and scale dependent. Accelerating ocean and atmospheric warming, changing water salinity (Cloern et al., 2011), fog, freshwater flow from tributaries, and SLR (IPCC, 2022) will alter the condition and distribution of marshes. These alterations can become “early indicators” of estuary change (Rogers et al., 2014; Garner et al., 2015).

Given that plant diversity and distribution influence ecosystem function, identifying the drivers of these patterns at multiple scales is paramount for understanding potential shifts in ecosystem function and managing for climate impacts. We conducted an analysis on a large vegetation, elevation, water level, and channel salinity dataset compiled over a decade to examine how gradients of flooding influence tidal marsh vegetation patterns across multiple scales in the San Francisco Bay Estuary, California, USA. Our questions were: (1) Which environmental gradients influence species diversity at the site and estuary scale? (2) Are species correlations impacted by environmental gradients? (3) Do species traits explain environmental drivers of diversity? and (4) Do differences in species rank and relative abundance influence the structure of marsh communities given the limited species pools?

2 Methods

2.1 Study sites

The San Francisco Bay Estuary (SFBE) in California is the second largest estuary in the United States and comprises nine counties with a population of over 8 million people (United States Census Bureau, 2021). The estuary has a Mediterranean climate with mild rainy winters and cool foggy summers. The weather is largely influenced by the cold water of the California Current flowing toward the equator year-round and the Davidson Current bringing warmer water toward the pole during the winter months. The SFBE is made up of multiple regions with different environments – South San Francisco Bay, Central San Francisco Bay, San Pablo Bay, Suisun Bay, and the Delta (Figure 1). In this inverted estuary, the Sacramento and San Joaquin Rivers flow through the Delta into brackish Suisun Bay and through the narrow Carquinez Strait into the greater San Francisco Bay embayment (Cloern and Jassby, 2012). Tidal marine waters are exchanged through the Golden Gate to the Pacific Ocean. The tidal regime is mixed semidiurnal with an average diurnal range of 2.6 m in South San Francisco (SF) Bay, 1.8 m in San Pablo Bay, and 1.2 m in the Delta (NOAA tide stations 9414509, 9415252, 9415316; https://tidesandcurrents.noaa.gov). Despite its highly urbanized landscape (Nichols et al., 1986), the SFBE is home to an array of wildlife that use tidal wetlands, including state and federally listed species such as the Chinook salmon (*Oncorhynchus tshawytscha*), California Ridgway's Rail (*Rallus longirostris obsoletus*), salt marsh harvest mouse (*Reithrodontomys raviventris*), Delta smelt (*Hypomesus transpacificus*), and longfin smelt (*Spirinchus thaleichthys*) (California Endangered Species Act 1970; Federal Endangered Species Act 1973; California Natural Diversity Database (CNDDB), 2023). It is important habitat for migratory and nesting birds, supporting more than 50% of the Pacific flyway waterfowl and millions of shorebirds (Takekawa et al., 2001). Tidal marshes in the more saline parts of the estuary generally lie above mean tide level (MTL) and are characterized by relatively flat elevation platforms occurring around mean high water (MHW) (Takekawa et al., 2013a). Extensive modifications of the estuary have resulted in 80% loss of historic tidal wetlands, but restoration efforts are ongoing (Marcus, 2000).

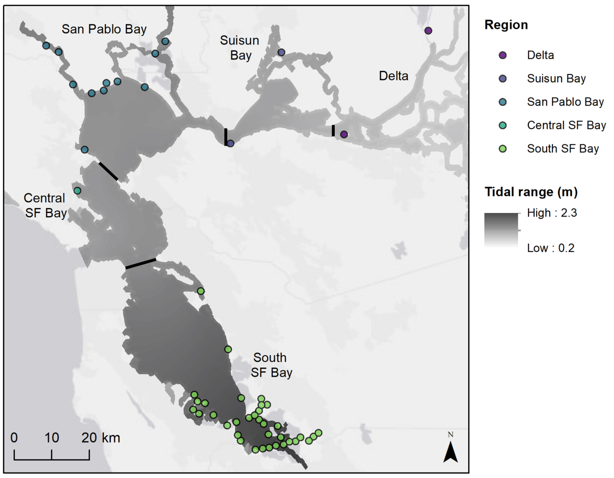

FIGURE 1
Map of study sites colored and labeled by region (sub-embayments). Tidal range is displayed in greyscale from low to high (NOAA VDATUM model; Parker et al., 2003).

For this effort, fifty-one tidal marsh sites across five regions (sub-embayments) were surveyed in the Delta, Suisun Bay, San Pablo Bay, Central SF Bay, and South SF Bay (Figure 1). These sites varied in geographic size, sample size, geomorphic setting, and tide range (Table S1). Some sites were close in proximity, such as many of the South Bay sites. However, sites were separated by large channels or land features that delineated their physical boundaries.

2.2 Field surveys and environmental data

Vegetation surveys spanned ten years, from July 2008 to October 2018 (Table S1). A total of 5,026 plots were surveyed. Most plots were positioned on transects along an elevation gradient, while non-transect plot placement was used at one site (Arrowhead Marsh) due to its small size and the desire to avoid endangered wildlife species. Most transects were evenly distributed across each site, where possible, to capture spatial variability along elevation and distance gradients. At each plot, percent cover of all plant species, bare ground, and litter was visually assessed within a 0.25 m^2 quadrat. Total plant cover in a plot could exceed 100 percent due to vegetation layering. Bare ground and litter cover was estimated as total area visible through the vegetation from above the plot. Vascular plant nomenclature followed Baldwin et al. (2012). Geographic position (in UTM) and elevation (North American Vertical Datum of 1988, NAVD88) were recorded at each plot. Sampling season was not expected to significantly influence species identification and cover estimates. The Mediterranean climate of the SFBE with short mild winters creates fairly unseasonal wetlands. Most of the wetland species are perennial and identifiable throughout the year.

Environmental gradients were selected based on previous studies that identified soil salinity and tidal inundation as the most influential drivers of tidal marsh vegetation structure (Engels and Jensen, 2009; Watson and Byrne, 2009; Janousek and Folger, 2014). Channel salinity was calculated at the site or multi-site scale (in PSU, Table S1) with data from locally deployed water sensors or from San Francisco Bay National Estuarine Research Reserve (NERR) sites (Takekawa et al., 2013a, Thorne et al., 2019; Table S2). Salinity dataloggers (Solinst and Odyssey) were programmed to record specific conductivity (in µS/cm) at 12-minute (Solinst) or 30-minute (Odyssey) intervals and were deployed for a minimum of one year. Annual mean salinity was calculated across the deployment period and converted to PSU. Salinity values were assigned to each marsh based on nearest available measurements, from either a NERR site or logger deployment. All salinity values represent marsh channel or creek conditions, and not soil porewater salinity.

A survey-grade Real Time Kinematic (RTK) global positioning systems (GPS) rover was used to measure location and elevation

(± 1 cm horizontal, ± 2 cm vertical manufacturer-stated accuracy; Leica Geosystems Inc., Norcross, Georgia). Rover positions were received in real time from the Leica Smartnet system using a CDMA modem (http://www.leica-geosystems.us/en/index.htm). The WGS 84 ellipsoid model was used for horizontal positioning and NAVD88 for vertical positioning. Rover accuracy and precision were evaluated by measuring positions at local National Geodetic Survey benchmarks; all errors were within the stated rover error. Elevation data was converted to z* ($z^* = [\text{NAVD88} - \text{MTL}]/[\text{MHHW} - \text{MTL}]$), a unitless measure of elevation relative to the local tidal frame which accounts for variation in tidal range and allows for direct comparison across sites (Swanson et al., 2014).

Local tidal datums were calculated from multiple sources including NOAA tide stations (https://tidesandcurrents.noaa.gov/), deployed water level loggers, and NOAA's VDATUM model (Parker et al., 2003; Table S2). Water loggers (Solinst) were deployed at select sites and programmed to record water level information at 6-minute intervals. Data were corrected for atmospheric pressure with barometric data from barometric dataloggers (Solinst; Takekawa et al., 2013a; Thorne et al., 2019). These water level values were used to calculate mean higher high water (MHHW) while mean tidal level (MTL) was estimated from NOAA's VDATUM model (Parker et al., 2003). At some sites, we used tidal datums from nearby NOAA tide gages where local loggers were absent (Table S2).

Distance to channel was calculated as the distance (in meters) between each plot and the digitalized boundaries of all nearby channels and bays. Channels were digitized based on 2020 NAIP imagery supplemented with LiDAR when necessary. The centerline was digitized on small channels (~1 – 2.5 m wide), while both edges were digitized on large channels (> 2.5 m), bays, and rivers.

2.3 Statistical analyses: site and estuary abundance models

To understand the relationship between plant communities and environmental gradients at different scales, generalized linear latent variable models (GLLVMs; Skrondal and Rabe-Hesketh, 2004) were analyzed in R version 4.2.2 (R Core Team, 2022; package 'GLLVM'; Niku et al., 2019; Niku et al., 2021) at the site and estuary levels. This type of model incorporates latent variables that quantify species response correlations and environment-trait interactions, known as fourth-corner terms (Skrondal and Rabe-Hesketh, 2004; Niku et al., 2021). At the site scale, GLLVMs were built with elevation (tidal position) and channel distance as environmental covariates. At the estuary scale, one model was built using all plot data. Site sampling intensity was accounted for by including row effects by site. Salinity was added as an environmental covariate to the estuary model as salinity data were collected at the site/multisite levels. All models were fit using negative binomial distributions. They identified species with strong associations, either negative or positive, between environmental covariates and species presence and abundance. Strong associations were defined by models with confidence intervals that did not overlap with zero. Associations were used to identify how elevation (tidal position), channel distance, and salinity influenced plant presence and abundance at the site and estuary scales. Species that changed associations between the site and estuary models were identified to examine scale-dependency.

Species associations from site and estuary abundance models were combined with percent cover values from field surveys to calculate site-specific cover of species with strong associations to each environmental variable. All species with strong associations (either negative or positive for each environmental covariate) were identified by site, and their mean percent cover values were added together to compute a total percent cover of strongly associated species. Sites with high total cover values indicate marsh communities most influenced by elevation, channel distance, or salinity.

2.4 Species correlations

To investigate the impacts of environment conditions on species interactions, species correlation matrices were compared between models with and without environmental predictors (elevation, channel distance, and salinity). Species positively correlated with each other could indicate facilitation while competition may be identified by negative correlations. Latent variables used in GLLVMs include correlation values across all model response variables used to create correlation matrices. Species relationship differences across environmental gradients were also identified by comparing correlation matrices from data subset along gradient thresholds.

2.5 Environment–trait interactions

To examine why species differ in their response to environmental drivers, species traits were incorporated into a "fourth corner" estuary model. Species traits included: California native/non-native status, wetland indicator status (upland – almost always occurs in upland habitat; facultative upland – usually occurs in upland habitat; facultative – equally likely in upland and wetland habitats; facultative wetland – usually occurs in wetlands; and obligate – almost always occurs in wetlands), and plant form (tree, shrub, forb/herb, and graminoid) (USDA, 2023; calflora.org; Baldwin et al., 2012). Strong environmental–trait interactions, or fourth corner terms, were identified from model coefficient plots.

2.6 Rank abundance curves

Differences in relative species abundance were examined by creating rank abundance curves (RACs) for each site and region as well as environmental covariates. Species richness and species evenness were evaluated by comparing RACs within regions and across the estuary. RAC differences were compared by site and region using R (package 'CODYN'; Hallett et al., 2020).

3 Results

3.1 Surveys

Eighty-one species were identified across all sites surveyed (Table S3). The number of species per site ranged from 1 to 31 with an average of 8.0 ± 6.5 species per site. Most plots were dominated by one or two plant species.

3.2 Site and estuary abundance models

At the site scale, elevation/tidal position (z*) was strongly associated with plant cover for more than half of the species (58%; Figure 2A). Most of these species (70%) had a positive association with elevation – they were more abundant at higher elevations. Some species that were more abundant at lower elevations included *Schoenoplectus americanus* and *Spartina foliosa*. Distance to channel had a weaker relationship with species abundance with an average association of 52%. Most of these species (73%) had a negative association with distance to channel indicating they were more abundant closer to a tidal channel or bay edge, such as *Spartina foliosa*.

At the estuary scale, environmental covariates (elevation/tidal position, distance to channel, and salinity) explained about 49% of the total community variation (Figure 2A). After incorporating region as a variable, the covariates explained about 65% of the variation. Of the three environmental covariates we examined, elevation and distance to channel had the strongest association with species composition. Elevation was associated with species abundance for 64% of the species, distance to channel for 57%, and salinity for 51% (Figure 2A). Coefficient estimates varied between site and estuary scale models as seen in 9 abundant species of interest in the estuary (Figure 2B).

Assigning a single environmental association for each species across the estuary, as opposed to each site, resulted in associations that were either confirmed (no association to positive or negative), changed (negative to positive or vice versa), or lost (positive or negative to no association) (Figure 3). With an increase in sample size, the estuary model confirmed existing positive associations to elevation (tidal position) for species such as *Atriplex prostrata* and *Frankenia salina* (Figure 3A). At the estuary level, *Typha* species had a negative association to elevation (tidal position) but at the site level these species had no strong association or even a positive association to tidal position in the Delta (Figure 3A). *Salicornia pacifica* had a negative association and no association to tidal position at multiple marsh sites (7 and 25 respectively of 49 sites), yet the estuary model identified a strong positive association (Figure 3A).

Schoenoplectus americanus had a strong association to tidal position at most of its marsh sites but did not have a strong association at the estuary scale (Figure 3A).

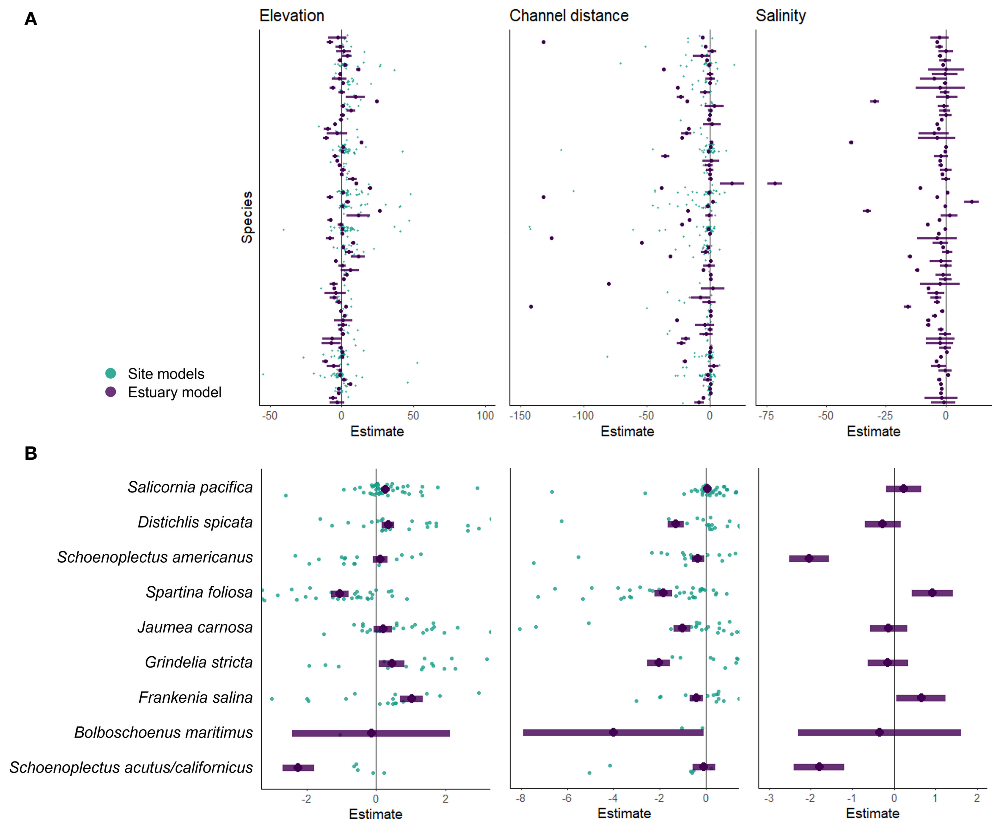

FIGURE 2
GLLVM species estimates for elevation, channel distance, and salinity covariates for all species **(A)** and 9 abundant species of interest **(B)**. Teal points are estimated coefficients modeled at the site scale. Purple points and lines are estimated coefficients with 95% confidence intervals modeled at the estuary scale (one value per species).

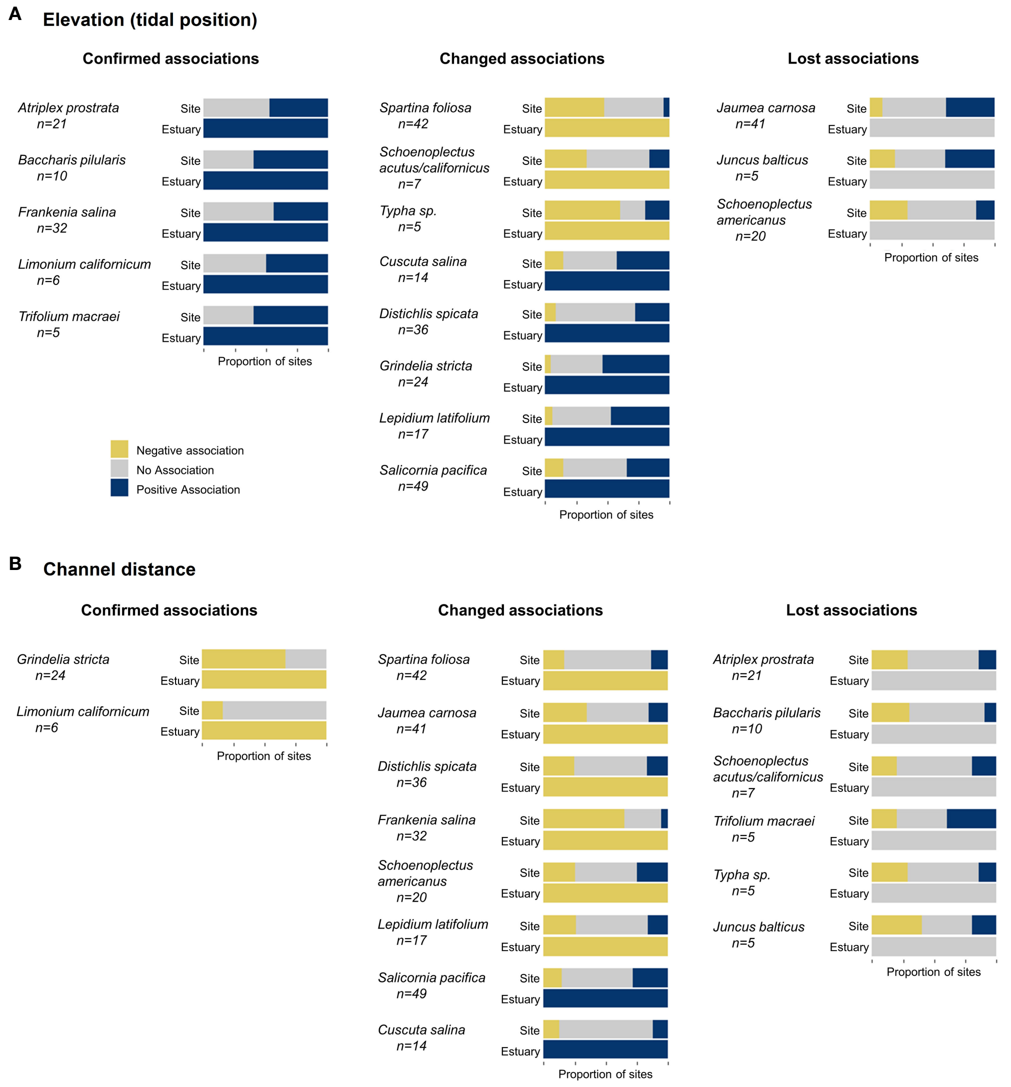

FIGURE 3
Proportion of marsh sites with negative and positive associations to elevation/tidal position **(A)** and channel distance **(B)** from site- and estuary-level modeling. Species are grouped by environmental association differences between scales, including those with confirmed associations (no association to positive or negative), changed relationships (positive to negative or negative to positive), and lost relationships (positive or negative to no association). Species shown here were located at a minimum of 5 marsh sites (total number of sites are listed below each species name).

Similar differences in species association to channel distance occurred between site and estuary models. The increased sample size confirmed negative associations for *Grindelia stricta* and *Limonium californicum*, but more species changed or lost associations between scales (Figure 3B). *Schoenoplectus americanus* had a strong positive association at 5 sites and no association at 10 sites (of 20 sites), yet a negative association at the estuary scale (Figure 3B). *Jaumea carnosa* had a positive association with channel distance at 7 of 41 sites, including all sites in the Delta and Suisun Bay where it was located, yet a negative association across the estuary. *Atriplex prostrata* had a strong association to channel distance at 9 of 21 marsh sites but did not have a strong association at the estuary scale (Figure 3B).

The total percent cover of species with strong association to these variables differed greatly by site (Figures 4A, C, Table S4). Sites with the highest percent cover of species associated with elevation were in Suisun Bay and the Delta, while the sites with the lowest percent cover were in South SF Bay (Figure 4A). Total percent cover of species associated with channel distance varied across the regions with the highest cover in Suisun Bay (Figure 4C). Given that species associations varied considerably between site models, associations at the site scale did not always correspond to associations at the estuary scale. Spatially, there was a narrower range in percent cover values across sites based on the estuary-wide model (Figures 4B, D, E, Table S4). Most sites had moderate to high cover of species strongly associated with elevation and channel distance (Figures 4B, D). The greatest cover of species associated with salinity occurred at more inland sites associated with freshwater sources in Suisun Bay, the Delta, and the southeastern area of South SF Bay (Figure 4E). More species had strong associations with elevation and channel distance when modeled at the estuary scale compared to the site

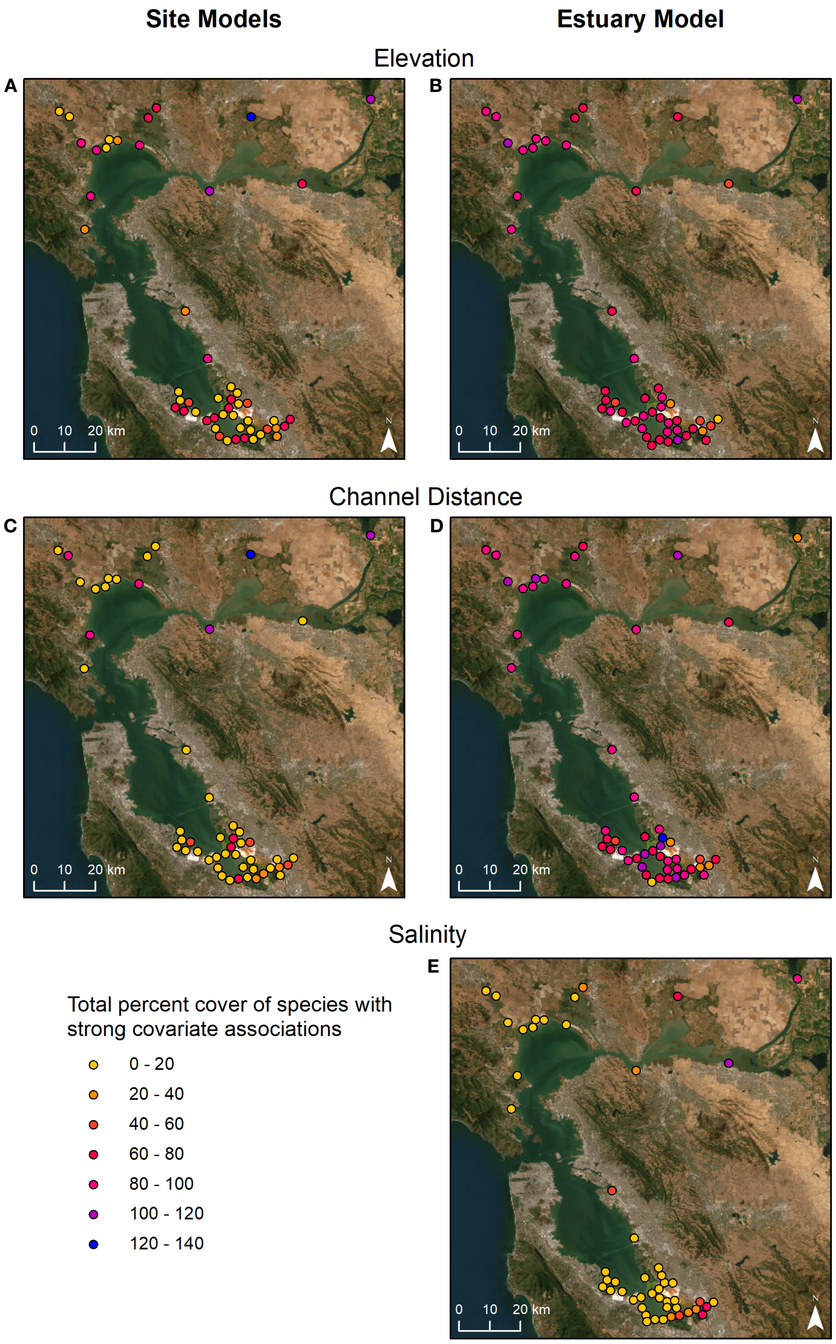

FIGURE 4
Marsh sites colored by total percent cover of plant species with strong associations to elevation, distance to nearest channel, and salinity modeled at the site **(A, C)** and estuary **(B, D, E)** scale.

scale (Figure S5). Species associations were less frequent for channel salinity (Figure S5).

3.3 Species co-occurrence patterns

Without accounting for environmental conditions, multiple positive species correlations were identified (Figure 5A). When environmental variables were incorporated into the model, almost no species correlations were observed (Figure 5A). Species were most likely found together because they had similar habitat preferences. The environmental gradients explained nearly all the species interactions when modeled across the entire estuary. However, species co-occurrence patterns did vary along the salinity gradient, where both positive and negative correlations were more common adjacent to less saline channels (Figure 5B). Species co-occurrence patterns appeared unaffected by position within the tidal frame and proximity to channel edge (Figure 5B).

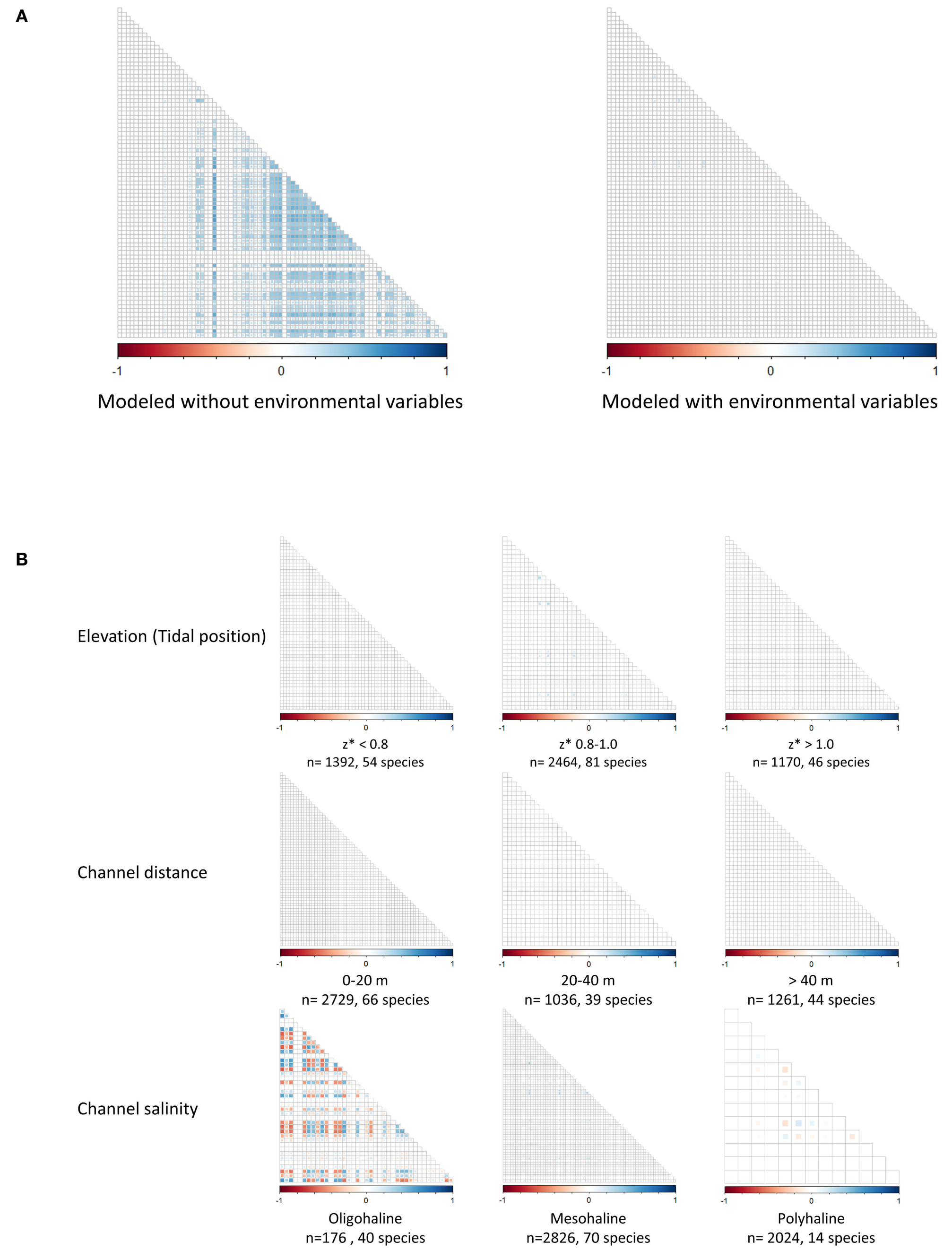

FIGURE 5
Species correlation matrices modeled with and without environmental variables **(A)** and along environmental gradients **(B)** (Elevation/tidal position, Channel distance, Channel salinity). Each gradient dataset includes sample size and number of species. Red squares indicate negatively correlated species, and blue squares indicate positive correlations.

3.4 Environment–trait interactions

Multiple environment–trait interactions were observed between regions and along environmental gradients (Figure 6). As expected, trees were more abundant higher in the tidal frame and farther from channel edges whereas shrubs, forbs/herbs, and graminoids were found closer to channels. Only forbs/herbs showed interactions along the salinity gradient as they were less abundant near saline channels. Species wetland status had no impact on abundance across the elevation gradient. All species had varying degrees of negative association to channel distance regardless of wetland status. Only upland species showed an interaction with salinity as they were more abundant near saline channels.

The influence of all species traits (form, wetland status, and native status) on abundance varied between regions (Figure 6). Trees were more abundant in San Pablo Bay and less abundant in Suisun Bay whereas shrubs had the opposite relationship. Forbs/herbs were more abundant in San Pablo Bay and graminids more abundant in South SF Bay. Obligate wetland species were less abundant in Central and South SF Bay. Facultative species were

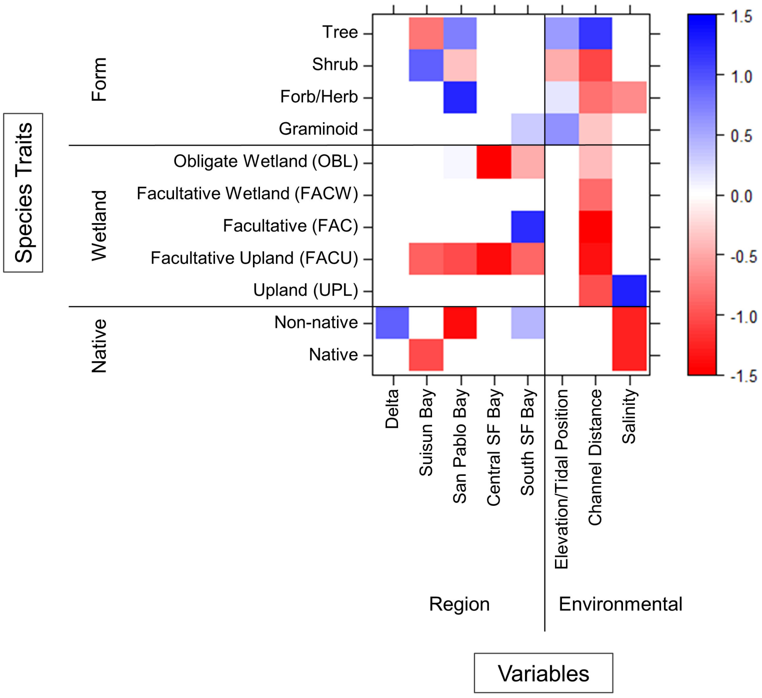

FIGURE 6
Environment–trait relationships that influence species abundance at the estuary scale. Interactions colored blue indicate positive associations and red indicate negative associations.

more abundant solely in South SF Bay. Facultative upland species were less abundant at all regions except for the Delta. Native plant species were less abundant in Suisun Bay. Non-native species were most abundant in the Delta and South SF Bay and less abundant in San Pablo Bay.

3.5 Rank abundance curves

RACs illustrated different levels of species dominance by site and region (Figure 7). Lower species evenness was observed at sites in San Pablo Bay, Central SF Bay, South SF Bay, and Delta. Most of these sites had similar species diversity, with *Salicornia pacifica* as the most abundant species (Figures 7B, D–F). The more inland sites at Suisun Bay exhibited higher evenness. Most sites in this fresher part of the estuary (Delta and Suisun Bay) did not have an individual species that accounted for over 50% of the proportional abundance (Figures 7A, B).

RACs by environmental gradients demonstrated a clear influence of flooding and salinity on species rank and abundance (Figure 8). Lower species evenness and similar dominant species (*Salicornia pacifica* and *Schoenoplectus acutus*) were measured at plots lower in the tidal frame ($z^* < 1.5$; Figure 8A). Plots higher in the tidal frame ($z^* > 1.5$) exhibited higher species evenness with variable dominant species (*Festuca microstchys* and *Baccharis pilularis*). There was no measurable difference in species rank or abundance by distance to channel (Figure 8B), *Salicornia pacifica* was always most abundant. The communities located near oligohaline channels with assumed lower soil salinity had more species evenness, while communities adjacent to more saline channels were dominated by *Salicornia pacifica* (Figure 8C).

Pairwise comparisons of site RACs revealed that sites differed most by species richness, calculated as the difference in richness between samples divided by the number of unique species in both samples (40%; Figure S6A). Species rank was the next most important measure of site difference (25%) followed by species number (22%) and evenness (15%; Figure S6A). Species number is calculated as the difference in species number between samples divided by the total number of species in both samples. While all sites were treated independently in the RAC comparison, sites within the same region would be expected to have similar RACs. The unequal number of sites by region could possibly affect which metric detected the most difference in RACs. However, when comparing differences by regional RACs, the order and magnitude of importance metrics were comparable (species richness – 49%, rank – 27%, species number – 26%, and evenness – 3%) (Figure S6B). Species richness and rank explained most of the variability in the plant communities across the estuary at the site and regional scale.

4 Discussion

Our results showed that vegetation communities were organized within marshes along expected gradients of abiotic drivers (i.e, elevation, flooding). This aligns with other marsh studies that found plant communities organized by climate and human impacts (Ewanchuk and Bertness, 2004), and flooding and salinity tolerances (Muench and Elsey-Quirk, 2019). Multiple

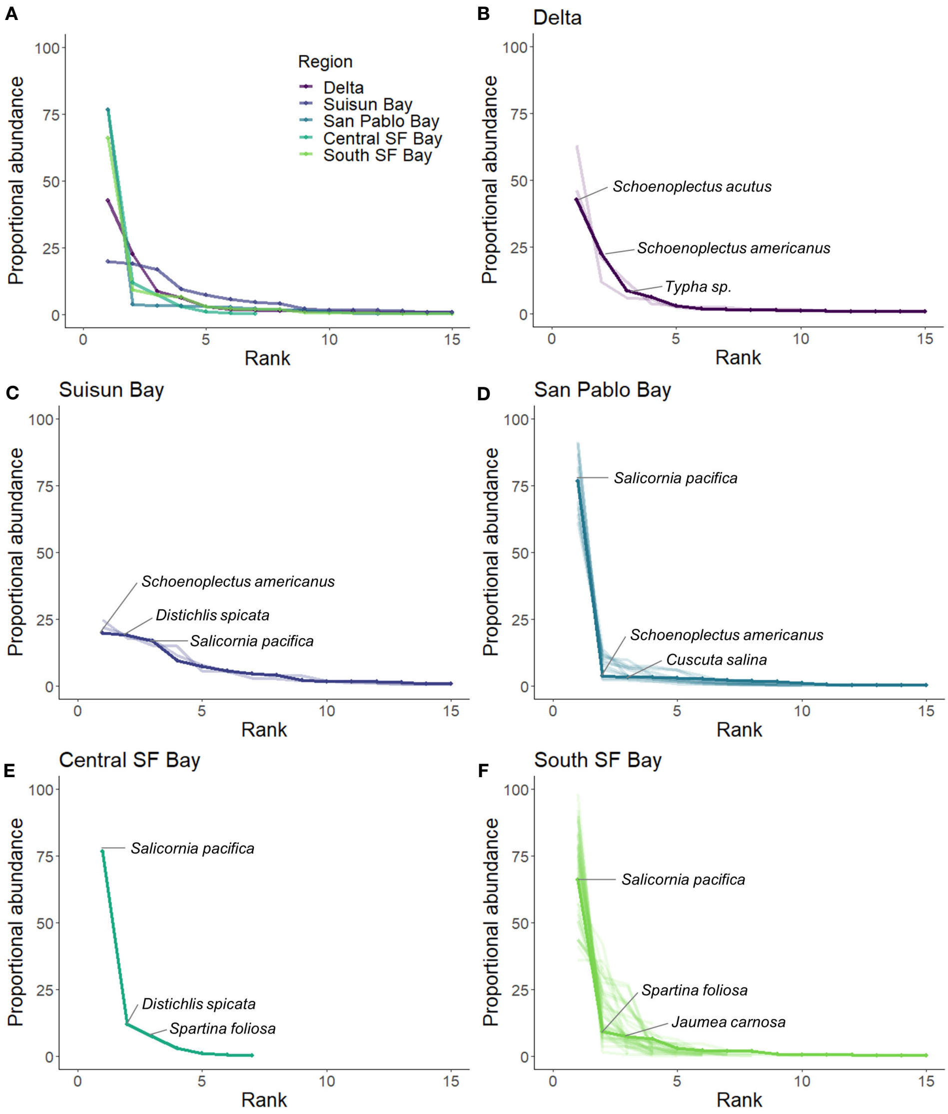

FIGURE 7
Rank abundance curves (RACs) calculated by region [solid lines; **(A–F)**] and sites within region [transparent lines; **(B–F)**]. The three most abundant species are labeled within region.

manipulation studies have demonstrated the importance of flooding and salinity tolerances to marsh plant distribution and abundance (e.g., Sharpe and Baldwin, 2012; Peng et al., 2018; Buffington et al., 2020). However, plant species differ in their tolerance of abiotic stress or deviation from the optimum conditions, enhancing plant species stratification within a site (e.g., Liancourt et al., 2005). While we found similar drivers of plant diversity at both the site and estuary levels, the magnitude of importance and direction of effects varied by scale, indicating context dependency (Figure 2). Regional or estuary-wide results are useful to identify trends but using them to inform management decisions at specific sites may not be ideal. Given that species associations change from site to estuary scales, local-scale processes and site variables should be investigated.

The *stress-gradient hypothesis* predicts that relative frequency of plant facilitation and competition will vary inversely with physical stress (Maestre et al., 2005) with the lower limit of marsh plant distribution set by abiotic stress and the upper limit set by biotic competition (Bertness and Ellison, 1987; Menge and Sutherland, 1987; Pennings et al., 2005), similar to our finding of abundant species correlations adjacent to oligohaline channels (Figure 5). Yet, species correlations were not observed higher in the tidal frame or further from channels, at the more stressful end of the inundation gradient (Figure 5). Species richness and evenness was quite high in the oligohaline marshes (Figures 5, 8). Less salt stress, abundant perennial and annual species, and lack of species dominance builds complex community structures in oligohaline marshes (Odum, 1988). This could result in multivariable biotic and abiotic interactions, making it difficult to identify competition and facilitation in these marshes. In the SFBE, plant species diversity decreased with salt tolerant species increase, presumably due to water diversion and dams (Goman et al., 2008). How stress gradients

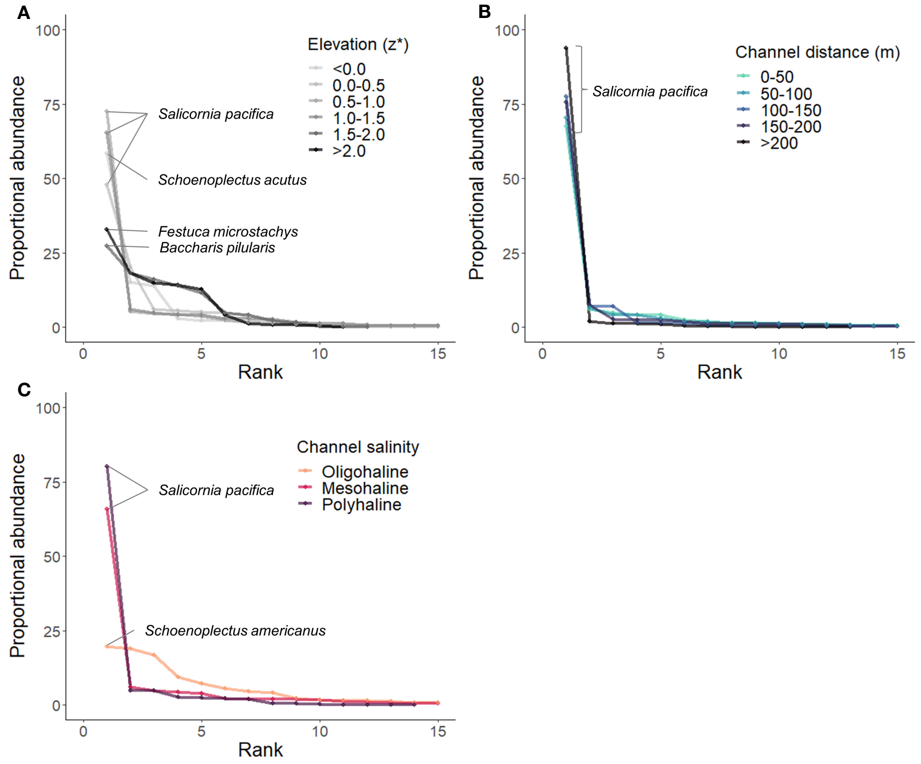

FIGURE 8
Rank abundance curves (RACs) calculated by stress gradient [**(A)** Elevation/tidal position, **(B)** Channel distance, **(C)** Salinity]. The topmost abundant species are labeled.

impact plant variability can be unpredictable as species abundance is not solely based on environmental interactions but also species–species interactions and environmental–trait interactions.

4.1 Species relationships are related to wetland structure

Within tidal marshes, plant functional traits have the potential to influence both marsh processes (e.g., accretion, channel formation) and species distributions (Schwarz et al., 2018). In our analysis, there was some variation between the environmental gradients and species trait relationships (Figure 6). Trait relationships varied between regions, possibly signaling additional environmental conditions that were not represented in the models or region-specific species responses. Tidal wetlands differ in channel structure, hydrology, elevation, and salinity which can result in variable relationships with common plant species (Watson and Byrne, 2009; Janousek and Folger, 2014). Understanding linkages between biogeomorphic features in estuaries and plant species composition is key to understanding vegetation community organization at small and large spatial scales (Van de Koppel et al., 2012). While all study sites were tidal with similar biogeomorphic features, the patterns of old dikes, berms, and levees throughout each site could have impacted plant communities at a much finer scale. Individually constructed earthen levees can impact ecosystem processes at coastal marshes long after abandonment (Hall et al., 2022). These "hidden levees" can cause a disconnect between channel distance, elevation, and inundation regime resulting in less flood tolerant vegetation and shallower organic rich soils landward of the abandoned levees (Hall et al., 2022). More research is needed on the impacts of past biogeomorphic features at these sites.

Our analysis showed that distance to channel and elevation relative to tidal flooding were the primary drivers for vegetation community structure and plant variability, but the magnitude of importance of these drivers varied by marsh site and scale. However, other factors related to flooding could be useful in determining stress gradient impacts, such as inundation frequency and duration. Future studies would benefit from more in-depth interaction measurements and species-specific responses to environmental stress gradients. Different halophyte plant species have varying tolerances to flooding; for example *Spartina foliosa* (California cordgrass) can tolerate extended flooding and *Salicornia pacifica* (pickleweed) is tolerant of higher salinities (Woo and Takekawa, 2012; Takekawa et al., 2013b; Gallego-Tévar et al., 2020). The spatial variability and distribution of plants by traits can be used to infer multiple habitat characteristics, but recent research suggests that there are limits to the extent to which traits can be related to ecosystem properties (Van der Plas et al., 2020).

4.2 Scale is important in spatial trends

This analysis identified elevation (tidal frame position), channel distance, and channel salinity as variables that strongly influenced abundance for more than half of the species at both the marsh site and estuary scales. Previous research found similarly strong responses of plant diversity to channel distance (Sanderson et al., 2001). The observed difference in magnitude of effect is supported by previous work which found plant diversity was dependent on scale (Jones et al., 2021; Korell et al., 2021), elevation (Janousek et al., 2019), and salinity (Bonin and Zedler, 2008). At the site scale, the highest total cover of species associated with elevation were in the Delta and Suisun Bay, possibly indicating more zonation in areas with lower tidal ranges and an increase in plant cover related to brackish and freshwater conditions; these marshes are dominated by grass and graminoid families such as Poacae (grasses), Cyperaceae (sedges), and Juncaceae (rushes). Sites with high cover associated with channel distance were spread across the estuary at both the marsh site and estuary scales. Many marshes have higher cover near channels due to the presence of *Grindelia stricta* (gumplant) and *Salicornia pacifica* (pickleweed). There are other additional factors with site-specific gradients, such as soil salinity, that may contribute to the importance of channel distance in species abundance. Sites with freshwater influence (the Delta, Suisun Bay, inland South SF Bay) had more species with abundance driven by channel salinity. Future studies should include soil salinity, rather than channel salinity, to capture site variability and improve site-level model coefficient strength.

As sea levels rise, marsh plant communities will shift from primarily high marsh species to low marsh species (Donnelly and Bertness, 2001; Wasson et al., 2013), significantly changing habitats. These types of plant species shifts have been projected under accelerating SLR scenarios, demonstrating drastic changes over the coming century with loss of relative elevation (Schile et al., 2014; Thorne et al., 2018; Buffington et al., 2021). At the site level, Miner Slough in the Delta and Coyote Creek in South SF Bay had the highest plant cover negatively associated with salinity. In other words, plant abundance was highest at low salinities throughout these sites, making them particularity vulnerable to saltwater intrusion from SLR. Miner Slough is a freshwater tidal marsh site located off the Sacramento River and the only freshwater Delta site in our study; therefore, a larger sample size of similar marshes is needed to determine if this pattern holds. Coyote Creek marsh is located on a large channel with freshwater input from an upland sewage treatment plant, and therefore, is a unique case study in SFBE.

Species were found to respond differently to environmental factors depending on the scale. For example, *Schoenoplectus americanus*, a bulrush native to CA, exhibited a strong positive association with elevation in the estuary scale model and in multiple, but not all, marsh site models. Strong negative associations to elevation were documented at the two Suisun Bay sites as well as half of the San Pablo Bay sites. Similar site-specific variations in plant vertical zonation have been previously observed along the Pacific coast (Janousek et al., 2019). As an obligate wetland species, *S. americanus* is expected to be more abundant closer to channels (as was seen in the estuary model), but some site models documented the opposite relationship (namely both Suisun Bay sites and a few sites in San Pablo Bay and South SF Bay). Species-environment associations that changed between site and estuary models indicate scale dependency for select species and environmental gradients (Figure 3). A combination of multiple environmental factors, rather than a single gradient, is likely responsible for marsh plant zonation (Eleuterius and Eleuterius, 1979; Silvestri et al., 2005). Other factors with the potential to influence plant diversity and composition at different scales include competition (Costa et al., 2003), microtopography (Courtwright and Findlay, 2011), soil salinity (He et al., 2011), herbivory (Rand, 2002; Elschot et al., 2017), geomorphic setting (Shipley, 2010), and local climate (De Leeuw et al., 1991). There could be fewer species capable of withstanding saline conditions, impacting diversity and rank abundance. Saltwater intrusion in some marshes has also been shown to strongly affect species composition rather than factors such as biomass production (Li and Pennings, 2019). More investigation is needed to understand ecosystem wide drivers of plant communities, which could be done with remote imagery (e.g., Li et al., 2005; Rosso et al., 2005; Adam et al., 2010) and long-term monitoring of abiotic drivers (Trowbridge et al., 2016).

The difference in plant associations from the site to estuary scales and overall trait interactions could be influenced by unequal samples within regions. South SF Bay had the most sites (35 sites; 1,567 plots) and San Pablo Bay had the most plots (11 sites; 2,864 plots) compared to Suisun Bay (2 sites; 176 plots), the Delta (2 sites; 88 plots), and Central SF Bay (1 site; 361 plots). The dataset also contained unequal covariate distributions with most plots existing close to channels, near MHHW ($z^* = 1$), and adjacent to mesohaline channels (Figures S1–S4). Given the deficient quantity of freshwater tidal marsh sites in the estuary due to development, there was not enough power to confidently detect the loss of rare plants, something common to freshwater systems since these communities experience drastic changes in response to shifting environmental gradients (Neubauer, 2013; Li et al., 2022).

Species associations with environmental gradients were sometimes stronger (larger coefficients and greater species cover; Figures 2, 4) at the site scale compared to the estuary scale, but when averaged across all sites, the estuary scale model had more species associations (Figure S5). Even though species pools were fairly similar across all sites (10 species made up 90% of occurrences), the relative abundance was determined by prevailing environmental conditions specific to the site. Local changes in environmental drivers influence plant communities within a small regional inference space, as seen in the variable RACs (Figures 7, 8). Understanding how local conditions influence plant variability is crucial in land management and conservation. At landscape scales, changes in vegetation patterns have been documented by large disturbance events (e.g., fire; Taylor et al., 2021) and human impacts (e.g., human pressure; Malavasi et al., 2016). Ecological studies at small scales would require different interpretations than a large-scale study.

4.3 Climate change relevance

There has been a growing interest in how best to track the effects of our changing climate. Increased flooding due to SLR can lead to vegetation loss and conversion of marsh to unvegetated mud flat (Orson et al., 1985; Morris et al., 2002), as well as an increase in erosion, creation of new channels, and the expansion of existing channels (Moffett and Gorelick, 2016). Increasing inundation can affect salinity concentrations leading to changes in plant communities, biomass, and productivity (Engels and Jensen, 2009; Ryan and Boyer, 2012; Janousek and Mayo, 2013; Snedden et al., 2015; Janousek et al., 2016). Previous modeling in California marshes showed drastic changes in marsh vegetation under SLR scenarios (Thorne et al., 2018); however, these models are based on generalizations of plant tolerances to flooding and focus on main functional plant groups, therefore missing plant community or diversity concerns that may manifest prior to state change from vegetated to unvegetated systems.

SLR impacts to marsh plant diversity are dependent on species associations and position along environmental gradients. Species more abundant at higher marsh elevations will be negatively impacted by rising sea levels due to loss of habitat, vegetation vigor, and soil condition from increased flooding time (Reed and Cahoon, 1992). If a physical barrier prevents upland migration, the marsh will experience a phenomenon known as "coastal squeeze" (Pontee, 2013). Species with abundance influenced by channel proximity may be negatively impacted as SLR inundates species near water forcing migration from channel widening (Hartig et al., 2002), which narrows existing habitat for species far from water. SLR will also expose more marsh plants to saline water, with saltwater intrusion predicted to be more common in the future (Cloern et al., 2011).

Future SLR is anticipated to lead to flooding, erosion, and saltwater intrusion (Cloern et al., 2011; Thorne et al., 2018). Sweet et al. (2022) project an increase in sea level between 0.3 m and 2.5 m by 2100 for the SFBE, depending on realized levels of global greenhouse gas emissions. The results from this study can be used when considering an unpredictable future related to SLR. Here we identified species community and abundance relationships across the SFBE and investigated how they relate to environmental variables. With rising sea levels, plant communities will shift lower in the tidal frame and experience more frequent saltwater intrusion. This shift is likely to result in less species evenness as select species become dominant in these lower and saltier environments (Figure 8). This type of information can be used by ecologists and wetland managers to project how vegetation communities will change in response to SLR and develop monitoring strategies that are scale dependent. Slight changes in vegetation composition or associations could be early indicators of change within the abiotic conditions of the estuary (Kearney et al., 2011; Schepers et al., 2017; Kutcher et al., 2022). This approach has been successfully deployed to monitor marsh restoration and holds the same premises (Handa et al., 2002).

Large scale analyses for abiotic drivers may be biased by other marsh associations and mask individual drivers at the local scale. At the local scale, site-specific drivers may dominate the influence on changes for species that were associated with high elevation, low salinity, and interior locations (Figure 2). At the regional or estuary scale, species may re-order to look more like the saline San Francisco Bay, dominated by a few species, and less like Suisun Bay with high evenness and patchiness (Jones et al., 2021). This has strong functional implications for carbon and nitrogen cycling (Knox et al., 2018; Windham-Myers et al., 2018; Baldocchi, 2020; Russell et al., 2023), habitat provisioning for threatened and endangered species (smelt, rails), recreation, and aesthetics.

Data availability statement

The datasets presented in this study can be found in online repositories. The names of the repository/repositories and accession number(s) can be found below: Lyndsay L. Rankin, Scott F. Jones, Christopher N. Janousek, Kevin J. Buffington, John Y. Takekawa, Karen M. Thorne, 2023, Marsh vegetation surveys across the San Francisco Bay Estuary, 2008–2018: U.S. Geological Survey Data Release, https://doi.org/10.5066/P94F802H.

Author contributions

SJ and KT conceived the research. LR analyzed the data. JT, CJ, KB, and KT collected the data. All authors contributed to the article and approved the submitted version.

Funding

The author(s) declare financial support was received for the research, authorship, and/or publication of this article. The project described in this publication was supported by funding from the U.S. Geological Survey National Climate Adaptation Science Centers, the National Oceanic and Atmospheric Administration (grant NA15NOS4780171), and the USGS Western Ecological Research Center.

Acknowledgments

We would like to thank land managers from the U.S. Fish and Wildlife Service, California State Parks, NOAA National Estuarine Research Reserve, California Department of Fish and Wildlife, Solano Land Trust, and East Bay Regional Parks District for granting site access to conduct this study. We express thanks to the countless field technicians who helped with these surveys. Thanks to Audrey Colley for ArcGIS assistance and Chase Freeman for data collection. Thanks to Robert Klinger for statistical advice and guidance. The project described in this publication was supported by funding from the U.S. Geological Survey National Climate Adaptation Science Centers, the National Oceanic and Atmospheric Administration (grant NA15NOS4780171), and the USGS Western Ecological Research Center. Any use of trade, firm, or product names is for descriptive purposes only and does not imply endorsement by the U.S. Government.

Conflict of interest

Publisher's note

Supplementary material

The Supplementary Material for this article can be found online at: https://www.frontiersin.org/articles/10.3389/fevo.2023.1215964/full#supplementary-material

References

Adam, E., Mutanga, O., and Rugege, D. (2010). Multispectral and hyperspectral remote sensing for identification and mapping of wetland vegetation: a review. *Wetlands Ecol. Manage.* 18, 281–296. doi: 10.1007/s11273-009-9169-z

Adam, P. (1993). *Saltmarsh ecology*. (Cambridge: Cambridge University Press).

Avolio, M. L., Carroll, I. T., Collins, S. L., Houseman, G. R., Hallett, L. M., Isbell, F., et al. (2019). A comprehensive approach to analyzing community dynamics using rank abundance curves. *Ecosphere* 10, e02881. doi: 10.1002/ecs2.2881

Baldocchi, D. D. (2020). How eddy covariance flux measurements have contributed to our understanding of Global Change Biology. *Global Change Biol.* 26, 242–260. doi: 10.1111/gcb.14807

Baldwin, B. G., Goldman, D. H., Keil, D. J., Patterson, R., and Rosatti, T. J. (2012). *The Jepson manual: vascular plants of California*. (Berkeley: University of California Press).

Barbier, E. B., Hacker, S. D., Kennedy, C., Koch, E. W., Stier, A. C., and Silliman, B. R. (2011). The value of estuarine and coastal ecosystem services. *Ecol. Monogr.* 810, 169–193. doi: 10.1890/10-1510.1

Bernhardt-Römermann, M., Baeten, L., Craven, D., De Frenne, P., Hédl, R., Lenoir, J., et al. (2015). Drivers of temporal changes in temperate forest plant diversity vary across spatial scales. *Global Change Biol.* 21, 3726–3737. doi: 10.1111/gcb.12993

Bertness, M. D. (1991). Interspecific interactions among high marsh perennials in a New England salt marsh. *Ecology* 72, 125–137. doi: 10.2307/1938908

Bertness, M. D., and Callaway, R. (1994). Positive interactions in communities. *Trends Ecol. Evol.* 9, 191–193. doi: 10.1016/0169-5347(94)90088-4

Bertness, M. D., and Ellison, A. M. (1987). Determinants of pattern in a New England salt marsh plant community. *Ecol. Monogr.* 57, 129–147. doi: 10.2307/1942621

Bertness, M. D., and Ewanchuk, P. J. (2002). Latitudinal and climate-driven variation in the strength and nature of biological interactions in New England salt marshes. *Oecologia* 132, 392–401. doi: 10.1007/s00442-002-0972-y

Bonin, C. L., and Zedler, J. B. (2008). Southern California salt marsh dominance relates to plant traits and plasticity. *Estuaries Coasts* 31, 682–693. doi: 10.1007/s12237-008-9057-4

Bridge, S. R. J., and Johnson, E. A. (2000). Geomorphic principles of terrain organization and vegetation gradients. *J. Vege. Sci.* 11, 57–70. doi: 10.2307/3236776

Brooker, R. W., Maestre, F. T., Callaway, R. M., Lortie, C. L., Cavieres, L. A., Kunstler, G., et al. (2008). Facilitation in plant communities: the past, the present, and the future. *J. Ecol.* 96, 18–34. doi: 10.1111/j.1365-2745.2007.01295.x

Buffington, K. J., Goodman, A. C., Freeman, C. M., and Thorne, K. M. (2020). Testing the interactive effects of flooding and salinity on tidal marsh plant productivity. *Aquat. Bot.* 164, 103231. doi: 10.1016/j.aquabot.2020.103231

Buffington, K. J., Janousek, C. N., Dugger, B. D., Callaway, J. C., Sloane, E., SChile-Beers, L., et al. (2021). Incorporation of uncertainty to improve projections of tidal wetland elevation and carbon accumulation with sea-level rise. *PloS One* 16, e0256707. doi: 10.1371/journal.pone.0256707

Busch, D. E., Loftus, W. F., and Bass, O. L. (1998). Long-term hydrologic effects on marsh plant community structure in the southern Everglades. *Wetlands* 18, 230–241. doi: 10.1007/BF03161658

California Natural Diversity Database (CNDDB). (2023). *Special Animals List* (Sacramento, CA: California Department of Fish and Wildlife).

Chaneton, E. J., and Facelli, J. M. (1991). Disturbance effects on plant community diversity: spatial scales and dominance hierarchies. *Vegetatio* 93, 143–155. doi: 10.1007/BF00033208

Clarke, P. J., Lawes, M. J., and Midgley, J. J. (2010). Resprouting as a key functional trait in woody plants—challenges to developing new organizing principles. *New Phytol.* 188, 651–654. doi: 10.1111/j.1469-8137.2010.03508.x

Cloern, J. E., and Jassby, A. D. (2012). Drivers of change in estuarine-coastal ecosystems: Discoveries from four decades of study in San Francisco Bay. *Rev. Geophys.* 50, RG4001. doi: 10.1029/2012RG000397

Cloern, J. E., Knowles, N., Brown, L. R., Cayan, D., Dettinger, M. D., Morgan, T. L., et al. (2011). Projected evolution of California's San Francisco Bay-Delta-River system in a century of climate change. *PloS One* 6, e24465. doi: 10.1371/journal.pone.0024465

Costa, C. S., Marangoni, J. C., and Azevedo, A. M. (2003). Plant zonation in irregularly flooded salt marshes: relative importance of stress tolerance and biological interactions. *J. Ecol.* 91, 951–965. doi: 10.1046/j.1365-2745.2003.00821.x

Courtwright, J., and Findlay, S. E. (2011). Effects of microtopography on hydrology, physicochemistry, and vegetation in a tidal swamp of the Hudson River. *Wetlands* 31, 239–249. doi: 10.1007/s13157-011-0156-9

Crain, C. M., Silliman, B. R., Bertness, S. L., and Bertness, M. D. (2004). Physical and biotic drivers of plant distribution across estuarine salinity gradients. *Ecology* 85, 2539–2549. doi: 10.1890/03-0745

Daniëls, F. J., de Molenaar, J. G., Chytrý, M., and Tichý, L. (2011). Vegetation change in Southeast Greenland? Tasiilaq revisited after 40 years. *Appl. Vege. Sci.* 14, 230–241. doi: 10.1111/j.1654-109X.2010.01107.x

De Leeuw, J., Van den Dool, A., De Munck, W., Nieuwenhuize, J., and Beeftink, W. G. (1991). Factors influencing the soil salinity regime along an intertidal gradient. *Estuarine Coast. Shelf Sci.* 32, 87–97. doi: 10.1016/0272-7714(91)90030-F

Donnelly, J. P., and Bertness, M. D. (2001). Rapid shoreward encroachment of salt marsh cordgrass in response to accelerated sea-level rise. *Proc. Natl. Acad. Sci.* 98, 14218–14223. doi: 10.1073/pnas.251209298

Eleuterius, L. N., and Eleuterius, C. K. (1979). Tide levels and salt marsh zonation. *Bull. Mar. Sci.* 29, 394–400.

Elmore, A. J., Mustard, J. F., and Manning, S. J. (2003). Regional patterns of plant community response to changes in water: Owens Valley, California. *Ecol. Appl.* 13, 443–460. doi: 10.1890/1051-0761(2003)013[0443:RPOPCR]2.0.CO;2

Elschot, K., Vermeulen, A., Vandenbruwaene, W., Bakker, J. P., Bouma, T. J., Stahl, J., et al. (2017). Top-down vs. bottom-up control on vegetation composition in a tidal marsh depends on scale. *PloS One* 12, e0169960. doi: 10.1371/journal.pone.0169960

Engels, J. G., and Jensen, K. (2009). Patterns of wetland plant diversity along estuarine stress gradients of the Elbe (Germany) and Connecticut (USA) rivers. *Plant Ecol. Divers.* 2, 301–311. doi: 10.1080/17550870903508947

Engels, J. G., Rink, F., and Jensen, K. (2011). Stress tolerance and biotic interactions determine plant zonation patterns in estuarine marshes during seedling emergence and early establishment. *J. Ecol.* 99, 277–287. doi: 10.1111/j.1365-2745.2010.01745.x

Ewanchuk, P. J., and Bertness, M. D. (2004). Structure and organization of a northern New England salt marsh plant community. *J. Ecol.* 92, 72–85. doi: 10.1111/j.1365-2745.2004.00838.x

Gallego-Tévar, B., Grewell, B. J., Futrell, C. J., Drenovsky, R. E., and Castillo, J. M. (2020). Interactive effects of salinity and inundation on native *Spartina foliosa*, invasive S. densiflora and their hybrid from San Francisco Estuary, California. *Ann. Bot.* 125, 377–389. doi: 10.1093/aob/mcz170

Garner, K. L., Chang, M. Y., Fulda, M. T., Berlin, J. A., Freed, R. E., Soo-Hoo, M. M., et al. (2015). Impacts of sea level rise and climate change on coastal plant species in the central California coast. *PeerJ* 3, e958. doi: 10.7717/peerj.958

Gedan, K. B., Silliman, B. R., and Bertness, M. D. (2009). Centuries of human-driven change in salt marsh ecosystems. *Annu. Rev. Mar. Sci.* 1, 117–141. doi: 10.1146/annurev.marine.010908.163930

Gilby, B. L., Weinstein, M. P., Baker, R., Cebrian, J., Alford, S. B., Chelsky, A., et al. (2021). Human actions alter tidal marsh seascapes and the provision of ecosystem services. *Estuaries Coasts* 44, 1628–1636. doi: 10.1007/s12237-020-00830-0

Goman, M., Malamud-Roam, F., and Ingram, B. L. (2008). Holocene environmental history and evolution of a tidal salt marsh in San Francisco Bay, California. *J. Coast. Res.* 24, 1126–1137. doi: 10.2112/08A-0005.1

Graham, R. L., Turner, M. G., and Dale, V. H. (1990). How increasing CO 2 and climate change affect forests. *BioScience* 40, 575–587. doi: 10.2307/1311298

Hall, E. A., Molino, G. D., Messerschmidt, T. C., and Kirwan, M. L. (2022). Hidden levees: Small-scale flood defense on rural coasts. *Anthropocene* 40, 100350. doi: 10.1016/j.ancene.2022.100350

Hallett, L., Avolio, M., Carroll, I., Jones, S., MacDonald, A., Flynn, D., et al. (2020). *Codyn: community dynamics metrics*. R package version 2.0.5. doi: 10.5063/F1N877Z6

Handa, I. T., Harmsen, R., and Jefferies, R. L. (2002). Patterns of vegetation change and the recovery potential of degraded areas in a coastal marsh system of the Hudson Bay lowlands. *J. Ecol.* 90, 86–99. doi: 10.1046/j.0022-0477.2001.00635.x

Hartig, E. K., Gornitz, V., Kolker, A., Mushacke, F., and Fallon, D. (2002). Anthropogenic and climate-change impacts on salt marshes of Jamaica Bay, New York City. *Wetlands* 22, 71–89. doi: 10.1672/0277-5212(2002)022[0071:AACCIO]2.0.CO;2

He, Y., Li, X., Craft, C., Ma, Z., and Sun, Y. (2011). Relationships between vegetation zonation and environmental factors in newly formed tidal marshes of the Yangtze River estuary. *Wetlands Ecol. Manage.* 19, 341–349. doi: 10.1007/s11273-011-9220-8

IPCC (2022). *Climate Change 2022: Impacts, Adaptation and Vulnerability. Contribution of Working Group II to the Sixth Assessment Report of the Intergovernmental Panel on Climate Change*. Eds. H.-O. Pörtner, D. C. Roberts, M. Tignor, E. S. Poloczanska, K. Mintenbeck, A. Alegría, M. Craig, S. Langsdorf, S. Löschke, V. Möller, A. Okem and B. Rama (Cambridge, UK and New York, NY, USA: Cambridge University Press), 3056. doi: 10.1017/9781009325844

Janousek, C. N., Buffington, K. J., Thorne, K. M., Guntenspergen, G. R., Takekawa, J. Y., and Dugger, B. D. (2016). Potential effects of sea-level rise on plant productivity: species-specific responses in northeast Pacific tidal marshes. *Mar. Ecol. Prog. Ser.* 548, 111–125. doi: 10.3354/meps11683

Janousek, C. N., and Folger, C. L. (2014). Variation in tidal wetland plant diversity and composition within and among coastal estuaries: assessing the relative importance of environmental gradients. *J. Vege. Sci.* 25, 534–545. doi: 10.1111/jvs.12107

Janousek, C. N., and Mayo, C. (2013). Plant responses to increased inundation and salt exposure: interactive effects on tidal marsh productivity. *Plant Ecol.* 214, 917–928. doi: 10.1007/s11258-013-0218-6

Janousek, C. N., Thorne, K. M., and Takekawa, J. Y. (2019). Vertical zonation and niche breadth of tidal marsh plants along the northeast Pacific coast. *Estuaries Coasts* 42, 85–98. doi: 10.1007/s12237-018-0420-9

Jones, S. F., Janousek, C. N., Casazza, M. L., Takekawa, J. Y., and Thorne, K. M. (2021). Seasonal impoundment alters patterns of tidal wetland plant diversity across spatial scales. *Ecosphere* 12, e03366. doi: 10.1002/ecs2.3366

Jones, S. K., Ripplinger, J., and Collins, S. L. (2017). Species reordering, not changes in richness, drives long-term dynamics in grassland communities. *Ecol. Lett.* 20, 1556–1565. doi: 10.1111/ele.12864

Kearney, M. S., Riter, J. A., and Turner, R. E. (2011). Freshwater river diversions for marsh restoration in Louisiana: Twenty-six years of changing vegetative cover and marsh area. *Geophys. Res. Lett.* 38 (16), L16405. doi: 10.1029/2011GL047847

Kirwan, M. L., and Guntenspergen, G. R. (2015). Response of plant productivity to experimental flooding in a stable and a submerging marsh. *Ecosystems* 18, 903–913. doi: 10.1007/s10021-015-9870-0

Knox, S. H., Windham-Myers, L., Anderson, F., Sturtevant, C., and Bergamaschi, B. (2018). Direct and indirect effects of tides on ecosystem-scale CO2 exchange in a brackish tidal marsh in Northern California. *J. Geophys. Res.: Biogeosci.* 123, 787–806. doi: 10.1002/2017JG004048

Korell, L., Auge, H., Chase, J. M., Harpole, W. S., and Knight, T. M. (2021). Responses of plant diversity to precipitation change are strongest at local spatial scales and in drylands. *Nat. Commun.* 12, 2489. doi: 10.1038/s41467-021-22766-0

Kutcher, T. E., Raposa, K. B., and Roman, C. T. (2022). A rapid method to assess salt marsh condition and guide management decisions. *Ecol. Indic.* 138, 108841. doi: 10.1016/j.ecolind.2022.108841

Li, F., Angelini, C., Byers, J. E., Craft, C., and Pennings, S. C. (2022). Responses of a tidal freshwater marsh plant community to chronic and pulsed saline intrusion. *J. Ecol.* 110, 1508–1524. doi: 10.1111/1365-2745.13885

Li, F., and Pennings, S. C. (2019). Response and recovery of low-salinity marsh plant communities to presses and pulses of elevated salinity. *Estuaries Coasts* 42, 708–718. doi: 10.1007/s12237-018-00490-1

Li, L., Ustin, S. L., and Lay, M. (2005). Application of multiple endmember spectral mixture analysis (MESMA) to AVIRIS imagery for coastal salt marsh mapping: a case study in China Camp, CA, USA. *Int. J. Remote Sens.* 26, 5193–5207. doi: 10.1080/01431160500218911

Liancourt, P., Callaway, R. M., and Michalet, R. (2005). Stress tolerance and competitive-response ability determine the outcome of biotic interactions. *Ecology* 86, 1611–1618. doi: 10.1890/04-1398

Lortie, C. J., and Callaway, R. M. (2006). Re-analysis of meta-analysis: support for the stress-gradient hypothesis. *J. Ecol.* 94, 7–16. doi: 10.1111/j.1365-2745.2005.01066.x

Maestre, F. T., Callaway, R. M., Valladares, F., and Lortie, C. J. (2009). Refining the stress-gradient hypothesis for competition and facilitation in plant communities. *J. Ecol.* 97, 199–205. doi: 10.1111/j.1365-2745.2008.01476.x

Maestre, F. T., Valladares, F., and Reynolds, J. F. (2005). Is the change of plant–plant interactions with abiotic stress predictable? *A meta-anal. Field results arid environ. J. Ecol.* 93, 748–757. doi: 10.1111/j.1365-2745.2005.01017.x

Maestre, F. T., Valladares, F., and Reynolds, J. F. (2006). The stress-gradient hypothesis does not fit all relationships between plant–plant interactions and abiotic stress: further insights from arid environments. *J. Ecol.* 94, 17–22. doi: 10.1111/j.1365-2745.2005.01089.x

Malavasi, M., Santoro, R., Cutini, M., Acosta, A. T. R., and Carranza, M. L. (2016). The impact of human pressure on landscape patterns and plant species richness in Mediterranean coastal dunes. *Plant Biosystems-an Int. J. Dealing All Aspects Plant Biol.* 150, 73–82. doi: 10.1080/11263504.2014.913730

Maliniemi, T., Kapfer, J., Saccone, P., Skog, A., and Virtanen, R. (2018). Long-term vegetation changes of treeless heath communities in northern Fennoscandia: Links to climate change trends and reindeer grazing. *J. Vege. Sci.* 29, 469–479. doi: 10.1111/jvs.12630

Marcus, L. (2000). Restoring tidal wetlands at Sonoma Baylands, San Francisco Bay, California. *Ecol. Eng.* 15, 373–383. doi: 10.1016/S0925-8574(00)00087-2

Marquer, L., Gaillard, M. J., Sugita, S., Poska, A., Trondman, A. K., Mazier, F., et al. (2017). Quantifying the effects of land use and climate on Holocene vegetation in Europe. *Quaternary Sci. Rev.* 171, 20–37. doi: 10.1016/j.quascirev.2017.07.001

Menge, B. A., and Sutherland, J. P. (1987). Community regulation: variation in disturbance, competition, and predation in relation to environmental stress and recruitment. *Am. Nat.* 130, 730–757. doi: 10.1086/284741

Michelsen, O., Syverhuset, A. O., Pedersen, B., and Holten, J. I. (2011). The impact of climate change on recent vegetation changes on Dovrefjell, Norway. *Diversity* 3, 91–111. doi: 10.3390/d3010091

Moffett, K. B., and Gorelick, S. M. (2016). Alternative stable states of tidal marsh vegetation patterns and channel complexity. *Ecohydrology* 9, 1639–1662. doi: 10.1002/eco.1755

Mokany, K., McCarthy, J. K., Falster, D. S., Gallagher, R. V., Harwood, T. D., Kooyman, R., et al. (2022). Patterns and drivers of plant diversity across Australia. *Ecography* 2022, e06426. doi: 10.1111/ecog.06426

Mora, J. W., and Burdick, D. M. (2013). Effects of man-made berms upon plant communities in New England salt marshes. *Wetlands Ecol. Manage.* 21, 131–145. doi: 10.1007/s11273-013-9285-7

Morris, J. T., Sundareshwar, P. V., Nietch, P. T., Kjerfve, B., and Cahoon, D. R. (2002). Responses of coastal wetlands to rising sea levels. *Ecology* 83, 2869–2877. doi: 10.1890/0012-9658(2002)083[2869:ROCWTR]2.0.CO;2

Morzaria-Luna, H. N., and Zedler, J. B. (2014). Competitive interactions between two salt marsh halophytes across stress gradients. *Wetlands* 34, 31–42. doi: 10.1007/s13157-013-0479-9

Muench, A., and Elsey-Quirk, T. (2019). Competitive reversal between plant species is driven by species-specific tolerance to flooding stress and nutrient acquisition during early marsh succession. *J. Appl. Ecol.* 56, 2236–2247. doi: 10.1111/1365-2664.13458

Neubauer, S. C. (2013). Ecosystem responses of a tidal freshwater marsh experiencing saltwater intrusion and altered hydrology. *Estuaries Coasts* 36, 491–507. doi: 10.1007/s12237-011-9455-x

Neumann, F. H., Scott, L., Bousman, C. B., and Van As, L. (2010). A Holocene sequence of vegetation change at Lake Eteza, coastal KwaZulu-natal, South Africa. *Rev. Palaeobotany Palynol.* 162, 39–53. doi: 10.1016/j.revpalbo.2010.05.001

Nichols, F. H., Cloern, J. E., Luoma, S. N., and Peterson, D. H. (1986). The modification of an estuary. *Science* 231, 567–573. doi: 10.1126/science.231.4738.567

Niku, J., Brooks, W., Herliansyah, R., Hui, F. K. C., Korhonen, P., Taskinen, S., et al. (2023). *gllvm: Generalized linear latent variable models*. R package version 1.4.3.

Niku, J., Hui, F. K. C., Taskinen, S., and Warton, D. I. (2019). gllvm - Fast analysis of multivariate abundance data with generalized linear latent variable models in R. *Methods Ecol. Evol.* 10, 2173–2182. doi: 10.1111/2041-210X.13303

Oakes, L. E., Hennon, P. E., O'Hara, K. L., and Dirzo, R. (2014). Long-term vegetation changes in a temperate forest impacted by climate change. *Ecosphere* 5, 1–28. doi: 10.1890/ES14-00225.1

Odum, W. E. (1988). Comparative ecology of tidal freshwater and salt marshes. *Annu. Rev. Ecol. Evol. Systs.* 19 (1), 147–176.

Oosterlee, L., Cox, T. J., Vandenbruwaene, W., Maris, T., Temmerman, S., and Meire, P. (2018). Tidal marsh restoration design affects feedbacks between inundation and elevation change. *Estuaries coasts* 41, 613–625. doi: 10.1007/s12237-017-0314-2

Orson, R. A., Panageotou, W., and Leatherman, S. P. (1985). Response of tidal salt marshes of the US Atlantic and Gulf coasts to rising sea levels. *J. Coast. Res.* 1, 29–37.

Parker, B., Milbert, D., Hess, K., and Gill, S. (2003). National VDatum–The implementation of a national vertical datum transformation database. Silver Spring: National Oceanic and Atmospheric Administration, National Ocean Service. 9.

Peng, D., Chen, L., Pennings, S. C., and Zhang, Y. (2018). Using a marsh organ to predict future plant communities in a Chinese estuary invaded by an exotic grass and mangrove. *Limnol. Oceanogr.* 63, 2595–2605. doi: 10.1002/lno.10962

Pennings, S. C., Grant, M. B., and Bertness, M. D. (2005). Plant zonation in low-latitude salt marshes: disentangling the roles of flooding, salinity and competition. *J. Ecol.* 93, 159–167. doi: 10.1111/j.1365-2745.2004.00959.x

Pontee, N. (2013). Defining coastal squeeze: A discussion. *Ocean Coast. Manage.* 84, 204–207. doi: 10.1016/j.ocecoaman.2013.07.010

Rand, T. A. (2002). Variation in insect herbivory across a salt marsh tidal gradient influences plant survival and distribution. *Oecologia* 132, 549–558. doi: 10.1007/s00442-002-0989-2

R Core Team (2022). *R: A language and environment for statistical computing* (Vienna, Australia: R Foundation for Statistical Computing). Available at: https://www.R-project.org/.

Reed, D. J., and Cahoon, D. R. (1992). The relationship between marsh surface topography, hydroperiod, and growth of Spartina alterniflora in a deteriorating Louisiana salt marsh. *J. Coast. Res.* 8, 77–87.

Rogers, K., Saintilan, N., and Woodroffe, C. D. (2014). Surface elevation change and vegetation distribution dynamics in a subtropical coastal wetland: implications for coastal wetland response to climate change. *Estuarine Coast. Shelf Sci.* 149, 46–56. doi: 10.1016/j.ecss.2014.07.009

Rogers, K., and Woodroffe, C. D. (2015). "Tidal flats and salt marshes," in *Coastal environments and global change*. ed. G. Masselink and R. Gehrels (West Sussex: John Wiley and Sons), 227–250. doi: 10.1002/9781119117261.ch10

Ross, M. S., Meeder, J. F., Sah, J. P., Ruiz, P. L., and Telesnicki, G. J. (2000). The southeast saline Everglades revisited: 50 years of coastal vegetation change. *J. Vege. Sci.* 11, 101–112. doi: 10.2307/3236781

Rosso, P. H., Ustin, S. L., and Hastings, A. (2005). Mapping marshland vegetation of San Francisco Bay, California, using hyperspectral data. *Int. J. Remote Sens.* 26, 5169–5191. doi: 10.1080/01431160500218770

Russell, S. J., Windham-Myers, L., Stuart-Haëntjens, E. J., Bergamaschi, B. A., Anderson, F., Oikawa, P., et al. (2023). Increased salinity decreases annual gross primary productivity at a Northern California brackish tidal marsh. *Environ. Res. Lett.* 18, 034045. doi: 10.1088/1748-9326/acbbdf

Ryan, A. B., and Boyer, K. E. (2012). Nitrogen further promotes a dominant salt marsh plant in an increasingly saline environment. *J. Plant Ecol.* 5, 429–441. doi: 10.1093/jpe/rts001

Sanderson, E. W., Foin, T. C., and Ustin, S. L. (2001). A simple empirical model of salt marsh plant spatial distributions with respect to a tidal channel network. *Ecol. Model.* 139, 293–307. doi: 10.1016/S0304-3800(01)00253-8

Schepers, L., Kirwan, M., Guntenspergen, G., and Temmerman, S. (2017). Spatio-temporal development of vegetation die-off in a submerging coastal marsh. *Limnol. Oceanogr.* 62, 137–150. doi: 10.1002/lno.10381

Schile, L. M., Callaway, J. C., Morris, J. T., Stralberg, D., Parker, V. T., and Kelly, M. (2014). Modeling tidal marsh distribution with sea-level rise: evaluating the role of vegetation, sediment, and upland habitat in marsh resiliency. *PloS One* 9, e88760. doi: 10.1371/journal.pone.0088760

Schile, L. M., Callaway, J. C., Suding, K. N., and Kelly, N. M. (2017). Can community structure track sea-level rise? Stress and competitive controls in tidal wetlands. *Ecol. Evol.* 7, 1276–1285. doi: 10.1002/ece3.2758

Schwarz, C., Gourgue, O., Van Belzen, J., Zhu, Z., Bouma, T. J., Van De Koppel, J., et al. (2018). Self-organization of a biogeomorphic landscape controlled by plant life-history traits. *Nat. Geosci.* 11, 672–677. doi: 10.1038/s41561-018-0180-y

Sharpe, P. J., and Baldwin, A. H. (2012). Tidal marsh plant community response to sea-level rise: a mesocosm study. *Aquat. Bot.* 101, 34–40. doi: 10.1016/j.aquabot.2012.03.015

Shipley, B. (2010). *From plant traits to vegetation structure: chance and selection in the assembly of ecological communities* (Cambridge: Cambridge University Press).

Silvestri, S., Defina, A., and Marani, M. (2005). Tidal regime, salinity and salt marsh plant zonation. *Estuarine Coast. shelf Sci.* 62, 119–130. doi: 10.1016/j.ecss.2004.08.010

Skrondal, A., and Rabe-Hesketh, S. (2004). *Generalized latent variable modeling: Multilevel, longitudinal, and structural equation models* (Boca Raton: CRC Press).

Snedden, G. A., Cretini, K., and Patton, B. (2015). Inundation and salinity impacts to above- and belowground productivity in Spartina patens and Spartina alterniflora in the Mississippi River deltaic plain:implications for using river diversions as restoration tools. *Ecol. Eng.* 81, 133–139. doi: 10.1016/j.ecoleng.2015.04.035

Song, Y., Jin, L., and Wang, H. (2018). Vegetation changes along the Qinghai-Tibet Plateau engineering corridor since 2000 induced by climate change and human activities. *Remote Sens.* 10, 95. doi: 10.3390/rs10010095

Sundaram, B., and Hiremath, A. J. (2012). Lantana camara invasion in a heterogeneous landscape: patterns of spread and correlation with changes in native vegetation. *Biol. Invasions* 14, 1127–1141. doi: 10.1007/s10530-011-0144-2

Swanson, K. M., Drexler, J. Z., Schoellhamer, D. H., Thorne, K. M., Casazza, M. L., Overton, C. T., et al. (2014). Wetland accretion rate model of ecosystem resilience (WARMER) and its application to habitat sustainability for endangered species in the San Francisco estuary. *Estuaries Coasts* 37, 476–492. doi: 10.1007/s12237-013-9694-0

Sweet, W. V., Hamlington, B. D., Kopp, R. E., Weaver, C. P., Barnard, P. L., Bekaert, D., et al. (2022). *Global and regional sea level rise scenarios for the United States: Updated mean projections and extreme water level probabilities along U.S. coastlines*. NOAA Technical Report NOS 01 (Silver Spring: National Oceanic and Atmospheric Administration, National Ocean Service), 111 pp. https://oceanservice.noaa.gov/hazards/sealevelrise/noaa-nostechrpt01-global-regional-SLR-scenarios-US.pdf.

Takekawa, J. Y., Thorne, K. M., Buffington, K. Y., Spragens, K. A., Swanson, K. M., Drexler, J. Z., et al. (2013b). Final report for sea-level rise response modeling for San Francisco Bay estuary tidal marshes *U.S. Geological Survey Open File Report 2013-1081*, 161 pp.

Takekawa, J. Y., Lu, C. T., and Pratt, R. T. (2001). Avian communities in baylands and artificial salt evaporation ponds of the San Francisco Bay estuary. *Hydrobiologia* 466, 317–328. doi: 10.1023/A:1014546524957

Takekawa, J. Y., Thorne, K. M., Buffington, K. J., Freeman, C. M., Powelson, K. W., and Block, G. (2013a). *Assessing marsh response from sea-level rise applying local site conditions: Humboldt Bay National Wildlife Refuge. Unpubl. Data Summary Report* (Vallejo, CA: USGS Western Ecological Research Center). 44pp + Appendices.

Takekawa, J. Y., Woo, I., Spautz, H., Nur, N., Grenier, J. L., Malamud-Roam, K., et al. (2006). Environmental threats to tidal-marsh vertebrates of the San Francisco Bay estuary. *Stud. Avian Biol.* 32, 176.

Tasser, E., and Tappeiner, U. (2002). Impact of land use changes on mountain vegetation. *Appl. vegetation Sci.* 5, 173–184. doi: 10.1111/j.1654-109X.2002.tb00547.x

Taylor, A. H., Poulos, H. M., Kluber, J., Issacs, R., Pawlikowski, N., and Barton, A. M. (2021). Controls on spatial patterns of wildfire severity and early post-fire vegetation development in an Arizona Sky Island, USA. *Landscape Ecol.* 36, 2637–2656. doi: 10.1007/s10980-021-01260-4

Thorne, K. M., Backe, K. E., Freeman, C. M., Buffington, K. J., Forstner, T. M., and Goodman, A. C. (2019). *Don Edwards National Wildlife Refuge Vegetation, Elevation, Inundation Inventory to Inform Sea-level Rise Vulnerability. Unpubl. Data Summary Report* (Davis, CA: USGS Western Ecological Research Center). 112pp.

Thorne, K., MacDonald, G., Guntenspergen, G., Ambrose, R., Buffington, K., Dugger, B., et al. (2018). U.S. Pacific coastal wetland resilience and vulnerability to sea-level rise. *Sci. Adv.* 4, eaao3270. doi: 10.1126/sciadv.aao3270

Trowbridge, P. R., Davis, J. A., Mumley, T., Taberski, K., Feger, N., Valiela, L., et al. (2016). The regional monitoring program for water quality in San Francisco Bay, California, USA: science in support of managing water quality. *Regional Stud. Mar. Sci.* 4, 21–33. doi: 10.1016/j.rsma.2015.10.002

United States Census Bureau (2021). *American Community Survey 5-year Data, (2009-2021)* (United States government). Available at: https://data.census.gov/cedsci/.

USDA, NRCS (2023). *The PLANTS Database* (Greensboro, NC USA: National Plant Data Team). Available at: http://plants.usda.gov.

Van de Koppel, J., Bouma, T. J., and Herman, P. M. (2012). The influence of local- and landscape-scale processes on spatial self-organization in estuarine ecosystems. *J. Exp. Biol.* 215, 962–967. doi: 10.1242/jeb.060467

Van Der Heijden, M. G., Bardgett, R. D., and Van Straalen, N. M. (2008). The unseen majority: soil microbes as drivers of plant diversity and productivity in terrestrial ecosystems. *Ecol. Lett.* 11, 296–310. doi: 10.1111/j.1461-0248.2007.01139.x

Van der Plas, F., Schröder-Georgi, T., Weigelt, A., Barry, K., Meyer, S., Alzate, A., et al. (2020). Plant traits alone are poor predictors of ecosystem properties and long-term ecosystem functioning. *Nat. Ecol. Evol.* 4, 1602–1611. doi: 10.1038/s41559-020-01316-9

Wasson, K., Woolfolk, A., and Fresquez, C. (2013). Ecotones as indicators of changing environmental conditions: rapid migration of salt marsh–upland boundaries. *Estuaries Coasts* 36, 654–664. doi: 10.1007/s12237-013-9601-8

Watson, E. B., and Byrne, R. (2009). Abundance and diversity of tidal marsh plants along the salinity gradient of the San Francisco Estuary: implications for global change ecology. *Plant Ecol.* 205, 113–128. doi: 10.1007/s11258-009-9602-7

White, J. R., Couvillion, B., and Day, J. W. (2023). Coastal wetland area change for two freshwater diversions in the Mississippi River Delta. *Ecol. Eng.* 186, 106819. doi: 10.1016/j.ecoleng.2022.106819

Windham-Myers, L., Bergamaschi, B., Anderson, F., Knox, S., Miller, R., and Fujii, R. (2018). Potential for negative emissions of greenhouse gases (CO2, CH4 and N2O) through coastal peatland re-establishment: Novel insights from high frequency flux data at meter and kilometer scales. *Environ. Res. Lett.* 13, 045005. doi: 10.1088/1748-9326/aaae74

Woo, I., and Takekawa, J. Y. (2012). Will inundation and salinity levels associated with projected sea level rise reduce the survival, growth, and reproductive capacity of *Sarcocornia pacifica* (pickleweed)? *Aquat. Bot.* 102, 8–14. doi: 10.1016/j.aquabot.2012.03.014

Xi, N., Chen, D., Bahn, M., Wu, H., Chu, C., Cadotte, M. W., et al. (2022). Drought soil legacy alters drivers of plant diversity-productivity relationships in oldfield systems. *Sci. Adv.* 8, eabn3368. doi: 10.1126/sciadv.abn3368

frontiers | Frontiers in Ecology and Evolution

TYPE Original Research
PUBLISHED 09 February 2024
DOI 10.3389/fevo.2023.1184918

OPEN ACCESS

EDITED BY
Ralf Ohlemuller,
University of Otago, New Zealand

REVIEWED BY
Xiaobin Hua,
University of Waikato, New Zealand
Gang Fu,
Chinese Academy of Sciences (CAS), China
Long Zhao,
Henan University of Science and Technology, China

*CORRESPONDENCE
Rob Klinger
✉ rcklinger@usgs.gov

RECEIVED 12 March 2023
ACCEPTED 26 May 2023
PUBLISHED 09 February 2024

CITATION
Klinger R, Stephenson T, Letchinger J, Stephenson L and Jacobs S (2024) The noise is the signal: spatio-temporal variability of production and productivity in high elevation meadows in the Sierra Nevada mountain range of North America.
Front. Ecol. Evol. 11:1184918.
doi: 10.3389/fevo.2023.1184918

The noise is the signal: spatio-temporal variability of production and productivity in high elevation meadows in the Sierra Nevada mountain range of North America

Rob Klinger[1]*, Tom Stephenson[2], James Letchinger[1], Logan Stephenson[1,2] and Sarah Jacobs[1]

[1]US Geological Survey, Western Ecological Research Center, Bishop, CA, United States, [2]Sierra Nevada Bighorn Sheep Recovery Program, California Department of Fish and Wildlife, Bishop, CA, United States

There are expectations that increasing temperatures will lead to significant changes in structure and function of montane meadows, including greater water stress on vegetation and lowered vegetation production and productivity. We evaluated spatio-temporal dynamics in production and productivity in meadows within the Sierra Nevada mountain range of North America by: (1) compiling Landsat satellite data for the Normalized Difference Vegetation Index (NDVI) across a 37-year period (1985–2021) for 8,095 meadows >2,500m elevation; then, (2) used state-space models, changepoint analysis, geographically-weighted regression (GWR), and distance-decay analysis (DDA) to: (a) identify meadows with decreasing, increasing or no trends for NDVI; (b) detect meadows with abrupt changes (changepoints) in NDVI; and (c) evaluate variation along gradients of latitude, longitude, and elevation for eight indices of temporal dynamics in annual production (mean growing season NDVI; MGS) and productivity (rate of spring greenup; RSP). Meadows with no long-term change or evidence of increasing NDVI were 2.6x more frequent as those with decreasing NDVI (72% vs. 28%). Abrupt changes in NDVI were detected in 48% of the meadows; they occurred in every year of the study and with no indication that their frequency had changed over time. The intermixing of meadows with different temporal dynamics was a consistent pattern for monthly NDVI and, especially, the eight annual indices of MGS and RSP. The DDA showed temporal dynamics in pairs of meadow within a few 100m of each other were often as different as those hundreds of kilometers apart. Our findings point strongly toward a great diversity of temporal dynamics in meadow production and productivity in the SNV. The heterogeneity in spatial patterns indicated that production and productivity of meadow vegetation is being driven by interplay among climatic, physiographic and biotic factors at basin and meadow scales. Thus, when evaluating spatio-temporal dynamics in condition for many high elevation meadow systems, what might often be considered "noise" may provide greater insight than a "signal" embedded within a large amount of variability.

KEYWORDS

consecutive disparity index, ecosystem function, geographically-weighted regression, heterogeneity, resistance, scale-dependent variability, state-space models, climate

Introduction

Alpine and subalpine ecosystems make up a small portion of the earth's surface (<6%; Testolin et al., 2020) but are widely distributed both latitudinally and longitudinally. The two characteristics these systems share across their broad geographic extent are extreme climatic conditions and isolation. Temperatures are very low and precipitation comes primarily as snow, and the systems can be envisioned as islands surrounded by forests. Distribution of vegetation at high elevations is controlled predominantly by temperature (Korner, 2003), so zonation of plant communities reflects the progressively harsher environmental conditions as elevation increases.

The extreme climatic conditions and isolation have given rise to plant species that have specialized adaptations to narrow climatic and high stress environments (Scherrer and Körner, 2011). This has resulted in relatively high degrees of endemism and species with restricted distributions (Packer, 1974). Consequently, high elevation plant communities in many mountain ranges are assumed to be vulnerable to shifts in climate (Dirnbock et al., 2003; Parmesan and Yohe, 2003; Krajik, 2004). There is evidence the relationship between climate and vegetation zonation in high elevation ecosystems has been, and continues to be, modified as temperatures have risen. Upward shifts in species distributions (Walther et al., 2005; Jurasinski and Kreyling, 2007; Lenoir et al., 2008; Felde et al., 2012) and changes in phenology (Huelber et al., 2006; Inouye, 2008) have been reported from mountain ranges in some parts of the world, as have encroachment of conifers and other woody species into subalpine meadows (Haugo et al., 2011; Brandt et al., 2013; Lubetkin et al., 2017). Together, these findings point toward the compression of plant species into even narrower ranges, changes in community composition by colonization and establishment of species from lower elevations, potential transformation of herbaceous-dominated to woody-dominated communities and altered dynamics of vegetation functional processes (Shen et al., 2014).

This perspective on change in structure, species composition, and function of high elevation plant communities not only has support, but intuitive and popular appeal as well (Krajik, 2004). Nevertheless, while it may not be inaccurate, this broad, temperature-centered outlook may also be overly simplistic (Malanson and Fagre, 2013). An increasing number of studies have reported regional and local variation driving changes in upward species expansion (Walther et al., 2005; Pauli et al., 2007, 2012), transitions in community composition (Randin et al., 2009; Kudo et al., 2010), and alteration of functional processes (Shen et al., 2014; Sun et al., 2016). An important regional factor underlying this variation is the role precipitation plays in structuring plant species distributions and community composition (Ding et al., 2007; Sun et al., 2013). It is common for snowpack to vary latitudinally and with elevation (Mote et al., 2004; Sun et al., 2016), resulting in regions where availability of moisture may offset presumed effects of temperature. Moreover, precipitation in mountainous regions occurs in seasons other than just winter, usually coinciding with periods when plants are actively growing (Ren et al., 2021). Local factors contributing to variation in species and community responses include heterogeneity in microclimate, nutrients, soils, and grazing (Boelman et al., 2003; Wang et al., 2012; Fu et al., 2013; Malanson and Fagre, 2013; Fu et al., 2015). These regional and local influences do not negate the importance of increased temperature on plant species distributions or community dynamics. They do suggest though that effects of temperature are likely to be modified by multiple factors operating at different scales, resulting in highly variable spatio-temporal patterns.

Vegetation in high elevation systems is comprised of different types, of which meadows are particularly important. They mainly occur on flat terrain in basins where runoff from snowmelt recharges shallow water tables, and are a good example of the strong influence precipitation exerts on assemblages of plants in the alpine and subalpine zones (Loheide and Gorelick, 2007; Ma et al., 2022). Meadows are recognized for their great hydrological (Loheide et al., 2009) and ecological importance (e.g., Hik et al., 2001; Wang et al., 2012), as well as the ecosystem services they provide to humans (Ganjurjav et al., 2016).

Variation among high elevation meadows in vegetation structure, species composition, and functional attributes can be large. This is because the communities have assembled and been maintained through a complex interplay of abiotic and biotic forces whose strengths vary greatly across the landscape. Abiotic factors are primarily related, directly or indirectly, to availability of water. These include snowmelt, watershed features (e.g., steepness of surrounding mountains), tributary characteristics (density, length and extent), and soils. Biotic factors include individual and interactive effects of competition, facilitation, and herbivory (Song et al., 2006, 2012; Niu et al., 2016). Within-meadow variation in vegetation composition can be considerable, primarily as a result of complex microtopography, herbivory, or both. Thus, meadows are often comprised of highly localized assemblages that sort along small-scale gradients in moisture, nutrients and grazing intensity (Li et al., 2021; Xiao et al., 2022).

Despite their worldwide distribution and the generally accepted view many will be altered to various degrees by shifts in climate, the geographic distribution of investigations into dynamics of high elevation meadows has been highly skewed (Verrall and Pickering, 2020). Studies of high elevation meadows in the mountain ranges of North America are underrepresented compared to the large number conducted in Europe and Asia (Verrall and Pickering, 2020). Meadows make up a small portion of the landcover in the Sierra Nevada range (SNV from hereon) of western North America (≈1%; Viers et al., 2013). That portion is higher in the sub-alpine and alpine zones (≈10%; Klinger et al., 2015), but the importance of meadows for hydrologic processes, as well as biological populations and communities, is far greater than the limited amount of land area they comprise (Patton and Judd, 1970; Allen-Diaz, 1991; Epanchin et al., 2010; Lowry et al., 2011; Klinger et al., 2015). Several studies have established clear links between water availability and the structure and composition of meadow vegetation in the SNV (Allen-Diaz, 1991; Lowry et al., 2011; McIlroy and Allen-Diaz, 2012; Roche et al., 2014). Those links suggest that climatically driven changes in hydrology would likely result in extensive shifts in vegetation composition and, implicitly, meadow condition (Loheide et al., 2009; Viers et al., 2013). Thus, climate shifts are widely regarded as one of the strongest forces of change in meadows in the subalpine and alpine zones of the SNV (Hayhoe et al., 2004; Loheide et al., 2009). Structure, composition, and function are different community attributes though, and changes in one will not necessarily be representative of change in others (Lamy et al., 2021). The potential direction and magnitude of change in vegetation condition in meadows in the high elevation zone of the SNV have been largely speculative, especially across large spatial scales and relatively long periods of time. This presents a significant gap in understanding of the degree of resistance high elevation meadows in the SNV might have to large-scale shifts in temperature and precipitation.

Our goal was to evaluate spatio-temporal dynamics in vegetation production and productivity for meadows in the subalpine and alpine zones of the SNV. Increasing summer temperatures and alterations to snowpack and hydrologic regimes have been occurring in the SNV for several decades (Cayan et al., 2001; Mote et al., 2005; Thorne et al., 2007; Stewart, 2009; Dettinger et al., 2018). An overwhelmingly strong climate signal would be expected to lead to largely consistent responses in meadow condition, but whether that response would translate to increased or decreased production and productivity is not known. Lower water tables in combination with higher temperatures could result in decreased production and productivity (Sun et al., 2013; Shen et al., 2014). But higher temperatures could lead to extended growing seasons and hence greater production and productivity (Ganjurjav et al., 2016; Wang et al., 2022). Moreover, there is high heterogeneity in topography, soils, climate, and hydrology throughout the SNV, all of which influence meadow condition (Viers et al., 2013). Finally, changes in production and productivity could be abrupt, possibly reflecting the existence of threshold effects (Hillebrand et al., 2020). Therefore, more than a largely consistent pattern of change in condition across meadows, there could be highly variable temporal and spatial responses that reflect the strong heterogeneity in environmental conditions.

We had three main objectives. The first was to identify the forms of temporal dynamics in terms of trends and variability over the last several decades. The second was to evaluate if there was a consistent pattern of increasing or decreasing production of vegetation biomass over the last several decades. The third was to identify the spatial pattern of variability in production and productivity (rate of biomass production) over the last several decades. We addressed five main questions: (1) Was there a consistent decreasing or increasing trend in production over the last four decades? (2) Were changes in vegetation production characterized primarily by steady trends or more abrupt changes? (3) Did abrupt changes tend to occur in different or the same periods of time? (4) Did meadows with higher or lower levels of production and/or productivity cluster in particular regions, or were they dispersed throughout the SNV? (5) Did meadows with greater or lower variability in production and productivity cluster in certain regions, or were they dispersed throughout the SNV?

Methods

Study region

The SNV is approximately 335 km east of the Pacific Ocean and located between the Central Valley of California and the Great Basin and Mojave Deserts (Figure 1). It is one of the major mountain ranges in North America, extending approximately 640 km in a north–south direction with a width of 80–130 km (east–west). Elevation initially increases from south to north until it reaches a maximum of 4,421 m in the central part of the range, then decreases again northward of that maximum. Its elevation and orientation results in the range intercepting winter storm systems from the Pacific Ocean, as well as moist airmasses from the Gulf of California during the monsoon season (mid-July to mid-September). Most of the annual precipitation above 1,800 m occurs as snow, with 90% of it falling between November and April (Storer et al., 2004). Monsoon rains are frequent and often intense, but are usually of short duration (1–3 cm in 1–2 h) and in total comprise <5% of total annual amounts. Precipitation has a pronounced rain shadow pattern, with the east side of the range receiving substantially less than the west.

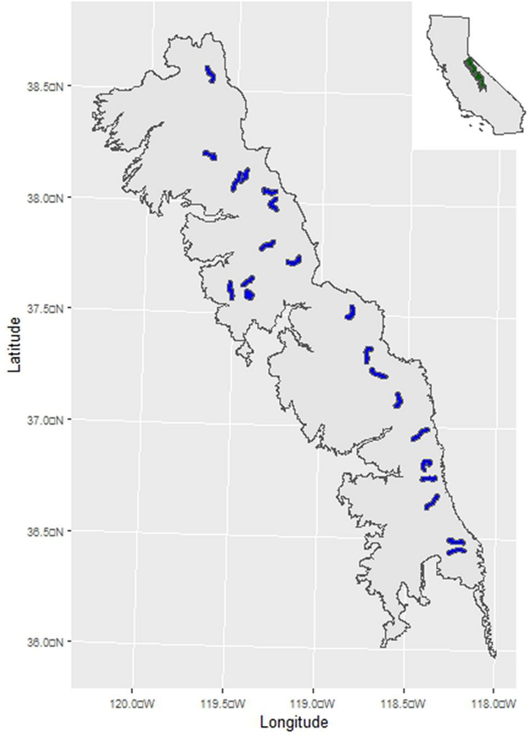

FIGURE 1
Location of the study region in the Sierra Nevada mountain range of North America. The inset shows the location of the study region (green polygon) in California, United States. The main map shows the geographical extent of the study region, and the blue polygons the locations of 21 randomly selected 10km^2 areas where herbaceous biomass samples were collected from 160 randomly located plots distributed among 60 randomly selected meadows >2,500m.

The study region spanned an elevation range of 2,500–4,000 m along a 350 km north–south gradient (≈3° of latitude) and encompassed virtually all of the alpine zone and a large portion of the sub-alpine zone (Figure 1). Transitions from the subalpine to alpine zones are not distinct, but vary with latitude and local topography (Fites-Kaufman et al., 2007). Thus, the existence of a distinct "treeline" between the subalpine and alpine zones is uncommon. Meadows tend to be surrounded by conifer stands in the lower and mid sub-alpine (Lubetkin et al., 2017), while in the upper sub-alpine conifers occur patchily in small, low-statured stands ("krummholz") scattered among a matrix of rock and meadows. Meadows comprise the main vegetation type in the alpine zone, but they occur patchily and in varying sizes among the dominant rocky features. There can be significant heterogeneity in soil moisture due to fine-scaled variation in topography, which is reflected in considerable within-meadow variation in species composition. Woody plants may be present in meadows (usually willows *Salix* spp.), but vegetation is overwhelmingly comprised of herbaceous plants.

Analysis overview

We based our analysis on monthly and annual satellite-derived indices of production and productivity. This allowed us to evaluate their temporal and spatial patterns throughout virtually all of the alpine zone and a substantial portion of the upper subalpine zone. The ability to analyze patterns across long temporal and large spatial scales is a clear advantage of satellite indices, but this depends on the accuracy of the indices. Therefore, our initial steps were to: (1) evaluate the accuracy of GIS polygons identified as meadows; and (2) relate data on biomass collected in the field to the satellite index of production (the Normalized Difference Vegetation Index; NDVI). After this, we partitioned the analysis into temporal and spatio-temporal dynamics. Monthly time series were used to investigate temporal dynamics of NDVI and variables derived from annual NDVI time series were used to examine spatio-temporal dynamics. We calculated the proportion of meadows with trends, abrupt changes (changepoints; Beaulieu et al., 2012), neither or both from time series of monthly NDVI. When there was evidence of abrupt changes, we determined the years they occurred. To analyze spatio-temporal dynamics, we derived indices of annual production and productivity, two measures of variability in annual production and productivity, and the overall change in annual production and productivity across years for each meadow. We used geographically weighted regression (GWR) to quantify the spatial distribution of meadows along gradients of latitude, longitude, and elevation for each annual index. We then conducted a distance-decay analysis to evaluate the relationship between similarity among annual temporal indices and distance among meadows. All analyses were conducted in R (R Core Team, 2022).

Data acquisition

Meadow boundaries

We used an Arc GIS shapefile of meadow polygons that was developed by integrating dozens of meadow shapefiles from multiple public and private organizations (Fryjoff-Hung and Viers, 2012). The polygons were for all meadows throughout the SNV, therefore we subset it to include only those ≥2,500 m and within the boundary of our study region. Elevation for each meadow was derived from a 30-m digital elevation model acquired from the US Geological Survey (USGS) National Map.[1]

NDVI

Satellite-derived indices have been used for monitoring vegetation biomass and phenology in an extensive range of ecosystems, including those at high elevation (Carlson and Ripley, 1997; Shen et al., 2011). Since the mid-1980's, NDVI has been perhaps the most widely used of those satellite indices (Pettorelli, 2013). We calculated monthly estimates (January 1985–December 2021) of NDVI from the US Geological Survey Analysis Ready Data archive (ARD; Dwyer et al., 2018). ARD are produced from Landsat 4–9 satellite images that have been accurately georegistered, calibrated, and pre-processed (both top of atmosphere and atmospheric correction). Because ARD are derived from multiple Landsat satellites, there are multiple images for each month (2–7 at 30 m resolution). Therefore, we used the terra package (Hijmans, 2022) in R to derive estimates of monthly maximum NDVI values. NDVI is a ratio between red (R) and near infrared (NIR) wavelengths, but the bands for these wavelengths differ between sensors (i.e., different Landsat satellites). We calculated NDVI as (Band 4 – Band 3)/ (Band 4 + Band 3) for Landsat 4–7 data, and (Band 5 – Band 4) / (Band 5 + Band 4) for Landsat 8 and 9 data. The calculations were done for images where cloud cover was ≤25%.

Because of the high proportion of rock in our study region, we wanted to confirm that NDVI was an accurate index of vegetation biomass. Therefore, we collected herbaceous biomass data that could be directly related to NDVI values. We established 21 randomly selected 10-km^2 units along a 270 km latitudinal gradient across the study region (Figure 1). The units consisted of 10 km transects with a 1-km buffer (500 m on each side of the transect) separated by a minimum of 5 km. The transects were on trails randomly chosen from a pool of 68 existing routes. Most of the transects traversed the crest of the SNV in a largely east–west orientation and avoided highly traveled routes such as the Pacific Crest Trail.

We randomly selected 60 meadows distributed among the 10-km^2 regions, then established 1–6 0.25 ha plots (50 m × 50 m) within each meadow ($N = 160$ plots). Plots within a meadow were separated by a minimum distance of 60 m, with plot centers located approximately in the center of a Landsat pixel. Herbaceous vegetation in four functional groups (forb, grass, rush, sedge) was clipped to ground level in four randomly located 900 cm^2 quadrats (30 cm × 30 cm) within each plot. The samples for each group were composited within each plot, weighed in the field, then oven dried and weighed in a USGS laboratory on the east side of the SNV (Bishop, California; 37.36° north, 118.40° west). Samples were collected from mid-July to late-August in 2010–2012 and 2014. Biomass (g 3,600 cm^2) was calculated as the weight of the composited samples after oven drying.

Analysis

Meadow boundaries

We assessed the accuracy of the meadow polygons with a two-stage ground-truth approach. The first stage consisted of visiting areas identified as meadows within the 21 randomly selected 10-km^2 regions. We used Arc GIS to calculate centroids for 1 to 9 randomly selected meadow polygons (median = 6) in each 10-km^2 region ($N = 126$ total). One of the authors (RK) then used a global positioning unit (GPS) to locate each centroid and classified the surrounding area into one of five landcover classes: meadow, shrub, conifer, mixed conifer-shrub, or rock. Visits to the centroids occurred from 2014 through 2016.

The second stage consisted of visiting an equal number ($N = 126$) of randomly selected points identified as landcover other than meadows and then classifying the surrounding area into one of the five landcover classes. These points were located in areas outside of but between the 10-km^2 regions. Visits to these points were made by RK between 2015 and 2019.

Accuracy assessment was made by collapsing the landcover classes into meadow and non-meadow, and then developing a confusion matrix based on the number of correct and incorrect classifications. We then calculated the true positive (sensitivity) and negative (specificity) rates, as well as overall accuracy of the meadow polygon delineations.

---

[1] https://apps.nationalmap.gov/downloader/

NDVI

We used ordinary least-squares regression (OLS) to model the relationship between NDVI and total herbaceous biomass (i.e., summed across the functional groups within each plot *i*). An exploratory analysis indicated there was a curvilinear relationship between NDVI and biomass (g 3,600 cm^2), so we log$_{10}$-transformed biomass and specified the model as:

$$NDVI_i \sim N\left(\mu_i, \sigma^2\right)$$

$$\mu_i = \alpha + \beta_1^* \log_{10}\left(\text{Biomass}\right)_i + \varepsilon_\text{i}$$

with $\alpha \sim N(0,\sigma^2)$, $\beta_1 \sim N(0,\sigma^2)$, $\varepsilon_\text{i} \sim N(0,\sigma^2)$.

Temporal dynamics

Because the cloud cover threshold (≤25%) resulted in months with missing data (median = 34 per meadow; range = 12–87), we interpolated and smoothed the raw monthly NDVI values with a state-space model. These are flexible hierarchical time series models where parameter estimation is based on an observation model that is linked to a state (process) model (Auger-Méthé et al., 2021). They have several advantages over other time series models (e.g., ARIMA), including; (1) the partitioning of state and observation variability results in estimates of process variation being less biased by sampling error; (2) the time series do not need to be stationary to estimate the parameters; and (3) missing values are accurately estimated through application of a recursive fitting and smoothing process (the Kalman filter). The structure of a state-space model with seasonality is (Shumway and Stoffer, 2011):

$$x_i = \text{B}_i x_{t-1} + u_i + \text{C}_i \text{c}_t + \text{w}_i \text{; the state process with } \text{w}_i \sim \text{MVN}\left(0, Q_i\right)$$

$$y_i = \text{Z}_i x_t + a_i + \text{D}_i \text{d}_t + \text{v}_i \text{; the observation process with } \text{v}_i \sim \text{MVN}\left(0, R_i\right)$$

where *x* and *y* are time series values for meadow *i* at time *t*, B and Z are parameters for *x* at time *t* or in the previous time step *t–1*, respectively, *u* and *a* are rate parameters, C and D are parameters associated with covariates for seasonality c and d, respectively (i.e., month), and *w* and *v* are the process and observation errors that are assumed to be multivariate normally (MVN) distributed with a mean of 0 and covariances *Q* and *R*, respectively. Because NDVI values are continuous and can be positive or negative, the assumption of MVN was justifiable. We used the imputeTS package (Moritz and Bartz-Beielstein, 2017) to interpolate missing NDVI values and the statespacer package (Beijers, 2022) to conduct the smoothing.

We analyzed temporal dynamics by comparing seven models of monthly NDVI for each meadow. The models included: (1) constant mean (null model: no trend or abrupt shifts in level); (2) 1-month autoregression (random walk); (3) 1-month autoregression and changepoints (random fluctuations between periods of abrupt shifts in level); (4) linear trend (steady increase or decrease over time); (5) 1-month autoregression and linear trend (random walk with drift); (6) linear trend with changepoints (steady increase or decrease between periods of abrupt shifts in level); and (7) 1-month autoregression, linear trend, and changepoints (random fluctuations or steady increase or decrease between periods of abrupt shifts in level). Detection of changepoints (number of changepoints and time, i.e., year) was based on a pruned exact linear time algorithm (PELT; Beaulieu and Killick, 2018). PELT searches for changes in mean and/or variance across sequential time segments using penalized likelihood ratio tests that evaluate where changepoints occur (Killick and Eckley, 2014). PELT assumes that the number of changepoints will increase with time series length, but it will not identify changepoints if the likelihood ratio tests indicate there are none. We specified 3 years as the minimum time segment length and used a modified Bayesian Information Criterion penalty for the likelihood ratio tests (Zhang and Siegmund, 2007; Beaulieu and Killick, 2018). Model comparisons were based on the biased-corrected version of Akaike's Information Criterion (AICc) and AICc weights (*w*AICc).

AICc is prone to identifying more complex models as having the most support even though some parameters may have little explanatory power (Ward, 2008). Therefore, we used dynamic linear regression (DLR; Zeileis et al., 2005) to calculate slope parameters for meadows identified by the PELT algorithm as having a trend. The incorporation of autoregressive effects into DLR makes it an appropriate tool for evaluating different types of dynamics, including the existence of linear trends. We used the dynlm package in R (Zeileis, 2019) to specify DLR models with trend and 1- and 12-month autoregression, then calculated the trend coefficients and their 95% confidence interval (CI). Based on the results of the PELT and DLR analyses, we assigned the temporal dynamics of each meadow into one of five classes (Table 1): significant decreasing trend in NDVI, negative but non-significant trend coefficient (the 95% CI of the slope coefficient from the DLR

TABLE 1 The number (N) and percentage of meadows >2,500 m in the Sierra Nevada mountain range of North America where changepoints were detected within five classes of trends between January 1985 and December 2021.

Trend class	Changepoints (%)		*N*	Percent
	Not detected	Detected		
Decrease	15.6	1.5	1385	17.2
Negative (NS)	7.8	2.9	862	10.6
No trend	0.0	19.7	1593	19.7
Positive (NS)	21.0	7.2	2276	28.1
Increase	7.1	17.4	1979	24.4
Total (%)	51.4	48.6		100.0
Total (N)	4163	3932	8095	

overlapped zero), no trend based on both the PELT and DLR analyses, a positive but non-significant trend (the 95% CI of the slope coefficient from the DLR overlapped zero), and a significant increasing trend in NDVI.

Spatio-temporal dynamics

We used the greenbrown package (Forkel et al., 2013, 2015) to derive an initial set of five indices of annual production and productivity from the monthly time series for each meadow. The indices included: mean growing season NDVI (MGS), peak growing season NDVI (Peak), low growing season NDVI (Trough), the amplitude in growing season NDVI (Amplitude; Peak–Trough), and the rate of spring greenup (RSP). We examined the intra-annual correlations among the indices and removed Peak and Trough because of their high correlations with MGS (mean $r = 0.97$ and 0.72, respectively), and Amplitude because of its high correlations with RSP (mean $r = 0.97$). The remaining variables provided indices of annual production (MGS, calculated as the mean NDVI value during the growing season) and productivity (RSP, calculated as the slope in NDVI between the beginning and peak of the growing season). We then calculated three other variables each for MGS and RSP: the coefficient of variation (CV) of temporal variation, the consecutive disparity index (D) of temporal variability, and the overall change in MGS or RSP over the 37-year period (ΔMGS and ΔRSP). The CV is a commonly used measure of temporal variability, but it is not independent of the mean of a time series and is sensitive to uncommon events (Fernández-Martínez et al., 2018). D takes into account the order of values in a time series, is independent of the mean, and not as sensitive to rare events as the CV (Fernández-Martínez et al., 2018). Since D is calculated as the mean rate of change of the log ratios of consecutive values, when $D = 1$, for example, this indicates that on average variability is ≈ 2.72 × greater than if a time series was constant. Thus, more than simply being an alternative to the CV, D provides additional insight into patterns of temporal variability. ΔMGS and ΔRSP were calculated as the sum of differences between years [e.g., $\Delta MGS = \Sigma(MGS_{year} - MGS_{year-1})$] and gave a measure of the net increase or decrease of MGS and RSP over the 37 years of the study.

We quantified the distribution of the annual indices along gradients of latitude, longitude and elevation with geographically weighted regression (GWR; Fotheringham et al., 2002). GWR is a variety of least-squares regression that examines how the relationship between dependent and predictor variables varies over space. Whereas traditional (i.e., non-spatial) least-squares would fit a global estimate of the relationship, GWR calculates an estimate for each data point. The non-spatial and spatially varying models can be compared with AICc, and if there is support for the spatial model the local coefficients can be mapped. The core of GWR is the development of a spatial kernel that is a moving window from point to point. The window includes a number of neighboring points determined by the bandwidth, which can be fixed or vary among points (an "adaptive kernel"); narrower bandwidths mean fewer neighboring points are used to calculate the local coefficients. We used the spgwr package (Bivand and Yu, 2020) to calculate the optimal bandwidth for adaptive kernels with a bisquare weighting function, then conducted the GWR for each MGS and RSP variable. We compared GWR and OLS models with *w*AICc and ANOVA (Fotheringham et al., 2002). We then classified local coefficients as increasing, decreasing or not changing based on the sign of the coefficient and if their 95% CIs overlapped zero.

We reasoned that if meadows with different spatio-temporal dynamics were segregated from each other this would translate to a well-defined distance-decay relationship. Conversely, if there was intermixing of meadows where spatio-temporal dynamics were unlike, then distance-decay relationships would be weak or non-existent. Therefore, we calculated distance matrices from each set of standardized MGS and RSP variables, then regressed those distance matrices against the geographic distances among meadows. We used Euclidean distance because some of the MGS and RSP variables had negative values. The large number of meadows (see Results) made pairwise comparisons of distances computationally unachievable using the full dataset, so we applied a randomization approach to compare slopes of the relationship between observed and permuted geographic distance. This entailed randomly selecting 1,000 meadows in each of 1,000 iterations, then estimating the slope and explained variation (R^2) from each iteration. We then calculated the slope based on 1,000 random permutations of the geographic distances within each iteration and compared the mean and 95% CIs of the observed and permuted values. The simba package (Jurasinski and Retzer, 2012) was used to create permutations and calculate slopes from the permuted distances.

Results

The meadow polygons were identified with a very high degree of accuracy. Sensitivity (98%; 123 meadows correctly identified as so) and specificity (97%; 122 points correctly identified as not being meadows) were nearly identical, and overall accuracy was 97.2% (95% CI = 94.4–98.9). A total of 8,149 meadows occurred within the study region. We removed 54 (<1%) from the dataset because sensible NDVI values could not be calculated for them, leaving a working set of 8,095.

There was a very strong relationship between NDVI and total herbaceous biomass ($r = 0.914$; Table 2 and Figure 2). The relationship was particularly strong in the middle range of biomass values, with a tendency of lower and higher estimates of NDVI than predicted for lower and higher values of biomass, respectively (Figure 2).

TABLE 2 Parameter estimates of the relationship between the Normalized Difference Vegetation Index (NDVI) and herbaceous biomass in 160 randomly located plots within 60 randomly selected meadows >2,500m in the Sierra Nevada mountain range of North America.

Parameter	Estimate	SE	LCL	UCL	*t*	*p*
Intercept	468.51	70.24	329.78	607.24	6.67	<0.0001
Biomass ($\log_{10}$)	2491.58	88.04	2317.69	2665.47	28.31	<0.0001

Biomass samples were collected once in four 900 cm^2 quadrats within each plot between 2010 and 2014. LCL and UCL are the lower and upper 95% confidence intervals of the parameter estimates.

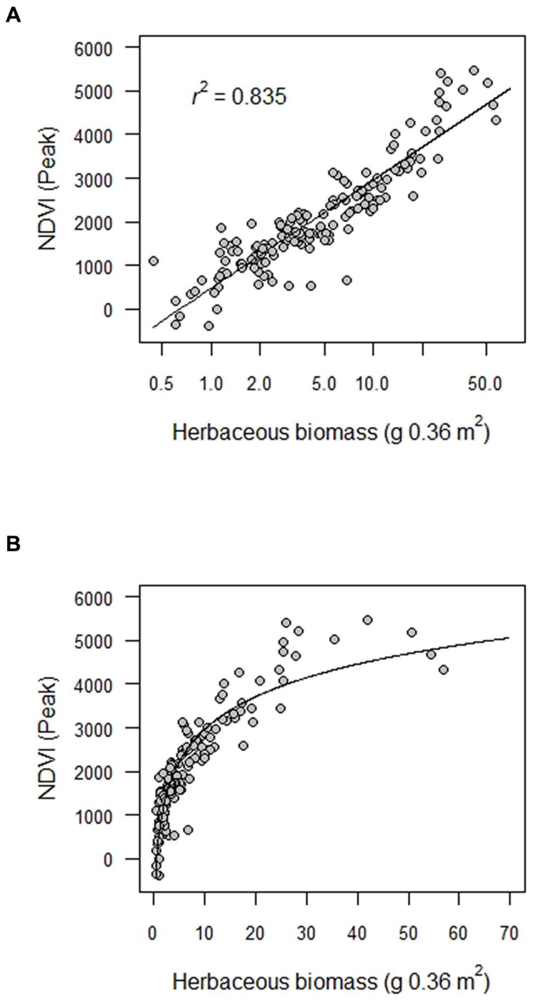

FIGURE 2
Estimated fit of the relationship between total herbaceous biomass (g per $0.36m^2$) and the Normalized Difference Vegetation Index (NDVI) in the Sierra Nevada mountain range of western North America. Biomass samples were collected once in either 2010, 2011, 2012 or 2014 from 160 plots distributed among 60 meadows along a 270km latitudinal gradient through the upper subalpine and alpine zones. Fitted values were derived from an ordinary least squares regression of $\log_{10}$ transformed biomass values **(A)**; panel **(B)** shows the curvilinear relationship for untransformed biomass values. NDVI was the peak growing season value associated with a plot in the year the biomass sample was collected.

Temporal dynamics

Temporal dynamics varied greatly among the meadows (Figure 3). Meadows with strong evidence of a positive trend comprised almost 25% of the total and were 1.5× more common than those with strong evidence of a negative trend (Table 1). Collectively, meadows classified as not having a long-term trend, having a positive but weak trend, or having a positive trend made up >70% of the total. There was marked mixing among the five trend classes when they were plotted along gradients of latitude, longitude, and elevation (Figure 4).

Changepoints occurred in every year (Figure 5) and were present in the dynamics of >48% of the meadows ($N = 3{,}932$). They occurred in 10.4 to 30.5% of the meadows across years, with no indication of a trend of them becoming less or more frequent over time (Figure 5). They also occurred in meadows in all five trend classes, particularly those with no evidence of a trend (100%) or strong evidence of a positive trend (71%) (Table 1).

Spatio-temporal dynamics

There was high heterogeneity in the spatial distribution of the MGS and RSP variables, with *w*AICc and ANOVA consistently supporting the GWR models for all eight variables (Table 3). The ranges of each of the local coefficients included negative and positive values, and while median values of those ranges were sometimes similar to the values of the global coefficients (MGS, CV of MGS, *D* for MGS, *D* for RSP), in other cases they were not (ΔMGS, RSP, CV of RSP; Table 3). Meadows representing the full range of predicted values for the MGS and RSP variables occurred throughout the study region, though there were also clear-cut clusters with similar values (Figures 6A,C, 7A,C, 8A,C, 9A,C).

The GWR model of the relationship between MGS and elevation explained a very high proportion of variation ($R^2 = 0.904$; Table 3), with 61.1% of the meadows having significantly negative coefficients (Table 4). Meadows with no indication of a relationship between MGS and elevation comprised 37.6% of the total (Table 4). Overall, meadows with coefficients of varying sign and strength for the relationship between MGS and elevation were intermixed throughout the study region (Figure 6B). The GWR model of the relationship between RSP and elevation explained a moderately high proportion of variation ($R^2 = 0.532$; Table 3), but in contrast with MGS the coefficients for 60.2% of the meadows indicated no significant relationship between RSP and elevation. Meadows with significant negative coefficients made up 28.2% of the total (Table 4). The meadows without significant coefficients were distributed throughout the study region, while those with significant negative coefficients were largely absent from the most northerly, southerly, and central areas of the region (Figure 6D). Meadows where there was a significant positive relationship between RSP and elevation made up 11.6% of the total and occurred patchily across the study region (Figure 6D).

The observed CV of MGS was highly skewed (Supplementary Figure S1). Approximately 90% of the values ranged between 0.127 and 0.844 and more than 99% were < 2, but the remainder went as high as 34. The relationship between the CV of MGS and elevation was weak ($R^2 = 0.107$; Table 3). Most meadows had no significant relationship with elevation (57.9%; Table 4) and occurred throughout the study region. However, there was notable geographic segregation of meadows with significantly positive coefficients for elevation (41.5%; Table 4 and Figure 7B). These meadows occurred throughout much of the study region but were particularly frequent in the central and southern parts (Figure 7B). The observed CV of RSP was not skewed, though there was one meadow with an extreme value; all other values were < 2 (Supplementary Figure S2). Coefficients in 55.8% of the meadows did not have a significant relationship with elevation, while 40.2% had a significant positive relationship (Tables 3, 4). The spatial distribution of the RSP-elevation relationship was similar to that of the MGS-elevation relationship, though there was a notable lack of

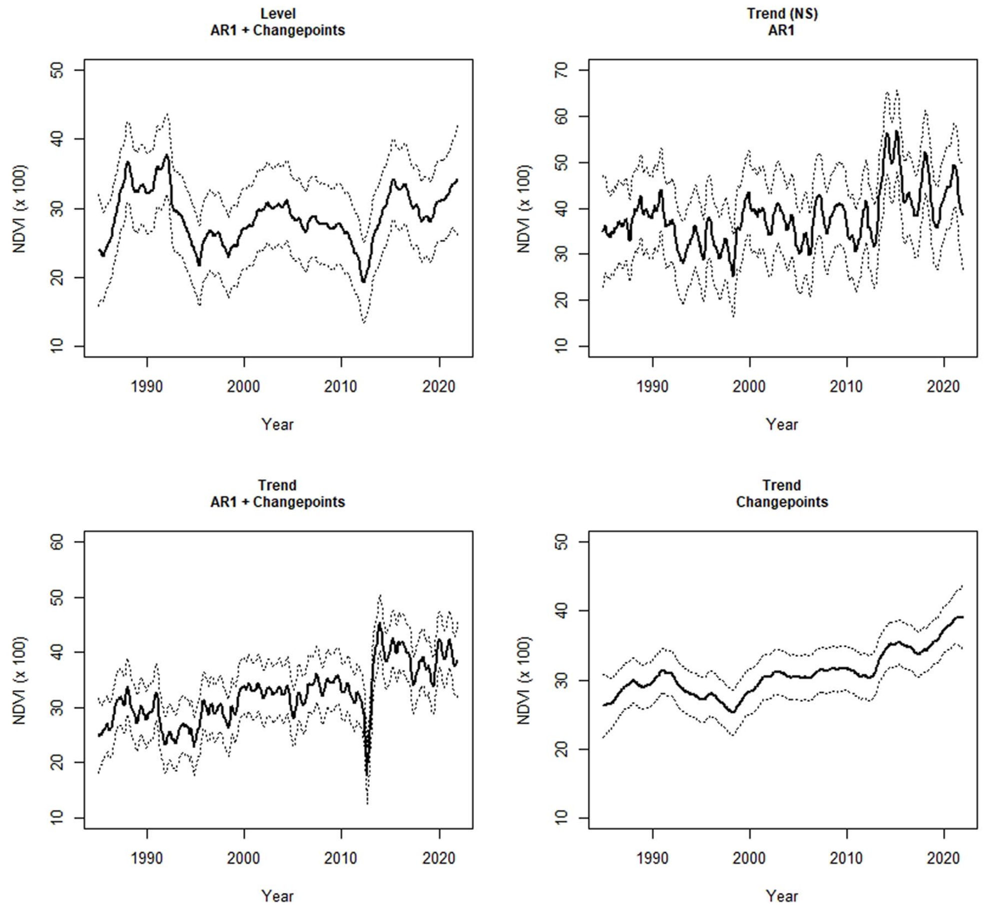

FIGURE 3
Four randomly selected examples of dynamics in monthly values of the Normalized Difference Vegetation Index (NDVI) from January 1985–December 2021 in meadows in the upper subalpine and alpine zones of the Sierra Nevada mountain range of western North America. The solid line is the smoothed estimate (±95% CI) from a state-space model. NS=a trend was identified as the best model (out of seven) but the 95% CI of the trend coefficient overlapped zero. AR1=1-month autoregression.

positive relationships in the central part of the study region (Figure 7D).

More than 75% of the values for *D* of MGS > 1 (Supplementary Figure S1). While this was indicative of relatively high inter-annual variability, its relationship with elevation was weak ($R^2 = 0.039$; Table 3). Nearly 75% of the meadows had coefficients with no significant relationship with elevation; those with coefficients indicating a significant positive relationship (22.2%) were almost 2× more frequent than those with significant negative coefficients (Table 4). Meadows with non-significant coefficients occurred throughout the study region (Figure 8B). Meadows with significant positive or negative coefficients had markedly different distributions; those with significant positive coefficients were almost entirely absent in the south part of the study region while those with significant negative coefficients were absent in the central part (Figure 8B). The values of *D* also pointed toward high inter-annual variability in RSP, with more than 70% > 1 (Supplementary Figure S2). Its relationship with elevation was weak ($R^2 = 0.137$; Table 3), with almost 73% of the meadows having coefficients indicating no significant relationship. There were more than 4× as many meadows with positive as negative coefficients for *D* of RSP (Table 4). The ones with positive coefficients occurred patchily throughout the study region, while those with negative coefficients were largely absent in the north (Figure 8D).

GWR R^2 values for ΔMGS and ΔRSP were 0.507 and 0.637%, respectively. The percentage of meadows with coefficients indicating no significant relationship with elevation was almost identical between ΔMGS and ΔRSP (Table 4). They occurred throughout the study region and were 2.4× to 10× more frequent as meadows with a significant positive or negative relationship (Figures 9B,D and Table 4). Meadows with a significant negative coefficient for ΔMGS (27.7%) occurred patchily throughout the region, as did those with significant positive coefficients for ΔRSP (28%; Figures 9B,D and Table 4). Meadows with significant positive ΔMGS coefficients (6.1%) were distributed sparsely throughout the study region, but those with significant negative ΔRSP coefficients (6%) were largely absent from the north (Figures 9B,D).

There was no indication of a meaningful distance-decay relationship for either the MGS or RSP matrices. Intercepts of the relationship indicated only moderate similarity among meadows even at very short distances, with extremely high variability across the entire range of geographic distances (Supplementary Figures S3, S4). The 95% CI of MGS slope parameters overlapped zero (Figure 10A)

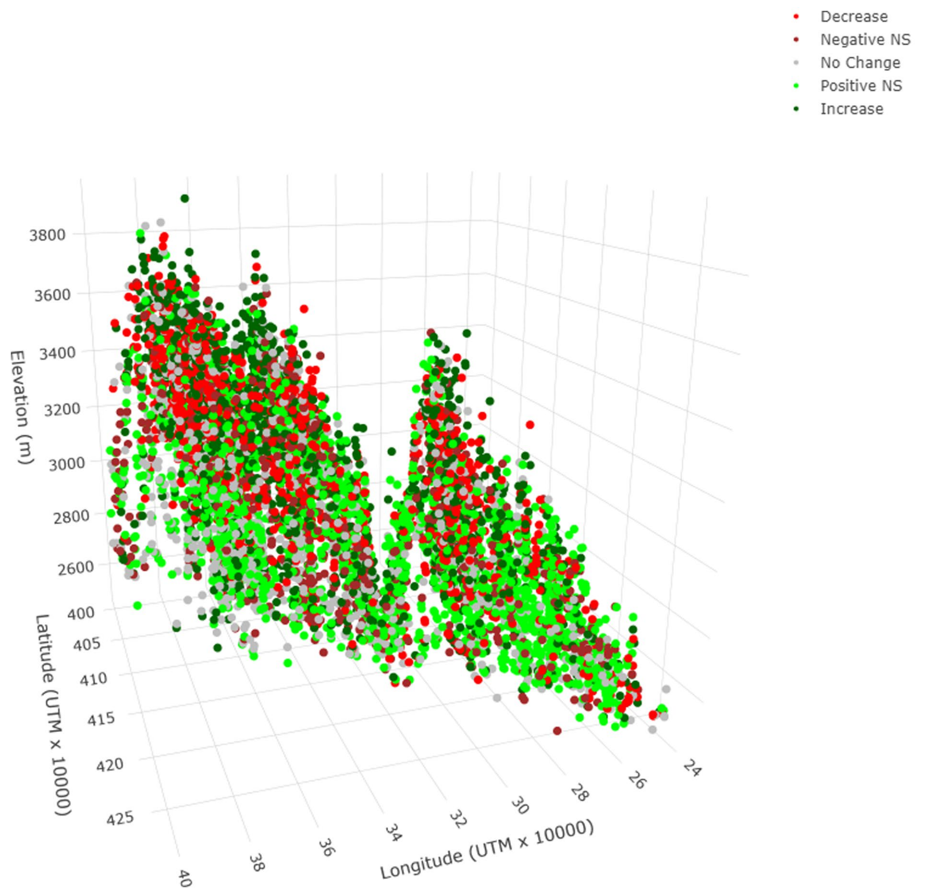

FIGURE 4
Spatial distribution of meadows in five trend classes in the upper subalpine and alpine zones of the Sierra Nevada mountain range of western North America. Classification of trend was based on smoothed time series of monthly values of the Normalized Difference Vegetation Index (NDVI) from January 1985–December 2021. NS=95% CI overlapped zero (non-significant).

and differences between pairwise and permuted slope values were essentially zero (Table 5). The 95% CI of RSP slope parameters was greater than zero (Figure 10B), but the effect size was negligible; differences between pairwise and permuted slope values were essentially zero (Table 5). The mean *p*-value and R^2 for the MGS permutations were 0.508 and 0.00087, respectively. Mean *p*-value and R^2 for RSP permutations were 0.503 and 0.00469, respectively.

Discussion

We focused the analyses in this study on spatio-temporal patterns so we would have a foundation for developing and testing hypotheses of more mechanistic relationships between environmental heterogeneity and dynamics in meadow condition. Based on the patterns we found, the analyses we conduct in the future will clearly need to focus on temporal variability and spatial heterogeneity more so than general trends. Across four decades and a spatial extent of hundreds of kilometers, we found indices of herbaceous production and productivity in meadows in the subalpine and alpine zones of the SNV pointed strongly toward high levels of variability in both temporal and spatial dynamics. A large portion of the meadows had either no trend or very weak ones, and where trends occurred they often differed in direction. Nearly half of the meadows had a rapid change in production in at least one of the 37 years of the study, but the changes were not associated with trend direction or periods of time with particular conditions (e.g., a series of drought or wet years). Indices of annual production and productivity had weak spatial associations with each other, and indices of net change in production and productivity had almost wholly opposing patterns. Two indices of temporal variability differed somewhat in their spatial pattern, but they were similar in highlighting the intermixing of meadows with different patterns of temporal variability and in having weak relationships with elevation.

NDVI is generally considered to be a useful index of vegetation production (Pettorelli, 2013) and has been used extensively to analyze climate effects on vegetation in high elevation zones of the Tibetan Plateau (Ding et al., 2007; Sun et al., 2013, 2016). It is particularly useful in studies such as ours where the focus is on large scale patterns. We found a strong relationship between herbaceous biomass and NDVI, so have little reason to think our findings could be an artifact of mismatch between plot-based and satellite-based measures of vegetation production. But we also think there are instances where NDVI needs to be used cautiously. In our case we simply wanted to ensure NDVI was an appropriate index of plant biomass in the meadows, so we specified it as being dependent on plant biomass. In other cases though the goal might be to predict herbaceous biomass

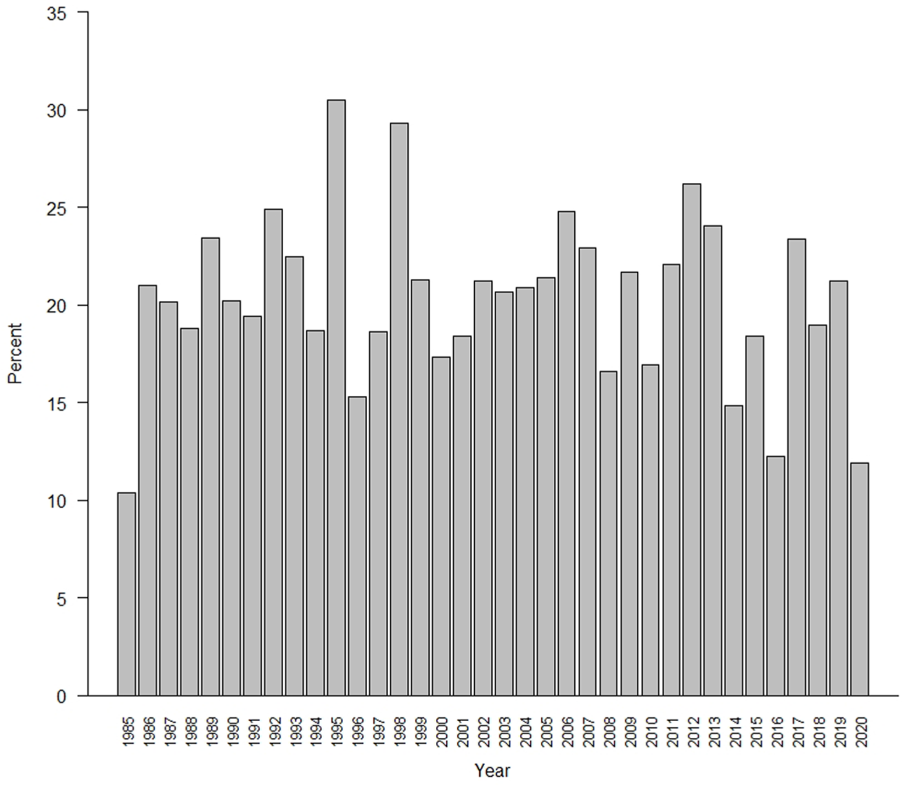

FIGURE 5
Percentage of meadows in the upper subalpine and alpine zones of the Sierra Nevada mountain range where abrupt changes (changepoints) in the Normalized Difference Vegetation Index (NDVI) were detected.

TABLE 3 Summary statistics for geographically weighted regressions (GWR) of eight indices of annual production (mean growing season value; MGS) and productivity (rate of spring greenup; RSP) in 8,095 meadows >2,500 m in the Sierra Nevada mountain range of North America.

MGS Bandwidth = 0.0021						
	DF	**SS**	**Mean Square**	***F***	***P***	***wAICc***
OLS Residuals	2	5769957694				
GWR Improvement	2374.6	4419502396	1861161			
GWR Residuals	5714.4	1350455298	236325	7.8754	0.0000	1
Parameters (quasi-R^2 = 0.906)						
	Minimum	**Median**	**Maximum**	**Global**		
Intercept	−55878.2	14573	63304.7373	13058.3142		
Elevation	−18.5	−3.9384	22.1745	−3.4349		
CV (MGS) Bandwidth = 0.0226						
	DF	**SS**	**Mean Square**	***F***	***P***	***wAICc***
OLS Residuals	2	4487.3				
GWR Improvement	292.91	282.4	0.96423			
GWR Residuals	7796.09	4204.9	0.53936	1.7877	0.0000	1
Parameters (quasi-R^2 = 0.111)						
	Minimum	**Median**	**Maximum**	**Global**		
Intercept	−14.8	−1.797	6.8458	−1.4542		
Elevation	−0.00197	0.0007	0.0051	0.0006		

(Continued)

TABLE 3 (Continued)

D (MGS) Bandwidth = 0.0558						
	DF	SS	Mean Square	*F*	*P*	*wAICc*
OLS Residuals	2	374.07				
GWR Improvement	118.1	14.62	0.123778			
GWR Residuals	7970.9	359.45	0.045095	2.7448	0.0000	1
Parameters (quasi-R^2 = 0.039)						
	Minimum	Median	Maximum	Global		
Intercept	0.323	1	2.3065	1.1266		
Elevation	−0.00038	0.000011	0.0003	0.00001		
ΔMGS Bandwidth = 0.0043						
	DF	SS	Mean Square	*F*	*P*	*wAICc*
OLS Residuals	2	1666748863				
GWR Improvement	1325	800621995	604256			
GWR Residuals	6764	866126868	128049	4.7189	0.0000	1
Parameters (quasi-R^2 = 0.507)						
	Minimum	Median	Maximum	Global		
Intercept	−26782.0	2390	16523.0	1458.5		
Elevation	−5.4	−0.6506	9.8475	−0.3523		
RSP Bandwidth = 0.0039						
	DF	SS	Mean Square	*F*	*P*	*wAICc*
OLS Residuals	2	699727891				
GWR Improvement	1459.2	352196283	241366			
GWR Residuals	6629.8	347531608	52419	4.6045	0.0000	1
Parameters (quasi-R^2 = 0.532)						
	Minimum	Median	Maximum	Global		
Intercept	−10045	2325	19520	1856.1588		
Elevation	−5.59	−0.3939	3.8569	−0.2448		
CV (RSP) Bandwidth = 0.0463						
	DF	SS	Mean Square	*F*	*P*	*wAICc*
OLS Residuals	2	101.159				
GWR Improvement	142.98	9.228	0.064545			
GWR Residuals	7946.02	91.931	0.011569	5.5789	0.0000	1
Parameters (quasi-R^2 = 0.107)						
	Minimum	Median	Maximum	Global		
Intercept	−0.381	0.104	0.9802	0.1319		
Elevation	−0.00025	0.000061	0.00020	0.00005		
D (RSP) Bandwidth = 0.0163						
	DF	SS	Mean Square	*F*	*P*	*wAICc*
OLS Residuals	2	359.77				
GWR Improvement	401.05	43.27	0.107882			
GWR Residuals	7687.95	316.5	0.041169	2.6205	0.0000	1

(Continued)

Parameters (quasi-R^2 = 0.137)						
	Minimum	**Median**	**Maximum**	**Global**		
Intercept	−1.831	0.789	3.0302	0.8241		
Elevation	−0.00058	0.000110	0.00095	0.0001		
ΔRSP **Bandwidth = 0.0035**						
	DF	**SS**	**Mean Square**	***F***	***P***	***wAICc***
OLS Residuals	2	530557176				
GWR Improvement	1569.4	310061341	197561			
GWR Residuals	6519.6	220495834	33821	5.8414	0.0000	1
Parameters (quasi-R^2 = 0.637)						
	Minimum	**Median**	**Maximum**	**Global**		
Intercept	−12917.0	−1241	15042	−1043.7		
Elevation	−4.32	0.3926	4.6282	0.3279		

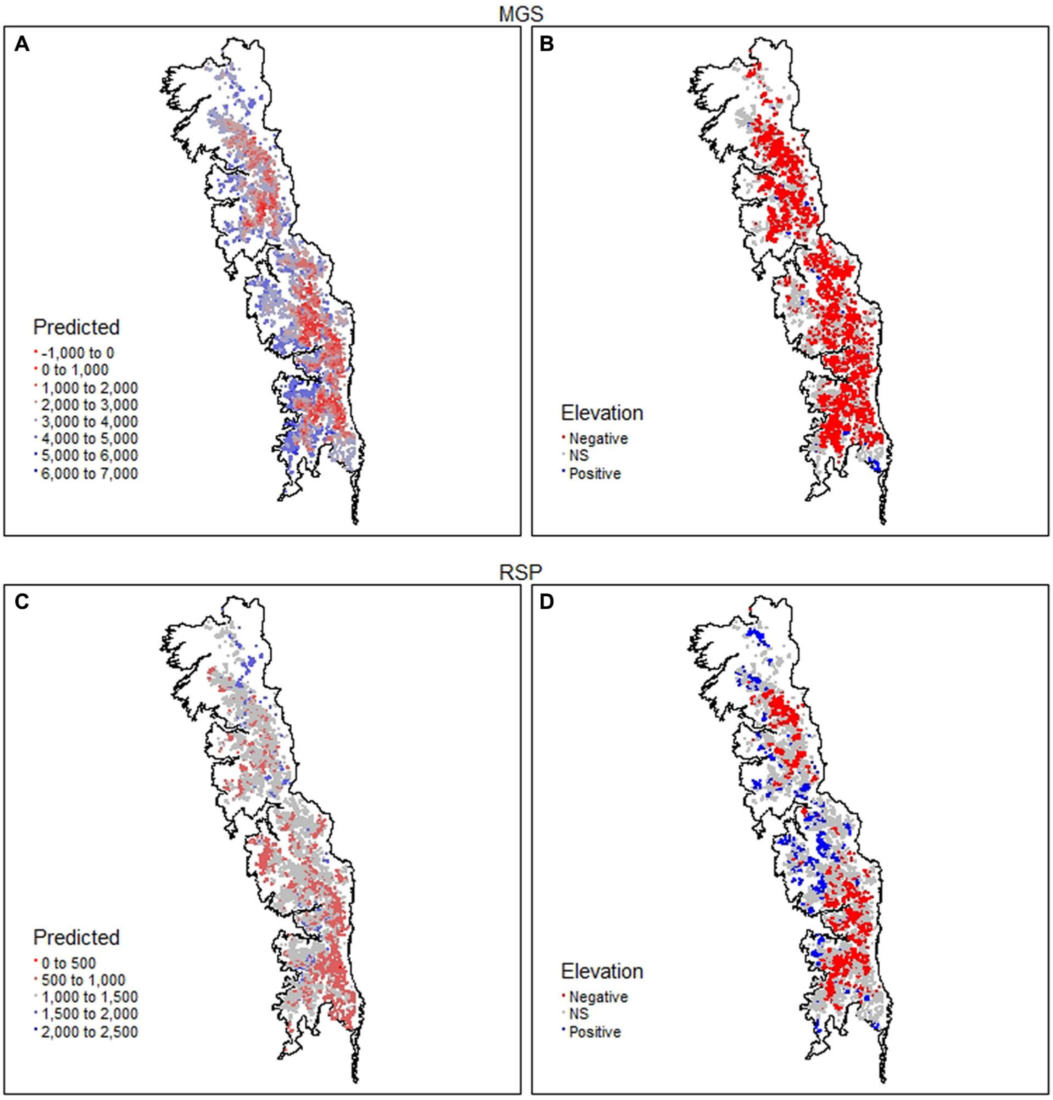

FIGURE 6
Spatial distribution of mean growing season (MGS) and rate of spring greenup (RSP) values in 8,095 meadows in the upper subalpine and alpine zones of the Sierra Nevada mountain range of western North America. MGS and RSP are annual indices derived from monthly time series (January 1985–December 2021) of the Normalized Difference Vegetation Index (NDVI) for each meadow. Panels **(A,C)** give predicted values and panels **(B,D)** direction and significance ($p<0.05$) of the relationship with elevation.

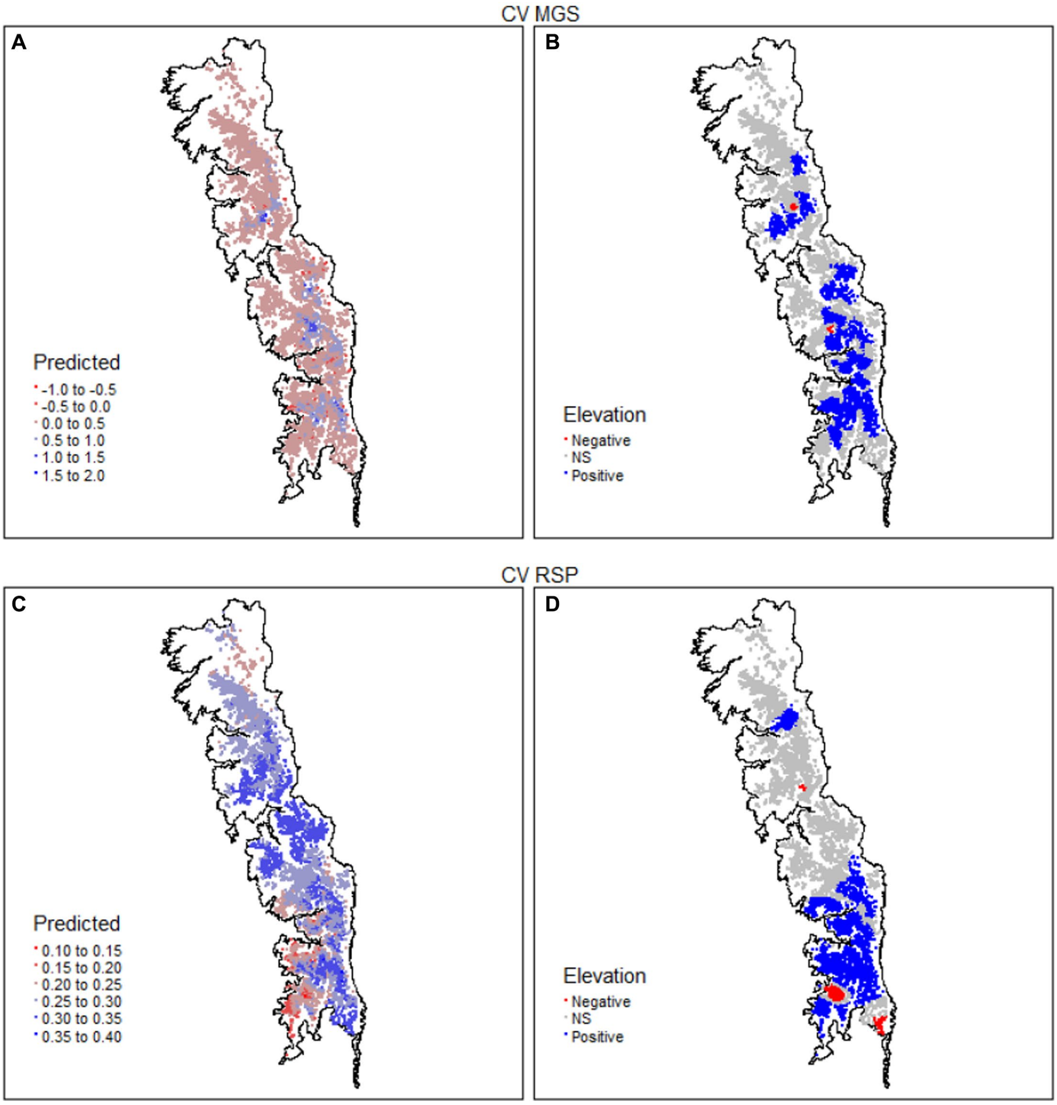

FIGURE 7
Spatial distribution of the coefficient of variation (CV) for the mean growing season (MGS) and rate of spring greenup (RSP) values of 8,095 meadows in the upper subalpine and alpine zones of the Sierra Nevada mountain range of western North America. MGS and RSP are annual indices derived from time series (January 1985–December 2021) of the Normalized Difference Vegetation Index (NDVI) for each meadow. Panels **(A,C)** give predicted values and panels **(B,D)** direction and significance ($p<0.05$) of the relationship with elevation.

from NDVI, hence biomass would be dependent on NDVI. In situations where there is a linear relationship between NDVI and biomass the predictions would be straightforward. But in circumstances such as ours where there was an asymptotic relationship between untransformed values, plant biomass would be underestimated at higher values of NDVI. A log transformation would linearize the relationship and put it on a multiplicative scale, but there would need to be an ecological justification, in addition to a statistical rationale, for doing so.

The larger proportion of meadows with increasing than decreasing trends in NDVI suggests warming is having greater positive than negative effects on meadow condition and is consistent with expectations of production increasing because of warmer conditions, a longer growing season, or both (Ganjurjav et al., 2016). However, many meadows had no trend or only a very weak trend. Thus, rather than temporal dynamics indicating a general prevalence of one pattern over others, the most ecologically appropriate interpretation appears to be recognition of a large diversity of patterns, none of which is dominant. The significance of this becomes even greater when spatial intermixing of the temporal dynamics is taken into account. Whether it was for the monthly time series of NDVI or indices of annual production and productivity, the close spatial association of meadows with different dynamics was the most consistent pattern we found. The lack of any meaningful distance-decay pattern was especially effective at showing this; meadows within a few 100 m of each other could have dynamics as dissimilar, or similar, as if they were hundreds of kilometers away. These patterns give a very strong indication of interplay between regionwide, basin, and meadow-scale factors, including climate patterns, snowpack, basin characteristics, topographic complexity, soils, and herbivory.

Intuitively, production and productivity should be greater where temperatures are higher and the growing season longer (Korner, 2003;

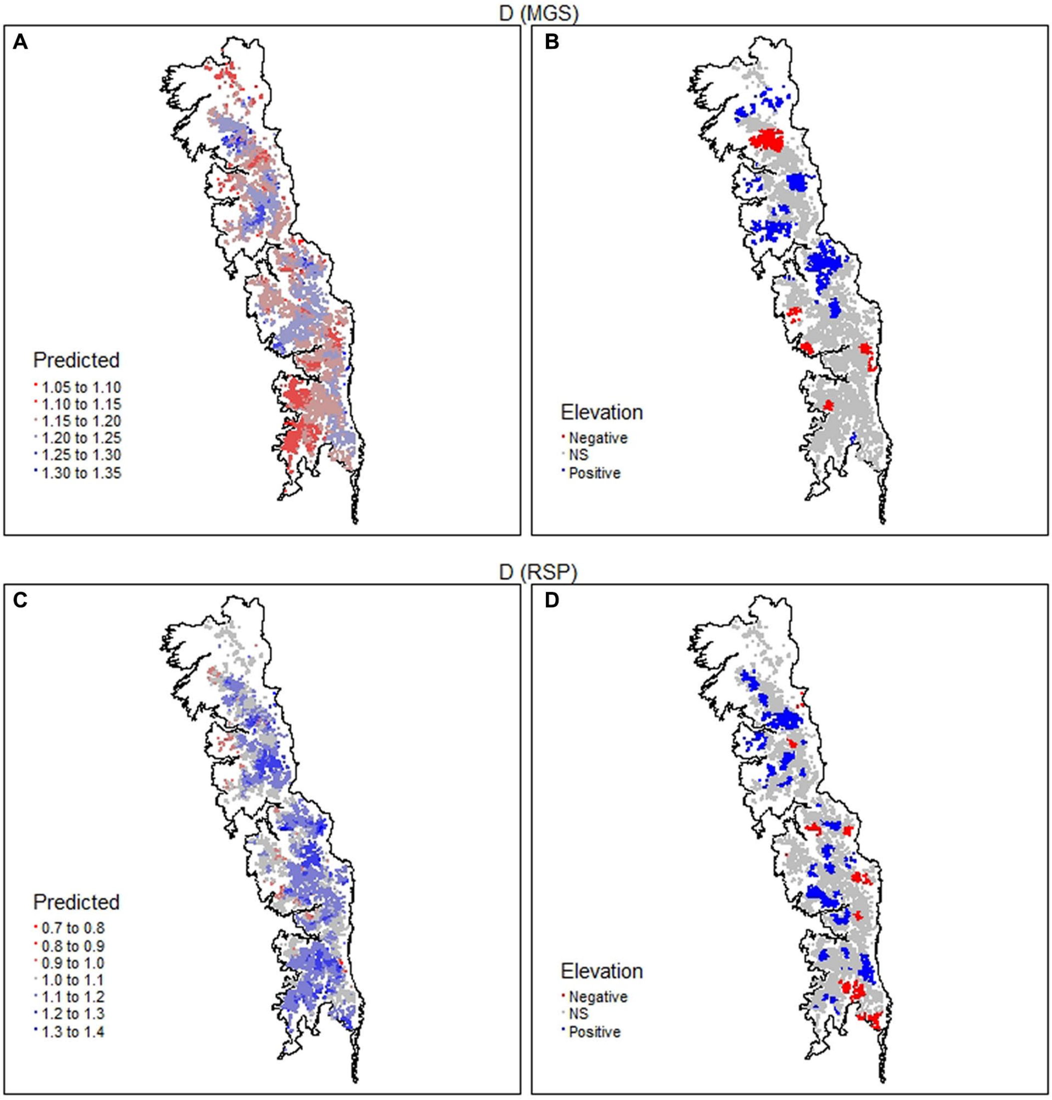

FIGURE 8
Spatial distribution of the consecutive disparity index (*D*) for the mean growing season (MGS) and rate of spring greenup (RSP) values of 8,095 meadows in the upper subalpine and alpine zones of the Sierra Nevada mountain range of western North America. MGS and RSP are annual indices derived from time series (January 1985–December 2021) of the Normalized Difference Vegetation Index (NDVI) for each meadow. Panels **(A,C)** give predicted values and panels **(B,D)** direction and significance ($p<0.05$) of the relationship with elevation.

Shen et al., 2014). The broad occurrence of the negative relationship between elevation and MGS was consistent, at least in part, with the expectation that temperature is setting limits on production. But the extensive distribution of meadows where this relationship was not present shows it is a variable and not completely predictable pattern. The relationship between elevation and RSP was much weaker than that of elevation and MGS, with the spatial distribution of productivity occurring in a patchwork varying greatly in strength and direction along latitudinal, longitudinal and elevation gradients. More so than just the dominance of temperature-related effects, this indicates joint effects of temperature and precipitation likely underlie the variability we observed in meadow production and productivity (Sun and Qin, 2016; Ma et al., 2022). The vast majority of precipitation in the SNV comes as snow, and snowpack is well-recognized to vary at multiple scales throughout the range (Lundquist and Lott, 2007). At a regional scale, differences among winter storm tracks are responsible for the uneven distribution of snow in different parts of the range (Kapnick and Hall, 2010) and likely contributes greatly to not just levels of MGS and RSP, but also the patchy distribution of their variability (CV and *D*). It is also important to recognize that snow occurs as a regime. Amount (magnitude) and duration are two components of that regime that are particularly relevant to variation in meadow condition in the SNV, but they are not independent and could even have opposite effects on production and productivity (Wang et al., 2017). Meltoff from large snowpacks would generally result in greater moisture availability and higher vegetation production, but larger snowpacks also persist longer. A more extended period of colder temperatures as well as a shortened growing season would be expected to lead to lower productivity, and if growing season length was shortened even further then production would decrease as well. The net effect over large

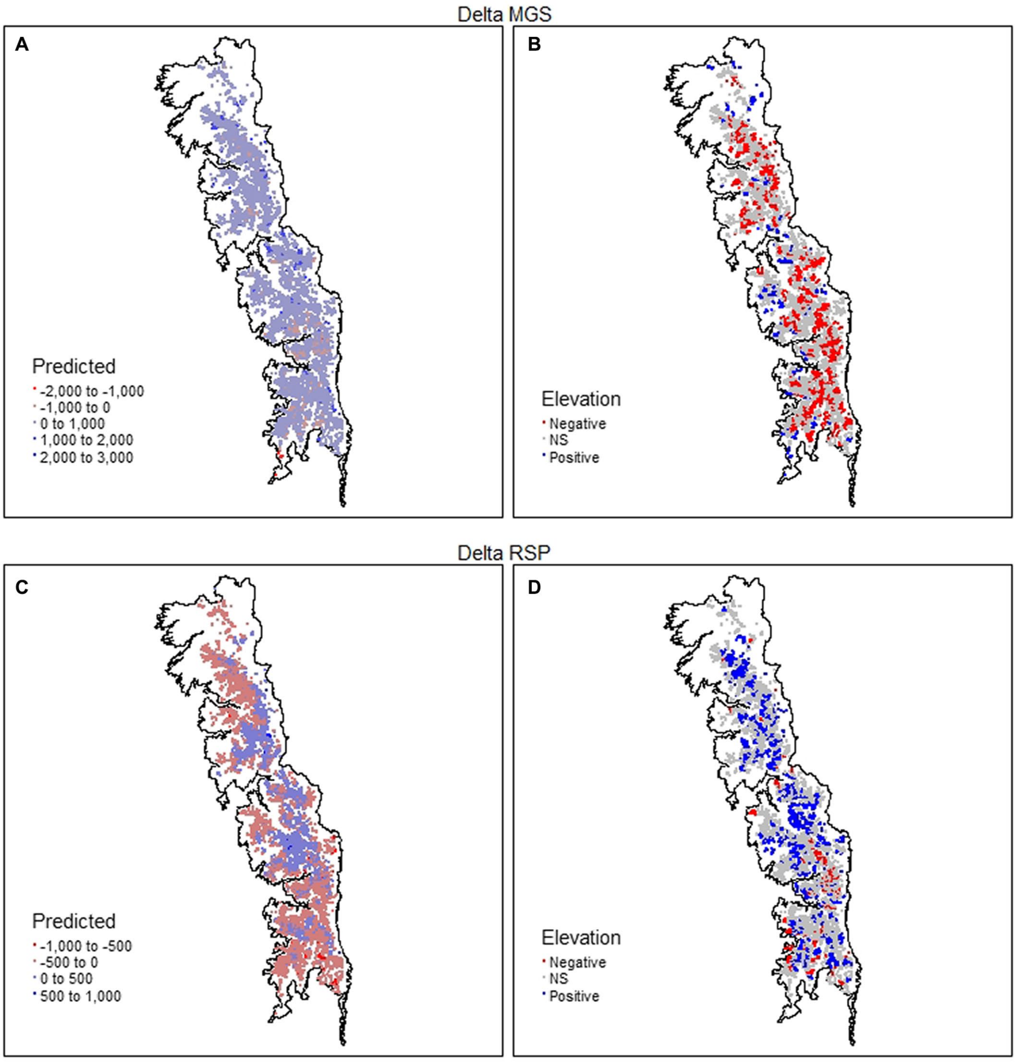

FIGURE 9
Spatial distribution of the net change (Delta) for mean growing season (MGS) and rate of spring greenup (RSP) values of 8,095 meadows in the upper subalpine and alpine zones of the Sierra Nevada mountain range of western North America. MGS and RSP are annual indices that are derived from time series (January 1985–December 2021) of the Normalized Difference Vegetation Index (NDVI) for each meadow. Panels **(A,C)** give predicted values and panels **(B,D)** direction and significance ($p<0.05$) of the relationship with elevation.

TABLE 4 The percentage of meadows (*N*=8,095) > 2,500m in the Sierra Nevada mountain range of North America with significantly negative or positive coefficients for eight indices of annual production (mean growing season value; MGS) and productivity (rate of spring greenup; RSP).

Variable	Negative	NS	Positive
MGS	61.1	37.6	1.3
CV (MGS)	7.0	57.9	41.5
D (MGS)	8.9	74.7	16.4
ΔMGS	27.7	66.2	6.1
RSP	28.2	60.2	11.6
CV (RSP)	4.0	55.8	40.2
D (RSP)	5.1	72.7	22.2
ΔRSP	6.0	66.0	28.0

CV=coefficient of variability in temporal dynamics (1985–2021) and *D*=the consecutive disparity index for the same period of time. ΔMGS and ΔRSP are the net change from 1985 to 2021.

spatial scales of this interplay between amount and duration of snow cover would be an increase in variation along geographic and elevation gradients. Thus, we hypothesize meadows with high production and high rates of productivity in the SNV are most likely to occur in areas where spring meltoff is relatively rapid and snowpacks are intermediate in size and duration.

Physiography and exposure to wind modify snow cover at the basin scale (Loheide et al., 2009; Stephenson et al., 2020; Rittger et al., 2021), which in turn results in variability in water table levels, soil moisture, and thus meadow condition (Lowry et al., 2011; Sun et al., 2016; Wang et al., 2017). Snow cover is more likely to persist longer on shadier slopes and in basins that are relatively protected from winds, resulting in variability along topographic gradients within and across basins. Composition, structure and condition of vegetation within meadows is influenced greatly by hydrology (Weixelman et al., 2011; Viers et al., 2013), and microtopography and soils can exert strong

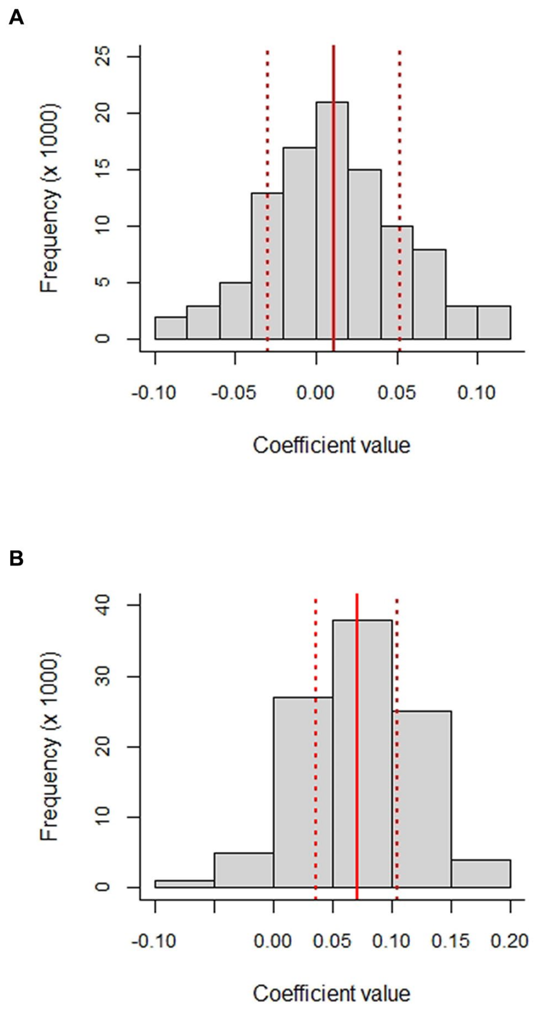

FIGURE 10
Histograms of slope parameters for the distance-decay relationship between the geographic distance between pairwise combinations of meadows in the upper subalpine and alpine zones of the Sierra Nevada mountain range of western North America and: **(A)** distance matrices derived from four variables related to the mean annual growing season value (MGS) of the Normalized Difference Vegetation Index (NDVI); and **(B)** distance matrices derived from four variables related to the rate of spring greenup (RSP). Parameter estimates were estimated from 1,000 random draws (*N*=1,000 per draw) from 8,095 meadows. The variables included MGS, the CV of MGS, the consecutive disparity index *D* of MGS, the net change in MGS from 1985 through 2021 (ΔMGS), RSP, and CV, *D*, and ΔRSP. Distance matrices were in Euclidean units. See text for further explanation of the variables and how they were derived. The solid red lines are the mean values and the dashed lines the 95% CIs.

effects on meadow hydrology (Allen-Diaz, 1991). Variation in microtopography is translated primarily to variation in snowpack accumulation while variation in soils primarily affects water table level, but their joint effects can lead to high within-meadow heterogeneity in vegetation condition (McIlroy and Allen-Diaz, 2012; Wang et al., 2017). It is important to note that there is greater likelihood of variation in microtopography and soils with increasing meadow area, therefore we expect within-meadow variation in production to vary greatly along a gradient from smaller to larger meadows.

TABLE 5 Summary statistics from distance-decay analyses based on matrices derived from variables related to annual herbaceous vegetation production (mean growing season value; MGS) and productivity (rate of spring greenup; RSP).

Distance matrix	ΔSlope	*p*	R^2
MGS	0	0.508 (0.478, 0.539)	0.00087 (0.00001, 0.004553)
RSP	0	0.503 (0.473, 0.533)	0.00468 (0.00001, 0.01551)

Besides MGS and RSP, the variables included the coefficient of variability in temporal dynamics (1985–2021), the consecutive disparity index in temporal dynamics (1985–2021), and the net change in MGS and RSP from 1985 to 2021 (*N*=4 variables per matrix). Pairwise geographic distances were calculated for 1,000 randomly selected meadows in each of 1,000 iterations. Differences in slope (ΔSlope) between observed values and 1,000 random permutations of the observed values were calculated within each iteration. A total of 8,095 meadows >2,500 m in the Sierra Nevada mountain range of North America were used in the analyses.

Herbivory by native and domestic mammals is known to shape vegetation patterns in alpine meadows (Li et al., 2021) and can modify climatic effects on meadow vegetation (Wang et al., 2012; Fu et al., 2015; Niu et al., 2016). A relatively large number of native mammalian herbivores occur in the high elevation zones of the SNV, including larger migratory species (bighorn sheep *Ovis canadensis*, mule deer *Odocoileus hemionus*) as well as smaller resident species (marmot *Marmota flaviventris*, pika *Ochotona princeps*, ground squirrels *Callospermophilus lateralis*, *Urocitellus beldingii*). Meadows are patches of highly nutritious forage for these species and are heavily used by them (Klinger et al., 2015; Stephenson et al., 2020). Widespread overgrazing by domestic sheep (*Ovis aries*) occurred in the SNV from the mid-19th century to early 20th century, and grazing by cattle was relatively common in some meadows from the mid to latter parts of the 20th century (Ratliff, 1985). In the last several decades, livestock grazing in the SNV has become more carefully managed, though damage to some meadows still occurs (McIlroy and Allen-Diaz, 2012; Roche et al., 2014). Virtually all of the meadows in our study region were on public lands administered by two federal agencies; US National Park Service (NPS) and US Forest Service (FS). Livestock are heavily regulated by NPS, with most grazing occurring intermittently from Equids (horses, mules) at light to moderate stocking levels in a relatively few designated areas (Klinger et al., 2015; Lee et al. 2017). Livestock grazing on FS lands is more extensive than on NPS lands, but it is still relatively light in the high elevation wilderness areas where our meadows occurred. We think it is likely historic and contemporary grazing are influencing at least some of the variability we observed in meadow condition, particularly in localized areas where meadows with opposite trends occurred in close proximity to one another. We also think it is likely that grazing effects are having a greater influence on variability in production and productivity (i.e., CV and *D*) than on levels of MGS and RSP or the net change in MGS and RSP. In general though, we strongly suspect the heterogeneity in abiotic conditions throughout the range plays a much larger role in structuring the spatial distribution of production and productivity in the SNV than biotic forces.

Outwardly, CV and *D* gave different impressions of spatial variability in annual production and productivity. The most obvious difference was the large clustering of positive relationships between CV and elevation in the southern and central parts of the SNV, while *D* had a much patchier distribution of that relationship. It is likely this pattern is an artifact of how the indices measure variability. Because the CV is sensitive to outliers and not independent of the mean, the clustering of positive relationships with elevation is indicative of more extreme values, lower overall values, or both. MGS and RSP decreased with elevation, and elevations are higher and there is more topographic variability in the southern and central parts of the SNV than the north. Therefore, it is not difficult to see why the CV would be greater in these conditions. In contrast, *D* is independent of the mean and far less sensitive to outliers, and it emphasizes the sequential differences in a series of values. Thus, the spatial distribution of *D* in the SNV contrasts the areas of high vs. low interannual variability in production and productivity. It is also important to bear in mind that the CV and *D* both indicated variability in the majority of meadows was not related to elevation. This implies factors other than temperature are responsible for the majority of the variability in production and productivity. These could be relatively localized processes such as heterogeneity in moisture and nutrients (Ren et al., 2010; Ma et al., 2022) or more complex, larger scale interactions between processes such as nitrogen deposition and phenological shifts (Zhang et al., 2015; Fu and Shen, 2017; Wang et al., 2022).

Implications

Temporal dynamics are often characterized by abrupt changes and being dependent on past conditions ("memory"; Beaulieu and Killick, 2018). Consequently, inferences based on dynamics from short-term studies are likely to be misleading, especially in regard to purported "trends." Ryo et al. (2019) proposed a hierarchical framework that accounts for complexity at different time scales resulting from varying numbers and types of perturbations. Because environmental conditions are highly changeable in most high elevation regions, this concept of scale-dependent variability should be a fundamentally appropriate one to help understand vegetation dynamics in these systems.

Implicitly or explicitly, the interpretation of responses to climate shifts have often been framed from "a big umbrella" perspective, with an emphasis on mean responses and much less on the variability around the mean response. An increasing amount of evidence from both experimental and observational studies indicates variable and complex responses are more likely than broadly consistent ones though, be they at species, community, or ecosystem levels (Klanderud, 2008; Randin et al., 2009; Ma et al., 2022). The diversity and intermixing of spatio-temporal patterns of meadow production and productivity we found is a strong indication "general trends" in meadow condition will be far less meaningful for understanding vegetation dynamics than local patterns resulting from strong heterogeneity in climate and physiognomy. In all likelihood, this will also pertain to montane systems besides the SNV. In conclusion, what is often considered "noise" may often be more informative than a "signal" embedded within a large amount of variability.

Author's Note

The use of trade, product, or firm names in this publication is for descriptive purposes only and does not imply endorsement by the US Government.

Data availability statement

The satellite data presented in the study are publicly available. The URL for the meadow polygons is https://meadows.ucdavis.edu/meadows/map. The URL for the NDVI data is https://earthexplorer.usgs.gov/.

Author contributions

RK designed the methodology, collected data with the field team, analyzed the data, and led the writing of the manuscript. TS and RK conceived the initial concept. TS provided review and modifications to drafts of the manuscript. JL, LS, and SJ acquired, processed, managed, and conducted preliminary analyses of the satellite data. All authors contributed to reviewing drafts of the manuscript and gave final approval for publication.

Funding

Major funding was provided by the USGS Ecosystems Program, with additional funding from Yosemite National Park and Sequoia and Kings Canyon National Parks.

Acknowledgments

We thank the USGS staff in Bishop, California for collecting the biomass data, especially Jennifer Chase, Ashley Beechan, Anna Godinho, Steven Lee, Lindsay Swinger, Stacey Huskins, Michael Cleaver, Laurel Triatek, Cody Massing, Jon Clark, Bridgett Downs, Drew Maraglia, Carli Morgan, and Brian Hatfield. Steven Lee, Peggy Moore, Sylvia Haultain, Kaitlin Lubetkin, and Jennifer Chase provided a number of important ideas and insights on the dynamics of high elevation meadows.

Conflict of interest

The authors declare that the research was conducted in the absence of any commercial or financial relationships that could be construed as a potential conflict of interest.

Publisher's note

Supplementary material

The Supplementary material for this article can be found online at: https://www.frontiersin.org/articles/10.3389/fevo.2023.1184918/full#supplementary-material

SUPPLEMENTARY FIGURE S1

Distributions related to four indices of annual mean growing season (MGS) values for herbaceous vegetation in 8,095 meadows > 2,500 m in the Sierra

Nevada mountain range of North America. CV = coefficient of variability in temporal dynamics (1985–2021) and *D* = the consecutive disparity index for the same period of time. ΔMGS is the net change from 1985 to 2021. Values were derived from monthly time series of the Normalized Difference Vegetation Index (NDVI) in each meadow.

SUPPLEMENTARY FIGURE S2

Distributions related to four indices of annual rate of spring greenup (RSP) values for herbaceous vegetation in 8,095 meadows > 2,500 m in the Sierra Nevada mountain range of North America. CV = coefficient of variability in temporal dynamics (1985–2021) and *D* = the consecutive disparity index for the same period of time. ΔRSP is the net change from 1985 to 2021. Values were derived from monthly time series of the Normalized Difference Vegetation Index (NDVI) in each meadow.

SUPPLEMENTARY FIGURE S3

Four examples of distance decay relationships for 1,000 randomly selected meadows > 2,500 m in the Sierra Nevada mountain range of North America. The meadows were selected from a total pool of 8,095. Points represent pairwise geographic distances and distances derived from annual herbaceous vegetation production (mean growing season value; MGS), coefficient of variability in temporal dynamics for MGS (1985–2021), the consecutive disparity index in temporal dynamics for MGS (1985–2021), and the net change in MGS from 1985 to 2021. The red horizontal line represents the fitted estimate.

SUPPLEMENTARY FIGURE S4

Four examples of distance decay relationships for 1,000 randomly selected meadows > 2,500 m in the Sierra Nevada mountain range of North America. The meadows were selected from a total pool of 8,095. Points represent pairwise geographic distances and distances derived from annual herbaceous vegetation productivity (rate of spring greenup; RSP), the coefficient of variability in temporal dynamics for RSP (1985–2021), consecutive disparity index in temporal dynamics for RSP (1985–2021), and net change in RSP from 1985 to 2021. The red horizontal line represents the fitted estimate.

References

Allen-Diaz, B. H. (1991). Water table and plant species relationships in Sierra Nevada meadows. *Am. Midl. Nat.* 126, 30–43. doi: 10.2307/2426147

Auger-Méthé, M., Newman, K., Cole, D., Empacher, F., Gryba, R., King, A. A., et al. (2021). A guide to state–space modeling of ecological time series. *Ecol. Monogr.* 91:e01470. doi: 10.1002/ecm.1470

Beaulieu, C., Chen, J., and Sarmiento, J. L. (2012). Change-point analysis as a tool to detect abrupt climate variations. *Philos. Trans. R. Soc.* 370, 1228–1249. doi: 10.1098/rsta.2011.0383

Beaulieu, C., and Killick, R. (2018). Distinguishing trends and shifts from memory in climate data. *J. Clim.* 31, 9519–9543. doi: 10.1175/JCLI-D-17-0863.1

Beijers, D. (2022). statespacer: state space modelling in R. R package version 0.4.1.

Bivand, R, and Yu, D. (2020). spgwr: geographically weighted regression. R package version 0.6-34. Available at: https://CRAN.R-project.org/package=spgwr

Boelman, N. T., Stieglitz, M., Rueth, H. M., Sommerkorn, M., Griffin, K. L., Shaver, G. R., et al. (2003). Response of NDVI, biomass, and ecosystem gas exchange to long-term warming and fertilization in wet sedge tundra. *Oecologia* 135, 414–421. doi: 10.1007/s00442-003-1198-3

Brandt, J. S., Haynes, M. A., Kuemmerle, T., Waller, D. M., and Radeloff, V. C. (2013). Regime shift on the roof of the world: Alpine meadows converting to shrublands in the southern Himalayas. *Biol. Conserv.* 158, 116–127. doi: 10.1016/j.biocon.2012.07.026

Carlson, T. N., and Ripley, D. A. (1997). On the relation between NDVI, fractional vegetation cover, and leaf area index. *Remote Sens. Environ.* 62, 241–252. doi: 10.1016/S0034-4257(97)00104-1

Cayan, D., Kammerdiener, S., Dettinger, M., Caprio, J., and Peterson, D. (2001). Changes in the onset of spring in the western United States. *Bull. Am. Meteorol. Soc.* 82, 339–415. doi: 10.1175/1520-0477(2001)082<0399:CITOOS>2.3.CO;2

Dettinger, M., Alpert, H., Battles, J., Kusel, Jonathan, Safford, Hugh, Fougeres, Dorian, et al., (2018). *Sierra Nevada summary report. California's fourth climate change assessment. Publication No. SUMCCCA4-2018-004*. Sacramento, CA: State of California. 94 p

Ding, M. J., Zhang, Y. L., Liu, L. S., Zhang, W., Wang, Z. F., and Bai, W. Q. (2007). The relationship between NDVI and precipitation on the Tibetan Plateau. *J Geogr Sci* 17, 259–268. doi: 10.1007/s11442-007-0259-7

Dirnbock, T., Dullinger, S., and Grabherr, G. (2003). A regional impact assessment of climate and land-use change on alpine vegetation. *J. Biogeogr.* 30, 401–417. doi: 10.1046/j.1365-2699.2003.00839.x

Dwyer, J. L., Roy, D. P., Sauer, B., Jenkerson, C. B., Zhang, H. K., and Lymburner, L. (2018). Analysis ready data: enabling analysis of the landsat archive. *Remote Sens.* 10:1363. doi: 10.3390/rs10091363

Epanchin, P. N., Knapp, R. A., and Lawler, S. P. (2010). Nonnative trout impact an alpine-nesting bird by altering aquatic-insect subsidies. *Ecology* 91, 2406–2415. doi: 10.1890/09-1974.1

Felde, V. A., Kapfer, J., and Grytnes, J.-A. (2012). Upward shift in elevational plant species ranges in Sikkilsdalen, Central Norway. *Ecography* 35, 922–932. doi: 10.1111/j.1600-0587.2011.07057.x

Fernández-Martínez, M., Vicca, S., Janssens, I. A., Carnicer, J., Martın-Vide, J., and Penuelas, J. (2018). The consecutive disparity index, D: a measure of temporal variability in ecological studies. *Ecosphere* 9:e02527. doi: 10.1002/ecs2.2527

Fites-Kaufman, J. A., Runel, P., Stephenson, N. L., and Weixelman, D. A. (2007). "Montane and subalpine vegetation of the Sierra Nevada and Cascade ranges" in *Terrestrial vegetation of California*. eds. M. G. Barbour, T. Keeler-Wolf and A. A. Schoenherr (University of California Press), 456–501.

Forkel, M., Carvalhais, N., Verbesselt, J., Mahecha, M. D., Neigh, C., and Reichstein, M. (2013). Trend change detection in NDVI time series: effects of inter-annual variability and methodology. *Remote Sens.* 5, 2113–2144. doi: 10.3390/rs5052113

Forkel, M., Migliavacca, M., Thonicke, K., Reichstein, M., Schaphoff, S., Weber, U., et al. (2015). Co-dominant water control on global inter-annual variability and trends in land surface phenology and greenness. *Glob. Chang. Biol.* 21, 3414–3435. doi: 10.1111/gcb.12950

Fotheringham, A.S., Brunsdon, C., and Charlton, M. (2002). *Geographically weighted regression: The analysis of spatially varying relationships*. Chichester: Wiley.

Fryjoff-Hung, A., and Viers, J.H. (2012). Sierra Nevada multi-source meadow polygons compilation (v 1.0), Center for Watershed Sciences, UC Davis. December 2012. Available at: http://meadows.ucdavis.edu/

Fu, G., and Shen, Z.-X. (2017). Response of alpine soils to nitrogen addition on the Tibetan Plateau: a meta-analysis. *Appl. Soil Ecol.* 114, 99–104. doi: 10.1016/j.apsoil.2017.03.008

Fu, G., Sun, W., Yu, C. Q., Zhang, X.-Z., Shen, Z.-X., Li, Y. L., et al. (2015). Clipping alters the response of biomass production to experimental warming: a case study in an alpine meadow on the Tibetan Plateau, China. *J. Mt. Sci.* 12, 935–942. doi: 10.1007/s11629-014-3035-z

Fu, G., Zhang, X., Zhang, Y., Shi, P., Li, Y., Zhou, Y., et al. (2013). Experimental warming does not enhance gross primary production and above-ground biomass in the alpine meadow of Tibet. *J. Appl. Remote. Sens.* 7:073505. doi: 10.1117/1111.jrs.1117.073505

Ganjurjav, H., Gaoa, Q., Gornish, E. S., Schwartz, M. W., Lianga, Y., Cao, X., et al. (2016). Differential response of alpine steppe and alpine meadow to climate warming in the Central Qinghai–Tibetan Plateau. *Agric. For. Meteorol.* 223, 233–240. doi: 10.1016/j.agrformet.2016.03.017

Haugo, R. D., Halpern, C. B., and Bakker, J. D. (2011). Landscape context and long-term tree influences shape the dynamics of forest-meadow ecotones in mountain ecosystems. *Ecosphere* 2:art91. doi: 10.1890/ES11-00110.1

Hayhoe, K., Cayan, D., Field, C. B., Frumhoff, P. C., Maurer, E. P., Miller, N. L., et al. (2004). Emissions pathways, climate change, and impacts on California. *Proc. Natl. Acad. Sci. U. S. A.* 101, 12422–12427. doi: 10.1073/pnas.0404500101

Hijmans, R. J. (2022). terra: Spatial Data Analysis. R package version 1.5-21. Available at: https://CRAN.R-project.org/package=terra

Hik, D. S., McColl, C. J., and Boonstra, R. (2001). Why are Arctic ground squirrels more stressed in the boreal forest than in alpine meadows? *Ecoscience* 8, 275–288. doi: 10.1080/11956860.2001.11682654

Hillebrand, H., Donohue, I., Harpole, W. S., Hodapp, D., Kucera, M, Lewandowska, A. M., et al (2020). Thresholds for ecological responses to global change do not emerge from empirical data. *Nat. Ecol. Evol* 4, 1502–1509. doi: 10.1038/s41559-020-1256-9

Huelber, K., Gottfried, M., Pauli, H., Reiter, K., Winkler, M., and Grabherr, G. (2006). Phenological responses of snowbed species to snow removal dates in the Central Alps: implications for climate warming. *Arctic Antarctic Alpine Res.* 38, 99–103. doi: 10.1657/1523-0430(2006)038[0099:PROSST]2.0.CO;2

Inouye, D. W. (2008). Effects of climate change on phenology, frost damage, and floral abundance of montane wildflowers. *Ecology* 89, 353–362. doi: 10.1890/06-2128.1

Jurasinski, G., and Kreyling, J. (2007). Upward shift of alpine plants increases floristic similarity of mountain summits. *J. Veg. Sci.* 18, 711–718. doi: 10.1111/j.1654-1103.2007.tb02585.x

Jurasinski, G., and Retzer, V. (2012). simba: a collection of functions for similarity analysis of vegetation data. R package version 0.3-5. Available at: https://CRAN.R-project.org/package=simba

Kapnick, S., and Hall, A. (2010). Observed climate–snowpack relationships in California and their implications for the future. *J. Clim.* 23, 3446–3456. doi: 10.1175/2010JCLI2903.1

Killick, R., and Eckley, I. A. (2014). changepoint: an R package for changepoint analysis. *J. Stat. Softw.* 58, 1, –19. doi: 10.18637/jss.v058.i03

Klanderud, K. (2008). Species-specific responses of an alpine plant community under simulated environmental change. *J. Veg. Sci.* 19, 363–372. doi: 10.3170/2008-8-18376

Klinger, R.C., Few, A.P., Knox, K.A., Hatfield, B.E., Clark, J., German, D.W., et al., (2015). *Evaluating potential overlap between pack stock and Sierra Nevada bighorn sheep (Ovis canadensis sierrae) in Sequoia and Kings Canyon National Parks, California*: Reston, VA: U.S. Geological Survey Open-File Report 2015-1102, 46.

Korner, C. (2003). *Alpine plant life: functional plant ecology of high mountain ecosystems. 2nd.* Springer, Berlin, Germany.

Krajik, K. (2004). All downhill from here? *Science* 303, 1600–1602. doi: 10.1126/science.303.5664.1600

Kudo, G., Kimura, M., Kasagi, T., Kawai, Y., and Hirai, A. S. (2010). Habitat specific responses of alpine plants to climatic amelioration: comparison of fellfield to snowbed communities. *Arctic Antarctic Alpine Res* 42, 438–448. doi: 10.1657/1938-4246-42.4.438

Lamy, T., Wisnoski, N. I., Andrade, R., Castorani, M. C. N., Compagnoni, A., Lany, N., et al. (2021). The dual nature of metacommunity variability. *Oikos* 130, 2078–2092. doi: 10.1111/oik.08517

Lee, S. R., Berlow, E. L., Ostoja, S. M., Brooks, M. L., Genin, A., Matchett, J. R. (2017). A multi-scale evaluation of pack stock effects on subalpine meadow plant communities in the Sierra Nevada. *PLoS ONE* 12:e0178536. doi: 10.1371/journal.pone.0178536

Lenoir, J., Gegout, J. C., Marquet, P. A., de Ruffray, P., and Brisse, H. (2008). A significant upward shift in plant species optimum elevation during the 20th century. *Science* 320, 1768–1771. doi: 10.1126/science.1156831

Li, J., Qi, H. H., Duan, Y. Y., and Guo, Z. G. (2021). Effects of plateau pika disturbance on the spatial heterogeneity of vegetation in alpine meadows. *Front. Plant Sci.* 12:771058. doi: 10.3389/fpls.2021.771058

Loheide, S. P., Deitchman, R. S., Cooper, D. J., Wolf, E. C., Hammersmark, C. T., and Lundquist, J. D. (2009). A framework for understanding the hydroecology of impacted wet meadows in the Sierra Nevada and Cascade Ranges, California, USA. *Hydrogeol. J.* 17, 229–246. doi: 10.1007/s10040-008-0380-4

Loheide, S. P., and Gorelick, S. M. (2007). Riparian hydroecology: a coupled model of the observed interactions between groundwater flow and meadow vegetation patterning. *Water Resour. Res.* 43:W07414. doi: 10.1029/2006WR005233

Lowry, C. S., Loheide, S. P., Moore, C. E., and Lundquist, J. D. (2011). Groundwater controls on vegetation composition and patterning in mountain meadows. *Water Resour. Res.* 47:W00J11. doi: 10.1029/2010WR010086

Lubetkin, K. C., Westerling, A. L., and Kueppers, L. M. (2017). Climate and landscape drive the pace and pattern of conifer encroachment into subalpine meadows. *Ecol. Appl.* 27, 1876–1887. doi: 10.1002/eap.1574

Lundquist, J. D., and Lott, F. (2007). Using inexpensive temperature sensors to monitor the duration and heterogeneity of snow-covered areas. *Water Resour. Res.* 44. doi: 10.1029/2008WR007035

Ma, Y., Tian, L., Qu, G., Li, R., Wang, W., and Zhao, J. (2022). Precipitation alters the effects of temperature on the ecosystem multifunctionality in alpine meadows. *Front. Plant Sci.* 12:824296. doi: 10.3389/fpls.2021.824296

Malanson, G. P., and Fagre, D. B. (2013). Spatial contexts for temporal variability in alpine vegetation under ongoing climate change. *Plant Ecol.* 214, 1309–1319. doi: 10.1007/s11258-013-0253-3

McIlroy, S. K., and Allen-Diaz, B. H. (2012). Plant community distribution along water table and grazing gradients in montane meadows of the Sierra Nevada Range (California, USA). *Wetlands Ecol. Manag.* 20, 287–296. doi: 10.1007/s11273-012-9253-7

Moritz, S., and Bartz-Beielstein, T. (2017). imputeTS: time series missing value imputation in R. *R J.* 9, 207–218. doi: 10.32614/RJ-2017-009

Mote, P. W., Clark, M., and Hamlet, A. F. (2004). Variability and trends in mountain snowpack in western North America. Preprints, 15th Symp. on global change and climate variations, Seattle, WA, Amer. Meteor. Soc. Vol. 5.

Mote, P., Hamlet, A., Clark, M., and Lettenmaier, D. (2005). Declining mountain snowpack in western North America. *Bull. Am. Meteorol. Soc.* 86, 39–49. doi: 10.1175/BAMS-86-1-39

Niu, K., He, J. S., and Lechowicz, M. J. (2016). Grazing-induced shifts in community functional composition and soil nutrient availability in Tibetan alpine meadows. *J. Appl. Ecol.* 53, 1554–1564. doi: 10.1111/1365-2664.12727

Packer, J. G. (1974). Differentiation and dispersal in alpine floras. *Arctic Alpine Res.* 6, 117–128. doi: 10.1080/00040851.1974.12003768

Parmesan, C., and Yohe, G. (2003). A globally coherent fingerprint of climate change impacts across natural systems. *Nature* 421, 37–42. doi: 10.1038/nature01286

Patton, D. R., and Judd, B. I. (1970). Role of wet meadows as wildlife habitat in southwest. *J. Range Manag.* 23, 272–276. doi: 10.2307/3896220

Pauli, H., Gottfried, M., Dullinger, S., Abdaladze, O., Akhalkatsi, M., Alonso, J. L. B., et al. (2012). Recent plant diversity changes on Europe's mountain summits. *Science* 336, 353–355. doi: 10.1126/science.1219033

Pauli, H., Gottfried, M., Reiter, K., Klettner, C., and Grabherr, G. (2007). Signals of range expansions and contractions of vascular plants in the high Alps: observations (1994-2004) at the GLORIA master site Schrankogel, Tyrol, Austria. *Glob. Chang. Biol.* 13, 147–156. doi: 10.1111/j.1365-2486.2006.01282.x

Pettorelli, N. (2013). *The normalized difference vegetation index*. New York: Oxford University Press. 224.

R Core Team (2022). *R: A language and environment for statistical computing*. R Foundation for Statistical Computing, Vienna, Austria.

Randin, C. F., Engler, R., Normand, S., Zappa, M., Zimmermann, N. E., Pearman, P. B., et al. (2009). Climate change and plant distribution: local models predict high-elevation persistence. *Glob. Chang. Biol.* 15, 1557–1569. doi: 10.1111/j.1365-2486.2008.01766.x

Ratliff, R.D. (1985). *Meadows in the Sierra Nevada of California: state of knowledge. Gen. Tech. Rep. PSW-GTR-84.* Berkeley, CA: U.S. Department of Agriculture, Forest Service, Pacific Southwest Forest and Range Experiment Station. 52 p.

Ren, Z., Li, Q., Chu, C., Zhao, L., Zhang, J., Ai, D., et al. (2010). Effects of resource additions on species richness and ANPP in an alpine meadow community. *J. Plant Ecol.* 3, 25–31. doi: 10.1093/jpe/rtp034

Ren, Y., Yang, K., Wang, H., Zhao, L., Chen, Y., Zhou, X., et al. (2021). The South Asia monsoon break promotes grass growth on the Tibetan plateau. *J. Geophys. Res.* 126:e2020JG005951. doi: 10.1029/2020JG005951

Rittger, K., Krock, M., Kleiber, W., Bair, E. H., Brodzik, M. J., Stephenson, T. R., et al. (2021). Multi-sensor fusion using random forests for daily fractional snow cover at 30 m. *Remote Sens. Environ.* 264:112608. doi: 10.1016/j.rse.2021.112608

Roche, L. M., O'Geen, A. T., Latimer, A. M., and Eastburn, D. J. (2014). Montane meadow hydropedology, plant community, and herbivore dynamics. *Ecosphere* 5:art150. doi: 10.1890/ES14-00173.1

Ryo, M., Aguilar-Trigueros, C. A., Pinek, L., Muller, L. A. H., and Rillig, M. C. (2019). Basic principles of temporal dynamics. *Trends Ecol. Evol.* 34, 723–733. doi: 10.1016/j.tree.2019.03.007

Scherrer, D., and Körner, C. (2011). Topographically controlled thermal-habitat differentiation buffers alpine plant diversity against climate warming. *J. Biogeogr.* 38, 406–416. doi: 10.1111/j.1365-2699.2010.02407.x

Shen, Z., Fu, G., Yu, C., Sun, W., and Zhang, X. (2014). Relationship between the growing season maximum enhanced vegetation index and climatic factors on the Tibetan plateau. *Remote Sens.* 6, 6765–6789. doi: 10.3390/rs6086765

Shen, M. G., Tang, Y. H., Chen, J., Zhu, X. L., and Zheng, Y. H. (2011). Influences of temperature and precipitation before the growing season on spring phenology in grasslands of the central and eastern Qinghai-Tibetan Plateau. *Agric. For. Meteorol.* 151, 1711–1722. doi: 10.1016/j.agrformet.2011.07.003

Shumway, R.H., and Stoffer, D.S. (2011). *Time series analysis and its applications: with R examples*. Springer: New York, USA.

Song, M. H., Hu, Q., Tian, Y., and Ouyang, H. (2012). Seasonal patterns of root and shoot interactions in an alpine meadow on the Tibetan Plateau. *J. Plant Ecol.* 5, 182–190. doi: 10.1093/jpe/rtq032

Song, M. H., Tian, Y. Q., and Xu, X. L. (2006). Interactions between root and shoot competition among four plant species in an alpine meadow on the Tibetan Plateau. *Acta Oecol.* 29, 214–220. doi: 10.1016/j.actao.2005.10.005

Stephenson, T. R., German, D. W., Cassirer, E. F., Walsh, D. P., Blum, M. E., Cox, M., et al. (2020). Linking population performance to nutritional condition in an alpine ungulate. *J. Mammal.* 101, 1244–1256. doi: 10.1093/jmammal/gyaa091

Stewart, I. T. (2009). Changes in snowpack and snowmelt runoff for key mountain regions. *Hydrol. Process.* 23, 78–94. doi: 10.1002/hyp.7128

Storer, T.I., Usinger, R.L., and Lukas, D. (2004). *Sierra Nevada natural history*. Berkeley: University of California Press. p. 592

Sun, J., Cheng, G. W., Li, W. P., Sha, Y. K., and Yang, Y. C. (2013). On the variation of NDVI with the principal climatic elements in the Tibetan Plateau. *Remote Sens.* 5, 1894–1911. doi: 10.3390/rs5041894

Sun, J., and Qin, X. (2016). Precipitation and temperature regulate the seasonal changes of NDVI across the Tibetan plateau. *Environ. Earth Sci.* 75:291. doi: 10.1007/s12665-015-5177-x

Sun, J., Qin, X., and Yang, J. (2016). The response of vegetation dynamics of the different alpine grassland types to temperature and precipitation on the Tibetan Plateau. *Environ. Monit. Assess.* 188:20. doi: 10.1007/s10661-015-5014-4

Testolin, R., Attorre, F., and Jiménez-Alfaro, B. (2020). Global distribution and bioclimatic characterization of alpine biomes. *Ecography* 43, 779–788. doi: 10.1111/ecog.05012

Thorne, J. H., Dobrowski, S., and Safford, H. D. (2007). *A 70-year review of landscape change across the Sierra Nevada* Ecological Society of America Annual Meeting Abstracts.

Verrall, B., and Pickering, C. M. (2020). Alpine vegetation in the context of climate change: a global review of past research and future directions. *Sci. Total Environ.* 748:141344. doi: 10.1016/j.scitotenv.2020.141344

Viers, J.H., Purdy, S.E., Peek, R.A., Fryjoff-Hung, A., Santos, N.R., Katz, J.V.E., et al., (2013). *Montane meadows in the Sierra Nevada: changing hydroclimatic conditions and concepts for vulnerability assessment. Center for Watershed Sciences Technical Report (CWS-2013-01)*, University of California, Davis, Davis. pp. 63.

Walther, G. R., Beissner, S., and Burga, C. A. (2005). Trends in the upward shift of alpine plants. *J. Veg. Sci.* 16, 541–548. doi: 10.1111/j.1654-1103.2005.tb02394.x

Wang, S. P., Duan, J. C., Xu, G. P., Wang, Y. F., Zhang, Z.-H., Rui, Y. C., et al. (2012). Effects of warming and grazing on soil N availability, species composition, and ANPP in an alpine meadow. *Ecology* 93, 2365–2376. doi: 10.1890/11-1408.1

Wang, J., Li, M., Yu, C., and Fu, G. (2022). The change in environmental variables linked to climate change has a stronger effect on aboveground net primary productivity than does phenological change in alpine grasslands. *Front. Plant Sci.* 12:798633. doi: 10.3389/fpls.2021.798633

Wang, S., Wang, X., Chen, G., Yang, Q., Wang, B., Ma, Y., et al. (2017). Complex responses of spring alpine vegetation phenology to snow cover dynamics over the Tibetan Plateau, China. *Sci. Total Environ.* 593-594, 449–461. doi: 10.1016/j.scitotenv.2017.03.187

Ward, E. J. (2008). A review and comparison of four commonly used Bayesian and maximum likelihood model selection tools. *Ecol. Model.* 211, 1–10. doi: 10.1016/j.ecolmodel.2007.10.030

Weixelman, D.A., Hill, B.A., Cooper, D.J., Berlow, E.L., Viers, J.H., Purdy, S.E., et al., (2011). *A field key to meadow Hydrogeomorphic types for the Sierra Nevada and southern Cascade ranges in California. Tech. Rep. R5-TP-034*. U.S. Department of Agriculture, Forest Service, Pacific Southwest Region Gen Vallejo, California, p. 34.

Xiao, J., Dong, S., Shen, H., Li, S., Wessell, K., Liu, S., et al. (2022). N addition overwhelmed the effects of P addition on the soil C, N, and P cycling genes in alpine meadow of the Qinghai-Tibetan Plateau. *Front. Plant Sci.* 13:860590. doi: 10.3389/fpls.2022.860590

Zeileis, A. (2019). dynlm: dynamic linear regression. R package version 0.3-6. Available at: https://CRAN.R-project.org/package=dynlm

Zeileis, A., Leisch, F., Kleiber, C., and Hornik, K. (2005). Monitoring structural change in dynamic econometric model. *J. Appl. Econ.* 20, 99–121. doi: 10.1002/jae.776

Zhang, N. R., and Siegmund, D. O. (2007). A modified Bayes information criterion with applications to the analysis of comparative genomic hybridization data. *Biometrics* 63, 22–32. doi: 10.1111/j.1541-0420.2006.00662.x

Zhang, X.-Z., Shen, Z.-X., and Fu, G. (2015). A meta-analysis of the effects of experimental warming on soil carbon and nitrogen dynamics on the Tibetan Plateau. *Appl. Soil Ecol.* 87, 32–38. doi: 10.1016/j.apsoil.2014.11.012

frontiers | Frontiers in Ecology and Evolution

TYPE Original Research
PUBLISHED 15 February 2024
DOI 10.3389/fevo.2024.1291310

EDITED BY
Robert Klinger,
United States Department of the Interior,
United States

REVIEWED BY
Kathryn Schoenrock,
University of Galway, Ireland
Aline Migné,
Sorbonne Université(CNRS), France
Fabio Abel Labra,
Universidad Santo Tomás, Chile
Dominique Davoult,
Sorbonne Universités, France

*CORRESPONDENCE
Stephen G. Whitaker
✉ Stephen_whitaker@nps.gov

RECEIVED 08 September 2023
ACCEPTED 19 January 2024
PUBLISHED 15 February 2024

CITATION
Whitaker SG, Raimondi PT, Smith JR, Lenihan HS, Gaines SD and Miller RJ (2024) Decline of a North American rocky intertidal foundation species linked to extreme dry, downslope Santa Ana winds.
Front. Ecol. Evol. 12:1291310.
doi: 10.3389/fevo.2024.1291310

Decline of a North American rocky intertidal foundation species linked to extreme dry, downslope Santa Ana winds

Stephen G. Whitaker[1,2,3]*, Peter T. Raimondi[4], Jayson R. Smith[5], Hunter S. Lenihan[1], Steven D. Gaines[1] and Robert J. Miller[3]

[1]Bren School of Environmental Science and Management, University of California, Santa Barbara, Santa Barbara, CA, United States, [2]Channel Islands National Park, U.S. National Park Service, Ventura, CA, United States, [3]Marine Science Institute, University of California, Santa Barbara, Santa Barbara, CA, United States, [4]Ecology and Evolutionary Biology Department, University of California, Santa Cruz, Santa Cruz, CA, United States, [5]Biological Sciences, California State Polytechnic University, Pomona, CA, United States

Foundation species are essential to ecosystem function, but their role as habitat providers is predicated on their spatial dominance. Worldwide, kelps, seagrasses, corals, and other marine foundation species have declined. This is true also for rockweeds, the canopy-forming analog of subtidal kelp forests in temperate rocky intertidal ecosystems. On the west coast of North America, dense beds of the rockweed *Silvetia compressa* occur across large biogeographic regions, benefitting numerous species by ameliorating physical stress caused by sun exposure, desiccation, heat, and wave disturbance. Like many rockweed species, *Silvetia* is long-lived, slow-growing, and short-dispersing – characteristics that reduce its resilience to disturbance. Using a generalized additive mixed-effects model with explicit spatial effects, we analyzed canopy cover data from 30 sites spanning 18 years, and we tested the hypothesis that *Silvetia* population trends are tightly linked to atmospheric climate conditions, particularly Santa Ana wind events (SAWs): strong, hot, and dry downslope winds that originate inland and move offshore. We found that the rockweed had declined markedly, particularly at sites south of the major biogeographic break, Point Conception (PC), including the California Channel Islands and southern California mainland, and a highly significant negative effect of dewpoint depression, a measure of moisture content in the atmosphere, on *Silvetia* cover across all three regions in this study. Our results suggest that any increases in the frequency or intensity of SAWs are likely to lead to large declines and possible extirpation of *Silvetia*, as well as the important ecological services the species provides.

KEYWORDS

ecosystem engineer, desiccation, rockweed, fucoid, offshore winds, prolonged desiccation events

1 Introduction

Foundation species define much of the structure of the community they occupy by modulating fundamental ecosystem processes and creating locally stable conditions for other species (Dayton, 1985; Ellison et al., 2005). Examples include mangroves (Duke et al., 2007), corals (Hughes et al., 2003), seagrasses (Short et al., 2006), kelps (Steneck et al., 2002), oysters (Lenihan et al., 2001), cordgrass (Zedler et al., 2001), and many tree species including redwood, hemlock, and birch (Ellison et al., 2005). These species share commonness and high local abundances, hence the tendency to name ecosystems after them – seagrass beds, kelp forests, oyster beds, and hemlock forests. Maintaining their foundational role in ecosystems, and the resulting effects on biodiversity, community composition, and ecosystem function, requires high local abundances, not simply species survival. However, many foundation species are declining due to coastal development (Zedler et al., 2001; Duke et al., 2007), pollution (Duke et al., 2007), invasive species (Steneck et al., 2002), introduced pathogens (Ellison et al., 2005), over-harvesting (Jackson et al., 2001; Steneck et al., 2002; Ellison et al., 2005), and climate change (Sagarin et al., 1999; Hughes et al., 2003), likely resulting in cascading impacts on associated communities (Sarà et al., 2021; Smale et al., 2022; Wernberg et al., 2023 and references therein).

In temperate rocky intertidal ecosystems, perennial fucoid macroalgae, commonly referred to as rockweeds, are often important foundation species (Chapman, 1995; Schiel and Foster, 2006). At low tide, rockweed canopies protect the substratum and communities beneath the canopy from sun exposure, desiccation, and heat stress (Bertness et al., 1999; Sapper and Murray, 2003; Råberg and Kautsky, 2007; Marzinelli et al., 2014) and thereby enhance biodiversity (Råberg and Kautsky, 2007; Marzinelli et al., 2014). Via this protection, as well as hydrodynamic effects, rockweed canopies also facilitate the recruitment of numerous intertidal species, including the rockweeds themselves (Bertness et al., 1999; Viejo et al., 1999), a positive feedback loop that likely contributes to their long-term population stability (Bertness et al., 1999). In addition to these ecosystem engineering effects, rockweeds are highly productive (Golléty et al., 2008; Tait and Schiel, 2010; Tait et al., 2014; Bordeyne et al., 2015), providing an important source of food for intertidal herbivores (Moore, 1977; Lubchenco, 1983; Steinberg, 1985; Bertness and Leonard, 1997; Jenkins et al., 2004; Hawkins et al., 2008) and detrital consumers (Bishop et al., 2010; Golléty et al., 2010; Renaud et al., 2015), and contributing to nutrient cycling (Schmidt et al., 2011).

Silvetia compressa (Agardh, 1824) (Phaeophyceae, hereafter *Silvetia*) is the dominant rockweed species in the northeast Pacific from Monterey County, California to Punta Baja, Baja California, Mexico (Abbott and Hollenberg, 1992; Silva et al., 2004; Skamarock and Klemp, 2008). *Silvetia* can live at least eight years (Gunnill, 1980) and is slow to recover from population declines due to the short-range dispersal of its gametes (Hays, 2006). Attaining frond lengths of 90 cm with up to 20 orders of branching (Silva et al., 2004), *Silvetia* can form large and dense beds (Figure 1) that harbor a diverse understory community. For example, Sapper and Murray (2003) documented 47 species of algae, 20 sessile and 44 mobile invertebrate species under the canopy formed by *Silvetia* at a rocky intertidal site in southern California.

Upper and middle intertidal rockweeds, including *Silvetia*, are regularly subjected to prolonged periods of aerial exposure (i.e., emersion) during low tides. Rapidly fluctuating atmospheric variables, such as temperature, irradiance, wind speed, and relative humidity, impose increasingly greater stress on intertidal biota as a function of shore height (e.g., Hawkins and Hartnoll, 1985). Physiological stress generally results in increased rates of mortality (Graham et al., 2000) and reduced physiological performance (Schonbeck and Norton, 1980), and individuals living higher on the shore often exhibit morphological differences in response, such as thickened and stunted body forms (Sideman and Mathieson, 1985; Davison and Pearson, 1996). As a result, stress from emersion, and particularly desiccation, is considered among the most important drivers of species performance and abundance in the rocky intertidal zone (Brinkhuis et al., 1976; Brawley and Johnson, 1993; Davison and Pearson, 1996; Stengel and Dring, 1998; Helmuth and Hofmann, 2001 and references therein).

The coast from central California to northern Baja California including southern California and the Channel Islands in the Southern California Bight is periodically exposed to strong, dry, and often warm downslope winds, commonly referred to as *Santa Ana* winds (SAWs) (Abatzoglou et al., 2021; Guirguis et al., 2023). These harsh winds result from sharp gradients between high-pressure systems across the interior of the western United States and low pressure at the coast. As the air masses move from the dry Great Basin to the west over the coastal mountain ranges, they are compressed down the mountains and through canyons where they accelerate, heat, and dry in the process termed downsloping. SAWs can reach sustained speeds of 7-13 m s^{-1} (and gusts of >25 m s^{-1}) and are characterized by low humidity (<15%) and warm air (>21° C) (Rolinski et al., 2019). SAWs can occur any time of the year, but they peak in late fall through early spring.

Recent modeling studies have revealed marked interannual variation in the frequency, intensity, and spatial coverage of SAWs (Jones et al., 2010; Abatzoglou et al., 2013; Guzman-Morales et al., 2016; Dye et al., 2020), and these temporal trends have been linked to variation in environmental indices, including the El Niño-Southern Oscillation (Raphael, 2003), Pacific Decadal Oscillation, and the Atlantic Multi-decadal Oscillation (Li et al., 2016). SAWs are well studied due to their impact on vegetation and catastrophic wildfire threats (e.g., Moritz et al., 2010; Dye et al., 2020), but research on their impacts on marine life and oceanographic patterns is scarce. Intertidal organisms in southern California are severely stressed in late fall and winter when SAWs frequently coincide with extreme low tides (Seapy and Hoppe, 1973; Gunnill, 1980; Littler, 1980), and die-backs of *Silvetia* and other species have been attributed to prolonged aerial exposure (Seapy and Littler, 1982).

According to the Santa Ana Wildfire Index, a model derived from the climatological data used in this study to generate time series representing the trend for SAWs from 1981-2016, the annual

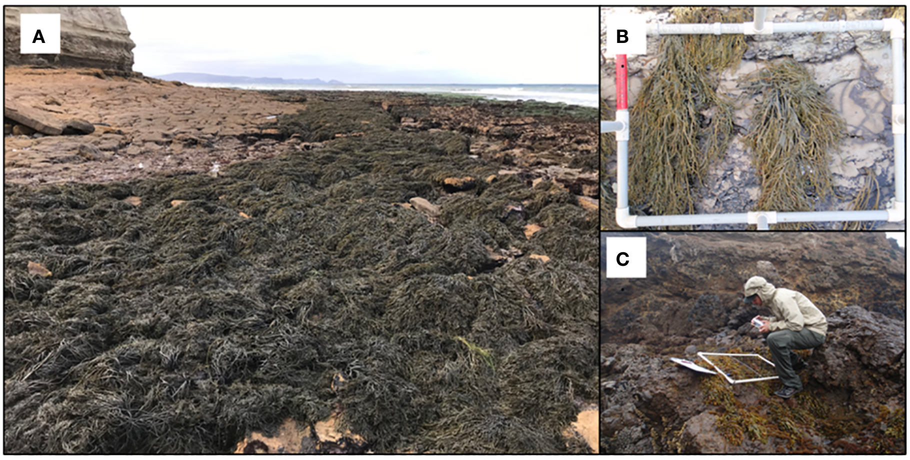

FIGURE 1
Rockweed, *Silvetia compressa*, forming large beds in the middle intertidal zone on the northwest side of Santa Rosa Island **(A)**; fixed plot established to document the percent cover of the rockweed, *Silvetia compressa* **(B)** (photos, S. Whitaker); lead author S. Whitaker scoring a fixed plot for rockweed **(C)** (photo, K. Chan).

frequency gradually increased beginning in 2000 (Li et al., 2016; see Figure 17 in Rolinski et al., 2019). By 2006, the mean number of SAW days had increased 54% from 46 days per year (1981-2005) to 71; a trend that persisted through the remainder of the climatology (Rolinski et al., 2019). This trend appears inversely proportionate to changes in *Silvetia* cover observed at numerous long-term monitoring study sites in the region affected by SAWs, with the most precipitous losses in cover occurring after 2005.

Here, we test the hypothesis that SAW events are driving declines in *Silvetia* populations in southern California. To perform our test, we used climatological time series data along with long-term monitoring data for *Silvetia* measured throughout much of its geographical range, extending across ca. 900 km of shoreline from Los Angeles, California to near the California/ Mexico border, including several of the offshore Channel Islands in southern California.

2 Materials and methods

2.1 Study sites

Thirty long-term monitoring sites (Figure 2; Supplementary Table S1) were established by the Multi-Agency Rocky Intertidal Network (MARINe; pacificrockyintertidal.org), a consortium of government agencies, academic institutions, and nonprofit groups, from 1981 to 1999 across *Silvetia's* range. Sites were established on bedrock benches with *Silvetia* beds. Refer to Engle et al. (2022) for detailed descriptions of methods.

Sites were grouped consistent with biogeographic regions described in Blanchette et al. (2008): central California (CEN, n = 4), defined as sites north of Point Conception (PC), a major biogeographic barrier separating the southern California sites (SOU, n = 10). Although located in the Southern California Bight, the offshore Channel Islands

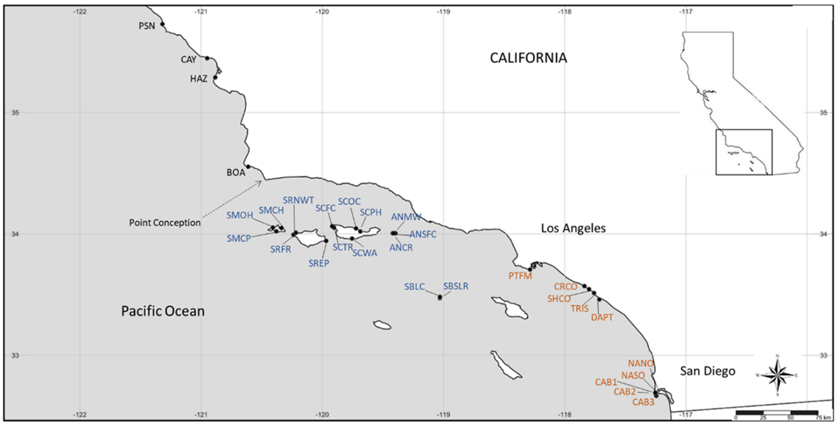

FIGURE 2
Map of long-term monitoring sites for *Silvetia compressa* used in this study. See Supplementary Table S1 for full site names and positions. Site abbreviations are color-coded by region (black = central California, blue = Channel Islands, orange = southern California).

are exposed to a latitudinal gradient in environmental and oceanographic conditions that differs from the mainland (Dailey et al., 1993; Harms and Winant, 1998; Kapsenberg and Hofmann, 2016). Therefore, we grouped the Channel Islands (CHA, n = 16) sites separately from the southern California mainland sites. The sites were primarily limited to the northern Channel Islands which are subjected to colder water temperatures than the southern Channel Islands.

2.2 Survey methods

At each of the sites, five fixed rockweed plots (50 x 75 cm) were established mostly in the mid-1980s to 1990s and were originally chosen haphazardly at each site in areas of high canopy cover of *Silvetia* (Engle et al., 2022) (Figure 1). Stainless steel hex bolts were installed in three corners of each rectangular plot so they could be relocated. Percent cover of *Silvetia*, as well as other species or bare substrate when *Silvetia* was absent, was scored in each plot using a point contact method with a grid of 100 points, either in the field or using a digital photo of the plot (Engle et al., 2022). Until 2015, fixed plots were photographed and sampled biannually in the spring (March–May) and fall (October – January) during daytime low tides. Beginning in 2015, plots were sampled annually to reduce survey effort since seasonal differences in *Silvetia* cover were not significant (Raimondi et al., 2018), and most annual monitoring was conducted during the fall period. The long-term monitoring, fixed-plot approach used by MARINe was established to support a reasonable sampling effort while providing effective statistical power to detect changes over space and time. To maximize spatial and temporal coverage, we included all data on *Silvetia* cover from 2002-2020. The initial year was chosen based on the period when protocols and the resolution of taxonomic identifications were standardized across monitoring sites.

2.3 Climatology

For each *Silvetia* monitoring site, daily mean and max statistics (3-km horizontal resolution) for dewpoint depression (D_d) (°C) and wind velocity (W_s) (km h^{-1}) were generated using a numerical weather prediction and atmospheric simulation system, the Weather Research and Forecasting (WRF) model (Rolinski et al., 2016). Daily values for D_d and W_s for each site were averaged between sampling events to provide a synopsis of the environmental conditions prior to measuring the percent cover of *Silvetia*. Dewpoint depression, the difference between air temperature and dewpoint temperature, together with near-surface wind gust time series, represents the drying process characteristic of synoptically driven offshore *Santa Ana* winds. Refer to Rolinski et al. (2016) and Skamarock et al. (2008) for detailed descriptions of how the atmospheric data used in this study were generated.

2.4 Statistical analysis

Data exploration of SAW patterns was carried out following the protocol described by Zuur et al. (2010). Dewpoint depression (D_d) and W_s climatological data were visually inspected using QQ plots, histograms, and a pair plot. Collinearity between D_d and W_s was assessed using scatterplots. Data transformations were deemed unnecessary, since the time series appeared approximately normally distributed, and various transformations including square root, cubic root, and logarithmic calculations did not significantly improve the linearity of the time series (Akaike, 1974). Data examination revealed nonlinear temporal and covariate effects.

To test for relationships between *Silvetia* cover and SAW time series data, trends in *Silvetia* populations were modeled as a function of the covariates using generalized additive mixed-effects models (GAMM) via restricted maximum likelihood (REML) in the mgcv package (Wood, 2011) using R Ver. 4.2.2 (R Core Team, 2022). Fixed covariates included *Season_number* (ordered integer with 36 levels), *Region* [categorical with three levels, central California (CEN), southern California (SOU), and the Channel Islands (CHA)], and a summary statistic (mean or maximum) for SAW time series data (D_d and W_s). *Site* (30 levels) was used as a random intercept to incorporate dependency among observations from the same site. A smoother for the *Site* spatial coordinates (*Xkm, Ykm*) was included to account for spatial dependency among sites.

We used interactions to test for regional differences in SAW time series data (e.g., $meanD_d \times Region$) and time (i.e., *Season_number* × *Region*) resulting in four full models: 1) interactions of *Region* with *maxW2*, *max*D_d, and *Season_number*, 2) interactions of *Region* with *mean*W_s, *mean*D_d, and *Season_number*, 3) interactions of *Region* with *max*W_s, *mean*D_d, and *Season_number*, and 4) interactions of *Region* with *mean*W_s, *max*D_d, and *Season_number*. We compared multiple reduced models based on the full models to test whether to include the interactions and both covariates (W_s and D_d) (Supplementary Table S2). The Akaike Information Criterion (AIC) and Bayesian Information Criterion (BIC) were used to identify the preferred model (i.e., lowest AIC and BIC) (Akaike, 1974; Schwarz, 1978). A beta distribution with a logistic link was used to ensure that the fitted values ranged from 0 to 1 for the response variable, mean percent cover of *Silvetia* [Equation (1)]. To account for the extremes 0 and 1, response variable data were transformed using $(y \cdot (n-1) + 0.5)/n$ where n is the sample size (Smithson and Verkuilen, 2006).

Using GAMM, we analyzed the following equation:

$$Cover_{ij} \sim Beta(\pi_{ij})$$

$$E(Cover_{ij}) = \pi_{ij}$$

$$Var(Cover)_{ij} = \pi_{ij} \times (1 - \pi_{ij})/(1 + \theta)$$

$$\begin{aligned} logit(\pi_{ij}) = {} & Intercept + Region_{ij} + s\left(Sample_{season_{number}} ij \times Region_{ij}\right) \\ & + s\left(D_d statistic \times Region_{ij}\right) + s\left(W_s statistic \times Region_{ij}\right) \\ & + s(Xkm \times Ykm) + Site_i \end{aligned}$$

$$Site_i \sim N(0, \sigma^2_{Site}) \tag{1}$$

where $Cover_{ij}$ is the *j*th observation in site *i*, and $i = 1, \ldots, 30$, θ is an unknown parameter controlling the variance, and $Site_i$is the random intercept, which is assumed to be normally distributed with mean 0 and variance σ^2.

To account for temporal dependency observed in the time-series data, we incorporated an autoregressive component [AR(1) correlation structure] into the model in which the random intercept *w_it* at time *t* and location *i* is similar to *w_i*, *t-1* at time *t-1* at location *i*. The AR(1) generates a latent variable that is spatially correlated, slowly changes over time, and captures any spatial and temporal patterns that are not modeled by the covariates. This latent variable ensures that the model residuals are independent and imposes a dependency structure on the response variable, *Silvetia* cover.

Underlying model assumptions including independence and absence of residual patterns were verified by plotting residuals versus fitted values and each covariate in the model. Temporal autocorrelation was assessed via partial autocorrelation function (PACF) plots of the model residuals. We then simulated 10,000 datasets from the preferred GAMM and calculated a frequency table for each simulated dataset. An average frequency table was generated from the simulated data and compared with the frequency table of the observed data.

Nonlinear trends and linear fits for *Silvetia* cover were generated at the region and site levels along with the regional relationship between *Silvetia* cover and *max*D_d using JMP Ver. 14.2.0 (SAS Institute Inc., 2018).

3 Results

3.1 Trends

Cover of the rockweed *Silvetia compressa* was highly variable in space and time across California. At the regional level, central California (CEN) *Silvetia* cover was relatively stable over time with slight declines until around 2009 and after 2015 (Figure 3). Channel Islands (CHA) *Silvetia* cover declined precipitously until around 2012 followed by a period of stabilization. Similarly, southern California (SOU) *Silvetia* cover followed a relatively steep negative trajectory but failed to recover.

Most sites (22 of 30) exhibited significant declines in rockweed cover over the study period. Declines were most prevalent south of Point Conception on the Channel Islands and the southern California mainland (Figure 4). The SOU sites exhibited high incidence (90% of sites) of decline, and nearly all declines exceeded 50% cover followed by minimal or no recovery. Within the CHA region, *Silvetia* cover decreased at all but five sites (ANSFC, SBLC, SBSLR, SRFR, SRNWT) with similar trajectories. CEN rockweed populations appeared most resilient, with one site (CAY) increasing in cover significantly during the study period and two sites (BOA, PSN) declining. The remaining sites across the three regions had relatively stable populations of rockweed over time (CEN 25%, CHA 25%, SOU 10%).

Most *Silvetia* declines occurred steadily after 2005 until approximately 2015 when *Silvetia* cover either slightly increased or continued declining for the remainder of the study period (Figures 3, 4). Sites that had stable or increasing *Silvetia* populations generally peaked in cover near the beginning of the study period and/or after 2015. Sites that precipitously declined more than 30% failed to recover.

3.2 Model results

The model (M17) with the lowest AIC and BIC included a smoother for time (i.e., *Season_number*) and an interaction with *Region* and a smoother for the covariate $maxD_d$ (Table 1; Supplementary Table S2). Based on ΔAIC, M9, M11 and M13 were considered comparable to M17 since AIC values for each were< 5 points apart. However, M9, M11 and M13 each were more complex than M17. Therefore, we identified M17 as the preferred

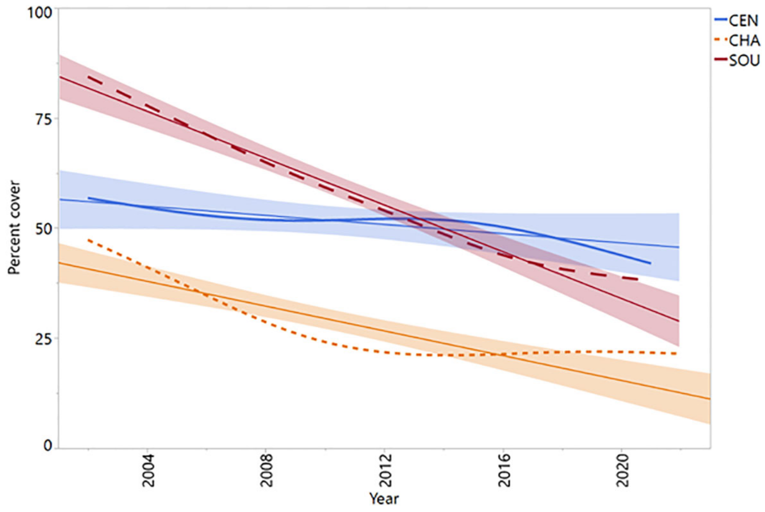

FIGURE 3
Mean annual percent cover data for *Silvetia* by region. Shade lines represent approximate linear fit. CEN, Central California region (P = 0.0982); CHA, Channel Islands region (P < 0.0001); SOU, Southern California region (P < 0.0001).

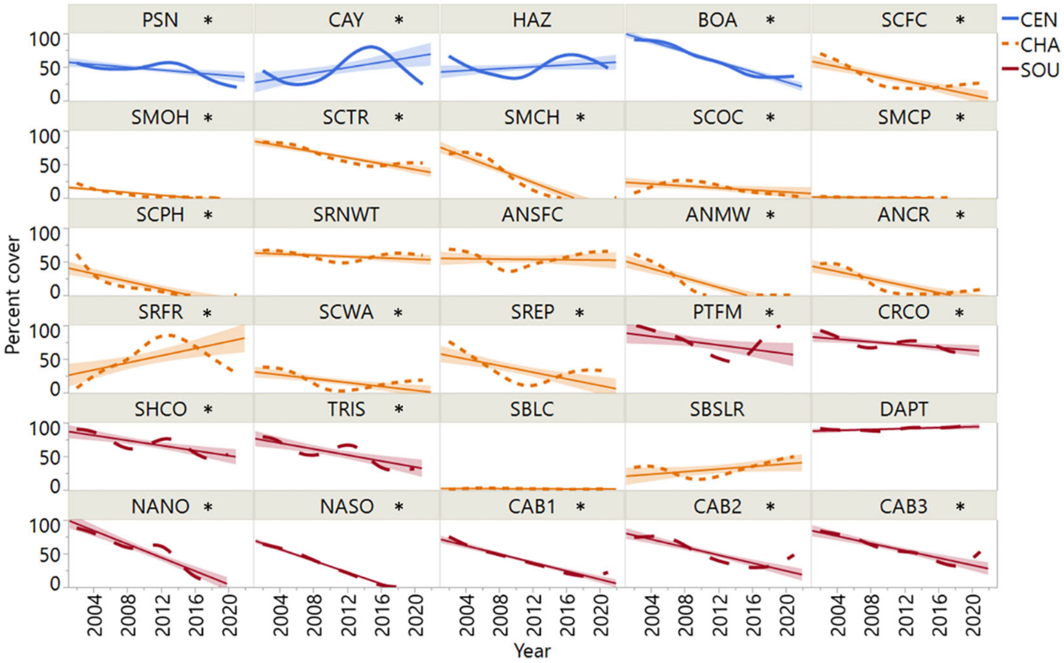

FIGURE 4
Mean annual percent cover data for *Silvetia* at each of the thirty sites arranged by latitude. Site codes are defined in Table 1. Asterisk denotes significance of the linear regression slope (P = <0.05). CEN, Central California region; CHA, Channel Islands region; SOU, Southern California region.

model. Based on Δ*BIC*, only one other model (M18) was comparable to the preferred model (M17).

Residuals from M17 met regression assumptions including normality and homogeneity of variance, and no clear patterns were seen when the residuals were plotted against covariates included and not included in the model. The AR(1) correlation structure markedly reduced the autocorrelation of the model residuals for M17 (Supplementary Figure S1). Residuals for the spatial coordinates represented variation in *Silvetia* cover not captured by covariates modeled with the GAMM (Supplementary Figure S2). Slightly higher residuals were observed in the middle latitudes corresponding with the CHA region. Lower residuals occurred in the southern latitudes near the lower portion of the SOU region. Low variability in the residuals was observed in the remaining study areas.

3.3 Dewpoint depression

Maximum dewpoint depression (maxD_d) was negatively correlated with *Silvetia* cover in all three regions (Table 1; Figures 5, 6). The relationship between *Silvetia* cover and maxD_d appeared nonlinear for the three regions (Figures 5, 6). Model selection indicated that an

TABLE 1 *Silvetia* cover GAMM (beta response distribution with logit link function) summary.

Component	Term	Estimate	Std Error	t-value	p-value	
A. parametric coefficients	(Intercept)	-0.227	1.475	-0.154	0.8780	
	georegionCHA	-1.504	1.379	-1.090	0.2759	
	georegionSOU	2.092	1.908	1.096	0.2733	
Component	**Term**	**edf**	**Ref. df**	**F-value**	**p-value**	
B. smooth terms	s(event):georegionCEN	1.944	2.459	1.076	0.2786	
	s(event):georegionCHA	3.355	4.271	26.697	0.0000	***
	s(event):georegionSOU	5.375	6.651	12.220	0.0000	***
	s(maxDD)	3.450	4.397	18.996	0.0000	***
	te(Xkm.std,Ykm.std)	3.000	3.000	1.809	0.1439	
	s(site_code)	22.412	25.000	12.131	0.0000	***

Signif. codes: 0 <= '***'.
Adjusted R-squared: 0.739, Deviance explained 0.835.
fREML : -57.440, Scale est: 1.000, N: 841.

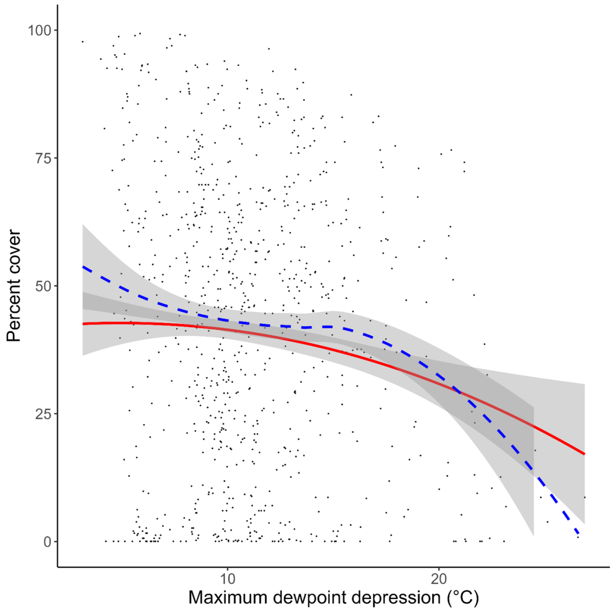

FIGURE 5
Effect of max dewpoint depression (maxD_d) on *Silvetia* cover at an average site and year plotted on the original scale. The blue dashed line represents a smoothed fit using the actual data. The red line represents a smoothed fit using the model (predicted data). The grey areas indicate the 95% confidence interval for the actual data and the modeled fit. Points denote measured data.

interaction between maxD_d and Region was not necessary since AIC for the full models was not substantially lower compared with the models excluding the interaction.

Simulating the preferred model (M17) 10,000 times, we found strong correspondence between the actual data and our modeled data (Figure 5). *Silvetia* cover across all three regions declined steadily as $maxD_d$increased according to the actual data and the modeled fit. At the regional level, *Silvetia* cover in CEN and SOU responded similarly to increasing $maxD_d$by decreasing precipitously until approximately 8°C then stabilizing (Figure 6). At the CHA region, *Silvetia* cover remained relatively stable until around 20°C before declining as $maxD_d$increased (Figure 6).

3.4 Wind

Mean near-surface wind gust (meanW_s) and max near-surface wind gust (maxW_s) were not significantly correlated with *Silvetia* cover in the three regions (Supplementary Table S2). Collinearity between D_d and W_s was low (Supplementary Figure S3). Model selection indicated that neither meanW_s nor maxW_s should be included in the preferred model based on AIC and BIC (Supplementary Table S2).

4 Discussion

We found large declines of the intertidal foundation species, *Silvetia* putatively driven by harsh, desiccating wind events across most of its geographical range, particularly the California Channel Islands and southern California mainland (Figures 3, 4). This pattern mirrors worldwide declines and range shifts in rockweeds and other fucoids (Bokn and Lein, 1978; Kautsky et al., 1986; Vogt and Schramm, 1991; Munda, 1993; Sagarin et al., 1999; Thompson et al., 2002; Lotze and Milewski, 2004; Keser et al., 2005; Torn et al., 2006; Airoldi and Beck, 2007; Ugarte et al., 2009; Lamela-Silvarrey et al., 2012; Martínez et al., 2012; Nicastro et al., 2013; Riera et al., 2015; Buonomo et al., 2018; Whitaker et al., 2023 and references therein). Spatio-temporal modeling revealed a pervasive trend of declining abundance for *Silvetia* populations at the Channel Islands and the California mainland south of Point Conception (PC), an important biogeographic break. Sites north of PC were characterized by a heterogeneous combination of trends, most of which indicated that *Silvetia* was relatively stable or increasing in cover during the study period.

Although declining rockweed populations were most prevalent in the southern California region, trends varied by site, and all three regions had examples of declining and stable sites (Figure 4). The possible causes of this complexity may, like the between-region patterns, reflect variability in meteorological and oceanographic climate, but on different spatial scales. The central California region is influenced primarily by the cool California current, while the California Current and the opposing, warmer Southern California Countercurrent (Hickey, 1979) combine to form a more complex seascape in the SCB (the region below PC including the islands). As a result, SST along the southern California mainland and the southern islands is consistently warmer, and onshore winds and fog are generally lighter relative to central California and the northwestern islands, San Miguel, and Santa Rosa Islands (Dailey et al., 1993). The islands in between occupy a transitional zone where these currents mix and SST can be highly variable (Dailey et al., 1993).

At the site level, variations in substratum aspect, slope (Harley, 2008) and extent (Gedan et al., 2011) interact with atmospheric and oceanographic variables to affect the conditions experienced by intertidal organisms including aerial temperature (Helmuth and Hofmann, 2001), wave energy (Harley and Helmuth, 2003), solar radiation (Schoch and Dethier, 1996), wind velocity, relative humidity and fog (Helmuth and Hofmann, 2001; Helmuth et al., 2006). A high degree of spatial heterogeneity exists across the network of sites in this study given its broad spatial scale, which likely corresponds to significant site-level variation in abiotic conditions (Choi et al., 2019). As a result, the mosaic of trends for *Silvetia* likely reflects environmental heterogeneity at both the local and regional levels, thereby influencing the population dynamics of *Silvetia*.

During the study period, sea surface temperatures (SST) rose more rapidly in southern California than in most other regions of the world (Hobday and Pecl, 2014). Anomalously high SSTs occurred in the northeastern Pacific Ocean during El Niño events in 2009-10 and 2014-16. The latter event, one of the strongest El Niño's in recent history (Huang et al., 2016), resulted in exceptionally high SST anomalies in part due to the concurrence of a widespread marine heat wave in the North Pacific (Jacox et al., 2016). In addition, the average annual air temperature in southern

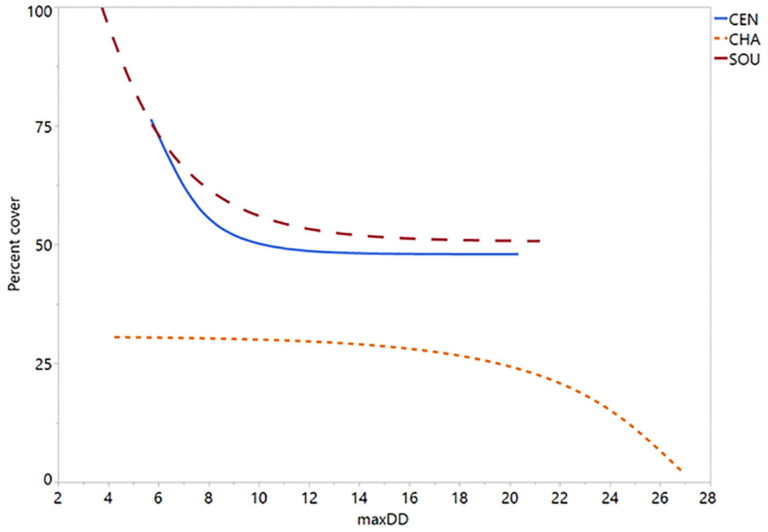

FIGURE 6
Silvetia percent cover plotted on scale of maximum dewpoint depression (°C). Regression slopes are all significant (P = 0). CEN, Central California; CHA, Channel Islands; SOU, Southern California.

California steadily increased from 1950 to 2010 (Gonzalez, 2020). Macroalgae including *Silvetia* can be stressed by oceanographic parameters including seawater temperature (Breeman, 1988; Wernberg et al., 2011; Hurd et al., 2014; Graham et al., 2018) and wave energy (Vadas et al., 1990), as well as by atmospheric conditions such as high temperatures (Bell, 1995) and high irradiance (Henley, 1992). These changes in regional atmospheric and oceanographic conditions are consistent with the general latitudinal pattern of trends we identified in *Silvetia* cover and suggest that declines in southern California may be linked to overall warming conditions both in the coastal ocean and on land.

Downsloping, offshore wind is a natural occurrence in western North America due to gradients between high-pressure systems in the inland Great Basin and low pressure over the Pacific Ocean. As low-pressure systems offshore of California pull air masses from inland desert areas, winds more than 25 m s^{-1} (56 mi h^{-1}) (Keeley et al., 2004; Cao and Fovell, 2013) are generated through canyons and mountain passes compressing, drying, and heating the air in the process. Below PC, these conditions are called Santa Ana winds (SAWs), and recent studies suggest that downslope wind systems in central and northern California coincide with SAWs (Gershunov et al., 2021; Guirguis et al., 2023). SAWs occur annually between September and June (Cao and Fovell, 2016). However, SAW frequency and intensity are greatest during the winter months of December and January, respectively, (Guzman-Morales et al., 2016) a time of year coincident with periods of day-time aerial exposure for intertidal ecosystems in southern California. More than any other environmental variable, the seasonal pattern of diurnal emersion has been attributed to changes in the abundances of intertidal algae in the Southern California Bight (SCB) (Emerson and Zedler, 1978; Gunnill, 1980; Seapy and Littler, 1982; Littler et al., 1991).

The Santa Ana Wildfire Index (SAWTI), a model generated from the climatological data used in this study, indicates that the monthly and seasonal SAW day counts were variable but mostly remained near average or below average from 1981 to the early 2000s (see Figure 17 in Rolinski et al., 2019). After 2006, the number of SAW days per season was significantly elevated for the remainder of the study period through 2016 (Rolinski et al., 2019). This trend corresponds with negative changes in *Silvetia* cover observed at many study sites in the two regions, Channel Islands (CHA) and southern California mainland (SOU) which exhibited gradual declines from the beginning of the study period through around 2015 with the most precipitous losses in percent cover occurring after 2005 (Figures 3, 4).

Despite rockweeds being very desiccation-resistant for a large frondose alga (Schonbeck and Norton, 1978), extreme conditions during warm and dry periods, especially with strong, dry winds, can be detrimental. During SAW events occurring during low tide periods, *Silvetia* is often observed exhibiting severe drying out with fronds turning crispy. Desiccation stress is known to affect various physiological processes and conditions in rockweeds and other fucoids, including oxidative damage (Martins et al., 2021), reduced net photosynthesis, survival, and growth (Dethier et al., 2005), increased susceptibility to loss from wave action (Haring et al., 2002), and limited recruitment success (Dudgeon and Petraitis, 2001). Over time, these effects are likely to cause population declines, as observed at our monitoring sites.

SAW activity has been linked with environmental cycles including the Atlantic multi-decadal oscillation (AMO), the PDO, and the ENSO, with elevated periods of SAW activity typically coinciding with cool phases of the PDO (Rolinski et al., 2019) and ENSO (Raphael, 2003; Rolinski et al., 2019), and the warm phase of the AMO (Li et al., 2016). Although Guzman-Morales et al. (2016) found seasonal SAW intensity to increase during the warm phases of the PDO and ENSO and vice versa. This information is critical for projecting SAW activity. However, it remains unclear how SAW events will change under anthropogenic climate warming conditions.

Projections of SAW activity due to climate change remain mixed due, in part, to differences in approaches used to distinguish and downscale the events (e.g., Miller and Schlegel, 2006; Hughes et al., 2011; Abatzoglou et al., 2013; Guzman-Morales et al., 2016). Some studies indicate a reduction of SAW events as anthropogenic warming increases due to a weakening in the temperature gradient between the ocean and the Great Basin (Hughes et al., 2009; Hughes et al., 2011; Guzman Morales, 2018). Others suggest that anthropogenic warming will increase the frequency of strong SAWs in late fall (Yue et al., 2014), or that more SAW days may occur at the beginning (September) and end (June) of the SAW season (Rolinski et al., 2019). Clearly, more research is needed to increase the accuracy of projecting SAW variability as climate warms. Based on patterns discussed here, however, any increases in the frequency or intensity of SAWs are likely to lead to large declines and possible extirpation of *Silvetia*, as well as the important ecological services the species provides.

Our results demonstrate that *Silvetia*, like many other fucoids throughout the world (Sagarin et al., 1999; Lamela-Silvarrey et al., 2012; Martínez et al., 2012; Nicastro et al., 2013; Riera et al., 2015), has declined significantly in southern California and the Channel Islands. This trend corresponds with elevated dewpoint depression, an indicator of SAW activity, which, in turn, may represent the phases of environmental cycles such as PDO, ENSO, and AMO that the data in this study were collected or anthropogenic forcing on SAW activity. Spatial and temporal patterns in rockweed populations, however, are complex, varying between sites as well as across regions. The network of long-term monitoring sites established by the Multi Agency Rocky Intertidal Monitoring Network (MARINe) that provided the data for this study is an ideal milieu for a detailed comparative and experimental program to elucidate the causes of rockweed declines. This information, along with more accurate future projections of SAW activity under climate change, are critical for informing conservation, and potentially restoration, of this important foundation species and the rocky intertidal biodiversity it supports.

5 Implications

Population dynamics are influenced by local- to regional-scale variability in environmental conditions across a broad range of temporal scales (Oro, 2013; Dallas and Kramer, 2022). Variations in environmental conditions arise from extensive habitat heterogeneity common in ecosystems (Tilman and Kareiva, 1997), including the rocky intertidal, where climatic variables range widely across regions to individual plots (Helmuth and Hofmann, 2001). Extreme variability in atmospheric factors such as air temperature, humidity, and wind, results from both continental scale differences in topographical landscapes composed of mountains, valleys, and plains (Keeley et al., 2004; Cao and Fovell, 2013), and microtopographical differences in substratum orientation, aspect, hue, and rugosity (Helmuth and Hofmann, 2001; Helmuth et al., 2006; Harley, 2008; Choi et al., 2019). Similarly, variance in oceanographic conditions such as temperature, pH, and wave energy, occurs across the large spatial scales of regional ocean currents and prominent land features such as headlands, to local offshore reefs and kelp forests (Harley and Helmuth, 2003). Temporally, rocky intertidal ecosystems vary as atmospheric and oceanographic conditions change on short- and long-term timescales due to tides, local weather patterns, season, and interannual and decadal climatological cycles such as the El Niño Southern Oscillation and the Pacific Decadal Oscillation (Wootton et al., 1996; Thompson et al., 2002; Menge et al., 2008). This variability presents complex challenges for ecologists testing broad-scale ecological hypotheses and forecasting population dynamics.

To account for high levels of spatial and temporal variability in environmental conditions in our study, we used long-term observational data at multiple spatial scales to test the simple hypothesis that canopy cover of the foundational rockweed *Silvetia* is reduced by dry air events associated with offshore Santa Ana winds. We found extensive spatial and temporal variability in *Silvetia* cover driven by a combination of large- and small-scale processes. Rockweed cover in all three regions of our study was significantly and often dramatically reduced by dry air events associated with Santa Ana winds, but the response of rockweed varied markedly by region. Rockweed in the southern and central study regions responded very differently depending on site, whereas the rockweed in the northern region was more stable and homogeneous across sites. Including ‘site’ as a random effect increased the deviance explained by approximately 10%, suggesting that local processes influence the dynamics of *Silvetia* cover, reducing or overriding the effects of regional scale factors including Santa Anas. Our results underscore the need for continued long-term monitoring of ecosystems across regions to capture both local and large-scale variation and effectively inform the conservation and restoration of important foundation species.

Data availability statement

The raw data supporting the conclusions of this article will be made available by the authors, without undue reservation.

Author contributions

SW: Conceptualization, Data curation, Formal analysis, Funding acquisition, Investigation, Methodology, Project administration, Resources, Software, Supervision, Validation, Visualization, Writing – original draft, Writing – review & editing. PR: Formal analysis, Writing – review & editing. JS: Writing – review & editing. HL: Writing – review & editing. SG: Writing – review & editing. RM: Funding acquisition, Supervision, Writing – review & editing.

Funding

The author(s) declare financial support was received for the research, authorship, and/or publication of this article. Funding for this work was provided by the California Ocean Protection Council (agreement C0302106), the NASA Biodiversity and Ecological

Forecasting Program (grant no. NNX14AR62A), the Bureau of Ocean Energy Management, Environmental Studies Program (BOEM Agreement MC15AC00006), the National Oceanic and Atmospheric Administration in support of the Santa Barbara Channel Marine Biodiversity Observation Network, and the National Park Service.

Acknowledgments

We are grateful to S. Capps, Principal of Atmospheric Data Solutions, for providing the climatological time series data used in this study. The biological data we analyzed were provided by the Multi-Agency Rocky Intertidal Network (MARINe). Funding for MARINe was contributed by Bureau of Ocean Energy Management, National Park Service, Partnership of Interdisciplinary Studies of Coastal Oceans and California Ocean Protection Council. We thank the National Park Service, the University of California Natural Reserve System and The Nature Conservancy for site access and logistical support. The authors also thank A. Zuur and L. Pandori for statistical advice, L. Kui for statistical assistance, and L. Lee, R. Gaddam and M. Miner for database assistance.

Conflict of interest

The authors declare that the research was conducted in the absence of any commercial or financial relationships that could be construed as a potential conflict of interest.

Publisher's note

Supplementary material

The Supplementary Material for this article can be found online at: https://www.frontiersin.org/articles/10.3389/fevo.2024.1291310/full#supplementary-material

References

Abatzoglou, J. T., Barbero, R., and Nauslar, N. J. (2013). Diagnosing Santa Ana winds in southern California with synoptic-scale analysis. *Weather Forecasting* 28 (3), 704–710. doi: 10.1175/WAF-D-13-00002.1

Abatzoglou, J. T., Hatchett, B. J., Fox-Hughes, P., Gershunov, A., and Nauslar, N. J. (2021). Global climatology of synoptically-forced downslope winds. *Int. J. Climatology* 41 (1), 31–50. doi: 10.1002/joc.6607

Abbott, I. A., and Hollenberg, G. J. (1992). *Marine Algae of California* (Stanford, California: Stanford University Press).

Agardh, C. A. (1824). *Systema algarum* (Lundae: Literis Berlingianis), 312 pp.

Airoldi, L., and Beck, M. (2007). Loss, status and trends for coastal marine habitats of Europe. *Oceanography Mar. Biol.* 45, 345–405. doi: 10.1201/9781420050943.ch7

Akaike, H. (1974). A new look at the statistical model identification. *IEEE Trans. Automatic Control* 19, 716–723. doi: 10.1109/TAC.1974.1100705

Bell, E. C. (1995). Environmental and morphological influences on thallus temperature and desiccation of the intertidal alga *Mastocarpus papillatus* Kützing. *J. Exp. Mar. Biol. Ecol.* 191, 29–55. doi: 10.1016/0022-0981(95)00037-R

Bertness, M. D., and Leonard, G. H. (1997). The role of positive interactions in communities: lessons from intertidal habitats. *Ecology* 78, 1976–1989. doi: 10.1890/0012-9658(1997)078[1976:TROPII]2.0.CO;2

Bertness, M. D., Leonard, G. H., Levine, J. M., Schmidt, P. R., and Ingraham, A. O. (1999). Testing the relative contribution of positive and negative interactions in rocky intertidal communities. *Ecology* 80, 2711–2726. doi: 10.1890/0012-9658(1999)080[2711:TTRCOP]2.0.CO;2

Bishop, M. J., Coleman, M. A., and Kelaher, B. P. (2010). Cross-habitat impacts of species decline: Response of estuarine sediment communities to changing detrital resources. *Oecologia* 163, 517–525. doi: 10.1007/s00442-009-1555-y

Blanchette, C. A., Melissa Miner, C., Raimondi, P. T., Lohse, D., Heady, K. E., and Broitman, B. R. (2008). Biogeographical patterns of rocky intertidal communities along the Pacific coast of North America. *J. Biogeography* 35 (9), 1593–1607. doi: 10.1111/j.1365-2699.2008.01913.x

Bokn, T. L., and Lein, T. E. (1978). Long-term changes in fucoid association of the inner Oslofjord, Norway. *Norway J. Bot.* 25 (1), 9–14.

Bordeyne, F., Migné, A., and Davoult, D. (2015). Metabolic activity of intertidal *Fucus* spp. communities: Evidence for high aerial carbon fluxes displaying seasonal variability. *Mar. Biol.* 162, 2119–2129. doi: 10.1007/s00227-015-2741-6

Brawley, S. H., and Johnson, L. E. (1993). Predicting desiccation stress in microscopic organisms the use of agarose beads to determine evaporation within and between intertidal microhabitats. *J. Phycology* 29, 528–535. doi: 10.1111/j.1529-8817.1993.tb00154.x

Breeman, A. M. (1988). Relative importance of temperature and other factors in determining geographic boundaries of seaweeds: Experimental and phenological evidence. *Helgoländer Meeresunters* 42, 199–241. doi: 10.1007/BF02366043

Brinkhuis, B. H., Tempel, N. R., and Jones, R. F. (1976). Photosynthesis and respiration of exposed salt-marsh fucoids. *Mar. Biol.* 34, 349–359. doi: 10.1007/BF00398128

Buonomo, R., Chefaoui, R. M., Lacida, R. B., Engelen, A. H., Serrão, E. A., and Airoldi, L. (2018). Predicted extinction of unique genetic diversity in marine forests of *Cystoseira* spp. *Mar. Environ. Res.* 138, 119–128. doi: 10.1016/j.marenvres.2018.04.013

Cao, Y., and Fovell, R. (2013). "Predictability and sensitivity of downslope windstorms in San Diego County," *Proc. 15th Conf. on Mesoscale Processes*. (Portland, OR: American Meteor Society), 7.6. Available at: https://ams.confex.com/ams/15MESO/webprogram/Paper228055.html.

Cao, Y., and Fovell, R. G. (2016). Downslope windstorms of San Diego County. Part I: A case study. *Monthly Weather Rev.* 144 (2), 529–552. doi: 10.1175/MWR-D-15-0147.1

Chapman, A. R. O. (1995). Functional ecology of fucoid algae: Twenty-three years of progress. *Phycologia* 34, 1–32. doi: 10.2216/i0031-8884-34-1-1.1

Choi, F., Gouhier, T., Lima, F., Rilov, G., Seabra, R., and Helmuth, B. (2019). Mapping physiology: Biophysical mechanisms define scales of climate change impacts. *Conserv. Physiol.* 7 (1), coz028. doi: 10.1093/conphys/coz028

Dailey, M. D., Reish, D. J., and Anderson, J. W. (1993). *Ecology of the Southern California Bight: A Synthesis and Interpretation* (Berkeley and Los Angeles, California: University of California Press).

Dallas, T. A., and Kramer, A. M. (2022). Temporal variability in population and community dynamics. *Ecology* 103 (2), e03577. doi: 10.1002/ecy.3577

Davison, I. R., and Pearson, G. A. (1996). Stress tolerance in intertidal seaweeds. *J. Phycology* 32, 197–211. doi: 10.1111/j.0022-3646.1996.00197.x

Dayton, P. K. (1985). Ecology of kelp communities. *Annu. Rev. Ecology Evol. Systematics* 16 (1), 215–245. doi: 10.1146/annurev.es.16.110185.001243

Dethier, M. N., Williams, S. L., and Freeman, A. (2005). Seaweeds under stress: manipulated stress and herbivory affect critical life-history functions. *Ecol. Monogr.* 75 (3), 403–418. doi: 10.1890/03-4108

Dudgeon, S., and Petraitis, P. S. (2001). Scale-dependent recruitment and divergence of intertidal communities. *Ecology* 82 (4), 991–1006. doi: 10.1890/0012-9658(2001)082[0991:SDRADO]2.0.CO;2

Duke, N. C., Meynecke, J. O., Dittmann, S., Ellison, A. M., Anger, K., Berger, U., et al. (2007). A world without mangroves? *Science* 317, 41–42. doi: 10.1126/science.317.5834.41b

Dye, A. W., Kim, J. B., and Riley, K. L. (2020). Spatial heterogeneity of winds during Santa Ana and non-Santa Ana wildfires in Southern California with implications for fire risk modeling. *Heliyon* 6, e04159. doi: 10.1016/j.heliyon.2020.e04159

Ellison, A. M., Bank, M. S., Clinton, B. D., Colburn, E. A., Elliott, K., Ford, C. R., et al. (2005). Loss of foundation species: consequences for the structure and dynamics of forested ecosystems. *Front. Ecol. Environ.* 3, 479–486. doi: 10.1890/1540-9295(2005)003[0479:LOFSCF]2.0.CO;2

Emerson, S. E., and Zedler, J. B. (1978). Recolonization of intertidal algae: an experimental study. *Mar. Biol.* 44, 315–324. doi: 10.1007/BF00390895

Engle, J. M., Anderson, L., Burnaford, J. L., Douglas, M., Lohse, D. P., and Parsons-Field, A. (2022). *Unified Monitoring Protocols for the Multi-Agency Rocky Intertidal Network* (Camarillo, California: BOEM Cooperative Agreement No. M19AC00023). Department of the Interior. Bureau of Ocean Energy Management. Pacific OCS Region. doi: 10.6085/AA/marine_ltm.15.3

Gedan, K. B., Bernhardt, J., Bertness, M. D., and Leslie, H. M. (2011). Substrate size mediates thermal stress in the rocky intertidal. *Ecology* 92, 576–582. doi: 10.1890/10-0717.1

Gershunov, A., Guzman Morales, J., Hatchett, B., Guirguis, K., Aguilera, R., Shulgina, T., et al. (2021). Hot and cold flavors of southern California's Santa Ana winds: Their causes, trends, and links with wildfire. *Climate dynamics* 57 (7-8), 2233–2248. doi: 10.1007/s00382-021-05802-z

Golléty, C., Migné, A., and Davoult, D. (2008). Benthic metabolism on a sheltered rocky shore: Role of the canopy in the carbon budget. *J. Phycology* 44, 1146–1153. doi: 10.1111/j.1529-8817.2008.00569.x

Golléty, C., Riera, P., and Davoult, D. (2010). Complexity of the food web structure of the Ascophyllum nodosum zone evidenced by a δ13C and δ15N study. *J. Sea Res.* 64 (3), 304–312. doi: 10.1016/j.seares.2010.04.003

Gonzalez, P. (2020). Human-caused climate change in United States national parks and solutions for the future. *Parks Steward. Forum* 36, 1–64. doi: 10.5070/P536248262

Graham, L. E., Graham, J. M., Wilcox, L. W., and Cook, M. E. (2000). *Algae, 2nd Edition* (Upper Saddle River: Prentice Hall).

Graham, S., Hong, B., Mutschler, S., Saunders, B., and Bredvik, J. (2018). Changes in abundance of Silvetia compressa at San Clemente Island before and during the 2015–2016 El Niño. *Western North Am. Nat.* 78 (4), 605–616. doi: 10.3398/064.078.0405

Guirguis, K., Gershunov, A., Hatchett, B. J., DeFlorio, M. J., Subramanian, A. C., Clemesha, R., et al. (2023). Subseasonal prediction of impactful california winter weather in a hybrid dynamical-statistical framework. *Geophys. Res. Lett.* 50 (23), 1729. doi: 10.1007/s00382-022-06361-7

Gunnill, F. C. (1980). Demography of the intertidal brown alga *Pelvetia fastigiata* in southern California, USA. *Mar. Biol.* 59, 169–179. doi: 10.1007/BF00396865

Guzman Morales, J. (2018). Santa Ana winds of southern California: historical variability and future climate projections [PhD thesis]. (San Diego: University of California), 68. Available at: https://escholarship.org/uc/item/6hm499nj.

Guzman-Morales, J., Gershunov, A., Theiss, J., Li, H., and Cayan, D. (2016). Santa Ana winds of southern California: Their climatology, extremes, and behavior spanning six and a half decades. *Geophysical Res. Lett.* 43, 2827–2834. doi: 10.1002/2016GL067887

Haring, R. N., Dethier, M. N., and Williams, S. L. (2002). Desiccation facilitates wave-induced mortality of the intertidal alga *Fucus gardneri*. *Mar. Ecol. Prog. Ser.* 232, 75–82. doi: 10.3354/meps232075

Harley, C. (2008). Tidal dynamics, topographic orientation, and temperature-mediated mass mortalities on rocky shores. *Mar. Ecol. Prog. Ser.* 371, 37–46. doi: 10.3354/meps07711

Harley, C. D. G., and Helmuth, B. S. T. (2003). Local- and regional-scale effects of wave exposure, thermal stress, and absolute versus effective shore level on patterns of intertidal zonation. *Limnology Oceanography* 48, 1498–1508. doi: 10.4319/lo.2003.48.4.1498

Harms, S., and Winant, C. D. (1998). Characteristic patterns of the circulation in the Santa Barbara Channel. *J. Geophysical Research: Oceans* 103, 3041–3065. doi: 10.1029/97JC02393

Hawkins, S., and Hartnoll, R. (1985). Factors determining the upper limits of intertidal canopy-forming algae. *Mar. Ecol. Prog. Ser.* 20, 265–271. doi: 10.3354/meps020265

Hawkins, S. J., Moore, P. J., Burrows, M. T., Poloczanska, E., Mieszkowska, N., Herbert, R. J. H., et al. (2008). Complex interactions in a rapidly changing world: Responses of rocky shore communities to recent climate change. *Climate Res.* 37, 123–133. doi: 10.3354/cr00768

Hays, C. (2006). *Ecological consequences of dispersal and gene flow in an intertidal alga - ProQuest* (Santa Cruz, Santa Cruz, CA: University of California).

Helmuth, B., Broitman, B. R., Blanchette, C. A., Gilman, S., Halpin, P., Harley, C. D. G., et al. (2006). Mosaic patterns of thermal stress in the rocky intertidal zone: Implications for climate change. *Ecol. Monogr.* 76, 461–479. doi: 10.1890/0012-9615(2006)076[0461:MPOTSI]2.0.CO;2

Helmuth, B. S. T., and Hofmann, G. E. (2001). Microhabitats, thermal heterogeneity, and patterns of physiological stress in the rocky intertidal zone. *Biol. Bull.* 201, 374–384. doi: 10.2307/1543615

Henley, W. J. (1992). Growth and photosynthesis of *Ulva rotundata* (chlorophyta) as a function of temperature and square wave irradiance in indoor culture. *J. Phycology* 28, 625–634. doi: 10.1111/j.0022-3646.1992.00625.x

Hickey, B. M. (1979). The California current system-hypotheses and facts. *Prog. Oceanography* 8, 191–279. doi: 10.1016/0079-6611(79)90002-8

Hobday, A. J., and Pecl, G. T. (2014). Identification of global marine hotspots: Sentinels for change and vanguards for adaptation action. *Rev. Fish Biol. Fisheries* 24, 415–425. doi: 10.1007/s11160-013-9326-6

Huang, B., L'Heureux, M., Hu, Z. Z., and Zhang, H. M. (2016). Ranking the strongest ENSO events while incorporating SST uncertainty. *Geophysical Res. Lett.* 43 (17), 9165–9172. doi: 10.1002/2016GL070888

Hughes, T. P., Baird, A. H., Bellwood, D. R., Card, M., Connolly, S. R., Folke, C., et al. (2003). Climate change, human impacts, and the resilience of coral reefs. *Science* 301, 929–933. doi: 10.1126/science.1085046

Hughes, M., Hall, A., and Kim, J. (2009). *Anthropogenic reduction of Santa Ana winds.* (Sacramento CA: California Energy Commission), 19. Available at: https://www.energy.ca.gov/2009publications/CEC-500-2009-015/CEC-500-2009-015-D.pdf.

Hughes, M., Hall, A., and Kim, J. (2011). Human-induced changes in wind, temperature and relative humidity during Santa Ana events. *Climatic Change* 109, 119–132. doi: 10.1007/s10584-011-0300-9

Hurd, C. L., Harrison, P. J., Bischof, K., and Lobban, C. S. (2014). *Seaweed Ecology and Physiology* (Cambridge, UK: Cambridge University Press).

Jackson, J. B. C., Kirby, M. X., Berger, W. H., Bjorndal, K. A., Botsford, L. W., Bourque, B. J., et al. (2001). Historical overfishing and the collapse of marine ecosystems. *Science* 293, 629–638. doi: 10.1126/science.1059199

Jacox, M. G., Hazen, E. L., Zaba, K. D., Rudnick, D. L., Edwards, C. A., Moore, A. M., et al. (2016). Impacts of the 2015–2016 El Niño on the California Current System: Early assessment and comparison to past events. *Geophysical Res. Lett.* 43 (13), 7072–7080. doi: 10.1002/2016GL069716

Jenkins, S. R., Norton, T. A., and Hawkins, S. J. (2004). Long term effects of *Ascophyllum nodosum* canopy removal on mid shore community structure. *J. Mar. Biol. Assoc. United Kingdom* 84, 327–329. doi: 10.1017/S0025315404009221h

Jones, C., Fujioka, F., and Carvalho, L. M. V. (2010). Forecast skill of synoptic conditions associated with Santa Ana Winds in Southern California. *Monthly Weather Rev.* 138, 4528–4541. doi: 10.1175/2010MWR3406.1

Kapsenberg, L., and Hofmann, G. E. (2016). Ocean pH time-series and drivers of variability along the northern Channel Islands, California, USA. *Limnolology Oceanography* 61, 953–968. doi: 10.1002/lno.10264

Kautsky, N., Kautsky, H., Kautsky, U., and Waern, M. (1986). Decreased depth penetration of Fucus vesiculosus (L.) since the 1940's indicates eutrophication of the Baltic Sea. *Mar. Ecol. Prog. Ser.* 28 (1/2), 1–8.

Keeley, J. E., Fotheringham, C. J., and Moritz, M. A. (2004). Lessons from the october 2003. Wildfires in Southern California. *J. Forestry* 102, 26–31. doi: 10.1093/jof/102.7.26

Keser, M., Swenarton, J. T., and Foertch, J. F. (2005). Effects of thermal input and climate change on growth of *Ascophyllum nodosum* (Fucales, Phaeophyceae) in eastern Long Island Sound (USA). *J. Sea Res.* 54, 211–220. doi: 10.1016/j.seares.2005.05.001

Lamela-Silvarrey, C., Fernández, C., Anadón, R., and Arrontes, J. (2012). Fucoid assemblages on the north coast of Spain: Past and preseny, (1977- 2007). *Botanica Marina* 55, 199–207. doi: 10.1515/bot-2011-0081

Lenihan, H. S., Peterson, C. H., Byers, J. E., Grabowski, J. H., Thayer, G. W., and Colby, D. R. (2001). Cascading of habitat degradation: oyster reefs invaded by refugee fishes escaping stress. *Ecol. Appl.* 11, 748–764. doi: 10.1890/1051-0761(2001)011[0764:COHDOR]2.0.CO;2

Li, A., Paek, H., and Yu, J. Y. (2016). The changing influences of the AMO and PDO on the decadal variation of the Santa Ana winds - *IOPscience. Environ. Res. Lett.* 11, 1–8. doi: 10.1088/1748-9326/11/6/064019

Littler, M. M. (1980). "*Overview of the rocky intertidal systems of Southern California*," in *The California Islands: Proceedings of a Multidisciplinary Symposium*, ed. D.M. Power (Santa Barbara: Santa Barbara Museum of Natural History), 265e306.

Littler, M. M., Littler, D. S., Murray, S. N., and Seapy, R. R. (1991). "Southern California rocky intertidal ecosystems," in *Ecosystems of the world. Volume 24. Intertidal and littoral ecosystems*, Eds. A.C. Mathieson and P.H. Nienhuis (Amsterdam: Elsevier), 273-296.

Lotze, H. K., and Milewski, I. (2004). Two centuries of multiple human impacts and successive changes in a North Atlantic food web. *Ecol. Appl.* 14, 1428–1447. doi: 10.1890/03-5027

Lubchenco, J. (1983). *Littornia* and *Fucus*: Effects of Herbivores, Substratum heterogeneity, and plant escapes during succession. *Ecology* 64, 1116–1123. doi: 10.2307/1937822

Martínez, B., Arenas, F., Rubal, M., Burgués, S., Esteban, R., García-Plazaola, I., et al. (2012). Physical factors driving intertidal macroalgae distribution: physiological stress of a dominant fucoid at its southern limit. *Oecologia* 170, 341–353. doi: 10.1007/s00442-012-2324-x

Martins, M., Soares, C., Figueiredo, I., Sousa, B., Torres, A. C., Sousa-Pinto, I., et al. (2021). Fucoid macroalgae have distinct physiological mechanisms to face emersion and submersion periods in their southern limit of distribution. *Plants* 10, 1892. doi: 10.3390/Plants10091892

Marzinelli, E. M., Campbell, A. H., Vergés, A., Coleman, M. A., Kelaher, B. P., and Steinberg, P. D. (2014). Restoring seaweeds: does the declining fucoid *Phyllospora comosa* support different biodiversity than other habitats? *J. Appl. Phycology* 26, 1089–1096. doi: 10.1007/s10811-013-0158-5

Menge, B. A., Chan, F., and Lubchenco, J. (2008). Response of a rocky intertidal ecosystem engineer and community dominant to climate change. *Ecol. Lett.* 11, 151–162. doi: 10.1111/j.1461-0248.2007.01135.x

Miller, N. L., and Schlegel, N. J. (2006). Climate change projected fire weather sensitivity: California Santa Ana wind occurrence. *Geophysical Res. Lett.* 33 (15), 1–5. doi: 10.1029/2006GL025808

Moore, P. G. (1977). "Organization in simple communities: observations on the natural history of Hyale nilssoni (Amphipoda) in high littoral seaweeds," in *Biology of Benthic Organisms. Presented at the 11th European Symposium on Marine Biology, Galway*. Eds. B. F. Keegan, P. O. Ceidigh and P. J. S. Boaden (Oxford: Pergamon Press), 443–451. doi: 10.1016/B978-0-08-021378-1.50050-6

Moritz, M. A., Moody, T. J., Krawchuk, M. A., Hughes, M., and Hall, A. (2010). Spatial variation in extreme winds predicts large wildfire locations in chaparral ecosystems. *Geophys. Res. Lett.* 37 (4), 1–5. doi: 10.1029/2009GL041735

Munda, I. M. (1993). Changes and degradation of seaweed stands in the Northern Adriatic. *Hydrobiologia* 260/261, 239–253. doi: 10.1007/BF00049025

Nicastro, K. R., Zardi, G. I., Teixeira, S., Neiva, J., Serrão, E. A., and Pearson, G. A. (2013). Shift happens: trailing edge contraction associated with recent warming trends threatens a distinct genetic lineage in the marine macroalga *Fucus vesiculosus*. *BMC Biol.* 11, 6. doi: 10.1186/1741-7007-11-6

Oro, D. (2013). Grand challenges in population dynamics. *Front. Ecol. Evol.* 1. doi: 10.3389/fevo.2013.00002

Råberg, S., and Kautsky, L. (2007). A comparative biodiversity study of the associated fauna of perennial fucoids and filamentous algae. *Estuarine Coast. Shelf Sci.* 73, 249–258. doi: 10.1016/J.ECSS.2007.01.005

Raimondi, P., Ammann, K., Gilbane, L., Whitaker, S., and Ostermann-Kelm, S. (2018). *Power analysis of the intertidal monitoring programs at Channel Islands National Park and the Bureau of Ocean Energy Management* (Fort Collins, Colorado: Natural Resource Report). NPS/MEDN/NRR—2018/1661. National Park Service.

Raphael, M. N. (2003). The Santa Ana winds of California. *Earth Interact.* 7, 1. doi: 10.1175/1087-3562(2003)007<0001:TSAWOC>2.0.CO;2

R Core Team. (2022). *R: A language and environment for statistical computing* (Vienna, Austria: R Foundation for Statistical Computing). Available at: http://www.R-project.org/.

Renaud, P. E., Løkken, T. S., Jørgensen, L. L., Berge, J., and Johnson, B. J. (2015). Macroalgal detritus and food-web subsidies along an Arctic fjord depth-gradient. *Front. Mar. Sci.* 2. doi: 10.3389/fmars.2015.00031

Riera, R., Sangil, C., and Sanson, M. (2015). Long-term herbarium data reveal the decline of a temperate-water algae at its southern range. *Estuarine Coast. Shelf Sci.* 165, 159–165. doi: 10.1016/j.ecss.2015.05.008

Rolinski, T., Capps, S. B., Fovell, R. G., Cao, Y., D'Agostino, B. J., and Vanderburg, S. (2016). The Santa Ana Wildfire Threat Index: Methodology and operational implementation. *Weather Forecast* 31, 1881–1897. doi: 10.1175/WAF-D-15-0141.1

Rolinski, T., Capps, S. B., and Zhuang, W. (2019). Santa Ana Winds: a descriptive climatology. *Weather Forecast* 34, 257–275. doi: 10.1175/WAF-D-18-0160.1

Sagarin, R. D., Barry, J. P., Gilman, S. E., and Baxter, C. H. (1999). Climate-related change in an intertidal community over short and long time scales. *Ecol. Monogr.* 69, 465–490. doi: 10.1890/0012-9615(1999)069[0465:CRCIAI]2.0.CO;2

Sapper, S. A., and Murray, S. N. (2003). Variation in structure of the subcanopy assemblage associated with southern California populations of the intertidal rockweed *Silvetia compressa* (Fucales). *Pacific Sci.* 57, 433–462. doi: 10.1353/psc.2003.0035

Sarà, G., Giommi, C., Giacoletti, A., Conti, E., Mulder, C., and Mangano, M. C. (2021). Multiple climate-driven cascading ecosystem effects after the loss of a foundation species. *Sci. total Environ.* 770, 144749. doi: 10.1016/j.scitotenv.2020.144749

SAS Institute Inc. (2018). *SAS Software, Copyright, SAS Institute Inc. SAS and all other SAS Institute Inc. product or service names are registered trademarks or trademarks of SAS Institute Inc.* (Cary, NC, USA).

Schiel, D. R., and Foster, M. S. (2006). The population biology of large brown seaweeds: ecological consequences of multiphase life histories in dynamic coastal environments. *Annu. Rev. Ecology Evolution Systematics* 37, 343–372. doi: 10.1146/annurev.ecolsys.37.091305.110251

Schmidt, A. L., Coll, M., Romanuk, T., and Lotze, H. K. (2011). Ecosystem structure and services in eelgrass *Zostera marina* and rockweed *Ascophyllum nodosum* habitats. *Mar. Ecol. Prog. Ser.* 437, 51–68. doi: 10.3354/meps09276

Schoch, G. C., and Dethier, M. N. (1996). Scaling up: The statistical linkage between organismal abundance and geomorphology on rocky intertidal shorelines. *J. Exp. Mar. Biol. Ecol.* 201, 37–72. doi: 10.1016/0022-0981(95)00167-0

Schonbeck, M., and Norton, T. A. (1978). Factors controlling the upper limits of fucoid algae on the shore. *J. Exp. Mar. Biol. Ecol.* 31 (3), 303–313. doi: 10.1016/0022-0981(78)90065-5

Schonbeck, M. W., and Norton, T. A. (1980). Factors controlling the lower limits of fucoid algae on the shore. *J. Exp. Mar. Biol. Ecol.* 43, 131–150. doi: 10.1016/0022-0981(80)90021-0

Schwarz, G. (1978). Estimating the dimension of a model. *Ann. Stat* 6 (2), 461–464.

Seapy, R. R., and Hoppe, W. J. (1973). Morphological and behavioral adaptations to desiccation in the intertidal limpet *Acmaea* (*Collisella*) *strigatella*. *Veliger* 16 (2), 181–188.

Seapy, R. R., and Littler, M. M. (1982). Population and species diversity fluctuations in a rocky intertidal community relative to severe aerial exposure and sediment burial. *Mar. Biol.* 71, 87–96. doi: 10.1007/BF00396995

Short, F. T., Koch, E. W., Creed, J. C., Magalhães, K. M., Fernandez, E., and Gaeckle, J. L. (2006). SeagrassNet monitoring across the Americas: case studies of seagrass decline. *Mar. Ecol.* 27, 277–289. doi: 10.1111/j.1439-0485.2006.00095.x

Sideman, E. J., and Mathieson, A. C. (1985). Morphological variation within and between natural populations of non-tide pool *Fucus distichus* (Phaeophyta) in New England. *J. Phycology* 21, 250–257. doi: 10.1111/j.0022-3646.1985.00250.x

Silva, P. C., Pedroche, F. F., Chacana, M. E., Aguilar-Rosas, R., Aguilar-Rosas, L. E., and Raum, J. (2004). Geographic correlation of morphological and molecular variation in *Silvetia compressa* (Fucaceae, Fucales, Phaeophyceae). *Phycologia* 43, 204–214. doi: 10.2216/i0031-8884-43-2-204.1

Skamarock, W. C., and Klemp, J. B. (2008). A time-split nonhydrostatic atmospheric model for weather research and forecasting applications. *J. Comput. Phys.* 227 (7), 3465–3485. doi: 10.1016/j.jcp.2007.01.037

Skamarock, W. C., Klemp, J. B., Dudhia, J., Gill, D. O., Barker, D., Duda, M. G., et al. (2008). *A description of the advanced research WRF version 3. NCAR Tech. Note NCAR/TN-475+STR* (University Corporation for Atmospheric Research), 113. doi: 10.5065/D68S4MVH

Smale, D. A., Teagle, H., Hawkins, S. J., Jenkins, H. L., Frontier, N., Wilding, C., et al. (2022). Climate-driven substitution of foundation species causes breakdown of a facilitation cascade with potential implications for higher trophic levels. *J. Ecol.* 110 (9), 2132–2144. doi: 10.1111/1365-2745.13936

Smithson, M., and Verkuilen, J. (2006). A better lemon squeezer? Maximum-likelihood regression with beta-distributed dependent variables. *psychol. Methods* 11 (1), 54. doi: 10.1037/1082-989X.11.1.54

Steinberg, P. D. (1985). Feeding preferences of *Tegula funebralis* and chemical defenses of marine brown algae. *Ecol. Monogr.* 55, 333–349. doi: 10.2307/1942581

Steneck, R. S., Graham, M. H., Bourque, B. J., Corbett, D., Erlandson, J. M., Estes, J. A., et al. (2002). Kelp forest ecosystems: biodiversity, stability, resilience and future. *Environ. Conserv.* 29, 436–459. doi: 10.1017/S0376892902000322

Stengel, D. B., and Dring, M. J. (1998). Seasonal variation in the pigment content and photosynthesis of different thallus regions of *Ascophyllum nodosum* (Fucales, Phaeophyta) in relation to position in the canopy. *Phycologia* 37, 259–268. doi: 10.2216/i0031-8884-37-4-259.1

Tait, L. W., Hawes, I., and Schiel, D. R. (2014). Shining light on benthic macroalgae: Mechanisms of complementarity in layered macroalgal assemblages. *PloS One* 9 (12), e114146. doi: 10.1371/journal.pone.0114146

Tait, L. W., and Schiel, D. R. (2010). Primary productivity of intertidal macroalgal assemblages: Comparison of laboratory and in *situ* photorespirometry. *Mar. Ecol. Prog. Ser.* 416, 115–125. doi: 10.3354/meps08781

Thompson, R. C., Crowe, T. P., and Hawkins, S. J. (2002). Rocky intertidal communities: Past environmental changes, present status and predictions for the next 25 years. *Environ. Conserv.* 29, 168–191. doi: 10.1017/S0376892902000115

Tilman, D., and Kareiva, P. (Eds.) (1997). *Spatial Ecology: The role of space in population dynamics and interspecific interactions (MPB-30)* (Princeton, New Jersey: Princeton University Press). Available at: http://www.jstor.org/stable/j.ctv36zpzm.

Torn, K., Krause-Jensen, D., and Martin, G. (2006). Present and past depth distribution of bladderwrack (*Fucus vesiculosus*) in the Baltic Sea. *Aquat. Bot.* 84, 53–62. doi: 10.1016/j.aquabot.2005.07.011

Ugarte, R. A., Critchley, A., Serdynska, A. R., and Deveau, J. P. (2009). Changes in composition of rockweed (*Ascophyllum nodosum*) beds due to possible recent increase in sea temperature in eastern Canada. *J. Appl. Phycology* 21, 591–598. doi: 10.1007/s10811-008-9397-2

Vadas, R. L., Wright, W. A., and Miller, S. L. (1990). Recruitment of *Ascophyllum nodosum*: wave action as a source of mortality. *Mar. Ecol. Prog. Ser.* 61, 263–272. doi: 10.3354/meps061263

Viejo, R. M., Cervin, G., and Lindegarth, M. (1999). The interactive effects of adult canopy, germling density and grazing on germling survival of the rockweed *Ascophyllum nodosum*. *Mar. Ecol. Prog. Ser.* 187, 113–120.

Vogt, H., and Schramm, W. (1991). Conspicuous decline of *Fucus* in Kiel Bay (western Baltic): What are the causes? *Mar. Ecol. Prog. Ser.* 69, 189–194. doi: 10.3354/meps069189

Wernberg, T., Russell, B. D., Thomsen, M. S., Gurgel, C. F. D., Bradshaw, C. J. A., Poloczanska, E. S., et al. (2011). Seaweed communities in retreat from ocean warming. *Curr. Biol.* 21, 1828–1832. doi: 10.1016/j.cub.2011.09.028

Wernberg, T., Thomsen, M. S., Baum, J. K., Bishop, M. J., Bruno, J. F., Coleman, M. A., et al. (2023). Impacts of climate change on marine foundation species. *Annu. Rev. Mar. Sci.* 16, 247–282. doi: 10.1146/annurev-marine-042023-093037

Whitaker, S. G., Ambrose, R. F., Anderson, L. M., Fales, R. J., Smith, J. R., Sutton, S., et al. (2023). Ecological restoration using intertidal foundation species: Considerations and potential for rockweed restoration. *Ecosphere* 14 (3), e4411. doi: 10.1002/ecs2.4411

Wood, S. N. (2011). Fast stable restricted maximum likelihood and marginal likelihood estimation of semiparametric Generalized Linear Models. *J. R. Stat. Soc. Ser. B Stat. Method.* 73 (1), 3–36. doi: 10.1111/j.1467-9868.2010.00749.x

Wootton, J. T., Power, M. E., Paine, R. T., and Pfister, C. A. (1996). Effects of productivity, consumers, competitors, and El Niño events on food chain patterns in a rocky intertidal community. *Proc. Natl. Acad. Sci. U. S. A.* 93 (24), 13855–13858. doi: 10.1073/pnas.93.24.13855

Yue, X., Mickley, L. J., and Logan, J. A. (2014). Projection of wildfire activity in southern California in the mid-twenty-first century. *Climate dynamics* 43, 1973–1991. doi: 10.1007/s00382-013-2022-3

Zedler, J. B., Callaway, J. C., and Sullivan, G. (2001). Declining biodiversity: Why species matter and how their functions might be restored in Californian tidal marshes: Biodiversity was declining before our eyes, but it took regional censuses to recognize the problem, long-term monitoring to identify the causes, and experimental plantings to show why the loss of species matters and which restoration strategies might reestablish species. *BioScience* 51, 1005–1017. doi: 10.1641/0006-3568(2001)051[1005:DBWSMA]2.0.CO;2

Zuur, A. F., Ieno, E. N., and Elphick, C. S. (2010). A protocol for data exploration to avoid common statistical problems. *Methods Ecol. Evol.* 1, 3–14. doi: 10.1111/j.2041-210X.2009.00001.x

Frontiers in Ecology and Evolution

TYPE Original Research
PUBLISHED 27 February 2024
DOI 10.3389/fevo.2024.1182021

EDITED BY
Robert Klinger,
United States Department of the Interior,
United States

REVIEWED BY
Roderick Gagne,
University of Pennsylvania, United States
Kristine Moody,
Oak Ridge National Laboratory (DOE),
United States

*CORRESPONDENCE
Ralph W. Tingley III
rtingley@usgs.gov

†PRESENT ADDRESS
Ralph W. Tingley III,
USGS Great Lakes Science Center,
Ann Arbor, MI, United States

RECEIVED 08 March 2023
ACCEPTED 01 February 2024
PUBLISHED 27 February 2024

CITATION
Tingley RW III, Infante DM, MacKenzie RA, Strauch AM, Foulk PB and Roth B (2024) Climate-driven differences in flow regimes alter tropical freshwater ecosystems with consequences for an endemic shrimp. *Front. Ecol. Evol.* 12:1182021. doi: 10.3389/fevo.2024.1182021

Climate-driven differences in flow regimes alter tropical freshwater ecosystems with consequences for an endemic shrimp

Ralph W. Tingley III[1*†], Dana M. Infante[1], Richard A. MacKenzie[2], Ayron M. Strauch[3], Patra B. Foulk[2] and Brian Roth[1]

[1]Department of Fisheries and Wildlife, Michigan State University, East Lansing, MI, United States, [2]United States Department of Agriculture (USDA) Forest Service, Pacific Southwest Research Center, Institute of Pacific Islands Forestry, Hilo, HI, United States, [3]University of Hawaii at Manoa, Department of Natural Resources and Environmental Management, Honolulu, HI, United States

Climate-driven shifts in the natural flow regime can threaten species persistence in stream systems, and anticipating such shifts before they occur is critical for conservation. We can explore how climate change may impact biota by examining natural systems that differ in terms of climate yet are similar in terms of other landscape features such as geology, size, and elevation. Across an established precipitation and hydrologic gradient on the east coast of Hawaii Island, we sampled stream habitat and populations of the endemic migratory mountain shrimp *Atyoida bisulcata* over three years and examined how habitat as well as population metrics and individual condition respond to differences in stream flow. Along the precipitation gradient, baseflow declined and streams shifted from run/riffle systems with moss cover to those with predominately pools and limited available habitat. Across years, baseflow conditions were relatively consistent within streams while measures of stream flow stability and the duration of high flows were more variable. Streams with high and persistent baseflow had greater atyid biomass density with larger individuals less prone to disease. Within-stream interannual variation in baseflow was low relative to differences across streams, and most *A. bisulcata* metrics also had low within-stream interannual variability, making average baseflow an appropriate surrogate for differences in suitability. However, extremes in annual rainfall may result in high variability in *A. bisulcata* metrics within a single stream due to seasonal drying or persistent high flows, highlighting the importance of long-term monitoring to fully understand population responses to climate-mediated stream flow. Our study suggests that changes in rainfall patterns will alter stream flow and may ultimately negatively influence tropical stream organisms.

KEYWORDS

climate change, Hawaii, *Atyoida bisulcata*, stream habitat, flow regime, rainfall, variability

1 Introduction

Aspects of stream flow influence aquatic biota by shaping the availability and quality of habitat (Poff et al., 1997). Many stream organisms are adapted to characteristics of natural flow regimes, and changes in flow outside the existing range of variability can have negative ecological consequences. Reductions in flow magnitude and increases in duration or frequency of low-flow events can, for example, reduce physical habitat and alter other physico-chemical conditions. Such changes can stress organisms and limit growth (Rolls et al., 2012) or result in unsuitable habitat (Canton et al., 1984). High flows can also act as a trigger for spawning or larval hatching (Naesje et al., 1995; Lytle and Poff, 2004), and changes in the magnitude or timing of high flow can negatively impact reproductive success. Conversely, increased frequency of floods can result in a temporary loss of species not adapted to high flows (e.g., Meffe and Minckley, 1987). The rate of change of stream flow can also affect organisms, stranding individuals in suboptimal habitats following quick flow recessions or flushing them downstream during freshets (e.g., Cushman, 1985; Bradford, 1997; Davey et al., 2006). Understanding what aspects of the stream flow regime influence species or populations is critical for their conservation, especially given anticipated impacts of climate change on stream flow via changes in rainfall timing and magnitude.

Alterations to the natural stream flow regime are a primary pathway through which climate change impacts stream species. For example, warmer air temperatures have increased winter and spring discharges and reduced summer flows in snowmelt-driven streams of the western United States (Leppi et al., 2012; Zeigler et al., 2012), limiting habitat for at-risk species like cutthroat trout (Isaak et al., 2012). In the Pacific Northwest, more frequent rainstorms and greater winter flow variability have been linked to reduced Chinook salmon reproduction (Ward et al., 2015). In the Rio Grande, warmer air temperatures have reduced spring discharges and increased interspecific competition among early life stages of stream fishes (Krabbenhoft et al., 2014). Collectively, such studies show clear widespread change that can inform future conservation action, but knowledge is missing for many regions and species. For example, documented effects of climate change on freshwater species are limited in tropical low-latitude ecosystems despite tropical species having potentially lower adaptive capacity (Comte et al., 2013; Myers et al., 2017; Krabbenhoft et al., 2020).

The lack of information on climate change impacts on tropical stream organisms is problematic for several reasons. First, seasonally- and regionally-specific changes in the timing and magnitude of rainfall are projected throughout the tropics (IPCC, 2013), altering flow regimes and threatening endemic species (Leong et al., 2014). Organisms that inhabit tropical island streams may be particularly vulnerable to such changes, as many streams require substantial rainfall to maintain baseflow (Craig, 2003). Additionally, many endemic tropical island stream species complete amphidromous life histories where larvae hatch in streams and drift downstream to the marine environment before migrating back upstream after the larval stage (Keith, 2003; Nishimoto and Fitzsimons, 2006; McDowall, 2007; Bauer, 2013). Reductions in streamflow can reduce or stall larval drift and slow or stop juvenile migration upstream (Gorbach et al., 2012; Walter et al., 2012; Leong et al., 2014). Further, stream flow reductions may reduce individual condition and growth by changing food availability (James et al., 2007). Thus, climate-driven changes in stream flow within tropical island systems could negatively impact populations.

The Hawaiian Islands are home to an endemic assemblage of amphidromous fish, shrimp and snails that are potentially threatened by climate change, including the atyid shrimp *Atyoida bisulcata*. *Atyoida bisulcata* can traverse most waterfalls and are found in many headwater streams, but they have been negatively impacted by widespread flow fragmentation and landscape degradation (Brasher, 2003). Climate-driven changes in flow are expected to further threaten these organisms through several mechanistic pathways. Like other amphidromous species, *Atyoida bisulcata* exist as a series of local populations within a larger metapopulation connected by mixing during the marine larval stage (Chubb et al., 1998; McRae, 2007). Reductions in baseflow may eliminate suitable juvenile and adult stream habitat and lower the likelihood of larval transport to the marine environment, making formally productive streams unsuitable. Sub-lethal effects also have the potential to influence individual condition and ultimately reproductive capacity. For example, lower baseflow and associated reductions in fine particulate organic matter (FPOM) as well as shifts from riffle/run to pool-dominated systems may reduce foraging opportunities for *Atyoida bisulcata*, which select for high velocity areas to filter feed and graze (Couret, 1976; Brasher, 1997). Diseases associated with less suitable habitats may also become more common, such as the chitinoclastic bacterial infection "brown spot disease" that is hypothesized to be the result of increased abrasion on *Atyoida bisulcata* exoskeletons in turbid high flow environments (Chan, 1978). Paired with climate change projections, increasing our understanding of the specific impacts of shifts in the stream flow regime on *Atyoida bisulcata* can improve our ability to project how individual local populations will be impacted in the upcoming decades.

The goal of our study was to examine how changes in the stream flow regime associated with lower rainfall influence *Atyoida bisulcata*. Using an established hydrologic and rainfall gradient, we tested the hypothesis that lower baseflow reduces *Atyoida bisulcata* habitat, population size, and individual condition. We predicted that lower baseflow would be associated with limited suitable habitat, lower population size and decreased individual condition. Our results can provide insight into the impact of climate change on runoff-driven stream ecosystems of Hawaii.

2 Materials and methods

2.1 Study area

Our study area occurs across the North Hilo coast of Hawaii Island where over a linear distance of less than 30 km, mean annual rainfall ranges from approximately 3,000 to 7,000 mm/year (Giambelluca et al., 2013; Figure 1). We evaluated 11 first- and second-order stream reaches between 400 and 510 m in elevation and bounded by waterfalls (Strauch et al., 2015). Study area catchments have minimal urban and agricultural land use, are composed primarily of mixed native and non-native forests (Price et al., 2012) and drain land on porous volcanic geology (Sherrod et al., 2008). Stream reaches at this elevation are inhabited by *A. bisulcata* and are above barrier waterfalls for most other amphidromous species (Tingley et al., 2019). Previous research in this study system indicates that stream flow is heavily dependent on precipitation, with baseflow positively correlated and flow variability negatively correlated with effective mean annual rainfall (rainfall below catchment elevations of 1,830 m; Strauch et al., 2015; Frauendorf et al., 2020). In turn, lower baseflow has been shown to reduce the quantity of FPOM available and the quality of food resources in a subset of these streams (i.e., shifts to leaf litter dominated systems; Frauendorf et al., 2019, 2020).

2.2 Data collection and processing

2.2.1 Stream flow data and the generation and selection of metrics

We obtained daily stream flow records for 2012, 2013, and 2014 water years from multiple sources. For a single study reach we downloaded data from the USGS National Water Information System (https://waterdata.usgs.gov/usa/nwis/16717000). For all other reaches, we averaged daily stream flow from 15-min interval instantaneous data collected at gaging stations installed between spring of 2011 and fall of 2012 (Strauch et al., 2015). In three study reaches we supplemented gaps in daily stream flow using a Distributed Hydrology Soil Vegetation Model for the North Hilo coast (DHSVM; Strauch et al., 2016).

We conducted a multi-step process to select a small number of minimally redundant flow metrics that vary across the study region and may influence available habitat and *A. bisulcata* populations. We first calculated all flow metrics available from the USGS

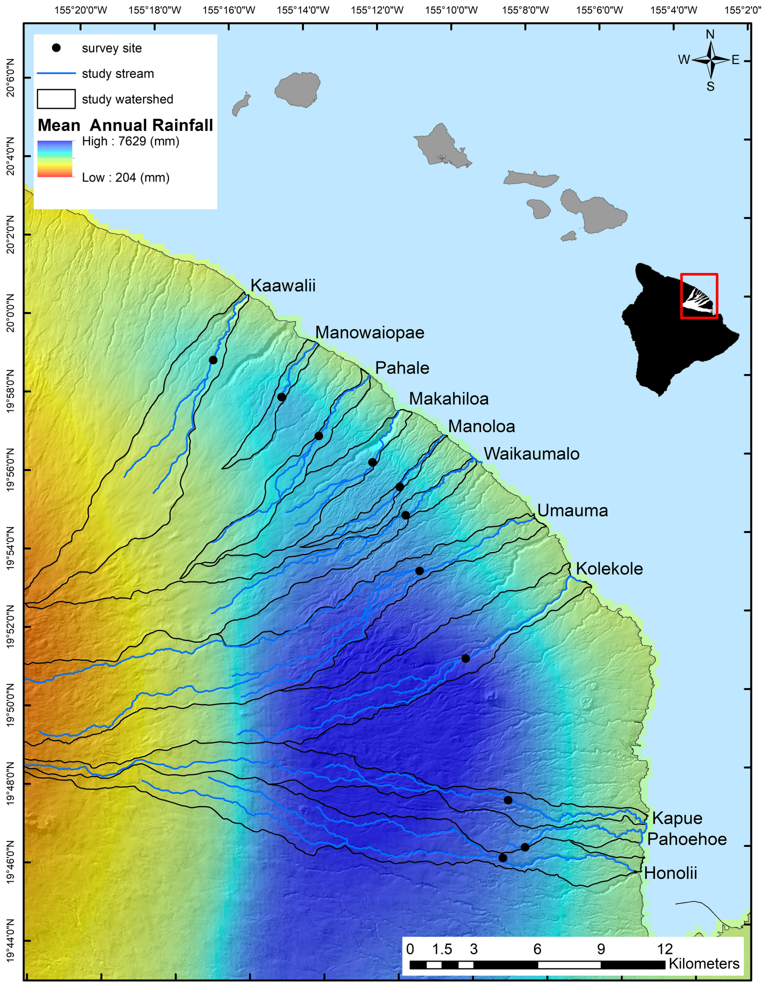

FIGURE 1
North Hilo coast of Hawaii Island and locations of study reaches along a gradient in mean annual rainfall. Study stream names are adjacent to their respective watersheds.

Hydrologic Index Tool (HIT; Henriksen et al., 2006) for the seven-month period (October – April) prior to the sample season (May-September). Next, we selected seven HIT metrics, one to two that were minimally redundant within each aspect of the flow regime (i.e., magnitude, duration, timing, frequency, rate of change; Poff et al., 1997), that are relevant to the flashy streams along the North Hilo coast (Supplementary Material Tables S1, S2). Metrics describing frequency of flow events included measures of low flow (total number of flow events below 5% of mean flow) and high flow (total number of flow events greater than the 25th percentile exceedance). Duration metrics included the mean length in days of high flows and the minimum 7-day mean flow normalized by effective catchment area. Timing was represented by the constancy of flow, or the stability in day-to-day stream flows over the study period, while rate of change was represented by the average rise rate of days with increased flow normalized by catchment area. Metrics describing flow magnitude included the coefficient of variability in daily flow and an additional metric calculated independently of the HIT tool; the 70th percentile exceedance value. Oki et al. (2010) found that the 70th percentile exceedance value is broadly representative of baseflow conditions in Hawaiian streams and we normalized it by effective catchment area to characterize potential differences across our study reaches.

Next, we used principal components analysis (PCA) to determine whether composite variables were useful for describing aspects of the flow regime across streams and years. The 70th percentile exceedance value (hereafter $Q_{70}Y$) and the minimum 7-day mean flow (hereafter DLY) were log-transformed to improve linearity, and all flow variables were centered and scaled. We performed a varimax rotation to increase interpretability, with variable loadings >0.6 on the rotated axes considered to be heavily weighted and representative of the principal component (PC). The first three PCs accounted for 84% of the total variation in the dataset and were retained for interpretation (Supplementary Material Table S3). The constancy of stream flow was positively associated with the first principal component (PC1; 51% variance explained) while rise rate normalized by catchment area, the frequency low flow events and the coefficient of variation in flow were negatively associated with the axis, suggestive of a gradient in flow stability ranging from stable conditions with few extreme flow events to flashy systems with many low flows events. Log-transformed DLY and $Q_{70}Y$ were strongly associated with PC2 (23% variance explained) while the duration of high flows (hereafter DH) and frequency of high flows were strongly associated with the third PC (10% variation explained). Given the results of the PCA, we chose to include three metrics that broadly reflect differences in the stream flow regime in further analysis: the composite PC representative of flow stability (PC1), $Q_{70}Y$ and DH. We chose to use the flow metrics $Q_{70}Y$ and DH because they contributed little to PC1 but were one of two metrics associated with the second and third PC, respectively. As expected, log-transformed $Q_{70}Y$ had a strong positive correlation with mean annual rainfall in each study season (r= 0.88, 0.93, 0.84), while DH (r = 0.20, 0.38, -0.33) and PC1 (r=-0.04, 0.05, 0.56) were variable in strength and direction of correlation (Supplementary Material Figure S1). PC1 had the lowest values (suggestive of unstable flow regimes) in streams with moderate levels of mean annual rainfall while DH did not show a clear relationship with mean annual rainfall (Supplementary Material Figure S1).

2.2.2 Stream reach abiotic and biotic data collection

We established study reach lengths equal to 20 times mean stream width (MSW) to capture a representative sample of habitat and biology (Kido, 2008, 2013). Transects lines were established once every MSW over study reaches. In a few instances, we truncated study reaches by up to 2 MSW due to limited length between unsurpassable upstream and downstream waterfalls.

In all sample years we estimated percent substrate, geomorphic units and channel dimensions to understand how habitat quality and quantity changes with stream flow and to infer potential drivers associated with changes in *A. bisulcata* metrics. Moving upstream, two researchers recorded the percent (± 5%) of substrate categories comprising the stream reach including silt, sand, gravel, cobble, boulder and bedrock (following Higashi and Nishimoto, 2007). Mean substrate size was calculated by multiplying the average percent substrate within a reach across transects by geometric mean of particle size range, with bedrock set to 5,656 mm (Kaufmann and Robinson, 1998). Percent of geomorphic units (e.g, pool, riffle, run) within 1 m of the transect line were visually estimated and averaged over the study reach (Higashi and Nishimoto, 2007). Wetted width was measured to the nearest 0.1 m, and maximum water depth along the transect line was measured to the nearest 0.01 m. Average wetted transect area was calculated by multiplying transect wetted width by one-half of maximum depth and averaging across transects (Knighton, 1998). In 2013 and 2014, we visually estimated the average percent (± 5%) substrate covered by aquatic moss and filamentous algae within 1 m of the transect line over the study reach. Aquatic moss is not a food resource for *A. bisulcata* (Riney, 2015) but it may act as high-quality habitat that traps FPOM and contains high levels of epiphytic microalgae, increasing foraging opportunities for grazers (Maurer and Brusven, 1983; Brusven et al., 1990; Bowden and Stream Bryophyte Group, 1999). Shifts to algal-dominated systems represents a potential reduction in available food for *A. bisulcata* (Riney, 2015).

We sampled *A. bisulcata* each year, approaching each transect from downstream with a hand seine net (2 mm mesh; 0.91 m wide; 0.45 m deep) and completing a single pass along the transect line. Individual transects were excluded if they were not able to be sampled effectively (e.g., debris in the transect, dry stream beds due to seasonal drought). The total numbers of *A. bisulcata* collected from each transect were recorded, and a subsample of all individuals were kept for further analysis (typically 75-125 individuals). In some sampling events, few atyids were captured and entire samples were processed. Given low samples sizes in some study reaches, we also collected individuals from the nearest plunge pool upstream to supplement analyses of individual condition. Plunge pools (>~2 m in depth) occurred below waterfalls and were not sampleable using our standard transect design. We seined 1 m^2 areas at 2 m intervals along the diameter of the pool to supplement our collection of individuals from the study reach. We included supplemental individuals from plunge pools only in streams with low rainfall (Supplementary Material Table S4). Based on the near absence of *A. bisulcata* from the study reach in these low rainfall streams, we assumed individuals collected from these plunge pools were representative of the stream population and individual condition could be compared to atyids subsampled from the entire reach in wetter systems.

We measured the post-orbital carapace (POC) length of atyids (i.e., the linear distance from the posterior of the ocular cavity to the posterior of the carapace) to the nearest 0.1 mm using an ocular micrometer and recorded individual wet weights to the nearest 0.001 g. Sex was determined based on shape of the endopod of the first pleopod and the presence of the *appendix masculina* on males (Couret, 1976; Chace, 1983). We recorded small specimens as juveniles if they did not show characteristics associated with either sex. In 2013 and 2014, we also inspected individuals for brown spot disease. We dried specimens at 60-105°C for at least 24 hours, reweighed, then combusted them at 500°C in a muffle furnace for at least 2.5 hours to obtain ash-free dry mass (AFDM; Benke et al., 1999). In a single stream in 2013, AFDM measurements were not available and were derived from dry weights. We calculated the average relative mass from length-mass relationships for each reach each year using the linear form of the basic length-mass model:

$$\log_{10} \mathrm{M} = \log a + b \log \mathrm{L}$$

where M is mass (AFDM; g), L is length (POC length; mm) and a and b are constants (Benke et al., 1999). Geometric means of a and b (a_m and b_m, respectively) were calculated from length-mass regressions from each reach each year (Froese, 2006). We calculated the relative mass (M_{rm}) of each individual as:

$$M_{rm} = 100 \frac{M}{a_m L^{b_m}}$$

We calculated average biomass (g/m^2) by finding the proportion of individuals in 0.5 mm POC length-classes in each reach each year. Abundance counts were multiplied by the size-class proportions to estimate the number of individuals within each 0.5 mm size-class at each transect (Cross et al., 2008). Length-mass regressions were used to predict an average AFDM for each size-class, which was multiplied by the size-class counts and summed then divided by wetted width to estimate biomass density at each transect.

We included three metrics of individual condition: POC length, presence of brown spot disease and percent relative mass (Froese, 2006). Females were excluded in calculation of POC length due to their low representation in samples and evidence of size stratification by sex. Females and juveniles were also excluded during analysis of brown spot disease presence and percent relative mass. Disease detection bias can result from post-egg release molting in females or high molting rates in juveniles (Couret, 1976; Chan, 1978; Nishimoto and Kuamo'o, 1996) while percent relative mass may be biased by differences in body shape among life stages and sexes as well as post-egg release declines (Froese, 2006). In two sampling events, low sample sizes restricted the calculation of average relative mass.

2.3 Data analysis

We tested for the effects of Q_{70}Y on the percent pools, percent riffles and wetted area averaged across each transect using the linear model:

$$H = ln(Q_{70}Y) + DA + Year + (1|Stream)$$

where DA is effective drainage area. We chose to use an average value of Q_{70}Y across years for each stream, as interannual variation in baseflow was relatively low within streams across our model system. Mean differences across years were tested using the difflsmeans function in R package lmerTest (Kuznetsova et al., 2017). For mean substrate size, percent algal cover and percent moss cover, we used the linear model:

$$H = ln(Q_{70}Y) * PC1 + DA + Year + (1|Stream)$$

which included the composite metric PC1 as flow stability likely influences the growth and retention of moss and algae and the movement of substrate within the stream channel.

We developed candidate models and used Akaike's Information Criterion (AIC) to determine which flow metrics, or interactions among them, explain the most variation in *A. bisulcata* populations and individual condition metrics (A). For biomass density, POC length and percent relative mass, we developed 6 models (Equations 1–6):

$$A = DA + Year + (1|Stream) \tag{1}$$

$$A = ln(Q_{70}Y) + DA + Year + (1|Stream) \tag{2}$$

$$A = PC1 + DA + Year + (1|Stream) \tag{3}$$

$$A = DH + DA + Year + (1|Stream) \tag{4}$$

$$A = ln(Q_{70}Y) * PC1 + DA + Year + (1|Stream) \tag{5}$$

$$A = ln(Q_{70}Y) * DH + DA + Year + (1|Stream) \tag{6}$$

with Model 1 as the null model. We included Year as a fixed term instead of a fully crossed random design because the number of factor levels (years) was less than five (Harrison et al., 2018). For models of atyid biomass density, we altered the random intercept term to allow transect estimates of biomass to be nested within streams (1|Stream/Transect). For percent relative mass we included 6 additional models (Equations 7–11):

$$A = ln(Q_{70}Y) * Year + DA + (1|Stream) \tag{7}$$

$$A = PC1 * Year + DA + (1|Stream) \tag{8}$$

$$A = DH * Year + DA + (1|Stream) \tag{9}$$

$$A = ln(Q_{70}Y) * PC1 * Year + DA + (1|Stream) \tag{10}$$

$$A = ln(Q_{70}Y) * DH * Year + DA + (1|Stream) \tag{11}$$

where we let the Year term interact with flow metrics after visually assessing differences in trends across sample years. We modeled atyid biomass, POC length and percent relative mass using a linear mixed model (LMM; lmer function, R package lme4; Bates et al., 2015) and used a generalized linear mixed model (GLMM; glmer function, R package lme4) assuming a binomial error distribution (logit link) for brown spot disease. Prior to analysis, we added a small amount (0.0001 g/m^2) to biomass density estimates and log-transformed to improve normality. We examined LMM residuals for deviations from normality prior to model interpretation. We considered all models<2 ΔAIC as "top-ranked" models with equivalent empirical support and interpreted predictors from the simplest top-ranked model for each *A. bisulcata* metric. We calculated intraclass correlation coefficients (ICC) to quantify the proportion of variation explained by grouping variables (stream, transect) and marginal and conditional R^2 to assess the relative contribution of fixed and random effects to variance explained (tab_model function, R package sjPlot; Nakagawa and Schielzeth, 2013).

3 Results

Associations between log-transformed $Q_{70}Y$ and habitat metrics indicate that habitat quality was highest in streams with the greatest mean annual rainfall and generally increased with baseflow (Supplementary Material Table S5). Wetted area (p=0.02), percent riffle habitat (p<0.01) and percent moss cover (p = 0.01) were positively associated with $Q_{70}Y$, while the percent of pool habitat decreased with greater values of $Q_{70}Y$ (p<0.01; Table 1). Wetted area was greater in 2012 than in 2013 (p=0.03) and 2014 (p=0.03), while the percent of pool habitat was lower in 2013 (p<0.01) and 2014 (p=0.01). The initial model of percent algal cover was singular and after removal of the grouping term there were no significant associations with predictor variables. Mean substrate size was significantly positively associated drainage area (p<0.01) and was not significantly associated with changes in stream flow stability or baseflow, but the interaction term was significant (p=0.02).

Mean biomass density (range 0.000 – 0.824 g/m^2), POC length (3.3 – 7.4 mm) and relative mass (68.5 – 120.1%) estimates were

TABLE 1 Parameter estimates, mariginal/conditional R^2 values, and intraclass correlation coefficients (ICC) for habitat metrics averaged across transects for each sampling event modeled by differences in the natural log of the 70th percentile exceedance of annual flow ($Q_{70}Y$) normalized by effective drainage area (DA).

	Riffle (%)		Pool (%)		Wetted area (m^2)	
	Estimate	CI	Estimate	CI	Estimate	CI
Intercept	9.24**	4.26 – 14.21	34.57**	20.33 – 48.80	2.11**	0.77 – 3.46
ln($Q_{70}Y$)	4.2**	2.50 – 5.90	-12.04**	-17.75 – -6.34	0.72*	0.12 – 1.32
DA	-1	-4.71 – 2.71	-6.16	-18.64 – 6.32	1.31*	0.00 – 2.63
2013	1.27	-4.38 – 6.93	13.18**	1.77 – 24.59	-0.68*	-1.04 – -0.32
2014	1.45	-4.20 – 7.11	12.91*	1.50 – 24.32	-0.47*	-0.83 – -0.11
PC1						
ln($Q_{70}Y$) × PC1						
ICC	0.32		0.66		0.96	
Marginal R^2/Conditional R^2	0.592/0.724		0.591/0.859		0.452/0.978	

Predictor	Substrate size (mm)		Algal cover (%)		Moss cover (%)	
	Estimate	CI	Estimate	CI	Estimate	CI
Intercept	2299.82**	1826.10 – 2773.53	8.83**	3.95 – 13.72	7.94*	0.60 – 15.27
ln($Q_{70}Y$)	-126.53	-335.23 – 82.17	-1.23	-3.00 – 0.53	4.34*	1.07 – 7.61
DA	758.96**	306.08 – 1211.85	-2.8	-6.26 – 0.67	-2	-9.11 – 5.11
2013	48.64	-169.27 – 266.54				
2014	413.38**	187.79 – 638.97	3.47	-3.85 – 10.78	-1.48	-5.47 – 2.51
PC1	106.59	-35.84 – 249.02	-3.79	-8.93 – 1.35	0.65	-3.66 – 4.97
ln($Q_{70}Y$) × PC1	-92.29*	-166.53 – -18.04	-0.8	-3.08 – 1.48	0.19	-1.12 – 1.50
ICC	0.89				0.91	
Marginal R^2/Conditional R^2	0.623/0.958		0.436/NA		0.482/0.951	

A composite metric of flow stability (PC1) was included for models of percent moss cover, percent algal cover and substrate size. Parameter estimates are noted when P values are<0.05 (*) and<0.01 (**). Yearly estimates are relative to the first year of sampling (2012 or 2013) as represented by the intercept value.

generally higher in streams with greater mean annual rainfall across years while the prevalence of brown spot disease was lower (0.0 – 50.0%; Supplementary Material Table S4). Baseflow, as represented by log-transformed $Q_{70}Y$, was a predictor in all top-ranked models, and the null model ΔAIC was >2 for all *A. bisulcata* metrics (Supplementary Material Table S6). In all cases, the simplest top-ranked model had the lowest AIC value. Models 2 (ΔAIC = 0) and 5 (ΔAIC = 1.5) were the top-ranked models for *A. bisulcata* biomass density. Fixed effects in Model 2 accounted for ~66% of the variation explained by the overall model (Marginal R^2/Conditional R^2 = 0.570/0.874; Table 2), with biomass density positively associated with baseflow and drainage area (Figure 2A). Model 11 was the only top-ranked model for percent relative mass, with fixed effects accounting for 63% of the total variation explained (Marginal R^2/Conditional R^2 = 0.211/0.332). Percent relative mass was positively associated with baseflow and DH, but the relationship with baseflow was influenced by year (Figure 2B). In 2014, average relative mass within streams did not increase with baseflow and was higher across streams (107.99 ± 2.02 standard error; SE) than in 2012 and 2013 (94.5 ± 3.62 SE and 96.2 ± 2.81 SE respectively; Supplementary Material Table S4). Model 6 was the sole top-ranked model for post-orbital carapace length with *A. bisulcata* length positively associated with baseflow (Figure 2C). The interaction of baseflow with DH indicates the duration of high flows has a negative effect on average length when baseflow is low but has limited impact on average length when baseflow is high (Supplementary Material Figure S2). Models 2 (ΔAIC = 0) and 6 (ΔAIC = 1.9) were the top-ranked models for predicting brown spot disease infection but fixed effects explained only a small amount of variation (Model 2 Marginal R^2 = 0.117). The probability of brown spot disease was lower in streams with high baseflow and disease was most common in drier systems (Table 2, Figure 2D). Metrics of individual condition were less similar within groups than biomass density, which had ICC values at the stream and transect level >0.5.

4 Discussion

Our results demonstrate that tropical island stream organisms are vulnerable to climate change, especially in systems where stream baseflow is primarily controlled by rainfall. Across the study system, baseflow magnitude as well as the amount and quality of habitat declined with mean annual rainfall, while the driest streams had prolonged periods of baseflow close to zero. Our hypothesis, that declines in stream flow negatively influence *A. bisulcata* habitat, population size and individual condition, was supported. Low *A. bisulcata* biomass densities in streams with low baseflow and limited physical habitat suggests that seasonal habitat loss limits population establishment in drier systems. However, populations in larger catchments may be less vulnerable to the impacts of prolonged low baseflow. Individual size and condition also generally decline with baseflow and may be driven by changes in

TABLE 2 Parameter estimates, mariginal/conditional R^2 values, and intraclass correlation coefficients (ICC) for *Atyoida bisulcata* population and individual condition metrics modeled by differences in the natural log of the 70th percentile exceedance of annual flow ($Q_{70}Y$) normalized by drainage area (DA) and the duration of high flows (days; DH) from 2012-2014.

	Biomass (g/m²)		Relative mass (%)		Post-orbital carapace length (mm)		Likelihood of brown spot disease	
	Estimate	CI	Estimate	CI	Estimate	CI	Odds Ratios	CI
Intercept	-4.8	-5.96 – -3.64	94.23	89.76 – 98.69	5.65	5.29 – 6.00	0.09	0.05 – 0.15
$\ln(Q_{70}Y)$	1.31	0.79 – 1.83	2.93	0.95 – 4.91	0.27	0.11 – 0.43	0.68	0.52 – 0.88
DA	1.34	0.22 – 2.45	-0.61	-4.46 – 3.25	-0.08	-0.43 – 0.27	1.08	0.62 – 1.86
DH			4.06	1.11 – 7.01	-0.32	-0.36 – -0.28		
2013	-0.27	-0.55 – 0.01	-1.22	-3.85 – 1.42	0.26	0.19 – 0.33		
2014	-0.25	-0.53 – 0.03	17.06	13.36 – 20.76	-0.06	-0.13 – 0.01	1.02	0.74 – 1.41
$\ln(Q_{70}Y) \times$ DH			-0.88	-1.86 – 0.09	0.08	0.07 – 0.09		
$\ln(Q_{70}Y) \times$ 2013			0.05	-1.09 – 1.19				
$\ln(Q_{70}Y) \times$ 2014			-3.45	-4.76 – -2.14				
DH × 2013			2.94	-2.89 – 8.76				
DH × 2014			4.86	-1.64 – 11.36				
$\ln(Q_{70}Y) \times$ DH × 2013			-0.24	-2.51 – 2.04				
$\ln(Q_{70}Y) \times$ DH × 2014			-0.67	-2.55 – 1.22				
ICC Stream	0.76		0.15		0.34		0.16	
ICC Transect	0.56							
Marginal R^2/Conditional R^2	0.570/0.874		0.211/0.332		0.335/0.563		0.117/0.261	

Parameter estimates for years 2013 and 2014 are relative to 2012 as represented by the intercept value. Parameters are presented from the simplest candidate model with ΔAIC<2.

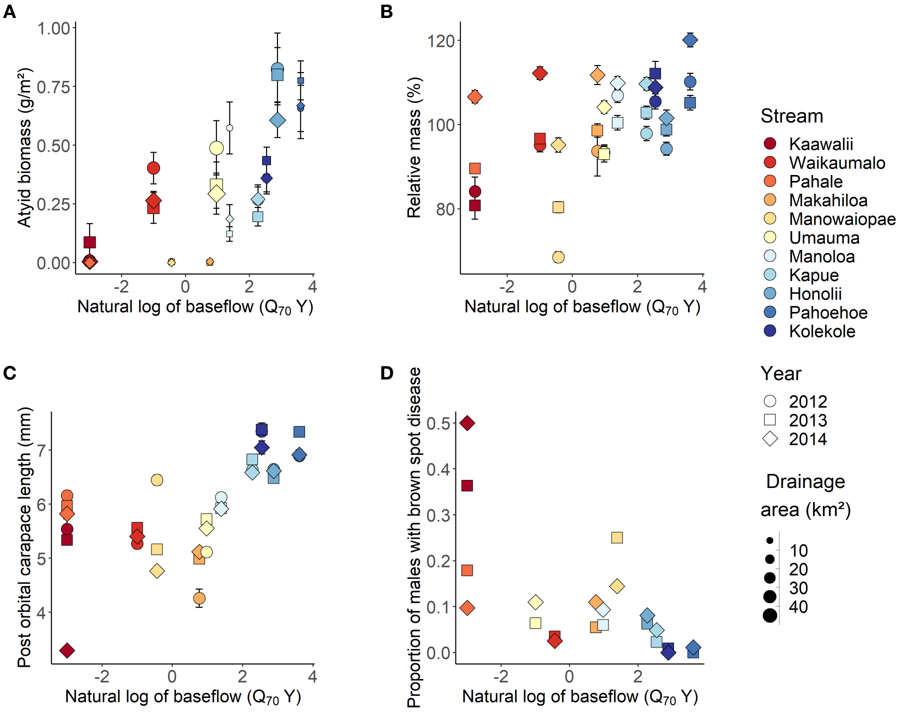

FIGURE 2
Atyoida bisulcata biomass density **(A)**, percent relative mass **(B)**, post orbital carapace length **(C)** and prevalence of brown spot disease **(D)** versus baseflow as represented by the natural log of the 70th percentile exceedance value ($Q_{70}Y$) of flow normalized by catchment area. The gradient in color represents differences in mean annual rainfall across study streams from lowest (dark red; Kaawalii stream) to highest (dark blue; Kolekole stream). Differences in drainage area size are represented by point size for biomass density only. Error bars are one standard error of the mean for transect values (biomass density) or individuals (percent relative mass, post orbital carapace length). Note that the sample size for the prevalance of brown spot disease in Kaawalii Stream in 2014 was only 2, while all other sample sizes were >10. See Supplementary Material Table S4 for additional information on sample size.

foraging opportunities as well as cyclical population loss and recolonization. Brown spot disease prevalence was lowest in streams with high baseflow and diverse habitats, and increased infection rates may indirectly be the result of higher turbidity and bacteria loads during high flow events in drier systems.

Changes in baseflow magnitude were associated with differences in the amount and type of physical stream habitat. This is not surprising, as baseflow changes stream habitat and reduces hydraulic habitat complexity (Rolls et al., 2012). In headwater streams of West Virginia, for example, low baseflow temporarily reduced riffle habitat within seven stream reaches by half but had no effect on total area of pools (Hakala and Hartman, 2004). The homogenization of habitat types in drier systems is apparent across our study area, with declines in baseflow coinciding with an increased prevalence of pools and the absence of riffles and runs. We also observed increases in the percent moss cover in streams with more stable and higher baseflow, which aligns with current understanding of flow controls on aquatic moss (Bowden and Stream Bryophyte Group, 1999). While our study design did not allow for hierarchical tests of stream flow on *A. bisulcata* through shifts in habitat, strong and consistent relationships between baseflow and habitat metrics suggests that *A. bisulcata* may be influenced in tandem by changes in the flow regime and habitat. Further research across a larger number of systems could provide more nuanced understanding of the hierarchical relationships between stream flow, habitat, and endemic fauna of Hawaiian streams.

Temporary loss of habitat may prevent the establishment of large *A. bisulcata* populations in streams with low rainfall. Prolonged periods of low flow can lead to temporary habitat desiccation, resulting in substantial loss of biomass within streams (Rolls et al., 2012). Stream macroinvertebrate communities can show trait-dependent threshold responses to increasing drought intensity, eventually resulting in population loss (Aspin et al., 2019). The driest (i.e., Kaawalii, Pahale) streams in our study system, which experience temporary cessation of stream flow in all study years, would likely be uninhabited by *A. bisulcata* if it were not for the presence of plunge pools below waterfalls (depth >~2 m). While these habitats encompass only a small amount of the entire channel in streams along the North Hilo Coast, they can act as semi-contained systems during low flows (McRae, 2007). Low flow river systems may therefore act as ecological “sinks” for the metapopulation of *A. bisulcata* and other migratory stream species, where larvae recruit during high flow events but have limited habitat capable of supporting juveniles and adults (McRae, 2007). While *A. bisulcata* in larger catchments appear to be more resilient to low baseflow due to an increase amount of instream habitat independent of plunge pools (i.e., Waikaumalo), these streams may still act as ecological sinks for the metapopulation. Larger catchment areas produce larger freshwater plumes, which attract more recruits from the nearshore environment (Nishimoto and Kuamoo, 1991). Large streams that are subject to prolonged low flows may attract high numbers of migratory organisms during high flow events. Cessation of flow could lead to population reductions or other limitations on productivity (i.e., fewer flow events that allow larval transport downstream, lower growth due to limited forage), which may result in an overall lower reproductive contribution to the metapopulation than smaller streams with sustained flow (McDowall, 2010). Quantifying the number of larvae transported to the marine environment across small and large catchments with differences in baseflow magnitudes could further test this hypothesis.

Variation in *A. bisulcata* biomass density estimates within individual sampling events was high, and standard errors often overlapped in streams with similar baseflows. This is not surprising, as macroinvertebrate density estimates are often highly variable and dependent on microhabitat selection (Rabeni, 1985; DiStefano et al., 2003). Because we saw such drastic variation in biomass density across the study region, we are still confident in observed differences in mean biomass resulting from reductions in suitable habitat. However, direct statistical comparisons of *A. bisulcata* biomass density between two streams with contrasting baseflow would be limited except for cases where differences in flow are extreme. Controlling for habitat in sample design could improve confidence in biomass estimates, but this proved difficult across our study system because of the drastic shifts in habitat (i.e., riffle-dominated to pool-dominated) and uncertainty in preferential habitat selection under different flow conditions. Increasing the number of transects sampled may be a more feasible approach when sampling across large gradients in stream flow. We conducted a power analysis (α=0.05, power=0.8) for biomass density comparisons between two streams, Umauma (moderate baseflow, large catchment) and Honolii (high baseflow, large catchment), for each year. Adequate sample sizes ranged from 15 – 35 transects, suggesting that doubling sampling effort could improve confidence in statistical comparisons across streams in future studies.

The positive relationship between baseflow and relative mass may be the result of higher food quantity and quality in systems with higher flow and more suitable habitat. Frauendorf et al. (2019) found that in four of the reaches included in this study, net-primary production was greater in high flow streams, that lower quality food resources (i.e., leaf litter) were predominant in low flow systems, and that suspended matter was 40x higher in streams with high baseflow compared to low flow systems. *Atyoida bisulcata* are opportunistic filterers/grazers assumed to filter FPOM in high velocity areas as well as graze on benthic resources (Couret, 1976). Reductions in high-velocity habitats (i.e., riffles and runs) in drier streams likely limits the amount of available habitat suitable for filtering FPOM. Simultaneously, residence time of coarse particular organic matter is expected to increase under lower flow conditions but Hawaiian streams lack a true shredder guild (Nakajima et al., 2006), and an increase in the availability of leaf litter does little for *A. bisulcata* food resources. However, average relative mass may be sensitive to increases in food availability resulting from temporary but sustained high flow. April runoff yield was consistently higher in 2014 than 2013 and 2012 (Tingley, 2017), coinciding with greater average relative mass across streams systems. Many studies have documented variability in organism condition with short-term or seasonal changes in food availability (e.g., Hakala and Hartman, 2004; Currinder et al., 2014; Miller et al., 2015), which may indicate differences in individual growth rates (Bentley and Schindler, 2013).

Average POC was highest in stable systems with high baseflow and, like observed differences in relative mass, may be due to higher growth in streams with higher food quantity and quality. Higher stream temperatures may also contribute to smaller *A. bisulcata* in streams with lower baseflow as increases in rearing temperature of ectotherms results in lower maximum adult size (as reviewed by Atkinson, 1994). Across several of our study reaches, Strauch et al. (2017) demonstrated that mean dry season water temperature increased as baseflow decreased. Given observed declines in adult POC length with declines in stream baseflow, higher average stream temperature may have contributed to lower maximum adult size. It is also likely that lower average sizes in streams with the lowest baseflows are the result of intermittent drying and iterative reductions in the standing stock of *A. bisulcata*, where few adults survive through dry periods, and streams may be recolonized by recruits moving upstream. This is partially supported by the observed interaction between baseflow and the duration of high flows; prolonged periods of high flow may attract new recruits to even low baseflow systems, resulting in populations dominated by small individuals. Future research could include the quantification of upstream migrant densities in addition to population demographics (length at age, maximum age) to fully explore this hypothesis. While it was beyond the scope of our study, direct age estimation techniques for some crustaceans are possible (e.g., Leland et al., 2015).

Brown spot disease was least prevalent in stream systems with high baseflow. Gagne and Blum (2016) had a similar finding of decreased parasite infection of a native amphidromous goby (*Awaous stamineus)* in streams with greater mean annual rainfall along the North Hilo coast. The exact mechanism causing increased prevalence of brown spot disease in drier streams is not clear, but previous research indicates that carapace surface abrasions increase susceptibility to chitinoclastic bacterial infection (Chan, 1978), and abrasive forces acting upon macroinvertebrates in streams increase during periods of high suspended sediment loads (Jones et al., 2012). Measures of turbidity from 2012-2014 in three reaches along the North Hilo coast did show higher sediment loads during flood events in streams receiving less annual precipitation (Strauch et al., 2018). Combined with higher bacterial loading during high flow events in drier streams (Strauch et al., 2014), it appears infection with chitinoclastic bacteria is more likely in systems with low baseflow and prolonged high flow events. While the strength of evidence from our study was relatively weak (null model ΔAIC = 3.1; Supplementary Material Table S6), the exact mechanism resulting in higher infection rates could be further explored by testing for differences in the effects of stream flow, turbidity and bacterial load in a controlled environment.

In Hawaii, precipitation is projected to increase in wet regions and decline in dry regions, following a general pattern observed in climate change projections (Elison Timm et al., 2015; Zhang et al., 2016). On windward facing slopes of Hawaii Island and Maui, rainfall is projected to increase significantly in the wet season, with total rainfall during the dry season changing little (Xue et al., 2020). However, the magnitude and timing of rainfall and its delivery to stream systems may ultimately impact stream ecosystems as rainfall intensity is also projected to increase (Fandrich et al., 2022). If streams dependent on persistent rainfall to maintain baseflow receive a higher proportion of rainfall during storm events, average baseflow conditions that result in lower numbers of atyids that are smaller, in poorer condition, and more susceptible to disease may still become more prominent even if mean annual rainfall does not change. Finer resolution projections of annual and daily rainfall paired with our results and additional studies on species-specific sensitivity to flow regime changes would improve the ability to predict climate change impacts on Hawaiian stream ecosystems.

The sustainable management of scarce resources necessitates a holistic perspective that incorporates future climate projections to protect the structure and function of ecosystems. Our results provide an initial understanding of the potential ramifications of climate change for tropical freshwater island streams as shifts in flow regimes alter such ecological processes as mortality, recruitment, and growth. Our results could also be used to understand climate change impacts in regions with the same ecological stream types, such as northeastern Maui (Tingley et al., 2019). Inference beyond similar stream types is not fully supported as broad-scale landscape controls (i.e., groundwater delivery, elevation) influence the relationship between rainfall and flow and the species assemblage present. However, understanding of how such fundamental ecological characteristics will shift across changing flow regimes is limited (Franklin and Gee, 2019), and our results may also have value in assessing how water management may promote critical life-history stages (Way et al., 1998) or how native communities will respond to introduced species (Brasher et al., 2006) in understudied tropical streams ecosystems.

4.1 Implications

Use of a space-for-time model allowed for the examination of how shifting flow regimes affect *A. bisulcata* populations but required careful consideration of interannual variation in flow within and across streams. Baseflow ($Q_{70}Y$) followed a predictable pattern with mean annual rainfall, and variation across streams was greater than within-stream interannual variation. Biotic metrics responded to differences in baseflow across streams as hypothesized, yet when we initially used year-specific baseflow as a predictor, slope estimates appeared erroneous and were sometimes opposite visual patterns observed across the study streams (e.g., POC length). Estimating slopes across years with only small variation in baseflow within streams (a grouping variable in our mixed effects models) seemingly captured spurious relationships between our primary predictor of interest and *A. bisulcata* populations. The presence of sign-reversal in parameter estimation is an observed phenomena resulting from confounding variables within groups (i.e., Simpson's paradox; Simpson, 1951), but aggregating $Q_{70}Y$ across years was the most appropriate approach for our study. An important assumption with the aggregation approach is that baseflow is a surrogate for differences in suitability that likely influence our biotic metrics over a timescale longer than a single year. We acknowledge that this assumption is dependent on yearly variation in rainfall. If we had sampled during an extremely dry year, we might have observed lower POC lengths and near-zero biomass density estimates in streams with moderate mean annual rainfall due to habitat loss and population die-off events. Continued sampling over many years would likely provide a greater range in baseflow conditions associated with climate extremes, making the use of yearly estimates of $Q_{70}Y$ more appropriate than an aggregation approach.

Data availability statement

The raw data supporting the conclusions of this article will be made available by the authors, without undue reservation.

Ethics statement

The manuscript presents research on animals that do not require ethical approval for their study.

Author contributions

RM conceptualized the model system; RM and DI developed the study. RM, DI and RT developed the survey design. RT, AS, PF, RM and DI conducted field sampling. RT, PF and AS processed data in the field and lab. RT, AS, RM, DI and BR contributed to data summary and analysis. RT led on development of figures, tables and initial drafts of the manuscript. RM, DI, AS, RT and BR contributed to critical review and finalization of the manuscript.

Funding

The author(s) declare financial support was received for the research, authorship, and/or publication of this article. We are thankful for financial support from the United States Department of Agriculture Forest Service (FS 12-JV-11272138-039), the US Fish and Wildlife Service via the Hawaii Fish Habitat Partnership (F12AC00708), and Michigan State University. Travel to present this research was also partially supported by the National Climate Change and Wildlife Science Center (now the US Geological Survey National Climate Adaptation Science Center) (G10AC00129).

Acknowledgments

We wish to thank Therese Frauendorf, Michael Riney, James Akau and Kristina Black for assistance in field sampling and laboratory analysis as well as Kevin McDonnell, Andrew Honsey, Robin Debruyne, Robert Klinger and the three individuals who provided initial reviews for edits that improved the manuscript.

Conflict of interest

The authors declare that the research was conducted in the absence of any commercial or financial relationships that could be construed as a potential conflict of interest.

Publisher's note

Supplementary material

The Supplementary Material for this article can be found online at: https://www.frontiersin.org/articles/10.3389/fevo.2024.1182021/full#supplementary-material

References

Aspin, T. W., Khamis, K., Matthews, T. J., Milner, A. M., O'Callaghan, M. J., Trimmer, M., et al. (2019). Extreme drought pushes stream invertebrate communities over functional thresholds. *Glob Chang Biol.* 25, 230–244. doi: 10.1111/gcb.14495

Atkinson, D. (1994). Temperature and organism size: A biological law for ectotherms? *Adv. Ecol. Res.* 25, 1–58. doi: 10.1016/S0065-2504(08)60212-3

Bates, D., Maechler, M., Bolker, B., and Walker, S. (2015). Fitting linear mixed-effects models using lme4. *J. Stat. Software* 67, 1–48. doi: 10.48550/arXiv.1406.5823

Bauer, R. T. (2013). Amphidromy in shrimps: a life cycle between rivers and the sea. *Lat. Am. J. Aquat. Res.* 41, 633–650. doi: 10.3856/vol41-issue4-fulltext-2

Benke, A. C., Huryn, A. D., Smock, L. A., and Wallace, J. B. (1999). Length-mass relationships for freshwater macroinvertebrates in North America with particular reference to the southeastern United States. *J. N. Am. Benthol. Soc* 18, 308–343. doi: 10.2307/1468447

Bentley, K. T., and Schindler, D. E. (2013). Body condition correlates with instantaneous growth in stream-dwelling Rainbow Trout and Arctic Grayling. *T. Am. Fish. Soc* 142, 747–755. doi: 10.1080/00028487.2013.769899

Bowden, W. B.Stream Bryophyte Group (1999). Roles of bryophytes in stream ecosystems. *J. N. Am. Benthol. Soc* 18, 151–184. doi: 10.2307/1468459

Bradford, M. J. (1997). An experimental study of stranding of juvenile salmonids on gravel ears and in side channels during rapid flow decreases. *Regul. River.* 13, 395–401. doi: 10.1002/(SICI)1099-1646(199709/10)13:5<395::AID-RRR464>3.0.CO;2-L

Brasher, A. M. (1997). *Habitat use by fish (o'opu), snails (hihiwai), shrimp ('opae) and prawns in two streams on the island of Moloka'i, University of Hawaii Cooperative National Park Resources Studies Unit Technical Report, 116* (Hawaii: Department of Biology).

Brasher, A. M. D. (2003). Impacts of human disturbances on biotic communities in Hawaiian streams. *BioScience* 11, 1052–1060. doi: 10.1641/0006-3568(2003)053[1052:IOHDOB]2.0.CO;2

Brasher, A. M. D., Luton, C. D., Goodbred, S. L., and Wolff, R. H. (2006). Invasion patterns along elevation and urbanization gradients in Hawaiian streams. *T. Am. Fish. Soc* 135, 1109–1129. doi: 10.1577/T05-083.1

Brusven, M. A., Meehan, W. R., and Biggam, R. C. (1990). The role of aquatic moss on community composition and drift of fish-food organisms. *Hydrobiologia* 196, 39–50. doi: 10.1007/BF00008891

Canton, S. P., Cline, L. D., Short, R. A., and Ward, J. V. (1984). The macroinvertebrates and fish of a Colorado stream during a period of fluctuating discharge. *Freshw. Biol.* 14, 311–316. doi: 10.1111/j.1365-2427.1984.tb00043.x

Chace, J. F. A. (1983). The atya-like shrimps of the Indo-Pacific Region (Decapoda: Atyidae). *Smithson. Contrib. Zool.* 384, 1–54. doi: 10.5479/SI.00810282.384

Chan, J. G. (1978). "Some aspects of a shell disease in the Hawaiian freshwater shrimp, *Atya bisulcata* (Randall)," in *Proceedings of the Second Conference in Natural Sciences Hawaii Volcanoes National Park*. Ed. C. W. Smith (Cooperative National Park Resources Study Unit, Hawaii), 42–50.

Chubb, A. L., Zink, R. M., and Fitzsimons, J. M. (1998). Patterns of mtDNA variation in Hawaiian freshwater fishes: the phylogeographic consequences of amphidromy. *J. Hered.* 89, 8–16. doi: 10.1093/jhered/89.1.8

Comte, L., Buisson, L., Daufresne, M., and Grenouillet, G. (2013). Climate-induced changes in the distribution of freshwater fish: observed and predicted trends. *Freshw. Biol.* 58, 625–639. doi: 10.1111/fwb.12081

Couret, J. C. L. (1976). The biology and taxonomy of a freshwater shrimp, Atyoida bisulcata randall, endemic to the Hawaiian islands. University of Hawai'i at Hilo, Hilo, HI.

Craig, D. A. (2003). Geomorphology, development of running water habitats, and evolution of black flies on Polynesian islands. *Bioscience* 53, 1079–1093. doi: 10.1641/0006-3568(2003)053[1079:GDORWH]2.0.CO;2

Cross, W. F., Covich, A. P., Crowl, T. A., Benstead, J. P., and Ramirez, A. (2008). Secondary production, longevity and resource consumption rates of freshwater shrimps in two tropical streams with contrasting geomorphology and food web structure. *Freshw. Biol.* 53, 2504–2519. doi: 10.1111/j.1365-2427.2008.02078.x

Currinder, B., Cecala, K. K., Northington, R. M., and Dorcas, M. E. (2014). Response of stream salamanders to experimental drought in the southern Appalachian Mountains, USA. *J. Freshw. Ecol.* 29, 579–587. doi: 10.1080/02705060.2014.938135

Cushman, R. M. (1985). Review of ecological effects of rapidly varying flows downstream from hydroelectric facilities. *N. Am. J. Fish. Manage* 5, 330–339. doi: 10.1577/1548-8659(1985)5%3C330:ROEEOR%3E2.0.CO;2

Davey, A. J. H., Kelly, D. J., and Biggs, B. J. F. (2006). Refuge-use strategies of stream fishes in response to extreme low flows. *J. Fish Biol.* 69, 1047–1059. doi: 10.1111/j.1095-8649.2006.01180.x

DiStefano, R. J., Gale, C. M., Wagner, B. A., and Zweifel, R. D. (2003). A sampling method to assess lotic crayfish communities. *J. Crustacean Biol.* 23, 678–690. doi: 10.1651/C-2364

Elison Timm, O., Giambelluca, T. W., and Diaz, H. F. (2015). Statistical downscaling of rainfall changes in Hawai'i based on the CMIP5 global model projections. *J. Geophys. Res-Atmos.* 120, 92–112. doi: 10.1002/2014JD022059

Fandrich, K. M., Ellison Timm, O., Zhang, C., and Giambelluca, T. W. (2022). Dynamical downscaling of near-term, (2026–2035) climate variability and change for the main Hawaiian islands. *J. Geophys. Res-Atmos.* 127, 1–18. doi: 10.1029/2021JD035684

Franklin, P., and Gee, E. (2019). Living in an amphidromous world: Perspectives on the management of fish passage from an island nation. *Aquat. Conserv.: Mar. Freshw. Ecosys.* 29, 1424–1437. doi: 10.1002/aqc.3049

Frauendorf, T. C., MacKenzie, R. A., Tingley, R.W., III, Frazier, A. G., Riney, M. H., and El-Sabaawi, R. W. (2019). Evaluating ecosystem effects of climate change on tropical island streams using high spatial and temporal resolution sampling regimes. *Glob. Change Biol.* 25, 1344–1357. doi: 10.1111/gcb.14584

Frauendorf, T. C., MacKenzie, R. A., Tingley, R.W., III, Infante, D. M., and El-Sabaawi, R. W. (2020). Using a space-for-time substitution approach to predict the effects of climate change on nutrient cycling in tropical island stream ecosystems. *Limnol. Oceanogr.* 65, 3114–3127. doi: 10.1002/lno.11577

Froese, R. (2006). Cube law, condition factor and weight-length relationships: history, meta-analysis and recommendations. *J. Appl. Ichthyol.* 22, 241–253. doi: 10.1111/j.1439-0426.2006.00805.x

Gagne, R. B., and Blum, M. J. (2016). Parasitism of a native Hawaiian stream fish by an introduced nematode increases with declining precipitation across a natural rainfall gradient. *Ecol. Freshw. Fish.* 25, 476–486. doi: 10.1111/eff.12228

Giambelluca, T. W., Chen, Q., Frazier, A. G., Price, J. P., Chen, Y. L., Chu, P. S., et al. (2013). Online rainfall atlas of Hawai'i. *B. Am. Meteorol. Soc* 94, 313–316. doi: 10.1175/BAMS-D-11-00228.1

Gorbach, K. R., Benbow, M. E., McIntosh, M. D., and Burky, A. J. (2012). Dispersal and upstream migration of an amphidromous neritid snail: implications for restoring migratory pathways in tropical streams. *Freshw. Biol.* 57, 1643–1657. doi: 10.1111/j.1365-2427.2012.02826.x

Hakala, J. P., and Hartman, K. J. (2004). Drought effect on stream morphology and brook trout (*Salvelinus fontinalis)* populations in forested headwater streams. *Hydrobiologia* 515, 203–213. doi: 10.1023/B:HYDR.0000027330.12182.24

Harrison, X. A., Donaldson, L., Correa-Cano, M. E., Evans, J., Fisher, D. N., Goodwin, C. E., et al. (2018). A brief introduction to mixed effects modelling and multi-model inference in ecology. *PeerJ* 6, e4794. doi: 10.7717/peerj.4794

Henriksen, J. A., Heasley, J., Kennen, J. G., and Nieswand, S. (2006). *Users' Manual for the Hydroecological Integrity Assessment Process Software (including the New Jersey*

Assessment Tools), U.S. Geological Survey, Biological Resource Discipline, Open File Report 2006-1093 (Washington DC: U.S.: Department of the Interior).

Higashi, G. R., and Nishimoto, R. T. (2007). "The point quadrant method: rapid assessment of hawaiian streams," in *Biology of Hawaiian Stream and Estuaries, Bishop Museum Bulletin in Cultural and Environmental Studies*. Eds. N. L. Evenhuis and J. M. Fitzsimons, 305–312.

IPCC (2013). "Climate Change 2013: The Physical Science Basis," in *Contribution of Working Group I to the Fifth Assessment Report of the Intergovernmental Panel on Climate Change*. Eds. T. F. Stocker, D. Qin, G. K. Plattner, M. Tignor, S. K. Allen, J. Boschung, A. Nauels, Y. Xia, V. Bex and P. M. Midgley (Intergovernmental Panel on Climate Change, United Kingdom and New York).

Isaak, D. J., Wollrab, S., Horan, D., and Chandler, G. (2012). Climate change effects on stream and river temperatures across the northwest US from 1980-2009 and implications for salmonid fishes. *Climatic Change.* 113, 499–524. doi: 10.1007/s10584-011-0326-z

James, A. B. W., Dewson, Z. S., and Death, R. G. (2007). The effect of experimental flow reductions on macroinvertebrate drift in natural and streamside channels. *River Res. Appl.* 24, 22–35. doi: 10.1002/rra.1052

Jones, J. I., Murphy, J. F., Collins, A. L., Sear, D. A., Naden, P. S., and Armitage, P. D. (2012). The impact of fine sediment on macro-invertebrates. *River Res. Appl.* 28, 1055–1071. doi: 10.1002/rra.1516

Kaufmann, P. R., and Robinson, E. G. (1998). "Physical Habitat Characterization," in *Environmental Monitoring and Assessment Program - Surface Waters: Field Operations and Methods for Measuring the Ecological Condition of Wadeable Streams*. Eds. J. L. Lazorchak, D. J. Klemm and D. V. Peck (Washington DC, U.S. Environmental Protection Agency), 77–93.

Keith, P. (2003). Biology and ecology of amphidromous Gobiidae of the Indo-Pacific and the Caribbean regions. *J. Fish Biol.* 63, 831–847. doi: 10.1046/j.1095-8649.2003.00197.x

Kido, M. H. (2008). A persistent species assemblage structure along a Hawaiian stream from catchment-to-sea. *Environ. Biol. Fishes.* 82, 223–235. doi: 10.1007/s10641-007-9276-8

Kido, M. H. (2013). A native species-based index of biological integrity for Hawaiian stream environments. *Environ. Monit. Assess.* 185, 4063–4075. doi: 10.1007/s10661-012-2849-9

Knighton, D. (1998). *Fluvial forms and processes: A new perspective* (London).

Krabbenhoft, T. J., Myers, B. J. E., Wong, J. P., Chu, C., Tingley, R. W.III, Falke, J. A., et al. (2020). FiCli, the Fish and Climate Change Database, informs climate adaptation and management for freshwater fishes. *Sci. Data.* 7, 1–6. doi: 10.1038/s41597-020-0465-z

Krabbenhoft, T. J., Platania, S. P., and Turner, T. F. (2014). Interannual variation in reproductive phenology in a riverine fish assemblage: implications for predicting the effects of climate change and altered flow regimes. *Freshw. Biol.* 59, 1744–1754. doi: 10.1111/fwb.12379

Kuznetsova, A., Brockhoff, P. B., and Christensen, R. H. B. (2017). lmerTest package: tests in linear mixed effects models. *J. Stat. Software* 82, 1–26. doi: 10.18637/jss.v082.i13

Leland, J. C., Bucher, D. J., and Coughran, J. (2015). Direct age determination of a subtropical freshwater crayfish (redclaw, Cherax quadricarinatus) using ossicular growth marks. *PloS One* 10. doi: 10.1371/journal.pone.0134966

Leong, J. A., Marra, J. J., Finucane, M. L., Giambelluca, T., Merrifield, M., Miller, S. E., et al. (2014). "Chapter 23: Hawai'i and U.S. Affiliated Pacific Islands," in *Climate Change Impacts in the United States: The Third National Climate Assessment U.S. Global Change Research Program*. Eds. J. M. Melillo, T. C. Richmond and G. W. Yohe (Government Printing Office, Washington DC: U.S), 537–556.

Leppi, J. C., DeLuca, T. H., Harrar, S. W., and Running, S. W. (2012). Impacts of climate change on August stream discharge in the Central-Rocky Mountains. *Climatic Change.* 112, 997–1014. doi: 10.1007/s10584-011-0235-1

Lytle, D. A., and Poff, N. L. (2004). Adaptation to natural flow regimes. *Trends. Ecol. Evol.* 19, 94–100. doi: 10.1016/j.tree.2003.10.002

Maurer, M. A., and Brusven, M. A. (1983). Insect abundance and colonization rate in *Fontinalis-neo-mexicana* (bryophyta) in an Idaho batholith stream. *U.S.A. Hydrobiol.* 98, 9–15. doi: 10.1007/BF00019246

McDowall, R. M. (2007). On amphidromy, a distinct form of diadromy in aquatic organisms. *Fish. Fish.* 8, 1–13. doi: 10.1111/j.1467-2979.2007.00232.x

McDowall, R. M. (2010). Why be amphidromous: Expatrial dispersal and the place of source and sink population dynamics? *Rev. Fish Biol. Fish.* 20, 87–100. doi: 10.1007/s11160-009-9125-2

McRae, M. G. (2007). "The Potential for source-sink population dynamics in Hawaii's amphidromous fishes," in *Biology of Hawaiian Stream and Estuaries, Bishop Museum Bulletin in Cultural and Environmental Studies 3*. Eds. N. L. Evenhuis and J. M. Fitzsimons, 87–98.

Meffe, G. K., and Minckley, W. L. (1987). Persistence and stability of fish and invertebrate assemblages in a repeatedly disturbed Sonoran desert stream. *Am. Midl. Nat.* 117, 177–191. doi: 10.2307/2425718

Miller, S. J., VanGenechten, D. T., and Cichra, C. E. (2015). Length weight relationships and an evaluation of fish size and seasonal effects on relative condition (K-n) of fishes from the Wekiva River, Florida. *Fla. Sci.* 78, 1–19.

Myers, B. J. E., Lynch, A. J., Bunnell, D. B., Chu, C., Falke, J. A., Kovach, R. P., et al. (2017). Global synthesis of the documented and projected effects of climate change on inland fishes. *Rev. Fish Biol. Fish.* 27, 339–361. doi: 10.1007/s11160-017-9476-z

Naesje, T., Jonsson, B., and Skurdal, J. (1995). Spring flood: A primary cue for hatching of river spawning Coregoninae. *Can. J. Fish. Aquat. Sci.* 52, 2190–2196. doi: 10.1139/f95-811

Nakagawa, S. N., and Schielzeth, H. (2013). A general and simple method for obtaining R2 from generalized linear mixed effects models. *MEE* 4, 133–142. doi: 10.1111/j.2041-210x.2012.00261.x

Nakajima, T., Asaeda, T., Fujino, T., and Nanda, A. (2006). Coarse particulate organic matter distribution in the pools and riffles of a second-order stream. *Hydrobiologia* 559, 275–283. doi: 10.1007/s10750-005-9127-6

Nishimoto, R. T., and Fitzsimons, J. M. (2006). "Status of native Hawaiian stream fishes, a unique amphidromous biota," in *Status, Distribution, and Conservation of Native Freshwater Fishes in Western North America*. Eds. M. J. Brouder and J. A. Scheurer (American Fisheries Society, Bethesda, Maryland), 21–27.

Nishimoto, R. T., and Kuamoo, D. G. K. (1991). "The occurrence and distribution of the native goby (*Lentipes concolor*) in Hawai 'i Island streams with notes on the distribution of other native fish species," in *New Directions in Research, Management and Conservation of Hawaiian Freshwater Stream Ecosystems: Proceedings of the 1990 Symposium on Freshwater Stream Biology and Fisheries Management*, Honolulu, HI. 77–95 (Division of Aquatic Resources).

Nishimoto, R. T., and Kuamo'o, D. G. K. (1996). Monitoring study of the endemic mountain shrimp, *Atyoida bisulcata* Randall, in Waikaumalo Stream, Hawaii Island. *Proc. West. Assoc. Fish Wildl. Agencies.* 76, 262–273.

Oki, D. S., Wolff, R. H., and Perreault, J. A. (2010). *Effects of surface-water diversion on streamflow, recharge, physical habitat, and temperature, Na Wai Eha, Maui, Hawaii, U.S. Geological Survey Scientific Investigations Report 2010–5011* (Virginia: U. S: Geological Survey).

Poff, N. L., Allan, J. D., Bain, M. B., Karr, J. R., Prestegaard, K. L., Richter, B. D., et al. (1997). The natural flow regime. *Bioscience* 47, 769–784. doi: 10.2307/1313099

Price, J. P., Jacobi, J. D., Gon, S.M., III, Matsuwaki, D., Mehrhoff, L., Wagner, W., et al. (2012). *Mapping plant species ranges in the Hawaiian Islands—Developing a methodology and associated GIS layers, U.S. Geological Survey Open-File Report 2012–1192* (Virginia: U.S.: Geological Survey).

Rabeni, C. F. (1985). Resource partitioning by stream dwelling crayfish: the influence of body size. *Am. Midl. Nat.* 113, 20–29. doi: 10.2307/2425344

Riney, M. H. (2015). The impacts of stream flow rate on food resource quality and diets of native endemic atyid shrimps (*Atyoida bisulcata*) in Hawaiian streams. University of Hawaii at Hilo, Honolulu, HI.

Rolls, R. J., Leigh, C., and Sheldon, F. (2012). Mechanistic effects of low-flow hydrology on riverine ecosystems: ecological principles and consequences of alteration. *Freshw. Sci.* 31, 1163–1186. doi: 10.1899/12-002.1

Sherrod, D. R., Robinson, J. E., Sinton, J. M., Watkins, S. E., and Brunt, K. M. (2008) *Database to accompany geologic map of the state of Hawaii*. Available online at: https://www.sciencebase.gov/catalog/item/60df56d5d34ed15aa3b8a39c (Accessed March 7, 2013).

Simpson, E. (1951). The interpretation of interaction in contingency tables. *J. R. Stat. Society Ser. B* 13, 238–241. doi: 10.1111/j.2517-6161.1951.tb00088.x

Strauch, A. M., Giardina, C. P., Mackenzie, R. A., Heider, C., Giambelluca, T. W., Salminen, E., et al. (2016). Modeled effects of climate change and plant invasion on watershed function across a steep tropical rainfall gradient. *Ecosystems* 19, 1–18. doi: 10.1007/s10021-016-0038-3

Strauch, A. M., Mackenzie, R. A., Bruland, G. L., Tingley, R. W., III, and Giardina, C. P. (2014). Climate change and land use drivers of fecal bacteria in tropical Hawaiian rivers. *J. Environ. Quality.* 43, 1475–1483. doi: 10.2134/jeq2014.01.0025

Strauch, A. M., MacKenzie, R. A., Giardina, C. P., and Bruland, G. L. (2015). Climate driven changes to rainfall and streamflow patterns in a model tropical island hydrological system. *J. Hydrol.* 523, 160–169. doi: 10.1016/j.jhydrol.2015.01.045

Strauch, A. M., MacKenzie, R. A., Giardina, C. P., and Bruland, G. L. (2018). Influence of declining mean annual rainfall on the behavior and yield of sediment and particulate organic carbon from tropical watersheds. *Geomorphology* 306, 2–39. doi: 10.1016/j.geomorph.2017.12.030

Strauch, A. M., MacKenzie, R. A., and Tingley, R.W., III (2017). Baseflow driven shifts in tropical stream temperature regimes across a mean annual rainfall gradient. *Hydrol. Process.* 31, 1678–1689. doi: 10.1002/hyp.11084

Tingley, R.W., III (2017). A multi-scaled research framework for conserving streams with changing climate. Michigan State University, East Lansing, Michigan.

Tingley, R.W., III, Infante, D. M., MacKenzie, R. A., Cooper, A. R., and Tsang, Y.-P. (2019). Identifying natural catchment landscape influences on tropical stream organisms: classifying stream reaches of the Hawaiian Islands. *Hydrobiologia* 826, 67–83. doi: 10.1007/s10750-018-3726-5

Walter, R. P., Hogan, J. D., Blum, M. J., Gagne, R. B., Hain, E. F., Gilliam, J. F., et al. (2012). Climate change and conservation of endemic amphidromous fishes in Hawaiian streams. *Endanger Species Rese.* 16, 261–272. doi: 10.3354/esr00404

Ward, E. J., Anderson, J. H., Beechie, T. J., Pess, G. R., and Ford, J. M. (2015). Increasing hydrologic variability threatens depleted anadromous fish populations. *Glob. Change Biol.* 21, 2500–2509. doi: 10.1111/gcb.12847

Way, C. M., Burky, A. J., Harding, J. M., Hau, S., and Puleloa, W. K. L. C. (1998). Reproductive biology of the endemic goby, Lentipes concolor, from Makamaka'ole Stream, Maui and Waikolu Stream, Moloka'i. *Environ. Biol. Fish.* 51, 53–65. doi: 10.1023/A:1007305917443

Xue, L., Wang, Y., Newman, A. J., Ikeda, K., Rasmussen, R. M., Giambelluca, T. W., et al. (2020). How will rainfall change over Hawai'i in the future? High-resolution regional climate simulation of the Hawaiian islands. *BAST* 1, 459–490. doi: 10.1007/s42865-020-00022-5

Zeigler, M. P., Todd, A. S., and Caldwell, C. A. (2012). Evidence of recent climate change within the historic range of Rio Grande Cutthroat Trout: Implications for management and future persistence. *T. Am. Fish. Soc* 141, 1045–1059. doi: 10.1080/00028487.2012.676589

Zhang, C., Wang, Y., Hamilton, K., and Lauer, A. (2016). Dynamical downscaling of the climate for the Hawaiian Islands. Part II: Projection for the late twenty-first century. *J. Climate.* 29, 8333–8354. doi: 10.1175/JCLI-D-16-0038.1

frontiers | Frontiers in Ecology and Evolution

TYPE Original Research
PUBLISHED 09 May 2024
DOI 10.3389/fevo.2024.1271824

Check for updates

OPEN ACCESS

EDITED BY
Daniel de Paiva Silva,
Goiano Federal Institute (IFGOIANO), Brazil

REVIEWED BY
Luciana Ghermandi,
National Scientific and Technical Research Council (CONICET), Argentina
Rafael Barbizan
Sühs, Federal University of Santa Catarina, Brazil

*CORRESPONDENCE
Steven Lee
✉ srlee@usgs.gov

RECEIVED 02 August 2023
ACCEPTED 02 April 2024
PUBLISHED 09 May 2024

CITATION
Lee S, Klinger R, Brooks ML and Ferrenberg S (2024) Homogenization of soil seed bank communities by fire and invasive species in the Mojave Desert. *Front. Ecol. Evol.* 12:1271824. doi: 10.3389/fevo.2024.1271824

Homogenization of soil seed bank communities by fire and invasive species in the Mojave Desert

Steven Lee[1,2]*, Robert Klinger[1], Matthew L. Brooks[1] and Scott Ferrenberg[3]

[1]U.S. Geological Survey, Western Ecological Research Center, Yosemite Field Station, Wawona, CA, United States, [2]Global Change Ecology Lab, Department of Biology, New Mexico State University, Las Cruces, NM, United States, [3]Department of Ecosystem and Conservation Science, University of Montana, Missoula, MT, United States

Soil seed banks help maintain species diversity through temporal storage effects and function as germination pools that can optimize fitness across varying environmental conditions. These characteristics promote the persistence of native plant communities, yet disturbances such as fire and associated invasions by non-native species can disrupt these reserves, fundamentally altering successional trajectories. This may be particularly true in deserts, where native plant communities are less adapted to fire. While studies of fire effects on desert plant communities are not uncommon, information regarding the short- and long-term effects of fire on seed banks is less available. To better understand the influence of fire and invasive species on desert seed banks, we investigated soil seed bank biodiversity from 30 wildfires that burned between 1972 and 2010 across the Mojave Desert ecoregion of North America. We assessed how characteristics of fire regimes (frequency, time since fire, and burn severity) interacted with climate and invasive plants on measures of α-, β-, and γ-diversities. Because β-diversity is a direct measure of community variability and reveals important information about biodiversity loss, we further examined the nestedness and turnover components of β-diversity. Mean α- and γ-diversities were generally higher for burned locations than in unburned reference sites, however individual fire variables had little influence on patterns of seed bank diversity. Burned area seed banks tended to be dominated by non-native invasive species, primarily two grasses, (*Bromus rubens*, *Bromus tectorum*), as well as an invasive forb (*Erodium cicutarium*). The most striking pattern we observed was a collective sharp decline in α-, β-, and γ-diversities with increased invasive species dominance, indicating the homogenization of seed bank communities with the colonization of invasive species after fire. Evidence of homogenization was further supported by reduced turnover and increased nestedness in burn areas compared to reference areas indicating potential biodiversity loss. Our findings highlight how biological processes such as plant invasions can combine with disturbance from fire to alter patterns of seed bank composition and diversity in desert ecosystems.

KEYWORDS

fire, invasives, seed banks, species diversity, desert, drylands, variability, beta diversity

1 Introduction

Disturbance plays a pivotal role in influencing biodiversity across ecosystems (Huston, 1979; Sousa, 1984). Characterized by heterogeneity in time and space, disturbances create a patchwork of varying resources and habitats that directly contribute to the maintenance of diversity (Petraitis et al., 1989). Ultimately, disturbances moderate the balance among deterministic (environmental and biotic filtering) and stochastic (random dispersal and recruitment) assembly processes that shape local ecological community composition and structure, and determine levels of similarity and turnover in species pools across communities (Chesson, 2000; Kraft et al., 2008; Ferrenberg et al., 2013). In light of global change pressures, including novel species introductions, and climate and land-use change that can rapidly alter disturbance regimes, understanding the effects of disturbance on species diversity remains crucial (Pulsford et al., 2016).

In western North America, global change pressures are reshaping historical fire regimes, increasing the frequency, severity, and extent of fires (Abatzoglou and Williams, 2016). A large proportion of this region is composed of arid desert ecosystems (Barbour and Billings, 2000). Lacking frequent exposure to fire over evolutionary time, native desert vegetation is thought to be less adapted and more vulnerable to fire compared to plants of more mesic fire-prone environments (Chambers and Wisdom, 2009; Brooks et al., 2018). As such, changes to the historical fire regimes in deserts can result in a long-term transformation of native vegetation and a shift in the trajectory of recovering post-fire plant communities. This has been well documented in the Mojave and Great Basin deserts, where disturbance to native woody plant cover and surface soils from fire has led to post-fire communities dominated by herbaceous plants, often non-native annual grasses of genus *Bromus*. The spread of *Bromus* has combined with climate and land-use change to alter the fire regime and promote positive feedback resulting in a “grass/fire cycle” that lead can to further invasions (D’Antonio and Vitousek, 1992; Brooks et al., 2004).

Introductions of non-native species like *Bromus* complicate the relationship between disturbance and plant diversity. Disturbance often reduces the abundance of competitively dominant species and increases the availability of limiting resources (Petraitis et al., 1989), which can promote colonization by less competitive species and lead to higher levels of diversity (Chesson and Huntly, 1997; Cadotte, 2007). However, the rapid spread of invasive annual grasses after fire can suppress the recruitment of native species and reduce overall diversity (Brooks, 2000; DeFalco et al., 2007). While extensive research has explored the link between disturbance, invasive plants, and their combined effects on native plant communities (Hobbs and Huenneke, 1992; McIntyre and Lavorel, 1994; Keeley et al., 2005), most studies focus on aboveground plant assemblages, often overlooking the crucial role of soil seed banks (Faist, 2013; Vandvik et al., 2016; Hosna et al., 2023). Seed banks, through dormancy strategies, enable plants to disperse across space and time, contributing to the maintenance of diversity via temporal “storage effects” (Chesson, 2000; Anderson et al., 2012). This is an important strategy in arid ecosystems where climatic conditions that promote successful recruitment may be sporadic across growing seasons and years (Gremer and Venable, 2014). The impact of altered disturbance regimes, coupled with non-native species introductions, on seed banks remains unclear for most ecosystems including deserts.

In this study, we assess the interactive roles of fire frequency, time since fire, burn severity, climate, topography, and the abundance of invasives on plant diversity in seed banks in the Mojave Desert, USA (Figure 1). Vegetation cover across the Mojave Desert varies as a function of local climate regimes (Aronson and Shmida, 1992; Rodríguez-Moreno and Bullock, 2014), with high aridity producing sparse, heterogeneous vegetation cover which translates to high spatial variability in both plant community types, and the risk and severity of fire (Abella, 2009). Patterns of diversity in aboveground vegetation and belowground seed banks are likely to reflect such variation (Engel and Abella, 2011). However, given temporal storage effects, the rate at which seed banks come to reflect aboveground vegetation patterns remains unclear. Following fires, plant diversity in the Mojave Desert is expected to vary as a function of the initial community, the dispersal potential of species in local and regional pools, local environmental characteristics, and the severity and time since fire as successional processes take place (Safford and Harrison, 2004; Keeley et al., 2005). Collectively, the combination of these factors determines diversity across different spatial scales while simultaneously shaping variability among vegetation communities (β-diversity). Consequently, observed aboveground plant diversity patterns in both burned and unburned landscapes can vary greatly based on annual and seasonal rainfall (Winkler and Brooks, 2020). Therefore, evaluations of seed banks provide temporally integrated insights into local communities, offering a more representative measure of potential plant diversity than short-term aboveground observations. To better understand how seed bank diversity varies with disturbance we specifically ask:

1. What relationship does seed bank diversity have with climate and topography?
2. How is seed bank diversity affected by the frequency, severity, and time since fire?
3. How is seed bank diversity influenced by invasive species with and without fire disturbance?

2 Materials and methods

2.1 Study sites

This study occurred in the Mojave Desert ecoregion of North America (Mojave hereafter). The Mojave is the smallest North American desert (≈152,000 km^2) but encompasses large variations in landforms and climate. Elevation ranges from −85 m to 3635 m with most of the ecoregion being between 600 m and 1600 m. A majority of precipitation, ~70%, occurs during the cool season between October and March with annual totals ranging from 50 to

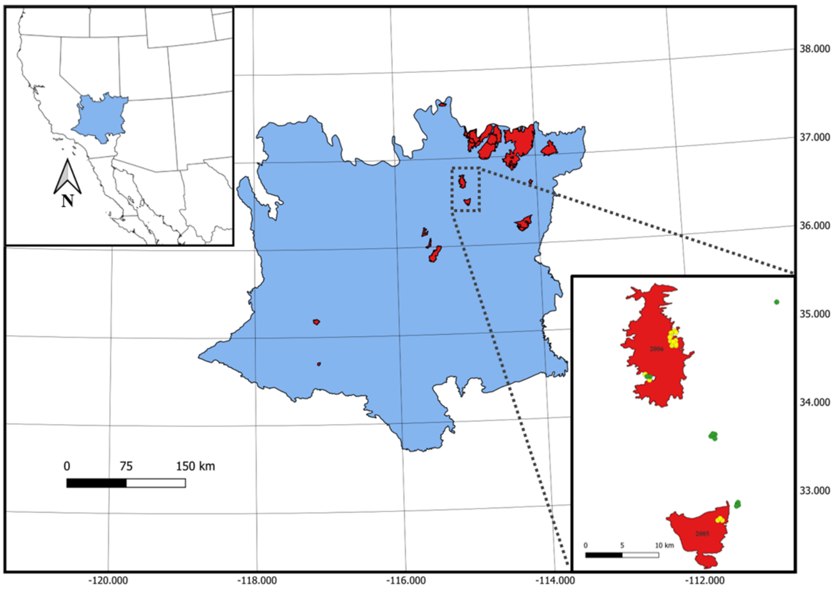

FIGURE 1
Burn perimeters (red) from 30 unique wildfires representing a chronosequence of fires that burned between 1972 and 2010 in the Mojave Desert of North America. Lower right inset panel shows an example of point locations for burned (yellow; total n = 432) and unburned (green; total n = 111) 0.1 ha plots where seed bank samples were collected. Mojave Desert Ecoregion and burn perimeter data provided by Klinger et al. (2022).

130 mm in lower elevations to 250–750 mm at higher elevations. Temperatures range from minimums of −20°C (high elevation) to −5°C (low elevation) during the winter and highs of 30°C (high elevation) to 50° C (low elevation) in the summer (Hereford et al., 2006; Tagestad et al., 2016). This large variation in climate and landform results in distinct vegetation communities across climatic and soil gradients: lower elevations (< 1200 m) feature low-stature shrubs with sparse herbaceous cover, mid-elevations (1200 to 1800 m) exhibit denser shrubs and increased herbaceous cover, and high elevations (> 1800 m) host a mix of large shrubs and small trees, with limited herbaceous vegetation and bare interspaces (Barbour and Billings, 2000).

2.2 Experimental design and soil sampling

Our seed bank study was conducted concurrently with assessments of above-ground vegetation response to fire and detailed descriptions of methods for site selection are given in Klinger and Brooks (2017) and Klinger et al. (2021). In brief, we acquired fire perimeters and burn severity (differenced normalized burn ratio; dNBR) from the Monitoring and Trends in Burn Severity program (MTBS; https://www.mtbs.gov) for fires ≥ 405 ha (the MTBS minimum fire size) that occurred throughout the Mojave from 1972–2010 (Eidenshink et al., 2007). We then used a Geographic Information System (GIS; ESRI http://www.esri.com/) to map fire frequency (number of times a site burned since 1972) by overlaying the perimeters and calculating their overlap through time. We then used GIS to randomly select sites within (burned) or adjacent (unburned) to the perimeters of 53 fires across the Mojave Desert. While fires in the Mojave spanned a large range of elevations, most occurred in middle to high-elevation zones (Brooks et al., 2018). We accounted for differences that may occur due to topography, soils, and land use history by randomly selecting 1 km^2 site polygons entirely within or outside the fire perimeters, then randomly selecting 3 to 7 plots within each site polygon. Each plot was 0.1 ha (32 m × 32 m) containing three randomly positioned, parallel 30 m transects. Five subplots of 1 m^2 were spaced at 5 m intervals along the three transects for a total of 15 subplots per plot (Figure 2). Visual assessments were conducted in the field to ensure that no unburned plots had evidence of burning to avoid inaccurate burn perimeters or smaller fires not reported in the MTBS database.

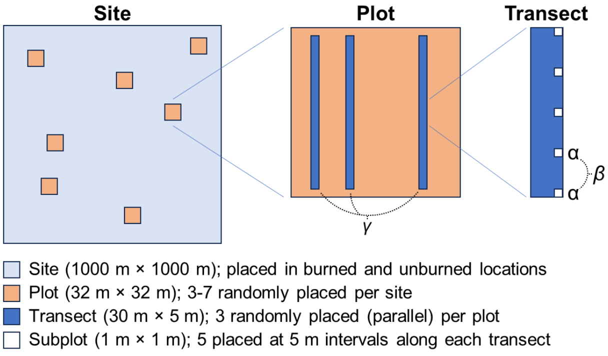

FIGURE 2
Conceptual diagram illustrating the scale and relationships between sampling sites, plots, transects, and subplots. Greek letters indicate the level at which each diversity metric was calculated, with alpha measuring species diversity of each subplot, beta diversity being calculated as the pairwise dissimilarities among the subplots, and gamma encompassing species diversity for plots.

Soil samples for seed bank assays were collected once from 432 burned plots across 30 unique fires and 111 unburned plots (N=543; Figure 1); this was a subset of the plots sampled in Klinger and Brooks (2017). Within each plot, we collected four samples from each subplot—one at each corner—that were pooled together. Each soil sample was collected using a cylindrical tin measuring 6.0 cm diameter × 4.4 cm deep (volume = 124.4 cm^3). This approach focused on the top 4 cm of soil where the bulk of viable seeds are located in desert soils (Young and Evans, 1975; Kemp, 1989; Ferrandis et al., 2001). Soil samples were collected in the fall (October-November) of 2009, 2011, and 2012, when annual plants had senesced, and the majority of seed bank inputs for the year had occurred. Seed bank samples were then stored in a cool (temperatures ranging from −10 to 20 degrees C), dry, dark location for two to three months, to maintain viability and aid germination (Baskin and Baskin, 1998).

We used an emergence method, where germinated seedlings are used as a surrogate for counting seeds, to determine seed bank composition and abundance. Individual soil samples were homogenized by crushing soil aggregates, removing rocks and litter >1 cm diameter, and thoroughly mixing. Soil on rocks and litter was brushed back into the samples to capture any seeds before discarding them. Litter with crevices or potentially seed-bearing surfaces was placed back into the soil sample. One-half cup of soil (~118 cm^3) from each sample was thoroughly mixed with ½ cup vermiculite to help with moisture regulation of the soils. Soil-vermiculite samples were then placed in plastic bulb pots (15.72 cm outside diameter × 9.21 cm height) and spread to approximately 2 cm deep on top of weed block fabric. Pots were arranged randomly on greenhouse benches and watered overhead using a gentle rain nozzle. Greenhouse temperature was maintained between 5 and 30°C.

Two consecutive germination trials, each lasting ~50 days, were completed with pots monitored every 1 to 3 days for seedlings and soil moisture. Pots were watered as needed (every 1 to 5 days) to maintain adequate moisture for seeds and seedling growth. Each trial was stopped once two weeks had passed with no new germination. Soils were then allowed to dry for three weeks between the first and second trials—an approach that simulates natural wetting from rainfall and is needed to break dormancy of some seeds (see Faist and Collinge, 2015; Haight et al., 2019). Seedlings were identified to species, counted, and plucked to quantify species abundance by subplot without allowing crowding or competition to reduce germination rates. Species not readily identifiable after germination were allowed to grow until features supported their identification. In cases where features remained non-descript, individuals were identified to *Genus* or higher taxonomic groups (this was the case for a very small number of seedlings). Because cheatgrass (*Bromus tectorum*) and red brome (*Bromus rubens)* are difficult to differentiate at the seedling stage, they were collectively identified as *Bromus* spp. Nomenclature for emerging species followed the U.S. Department of Agriculture, Natural Resource Conservation Service (plants.usda.gov; 2013).

2.3 Data analysis

2.3.1 Diversity indices

Using count data of species emergence from our subplot samples, we partitioned diversity into plot-scale α, β, and γ components and constructed diversity profiles for each based-on Hill numbers (Hill, 1973) of diversity using the 'entropart' package (Marcon and Hérault, 2015) for R. Hill numbers are a parametric family of diversity indices that incorporate species richness and relative abundance information to quantify diversity (Jost, 2007). These are broken into three primary orders (q): q0, species richness; q1, the exponential of Shannon entropy; and q2, the inverse of Gini-Simpson index. An advantage of assessing diversity via Hill numbers is that each diversity metric is expressed in units of effective numbers of species (i.e., the number of equally abundant species that would be needed to give an equivalent measure of diversity; Chao et al., 2014). We focused our assessment of diversity across the Mojave landscape at the order of q1, which is considered "true diversity" or the effective number of species in a community (Jost, 2013). We did this because these metrics are generalizable across samples and have intuitive interpretations of our dataset: α-diversity for q1 is the mean effective number of species across 1-m^2 subplots within a plot; γ-diversity is the effective number of species for the entire 0.1 ha plot, and β-diversity represents the effective number of distinct localized communities within a plot, a direct measure of community variability (Jost, 2007; Silva Pedro et al., 2016).

Beta diversity was calculated following Whittaker (1972) multiplicative law ($\alpha \times \beta = \gamma$), which, when combined with Hill numbers, produces a β independent of the plot α values (Jost, 2007). Additionally, utilizing the subplots as individual samples, we decomposed β-diversity via Sørensen dissimilarity into plot-level nestedness (i.e., the degree to which species losses are a function of being a subset of a larger community) and turnover (i.e., species replacement across local assemblages) components using the 'nestedbetasor' function in the 'vegan' package (Oksanen et al., 2020). Separating β-diversity into various components may help determine whether local community variability is the result of environmental and dispersal processes thought to reflect species turnover versus patterns of local colonization and extinction that can influence levels of species nestedness (Soininen et al., 2018). We derived β at the 0.1 ha (plot) scale to characterize variability within the seed bank at a spatial scale relevant to potential biological processes and interactions (e.g., species competition, nurse plant effect). Furthermore, by having a measure of variability at the plot scale, we could then model β as a response to environmental, fire, and biotic factors.

2.3.2 Explanatory variables

We identified 10 explanatory variables across four categories influencing diversity in the Mojave landscape: climate, topography, biotic, and fire (see Table 1). Climate variables included 30-year normals (1984–2014) for mean annual precipitation (MAP) and

TABLE 1 Variables used to assess patterns of soil seed bank diversity across the Mojave Desert ecoregion, USA.

	Variable	Source
Climate	30-year mean annual precipitation (MAP)	PRISM Climate Group, Oregon State University, Corvalis, Oregon (http://www.prismclimate.org
	30-year mean July maximum temperature (tmax7)	PRISM Climate Group, Oregon State University, Corvalis, Oregon http://www.prismclimate.org
Topography	Elevation (Elev)	30-meter Digital Elevation Model (National Elevation Dataset, https://www.usgs.gov/programs/national-geospatial-program/national-map).
	Hillshade (Hllshd)	Derived from DEM
	Terrain Ruggedness Index (TRI)	Derived from DEM; Wilson et al., 2007
Biotic	Relative cover of above ground woody plants (prWoody)	Klinger and Brooks, 2017, Cover of woody and herbaceous functional groups in burned and unburned plots, Mojave Desert, 2009–2013: U.S. Geological Survey data release, https://doi.org/10.5066/F79022PZ.
	Relative abundance of non-native plants from seed bank (prAlien)	reported here
Fire	Number of times burned 1984–2010 (Freq)	Klinger et al., 2022, Fire regimes in the Mojave Desert (1972–2010): U.S. Geological Survey data release, https://doi.org/10.5066/P99YGHSJ.
	Burn Severity (dNBR)	Klinger et al., 2022, Fire regimes in the Mojave Desert (1972–2010): U.S. Geological Survey data release, https://doi.org/10.5066/P99YGHSJ.
	Years post fire (YPF)	Klinger et al., 2022, Fire regimes in the Mojave Desert (1972–2010): U.S. Geological Survey data release, https://doi.org/10.5066/P99YGHSJ.

maximum July temperature (tmax7) using PRISM data. (PRISM Climate Group, Oregon State University, http://prism.oregonstate.edu, accessed 19 August 2019). Topographic variables included elevation, hillshade (an index of solar radiation that utilizes aspect and slope) and a terrain ruggedness index (TRI; Wilson et al., 2007). Due to the strong correlation between elevation and temperature (r > 0.8; Appendix 1), we withheld temperature in favor of elevation in our analyses for its significant role in determining both climate and landscape position. Interactions among plant species can strongly influence pattern diversity in vegetation communities (McIntire and Fajardo, 2014; Lucero et al., 2020). To address this, we incorporated the relative cover of above-ground woody vegetation (shrub and tree cover) and the relative abundance of non-native plants from soil seed bank greenhouse trials as biotic factors. Woody cover plays a crucial role in shaping plant composition patterns in desert ecosystems (Schade et al., 2003; Haas-Desmarais and Lortie, 2023), and non-native species can impact biodiversity (Underwood et al., 2019). We classified each species as either native or non-native (alien), and calculated the relative abundance of non-native plants for each plot. Fire variables included burn severity (dNBR), years' post-fire (YPF), and fire frequency (0,1 vs 2–3 times since 1972). YPF was transformed as 1 divided by the time since the last burn, establishing a gradient supporting theoretical successional states along a directional time axis. Unburned plots were assigned a YPF value of 0, facilitating the inclusion of burned and unburned plots in the same model along a time since disturbance gradient. Data on burn severity and fire history can be found in Klinger et al. (2022).

2.3.3 Diversity modelling

We used generalized linear mixed models (GLMMs) to examine the relationship between plot-level diversities and various climate, topography, biotic, and fire-related variables (Table 1). We constructed individual GLMMs incorporating a gamma distribution and log link function for the q1 order α-, β-, and γ-diversities, designating "site" as a random effect. Additionally, we developed individual GLMMs for the decomposed nestedness and turnover components of Sørensen dissimilarity, using a Gaussian distribution and identity link function, with site specified as a random effect. For each model, we employed model averaging using the MuMin package (Bartoń, 2020) to estimate 95% confidence intervals of standardized parameter estimates (β coefficients) for each explanatory variable. We considered variables ecologically significant if their 95% CIs did not overlap zero. The use of multi-model inference allowed us to assess the relative importance of each variable. To address non-linear relationships identified in preliminary analyses between diversity responses and the relative abundance of non-native species, as well as mean annual precipitation (MAP), we incorporated quadratic terms for these variables into each model. We used the lme4 package (Bates et al., 2015) to construct all GLMMs and model fits were checked (Appendices 2–4) using the DHARMa (Hartig, 2022) and performance packages (Lüdecke et al., 2020). We assessed possible collinearity issues between fixed effects by estimating the variance inflation factors (VIF) for each model (Appendix 5). VIF values were <5, indicating little collinearity among predictors (Akinwande et al., 2015). All analyses were run with R 4.3.1 (R Core Team, 2023).

3 Results

We recorded the emergence of 173 unique plant species from the soil seed bank, the majority of which were native annual plants. We documented 14 non-native species, the most abundant being the invasive annual grasses *B. tectrorum* and *B. rubens* and the annual forb *Erodium cicutarium* (Appendix Table 1). In general, plot level species richness (γ at q0) was higher in burned areas, 9.61 (95% CI = 8.50–10.57), than in unburned areas, 6.75 (95% CI =

6.00–7.37; Figure 3). In terms of true diversities (q1), a subset of explanatory variables tended to have significant influences on seed bank diversity at subplot (α) and plot (γ) scales, as well as plot-scale community variability (β), nestedness, and turnover. Additionally, all measures of diversity had a non-linear relationship with the relative abundance of non-native plants found within the seed bank, particularly in burned sites, where measures of diversity initially increased with non-native abundance before peaking and rapidly declining as non-native plants became dominant (Figure 4).

3.1 Alpha diversity

At the local 1 m^2 subplot scale, the effective number of species (α-diversity at q1) tended to be greater in areas that burned, 1.92 (95% CI = 1.79–2.05), than in unburned areas, 1.56 (95% CI = 1.45–1.68). Our GLMM was able to explain roughly half of the variation in α-diversity ($R^2 = 0.51$). Alpha diversity had a significant positive relationship with topographic complexity (TRI) and burn frequency, and a negative relationship with relative cover of woody plants and elevation (Figure 3). However, the largest influence on local α-diversity was the relative abundance of non-native plants within the seed bank, which had a strong non-linear relationship with α-diversity across both burned and unburned locations (Figures 4, 5).

3.2 Beta diversity

Plot-scale variability in community composition among (β-diversity at q1) was generally lower in burned sites, 1.87 (95% CI = 1.72–2.05), than in unburned sites, 2.47(95% CI = 2.31–2.65; Figure 3). Our GLMM explained a relatively high amount of variation in β-diversity ($R^2 = 0.62$). Beta diversity had a significant positive relationship with relative cover of woody vegetation and a negative relationship with burn frequency. Similar to α-diversity, β-diversity had a non-linear relationship with the relative abundance of non-native plants within the seed bank (Figure 4).

Plot-scale Sørensen dissimilarity was similar across burned (μ = 0.74, 95% CI = 0.65–0.83) and unburned (μ = 0.78, 95% CI

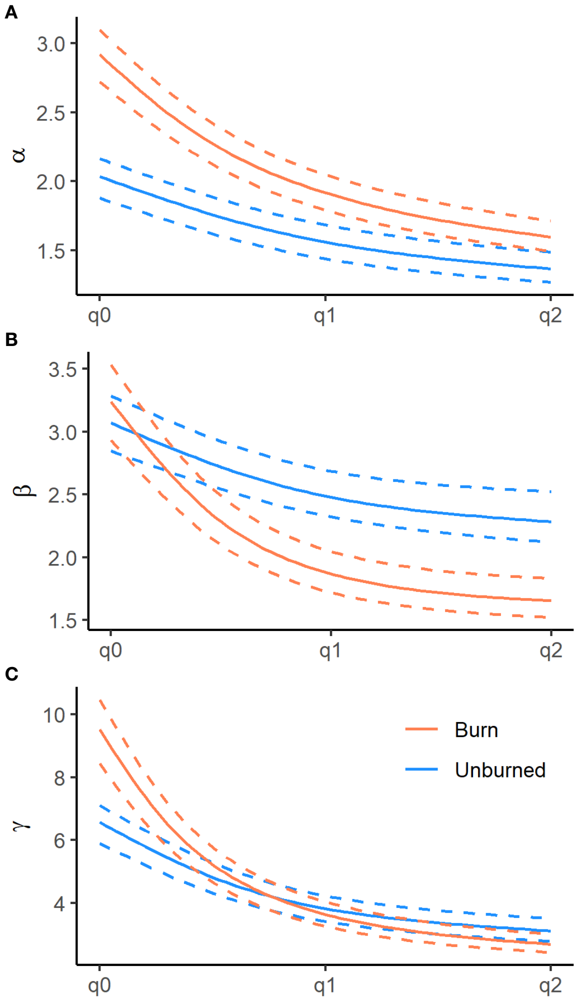

FIGURE 3
Diversity profiles for alpha (α, panel **A**), beta (β, panel **B**), and gamma (γ, panel **C**) diversities of burned (red) and unburned (blue) plots from the Mojave Ecoregion. Diversity orders range across species richness (q0), exponent of Shannon's entropy (q1) and the Gini-Simpson index (q2). Dashed lines indicate 95% confidence intervals.

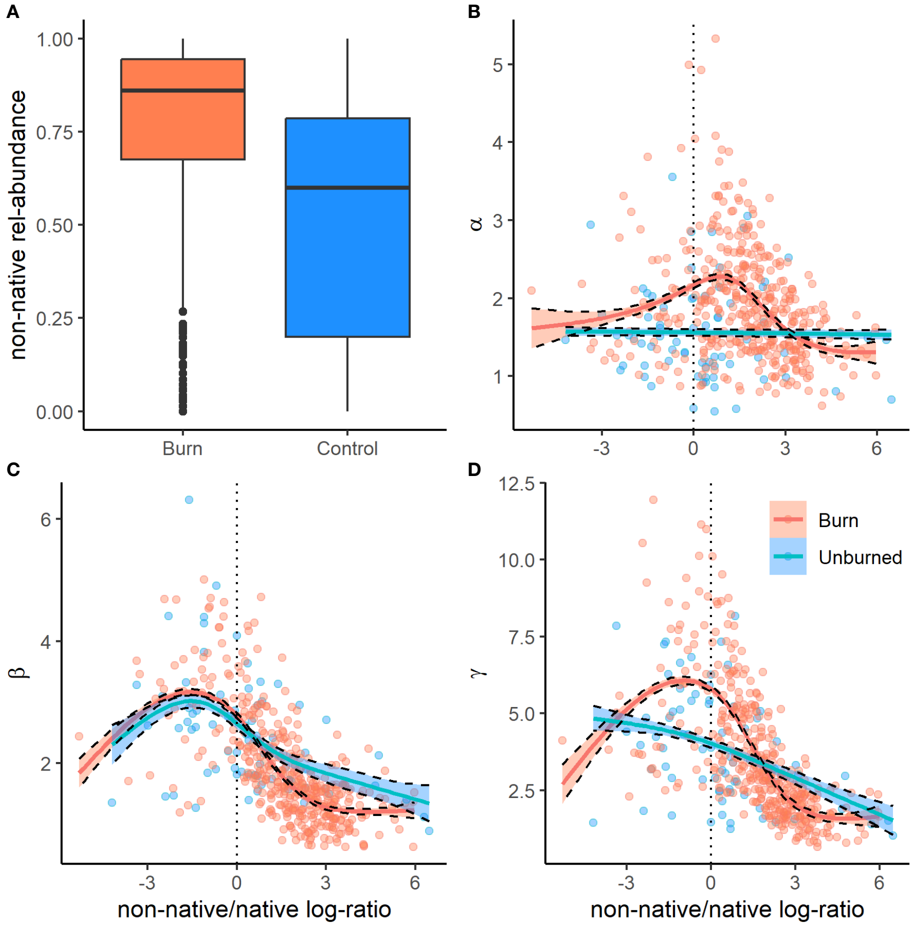

FIGURE 4
Box and whisker plots **(A)** of the relative abundance of non-native germinates from seed bank samples from burned (red) and unburned (blue) sites from across the Mojave Desert. Bold lines represent the median, boxes the upper and lower quartiles (interquartile range), whiskers 1.5× the interquartile range, and points outliers. Panels **(B–D)** show the relationship of α **(B)**, β **(C)**, and γ **(D)** diversity with the ratio (log) of non-native to native seed bank abundance.

= 0.65–0.90) sites, with the majority of dissimilarity contributed to by species turnover (losses and gains that appear as "replacements" in species composition) as opposed to nestedness (changes in abundance where local communities are subsets of the larger, regional or site-level pool). Species turnover was higher across unburned (87% of dissimilarity) than burned locations (72% of dissimilarity). Accordingly, species nestedness was twice as high in burned (28%) compared to unburned plots (13%), indicating that a greater proportion of observed differences in composition within burn plots was composed by variable subsets of local species pools with a shrinking role of replacement via turnover (Figure 6). The GLMMs explained slightly less of the total variation in plot-scale dissimilarity for both nestedness (R^2 = 0.42) and turnover (R^2 = 0.44) than standard measures of diversity. However, both turnover and nestedness had similar, non-linear relationships with the relative abundance of non-native plants (Figure 6). Turnover exhibited a negative relationship with burn frequency and a positive relationship with the relative cover of woody vegetation. Nestedness had a significant positive relationship with the relative cover of woody vegetation, and a negative relationship with burn frequency.

3.2 Gamma diversity

The effective number of species at the plot scale (γ at q1) was similar for burned and unburned sites. Mean γ-diversity was 3.63 (95% CI = 3.26–4.04) for burned and 3.82 (95% CI = 3.41–4.24) for unburned plots. Similar to α- and β-diversity models, the model explained a little over half of the variation in γ-diversity (R^2 = 0.55; Figure 5). Gamma diversity was significantly and positively related with tmax7 and negatively related with Hillshade. Also similar to the other diversity measures, γ-diversity had a strong non-linear relationship with the relative abundance of non-native species.

4 Discussion

Fire, while historically rare and infrequent across North American deserts (Wright and Bailey, 1982), has become an increasingly significant disturbance on the landscape. An examination of Mojave fires over the last four decades indicates a highly heterogeneous regime with varying frequency, severity, and size (Klinger et al., 2021). Shifts in fire frequency and severity can

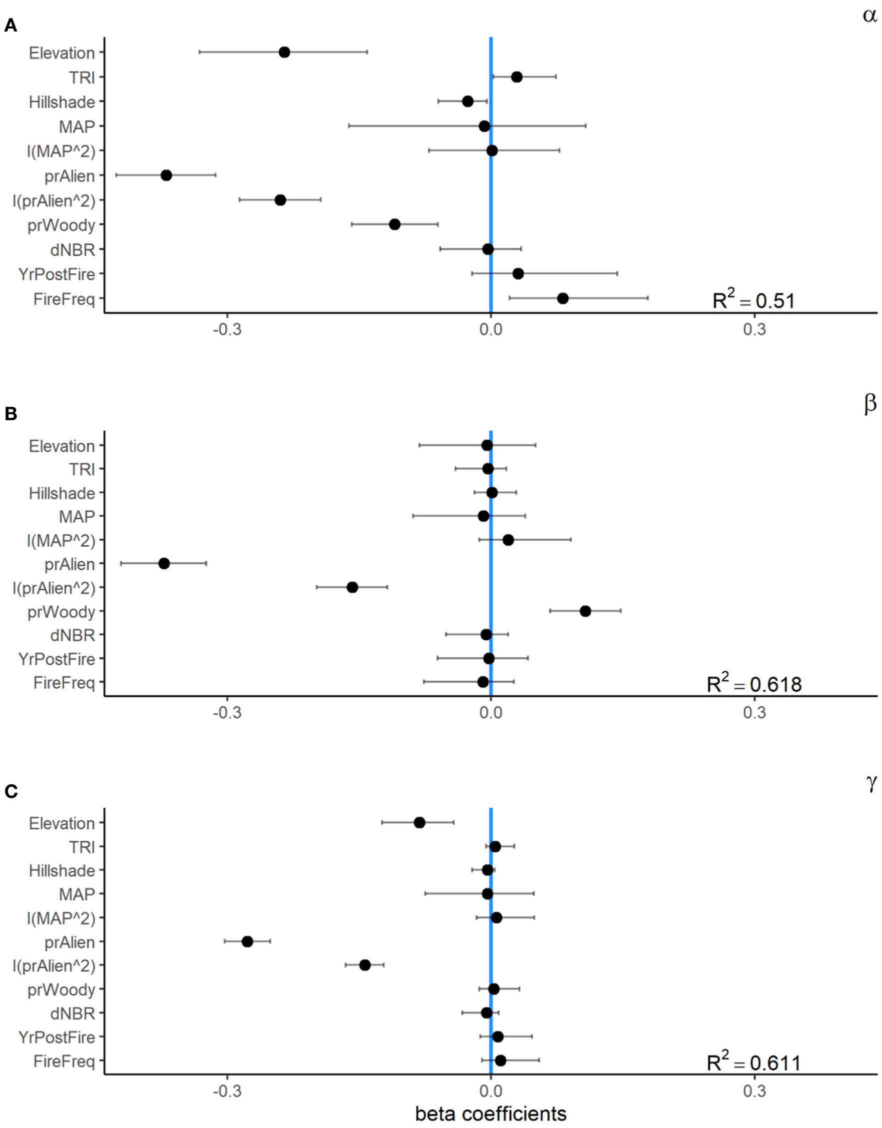

FIGURE 5
Standardized beta coefficients for fixed effects from generalized linear mixed effect models (GLMMs) for seed bank alpha **(A)**, beta **(B)**, and gamma **(C)** diversity from a 35-year chronosequence of burned locations from across the Mojave Desert. Error bars indicate 95% confidence intervals.

promote transitions toward communities dominated by herbaceous and non-native plants (Brooks et al., 2004; Klinger and Brooks, 2017). Notably, certain *Bromus* grass species, once introduced, exhibit explosive invasiveness in post-fire areas in the Mojave and other regions (Reid et al., 2006). The rapid alteration of local plant community dynamics by invasives raises concerns about the emergence of persistent alternative ecological states. Our findings in the Mojave indicate that fire can increase seed bank species richness (γ at q0) and the effective number of species (α & γ at q1) at relatively small subplot (1 m) and plot (0.1 ha) spatial scales. This likely underscores the crucial role of disturbance in promoting variability in resources that sustain plant diversity within this ecoregion. However, seed bank diversity was minimally influenced by measures of fire severity, frequency, and YPF. Instead, diversity was strongly shaped by the invasion severity of non-native plants and the cover of woody perennial plants—factors reflecting the long-term effects of climate and disturbance history on plant communities. Effectively, invasion of the Mojave ecoregion by non-native annual plants homogenizes the soil seed bank by rapidly driving a decline in native plant diversity beyond a critical threshold in non-native plant relative abundance, and a concomitant decrease in the compositional variability of the seed bank across the landscape (i.e., a decrease in β-diversity). While unburned locations also host non-native plants at lower abundance than burned, fire disturbances allow for a rapid increase in the relative abundance of non-native plants, driving more rapid losses of native diversity and resulting in greater homogenization across space. Further efforts to quantify this threshold will be pivotal for developing management strategies and designating urgent restoration zones to support native plant biodiversity in the Mojave system.

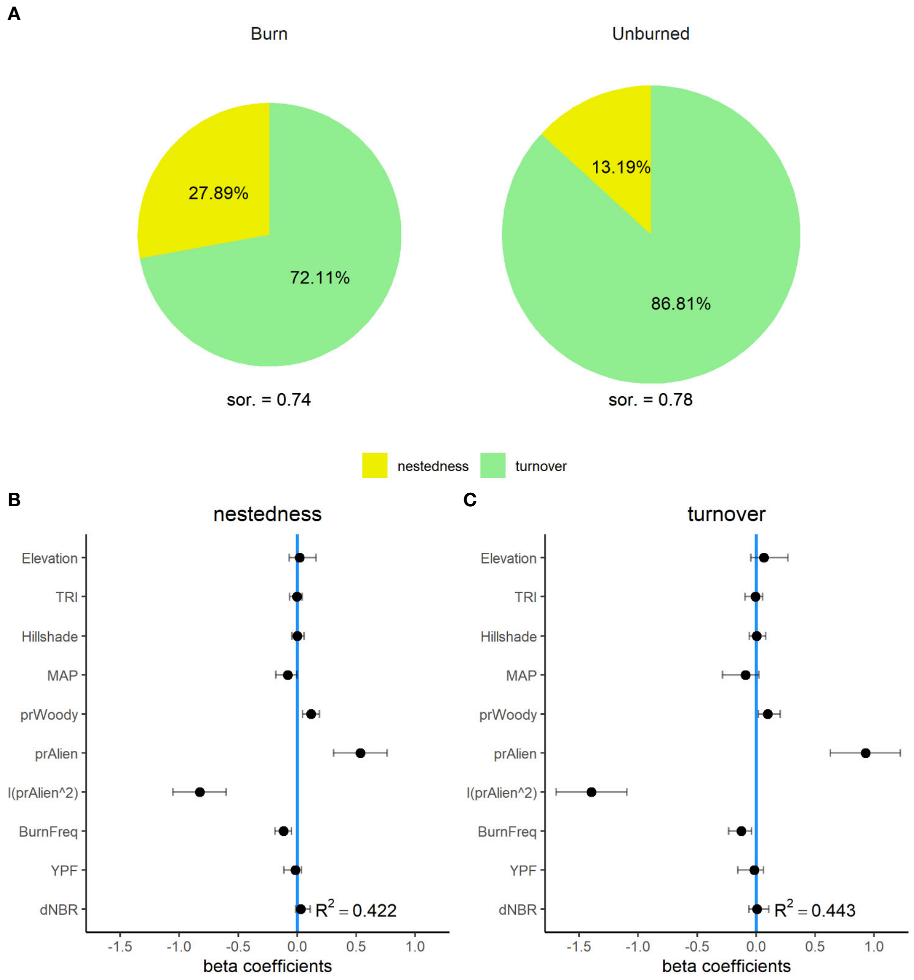

FIGURE 6
Nestedness and turnover components of beta diversity for burned and unburned sites across the Mojave Desert **(A)**. Percent values within each pie chart represent the proportion of mean plot-level Sørensen dissimilarity (sor.) portioned into either nestedness (yellow) or turnover (green). Panels **(B, C)** are the standardized beta coefficients for fixed effects (see Table 1) from generalized linear mixed effect models (GLMMs) for seed bank nestedness **(B)**, and turnover **(C)** from a 35-year chronosequence of burned locations from across the Mojave Desert. Error bars indicate 95% confidence intervals.

4.1 Disturbance and changes in native plant species diversity

Measures of q1 diversity (i.e., effective number of species) at the subplot (α; 1m^2) and plot (γ; 0.1 ha) scale were higher in burned than unburned areas. The effective number of species in burned areas, however, was not significantly influenced by the severity, frequency, or years since fire such that areas that burned once differed little from sites that burned multiple times over the data timeline.

The seemingly weak influence of fire variables on the effective number of species at local subplot and plot scales may also be because the strongest influence we observed in determining diversity at both scales was the abundance of non-native alien species within the seed bank. This relationship was variable across unburned and burned sites but was non-linear and often parabolic. The relationship was consistent in that the effective diversity initially increased as the relative abundance of non-native species in the seed bank increased before reaching a threshold peak that was followed by a rapid loss of diversity at higher non-native seed abundance. This relationship was strongest in burned sites—an outcome that was expected given the positive influence of disturbance on the abundance of non-native plants in the Mojave and other ecoregions. While the common non-native plants of the Mojave benefit from disturbances, these species can still invade unburned sites where they persist at lower abundances than in more heavily disturbed locations. For example, the earlier emergence of *B. tectoroum* from the seed bank relative to native plants allows it to capture greater amounts of soil nitrogen, increasing its abundance while elevating resource competition that causes a decline in native plant diversity (Prevéy and Seastedt, 2014). Similar plant community responses and outcomes of soil nutrient pulses have been documented in other prolific plant invaders (Besaw et al., 2011). *Bromus tectorum*, and some other non-native annual plants, have also been shown to capitalize on resources provided by soil-surface biocrust communities (Ferrenberg et al., 2018; Havrilla et al., 2019) which are more common and widespread in less frequently disturbed locations of drylands (Weber et al. 2022). Fire effects on vegetation and soils typically cause short-duration pulses in soil inorganic nitrogen, which have been shown to amplify non-native plant invasion in the Mojave Desert (Esque et al., 2010).

We also found a negative relationship between the effective number of species and woody plant cover at the local, subplot scale. This result seems contrary to expectations of shrubs and trees acting as "nurse plants" that promote species diversity in arid ecosystems (Madrigal-González et al., 2020). However, an overwhelming majority of nurse plant studies report patterns derived from aboveground plant assemblages and are not measures based on the larger plant community found in soil seed banks which can harbor additional species diversity (Hosna et al., 2023). Woody plant cover is also correlated to local climate and disturbance histories; areas with more woody plants are likely to have experienced fewer or less severe disturbances over time (Sühs et al., 2020). In the context of our study, the presence of woody vegetation in burned areas likely reflects the natural heterogeneity in fire effects across study sites and transects, impacting local vegetation community structure and the average age/size of shrubs. This aligns with findings in the Chihuahuan Desert, where nurse plant effects depend on shrub size and species, emphasizing the role of both floristic composition and disturbance regimes in shaping the plant diversity of arid systems (Ferrenberg et al., 2023).

4.2 Fire as a homogenizing influence on soil seed banks

Disturbance is expected to alter β-diversity in several ways. In the short term, fire may increase β-diversity by altering environmental heterogeneity, reducing local α-diversity, and pushing fire intolerant species to be more clumped or in "patches" (Myers et al., 2015). Under classical post-disturbance recovery models, β-diversity would have a trajectory towards pre-disturbance levels as time passed. However, invasion can disrupt this process (e.g., Kuebbing et al., 2014). We observed that the abundance of native species represented in the seed bank declined linearly with non-native relative abundance at burned sites, but not at unburned sites. β-diversity similarly declined, although non-linearly, with the increase in relative abundance of invasives. This nonlinear relationship might reflect changes in biotic interactions (e.g., competitive or facilitative effects), environmental filtering, or responses by plants to localized resource pools. This relationship might also reflect stochastic influences on seed bank community assembly, particularly dispersal processes and the effects of fire disturbance on the probability of seed movements among heterogenous resource and vegetation patches (Applestein et al., 2022).

The decline in both α- and β-diversity indicates that the seed bank communities of this system are being homogenized by non-native plant invasion. Fire disturbance plays an important role in the progress of seed bank homogenization: we observed a relative reduction in species turnover and a greater than 200% increase in species nestedness in burned compared to unburned sites. Thus, across burned sites, seed banks experience less species turnover (replacements) while dwindling toward a subset of plants found in the more diverse γ-level communities. This increased similarity in community composition is produced by the loss of species from a community and the non-random replacement of those species by more widespread occurring species (Clavel et al., 2011). This phenomenon has been documented widely across biota and ecosystems in response to the proliferation of invasive non-native species (Olden and Poff, 2003). This occurs in the Mojave, where the suppression of recruitment of native species by invasive annual grass and forb species has been observed (Brooks, 2000; DeFalco et al., 2007). Meanwhile, the greatest difference in turnover was driven by fire frequency with two or more fires increasing turnover suggesting that ongoing increases in fire frequency are likely to produce alternate community states within soil seed banks.

Beta diversity is a crucial concept in ecology, representing variation in species composition between different ecological communities. Beta diversity is important as it provides insights into the mechanisms of community assembly and biodiversity patterns across different habitats or environmental gradients. For, instance, studies have shown that beta diversity can vary with elevation (Kraft et al., 2011) and shift in response to fire disturbance and time since fire (Ferrenberg et al., 2013). This variation in beta diversity across elevations or disturbed habitats can indicate the influence of various ecological processes, such as environmental filtering, species interactions, or spatial constraints on community composition. Understanding these patterns is vital, as it helps in identifying drivers of biodiversity and understanding the impact of environmental changes on plant communities.

5 Conclusions

Variability and maintenance of native species in local plant assemblages has important implications for the conservation and ecological integrity of Mojave Desert ecosystems. We measured the effects of fire severity, frequency, and history on seed bank species diversity. We found that invasive plants are driving a homogenization process of desert plant communities, which is amplified by the positive effects of fire disturbance on the abundance of key invaders, particularly annual *Bromus* grasses. Such homogenization could have profound impacts on the maintenance of regional biodiversity pools, including across trophic levels where numerous species, such as the threatened desert tortoise (*Gopherus agassizii*), are already taxed by habitat alteration. Understanding the mechanistic pathways through which plant invasion and disturbance combine to alter seed bank composition and abundance patterns, and what role direct and indirect effects of disturbance on soil systems play in seed bank homogenization, is crucial for identifying targets for restoration as well as conservation goals.

Data availability statement

The raw data supporting the conclusions of this article will be made available by the authors, without undue reservation.

Author contributions

SL: Data curation, Formal analysis, Investigation, Methodology, Supervision, Visualization, Writing – original draft, Writing – review & editing. RK: Conceptualization, Data curation, Funding acquisition, Methodology, Project administration, Resources, Supervision, Validation, Writing – review & editing. MB: Conceptualization, Funding acquisition, Investigation, Project administration, Resources, Supervision, Validation, Writing – review & editing. SF: Conceptualization, Investigation, Resources, Supervision, Writing – original draft, Writing – review & editing.

Funding

The author(s) declare financial support was received for the research, authorship, and/or publication of this article. Research was funded by the United States Strategic Environmental Research & Development Program (SERDP grant 10 SI01-016), U.S. Joint Fire Science Program (JFSP project number 10-1-04-21), and US Geological Survey Invasive Species Program.

Acknowledgments

We thank the Strategic Environmental Research & Development Program (SERDP, Department of Defense), Joint Fire Science Program (JFSP, Department of Interior), and U.S. Geological Survey Invasive Species Program for funding. We thank the USGS staff in Bishop, California for collecting soil seed bank samples, especially, Michael Cleaver, Sunny Sawyer, Robyn Lee, Laurel Triatik, Elizabeth Moore, Lindsay Swinger, and Stacey Huskins. Laurel Triatik helped immensely with the greenhouse work. Any use of trade, firm, or product names is for descriptive purposes only and does not imply endorsement by the U.S. Government.

Conflict of interest

The authors declare that the research was conducted in the absence of any commercial or financial relationships that could be construed as a potential conflict of interest.

Publisher's note

Supplementary material

The Supplementary Material for this article can be found online at: https://www.frontiersin.org/articles/10.3389/fevo.2024.1271824/full#supplementary-material

References

Abatzoglou, J. T., and Williams, A. P. (2016). Impact of anthropogenic climate change on wildfire across Western US forests. *Proc. Natl. Acad. Sci. U.S.A.* 113, 11770–11775. doi: 10.1073/pnas.1607171113

Abella, S. R. (2009). Post-fire plant recovery in the Mojave and Sonoran deserts of western North America. *J. Arid Environ.* 73, 699–707. doi: 10.1016/j.jaridenv.2009.03.003

Akinwande, M.O., Dikko, H.G., and Samson, A. (2015). Variance Inflation Factor: As a Condition for the Inclusion of Suppressor Variable(s) in Regression Analysis. *Open J Stat.* 5, 754.

Anderson, T. M., Schütz, M., and Risch, A.C. (2012). Seed germination cues and the importance of the soil seed bank across an environmental gradient in the Serengeti. *Oikos* 121, 306–312. doi: 10.1111/j.1600-0706.2011.19803.x

Applestein, C., Caughlin, T. T., and Germino, M. J. (2022). Post-fire seed dispersal of a wind-dispersed shrub declined with distance to seed source, yet had high levels of unexplained variation. *AoB Plants* 14, plac045. doi: 10.1093/aobpla/plac045

Aronson, J., and Shmida, A. (1992). Plant species diversity along a Mediterranean-desert gradient and its correlaiton with interannual rainfall fluctuations. *J. Arid Environ.* 23, 235–247. doi: 10.1016/S0140-1963(18)30513-5

M. G. Barbour and W. D. Billings (Eds.) (2000). *North American terrestrial vegetation. 2nd ed.* (Cambridge and New York: Cambridge University Press).

Bartoń, K. (2020) *MuMIn: multi-model inference.* Available at: https://CRAN.R-project.org/package=MuMIn.

Baskin, C. C., and Baskin, J. M. (1998). *Seeds: ecology, biogeography, and evolution of dormancy and germination* (San Diego, California, USA: Academic Press).

Bates, D., Maechler, M., Bolker, B., and Walker, S. C. (2015). Fitting linear mixed-effects models using lme4. *J. Stat. Software* 67, 1–48. doi: 10.18637/jss.v067.i01

Besaw, L. M., Thelen, G. C., Sutherland, S., Metlen, K., and Callaway, R. M. (2011). Disturbance, resource pulses, and invasion: short-term shifts in competitive effects, not growth responses, favour exotic annuals. *J. Appl. Ecol.* 48, 998–1006. doi: 10.1111/jpe.2011.48.issue-4

Brooks, M. L. (2000). Competition between alien annual grasses and native annual plants in the Mojave Desert. *Am. Midland Nat.* 144, pp.92–pp108. doi: 10.1674/0003-0031(2000)144[0092:CBAAGA]2.0.CO;2

Brooks, M. L., D'Antonio, C.M., Richardson, D.M., Grace, J.B., Keeley, J.E., DiTomaso, J.M., et al. (2004). Effects of invasive alien plants on fire regimes. *BioSience* 54, 677–688. doi: 10.1641/0006-3568(2004)054[0677:EOIAPO]2.0.CO;2

Brooks, M. L., Minnich, R., and Matchett, J. R. (2018). *Southeastern deserts bioregion.* Fire in California's Ecosystems. *2nd. Ed.* Eds. J. W. V. Wagtendonk, N. G. Sugihara, S. L. Stephens, A. E. Thode, K. E. Shaffer and Fites-Kaufman, (Berkeley, CA, USA: University of California Press).

Cadotte, (2007). Concurrent niche and neutral processes in the competition-colonization model of species coexistence. *Proc. R. Soc B.* 274, 2739–2744. doi: 10.1098/rspb.2007.0925

Chambers, J. C., and Wisdom, M. J. (2009). Priority research and management issues for the imperiled great basin of the western United States. *Restor. Ecol.* 17, 707–714. doi: 10.1111/j.1526-100X.2009.00588.x

Chao, A., Gotelli, N. J., Hsieh, T. C., Sander, E. L., Ma, K. H., Colwell, R. K., et al. (2014). Rarefaction and extrapolation with Hill numbers: a framework for sampling and estimation in species diversity studies. *Ecol. Monogr.* 84, 45–67. doi: 10.1890/13-0133.1

Chesson, P. (2000). Mechanisms of maintenance of species diversity. *Annu. Rev. Ecol. Syst.* 31, 343–366. doi: 10.1146/annurev.ecolsys.31.1.343

Chesson, P. L., and Huntly, N. (1997). The roles of harsh and fluctuating conditions in the dynamics of ecological communities. *Am. Nat.* 150, 519–553. doi: 10.1086/286080

Clavel, J., Julliard, R., and Devictor, V. (2011). Worldwide decline of specialist species: toward a global functional homogenization? *Front. Ecol. Environ.* 9, 222–228. doi: 10.1890/080216

D'Antonio, C. M., and Vitousek, P. M. (1992). Biological invasions by exotic grasses, the grass/fire cycle and global change. *Annu. Rev. Ecol. Syst.* 23, 63–87. doi: 10.1146/annurev.es.23.110192.000431

DeFalco, L. A., Fernandez, G. C., and Nowak, R. S. (2007). Variation in the establishment of a non-native annual grass influences competitive interactions with Mojave Desert perennials. *Biol. Invasions* 9, 293–307. doi: 10.1007/s10530-006-9033-5

Eidenshink, J., Schwind, B., Brewer, K., Zhu, Z.-L., Quayle, B., and Howard, S. (2007). A project for monitoring trends in burn severity. *Fire Ecol.* 3, 3–21. doi: 10.4996/fireecology.0301003

Engel, E. C., and Abella, S. R. (2011). Vegetation recovery in a desert landscape after wildfires: influences of community type, time since fire and contingency effects. *J. Appl. Ecol.* 48, 1401–1410. doi: 10.1111/j.1365-2664.2011.02057.x

Esque, T. C., Kaye, J. P., Eckert, S. E., DeFalco, L. A., and Tracy, C. R. (2010). Short-term soil inorganic N pulse after experimental fire alters invasive and native annual plant production in a Mojave Desert shrubland. *Oecologia* 164, 253–263. doi: 10.1007/s00442-010-1617-1

Faist, A. M. (2013). Banking on the past: seed banks as a reservoir for rare and native species in restored vernal pools. *Aob Plants* 5, plt043. doi: 10.1093/aobpla/plt043

Faist, A. M., and Collinge, S. K. (2015). Seed bank composition varies along invasion and inundation gradients in vernal pool wetlands. *Plant Ecol.* 216, 553–564. doi: 10.1007/s11258-015-0458-8

Ferrandis, P., Herranz, J. M., and Martinez-Sanches, J. J. (2001). Response to fie of a predominantly transient seed bank in a Mediterranean weedy pasture (eastern-central Spain). *Ecoscience* 8, 211–219. doi: 10.1080/11956860.2001.11682647

Ferrenberg, S., Faist, A. M., Howell, A., and Reed, S. C. (2018). Biocrusts enhance soil fertility and Bromus tectorum growth, and interact with warming to influence germination. *Plant Soil* 429, 77–90. doi: 10.1007/s11104-017-3525-1

Ferrenberg, S., Faist, A., Osborne, B., and Lee, S. (2023). Quantifying potential abiotic drivers of the nurse-plant effect in two dominant shrub species of the northern Chihuahuan Desert. *bioRxiv*, 2023–2011. doi: 10.1101/2023.11.16.567462

Ferrenberg, S., O'Neill, S. P., Knelman, J. E., Todd, B., Duggan, S., Bradley, D., et al. (2013). Changes in assembly processes in soil bacterial communities following a wildfire disturbance. *ISME J.* 7, 1102–1111. doi: 10.1038/ismej.2013.11

Gremer, J. R., and Venable, D. L. (2014). Bet hedging in desert winter annual plants: optimal germination strategies in a variable environment. *Ecol. Lett.* 17, 380–387. doi: 10.1111/ele.12241

Haas-Desmarais, S., and Lortie, C. J. (2023). Direct and indirect interactions between shrubs and the flowering annual community in an arid ecosystem. *Flora* 298, 152202. doi: 10.1016/j.flora.2022.152202

Haight, J. D., Reed, S. C., and Faist, A. M. (2019). Seed bank community and soil texture relationships in a cold desert. *J. Arid Environ.* 164, 46–52. doi: 10.1016/j.jaridenv.2019.01.008

Hartig, F. (2022). DHARMa: Residual diagnostics for hierarchical (multi-level /mixed) regression models. *R package version 0.4.5.*

Havrilla, C. A., Chaudhary, V. B., Ferrenberg, S., Antoninka, A. J., Belnap, J., Bowker, M. A., et al. (2019). Towards a predictive framework for biocrust mediation of plant performance: A meta-analysis. *J. Ecol.* 107, 2789–2807. doi: 10.1111/1365-2745.13269

Hereford, R., Webb, R. H., and Longpre, C. I. (2006). Precipitation history and ecosystem response to multidecadal precipitation variability in the Mojave Desert region 1893–2001. *J. Arid Environ.* 67, 13–34. doi: 10.1016/j.jaridenv.2006.09.019

Hill, M. O. (1973). Diversity and evenness: A unifying notation and its consequences. *Ecology* 54, 427–432. doi: 10.2307/1934352

Hobbs, R. J., and Huenneke, L. F. (1992). Disturbance, diversity, and invasion: implications for conservation. *Conserv. Biol.* 6, 324–337. doi: 10.1046/j.1523-1739.1992.06030324.x

Hosna, R. K., Reed, S. C., and Faist, A. M. (2023). Long-term relationships between seed bank communities and wildfire across four North American desert sites. *Ecosphere* 14, e4398. doi: 10.1002/ecs2.4398

Huston, M. (1979). A general hypothesis of species diversity. *Am. Nat.* 113, 81–101. doi: 10.1086/283366

Jost, L. (2007). Partitioning diversity into independent alpha and beta components. *Ecology* 88, 2427–2439. doi: 10.1890/06-1736.1

Jost, L. (2013). "Effective number of species," in *The new synthesis of diversity indices and similarity measures*. Available at: http://www.loujost.com/Statistics%20and%20Physics/Diversity%20and%20Similarity/EffectiveNumberOfSpecies.htm.

Keeley, J. E., Baer-Kelley, M., and Fotheringham, C. J. (2005). Alien plant dynamics following fire in Mediterranean-climate California shrublands. *Ecol. Appl.* 15, 2109–2125. doi: 10.1890/04-1222

Kemp, P. R. (1989). "Seed banks and vegetation processes in deserts," in *Ecology of soil seed banks*. Eds. M. A. Leck, V. T. Parker and Hanneke, (Academic, New York), 257–282.

Klinger, R., and Brooks, M. (2017). Alternative pathways to landscape transformation: invasive grasses, burn severity and fire frequency in arid ecosystems. *J. Ecol.* 105, 1521–1533. doi: 10.1111/1365-2745.12863

Klinger, R., Underwood, E. C., McKinley, R., and Brooks, M. L. (2021). Contrasting geographic patterns of ignition probability and burn severity in the Mojave Desert. *Front. Ecol. Evol.* 9, 79. doi: 10.3389/fevo.2021.593167

Klinger, R. C., Underwood, E. C., McKinley, R., and Brooks, M. L. (2022). *Fire regimes in the Mojave Desert (1972-2010): U.S. Geological Survey data release*. doi: 10.5066/P99YGHSJ

Kraft, N. J. B., Comita, L. S., Chase, J. M., Sanders, N. J., Swenson, N. G., Crist, T. O., et al. (2011). Disentangling the drivers of beta diversity along latitudinal and elevational gradients. *Science* 333, 1755–1758. doi: 10.1126/science.1208584

Kraft, N. J., Valencia, R., and Ackerly, D. D. (2008). Functional traits and niche-based tree community assembly in an Amazonian Forest. *Science* 322, 580–582. doi: 10.1126/science.1160662

Kuebbing, S. E., Souza, L., and Sanders, N. J. (2014). Effects of co-occurring non-native invasive plant species on old-field succession. *For. Ecol. Manage.* 324, 196–204. doi: 10.1016/j.foreco.2013.10.031

Lucero, J. E., Seifan, M., Callaway, R. M., and Lortie, C. J. (2020). Positive associations with native shrubs are intense and important for an exotic invader but not the native annual community across an aridity gradient. *Divers. Distrib.* 26, 1177–1197. doi: 10.1111/ddi.13111

Lüdecke, D., Makowski, D., Waggoner, P., and Patil, I. (2020). performance: assessment of regression models performance. *R Package Version 0.4. 7. Appl. Stat. Using R* 440, 5.

Madrigal-González, J., Cano-Barbacil, C., Kigel, J., Ferrandis, P., and Luzuriaga, A. L. (2020). Nurse plants promote taxonomic and functional diversity in an arid Mediterranean annual plant community. *J. Vegetation Sci.* 31, pp.658–pp.666. doi: 10.1111/jvs.12876

Marcon, E., and Hérault, B. (2015). entropart: an R package to measure and partition diversity. *J. Stat. Software* 67, 1–26. doi: 10.18637/jss.v067.i08

McIntire, E. J. B., and Fajardo, A. (2014). Facilitation as a ubiquitous driver of biodiversity. *New Phytol.* 201, 403–416.-416. doi: 10.1111/nph.12478

McIntyre, S., and Lavorel, S. (1994). Predicting richness of native, rare, and exotic plants in response to habitat and disturbance variables across a variegated landscape. *Conserv. Biol.* 8, 521–531. doi: 10.1046/j.1523-1739.1994.08020521.x

Myers, J. A., Chase, J. M., Crandall, R. M., and Jimenez, I. (2015). Disturbance alters beta-diversity but not the relative importance of community assembly mechanisms. *J. Ecol.* 103, 1291–1299. doi: 10.1111/1365-2745.12436

Oksanen, J., Blanchet, F. G., Friendly, M., Kindt, R., Legendre, P., McGlinn, D., et al. (2020). Vegan: community ecology package version 2.5-7. *R Project for Statistical Computing*. Vienna, Austria.

Olden, J. D., and Poff, L. (2003). Toward a mechanistic understanding and prediction of biotic homogenization. *Am. Nat.* 162, 442–460. doi: 10.1086/378212

Petraitis, P. S., Latham, R. E., and Niesenbaum, R. A. (1989). The maintenance of species-diversity by disturbance. *Q. Rev. Biol.* 64, 393–418. doi: 10.1086/416457

Prevéy, J. S., and Seastedt, T. R. (2014). Seasonality of precipitation interacts with exotic species to alter composition and phenology of a semi-arid grassland. *J. Ecol.* 102, 1549–1561. doi: 10.1111/1365-2745.12320

Pulsford, S. A., Lindenmayer, D. B., and Driscoll, D. A. (2016). A succession of theories: purging redundancy from disturbance theory. *Biol. Rev.* 91, 148–167. doi: 10.1111/brv.12163

R Core Team (2023). *R: A language and environment for statistical computing* (Vienna, Austria: R Foundation for Statistical Computing). Available at: https://www.R-project.org.

Reid, C. R., Goodrich, S., and Bowns, J. E. (2006). "Cheatgrass and red brome; History and biology of two invaders," in *Proceedings–shrublands under fire: disturbance and recovery in a changing world* (Fort Collins, Colorado: US Department of Agriculture, Forest Service, Rocky Mountain Research Station), 27–32.

Rodríguez-Moreno, V. M., and Bullock, S. H. (2014). Vegetation response to hydrologic and geomorphic factors in an arid region of the Baja California Peninsula. *Environ. Monit. Assess.* 186, 1009–1021. doi: 10.1007/s10661-013-3435-5

Safford, H., and Harrison, S. (2004). Fire effects on plant diversity in serpentine and sandstone chaparral. *Ecology* 85, 539–548. doi: 10.1890/03-0039

Schade, J. D., Sponseller, R., Collins, S. L., and Stiles, A. (2003). The influence of *Prosopis* canopies on understorey vegetation: Effects of landscape position. *J. Vegetation Sci.* 14, 743–750. doi: 10.1111/j.1654-1103.2003.tb02206.x

Silva Pedro, M., Rammer, W., and Seidl, R. (2016). A disturbance-induced increase in tree species diversity facilitates forest productivity. *Landscape Ecol.* 31, 989–1004. doi: 10.1007/s10980-015-0317-y

Soininen, J., Heino, J., and Wang, J. (2018). A meta-analysis of nestedness and turnover components of beta diversity across organisms and ecosystems. *Global Ecol. Biogeography.* 27, 96–109. doi: 10.1111/geb.12660

Sousa, W. P. (1984). The role of disturbance in natural communities. *Annu. Rev. Ecol. Syst.* 15, 353–391. doi: 10.1146/annurev.es.15.110184.002033

Sühs, R. B., Giehl, E. L. H., and Peroni, N. (2020). Preventing traditional management can cause 1468 grassland loss within 30 years in southern Brazil. *Sci. Rep.* 10, 783. doi: 10.1038/s41598-020-57564-z

Tagestad, J., Brooks, M., Cullinan, V., Downs, J., and McKinley, R. (2016). Precipitation regime classification for the Mojave Desert: implications for fire occurrence. *J. Arid Environ.* 124, 388–397. doi: 10.1016/j.jaridenv.2015.09.002

Underwood, E. C., Klinger, R. C., and Brooks, M. L. (2019). Effects of invasive plants on fire regimes and postfire vegetation diversity in an arid ecosystem. *Ecol. Evol.* 9, 12421–12435. doi: 10.1002/ece3.5650

Vandvik, V., Klanderud, K., Meineri, E., Måren, I. E., and Töpper, J. (2016). Seed banks are biodiversity reservoirs: species–area relationships above versus below ground. *Oikos* 125, 218–228. doi: 10.1111/oik.02022

Weber, B., Belnap, J., Büdel, B., Antoninka, A. J., Barger, N. N., Chaudhary, V. B., et al. (2022). What is a biocrust? A refined, contemporary definition for a broadening research community. *Biol. Rev.* 97, 1768–1785. doi: 10.1111/brv.12862

Whittaker, R. H. (1972). Evolution and measurement of species diversity. *Taxon* 21, 213–251. doi: 10.2307/1218190

Wilson, M. F. J., O'Connell, B., Brown, C., Guinan, J. C., and Grehan, A. J. (2007). Multiscale terrain analysis of multibeam bathymetry data for habitat mapping on the continental slope. *Mar. Geodesy* 30, 3–35. doi: 10.1080/01490410701295962

Winkler, D. E., and Brooks, E. (2020). Tracing extremes across iconic desert landscapes: socio-ecological and cultural responses to climate change, water scarcity, and wildflower superblooms. *Hum. Ecol.* 48, 211–233. doi: 10.1007/s10745-020-00145-5

Wright, H. E., and Bailey, A. W. (1982). *Fire ecology, United States and Canada* (New York, USA: Wiley, New York).

Young, J. A., and Evans, R. A. (1975). Germinability of seed reserves in a big sagebrush communitiy. *Weed Sci.* 23, 358–364. doi: 10.1017/S0043174500062664

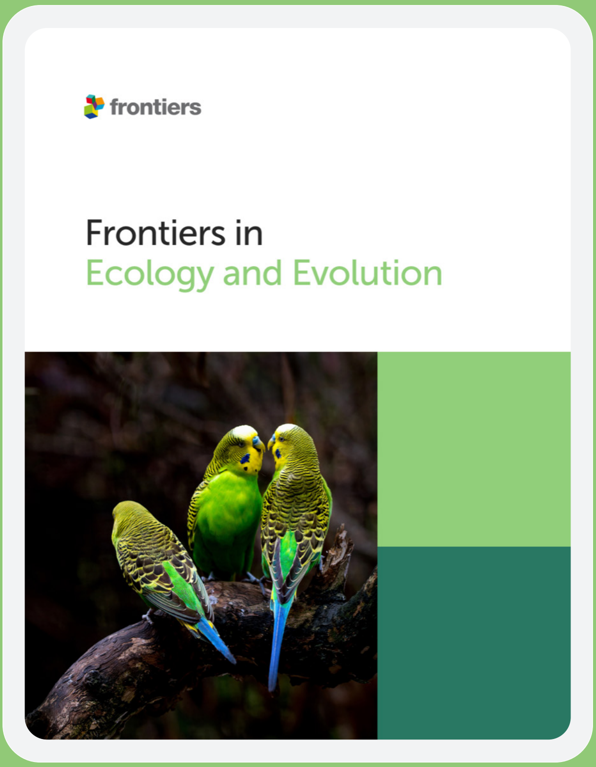

Frontiers

Avenue du Tribunal-Fédéral 34
1005 Lausanne, Switzerland
frontiersin.org

Contact us

+41 (0)21 510 17 00
frontiersin.org/about/contact